

THE GLACIAL WORLD ACCORDING TO WALLY

W.S. BROECKER

ELDIGO PRESS
2002

THE GLACIAL WORLD ACCORDING TO WALLY

W.S. BROECKER
LAMONT-DOHERTY EARTH OBSERVATORY
OF COLUMBIA UNIVERSITY
Palisades, NY 10964

September 1992

Second Revised Edition June 1995

Third Revised Edition August 2002

FOREWORD

In 1990 I started a book on glacial climates. I planned four sections, one on indicators, one on clocks, one on records and finally, one on the physics of the system. After completing the first three of these, I got stuck in my attempt to come up with a conceptual view of what might be driving these changes. However, having taught a course on climate change for many years, I know that much of the information one needs is not available in textbook form. Instead, we all depend heavily on reprints. As this proves to be an inefficient route for students interested in learning the basics of our field, I have tried to capture many of these basics in the first three sections of my would-be book. As I realized that it would be several years before I completed this project, I thought it might be useful to the community if I were to make available the three largely completed sections. This was done in 1992. In preparation for use in a short course to be taught at the Geological Society of America in November 2002, I undertook an effort to update the first three sections and the references during the early part of 2002.

I encourage purchasers of the book to make as many copies as they wish for use by students and colleagues. The spiral binding is easily removed so as to facilitate duplication.

Library-bound copies are also available.

DEDICATION

To
Gary Comer
A newfound friend and patron of young abrupt-change researchers.

.....

This book is available at a cost of \$50 for the spiral-bound version or \$70 for the hard-bound version (shipping included) Pre-payment is preferred. Checks in US\$ should be made out to Trustees of Columbia University.

To purchase contact
Patty Catanzaro
Eldigio Press
Lamont-Doherty Earth Observatory
of Columbia University
Palisades, NY 10964 USA
Tel.: (845) 365-8515; Fax: (845) 365-8155; e-mail: pcat@ldeo.columbia.edu

Copyright 1993

TABLE OF CONTENTS

PROLOGUE

INDICATORS

INTRODUCTION	1
ICE VOLUME	1
Glacial Moraines.....	2
Shorelines.....	4
Oxygen Isotopes.....	13
Summary	21
TEMPERATURE	21
Mountaintop Temperatures.....	23
Polar Temperatures	25
Sea Surface Temperatures.....	31
Continental Temperatures.....	45
The Tropical Temperature Dilemma	55
ARIDITY	56
Precipitation	58
Rock Varnish	61
Dust	63
ATMOSPHERIC GAS COMPOSITION.....	67
Carbon Dioxide.....	67
Methane.....	75
Isotopic Composition of Atmospheric Gases	77
OCEANIC CHEMISTRY.....	83
Trace Metals.....	83
Carbon Isotopes	96
RATE OF DEEP SEA VENTILATION.....	105
CO ₃ Concentration	109
Paleo pH.....	119
CLOCKS	
INTRODUCTION	1
THE RADIOCARBON CLOCK.....	1
ANNUAL CLOCKS	5
THE URANIUM-THORIUM CLOCK	15
CLOCKS READING MORE THAN 50,000 YEARS	29
THE POTASSIUM-ARGON CLOCK	35

TABLE OF CONTENTS

(continued)

IN SITU PRODUCTION CLOCKS	39
PLANETARY CLOCKS	40
SUNDIALS	41
RECORDS	
55 MILLION YEARS OF POLAR COOLING	1
MILANKOVITCH CYCLES	12
THE RECORD IN ANTARCTIC ICE	24
THE LAST 160,000 YEARS	26
THE LAST TERMINATION	37
DANSGAARD-OESCHGER EVENTS	63
HEINRICH EVENTS	69
RELATIONSHIP BETWEEN DANSGAARD-OESCHGER EVENTS AND HEINRICH EVENTS	79
MECHANISMS	
INTRODUCTION	1
FORCINGS	1
INSOLATION SEASONALITY CYCLES	1
THERMOHALINE CIRCULATION REORGANIZATIONS	2
FLUCTUATIONS IN SOLAR ENERGY OUTPUT	3
THE BIPOLAR SEESAW	6
AMPLIFIERS	6
WATER VAPOR	8
CLOUD COVER	9
TERMINATIONS	9
SUMMARY	10
FOSSIL FUEL CO ₂	11
BIBLIOGRAPHY	

PROLOGUE

In the debate regarding the possible consequences of the ongoing buildup of greenhouse gases, the climate record for the past hundred-thousand years sends us an important message. Contrary to the view held by those who downplay the consequences of fossil fuel burning, the paleorecord clearly demonstrates that the Earth's climate system is far from self stabilizing. Rather, it has undergone large responses to seemingly small forcings. Not only have major changes occurred, but some of the largest have taken place on the time scale of a few decades. Further, the magnitude of these shifts is far greater than expected from any known forcing (i.e., fluctuations in solar output, variable interception of sunlight by dust and aerosols, changes in seasonality resulting from variations in the Earth's orbital parameters...). Thus I am driven to the conclusion that the Earth's climate system has several distinct modes of operation.

To date, no Earth system model has been able to adequately account for the growth and maintenance of large ice sheets which occupied most of Canada and Scandinavia during peak glacial time. Nor has any model been able to adequately account for the atmosphere's low CO₂ content and high dust content during these times. Nor has any model been able to reproduce the rectangular character of past climate changes. We do, however, have one valuable clue in this regard. Models clearly demonstrate that the ocean's thermohaline circulation has a number of quasi-stable modes of operation. Further, these models show how the ocean might be triggered to jump from one of these modes to another. But to date, no clear explanation has been given as to how these changes in ocean operation translate into the globe-encompassing atmospheric changes recorded in the paleoclimate record.

The paleoclimatic record challenges us by demonstrating that much more must be learned about the Earth's climate system before we can have any confidence in model-based predictions of the changes which will result from the buildup of CO₂ and other

greenhouse gases in our atmosphere. If we are to take full advantage of the information offered by experiments carried out in the past, we must develop the capability to properly read the record kept in sediment and ice. Such a reading requires that we fully understand how each of our proxies responds to changes in environmental conditions. It also requires that we develop the capability to precisely correlate records from different places. To this end, the first two sections of this book deal with “Indicators” and “Clocks”. In the first, I attempt to depict the strengths and weaknesses of the many climate proxies currently under investigation. In the second, I do the same for radioisotope dating methods. Then, in the third section, entitled “Records”, I summarize what I consider to be the most informative of the proxy versus time curves. Finally, in the fourth section, entitled “Mechanisms”, I provide a scenario designed to explain what I consider to be the most important features of the record.

While in the text and captions I refer to by name some of the key contributors to this subject, these references are sparse compared to what would be found in a review article. While those of us in the field are extremely conscious of who did what and when they did it, my aim in writing this book is to introduce people to the subject. Detailed referencing would only interfere with this mission. Instead, I have put together a bibliography arranged by subject, and for a given subject, by publication date. By scanning these lists, one can see not only who did the work but also how the subject has evolved. As thousands of articles have been written on subjects included in this book, the bibliography is by no means comprehensive. Rather, it reflects my own reading.

INDICATORS

INTRODUCTION

Except for the observations made over the last 130 or so years at weather stations and on ships, our knowledge of past climates is based on records kept in sediment and ice. The task of the paleoclimatologist is to decipher the proxies contained in these records. This has proven a complex task for every proxy is influenced by more than one climatic variable. While much progress has been made toward isolating the influence of these competing contributions, the task has proven to be a very tough one. For convenience, these proxies can be divided into five major groups; i.e., those which carry information regarding: 1) ice volume, 2) temperature, 3) aridity, 4) atmospheric composition, and 5) ocean chemistry.

Emphasis is placed on reconstructing the conditions which prevailed during the peak of the last glaciation. Discussion of the time sequence of climate changes appears in the section entitled “Records”.

ICE VOLUME

When we speak of glaciation, we think mainly of the expansion and contraction of the great ice sheets which as recently as 20,000 years ago covered much of Canada and Scandinavia. Hence of primary interest to the study of glacial cycles is the volume of these ice masses. Emphasis is placed on volume rather than area because of its tie to sea level: the bigger the ice sheets, the lower the level of the sea. Estimates of the volume of ice on continents at any given time has been pieced together from three quite different sources of information, moraines which mark the perimeter of the ice sheets, shorelines which mark the level of the sea, and the ratio of ^{18}O to ^{16}O in benthic foraminifera which depend on ice volume. As each source has its limitations and ambiguities, only by considering the three together can we get the information we seek.

Glacial Moraines

The primary information regarding the volume of ice comes from deposits produced by the glaciers themselves. Moraines, i.e. debris bulldozed into place by the advancing ice front, mark the perimeter of the ice. Most important in this regard are those features created when the ice sheets of the last glacial period reached their maximum extent. We know from marine oxygen isotope records (see below) that each of the great ice ages culminated with about the same ice volume. Assuming that for each cycle the geometry of the ice sheets was more or less the same, the moraines formed during the last glacial maximum tell us where the major ice masses were located, not only during the last cycle but also during the previous ones (see figure 1). Indeed, where moraines from earlier ice maxima are preserved, they support this supposition.

While the location of the southern margins of the North American and Eurasian ice sheets is clearly defined by moraines, serious debate exists concerning the extent of ice along their northern perimeters. One school is convinced that large ice sheets were centered over the shelves of arctic Canada, Scandinavia, and Siberia. Another school is convinced that ice cover in these areas was minor, being confined to a few small island-based caps. The problem is that deposits similar to those that mark the edges of the southern margin of the Laurentide and Eurasian ice caps are absent in the Arctic. The big-ice school contends that they lie beneath the sea on the continental shelves. They point instead to the raised shorelines which ring the Arctic Islands. The height of these shorelines argues strongly for rebound triggered by the melting of large rather than small caps.

Were no information other than the position of the ice margins available, estimates of the volume of ice at glacial maxima would have to be obtained from computer simulations designed to yield the height and contour of the ice caps fitted to these boundaries. Even though these simulations are constrained by studies of the existing ice caps on Greenland and Antarctica, the uncertainties associated with such

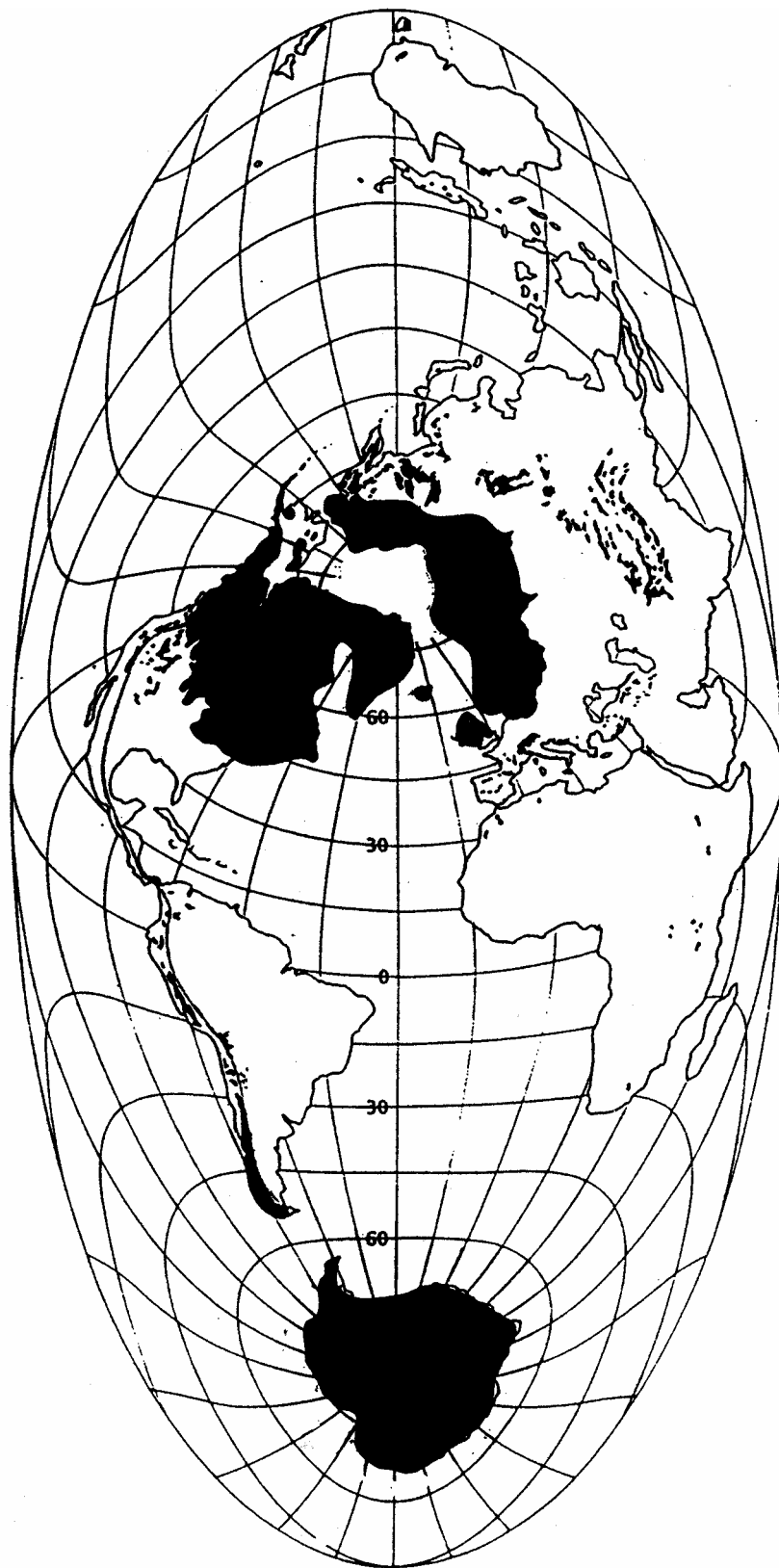


Figure 1. Map showing the extent of ice sheets during peak glacial time as viewed by the big-ice school.

estimates are on the order of $\pm 30\%$. Part of this uncertainty relates to the debate about the position of the northern perimeter of these ice sheets. Equally important are uncertainties regarding the snow fall rate during glacial time and the magnitude of the friction at the base of the glacial caps. The former is important because the higher the precipitation rate, the thicker an ice sheet will have to be in order to force the ice to flow toward its margins at a rate matching that at which snow accumulates in its interior. The latter is important because in some cases ice caps are frozen to the underlying terrain; while for others, geothermal heat melts the base of the ice allowing it to glide smoothly over the underlying rock. Clearly a glacier which moves over the underlying terrain like a hovercraft will be thinner than one which is firmly locked to its rock base.

Shorelines

On the time scales of interest (i.e. less than one million years), global sea level can change only in response to the amount of water stored in ice caps. Hence by dating shorelines formed in the past, it should be possible to directly assess the amount of water tied up in ice caps at that time. Despite the seeming simplicity of this approach, in practice it has proven exceedingly difficult. The primary reason is that the glacial-age shorelines we wish to study lie beneath the sea. Conducting underwater the geologic studies required to establish the relationship between the elevation of the sample to be dated and the elevation of the sea at the time it formed is not easy. The problem is that the action of waves and currents on submerged shorelines has often moved things ‘downhill.’ Successes have been rare. Only during the last 30 or so meters of the transgression of the sea accompanying the last deglaciation when the sea invaded estuaries and salt marshes were extensive deposits easily accessible to geologists produced. Unfortunately, the elevation of the shoreline of most interest, i.e., that formed at the time of maximum glacial extent, until recently has remained elusive.

A further complication associated with reconstruction of past sea levels stems from the fact that no place on the Earth's surface can be assumed to have remained at its

present elevation even on the time scales of a single glacial cycle. One reason is that as the Earth's great crustal plates lumber along, they induce tectonic movements which gradually elevate some shore zones and gradually submerge others. In the extreme, the rates of these movements reach several meters per 1000 years. The other reason is related to shifting water and ice loads. The growth of several kilometer-thick ice caps not only elastically warps the underlying crust but also induces lateral transport in the underlying mantle extending tens of thousands of kilometers away from the perimeter of the ice sheets. This extruded material lifts the ocean floor. At isostatic equilibrium a 3000-meter-thick ice cap would displace a layer of underlying mantle material 835 meters thick. Correspondingly, a 120 meter lowering of sea level should cause the sea floor to rise by about 36 meters relative to the adjacent ice-free continents (see figure 2). As it takes many thousands of years to reestablish isostatic equilibrium, the viscous mantle never quite catches up with the ever changing glacial load. Rather the cycles of glaciation keep the Earth's mantle in a continuing state of flux. Even now, no spot on Earth is entirely free of these effects. Hence if we are to transform shoreline elevations to global ice volume, careful account must be taken of both tectonic and ice-load effects.

It turns out that this problem has been largely solved by the patient unraveling of a host of evidence. A breakthrough in this regard came when $^{230}\text{Th}/^{234}\text{U}$ ages on corals from raised shorelines from many places in the tropics revealed a prominent high stand of the sea with an age of about 124,000 years. A pattern appeared in the elevation of this strand (see figure 3). At localities far removed from the margins of tectonic plates (i.e., in tectonic quiet zones), the crest of this reef lies several meters above sea level. The broad consistency of these elevations has led to the conclusion that this reef formed during a time when global ice volume was slightly smaller than today's. The fact that the age of this reef corresponds to that for an interglacial peak recorded by ^{18}O in deep sea sediments strengthens this conclusion.

The value of this finding was that the elevation of the 124,000 year-old shoreline

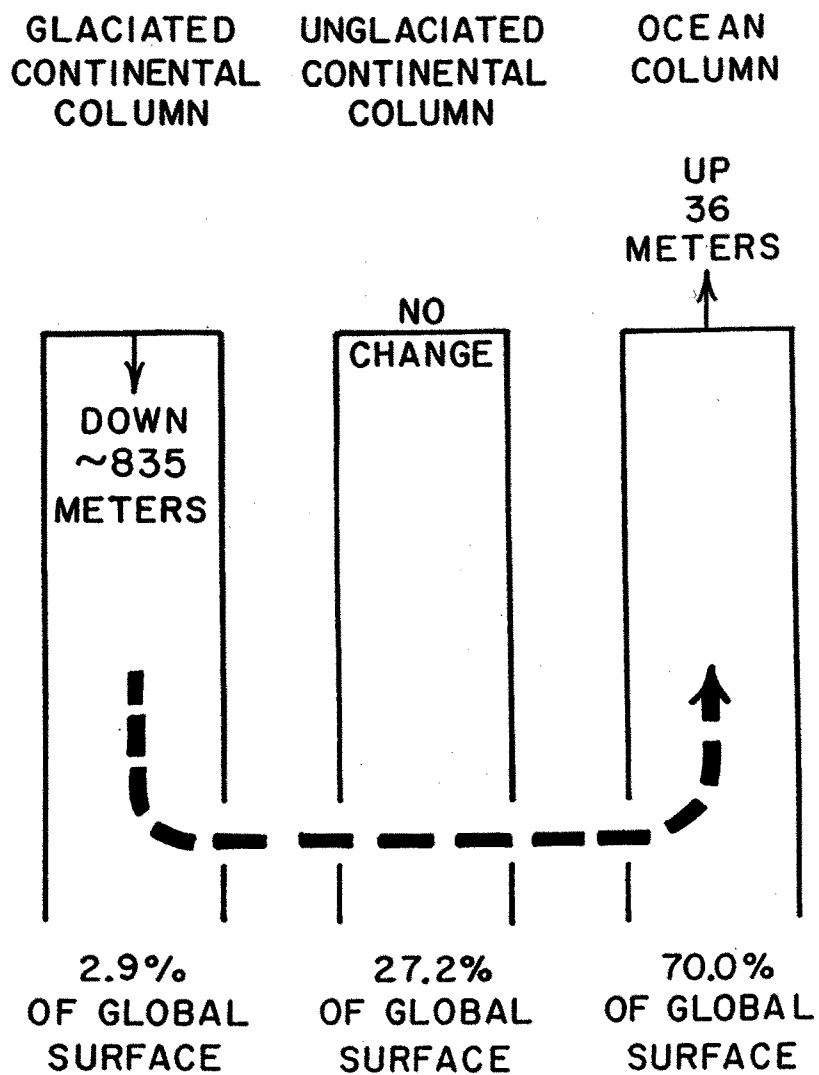


Figure 2. When a 120 meter thick layer of sea water (density 1.0 gm/cm^3) is stacked up as 3000 meter thick ice cap (density 0.92 gm/cm^3), gravitational balance is restored by the lateral flow of material in the Earth's mantle (density 3.3 gm/cm^3). Were isostatic equilibrium to be achieved, the land beneath the ice would drop 835 meters (i.e. $3000 \times 0.92/3.3$) and the sea floor would rise by 36 meters (i.e. $120 \times 1.00/3.3$). In other words, a layer of mantle material 835 meters thick would be squeezed from beneath the glaciated regions (2.9% of the earth's surface) and spread uniformly beneath the sea (70.0% of the Earth's surface).

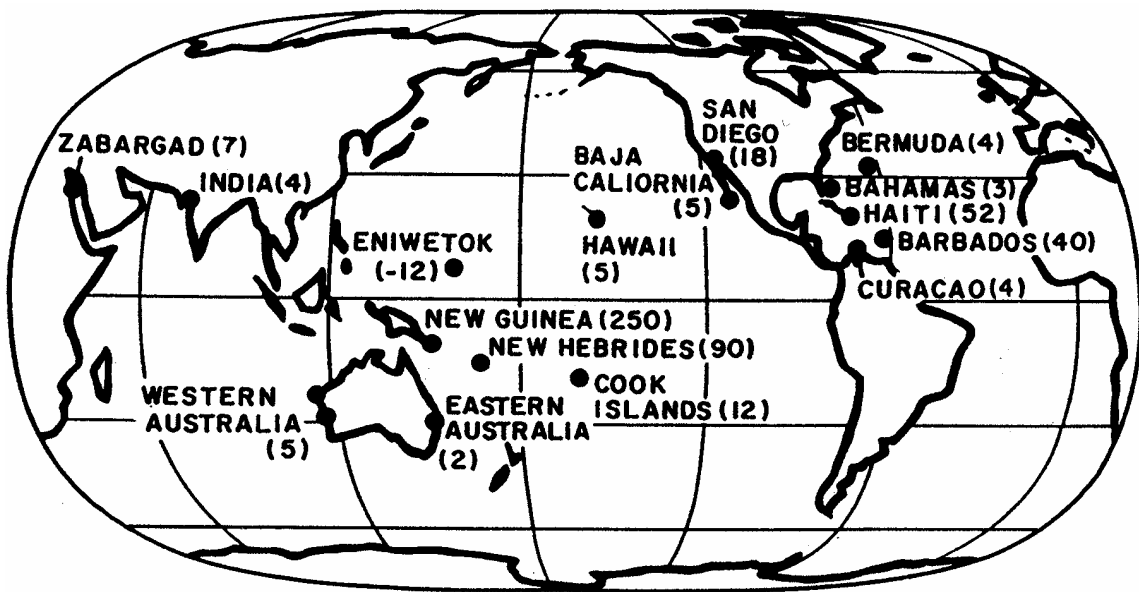


Figure 3. Map showing locations and elevations (in meters) of radiometrically dated coral reefs formed during the last interglaciation (i.e., ~124,000 years ago). At localities like New Guinea, New Hebrides, San Diego, Barbados and Haiti which are subject to intense tectonic activity, these shorelines have been uplifted by several to many 10's of meters. In others, like Eniwetok, it has subsided. But at some (i.e., western and eastern Australia, northwestern India, Hawaii, the Bahamas, Bermuda, Baja California, and Curacao), it has undergone only minor elevation change since the last interglacial sea level maximum.

in areas subject to tectonic deformation provides a measure of the rate of movement. This proves important because in areas of rapid tectonic uplift, some of the shorelines formed at times of greater than present ice volume have been lifted above the sea and therefore can be effectively inspected and sampled.

The first application of this approach was by Robley Matthews on the island of Barbados in the eastern Caribbean. This island sits on a great mass of sediment which is being scraped off the Atlantic Ocean plate and subducted beneath the Caribbean Arc. On Barbados the 124,000 year old reef is found at an elevation averaging 40 meters, suggesting that Barbados is being lifted out of the sea at the rate of about 0.3 meters per thousand years (i.e., $[40-3]/124$). Lying between this 124,000 year old reef and present sea level are two other reefs, one dating about 104,000 and the other about 83,000 years (see figure 4). If the assumption is made that Barbados has over the last 124,000 years been rising at constant rate (at least when averaged over several thousand years), then it is possible to correct for the extent to which the 83,000 and 104,000 year coral reefs have been elevated. When this is done, the result is obtained that both formed when sea level was about 16 meters lower than today's (see figure 4).

As already mentioned, one major goal of sea level research was proven elusive, namely, establishing the level of the sea at the peak of the last glaciation. The reason is that these shorelines formed 100 or so meters below the present sea surface. Nowhere has tectonic uplift proceeded at a fast enough rate to hoist these strands above the present level of the sea. While many attempts have been made to establish the elevation of this horizon by dating materials dredged or cored from continental margins, the results are so inconsistent that none were taken seriously. The estimates ranged from 60 to 150 meters.

Finally in 1988 a set of samples was obtained that changed all this. Richard Fairbanks developed a means to make borings into submerged coral reefs. He implemented this technique off the coast of the island of Barbados and obtained sequences of a species of coral, *Acrapora palmata*, known to live only within a few

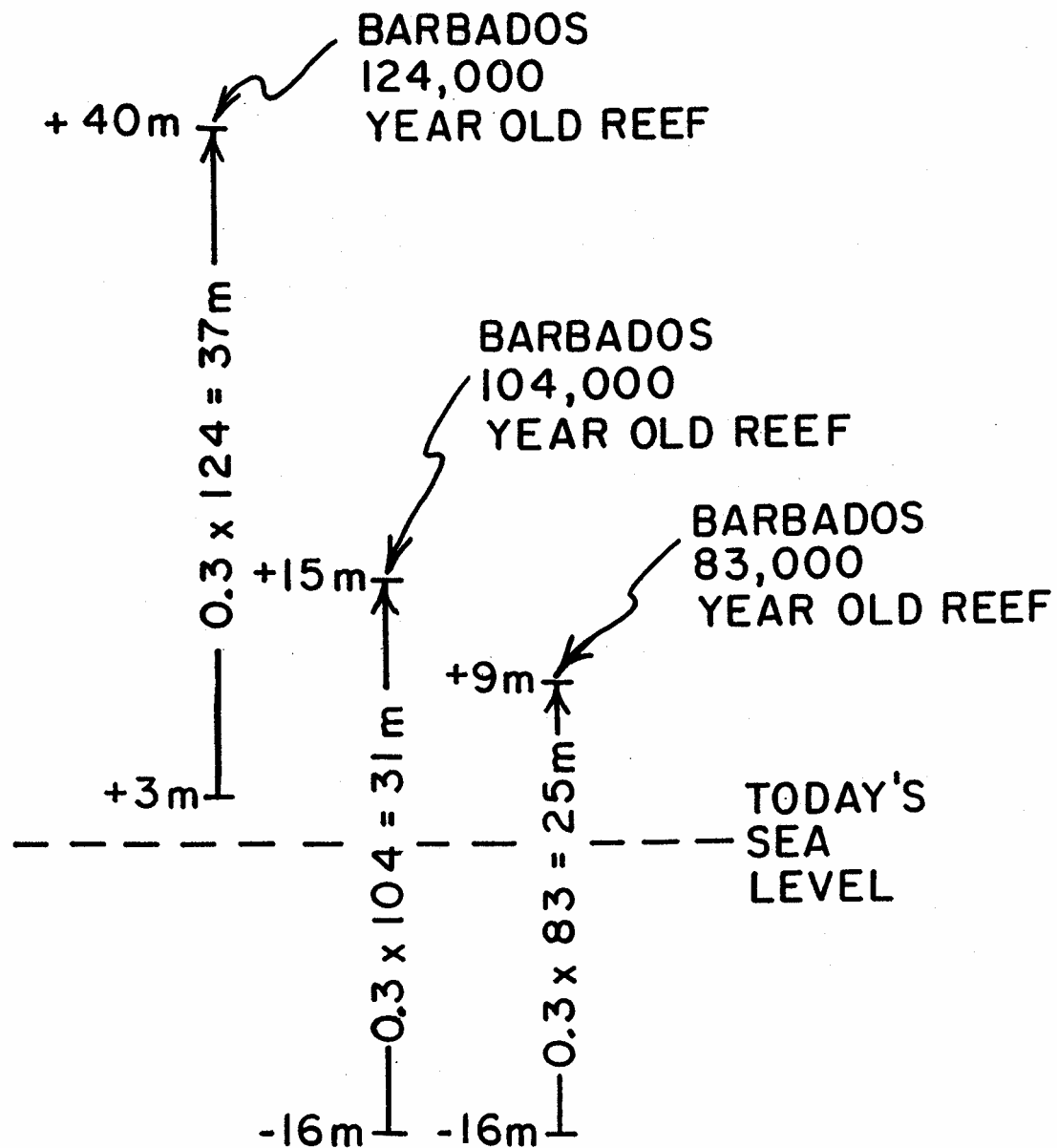


Figure 4. Diagram showing the relationship between the elevations of the crests of coral reefs on Barbados and the sea level at the time they formed. Because the true sea level (+3 meters) at the time the 124,000 year old reef formed is known, the uplift rate (0.3 meters per 1000 years) for Barbados can be established. This permits the elevations of the sea (-16 meters in both cases) to be reconstructed for the times when the 104,000 and 83,000 year old reefs formed on Barbados.

meters of the sea surface. By radiocarbon dating of these corals, he was able to establish that the sea stood at least 120 meters lower than today during peak glacial time (see figure 5). Even though Barbados is undergoing tectonic uplift at the rate of 0.3 meters/1000 years, the correction is only 5 meters for the 18,000 year-old corals which mark the level of the glacial sea. Also, Barbados is nicely situated with regard to the deformation resulting from ice loading. Models of global deformation caused by the glacial ice load suggest that it has moved by only about 10 meters since glacial time. Fairbanks' accomplishment constitutes a major step toward the goal of disentangling the highly interwoven factors influencing paleoclimatic indicators.

The reason that Fairbanks results yield only a lower limit on the maximum extent of sea level lowering is that his oldest *Acrapora palmata* corals do not extend back to the time of the glacial maximum. Fortunately, rooted terrestrial mangrove plants dating 21,000 calendar years have been recovered by dredging of the Sunda Shelf. They yield a sea level lowering of 115 meters.

Another quite different type of shoreline led to a breakthrough in understanding the rate of deformation created by ice unloading. These shorelines are found in areas covered by thick ice sheets during the last glaciation. They most often appear in staircase-like flights extending several hundred meters above the present day shoreline. Each successive 'step' has an older radiocarbon age (see example in figure 6). The highest shorelines have ages in the range 7000 and 12,000 ^{14}C years corresponding to the time the locale became ice free. Clearly the uplift of the land which produced these 'flights' was caused by the removal of the ice load. Geologists refer to this uplift as glacial rebound.

Geophysicists interested in modeling the deformation of our planet resulting from ice loading were quick to realize that sea level histories obtained at many points on the planet for the last ten or so thousand years are a valuable resource. Not only could this information be used to constrain the elastic properties of the Earth's lithosphere and the

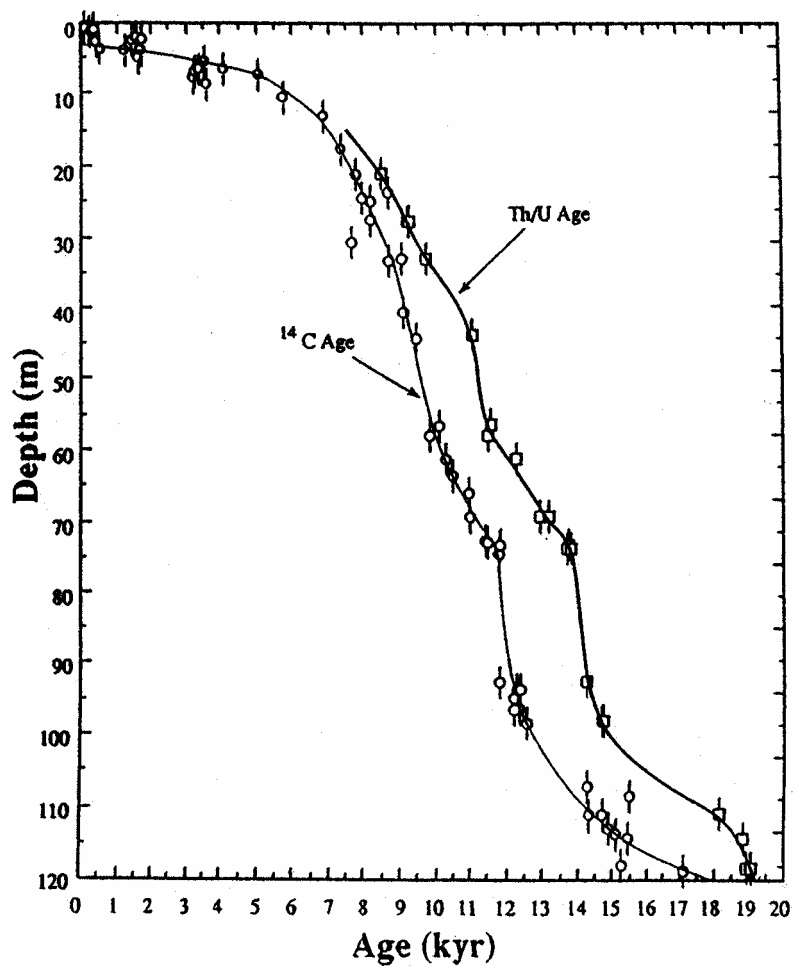


Figure 5. Radiocarbon and uranium thorium ages on corals from borings made off the coast of Barbados (Bard et al., 1990). The *Acropora palmata* samples on which the age determinations were made are thought to have grown within a few meters of sea level. The difference between the radiocarbon scale and the calendar scale is discussed in the section entitled "Clocks."

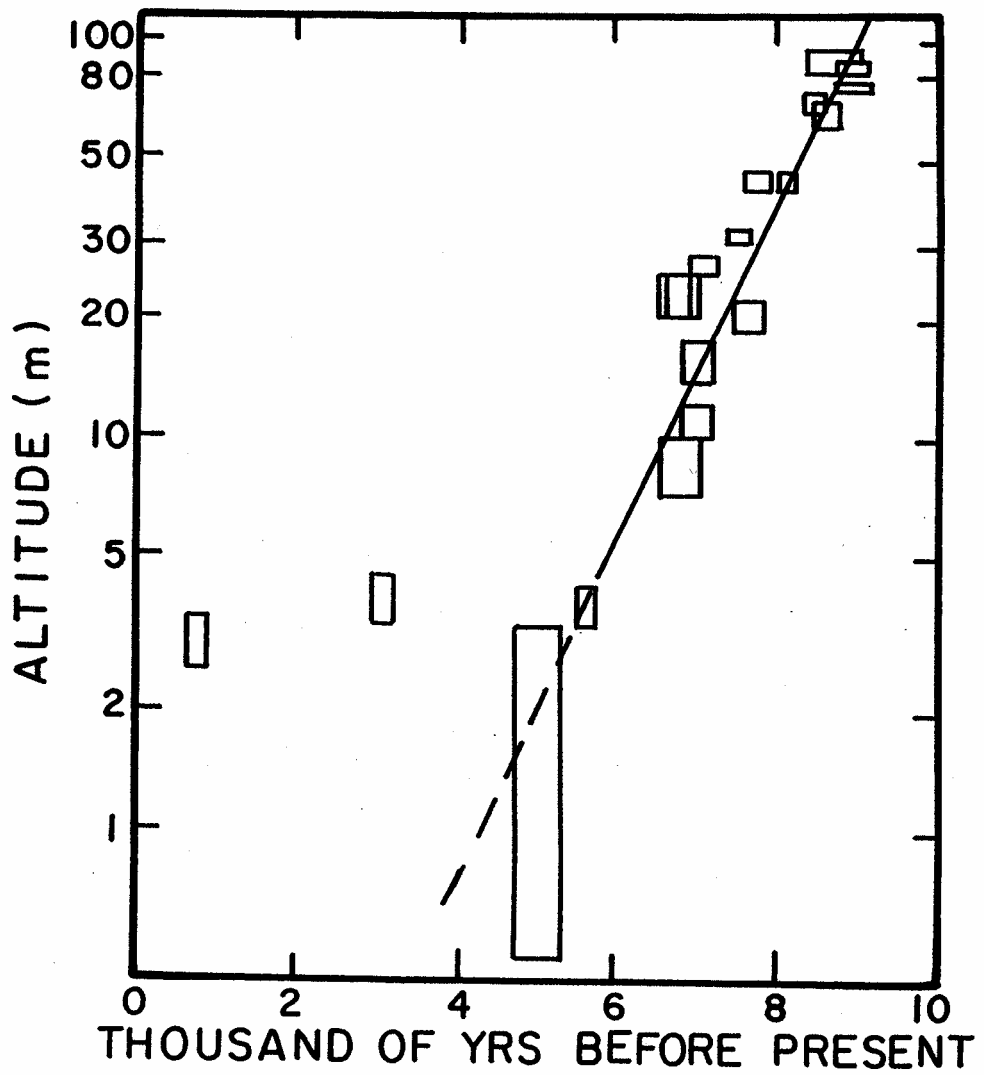


Figure 6. Radiocarbon ages for shells from a flight glacially rebounded shorelines in northeastern Greenland (Washburn and Stuiver, 1962). Note that elevation scale is logarithmic. The straight line indicates that the uplift followed the relationship

$$U = U_{\max} (1 - e^{-t/\tau})$$

where τ is the e - folding time for rebound, which in this case is about 1000 years.

viscus properties of its mantle, but also to better define the distribution and magnitude of the ice loads of the last glaciation. Toronto's Richard Peltier and his associates have exploited this information. Their strategy was to create a model of our planet which when perturbed by the glacial load reproduced the observed shoreline records. This exercise proved highly successful. Among other things, it provided strong support for the existence of large ice sheets around the perimeter of the Arctic Ocean.

Oxygen Isotopes

For every 500 water molecules in the sea, one bears the heavy isotope ^{18}O . The ^{16}O to ^{18}O ratio in sea water typifies our solar system and bears witness to the fact that nuclei (such as ^{16}O) consisting of an integral number of helium nuclei are manufactured with great preference in the centers of stars. We know from measuring the ratio of light oxygen atoms (^{16}O) to heavy oxygen atoms (^{18}O) in a wide variety of Earth substances that while the ratio is always close to 500, it varies over a range of several percent. For instance, the calcium carbonate manufactured by marine organisms has on the average four percent more heavy oxygen than sea water and the snow falling at high elevations on the Antarctic ice cap has on the average four percent less heavy oxygen than sea water. These differences reflect the fact that while chemically similar, the isotopes of any given element are not chemically identical. For example, water made with the heavy oxygen isotope has a one percent lower vapor pressure than water made with the light oxygen isotope.

The separation of oxygen isotopes plays an important role in paleoclimatology providing information both about past ice volumes and about past temperatures. As this section concerns ice volume, we will consider this application first. On the time scale of one million years or less, only one means exists to change the average isotopic composition of the water in the sea, i.e., the growth and retreat of ice caps. The tie between the isotopic composition of ocean water and ice volume stems from the fact that the snow which accumulates to make ice caps is depleted by several percent in heavy

oxygen. We know this from measurements on recent snow from Antarctica and Greenland (see figure 7). We also understand why this is the case. As illustrated in figure 8, this depletion is created because the water which condenses to form precipitation in a cooling air mass is enriched in the heavy isotope. The light isotope is correspondingly enriched in the residual vapor. Because of this, the residual water vapor in the airmass becomes progressively depleted in the heavy isotope. By the time air masses reach the very cold regions atop the Greenland and Antarctic ice caps, this depletion in the heavy isotope has reached several percent. Because of this, the ice which forms these caps (and also the ice which formed the great caps of glacial time) is depleted in heavy water. These missing heavy molecules are stored in the sea, giving it a slightly higher ^{18}O to ^{16}O ratio. Thus the greater the volume of ice on the continents, the higher the ^{18}O to ^{16}O ratio in sea water. For example, if the snow which accumulated to form the ice sheets of last glaciation were on the average 3.5 percent depleted in ^{18}O (i.e., $\delta^{18}\text{O} = -35\text{\textperthousand}$), then the magnitude of the enrichment in the sea is easily estimated. The ocean has a mean depth of 3800 meters, so the removal of a 120 meter thick layer of water with 35‰ lower ^{18}O content would leave the water remaining behind enriched by about

$$\frac{120}{3800} \times 35\text{\textperthousand} \text{ or } 1.1\text{\textperthousand}$$

We use per mil (i.e. parts per 1000) instead of percent (i.e. parts per 100) in this calculation to conform to the standard notation adopted by those who make oxygen isotope measurements on Earth materials (see figure 7 caption). Average ocean water constitutes the zero on this scale.

As the oxygen atoms in the CaCO_3 deposited by marine organisms come from the oxygen in sea water, these shells must record changes in the ^{18}O to ^{16}O ratio in the sea. Thus, down core series of oxygen isotope ratios on the microscopic shells of foraminifera found in deep sea sediments should provide a record of changes in ice volume on the

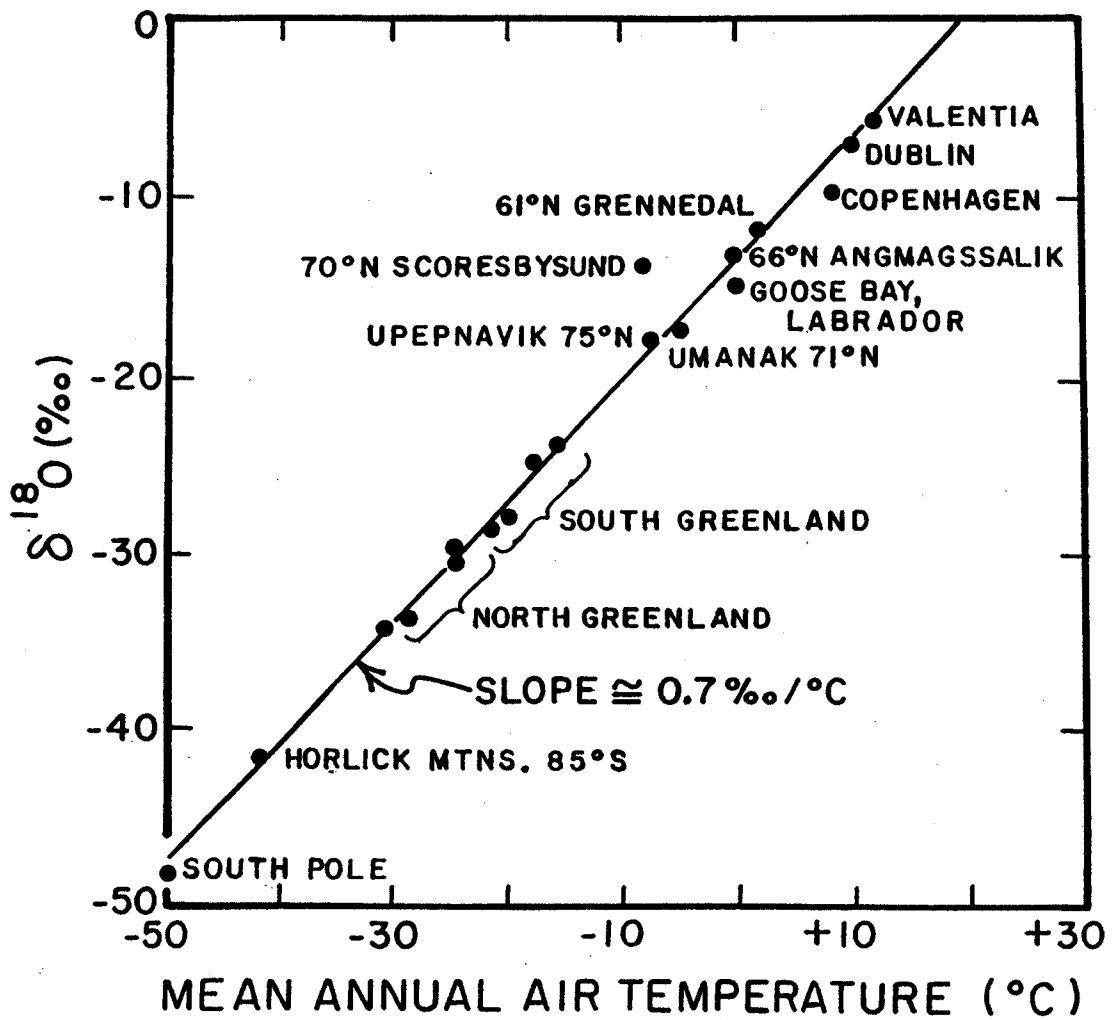


Figure 7. Observed $\delta^{18}\text{O}$ in average annual precipitation as a function of mean annual air temperature (Dansgaard, 1964). Note that all the points on this graph are for high latitudes ($>45^{\circ}$). The $\delta^{18}\text{O}$ values are calculated as follows:

$$\delta^{18}\text{O} = \frac{{}^{18}\text{O}/{}^{16}\text{O}_{\text{sample}} - {}^{18}\text{O}/{}^{16}\text{O}_{\text{std.}}}{{}^{18}\text{O}/{}^{16}\text{O}_{\text{std.}}} \times 1000$$

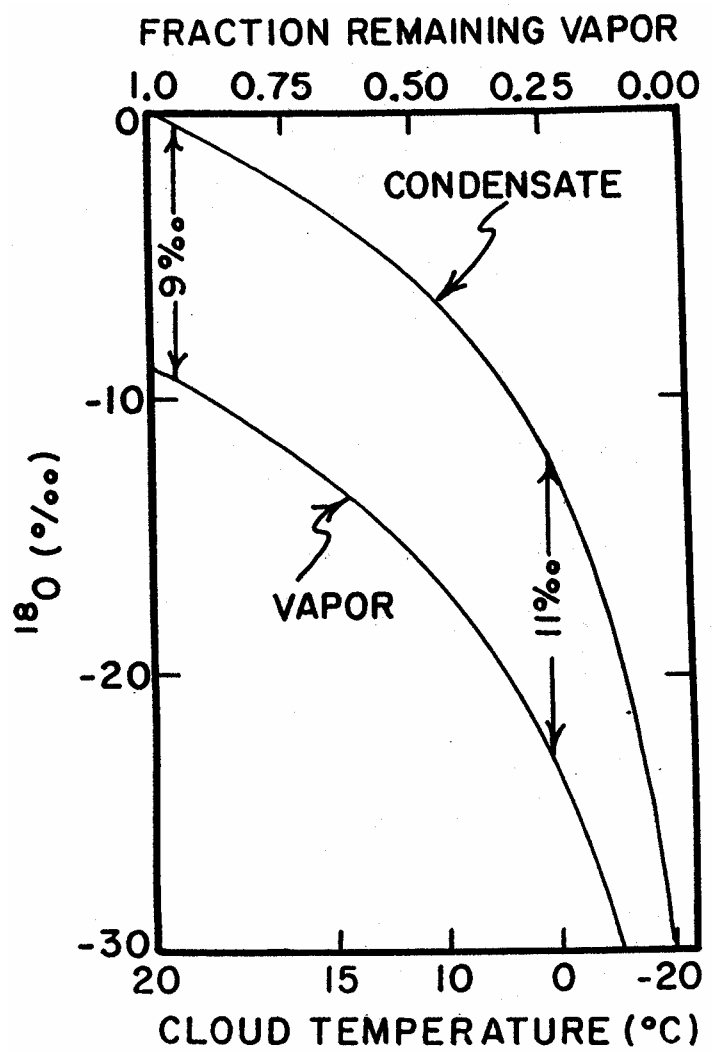


Figure 8. $\delta^{18}\text{O}$ in cloud vapor and condensate plotted as a function of the fraction of remaining vapor in the cloud for a Rayleigh process. The temperature of the cloud is shown on the lower axis. The increase in isotope fractionation with decreasing temperature has been taken into account (Dansgaard, 1964).

continents! Indeed, changes in ice volume constitute the largest contributor to the record kept by foraminifera shells. Unfortunately, it is not the only contributor. Two other influences must be considered. The first of these has to do with the fact that the ocean's ^{18}O is not uniformly distributed. The same meteorologic forces which cause the snow which falls on polar caps to be depleted in ^{18}O redistribute ^{18}O across the sea surface (see figure 9). Those regions of the surface which lose more water to evaporation than they gain from precipitation (and from the runoff from adjacent rivers) are enriched in ^{18}O as well as in salt. The opposite is true for areas of low salinity where precipitation and runoff exceed evaporation. The range of these changes in today's open ocean surface waters is as large as the signal imprinted by ice volume changes. Thus possible changes in the distribution of ^{18}O within the sea with changing climate must be considered. Fortunately, a means exists to avoid this problem. Rather than relying on the record kept by the shells of planktonic foraminifera which inhabit surface water, attention is focused on the record kept by the shells of benthic foraminifera which live on the sea floor. As most of the ocean's water resides in the deep sea, redistribution of ^{18}O will create much smaller changes in this reservoir than at the ocean's surface. Also the ^{18}O content of deep sea waters is far more homogeneous than that of surface water. In particular, the deep Pacific (the largest of the ocean's reservoirs) is uniform isotopically both with location and depth. Thus, measurements made on benthic foraminifera shells picked from cores from the floor of the deep Pacific should not be significantly affected by changes in the distribution of ^{18}O within the sea.

The other source of change in the ^{18}O content of CaCO_3 precipitated in sea is temperature. We have already mentioned that the ^{18}O to ^{16}O ratio in shells is on the average 40‰ higher than that in the water in which the shell grows. The complication is that the magnitude of the isotope separation between water oxygen and shell oxygen depends on temperature. For each degree Celsius the temperature cools, heavy oxygen is enriched in the shell by an additional 0.25‰. Hence a three degree

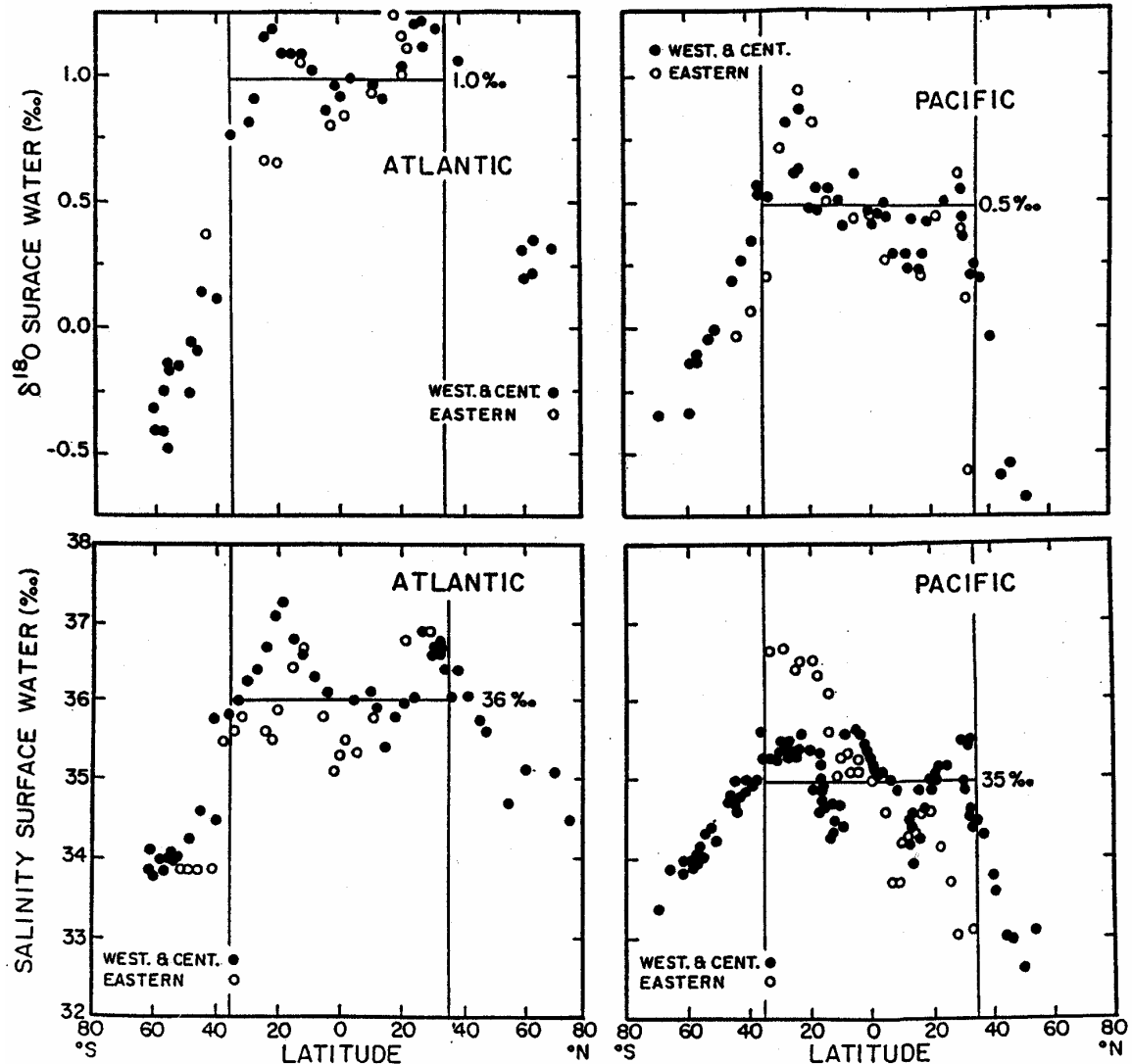


Figure 9. Latitude dependence oxygen isotope composition (upper) and salinity (lower) as measured by Harmon Craig on samples of surface waters in the open Atlantic and Pacific Oceans obtained during the GEOSECS expeditions.

centigrade cooling of the water in which the shells grow leads to nearly as large an isotope shift (i.e., 3×0.25 or $0.75\text{\textperthousand}$) as that thought to be produced by the growth of the ice caps (i.e., $1.1\text{\textperthousand}$). Since the planet was cooler during glacial time, ice volume and temperature worked together to raise the ^{18}O to ^{16}O ratio in marine shells.

Again the deep Pacific proves to be the most favored place to find shells least subject to temperature contribution to oxygen isotope shifts. Not only is temperature quite uniform with depth and geographic location, but more important, it is the coldest of the deep ocean reservoirs. This proves to be important because the already very cold polar regions from which the deep seas are ventilated could not have been much colder during glacial time. Nevertheless, the results of measurements on benthic foraminifera from the deep sea (see figure 10) show that shells formed during full glacial time had $1.75\text{\textperthousand}$ higher ^{18}O to ^{16}O ratio than shells formed during peak interglacial time. This is $0.65\text{\textperthousand}$ more than would be expected from the ice volume change alone ($1.10\text{\textperthousand}$), suggesting that deep Pacific water was 2.5°C cooler during glacial time than now. Unfortunately, the extent of cooling of the deep Pacific in all likelihood was not simply proportional to the extent of ice growth. In other words, the proportion of the change resulting from ice volume on the one hand and water temperature on the other was not always the same as it was at the time of the glacial maximum. Hence, in order to untangle the temperature component from the ice volume component in oxygen isotope records for benthic foraminifera from the deep Pacific Ocean, additional information is needed.

Harvard's Dan Schrag proposed a means to more firmly establish the ^{18}O to ^{16}O ratio change attributable to ice volume. He showed that it is recorded in the pore waters of marine sediments. At several sites on the sea floor, he measured oxygen isotope ratios on pore water squeezed from sediments from a series of depths recovered by the Ocean Drilling Program. An example is shown in figure 11. The maximum in $\delta^{18}\text{O}$ at about 40 meters depth reflects the high ^{18}O of glacial time. The reason that it is only

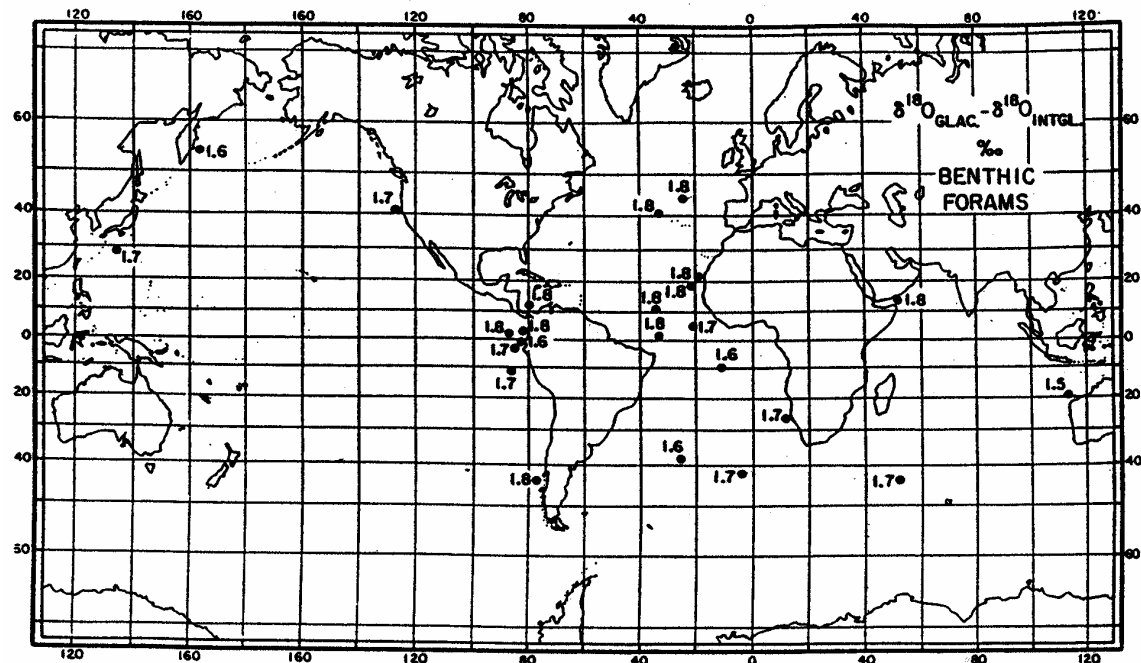


Figure 10. Glacial to interglacial change in the oxygen isotope composition of benthic forams at various sites in the deep ocean.

about one third the expected amplitude is that diffusion of water within the pores has gradually replaced the glacial age water molecules with post glacial ones. From a knowledge of the molecular diffusion rate and the time history of the ice volume, it is possible to deconvolve the actual isotopic composition of the glacial age bottom water. Based on these measurements, Schrag concluded that the ice volume effect is $1.0 \pm 0.1\text{\%}$. Hence he would conclude that the average isotopic composition of the glacial age ice was $-32 \pm 3\text{\%}$.

Summary

The reconstruction of past ice cover requires the use of information from several sources. Moraines tell us the location of the ice margin for those regions of the ice sheet perimeter now above sea level. The shoreline record for post-glacial time aids in the reconstruction of the extent of ice cover in the Arctic where the glacial maximum moraines now lie beneath the sea. The total volume of the ice residing within this perimeter is given by the depth of the glacial-age mangrove wood. Finally, ^{18}O measurements on sediment pore waters allow the ice volume contribution to the benthic ^{18}O change to be isolated. We return to this subject in the section on “Records”.

TEMPERATURE

Accurate paleothermometry has proven to be a tall order. In the case of ice volume, we sought a single number for peak glacial time. In the case of temperature, we would like to have a world map for peak glacial time. Two recorders of temperature information are friends from the previous section: moraines (in this case those created by mountain glaciers) and oxygen isotope ratios (in this case in glacial ice). In addition, temperature information is available from the relative abundances of shells formed by different species of planktonic foraminifera, from the concentrations of the noble gases dissolved in the glacial age water in continental aquifers, from the ratio of two alkenones found in marine organic material and from magnesium to calcium ratios in foraminifera shells.

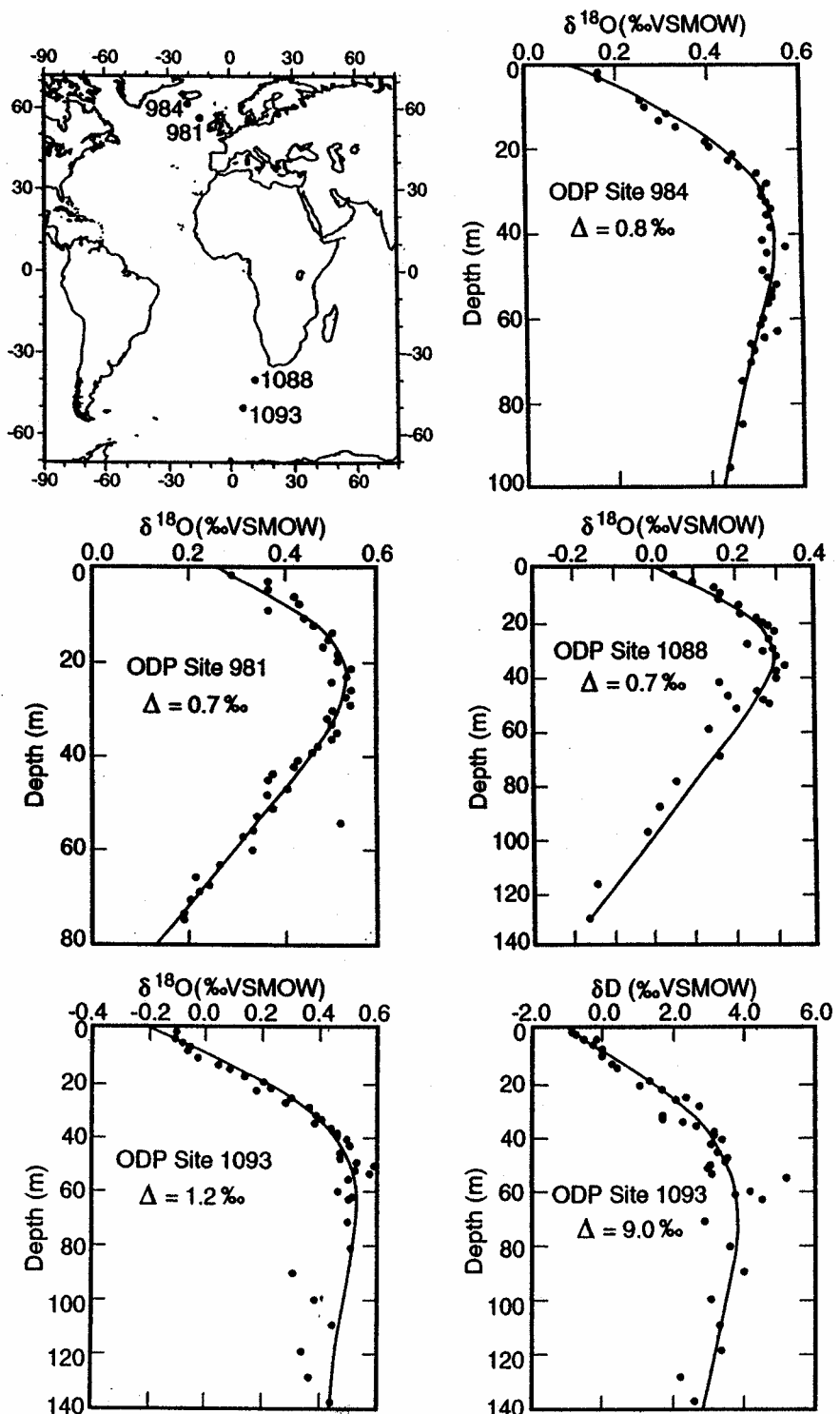


Figure 11. Stable isotope composition of sediment pore waters as summarized by Schrag et al., 2002. In each case, the bulge toward heavier values reflects the memory of the enrichment of the heavy isotopes in the ocean as the result of the existence during glacial time of ice sheets depleted in the heavy isotopes. The Δ values are Schrag et al.'s best estimate of the deconvolved deep-water isotope enrichment during peak glacial time. The Atlantic Δ values are smaller than that for the whole ocean because its waters are currently enriched in ^{18}O relative to the rest of the deep ocean. Of the four records reproduced here, only that for site 1093 reflects the rest of the ocean. The other three are bathed in Atlantic water.

Mountaintop Temperatures

Even in the tropics, the highest mountains are capped by ice. The reason is that as everywhere on Earth, air temperature decreases with altitude. Thus, if one goes high enough in the atmosphere, freezing temperatures will be encountered. The boundary between elevations where snowfall exceeds melting and elevations where melting exceeds snowfall corresponds roughly to the position of the mean annual zero degree Celsius isotherm. The horizon is referred to as the equilibrium snowline. On all of the world's snow capped mountains, moraines left behind by glaciers more extensive than the current ones are easily identified. Radiocarbon and cosmogenic isotope dating demonstrate that these moraines formed during the peak of the last glaciation. Through careful mapping of these features, it has been possible to reconstruct the elevation of the peak glacial equilibrium snowline. In most places, the extent of lowering lies in the range 950 ± 70 meters (see figure 12 for partial summary). After correction for the contribution of lowered sea level, this drop becomes 830 ± 70 meters. Included on the list are several tropical mountains (Wilhelm in New Guinea, Mauna Kea on Hawaii, and Kenya in east Africa) and quite a number of temperate mountains (the American cordillera, the Swiss Alps, the southern Andes, and the New Zealand Alps). The conclusion appears to be inescapable, for mountains from 45°N to 45°S located both on oceanic islands and on continental interiors, the temperature was considerably colder during peak glacial time than now. Lapse rates (i.e., temperature gradients) at elevations corresponding to today's zero degree centigrade isotherm average about 5.5°C per kilometer. Hence these moraines appear to be telling us that it was at least 4.5°C colder on high mountains then, compared to now. I say 'at least' because the rate of snowfall also plays a role in setting the elevation of the snowline. The higher the snowfall rate, the greater the displacement of the snowline below the zero degree isotherm. As the water vapor content of the atmosphere scales with sea surface temperature, the colder the air the less vapor and hence the lower the snowfall. Hence, the changes in snowfall tend to

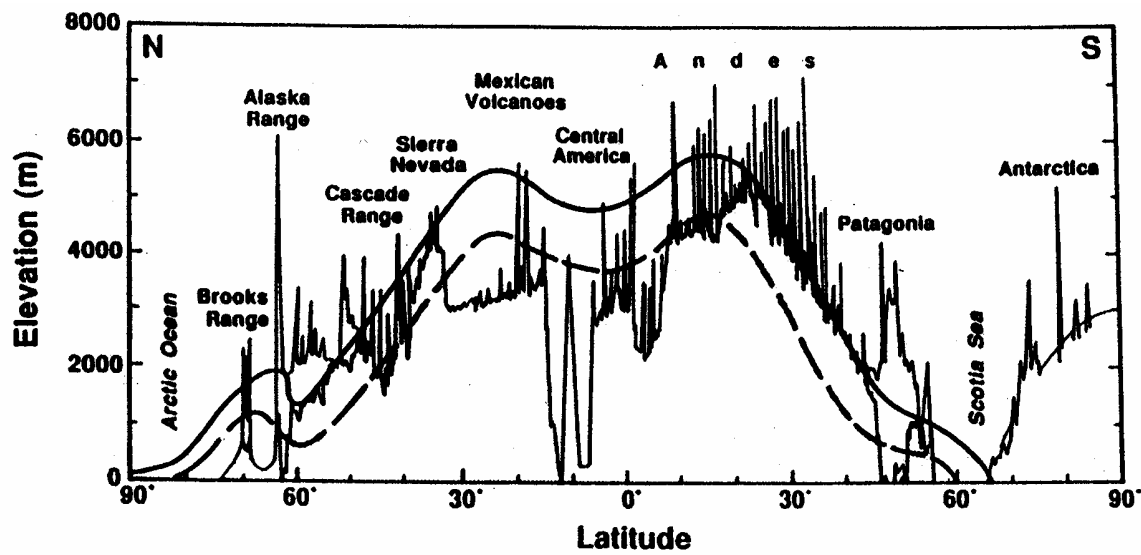


Figure 12. Topographic transect along the cordillera of North and South America. The position of the present-day snowline is shown by the heavy line. The depressed snowline of the last glacial maximum is shown by the dashed line.

counteract the cooling. While uncertain, the magnitude of the snowfall impact is on the order of 20 percent that of the cooling itself. If so, the 4.5°C estimate must be increased to 5.4°C glacial cooling.

During glacial time, vegetation zones on mountain sides also underwent a shift to lower elevation. This shift has been demonstrated by studies of the pollen grains extracted from the sediments of mountainside lakes and bogs. Whereas Holocene sediments contain pollen representative of the vegetation currently populating the immediate surroundings, glacial age sediments have pollen assemblages representative of the plants now living at elevations roughly one kilometer above that of the lake or bog of interest.

Polar Temperatures

Deep borings in both the Greenland and Antarctica caps encounter ice which formed during glacial time. The dating is surprisingly good. For the summit Greenland cores, age estimates based on annual layer counting are thought to be accurate to plus or minus two percent back to 40,000 years. As will be discussed below, ice core records can be correlated with one another based on measurements of two globally uniform but temporally varying properties of air trapped in the ice (i.e., CH₄ concentrations and ¹⁸O to ¹⁶O ratios in O₂). Thus, a very accurate chronology developed for any one ice core can be transferred to all the other ice cores. The ¹⁸O to ¹⁶O ratio for glacial age ice is consistently lower than that for ice formed during the present interglacial. Except for the Camp Century core in northern Greenland, these differences range from 5 to 7‰ (see table 1). To these differences must be added the 1.1‰ glacial to interglacial change in the isotopic composition of sea water. Then, based on the very tight correlation between the ¹⁸O to ¹⁶O in mean annual snowfall and mean annual temperature for polar regions of 0.7‰ per °C (see figure 7), the oxygen isotope shifts observed in the ice core can be transformed into temperature differences. Putting aside Camp Century, the results point to 9 to 11°C colder temperatures during glacial time.

Table 1. Interglacial to glacial $\delta^{18}\text{O}$ differences for the Andean glacier Huascarán compared with that for six polar ice cores. The temperature change is based on today's 0.7‰ per °C slope in the mean annual temperature - mean annual $\delta^{18}\text{O}$ trend observed for high latitudes.

LOCATION	$\Delta\delta^{18}\text{O}$ ‰	$\Delta\delta^{18}\text{O}^*$ ‰	ΔT °C
Camp Century, Northern Greenland	11	12	~17
Summit, Central Greenland	7	8	~11
Dye 3, Southern Greenland	6	7	~10
Devon Island	7	8	~11
Byrd Station, Antarctica	5	6	~ 9
Vostok, Antarctica	5	6	~ 9
Hauscarán, Peru (9°S)	7	8	~11

*Corrected for the change in the isotopic composition of sea water.

A surprise came when it was shown by a completely different method that the actual glacial to post glacial change in air temperature must have been twice as large (i.e., 22°C rather than 11°C). This method is analogous to that used by Dan Schrag to reconstruct the ^{18}O to ^{16}O ratio in glacial-age sea water. The holes created by the deep borings into the Greenland ice cap were filled with a fluid whose freezing point lay well below that of the coldest temperature encountered in the ice. The idea was to prevent the hole from closing. The hole was then capped and the fluid allowed to come to thermal equilibrium with the surrounding ice. Then a very accurate thermister was lowered into the hole to log the ice temperature versus depth record. As was the case with the oxygen isotope record in sediment pore waters, a remnant of the very cold glacial temperature was found (see figure 13). And again, as for the ^{18}O record, this memory is gradually being erased by the diffusion of ‘warmth’ from the post-glacial atmosphere down through the ice. Having a knowledge of the rate at which heat diffuses in ice and time history of the shape (but not the absolute amplitude) of the temperature change (from the ^{18}O record in the ice), the magnitude of the glacial cooling could be deconvolved.

The problem then became to explain the twofold disagreement between the ^{18}O and thermal profile temperature reconstructions. A possible answer comes from simulations of glacial precipitation carried out in atmospheric models. They show that unlike today’s snowfall on Greenland which is spread over the entire year, during the periods of extreme glacial cold almost no snow fell during the winter months. Hence, while the ^{18}O record yields something close to mean annual temperatures for post-glacial time, it yields something closer to summer temperature during times of glaciation. Of course, as the thermal record can have no seasonal bias, it wins hands down.

A potentially important consideration is the possibility that the Greenland and Antarctic ice caps stood higher during glacial time. If higher, the air temperature would have been colder. As the size of both of these caps is currently limited by the proximity to the sea, with lowered sea levels the perimeters would have been larger. Were the other

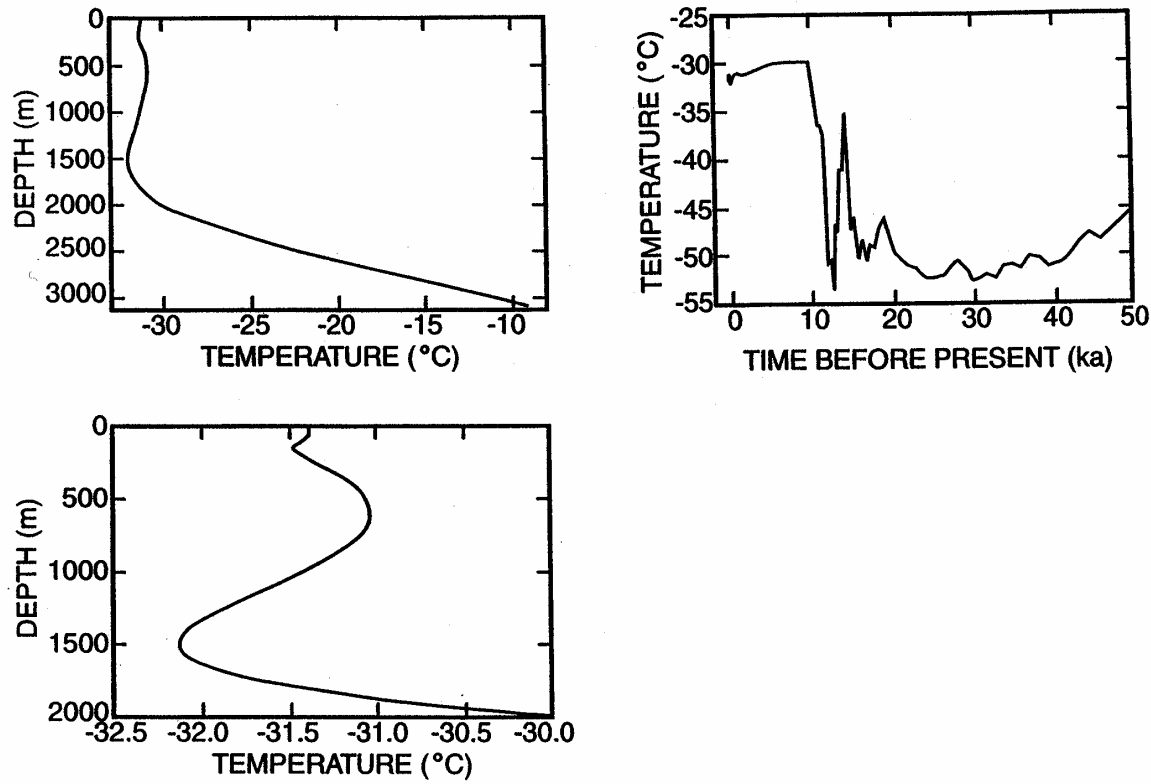


Figure 13. Upper left: temperature versus depth in the bore hole created by the recovery of the GISP2 Greenland Summit ice core. Lower left: Detail of the upper 2000 meters of the above record. Upper right: the air temperature record deconvolved from the thermal profile. These results were provided by Gary Clow of the USGS Denver Branch.

factors influencing the ice caps the same, then a larger perimeter would translate into higher elevations for the interior plateau. But several lines of evidence suggest that this was not the case. First of all, accumulation rates on today's caps drop systematically with air temperature. The colder the air, the less moisture it contains and hence, the less potential it has to generate snow. If the same rules are applied for glacial time, then the 22°C colder temperatures would translate to a several fold reduction in accumulation rate. This conclusion receives support from the higher concentrations of cosmogenic ^{10}Be in the interglacial glacial ice. The point is that the equilibrium height of the ice sheets must be such that the lateral pressure gradients are large enough to promote a flow toward the edges matching the snow accumulation in the interior. Hence, lower glacial accumulation rates would have led to thinner ice caps.

Direct evidence for the height of the glacial ice is available in Antarctica. Trim lines marking the height to which mountains projecting through the cap were scraped by passing glaciers can be traced from the edge of the ice cap inward toward the polar plateau. While these reconstructions reveal thicker ice than now near the edges of the cap (consistent with lowered sea level and larger ice perimeter), when traced toward the interior, the trim lines merge with the present ice surface suggesting that during glacial time the center of the cap was at today's elevation or perhaps even a bit lower. This picture is consistent with the combination of larger perimeter and lower accumulation rate. In Antarctic the two changes appear to have compensated one another.

It is possible that the ice itself retains a measure of its elevation at the time it formed. As snow is lithifies, small vesicles become sealed off, trapping air in the ice. When lithification is complete, the ice has about 10% by volume air-filled voids (see figure 14). Of course, as the ice becomes more deeply buried, these voids are gradually squeezed down in size. As the air cannot escape under sufficiently high pressure, it crystallizes. Assuming that the amount of void space in ice is independent of the environmental conditions, then the amount of air contained in an ice sample could serve

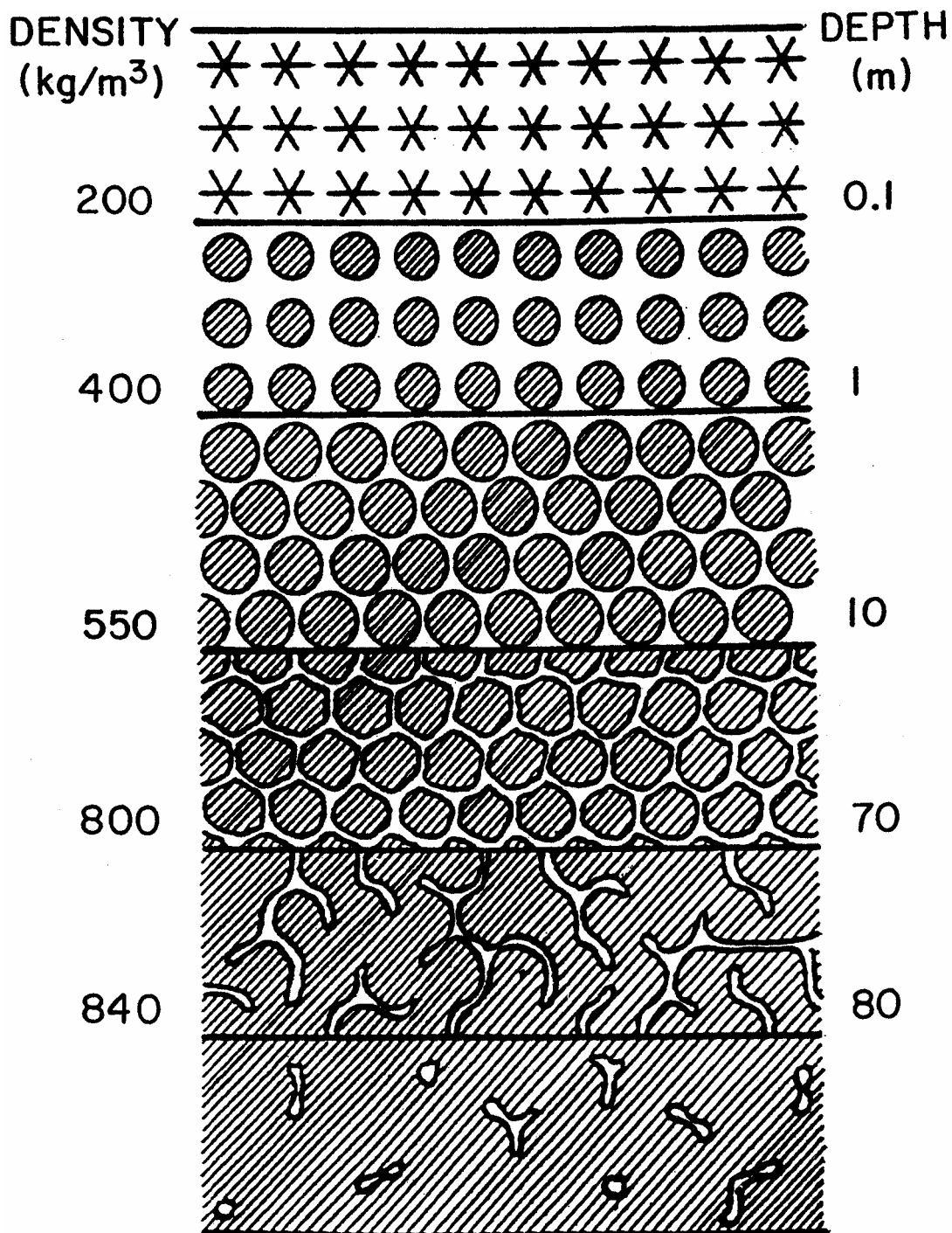


Figure 14. Diagrammatic depiction of the gradual lithification of the snow which falls on polar ice caps. The snow recrystallizes to firn which has passages through which air can circulate. When the firn is fully lithified, the air passages are sealed off becoming bubbles.

as an altimeter. Measurements made on Antarctic ice of glacial age do reveal more air per unit of weight of glacial ice than is found in recently lithified ice, suggesting that the elevation of the ice was not as great during glacial time as it is now. However, until the rules regarding the dependence of the pore volume on temperature and accumulation rate are better understood, air content-based paleoaltitude estimates must be considered tentative.

Pioneering ice coring in the world's high mountain regions by Ohio State University's Lonnie Thompson hit pay dirt when he was able to penetrate ice of last glacial age at 8°S in the high Peruvian Andes. This ice core recovered at 6030 meters elevation showed an 8‰ change in $\delta^{18}\text{O}$ between late glacial and early Holocene time. Thompson had previously obtained a similar ^{18}O shift for a core recovered in the eastern part of the Tibetan Plateau. The bottom line is that the ice polar plateaus of Greenland and Antarctica and high mountain elevations across the planet were much colder during glacial time than they are today. But again, the ^{18}O results for mountain ice are not consistent with independent temperature reconstructions based on snowline lowering. In this case, the ^{18}O based estimates are larger than those based on snowline lowering. The reason for this is not clear.

Sea Surface Temperatures

In each region of the ocean, certain species of planktonic foraminifera shells flourish while others are rare or absent. John Imbrie and Nilva Kipp took the trouble to determine the relative abundances of shells of each of these species in core top sediment samples from throughout the Atlantic Ocean. Their maps (see figure 15) confirmed what marine biologists had long believed. The contours of abundance closely parallel those of surface water temperature. This correlation led to the speculation that water temperature plays a key role in the competition among species. Perhaps each species has enzymes tuned to an optimal temperature. For example, the left coiling variety of *N. pacyderma* is the only species capable of flourishing at temperatures lower than 5°C.

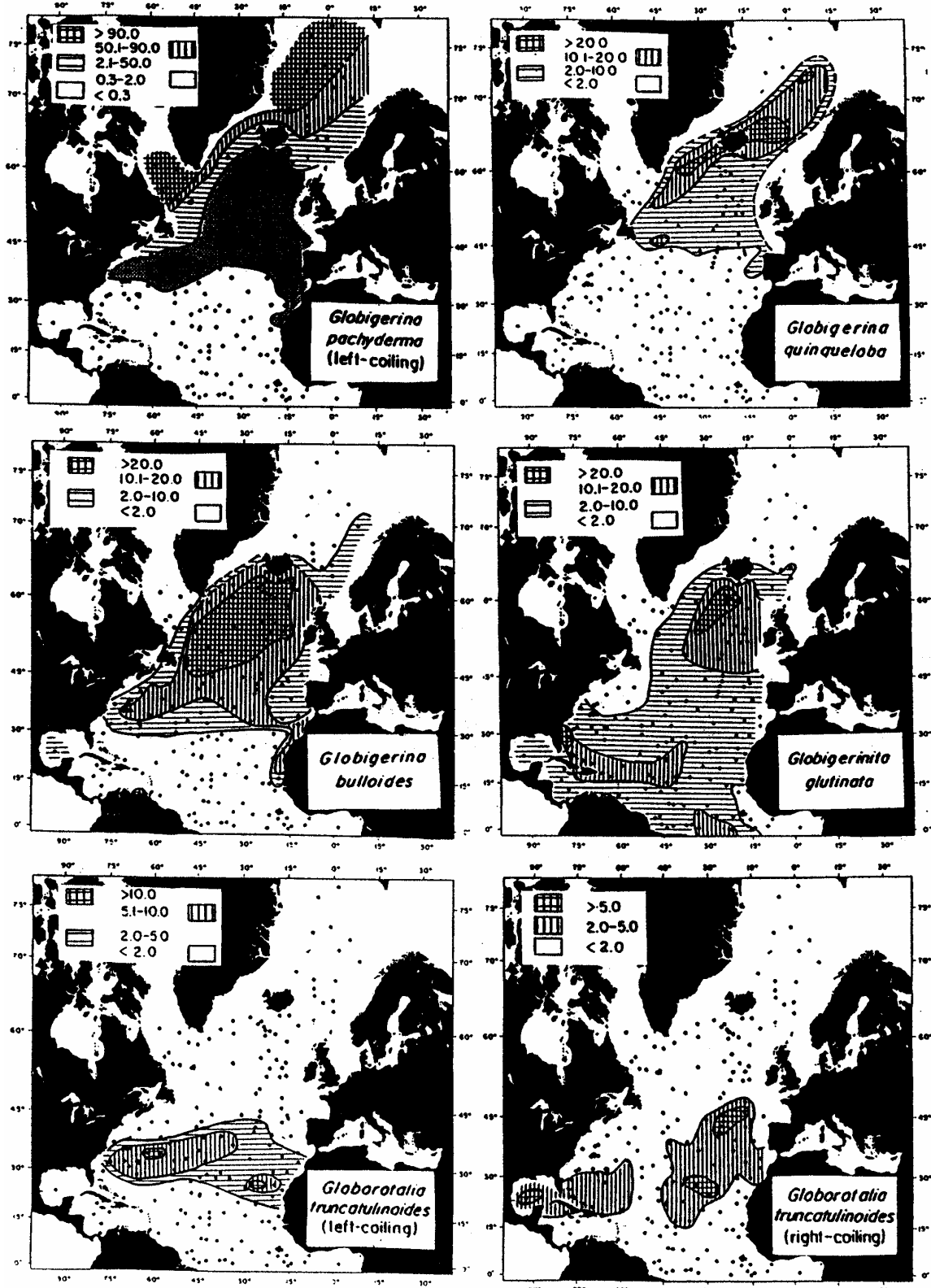


Figure 15. Maps showing the relative abundance patterns for the shells of six species of foraminifera in core top samples from the northern Atlantic (Kipp, 1976).

Imbrie developed a means to quantify the relationship between water temperature and relative abundance. He employed a technique called principle component analyses which allowed those aspects of the abundance patterns which correlate with water temperature to be mathematically isolated from those aspects which owe their origin to other influences. He demonstrated that the equations developed to relate water temperature to abundance does a remarkably good job. The mean deviation between calculated and observed temperature is only 1°C (see figure 16).

So Imbrie proposed to use his method to reconstruct surface ocean temperatures for peak glacial time. A group of marine geologists and geochemists in a program named CLIMAP identified the horizon corresponding to peak glacial time in hundreds of sediment cores from throughout the world ocean. The relative abundances of planktonic foraminifera were determined for the glacial horizon from each core. When temperatures were calculated using Imbrie's equations, an amazing, and to a large extent unexpected, result was found. Tropical ocean temperatures during glacial time were found to be nearly identical to those during interglacial time! This finding became the subject of considerable debate.

To understand why, we must first keep in mind that the coldest parts of today's surface ocean could have been no colder during glacial time. The reason is obvious; they contain floating ice. Thus one end of the temperature spectrum for the glacial ocean water is fixed at minus 1.8°C, the freezing point of sea water. The important discovery by the CLIMAP group was that little change occurred at the other end of the temperature spectrum. When analyzed by Imbrie's equations, glacial samples from throughout the tropical ocean showed deviations from contemporary temperature generally no bigger than the 1°C. So despite the fact that the snowlines on mountains rising out of the tropical ocean dropped by 950 meters, the temperatures at sea level appeared to the CLIMAP group to have remained unchanged.

The fact that the low and high ends of the range remained unchanged does not

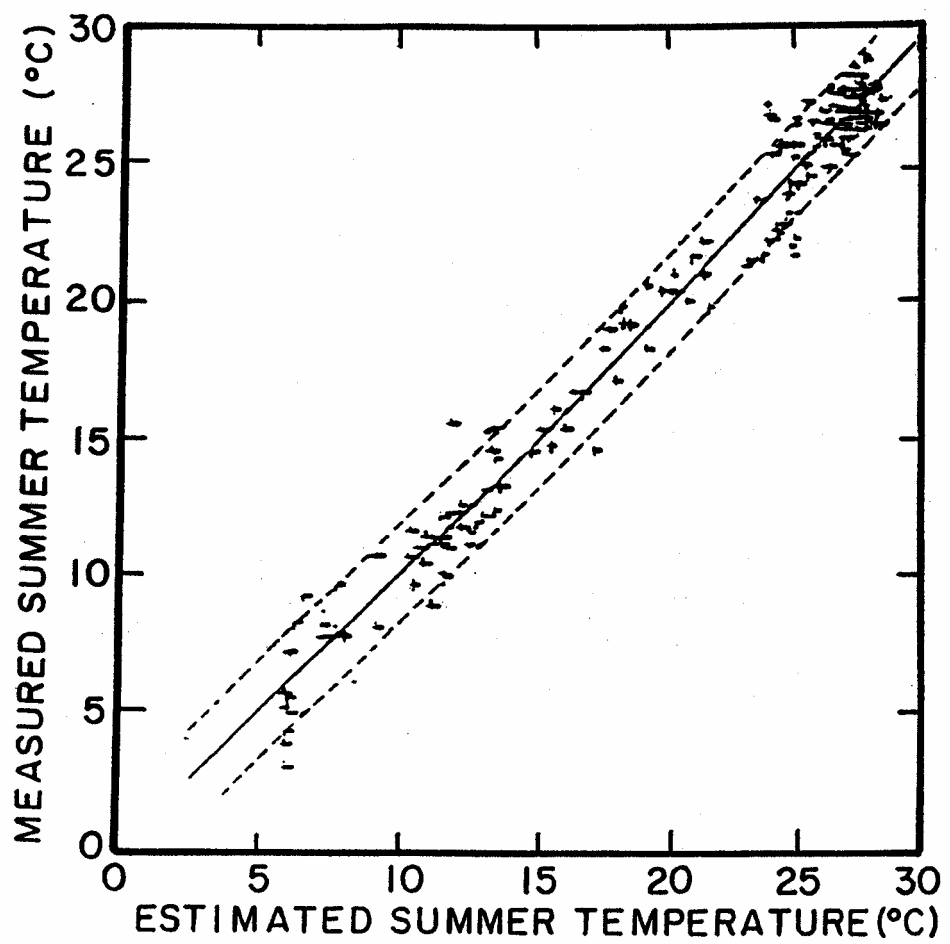


Figure 16. Comparison of temperatures calculated from core top foraminifera assemblages and observed sea surface temperatures (Kipp, 1976).

require that everywhere in the glacial ocean surface temperatures were the same as today's. Not at all. A look at the maps in figure 17 shows that the gradient in temperature between poles and tropics did change. The realm of cold water was expanded at the expense of the realm of warm water. Taken together with the temperature change at high elevation, this seems to be telling us that the Earth's cold sphere moved in on the Earth's warm sphere both from above and from the poles. Further, it must be kept in mind that while the temperature of ocean water cannot drop below -1.8°C , the air over the ocean can be far colder. The reason is that sea ice forms insulating the underlying water from the overlying air. Hence, as seen from the Antarctica - Greenland ice core records, air temperatures in the polar regions were far colder than now during glacial time. Imbrie's foraminiferal temperatures for the tropical ocean during glacial time found support from ^{18}O to ^{16}O ratios measured in planktonic foraminifera. The approach is to subtract from the glacial to interglacial oxygen isotope composition difference measured in planktonic foraminifera the contribution attributable to ice volume. The residual should be due to temperature. We've already shown that when the Barbados coral based sea level lowering of 120 meters is combined with an ^{18}O depletion in the glacial ice caps of 35‰, then the ice volume contribution to the oxygen isotope change would be 1.1‰. As shown in figure 18, the observed ^{18}O difference between glacial and post glacial planktonic foraminifera in the Atlantic and Indian Oceans averages 1.72‰, yielding an excess attributable to temperature of 0.62‰. Such a change suggests a 2.5°C cooling. For the Pacific Ocean (see figure 16), the observed change is about 1.25‰ leaving only an 0.15‰ residual, suggesting that surface water temperatures were only 0.6°C colder during glacial time. Averaging these results (i.e., -2.5°C for the Indian and Atlantic and -0.6°C change for the Pacific), the tropical ocean was only 1.5°C cooler during glacial time than today. This result agrees with that based on Imbrie's planktonic abundance thermometer.

Howard Spero and his colleagues came upon an isotope effect which might give

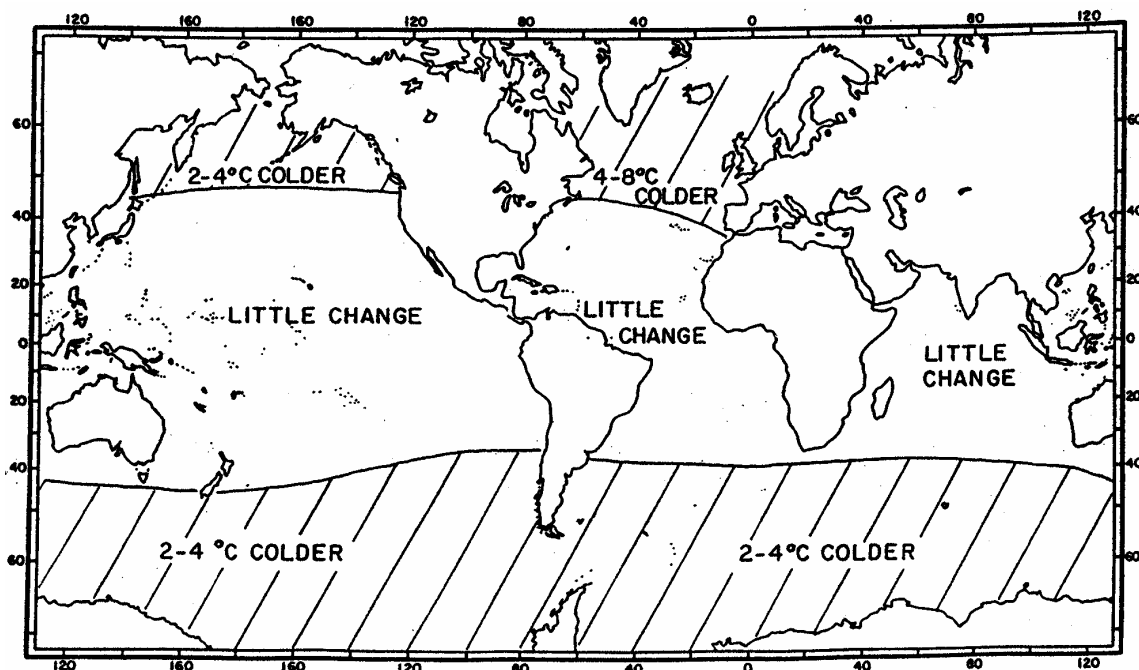


Figure 17. Summary of the findings of the CLIMAP program. While at mid to low latitudes, ocean temperatures appear to have been no more than 2°C colder during peak glacial than during peak interglacial time; at mid to high latitudes, clear evidence for cooling is seen. This cooling is especially pronounced in the northern Atlantic reaching as much as 8°C.

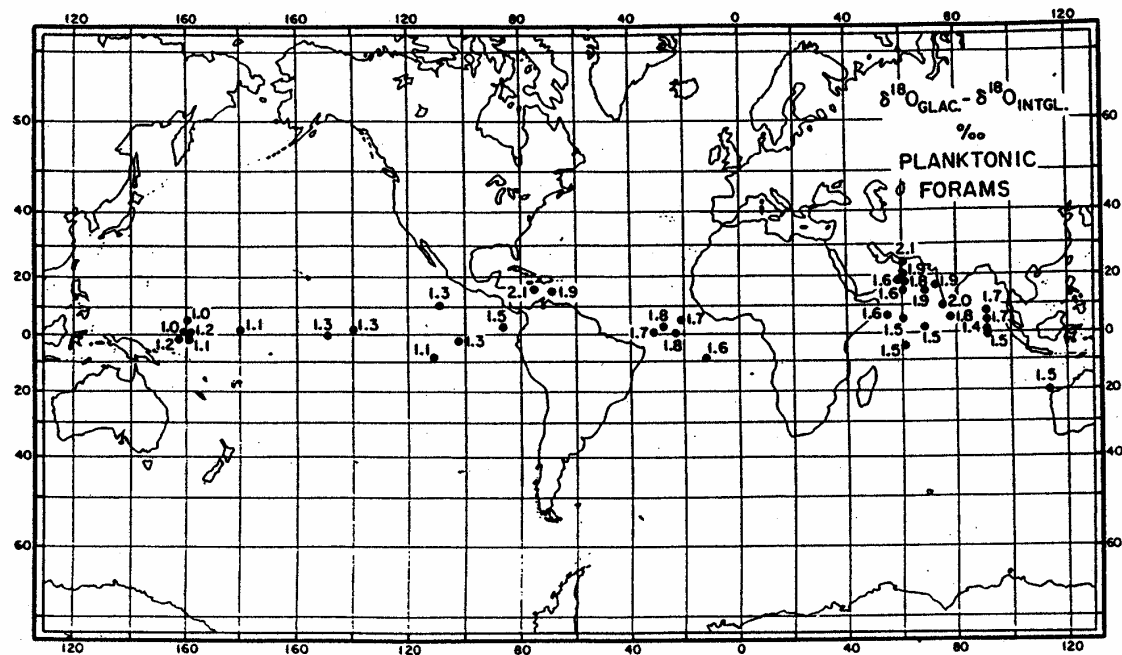


Figure 18. Glacial to interglacial differences in the oxygen isotope composition of planktonic foraminifera shells.

rise to yet another degree Celsius to the magnitude of the glacial to interglacial temperature change for the tropical ocean. Working at a marine laboratory on Santa Catalina Island, they grew the planktonic species *Orbulina universa* at a series of pHs. They were surprised to find that the higher the pH, the lower the $\delta^{18}\text{O}$ of the shell CaCO_3 . As we shall see later in this section based on measurements made on gases trapped in ice cores, the atmospheres pCO_2 was 30% lower during peak glacial time than prior to the onset of the Industrial Revolution. For this to have been the case, the pH of the surface ocean must have been 0.15 units higher at that time. If the pH dependence found by Spero et al. applies to all planktonics, then this pH difference would cause a $\delta^{18}\text{O}$ lowering of about 0.32‰. This is equivalent to a bit over 1.4°C. Thus the oxygen isotope-based estimates for the glacial to interglacial temperature change for the tropics would have to be increased from 1.5 to about 3°C. This is outside the range permitted by Imbrie's planktonic abundance method.

In recent years support for an approximately 2°C glacial to interglacial change in tropical ocean temperatures has come from alkenone molecules manufactured by marine plants. While the no firm biochemical explanation has been put forward, as shown in figure 19, a strong empirical relationship has been found between the ratio of two 37 carbon atom molecules and the temperature at which the plants (mainly the coccolithophorid *Emiliania huxleyi*) which manufactured them grew. The colder the water the higher the proportion of the diunsaturated molecule relative to the triunsaturated alkenone molecule. Fortunately, as alkenones are very resistant to degradation, they are preserved in marine sediments. As they are nearly identical chemically, presumably the ratio of the alkenone molecules of interest remains unchanged even if partial degradation has occurred. Down core alkenone measurements for the tropical Pacific and Indian Oceans suggest a temperature drop of about two degrees centigrade during peak glacial time (see example in figure 19).

This seemingly strong case for nearly constant tropical ocean temperatures has

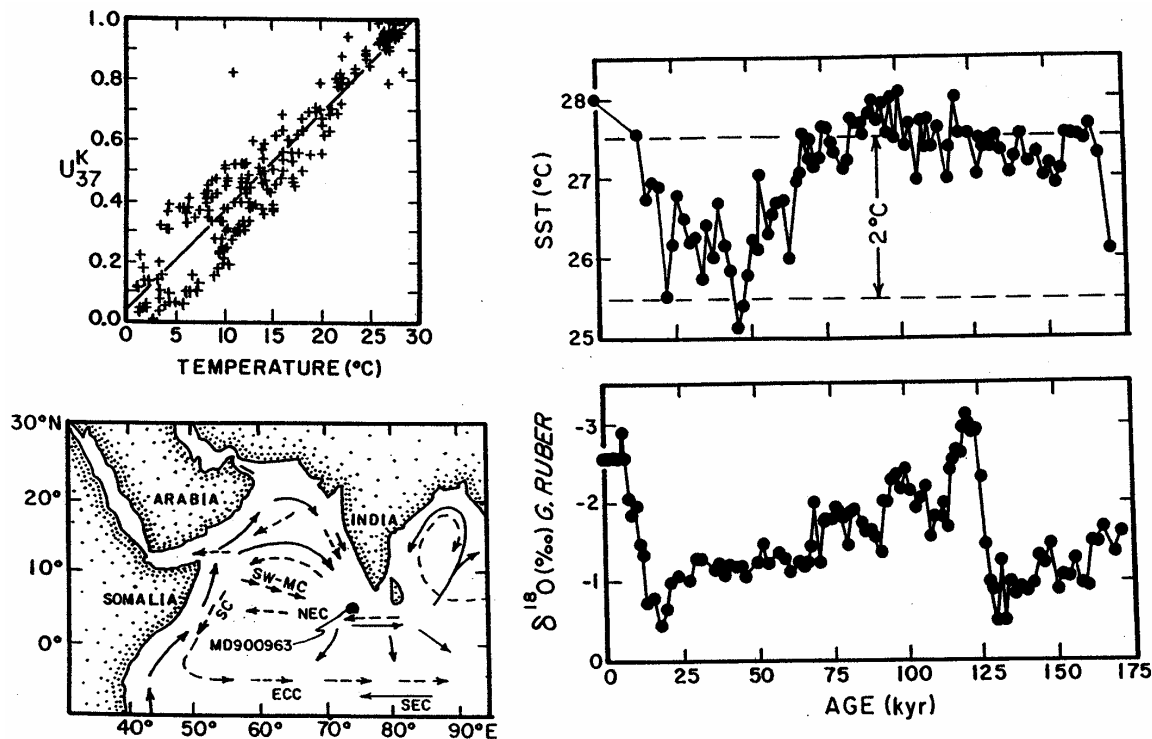


Figure 19. The plot in the upper left hand corner shows the field evidence compiled by Simon Brassel supporting the dependence of the alkenone composition index U_{37}^K on growth temperature. Based on this calibration, measurements on cores from the tropical ocean have been used to reconstruct surface ocean temperatures. As can be seen in the example from the central Indian Ocean, temperatures during the last glacial period averaged two degrees lower than those for interglacial time.

not gone unchallenged. The first challenge comes from measurements of strontium to calcium ratios in fossil corals. As early as 1979, Steve Smith and his colleagues at the University of Hawaii found that the Sr/Ca ratio in scleractinian corals decreased by about 0.8% per °C. However it was not until 1992 when a very accurate series of measurements made by Warren Beck and his colleagues at the University of Minnesota using isotope dilution mass spectrometry were published that the paleoclimate community took active notice. Beck showed that the Sr to Ca ratio across annual growth bands in living corals very nicely followed the seasonal temperature cycle (see figure 20). He also presented results for a fossil coral with a radiocarbon age of 10,000 years from the island of Vanautu (16°S in the western Pacific) which showed clear Sr/Ca cycles associated with seasonal banding and suggested mean surface water temperatures 5°C colder than today's!

Following the Minnesota group's lead, Rick Fairbanks and his colleagues at Lamont-Doherty analyzed a series of corals from borings off the island of Barbados (13°N in the Atlantic) ranging in age from 15,000 to 8000 radiocarbon years. Their results suggest that surface ocean temperatures were 4 to 5° colder during peak glacial than during early Holocene time (see figure 21).

Yet another recently developed marine paleothermometer may well eclipse the others. It is the magnesium to calcium ratio in planktonic foraminifera. As shown in figure 22, the amount of Mg incorporated into the shells of the species *G. ruber* is a strong function of temperature ranging from 4.0 mmol Mg/mol Ca at 29°C to 2.5 mmol Mg/mol Ca at 24°C. David Lea and his coworkers applied this method to a number of cores in the equatorial Pacific and obtained a late glacial to Holocene surface temperature change of 2.6°C. (see table 2)

One drawback of this method is that partial dissolution of the shells after they reach the sea floor reduces the Mg to Ca ratio thereby lowering the temperature they record. Part of this preferential removal of magnesium relative to calcium during

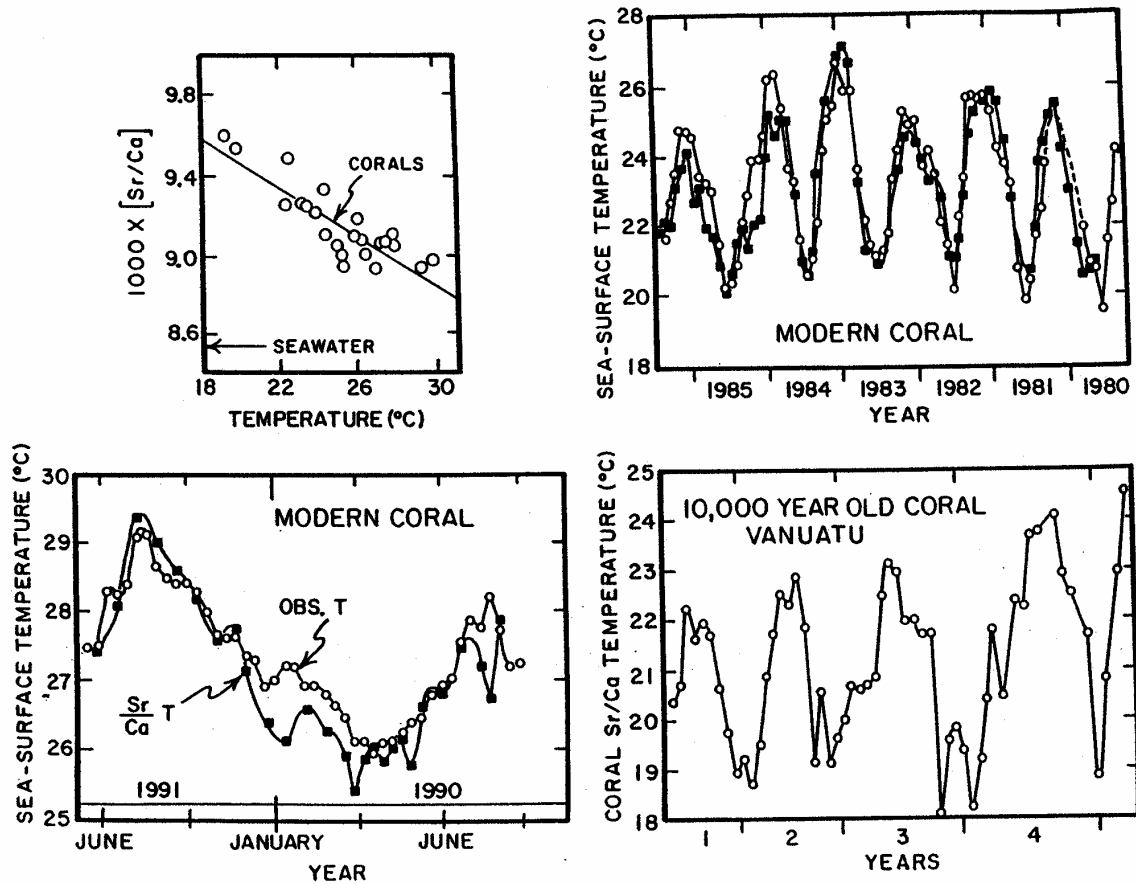


Figure 20. In the upper left hand corner is shown the original data of Smith et al. (open circles) and the more recent high precision data of Beck et al. (solid line) which demonstrates that the Sr to Ca ratio in corals depends on temperature. Also shown are two checks on this calibration made by comparing the Sr/Ca-based temperatures with observed water temperatures across annual growth bands in modern corals. Finally, shown at the lower right are Sr/Ca temperatures obtained by Beck and his colleagues on a coral from the island of Vanuatu (19°S in the western Pacific Ocean) with a ^{14}C age of 10,000 years. This coral shows a larger seasonal amplitude and a 5°C lower mean annual temperature than found at Vanuatu today.

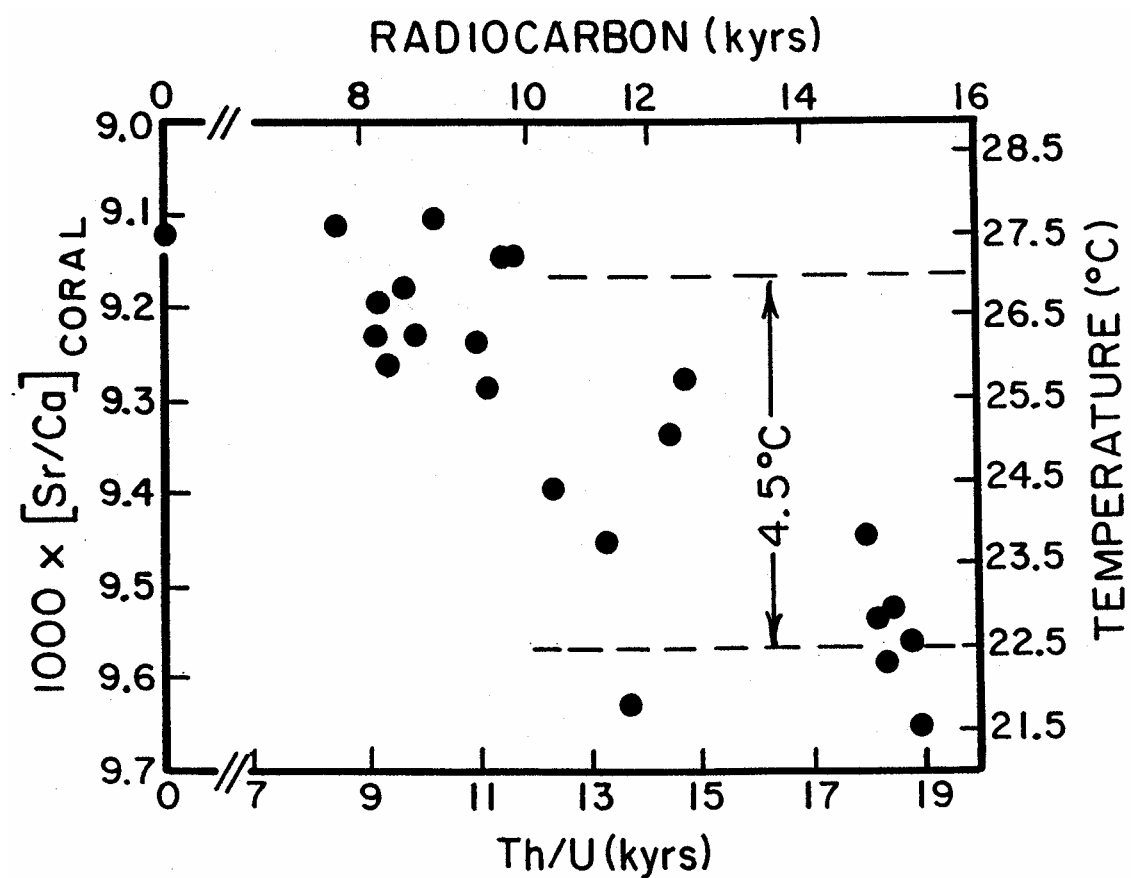


Figure 21. Sr-Ca temperatures obtained by Guilderson and Fairbanks for a series of Barbados corals spanning in age the transition from the late glacial to the early Holocene interglacial. As can be seen, the temperature ranges from an average of about 22.5°C during glacial time to about 27.0°C during early Holocene time, a difference of 4.5°C .

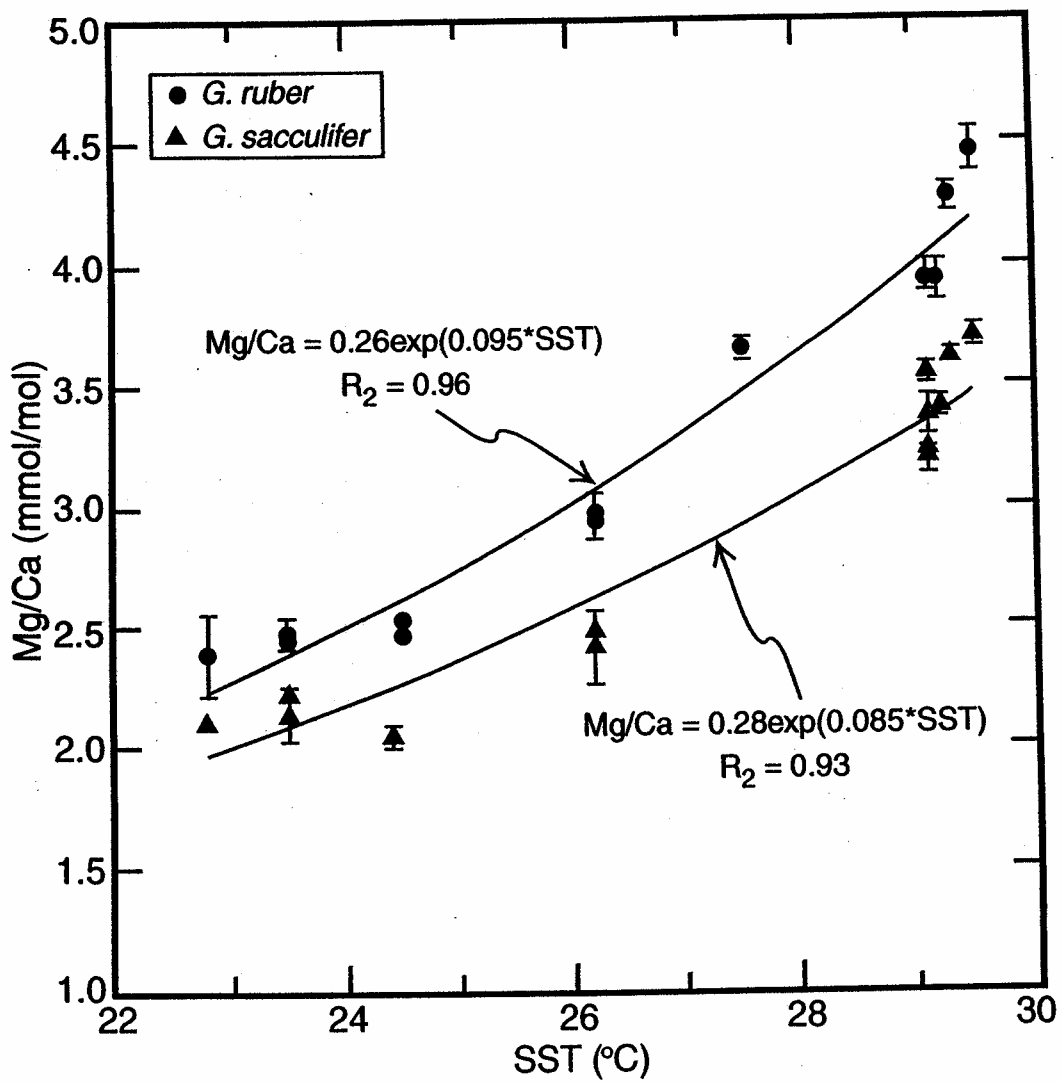


Figure 22 Tropical Pacific core-top *G. ruber* and *G. sacculifer* calibration for Mg/Ca versus mean annual SST (Levitus, 1994, World Ocean Atlas). Each point is the average of 1-4 analyses, with standard deviations shown. The range of core-top depths for *G. ruber* is 1625-3200m and for *G. sacculifer*, 1625-4445m. The standard errors of the exponential fits are $\pm 0.5^\circ\text{C}$ for *G. ruber* and $\pm 0.7^\circ\text{C}$ for *G. sacculifer*. Data are from Lea et al. (2000), Dekens et al. (2002) and Lea (UCSB), unpublished.

Table 2. Results of Mg/Ca ratio measurements on late glacial and Holocene *G. ruber* from cores from the equatorial Pacific (Lea et al., 2000).

Lat.	Long.	Depth km	Today's Temp. °C	Mg/Ca Core top -----mmol/mol-----	Mg/Ca Late G.	ΔT G. → H. °C
2.8°N	89.9°W	2.03	26.2	3.15	2.39	2.6
2.3°N	91.0°W	2.35	26.2	2.99	2.38	2.6
0.5°N	92.4°W	2.83	24.5	2.70	2.18	2.4
0.3°N	159.4°E	2.52	29.2	3.97	3.10	2.8

dissolution is thought to reflect the selective loss of ontogenetic shell material which because it forms in the warm oceanic mixed layer is more enriched in magnesium. However, recent studies by Harry Elderfield indicate that the situation is more complex. A series of measurements on core top *G. ruber* from a series of water depths on the Ontong Java Plateau suggest that the bias introduced in this way increases by -1.3°C per kilometer water depth reflecting the increase in the solubility of calcite with pressure.

An advantage of the Mg/Ca method over the alkenone method is that the ^{18}O to ^{16}O measurements can be made on the same shells as the Mg/Ca measurements. This allows the temperature contribution to the ^{18}O signal to be reliably estimated, for the impact of any seasonal or water depth temperature impacts would apply equally to both measurements. Hence the temperature corrected ^{18}O record should provide a reliable estimate of the glacial to Holocene change in the isotopic composition of the local surface water. For the Cocos Ridge site (91°W), the decrease in $\delta^{18}\text{O}$ from peak glacial to Holocene obtained in this way by Lea et al. (2000) was $1.7\text{\textperthousand}$, a value substantially larger than that expected for ice volume alone (i.e., $1.1\text{\textperthousand}$). In contrast, the change for the Ontong Java Plateau was only $0.7\text{\textperthousand}$ (i.e., substantially lower than that due to ice volume). Clearly, this implies a reduction in the salinity contrast between the western and eastern equatorial Pacific during glacial time. But until a better understanding of the differential dissolution of Mg relative to Ca is obtained, these results must be taken with a grain of salt.

Continental Temperatures

Except for high mountain regions, little precise paleotemperature information exists for the continents. The obvious source of such information is the fossil remains of plants and animals. Indeed a wealth of measurements regarding the relative abundances of pollen grains has been collected over the last century. However, the Imbrie approach to analyzing this information has not proven particularly successful. Unlike the sea which is everywhere wet, the topography of the continents strongly influences the

availability of water. Plant communities are attuned to these differences in moisture availability. Hence plant communities respond as much to changes in rainfall and humidity as they do to changes in temperature. Reliable separation of these two influences has proven very difficult. The problem is compounded by the large seasonality in temperature and rainfall. Because of this, two locales with the same mean annual temperature and rainfall may have quite different plant cover. Thus, while in a historical sense pollen abundances have provided very valuable qualitative evidence with regard to changing climates, no means yet exists to convert these results into reliable absolute temperature changes.

Another problem is that while ocean sediments accumulate almost everywhere on the sea floor, pollen-bearing sediments are found only in lakes and bogs. The closed depressions which contain these water bodies are not uniformly distributed across the continents. The hummocky topography created during the retreat of the glaciers hosts most of the world's lakes and bogs. While providing an excellent record of the post glacial succession of plants, these lakes and bogs tell us nothing about continental environments during peak glacial time, for these water bodies had not yet come into existence!

In the non-glaciated regions of the world, lakes and bogs are far less numerous, for erosion long ago breached the rims of most closed basins. The lakes that do exist are hosted by sink holes which form in limestone terrain, in the craters of young volcanoes, and in between fault blocks in tectonically active areas. As most of these features are ephemeral, the number of records extending back several glacial cycles is quite small. For example, only 6 pollen records for glacial time have been obtained in the entire Amazon basin and none of these cover the entire interval from 30,000 years to present.

In recent years, Linda Heusser has extended pollen studies to deep ocean sediments adjacent to the margin of continents. Not only are these records continuous, but also, it has allowed Heusser, working with Cambridge University's Nick Shackleton,

to directly compare the terrestrial pollen with the marine oxygen isotope records. Such comparisons are very revealing, for they allow the local vegetation history to be compared with the global ice volume record kept by benthic foraminifera. One important result from these studies is the finding that pollen records from both hemispheres mirror the marine ^{18}O record clearly indicating that the glacial-interglacial climate cycles are globally synchronous.

One very interesting attempt to overcome these difficulties associated with pollen is based on the remains of beetles (*Coleoptera*). Unlike plants whose ecology is highly moisture dependent, beetle ecology depends mainly on temperature (including its seasonal span). Unlike pollen grains which can be carried long distances by the wind, the beetles remains found in peat lived on the vegetation growing in the bog itself. For pollen, transport biases are reduced by obtaining the glacial and interglacial samples from the same site. By contrast, because no transport bias exists, beetle populations can be reconstructed from deposits at a number of different localities and sequenced by radiocarbon dating. To date, the most extensive study of the beetle record has been carried out in Great Britain. The results suggest glacial temperatures 10°C colder than today's for the summer months and an even larger cooling for the coldest winter months.

The oxygen isotope method, so useful in marine sediments and ice cores, while potentially applicable to lake sediments, has not produced useful temperature data. One reason is that lake sediments are often too acid to preserve the CaCO_3 . Even in those situations where CaCO_3 is preserved, the task of extracting temperature information proves to be difficult. The interplay of changing isotopic composition of precipitation, fractionation during evaporation and seasonal temperature swings proves to be too complex to unravel. Seemingly, a way around this complexity would be to find environments where evaporation and seasonality do not play strong roles. Such environments must, by definition, be removed from active contact with the atmosphere.

Caves are an obvious choice, for well away from their portals, temperature stays close to its annual mean.

Even so, even for caves a major complication exists. The water from which speleothems form comes from the rain and snow which falls on the overlying land surface. The isotopic composition of the precipitation itself depends on temperature. We have already seen that in the polar regions the H_2^{18}O content of the snow decreases 0.7‰ per °C of cooling. If the same coefficient were to apply to lower latitudes (which it doesn't), then the isotopic composition change produced by the rainfall composition change would be about three times (0.70‰/0.23‰) as great as that produced by the temperature impact on the isotope fractionation during growth of the calcite in the cave. In reality, the temperature dependence of the isotopic composition of rain is smaller (averaging perhaps 0.4 to 0.5‰ in temperate regions). In such regions a one degree cooling would deplete the isotopic composition of the ^{18}O in rain by 0.46‰ but would increase the ^{18}O in the CaCO_3 relative to cave water by 0.23‰. The net change in CaCO_3 would be a drop in the ^{18}O content of the calcite oxygen by 0.23‰ (i.e., 0.46‰ - 0.23‰). So in a sense, any temperature information to be obtained from cave deposits will reflect more the temperature dependence of the isotopic composition of the local precipitation rather than the actual cave temperature. The problem with this is that at lower latitudes the tie between the annual means for temperature and for isotope composition of the precipitation is not nearly so tight as it is in polar regions. Factors such as seasonality of rain and source of the water in the air masses which bring the rain and evaporation from soils bias the local oxygen isotope composition. A further correction must be made. During peak glacial time, the $\delta^{18}\text{O}$ for sea water was higher by 1.1‰; hence the actual change at our hypothetical site would be a rise in $\delta^{18}\text{O}$ of about +0.87‰ (i.e., -0.23 + 1.10‰). Because of this, even in the most favorable situations, the isotopic composition of cave calcite is difficult to interpret. However, as we shall see, because stalagmites can be dated with extremely high accuracy (by the ^{230}Th - ^{234}U

method) and do show ^{18}O to ^{16}O ratio changes with time, they provide an excellent means of establishing to what extent the impacts of millennial duration climate changes, so beautifully recorded in the glacial section of Greenland ice and in high accumulation-rate continental-margin sediments, extend across the continents.

Fortunately, a far better means for reconstructing absolute mean annual temperatures for the continents exists. It involves the measurement of noble gas concentrations in waters from deep aquifers. The amounts of neon, argon, krypton and xenon dissolved ground water depend on temperature at the water table from which the aquifer is charged (see figure 23). As these gases are chemically inert once the water leaves the vicinity of the water table, their concentrations cannot change. Hence, the concentration of each of the four gases constitutes a paleothermometer.

The water table at which the gas content of ground waters is set marks the transition from pore space filled with air to pore space filled with water. Until it descends beneath the water table, the fluid is free to exchange its gases with air present in the adjacent pores. The important point is that since the water table generally lies several meters below the surface, its temperature remains very close to the annual mean. This eliminates the seasonality problem which plagues most other attempts to establish past temperatures on the continents.

Once beneath the water table, this water moves slowly downward under the influence of gravity (see figure 24). In some cases, this ground water follows a short pathway to a nearby stream. In others, it follows a pathway hundreds of kilometers in length before re-emerging. It is these long pathways in which we are interested, for along them, waters of glacial age are often found. The long distance channels along which glacial age waters are found often lie in a porous sandstone horizon sandwiched between two impermeable shale beds. Water enters the aquifer where the sandstone layer is exposed at the surface (for example, along the front of a mountain range). The water moves down dip through the sandstone toward some distant place where the sandstone

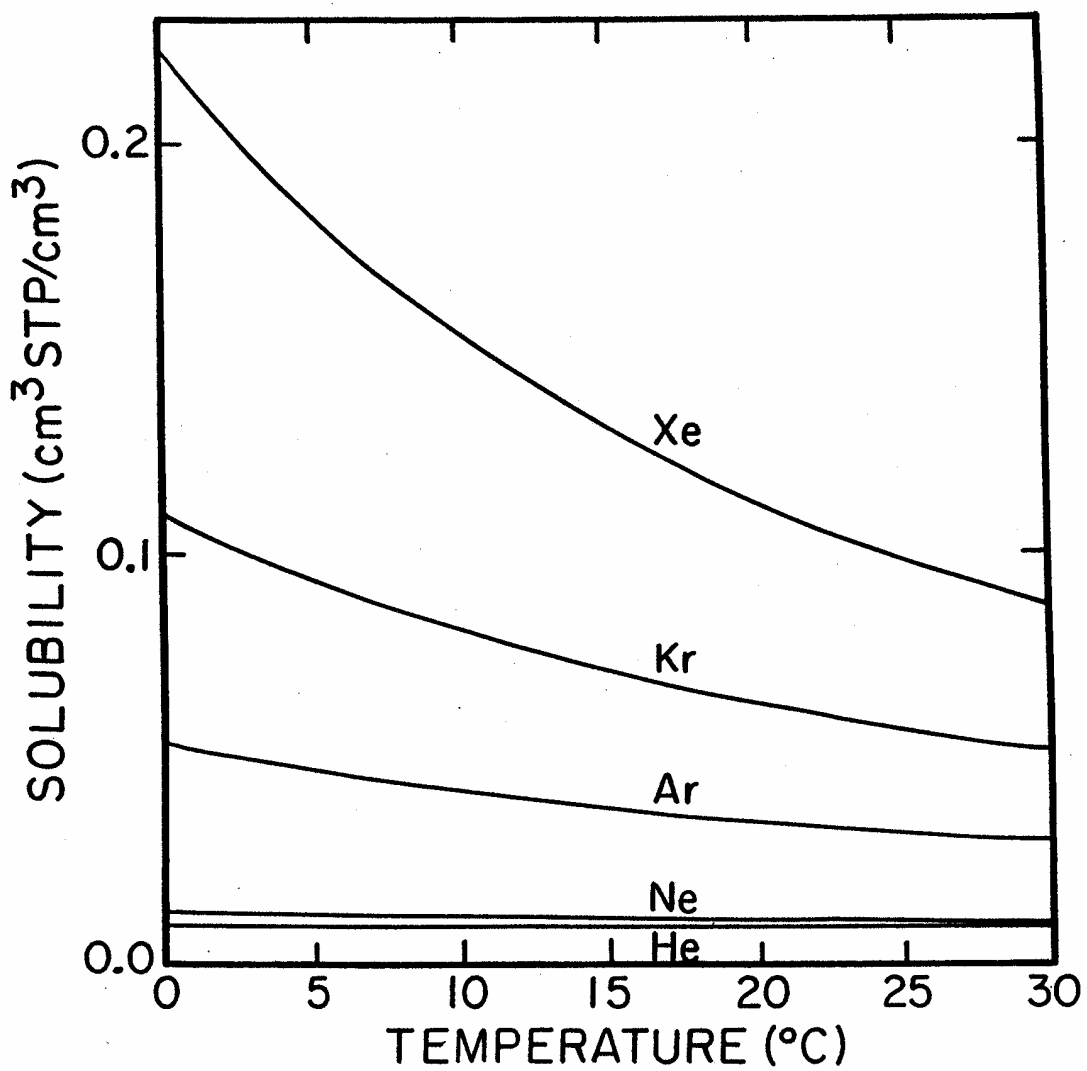


Figure 23. Solubilities of the noble gases as a function of temperature. The He and Ne values are from Weiss (1971) and the Ar, Kr and Xe values from Cleve (1979).

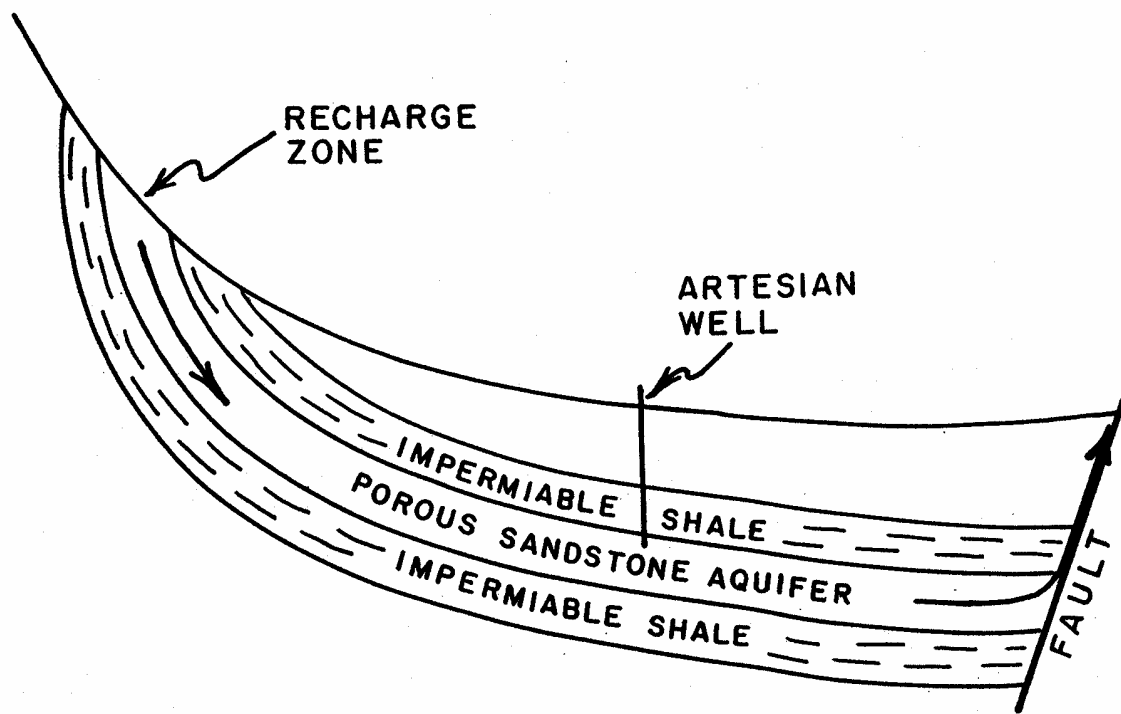


Figure 24. Idealized diagram showing a sandstone aquifer confined between impermeable beds of shale. Waters enter the aquifer where it outcrops at a mountain front and flows through it until it reaches a fault where it returns to the surface. If the aquifer is long enough, its distill region may contain water of glacial age.

horizon is cut by a fault, a river valley or a continental margin. Here the water exits. Provided the capping by the shale is tight, precipitation falling on the overlying surface cannot penetrate down into the sandstone. Thus the only water in the aquifer is that which entered along the mountain front outcrop (see figure 24).

As sandstones are generally free of soluble salts, such aquifers provide excellent sources for drinking water. Further, as the water in the aquifer is under a head of pressure supplied by the extra elevation of its mountain front recharge zone, no pumps are needed. Hence artesian wells have been drilled into such aquifers. Geochemists in their search for glacial water have only to sample a traverse of such wells along the aquifer's course. Radiocarbon ages obtained on the HCO_3^- dissolved in the aquifer water increase with distance from the recharge zone. But because these waters often dissolve or exchange with CaCO_3 minerals, radiocarbon measurements on dissolved carbon provide only an approximate measure of the time elapsed since the water descended from the recharge zone. However, these ages are good enough to distinguish waters of Holocene age (i.e., <10,000 radiocarbon years) from waters of glacial age (14,000 to 25,000 radiocarbon years). In most cases, this assessment is confirmed by a change in the oxygen isotope ratios in the water corresponding to the transition between waters of Holocene and glacial age. While aquifers fulfilling these requirements are found on every continent, to date, noble gas studies have been made on only a few (see figure 25).

The noble gas method is not without complications. One stems from the observation that aquifer waters are supersaturated with all gases. In other words, more gas exists than would be expected for the temperature at the groundwater table in the recharge zone. This has been demonstrated by sampling waters close to the recharge zone. The explanation for the supersaturation is that air bubbles become entrapped in the water in the vicinity of the water table (much as air bubbles become entrapped in ice). If this air doesn't diffuse out, it eventually will be forced into solution by the weight of the overlying water. Fortunately, the concentration of the gas neon can be used to assess the

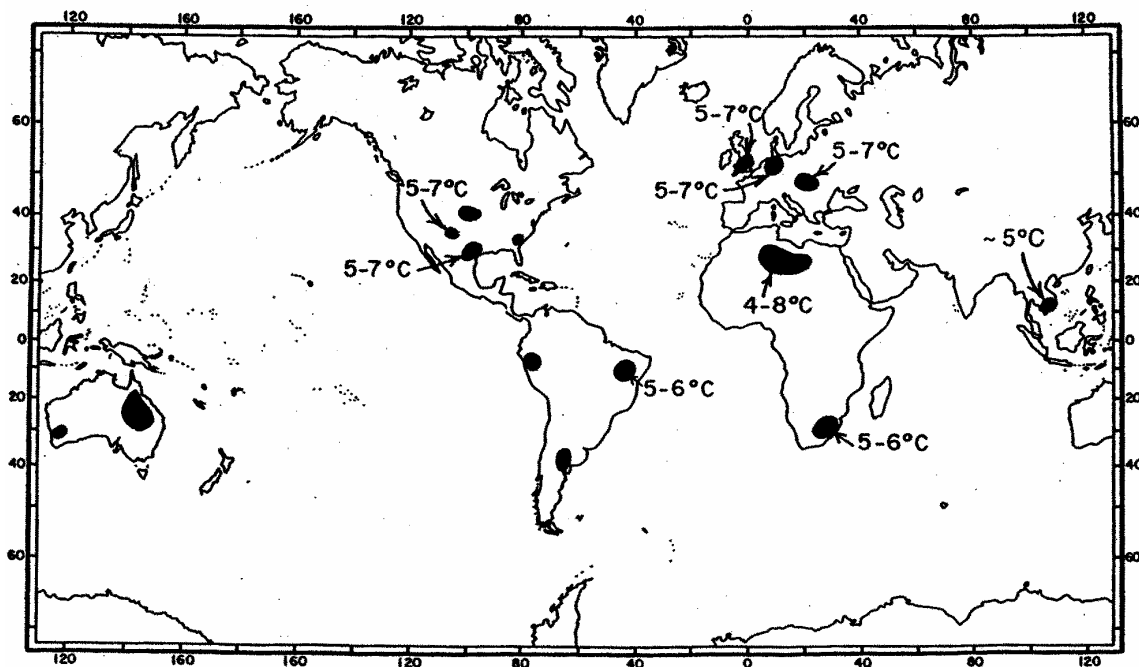


Figure 25. Locations of aquifers known to contain glacial age water. Temperature differences (i.e. Holocene - glacial) are shown for those aquifers on which gas concentration studies have been conducted. As explained in the text, the temperatures are for the water table in the recharge area for the aquifer. They are mean annual temperature.

extent of supersaturation. This correction owes its effectiveness to the fact that neon is the least soluble of the noble gases (see figure 23). Hence, when air bubbles are forced into solution in ground water, they make a far greater fractional change in the concentration of neon than they do for xenon. For example, were air bubble injection to raise the concentration of neon by 30% (a typical value), the concentration of xenon would be raised by only about 1%. Fortunately, the temperature dependence of neon is very small (see figure 23) making it easy to separate the impacts of supersaturation and temperature. Thus from each sample, three independent temperatures can be obtained from the concentrations of Ar, Kr and Xe. When measured by state of the art mass spectrometry, the noble gases offer temperatures precise to one half degree centigrade! So far, most of the results have been obtained from aquifers in zones of temperate climate (northern Europe, the Sahara, South Africa, and the southwestern USA). All show glacial to Holocene temperature changes of 5°C or more (see figure 25). Hence, it appears that for mid-latitude continents, the glacial cooling was of similar magnitude to that for high elevations everywhere in the world. Martin Stute and his colleagues at Columbia's Lamont-Doherty Earth Observatory have obtained results for an aquifer at 7°S in Brazil which suggest a $5.4 \pm 0.5^\circ\text{C}$ lower soil temperature for glacial time. This new result is consistent with the coral-based temperature change for Barbados at nearly the same longitude but at 13°N. One caveat must be added; the ground water results for Brazil are subject to a complication not encountered in temperate climate aquifers; namely, the neon-based correction for supersaturation does not lead to concordant temperatures for the other gases. The pattern of the anomalies among the argon-, krypton- and xenon-based temperatures is such that it appears that once incorporated into the water, part, but not all, of the excess gas diffused back through the water table into the overlying airspace. Indeed, when a correction for such a loss is made (based on the molecular diffusivities of the four gases), the temperatures come into agreement. However, in doing this, one more piece of information is utilized. Thus only two

independent temperature estimates remain (i.e., only one cross check rather than two is available). This situation is aggravated by the fact that the amount of excess gas is much larger in the Brazilian aquifer than in temperate aquifers. It reaches threefold for neon in glacial age waters. So not only is the correction scheme more complicated but also the corrections are larger. Stute proposes that the extent of supersaturation increases with aridity. In arid regions, the rainfall tends to be highly seasonal creating sizable fluctuations in the level of the ground water table. Each upward excursion leads to the incorporation of bubbles and hence the injection of excess gas. If this hypothesis is correct, then the ground waters store not only information about past temperatures but also a qualitative indication regarding past aridities. In the case of eastern Brazil, the suggestion is that the climate was more arid during glacial time.

The Tropical Temperature Dilemma

So we have a big problem on our hands. How can the diverse temperature estimates presented above for tropical regions be reconciled? One obvious conclusion would be that all are correct. If so, as demanded by the magnesium to calcium and alkenone results during peak glacial time most of the tropical sea surface cooled by 2 to 3°C. The exceptions would be those oceanic regions in the vicinity of Barbados and Vanuatu which according to the strontium to calcium results on glacial age corals have been as much as 5°C cooler. Further, as suggested by the noble gas data from the Brazilian aquifer, the Barbados cold anomaly would have to have extended southward onto the South American continent. A seeming problem with this interpretation is that it requires large longitudinal gradients in tropical temperatures. However, while longitudinal temperature gradients are a theoretical no-no at mountain top elevations, substantial gradients are permitted at low elevations. For example, the western equatorial Pacific has temperatures averaging 5°C warmer than those in the eastern equatorial Pacific. So, one cannot reject on theoretical grounds glacial reconstructions which require regional differences in ΔT . What can be said at this point is that equatorial

temperatures likely cooled by 2 to 3°C over large regions and perhaps by 3 to 5° in smaller regions. Atmospheric models suggest that a three-degree glacial cooling is consistent with the extent of snowline lowering in tropical mountains. Further, it is clear that the polar atmosphere cooled far more than the tropical atmosphere.

The relationship between the greater glacial cooling at the elevation tropical snowline (5 to 6°C) and that for the tropical sea surface (2 to 4°C) can be explained as follows. For any given tropical temperature change, the altitude of the 0°C isotherm sets the difference in water vapor content between air at sea level and air at the snowline. As tropical sea surface temperature reaches 26°C and as the adiabatic cooling of air between sea level and 5.3 km is 53°C, in order for the temperature at 5.3 km to be 0°C, the air must be warmed through condensation by 25°C (i.e., $0^\circ = 26^\circ - 53^\circ + 27^\circ$). For this to happen, 17.6×10^{-3} moles H₂O per mole of air must be lost to precipitation during its ascent (see table 3). As air at 5.3 km is observed to be about 65% saturated with water vapor (i.e., it contains 7.6×10^{-3} moles H₂O/mole air), then the sea level water vapor content must have had about 25.2×10^{-3} miles H₂O per mole air. As at 26°C the saturation water vapor content is 33.2×10^{-3} moles H₂O per mole of air, this requires a sea level relative humidity of 76%, a value close to the observed. Now, let's turn our attention to glacial time when the snowlines were 4.5 km above sea level. In this situation the adiabatic cooling would be 45°C. Assuming the relative humidity at the 0°C isotherm to have been the same then as now, a 3°C cooler tropical sea surface temperature would be required were the sea surface relative humidity to have been similar to today's. Hence, cooling aloft is greater than cooling of the sea surface!

ARIDITY

Clearly, if we are to characterize the climates of the past, we need to reconstruct precipitation as well as temperature. This turns out to be an extremely difficult task. The little information we have comes mainly from the fluctuations in size of closed basin lakes and from the rate of accumulation of wind transported debris. As already discussed,

Table 3. Possible combinations of sea surface temperature and relative sea surface humidity capable of producing an 800-meter reduction in the elevation difference between tropical snowlines and sea level. For each of the six glacial sea surface temperatures, the required condensation-induced warming and the corresponding difference in water vapor content between sea level and the snowline air is given. If, as now, air at the glacial age snowline had a relative humidity of 65%, then this air must have had a water vapor content of 6.9×10^{-3} moles H₂O per mole of air. Summing this residual vapor with the amount lost to condensation gives the water vapor content of sea level air and, in turn, the relative humidity at sea level for each scenario.

0°C Iso therm Elev	ΔT^{\dagger} Sea Surf	T Sea Surf	ΔT Adia Cool	ΔT^* Cond Warm	ΔQ^{**} Cond	Q Snow line	Q Sea Lev	Q Sea Lev Sat	Rel Hum Sea Lev
km		°C				10 ⁻³ moles H ₂ O/mole air			%
<i>Holocene: P = 390 mm Hg; Snowline R.H. = 65%</i>									
5.3	–	26	-53	27	17.6	7.6	25.2	33.2	76
<i>Glacial: P = 433 mm Hg; Snowline R.H. = 65%</i>									
4.5	0	26	-45	19	12.4	6.9	19.3	33.2	58
4.5	-1	25	-45	20	13.0	6.9	19.9	31.3	64
4.5	-2	24	-45	21	12.7	6.9	20.6	29.4	70
4.5	-3	23	-45	22	14.3	6.9	21.2	27.7	77
4.5	-4	22	-45	23	15.0	6.9	21.9	26.1	84
4.5	-5	21	-45	24	15.7	6.9	22.6	24.5	92

*Required to yield T = 0°C at the snowline elevation.

** ΔQ (in 10⁻³moles H₂O/mole air) = .653 ΔT (in °C).

†Interglacial to glacial.

the use of pollen records for this purpose is difficult because of the problem of separating influences of temperature and moisture. An additional problem arises due to the fact that the CO₂ content of the atmosphere was lower during glacial time. Because of this, plants had to 'spend' more water in order to take in the CO₂ needed for growth. Because of this, the drop in moisture availability suggested by the paleovegetation may not be a valid indicator of paleorainfall. Rather, it may reflect in part the atmosphere's low CO₂ content.

Precipitation

Indicators of past precipitation rates are at best qualitative. Only for the closed drainage basins does a means exist to quantify changes in the moisture budget. The size of water bodies such as Great Salt Lake, the Dead Sea, and the Caspian Sea change with climate. The reason is that all the water which currently enters these lakes via rain and via rivers must leave by evaporation. Hence, during times of higher rainfall, these lakes expand in area until evaporation matches the enhanced input of water to the lake. Accompanying the expansion in area is a rise in lake level. Thus shorelines marking times when a closed basin lake stood higher record times of greater precipitation. These lakes exist only in desert areas (see figure 26). Under more moist conditions, the area of water surface required to evaporate the incoming water exceeds the size of the entire drainage basin. Hence, all lakes in humid regions have developed outlets that allow the excess water to flow to the ocean.

While simple in concept, the reconstruction of precipitation rates from shoreline elevations has many pitfalls. Some of these are meteorologic. The hydrographically closed basins in which the lakes are located are most often bounded by mountains. Because of this, precipitation directly over the lake surface is often of minor importance compared to that by rivers which head in mountains where most of the precipitation falls. So in a sense, the lake level based record has more to say about precipitation in the neighboring mountains than about that in the region immediately surrounding the lake.

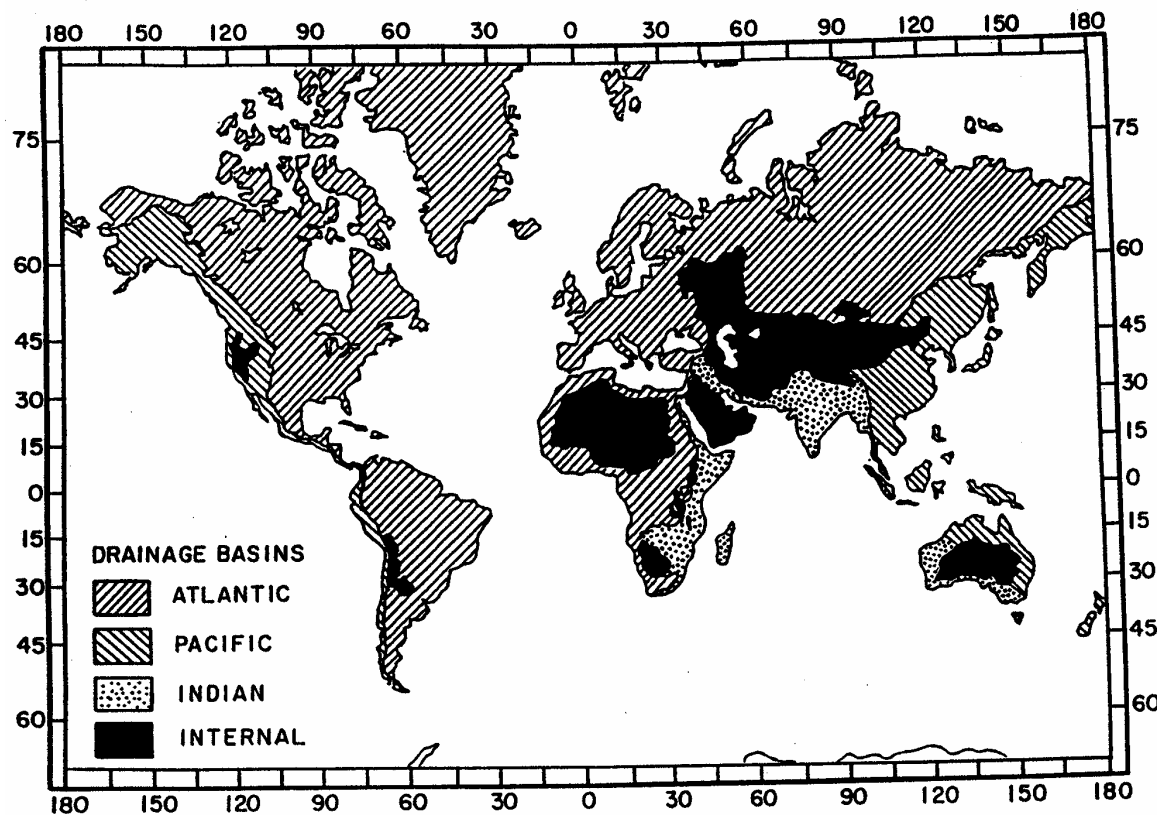


Figure 26. Map showing the internal drainage areas of the Earth (in black). Rainfall onto these areas is lost entirely by evaporation (i.e., none of the water escapes to the sea via rivers). In each are found closed basin saline lakes fed by rivers draining local highlands. The size of these water bodies changes with changing precipitation.

While no one would debate that increased rainfall leads to increased riverflow, the dependence is not a simple one. The reason is that the fraction of the rain water which reaches the lake changes with climate. The lower the rainfall, the greater the fraction of the water which either evaporates from the soil or is transpired by the plants. Reevaporation can become so efficient that, under very arid conditions, as little as 10 percent of the water delivered by rainfall to the drainage basin reaches rivers. By contrast, in areas with abundant rainfall, roughly 50 percent of the precipitation runs off. The remaining 50 percent is lost through transpiration by the vegetation. Hence an amplification occurs, the higher the precipitation, the greater the fraction of the water which reaches the lake. Also the higher the rainfall, the higher the humidity, and hence, the lower the rates of evaporation over the lake itself. While it is not possible to quantify the impact of these amplifiers, it is clear that if precipitation is assumed to be linearly related to lake area, only a gross upper limit on the precipitation rate change would be obtained. Despite these complications, the size of closed basin lakes is by far our best paleoprecipitation proxy.

In addition to meteorologic problems, geomorphic problems exist in interpreting closed lake records. All lakes have two elevation limits. One is reached when the rainfall becomes so great that the lake rises to its overflow point and the basin is no longer closed. In this situation, the excess water flows into some neighboring basin or to the sea. Late in glacial time, Lake Bonneville, the much larger glacial equivalent of today's Great Salt Lake, spilled over a lip in its basin and cut a deep channel which now sets the maximum size this lake can achieve. The other limit is reached when the lake becomes so shallow that it can dry up during periods of drought or even during the dry season of a single year. Such ephemeral lakes are called playas. They have standing water only during wet periods (or wet seasons). So any given lake provides a record of precipitation only over a finite range; if conditions become too wet or too dry, the recorder fails.

Most published records are for lake elevation versus time, rather than lake area versus time. The reason is that adequate maps of the paleoshorelines are often not available. As the relationship between area and elevation is usually not a simple one, it is essential to map the paleoshorelines in order to generate an improved tie to paleoprecipitation.

Those closed basin lakes which were larger than now during late glacial time are located in regions beneath the descending limbs of the Hadley cell. Included are Lakes Lahontan and Bonneville in the western USA (see figure 27) and the Lake Lison in Israel's Dead Sea graben. By contrast, lakes like Victoria in equatorial Africa's rift valley were much smaller during late glacial time. The impression given from this and other evidence is that during late glacial time the tropics were less wet and the subtropics less dry than now.

Rock Varnish

Iron-manganese patens often coat rock surfaces in desert regions. The chemical composition of this so-called 'varnish' depends on climate. During dry periods, the varnish is richer in manganese (and barium), while during wet periods, the opposite is true. This chemical layering can be studied optically in ultra thin sections; the manganese poor layers are orange while the manganese-rich layers are black. Tanzhou Liu, while a graduate student, developed a thin sectioning technique which yields such high resolution of the color record that wet and dry alternations taking place even on millennia time scales can be resolved. This is amazing because the growth rate of the varnish is very slow, averaging only a few microns per thousand years. Liu is able to define layers as thin as a few microns. Although this approach yields only a qualitative index of wetness, when combined with shoreline elevation studies, it offers a powerful means of creating a high resolution climate history for desert regions throughout the world.

One problem associated with varnish is establishing its chronology. As of now,

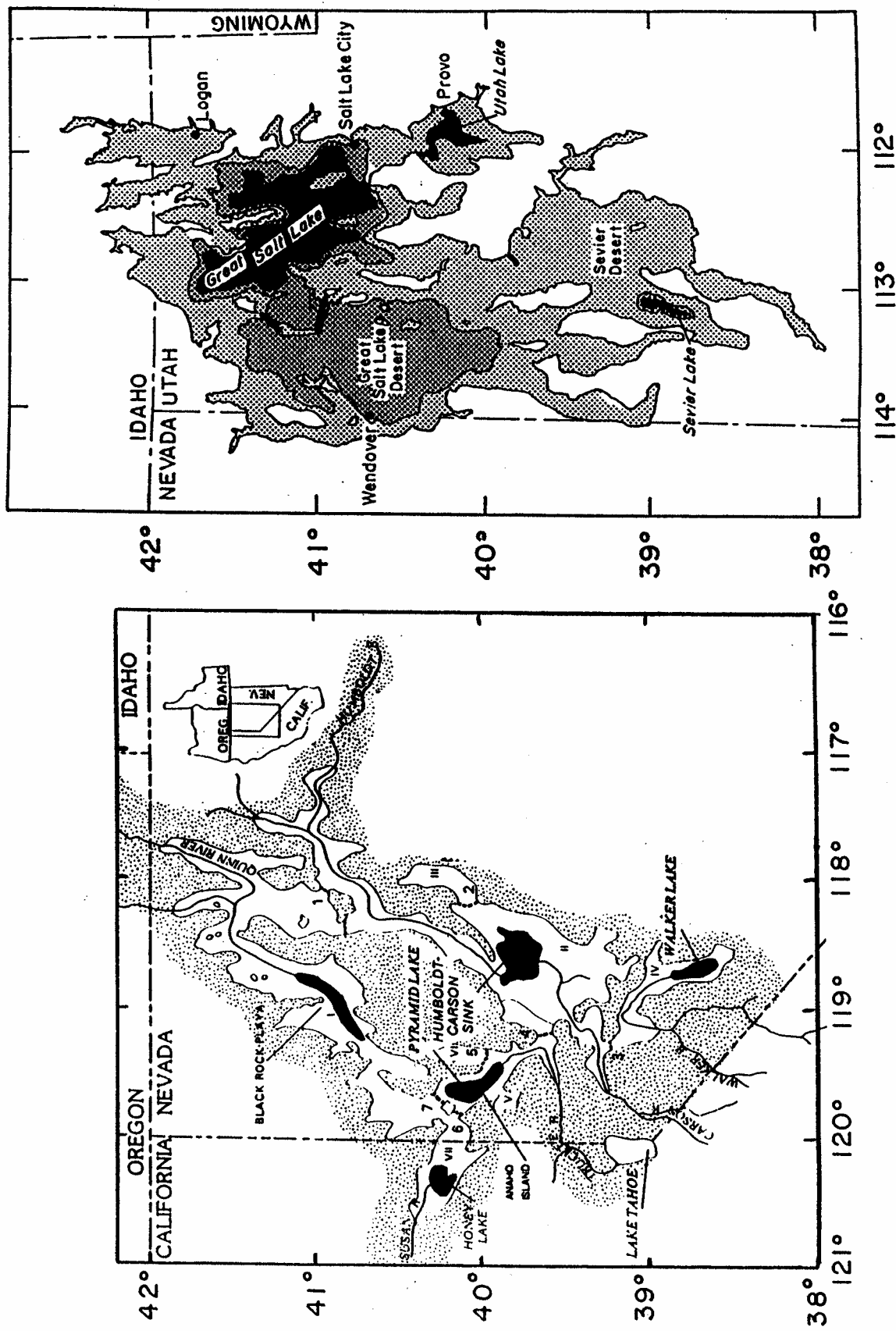


Figure 27. Comparison between the maximum size reached by lakes Lahontan (white area in left-hand panel) and Bonneville (stippled areas in right-hand panel) with that of the present day remnants (Honey, Pyramid and Walker Lakes in the western Great Basin and Great Salt, Utah and Sevier Lakes in the eastern Great Basin).

no means has been found to date the varnish itself. Although rich in uranium, varnish is equally rich in thorium. Hence, the ^{230}Th method is not applicable. Further, there is no measurable carbon in or beneath varnish. Hence, the ^{14}C cannot be used. However, it is possible to obtain at least an upper limit on the basal varnish age by establishing the geomorphic age of the substrate on which varnish formed. In the case of late glacial shorelines of closed basin lakes, this can often be done by ^{14}C dating of algal carbonates. For boulders exposed in moraines and for lava flows, it can be accomplished measuring the buildup of cosmogenic isotopes (^{10}Be , ^{26}Al , ^{36}Cl , ^{14}C). I say ‘upper limit’ because this approach leaves open the question regarding the time lapse between the emplacement of the host rock and the nucleation of the varnish.

Dust

Arid areas are frequented by dust storms. The sparsity of vegetation permits the wind to entrain material from soils, alluvial fans and playas. The particles lofted by these events must eventually return to the Earth's surface. In those circumstances, where this wind-carried debris accumulates without subsequent disturbance, it is possible to determine how the rate of fall (and hence, presumably, also the rate of dust entrainment) changed from glacial to interglacial time. A consistent global picture emerges. At temperate and high latitudes the rate of dust accumulation was about one order of magnitude greater during glacial than during interglacial time. While this result suggests less vegetative cover and hence higher desert aridity during glacial time, storminess is likely the most important factor. As dust entrainment is thought to vary with the cube of wind velocity, a tenfold increase in dust accumulation would, in the absence of vegetation change, require glacial wind speeds at least twofold higher than those for interglacial time! As simulations of glacial climates conducted in atmospheric models yield winds of comparable strength to today's, the more likely cause is that storms capable of lofting dust high into the atmosphere were far more frequent during glacial time. Support for this comes from the finding in ice cores from both Greenland and

Antarctica that NaCl also accumulated an order of magnitude faster during late glacial time. As the likely source of this NaCl was sea spray, its glacial increase cannot be blamed on aridity and vegetation. If indeed storm frequency is the driver, then the obvious explanation is that it depends strongly on the latitudinal thermal gradient which as we have already seen was stronger during glacial time.

Evidence for higher glacial dust accumulation rates comes from the continents, the sea floor and polar ice caps (see figure 28). Measurement of the concentration of particulate matter in ice reveal that both in Greenland and in Antarctica, the concentration was about 20 times higher in ice formed during peak glacial time than in ice formed during peak interglacial time. As the accumulation of snow was only about half as great during glacial time, this twenty-fold increase in concentration translates into a tenfold increase in the rate of dust fall.

The most famous of the areas of continental dust deposition is central China. Here dust has accumulated continuously for the past 2.5 million years to create a mantle of loess 150 meters in thickness. A clever means has been developed to assess changes over time in the accumulation rate of this material. It involves measuring the magnetic susceptibility of the sediment. This measurement yields the concentration of ultra fine-grained magnetite. The results reveal that during times of glaciation, the susceptibility averaged about one sixth that during times of interglaciation. Two lines of evidence suggest the changes in susceptibility were the result of changes in the rate of dust deposition (i.e., the rate of accumulation of ultra fine-grained magnetic minerals remained more nearly constant). One line of evidence is the observation that the integrated amount of magnetic material at sites with higher than average overall loess accumulation is nearly the same as that at sites with lower than average loess accumulation. The other line of evidence is that when the susceptibilities are plotted against time, assuming a constant rate of accumulation of the magnetic material, the pattern becomes nearly identical to that for the marine oxygen isotope records (see figure

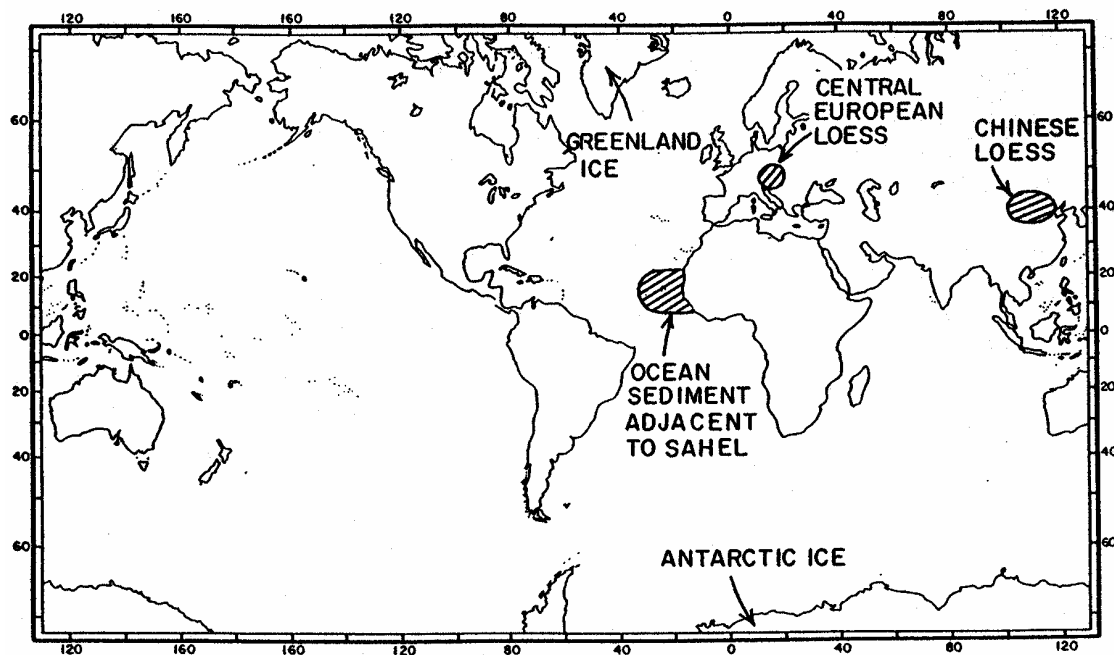
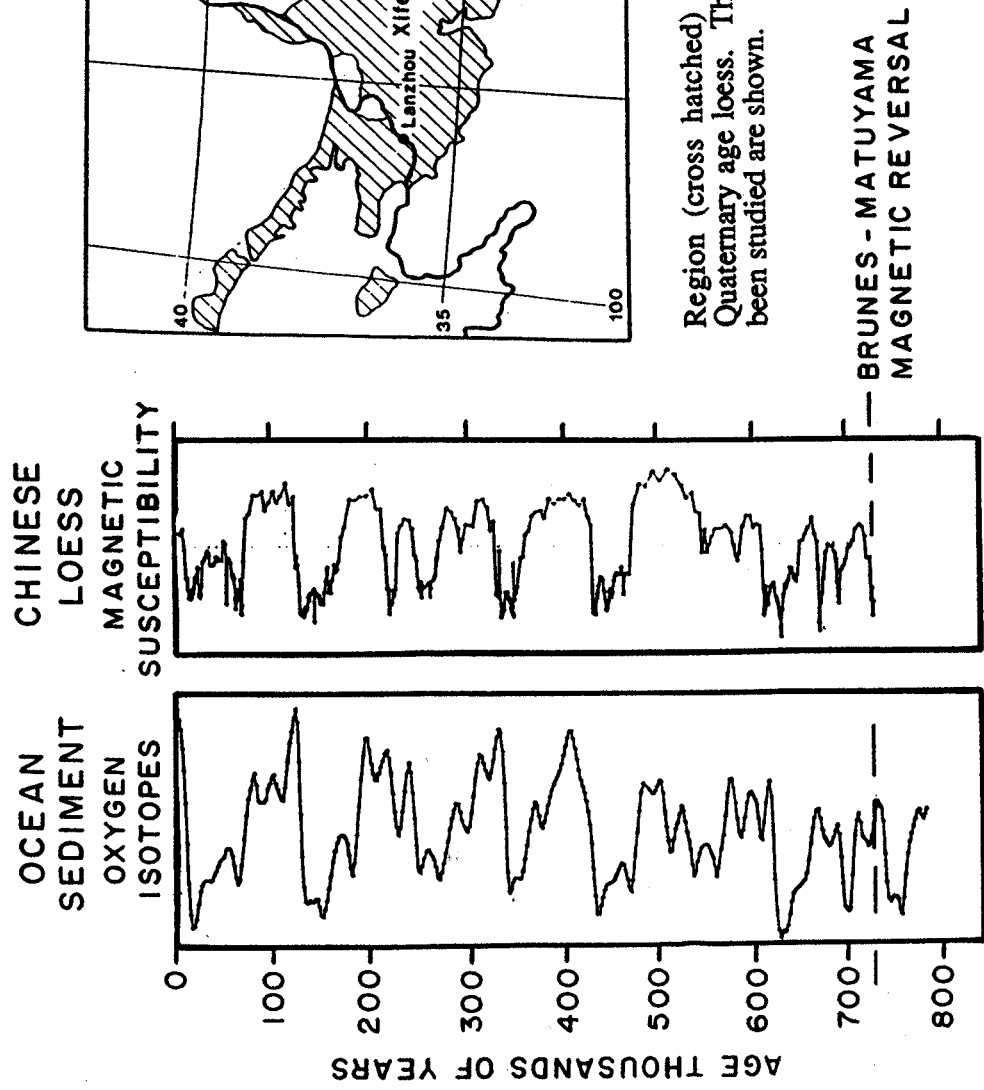


Figure 28. Map showing regions of the Earth where it has been possible to demonstrate that the rate of dust fall was on order of magnitude greater during times of peak glaciation than during times of peak interglaciation.



Region (cross hatched) of central China covered with a blanket of Quaternary age loess. The four sites at which the loess stratigraphy has been studied are shown.

Figure 29. Comparison between the oxygen isotope record for the ocean and the loess record from Xifeng China. The Brunhes-Matuyama magnetic reversal is present in both creating a firm tie point. The accumulation rate for the loess is assumed to be inversely proportioned to the magnetic susceptibility allowing depth to be converted to time.

29). If instead, the accumulation rate were assumed constant, then the duration of the interglacials would be too small and that of glacials too large.

For the ocean, the most dramatic dust rain record comes from the area in the eastern Atlantic adjacent to the bulge of Africa. This region is subject to frequent dust storms originating in the Sahel (see figure 30). Deep sea cores from this region have CaCO_3 contents ranging from about 50% during peak interglacial time to about 3% during peak glacial time. If the accumulation rate of CaCO_3 is assumed to have remained more or less constant with time (an assumption borne out of radiocarbon studies of other tropical Atlantic cores), then the accumulation rate of the noncarbonate material (largely wind blown) must have been about 15 fold higher during peak glacial than during peak interglacial time.

ATMOSPHERIC GAS COMPOSITION

All atmospheric gases whose molecules contain three or more atoms capture quanta of infra red light given off by the warm surface of the Earth. This interception acts as a blanket warming the Earth's surface. Because of this, H_2O , CO_2 , CH_4 and N_2O are referred to as greenhouse gases. As the concentrations of all these gases are subject to change it is important to establish their concentrations for glacial time. CO_2 , CH_4 and N_2O are recorded in air bubbles trapped in polar ice, but, unfortunately, for H_2O , the king of greenhouse gases, no way currently exists to reconstruct its past concentration.

Carbon Dioxide

Until 1980, no clue existed regarding atmosphere's carbon dioxide content during glacial time. This changed when scientists in Bern, Switzerland and in Grenoble, France independently demonstrated that air trapped in bubbles contained in ice formed during glacial time had a lower CO_2 content than does today's atmosphere. Based on these measurements, both groups concluded that the CO_2 content of the glacial atmosphere was about 70 percent (i.e., ~195 ppm) that which the atmosphere had prior to the onset of the Industrial Revolution (i.e., ~280 ppm). Since this discovery, thousands of such

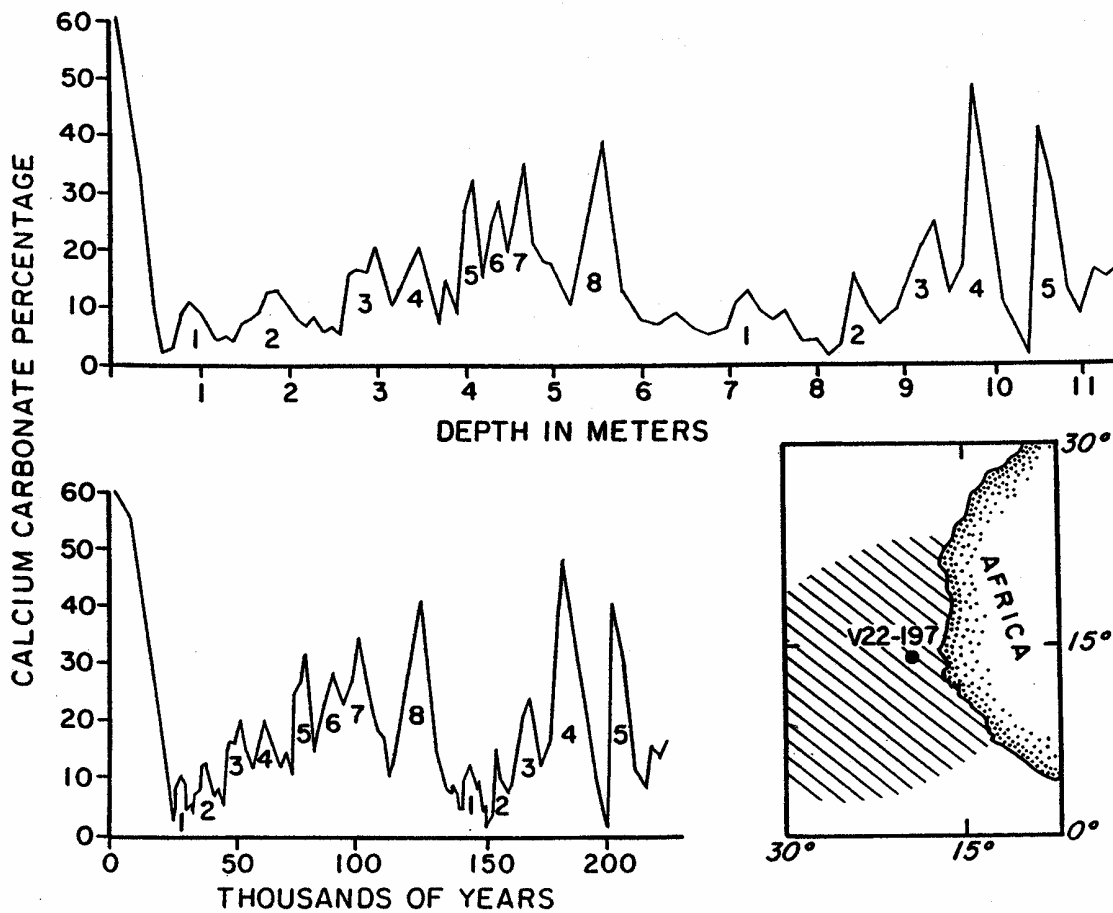


Figure 30. Calcium carbonate content of deep sea core V22-197 from the eastern Atlantic off the bulge of Africa (Hays and Perruzza, 1972). In the upper panel, the percentage CaCO_3 is plotted versus depth. In the lower panel, it is plotted versus time based on the assumption that CaCO_3 accumulated at a constant rate and that peak 8 corresponds to the peak of the last interglacial (i.e., 124,000 years ago). The small map shows region of frequent dust storms and location of core.

measurements have been made on ice from a number of borings in both Greenland and Antarctica. A consistent picture has emerged. During peak glacial time, the concentration was 195 ± 15 ppm and during the Holocene, 270 ± 10 ppm.

What caused the CO₂ content to change? This is a subject which will be treated later in the book. But because it is so complex a problem, some words here will help to pave the way. The magnitude of CO₂ increase from late glacial time to the Holocene is so large and occurred so rapidly that it has proven very difficult to find a satisfactory mechanism to explain it. However, almost all those who have worked on this problem agree that the cause must lie in the ocean. The reason is that the amount of carbon dissolved in the ocean exceeds that in the atmosphere by about a factor of 60. Because of this, the atmosphere's CO₂ content is dictated by the chemical state of the ocean. As the rates of supply of CO₂ to the ocean-atmosphere system through planetary degassing is too slow to account for the rapidity of the glacial to interglacial atmospheric CO₂ change, the explanations which have been proposed involve redistributions of carbon among the active reservoirs (i.e., upper ocean, deep ocean, forests, terrestrial humus, marine humus and CaCO₃ in deep sea sediments). A number of quite different scenarios by which the job could have been done have been proposed. Each of these mechanisms predicts its own unique imprint on the ocean sediment record. The problem is that this record, at least as we now know it, is not entirely consistent with any of the scenarios put forward to date.

The simplest scenario in this regard involves the transfer of carbon between the combined ocean-atmosphere reservoir on one hand and the forest-humus reservoir on the other. The idea is that more carbon was stored as organic matter in these reservoirs during glacial time than today. However, two observations strongly suggest that the opposite was true; i.e., during glacial time the storage of carbon in organic form was smaller rather than larger than today. One observation is that the northern temperate forests which contain nearly half of today's wood did not exist during glacial time. The

areas in which they are now located either lay beneath the ice caps or were vegetated with cold climate shrubs. There are also suggestions that the tropical forests which contain most of the other half of today's wood were more restricted in extent than today. The second observation has to do with isotope measurements on benthic foraminifera shells. These measurements suggest that the ratio of ^{13}C to ^{12}C in the carbon dissolved in the sea was about 0.35‰ lower during glacial than during interglacial time. This change could be explained if an amount of organic carbon equal to roughly one third that in today's combined wood and soil humic reservoir were during glacial time to have been converted to CO_2 and added to the ocean-atmosphere carbon reservoir. Because organic matter has on the average 25‰ less ^{13}C than ocean carbon, by transferring an amount of biogenic carbon equal to one seventieth its present ocean-atmosphere inventory, the carbon isotope ratio would drop by 0.35‰ (i.e., 25‰/70). Taken together, these two observations suggest that transfers of carbon in and out of organic reservoirs appears to have changed the atmosphere's CO_2 content in the wrong direction! Were it the sole cause of change, the CO_2 content of the atmosphere would have been higher during glacial time. Not only is some other mechanism required to explain the drop in atmospheric CO_2 content between interglacial and glacial time but it has to produce an even larger change so as to counteract the CO_2 content increase caused by the reduction in size of the terrestrial organic reservoir as well! (see figure 31)

The CO_2 content of the ocean's surface waters also depends on salinity. The 120 meter lowering of sea level during full glacial time would have raised the ocean's salt content by about 3% (i.e., from 35 gm/liter to 36 gm/liter). This salinity increase would cause the atmosphere's CO_2 content to rise by about 11 μatm . Like the terrestrial biosphere effect, this one is also in the wrong direction.

One way in which a reduction in atmospheric CO_2 content could have been accomplished is through a cooling of the surface ocean. The partial pressure of CO_2 gas in sea water drops by about 4% for each degree of cooling. The problem is that to explain

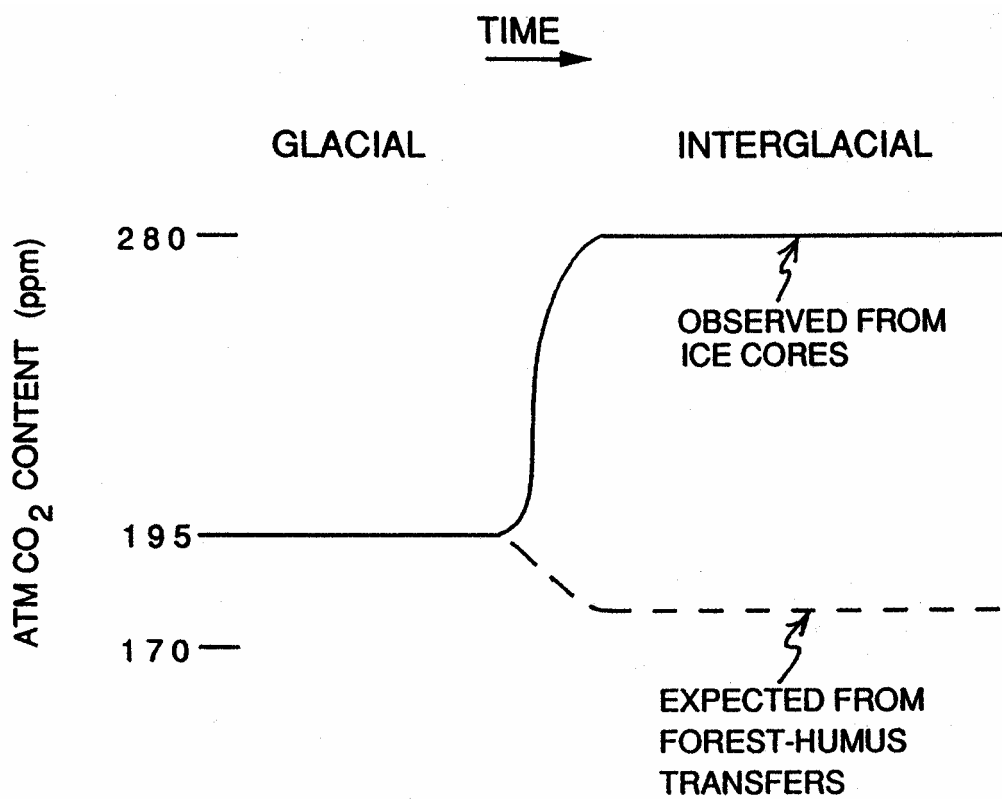


Figure 31. Comparison of the CO₂ record observed in air extracted from ice cores with that expected if the only change were that induced by the regrowth of forests (followed by compensation of the ocean's CaCO₃ cycle).

the 30% decrease in the CO₂ content of the atmosphere, the surface ocean would have had to have been about 9°C colder during glacial time than it is today. As we have already seen, the results of magnesium to calcium and alkenone measurement studies suggest that the actual cooling was only about 3°C. This cooling would cause only a 33 μatm drop in atmospheric CO₂ pressure. Taken together, the change related to the decrease in the terrestrial biomass (+15 ppm), the increase in ocean salinity (+11 ppm), and the 3°C cooling (-33 ppm) leave the atmosphere CO₂ content very close to its pre-industrial level. Forced to put aside these more obvious explanations, geochemists turned to more subtle ones which have to do with what is referred to as the ocean's biological pump. Marine plants remove CO₂ from the ocean's surface waters and convert it to organic tissue. Part of this material sinks into the deep sea before it is eaten (i.e., is oxidized back to CO₂). As organisms capable of converting CO₂ to organic matter require light, they live only in the upper 100 meters of the sea. Thus the photosynthesis-respiration cycle acts as a pump which drives CO₂ from the sea's surface to its interior. Hence, changes in the power of this pump could be responsible for the glacial to interglacial atmospheric CO₂ change.

Two limits exist on the changes in atmospheric CO₂ attributable to the strength of this biological pump (see figure 32). The upper limit is the CO₂ content the atmosphere would achieve were the pump to shut down altogether. We might refer to this as a Dr. Strangelove ocean where life had been snuffed out. In this case, the CO₂ content of the atmosphere would rise to half again its present value. The lower limit on the CO₂ content, the atmosphere would be that if the biological pump were to operate at full strength. The limiting chemical constituents for plants in today's ocean are phosphorus and nitrate. Without them, plants can't grow. So if all the NO₃ and PO₄ made available to plants by water upwelling to the surface were utilized, maximum pumping power would be achieved. Much of today's surface ocean is already depleted in NO₃ and PO₄ (see figure 33). In these places, the biological pump is functioning at maximum capacity.

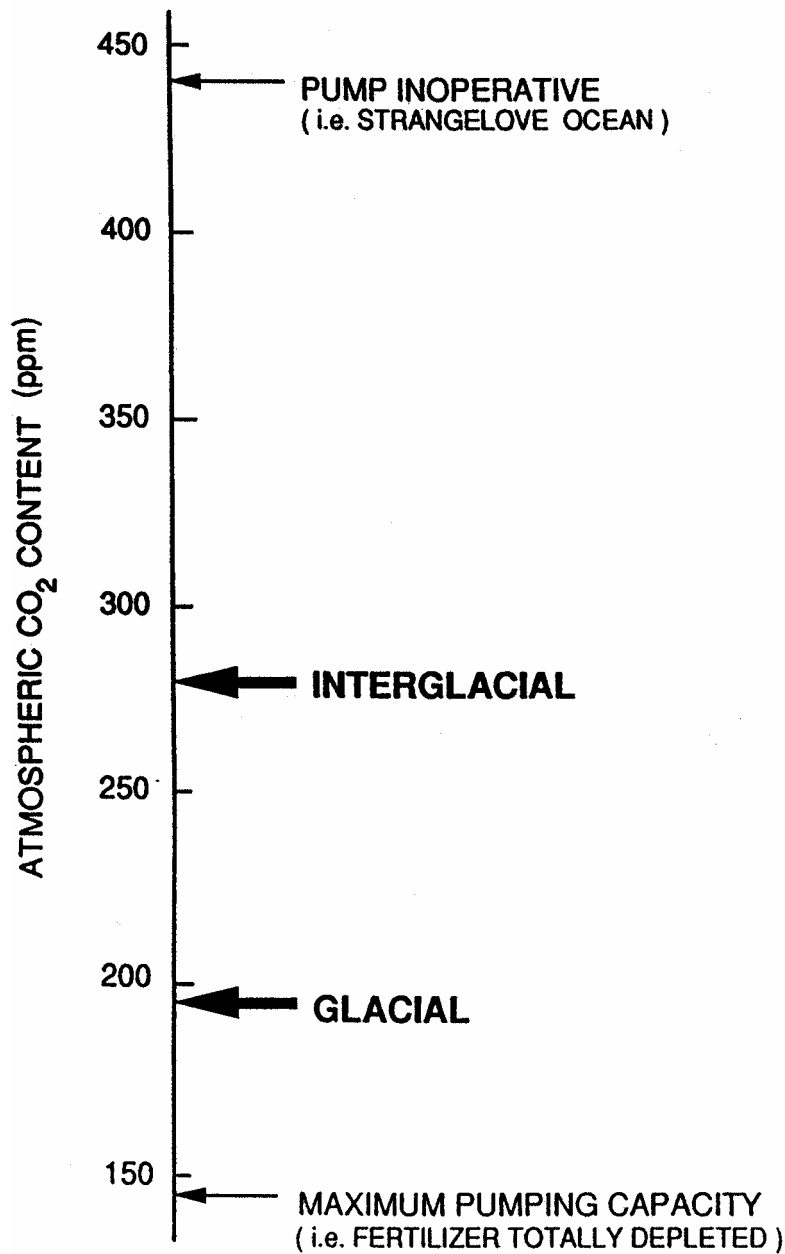


Figure 32. Range of atmospheric CO₂ content of the ocean permitted by changing the strength of the biological pump. The glacial value, as reconstructed from measurements on ice cores falls closer to the limit of maximum pumping power.

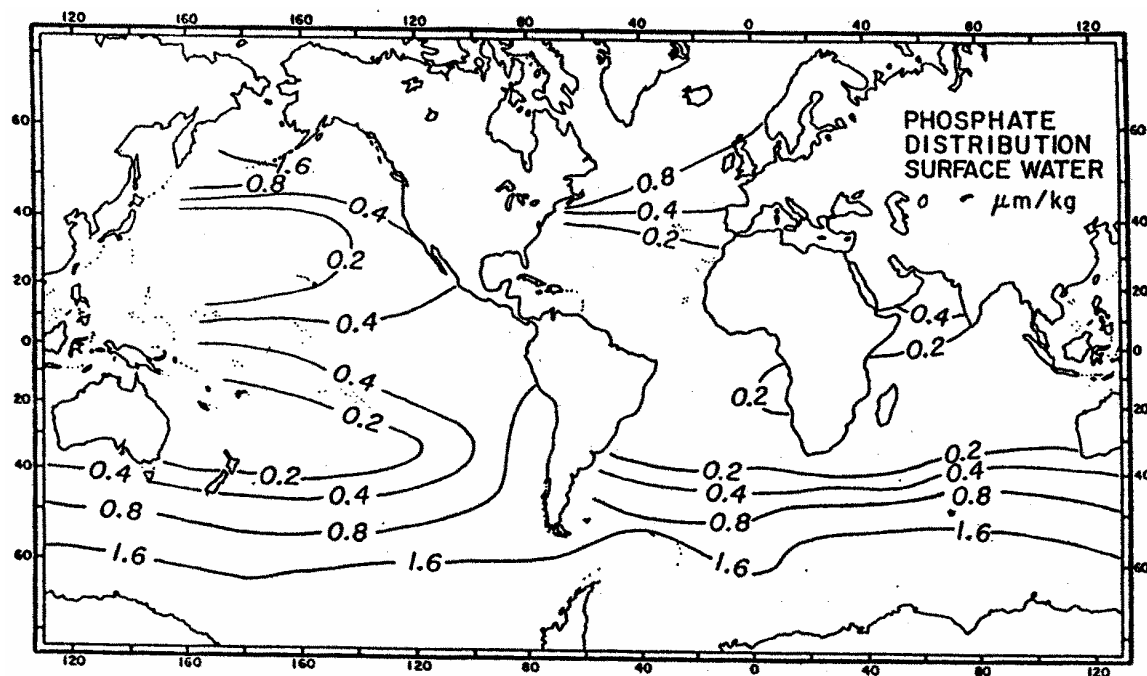


Figure 33. Contours of the phosphate content of surface water. For the northern Atlantic the values are for the winter period. In other high latitude regions, they represent summer values (and hence, minimum values for the winter period).

However, at high latitudes where the light is weak, the water cold, and the upwelling strong, much of the fertilizer goes unused (see figure 33). If plants were to utilize all the available high latitude fertilizer, the CO₂ pressure in the atmosphere could fall to about one half its present day value. Thus one might say that today the ocean's biological pump is working at roughly 40 percent its capacity. Thus, if for some reason during glacial time, the pumping power were increased to 85 percent of its capacity, then the low glacial atmospheric CO₂ content could be explained.

In recent years, the important biological role of the element iron has been demonstrated. Purposeful additions of iron to waters in the eastern equatorial Pacific and Southern Ocean where currently substantial amounts of NO₃ and PO₄ go unused prove that, given iron, the organisms can increase their utilization of these key nutrients. As already discussed, far more dust than now reached the ocean during glacial time. The extra iron provided by this dust likely played an important role in strengthening the ocean's biological pump.

Another mechanism has to do with the cycle of CaCO₃ in the sea. Organisms living in surface water produce shells made of calcite and aragonite. Much of this CaCO₃ dissolves after falling to the deep sea. Only about twenty percent survives and is stored in the sediment. As the production of CaCO₃ in surface waters, mole for mole, is accompanied by a generation of CO₂, in a sense the CaCO₃ 'pump' opposes the organic matter 'pump.' The latter drives down the atmosphere's pCO₂ and the former drives it up.

Methane

A record of past concentrations of a second greenhouse gas, methane, is also available from ice cores. Air from glacial age ice turns out to have only half the methane content of air from Holocene ice (see table 4). Methane differs from CO₂ in an important way; while CO₂ is chemically stable, methane molecules are not. Methane reacts with O₂ (through catalytic intermediaries) to form CO₂ and H₂O. One such

Table 4. Greenhouse gas contents reconstructed from ice cores compared with the anthropogenically-altered values for 2001.

	GLACIAL	INTERGLACIAL	TODAY
CO ₂ (ppm)	195	280	370
CH ₄ (ppm)	0.4	0.8	1.8

pathway to destruction involves the web of chemical reactions related to the ozone cycle. Another involves diffusion into the pore space of oxygenated soils where CH₄ is consumed by bacteria. Currently, the atmospheric lifetime of a methane molecule is about one decade. Thus an amount of methane equal to that in the atmosphere must be produced each decade in order to maintain the atmosphere's inventory. The major source for this methane is bacterial degradation of organic matter in anaerobic environments. Key among these environments are water-logged swamps and rice paddies, and the stomachs of ruminant animals (i.e., cows, buffalo, sheep...). In today's anthropogenically modified environment, rice paddies and domestic cattle each account for about one quarter of the production of CH₄. A third quarter comes from swamps and the remaining quarter is from forest fires and leaky transmission pipes. The extra anthropogenic inputs have caused the atmosphere's methane content to more than double since the year 1800.

Based on our knowledge of the present day methane cycle, we surmise that the lower methane content of the glacial atmosphere was the result of reduced acreage of swamps. Many of the currently swampy areas were either buried beneath ice caps or frozen during glacial time. Further, the drop in sea level allowed coastal swamps to drain. Thus unlike CO₂ which records changes in ocean operation, changes in CH₄ are the result of things that happened to the continents.

Isotopic Composition of Atmospheric Gases

The isotopic composition of the gases trapped in ice offers additional information about glacial climate. Of great importance in this regard is the carbon isotope composition of CO₂. Measurements by the late Uli Siegenthaler and his coworkers in Bern on gas extracted from polar ice cores suggest that glacial age CO₂ was 0.3±0.2‰ more depleted in ¹³C than Holocene CO₂. Earlier in this section, we mentioned that based on measurements on benthic foraminifera, the ¹³C/¹²C ratio in the ocean carbon appears to have been 0.35‰ more negative during glacial time than now. Thus the shift in the carbon isotope composition of atmospheric CO₂ is of the same magnitude as that

for deep ocean ΣCO_2 . This agreement may, however, be fortuitous for two other factors come into play. One is a shift in the surface to deep ocean carbon isotope ratio difference caused by change in strength of the biologic pump. The other is a shift in the carbon isotope composition difference between surface ocean (ΣCO_2) and atmosphere (CO_2) caused by the change in surface ocean temperature.

Let us first consider the atmosphere-surface ocean difference. For each $^{\circ}\text{C}$ the ocean cools, the fractionation between surface ocean carbon and atmospheric carbon increases by 0.1% . The sense of the fractionation is to deplete the ^{13}C in atmospheric CO_2 as the ocean cools. As the ocean contains 60 times more carbon than the atmosphere, $59/60$ ths of the isotopic shift will appear in the atmosphere and only $1/60$ th in the ocean. If the estimate of about 3°C for the cooling of the surface ocean during late glacial time is correct, then for this reason alone, the atmosphere CO_2 should have been 0.3% more deficient in ^{13}C during glacial time.

The surface ocean to deep ocean carbon isotope ratio difference reflects the strength of the biological pump. The reason is that the carbon extracted from the sea to form plant tissue is depleted in the heavy isotope by about 20% . In today's ocean, the heavy carbon left behind in surface water as the result of photosynthetic fractionation enriches surface water ΣCO_2 by about 2% in ^{13}C with respect to deep water ΣCO_2 . If the ocean's biological pump were stronger during glacial time, then even more ^{13}C should have been left behind in surface water than today. This would bring about an increase in the surface ocean-deep ocean carbon isotope ratio difference. Since the deep sea is a far larger reservoir than the surface sea, this change would cause the $^{13}\text{C}/^{12}\text{C}$ ratio in surface water ocean carbon to rise. An estimate of the surface ocean to deep ocean carbon isotope difference has been made from measurements on planktonic and on benthic forams. These results suggest that the difference was about 0.35% larger during glacial than during interglacial time. Thus for the surface ocean, the carbon isotope shift resulting from the change in terrestrial organic storage appears to have been compensated

by the change in the power of the biologic pump. If this proves to be correct, then the change in the ^{13}C to ^{12}C ratio in atmospheric CO_2 provides a direct measure of the change between glacial and interglacial time of the temperature of surface ocean water. As summarized in figure 34, a lowering in surface ocean temperature during glacial time of $3\pm2^\circ\text{C}$ is suggested by the carbon isotope measurements on CO_2 extracted from polar ice. While yielding a result consistent with proxies for tropical ocean temperature during glacial time, the error in the ^{13}C -based estimate is too large to permit its use as a rigorous tropical paleothermometer.

The only other isotopic measurements currently available on gases from ice are those on N_2 and O_2 . Although biochemical fractionation of nitrogen isotopes akin to that for carbon isotopes exist, the amount of N_2 in the atmosphere is so much greater than the amount of NO_3^- dissolved in the sea or the amount of NH_3 contained in the terrestrial biosphere that these fractionations do not leave a measurable imprint on the ^{15}N to ^{14}N ratio in atmospheric N_2 . Yet the ^{15}N to ^{14}N in air of all ages extracted from ice averages 1‰ greater than that for atmospheric N_2 . This enrichment is the result of a gravitational separation of heavier gases from lighter gases in the 70 or so meter-thick firn. Because the pores in the partially lithified ice are narrow and tortuous, significant convective transport of air does not take place. Hence communication with the surface is by molecular diffusion alone. Under these circumstances, the influence of gravity causes N_2 at the base of the firn to become enriched in molecules containing a heavy nitrogen atom (i.e., $^{15}\text{N}^{14}\text{N}$ molecules). Although a curiosity rather than a climate indicator, the enrichment of heavy nitrogen molecules in the ice provides a means to correct for gravitational enrichment the isotopic ratios measured in other gases which do carry climatic information. For example, the Bern group made this correction on the carbon isotope measurements on ice core CO_2 .

Even after correction for gravitational enrichment, clear differences are seen between the isotopic composition of O_2 extracted from glacial age ice compared with that

← EXPECTATION → OBS.

WHOLE OCEAN	SURF SEA	SURF SEA
ΣCO_2	ΣCO_2	TEMP

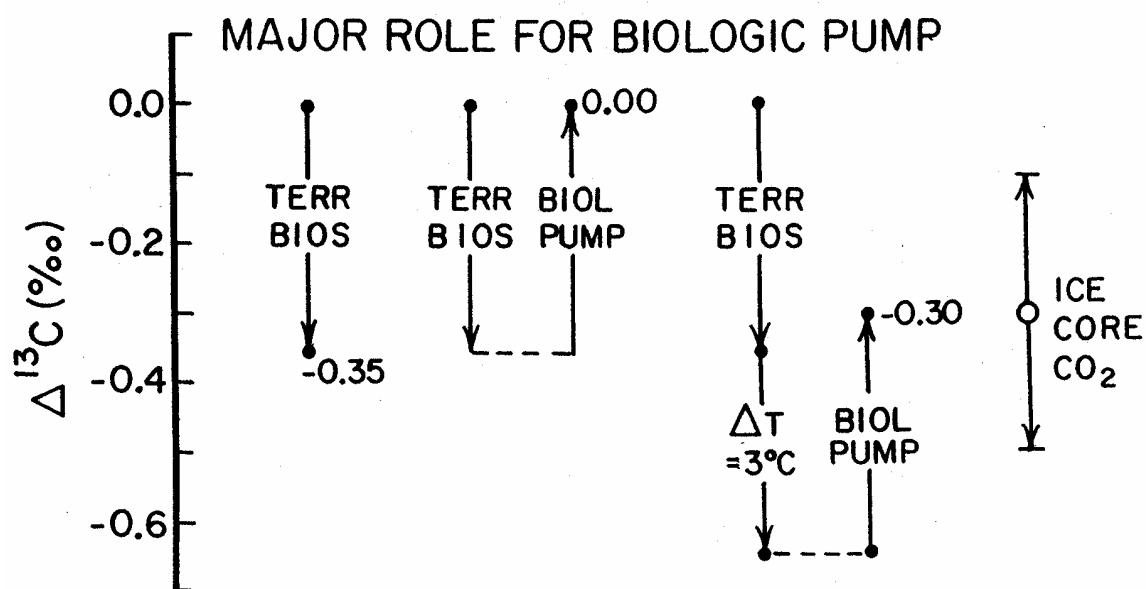


Figure 34. Predicted change in the $\delta^{13}\text{C}$ for atmospheric CO₂ during glacial time assuming that a strengthening of the biological pump was responsible for the lower atmospheric CO₂ content. The change estimated from measurements on CO₂ extracted from ice cores (Leuenberger et al., 1992) is shown at the right. The ice core results support the biological pump mechanism.

for O₂ extracted from interglacial ice. Sowers and Bender show that the O₂ in peak glacial ice is about 1.3% richer in ¹⁸O than the O₂ in interglacial ice. To understand the cause of this shift, we must learn a bit about what causes the ¹⁸O to ¹⁶O ratio in atmospheric O₂ to be 23.6‰ higher than that in sea water. This enrichment occurs because isotopically light O₂ (i.e., ¹⁶O¹⁶O) is consumed in preference to isotopically heavy O₂ (i.e., ¹⁸O¹⁶O) during the oxidation of organic matter (i.e., during respiration). By contrast, no fractionation occurs when O₂ is manufactured during photosynthesis. This situation is the reverse of that for carbon; ¹³C is depleted during photosynthesis but is unchanged during respiration. To offset the fractionation during respiration, a compensating excess of ¹⁸O has built up in the atmosphere's O₂. In the presence of this isotopic offset, the isotopic composition of the O₂ removed from the atmosphere as the result of respiration is identical to that of the O₂ added during photosynthesis.

The oxygen atoms in the O₂ produced during photosynthesis come from the plant's water. For marine plants the source is surface ocean water. For terrestrial plants, the source is rain water. Today roughly half the world's photosynthesis takes place in the ocean and roughly half on land. As we have seen, during glacial time sea water had about 1.1‰ more ¹⁸O than it does now; so also must the average rain and snow which fell onto the continents. Hence the isotopic composition of O₂ produced by photosynthesis should have been on the average 1.1‰ more ¹⁸O rich during glacial time. This is close to (but not exactly) the glacial to interglacial difference found by Sowers and Bender based on their isotopic measurements on O₂ from the Vostok Antarctica ice.

The importance of this finding is that it permits the correlation of the ice core record from Antarctica with that from Greenland and also with the ¹⁸O record for benthic foraminifera. This is possible since the ¹⁸O offset in atmospheric O₂ lags only about 1000 years behind the changes in $\delta^{18}\text{O}$ for sea water. The lag represents the time required for plants to produce an amount of O₂ equal to that contained in the atmosphere.

A complication in this approach has to do with offset in the record kept by gases in ice from the record kept by the ice itself. The reason is that the air bubbles do not close off until the snow has been buried about 70 meters below the surface. On the Greenland plateau where the accumulation rates average 25cm/yr., this means that the gas bubbles currently being incorporated into the ice are about 280 years older than the ice itself. The offset is much larger for cores from the Antarctic plateau where the accumulation rates average only a few centimeters per year. Here the gas bubbles are several thousand years younger than the ice in which they are contained. So while the oxygen isotope measurements on O₂ provide a direct means of correlating the CO₂ and CH₄, records kept in ice with the marine oxygen isotope record a further correction has to be made before the correlation can be extended to the ¹⁸O/¹⁶O and the dust signals recorded in the ice itself.

Of course, as the accumulation rate of snow varies with climate and so also does the thickness of the firn, the magnitude of the time offset between the age of the gas bubbles and that of the ice in which they reside was not the same during glacial time as today. Jeff Severinghaus came upon an extremely clever application of nitrogen isotope ratios to directly determine the magnitude of the time offset at specific times in the past. He took advantage of the large and abrupt warnings which terminated each of the millennium duration temperature cycles recorded in Greenland ice (see below). He reasoned that an abrupt change in air temperature would have set up a thermal gradient in the firn and that because frozen snow is an excellent thermal insulator that a century or more would elapse before the warmth penetrated to the base of the firn. During the interim, a process called thermal diffusion would come into play. This process leads to a separation of heavy and light molecules with the heavy ones being preferentially concentrated at the cold end of the temperature gradient. Hence, the sudden warming of the air temperature should further enrich the heavy nitrogen molecule (i.e., ¹⁵N¹⁴N) in the air at the base of the firn. Lo and behold, Severinghaus' prediction turned out to be

correct for he was able to document the predicted ^{15}N shift (see figure 35). As the Greenland ice cores have clearly discernible annual layers, he was able to count the years separating the shift in ^{18}O which marked the warming in the ice and the shift in ^{15}N which marked the warming in the gas bubbles. As a bonus, Severinghaus showed that when combined with ^{40}Ar to ^{36}Ar measurements the magnitude of the ^{15}N shift could be used to determine the magnitude of the warming.

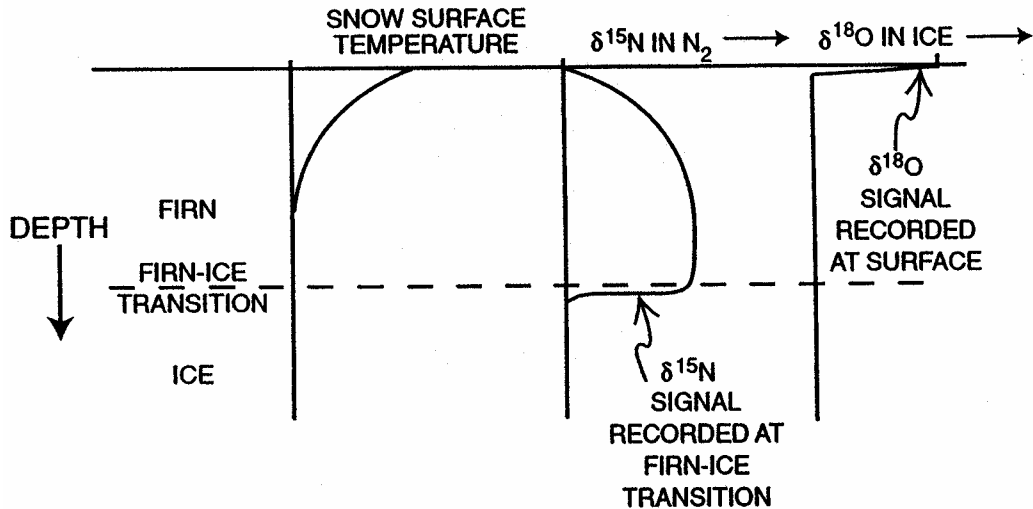
OCEANIC CHEMISTRY

The ocean influences climate in two major ways. One has to do with the heat carried by ocean currents from the warm to the cold regions of the planet. So important is this transport that changes in ocean circulation have the potential to produce important modifications in the climate at high latitudes. We have already seen that the amount of CO_2 in the atmosphere is influenced by the strength of the ocean's biological pumps. Fortunately, information is contained in ocean sediments which tells us about the pattern of the heat-bearing currents and about the strength of the biological pumps. We have already seen that the carbon isotope ratio difference between planktonic and benthic foraminifera provides a measure of the amount of CO_2 extracted from surface waters by plants. Intercean differences of carbon isotope ratios (and also the concentrations of Cd, Ba and Zn in benthic foraminifera) tell us something about the pathways followed by heat transporting currents. Radiocarbon measurements on coexisting planktonic and benthic foraminifera from sediments and also on ^{230}Th dated benthic corals place constraints on how rapidly the deep ocean was ventilated during glacial time. Measurements of the isotope ratios of boron contained in foraminifera shells offer a means of reconstructing pH of the glacial ocean. Finally, changes in the extent of dissolution of the CaCO_3 entities allow past deep sea carbonate ion concentrations to be reconstructed.

Trace Metals

One set of indicators of the pattern of large scale ocean circulation is the concentrations of the trace metals, cadmium, barium and zinc in the shells of benthic

TEN YEARS AFTER ABRUPT WARMING:



THOUSANDS OF YEARS LATER, IN AN ICE CORE:

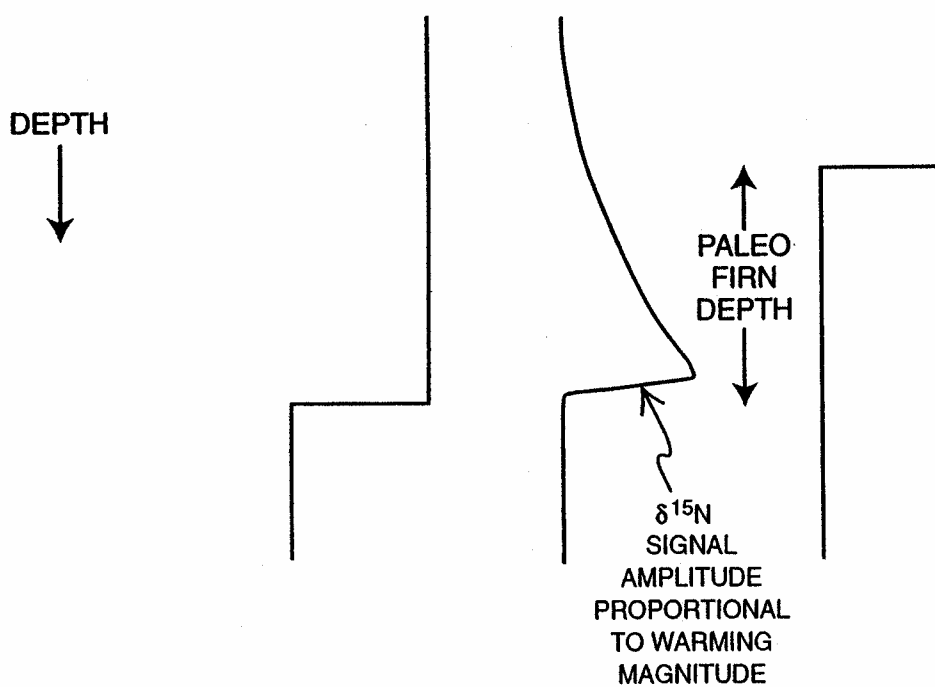


Figure 35. The imprint of an abrupt rise in air temperature on the ^{18}O to ^{16}O ratio in the ice and ^{15}N to ^{14}N ratio in the N_2 trapped in bubbles. The former is imprinted at the top of the firn and the latter is imprinted at the base of the firn. The enrichment of ^{15}N is the result of the thermal gradient in the firn. This ^{15}N enrichment gradually diminishes as the firn temperature equilibrates with that in the atmosphere but its imprint in the bubbles remains. The offset in depth between the ^{18}O change and the ^{15}N change records the paleothickness of the firn. By counting the number of annual layers in this interval, it is possible to determine the time offset between the gas record and ice record.

foraminifera. To understand this, it is necessary to be reminded that those constituents of sea salt which participate in marine biological cycles are depleted in surface water and enriched in deep water (see figure 36). These vertical gradients are maintained by the fall and subsequent remineralization of particulate organic matter created by surface dwelling plankton. The interaction between downward transport of particles and lateral transport in deep currents produces differences in the concentrations of these substances between the Atlantic and Pacific Oceans (see figure 37). To understand this, it is necessary to be aware that the ocean has preferred states of circulation involving conveyor-like currents which run from one end of the ocean to the other. One limb of the conveyor moves through the upper ocean and the other through the deep ocean. Today, the lower limbs of the Indian and Pacific conveyors run northward from the Antarctic and the upper limbs back to the south. By contrast, the Atlantic's conveyor flows in the opposite sense; the upper limb flows to the north and the lower limb to the south. The southern ends of the three conveyors are linked by the rapidly flowing circum-Antarctic current.

When coupled with the biological cycle, this global flow pattern tends to deplete the deep Atlantic in biologically utilized constituents. For example, in today's ocean, NO_3 and PO_4 , have twice the concentration in deep tropical Pacific and Indian Oceans as in deep tropical Atlantic (see figure 37). Were, instead, all three oceans to have conveyors running in the same sense (i.e., south to north in the deep ocean and north to south in the upper ocean), then one would expect the nitrate and phosphate concentrations to be more uniformly spread among the three oceans. Thus if we were able to reconstruct the distribution of biologically utilized constituents of the ocean during glacial time, we could say something about the sense of the ocean's three conveyor systems at that time.

Ed Boyle, a geochemist at MIT, came up with an exciting means to make such a reconstruction. He was inspired by the observation that in today's ocean the distribution of the metal cadmium parallels that of phosphate (see figure 38). As is the case for PO_4 ,

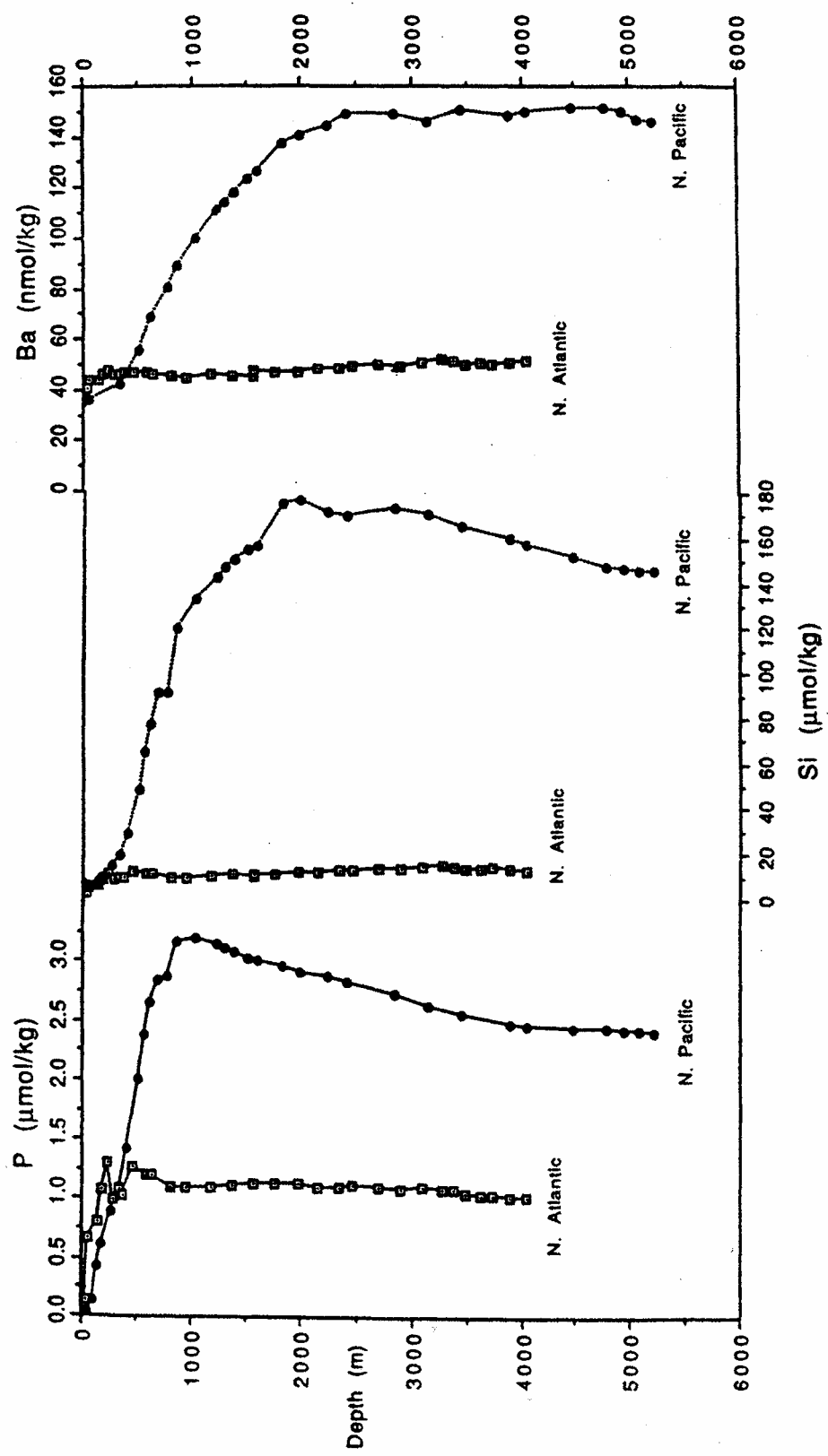


Figure 36. Phosphate, silica and barium profiles from GEOSECS stations in the North Atlantic (St. 3: $54^{\circ}5'N$, $42^{\circ}57'W$) and North Pacific (St. 204: $31^{\circ}22'N$, $150^{\circ}2'W$). Data from Bainbridge et al., 1981, Broecker et al., 1982 and Ostlund et al., 1987.

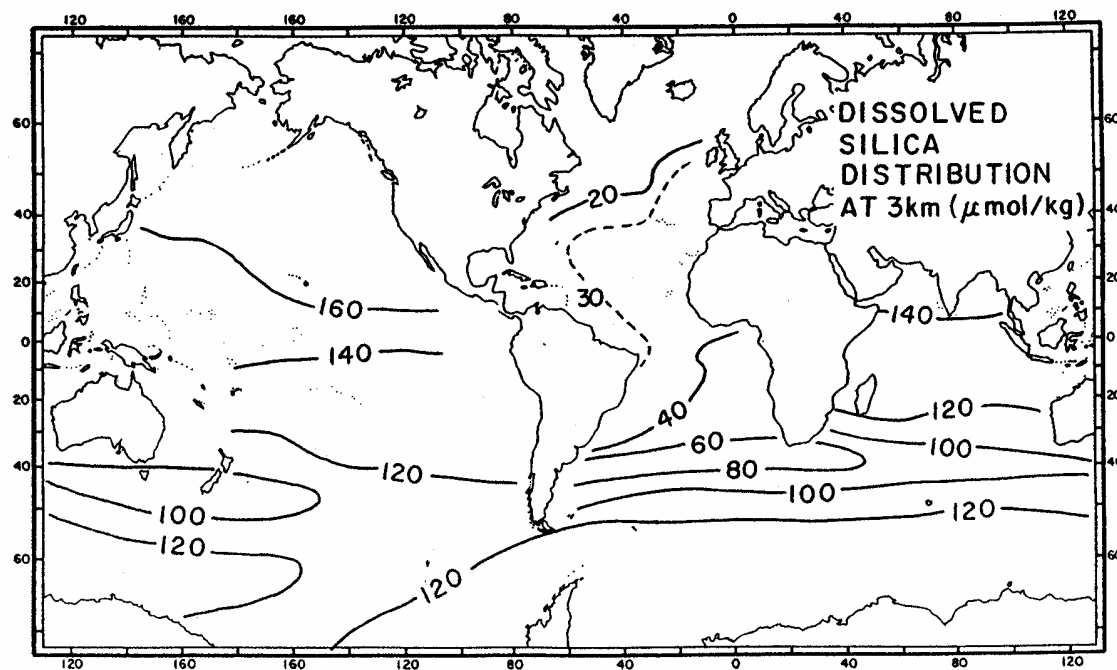
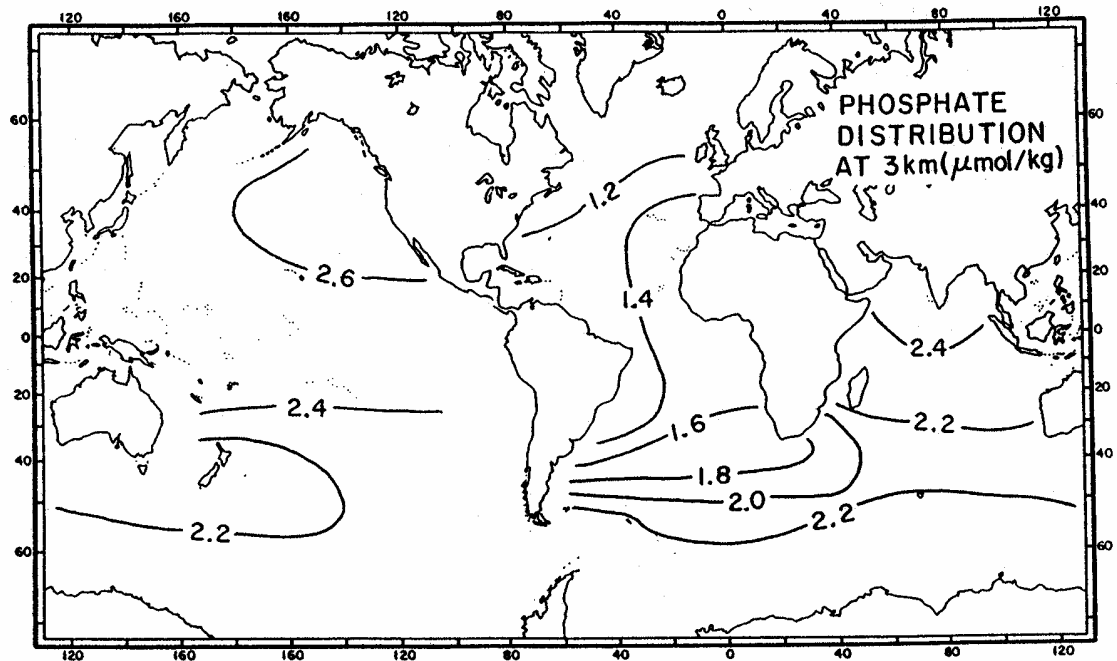


Figure 37. Maps showing the distribution of PO_4 and SiO_2 in the deep sea (at a depth of 3 km).

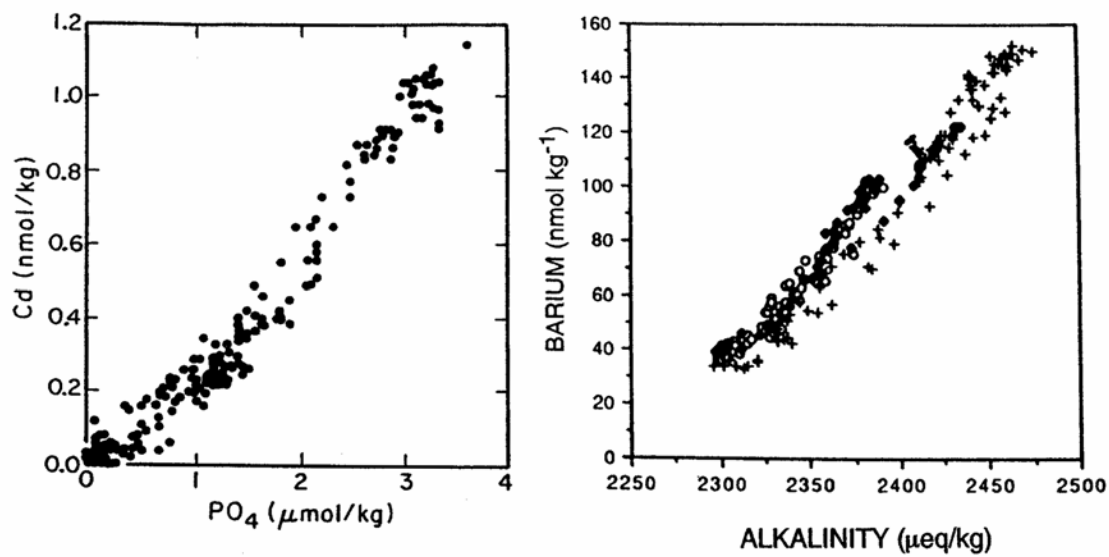


Figure 38. Cadmium versus phosphate concentration in sea water samples from throughout the world ocean (upper panel). Similar plot for barium versus salinity-normalized alkalinity.

surface waters in the warm ocean have the lowest cadmium content and deep waters in the northern Pacific the highest, and the concentration in deep Atlantic waters falls midway between these extremes. Boyle realized that cadmium and calcium were sufficiently similar chemically that cadmium could substitute for calcium in the calcite produced by benthic foraminifera. Both elements exist as doubly charged cations when dissolved in water. They have similar ionic radii. Because of this, the cadmium to calcium ratio in foraminifera shells should be proportional to the cadmium to calcium ratio in the sea water in which the shell formed. Since the Ca content of sea salt is nearly constant from place to place and since calcium has a million year long residence time in the sea, any changes in the cadmium to calcium ratio between glacial and interglacial time must be the result of changes in cadmium content of the sea water in which the shells formed. Further, since cadmium itself has a residence time in the sea of several tens of thousands of years, its inventory in the ocean should not have changed significantly over the 10,000 year long interval separating times of peak glaciation from times of peak interglaciation. Rather, glacial to interglacial changes in the cadmium content of foraminifera shells are more likely the result of the redistribution of cadmium within the sea.

Boyle developed methods to rid benthic foraminifera shells recovered from deep sea sediments both of clay minerals which often fill their chambers and of the manganese-iron oxides which often coat their chambers. The idea was to make sure that the cadmium he eventually measured was that contained within the shell itself. He was pleased to find that indeed benthic foraminifera shells from recent sediments displayed cadmium to calcium ratios concordant with those in the deep water in which they grew. In other words, when the Ca to Cd ratio in the shells was plotted against the ratios for the corresponding water samples, the points scattered about a straight line with a slope of about 2.8 (see figure 39). That the slope differs from unity is not surprising. Although chemically similar, the two ions are not identical. Hence, like isotopes, these two metals

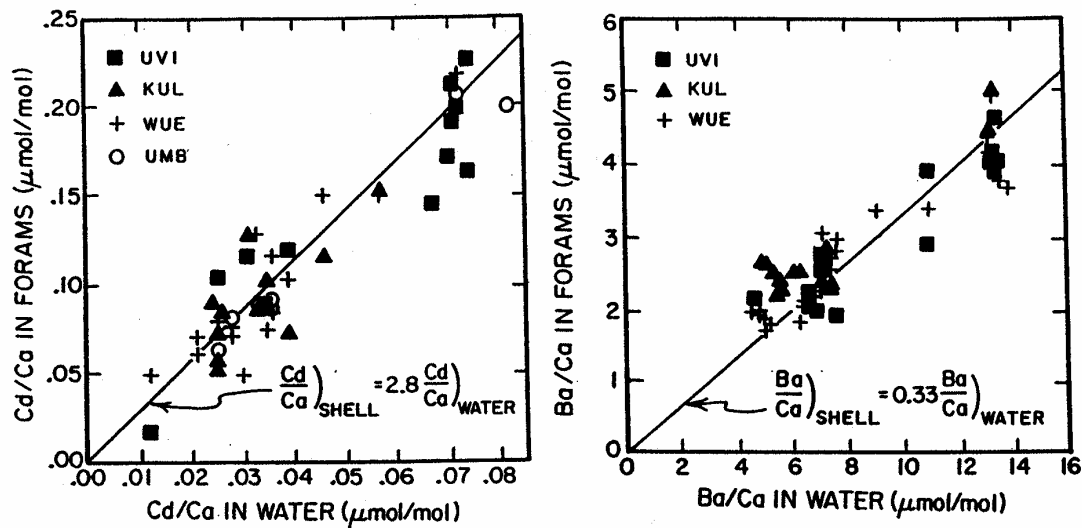


Figure 39. Cadmium content (left) of four different species of benthic foraminifera from the tops of deep sea sediment cores plotted against the cadmium to calcium ratio in overlying sea water. Similar plot for barium (right).

are separated from one another during chemical reactions. Since these element to element chemical differences are much larger than isotope to isotope chemical differences, separation factors for elements are much larger than for isotopes. Based on these results, Boyle initially concluded that all he had to do to estimate the cadmium content at a given place and time in the ocean was to analyze shells which grew there and then divide the measured Cd/Ca ratio by 2.8. Since the calcium content was nearly the same then as now, he could convert this ratio into a cadmium concentration.

Although more recent studies have shown that the distribution coefficient depends on temperature and on pressure making the situation a bit more complicated, the utility of the cadmium proxy has not been diminished. The glacial to interglacial changes in deep sea temperature are too small to be significant and, of course for a given deep sea core, the sea level-generated glacial to interglacial pressure change is also negligible.

Once Boyle had demonstrated that his method worked, he set out to map the distribution of cadmium in the glacial ocean as a function of both geographical location and water depth. He uncovered some fascinating differences. First, the contrast between the deep Pacific and deep Atlantic was smaller during glacial time than today (see figures 40 and 41). Second, the vertical gradients in the deep sea were steeper during glacial time. This is dramatically shown by a set of cores from the North Atlantic (see figure 42). During Holocene time, benthic forams from cores covering a range of water depth have nearly the same cadmium content (consistent with depth profiles in today's deep water). By contrast, in the glacial Atlantic, Boyle's results reveal what appeared to be two distinct deep water masses, an upper one with lower cadmium concentrations and a deep lower one with higher cadmium contents. The observation that the Atlantic-Pacific cadmium difference was substantially reduced is consistent with a weakening of the Atlantic's conveyor during glacial time. The observation that the deep glacial Atlantic was stratified was unforeseen.

In order to obtain a confirmation of the conclusions drawn from his cadmium

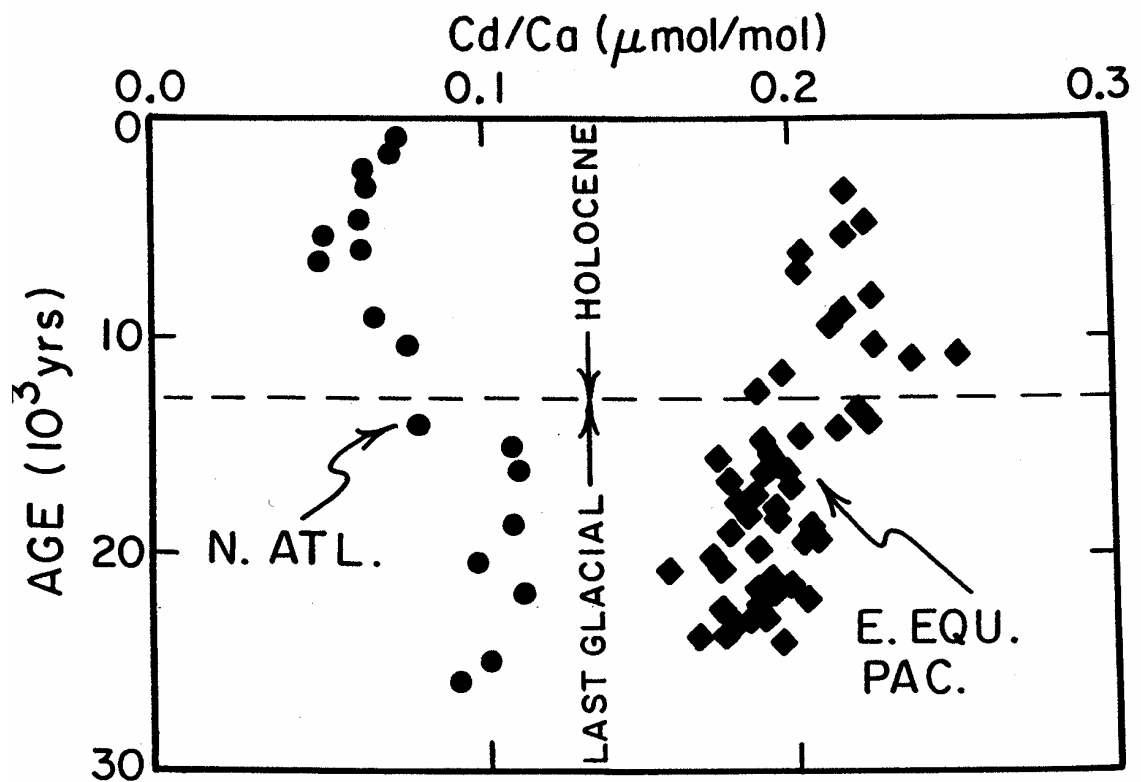


Figure 40. Comparison of the time histories of the cadmium content in an Atlantic core with that in a Pacific core. As can be seen interocean, the contrast was smaller during glacial time than during interglacial time.

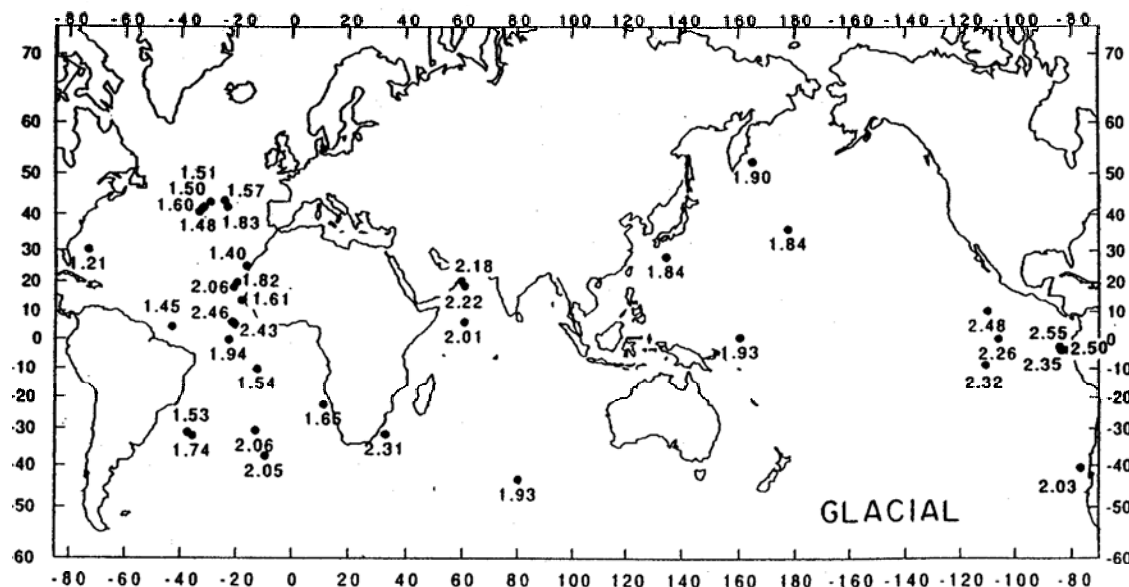
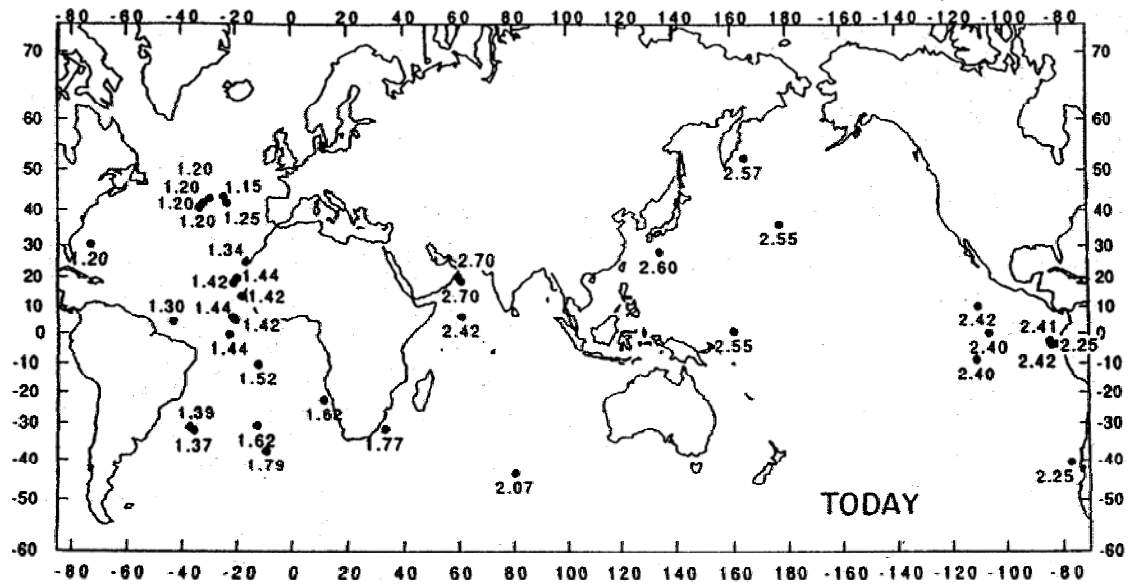


Figure 41. Comparison of glacial and modern phosphorus ($\mu\text{mol/kg}$) distributions at mid-depths (2400-3800 m). The modern distribution is based on GEOSECS data extrapolated to core locations; the glacial distribution is based on benthic foraminiferal Cd/Ca data from sediment cores, converted to equivalent levels of phosphorus based on the modern global Cd-P correlation.

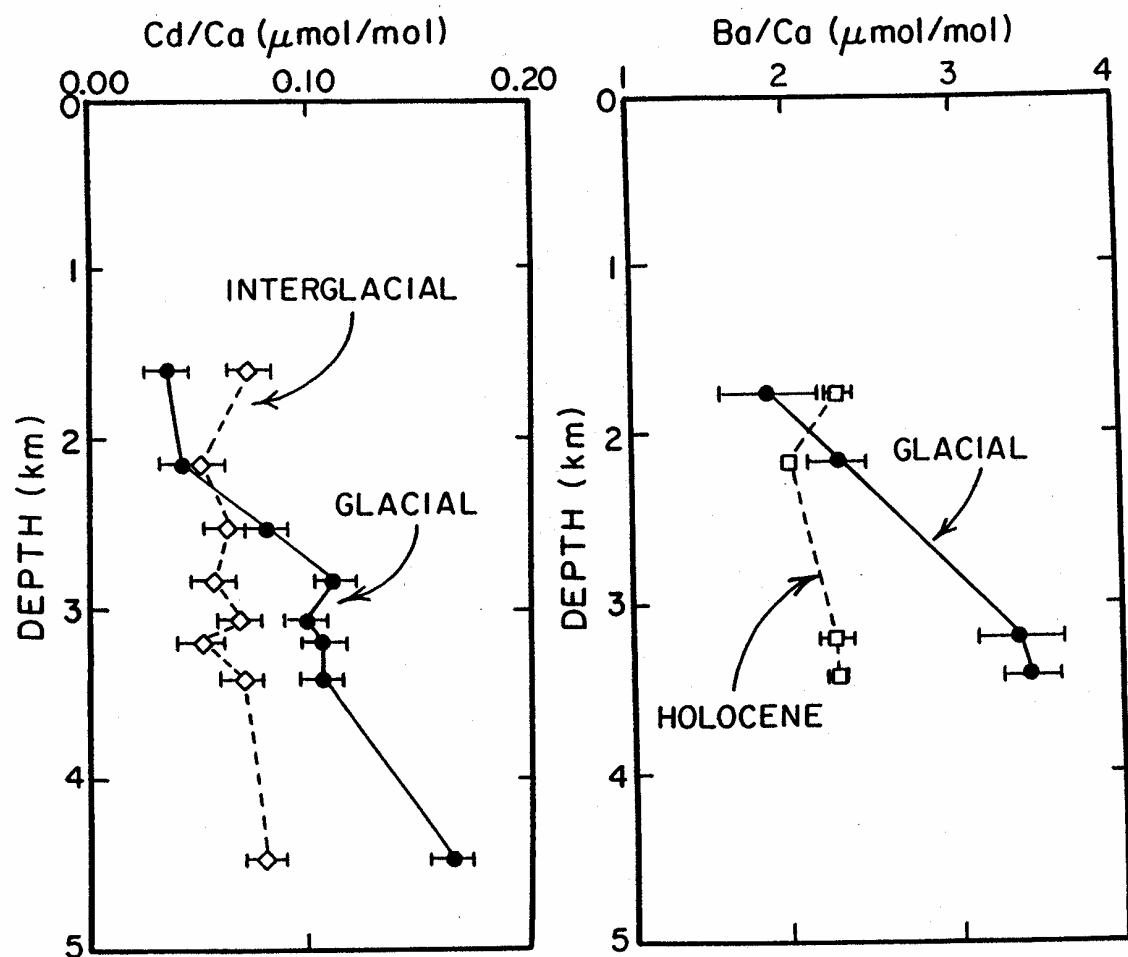


Figure 42. Comparison of interglacial and glacial trends with water depth in the North Atlantic of the cadmium and barium contents of benthic foraminifera. The interglacial trend agrees with that obtained from measurements of cadmium and barium (also of NO_4 and PO_4) on water samples.

measurements, working with David Lea, Boyle turned his attention to the metal barium whose distribution in the ocean is also influenced by biological cycling. Barium sulfate crystals form in the tissue of some marine microorganisms. These crystals fall to the sea floor and largely dissolve returning the barium to solution. This cycle produces a pattern barium distribution in the sea akin to, but not identical to, that of cadmium. Surface waters are the most depleted, deep northern Pacific waters the most enriched, with deep Atlantic waters falling in between. The major difference is that the concentration of barium in warm surface water does not drop to near zero values. Another difference is that the extent of enrichment of barium in the deep Pacific relative to the deep Atlantic is greater than for cadmium. While the distribution of cadmium in today's ocean follows that of NO_3 and PO_4 , the distribution of barium more nearly follows that of salinity-normalized alkalinity. The reason for this close tie is not known. The best explanation is that the ratio of barite to organic matter falling to the deep sea floor is fairly uniform across the ocean. Dissolution of barite supplies barium. Bacterial destruction of the organic matter produces respiration CO_2 which is neutralized by CaCO_3 dissolution. The dissolution of CaCO_3 adds to the ocean's alkalinity. Like cadmium, barium substitutes for calcium in the CaCO_3 shells manufactured by foraminifera. In this case, Lea found that the line relating the Ba to Ca ratio in foraminifera shells to the barium to calcium ratio in sea water has a slope of about 0.33. So while cadmium is enriched relative to calcium by threefold in the calcite manufactured by foraminifera, barium is depleted by threefold.

Barium measurements on benthic foraminifera shells from glacial time lead to much the same conclusions as those based on cadmium. The Pacific-Atlantic deepwater difference was reduced and the deep Atlantic was stratified into an upper and lower deep water mass. (see figure 42).

While a graduate student in the MIT-WHOI program, Tom Marchitto demonstrated that the element zinc serves as a stand-in for silica in today's ocean and

also that its concentration in benthic foraminifera could be used as a paleo-silica proxy. However, he introduced yet another complication regarding the use of trace metal proxies by suggesting that the distribution coefficients of both cadmium and zinc depended on carbonate ion concentration.

Carbon Isotopes

The distribution of carbon isotope ratios in today's ocean is the near mirror image of that for the nutrients NO_3 and PO_4 (and hence, also that for cadmium). The reason is that the organic tissue manufactured by ocean plants is depleted by about 20‰ in carbon's heavy isotope. Hence, the photosynthesis-respiration cycle leads to an enrichment in ^{13}C in those waters where photosynthesis occurs, and a depletion in those waters in which respiration occurs (see figures 43 and 44). This isotopic separation produces a range in carbon isotope composition of about 3‰, with warm surface water ΣCO_2 having the highest ^{13}C contents and deep Pacific water ΣCO_2 having the lowest. As would be expected, the lower the PO_4 content of the sea water, the higher the ^{13}C to ^{12}C ratio and vice versa. In fact, when $\delta^{13}\text{C}$ is plotted against PO_4 , the values fall close to a straight line with a slope close to -1‰ $\delta^{13}\text{C}$ change per $\mu\text{m}/\text{kg}$ PO_4 change (see figure 44). This raises the possibility that the carbon isotope ratios in planktonic and benthic shells could be used in the same way as are the cadmium and barium concentrations. Working in favor of this application is the fact that the fractionation of carbon isotopes during the formation of CaCO_3 is quite small. Because of this, water temperature has almost no influence on the carbon isotope composition of marine calcite. Rather, glacial to interglacial changes in the $^{13}\text{C}/^{12}\text{C}$ ratio in foraminifera shells should reflect only changes in the carbon isotope ratio in water in which they grew.

Unfortunately, this ideal situation is marred by small amounts of ^{13}C deficient respiration CO_2 which become incorporated into the shells of both planktonic and benthic foraminifera. As this carbon is depleted in ^{13}C , its incorporation complicates the interpretation of carbon isotope measurements on foraminifera shells. For benthic

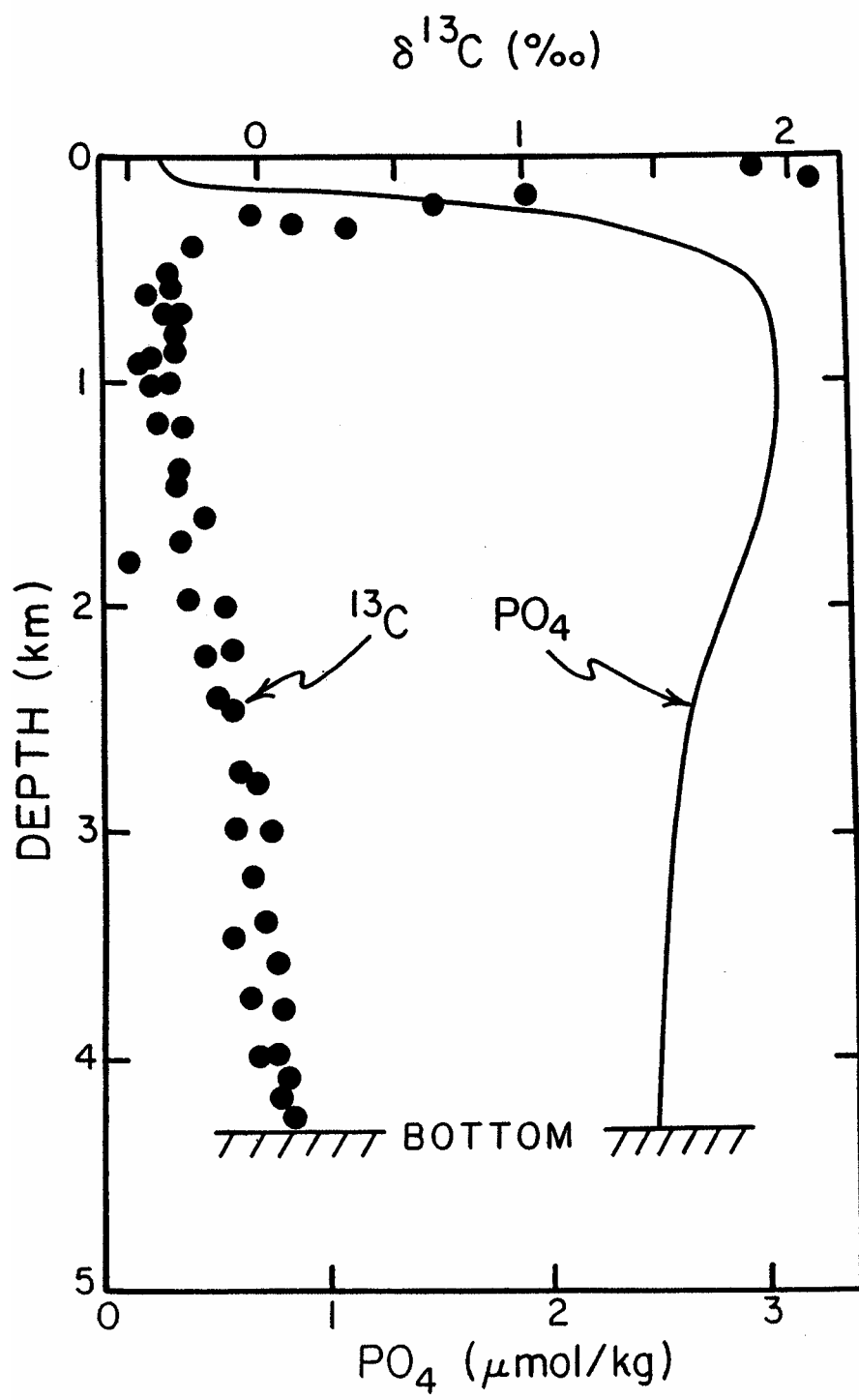


Figure 43. Plots of $\delta^{13}\text{C}$ and PO₄ versus depth at GEOSECS station 346 (28°N, 121°W) in the northwestern Pacific Ocean. The carbon isotope analyses were made by Craig and Kroopnick at the Scripps Institution of Oceanography and the PO₄ analyses as part of the GEOSECS program.

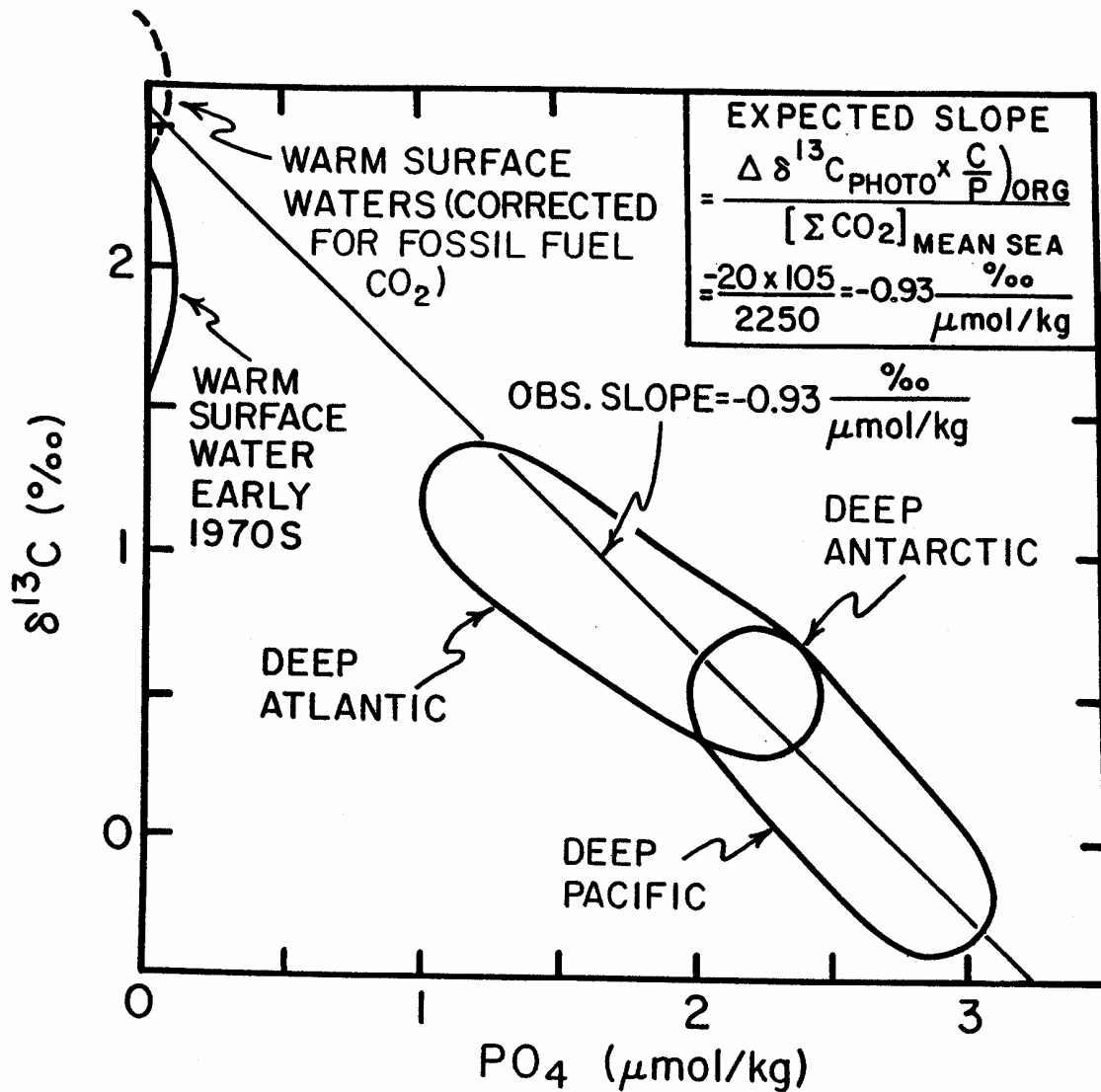


Figure 44. Relationship between $\delta^{13}\text{C}$ and PO_4 in the world ocean. The $\delta^{13}\text{C}$ values for warm ocean water have been corrected by 0.6‰ to remove the decrease which has taken place over the last century as the result of the invasion of CO_2 produced by the burning of fossil fuels and the decline of the terrestrial wood and humus reservoirs. The slope defined by these results is close to that expected from photosynthesis and respiration cycle (i.e., -0.93‰/°C). The ±13 C data on which this diagram is based were obtained in the laboratories of Harmon Craig at the Scripps Institution of Oceanography and of Peter Kroopnick at the University of Hawaii.

foraminifera, the incorporation of respiration CO₂ manifests itself in a difference between the carbon isotope ratios in species which live on the sediment surface (the epifauna) and in species which live within the upper few centimeters of the sediment (the meiofauna). Measurements on dissolved inorganic carbon from pore waters show why this is the case (see figure 45). Bacteria living within the sediment raise the ΣCO₂ content of the pore waters. Since respiration CO₂ is ¹³C deficient, pore waters have lower ¹³C/¹²C ratios than the overlying bottom water. So also do the shells formed by benthic foraminifera living within these pores (see figure 46). To avoid the bias introduced in this way, carbon isotope measurements are generally made on the shells manufactured by epifauna (usually on the species *C. wuellerstorfi*). A surprising finding in this regard is that despite large pore water excesses of dissolved cadmium (see figure 45), species to species differences in the cadmium content of co-existing benthic foraminifera have not been found.

For planktonic foraminifera, the presence of respiration CO₂ reveals itself in quite a different way. In this case, a correlation exists between the size of a shell and its carbon isotope ratio (see figure 47). The very small shells of juvenile organisms have ¹³C/¹²C ratios as much as 2‰ lower than expected from the isotopic composition of the ΣCO₂ in the water in which the shells grew. Apparently, during their infancy, a fairly large fraction (~10%) of the carbon used to make shell material comes from respiration CO₂. As the shell grows larger, its aggregate carbon isotope ratio approaches the value representing equilibrium with sea water ΣCO₂. Hence the contribution of respiration CO₂ decreases as the organism approaches maturity. In order to reduce the bias introduced by respiration CO₂ incorporation, carbon isotope measurements are made on a restricted size range of large (i.e., mature) planktonic shells.

We have already discussed the fact that a change in ¹³C to ¹²C ratio in deep sea water averaged about 0.35‰ lower during glacial than interglacial time. This result was obtained by suitably averaging the carbon isotope measurements on benthic foraminifera

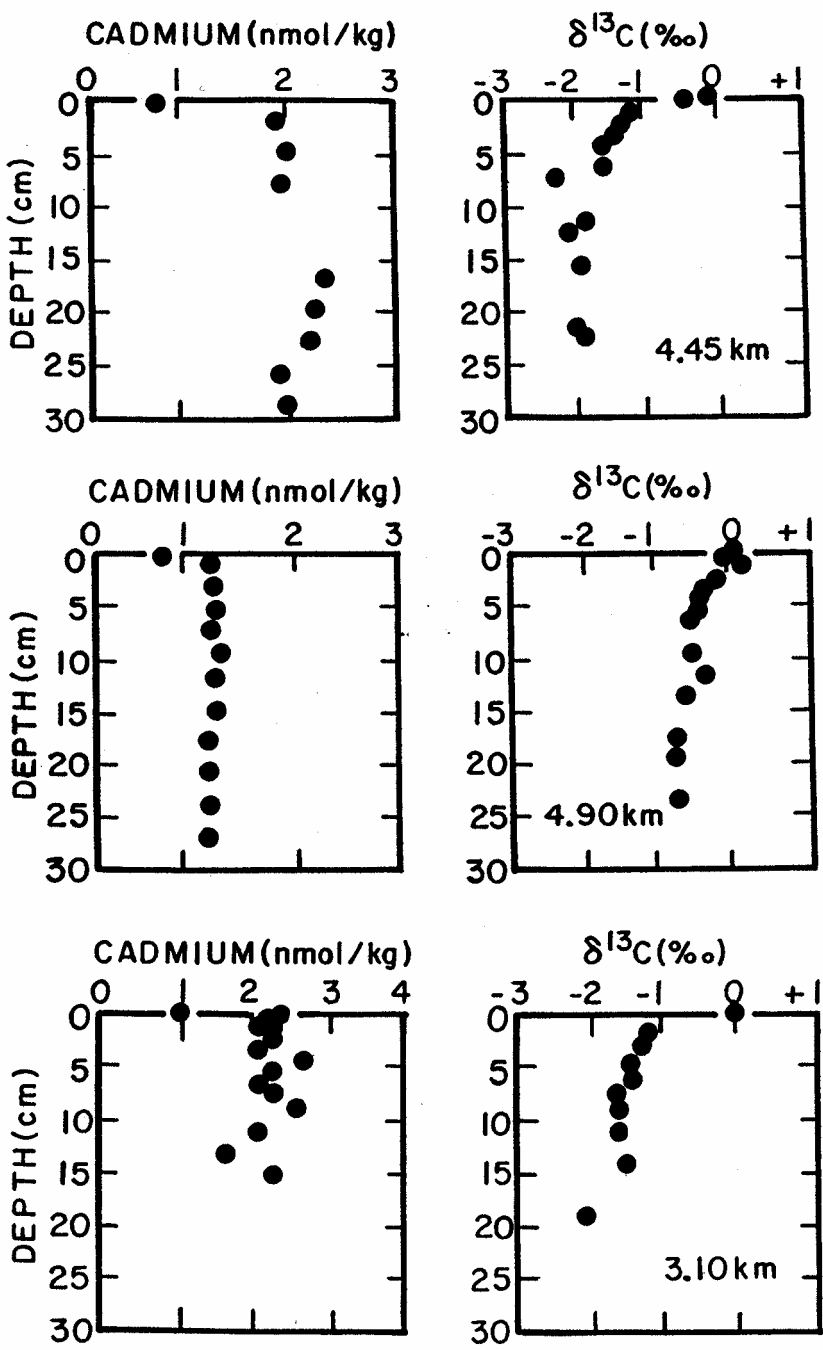


Figure 45. Comparison of pore water profiles for cadmium (by Klinkhammer) and for carbon isotopes (by McCorkle) in three deep sea cores from the Pacific Ocean. In all three, the cadmium of the pore waters is higher than content and that in bottom water and $^{13}\text{C}/^{12}\text{C}$ ratio is lower.

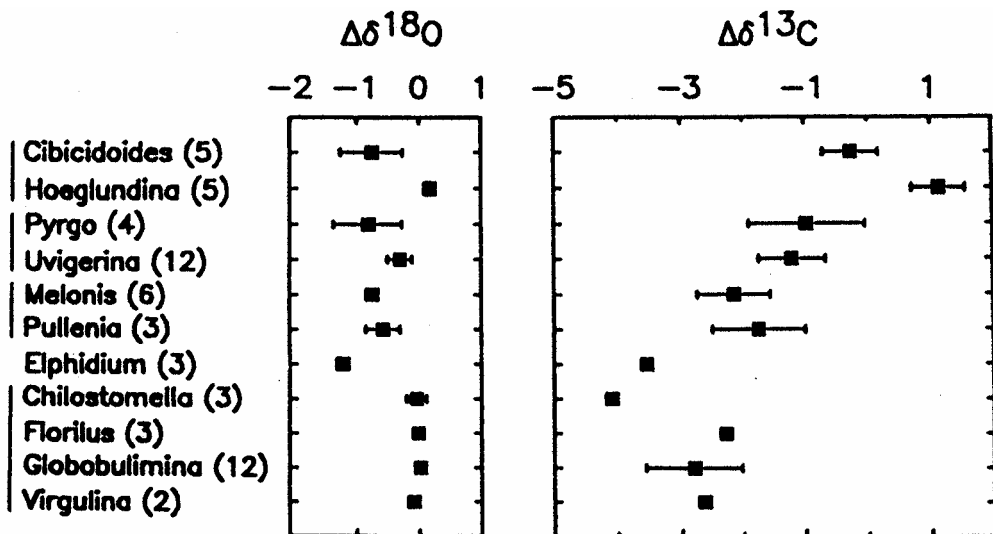


Figure 46. Difference between oxygen and carbon isotope ratios measured in various taxa of benthic foraminifera and the values expected were the CaCO_3 to have been deposited from bottom waters. The species are arranged in order of depth habitat in the sediments. The oxygen isotope results are consistent with the fact that no significant isotope gradient exists in the pore water oxygen. The decrease in $^{13}\text{C}/^{12}\text{C}$ ratio is the result of the input of ^{13}C deficient respiration CO_2 to the sediment pore waters.

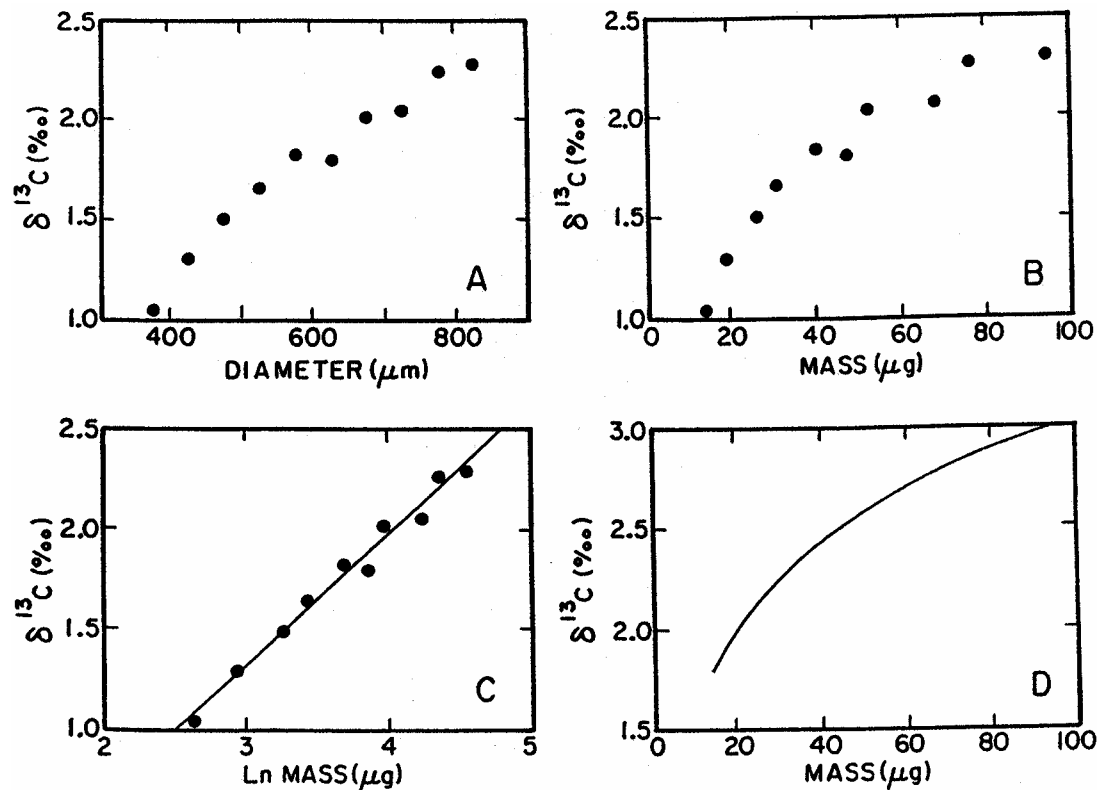


Figure 47. Carbon isotope measurements (by Oppo and Fairbanks) on shells of *G.sacculifer* (without sac) from 121 cm depth in a deep sea core, V28-122, from the Caribbean Sea. In A, the results are plotted as a function of diameter of the shell; in B, as a function of the mass of the shell; in C, as the logarithm of the mass. In D, the $^{13}\text{C}/^{12}\text{C}$ ratio for the mass added is shown.

shells from cores taken from various oceanic regions and of water depths.

In addition to providing a measure of the change in carbon isotope composition for the sea as a whole, measurements on benthic foraminifera shells offer information similar to that obtained from cadmium, barium and zinc. Ideally the results of carbon isotope ratios in foraminifera of glacial age should tell the same story. To a large extent these cross-checks have proven positive. The carbon results indicate both a smaller deep Pacific to deep Atlantic nutrient difference and larger nutrient gradients in the deep Atlantic Ocean during glacial time. However, in one region, the Antarctic, the two indicators yield quite different pictures. As illustrated in figure 48, larger carbon isotope differences between glacial and interglacial are found in the Antarctic than in any other place in the ocean. By contrast, Boyle found no significant glacial to interglacial cadmium differences for either planktonic or benthic foraminifera from Antarctic cores. Nor has Lea found significant differences for barium. Until the cause of this fundamental disagreement between the two indicators has been established, the utility of both methods as paleoceanographic indicators remains somewhat in limbo.

One possible explanation presents itself. The carbon isotope distribution in the sea is subject to an influence not shared by cadmium or by barium. CO_2 can be transferred through the atmosphere from one region of the ocean to another. Such transfers have potential significance to the distribution of ^{13}C within the sea. The reason is that the isotope fractionation between gaseous CO_2 in the atmosphere and dissolved ΣCO_2 in the surface sea is temperature dependent, being greater for cold than for warm water. So large is this effect that were the cold waters in the polar ocean to achieve isotopic equilibrium with the warm waters in the tropical ocean, the ΣCO_2 in the cold waters would have a $\delta^{13}\text{C}$ value 2.5‰ greater than that for the ΣCO_2 in the warm water, i.e., roughly equal in magnitude to the difference related to the photosynthesis-respiration cycle. The problem is that surface waters don't remain in place nearly long enough for this equilibrium to be achieved. Rather, isotope exchange through the atmosphere makes

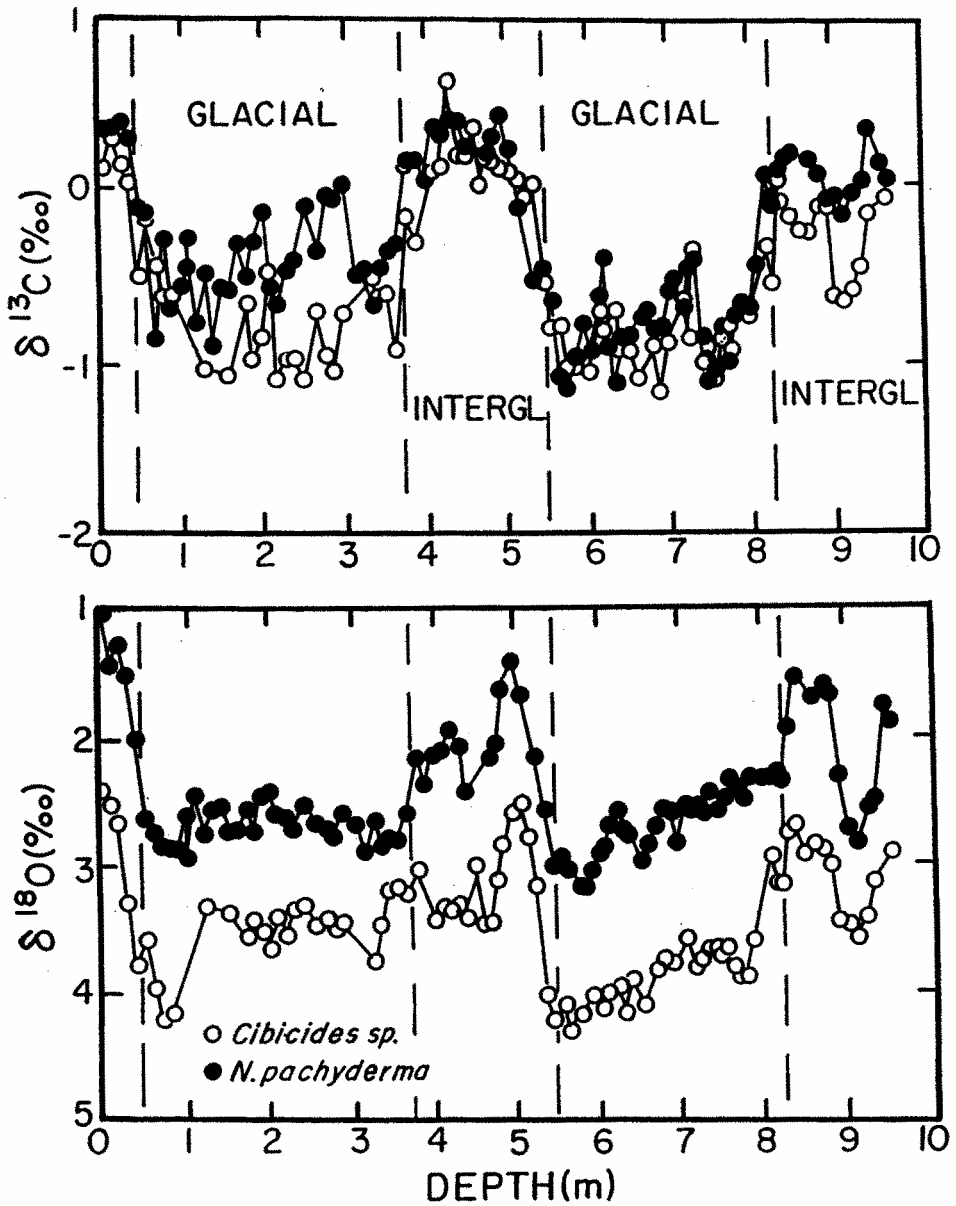


Figure 48. Oxygen and carbon isotope records for benthic (open circles) and planktonic (closed circles) from core V22-108 from the Antarctic Ocean (Charles and Fairbanks 1990).

only a small contribution to the distribution of $\delta^{13}\text{C}$ to $\delta^{12}\text{C}$ ratios in the sea. Nevertheless, this process produces a significant deviation from the linear $\delta^{13}\text{C}-\text{PO}_4$ established for deep waters in the Pacific and Indian Oceans (see figure 49). Newly formed deep water in the northern Atlantic has a 0.5‰ lower $\delta^{13}\text{C}$ value than expected from its PO_4 content. The reason is that North Atlantic Deep Water is the product of the rapid cooling of warm waters carried northward by the upper limb of the Atlantic's conveyor; hence, its carbon isotope signature reflects contact of warm water with the atmosphere and is shifted toward the $\delta^{13}\text{C}$ deficient side of the global $\text{PO}_4-\delta^{13}\text{C}$ trend. Thus it is possible that the discordance between the distributions of cadmium and carbon isotopes reconstructed for glacial time by measurements on benthic foraminifera reflects changes in the air-sea exchange imprint.

Howie Spero of University of California, Davis and David Lea of University of California, Santa Barbara working in cooperation with scientists in from the Alfred Wegner Institute in Bremerhaven have cultured the planktonic foraminifera, *O. universa*, at several different pHs. To the surprise of all, they observed a strong isotope dependence, the higher the pH, the lower both the $\delta^{13}\text{C}$ and the $\delta^{18}\text{O}$ value for the shell material. Were this dependence to apply to all planktonics, then a correction would have to be made on the results for glacial age samples. As the atmosphere's CO_2 content was 30% lower during glacial time, the surface ocean pH must have been 0.15 units higher. This means that the $\delta^{18}\text{O}$ for planktonic shells formed during glacial time was about 0.2‰ more negative than would have been the case had the pH remained unchanged. The 0.2‰ $\delta^{18}\text{O}$ shift is equivalent to a 1°C cooling. Hence 1° would have to be added to the glacial to interglacial temperature difference derived from oxygen isotope measurements on planktonic foraminifera.

RATE OF DEEP SEA VENTILATION

The best indicator of the current rate of deep sea ventilation (i.e., renewal by water descending from sea surface) is the distribution of radiocarbon within the sea.

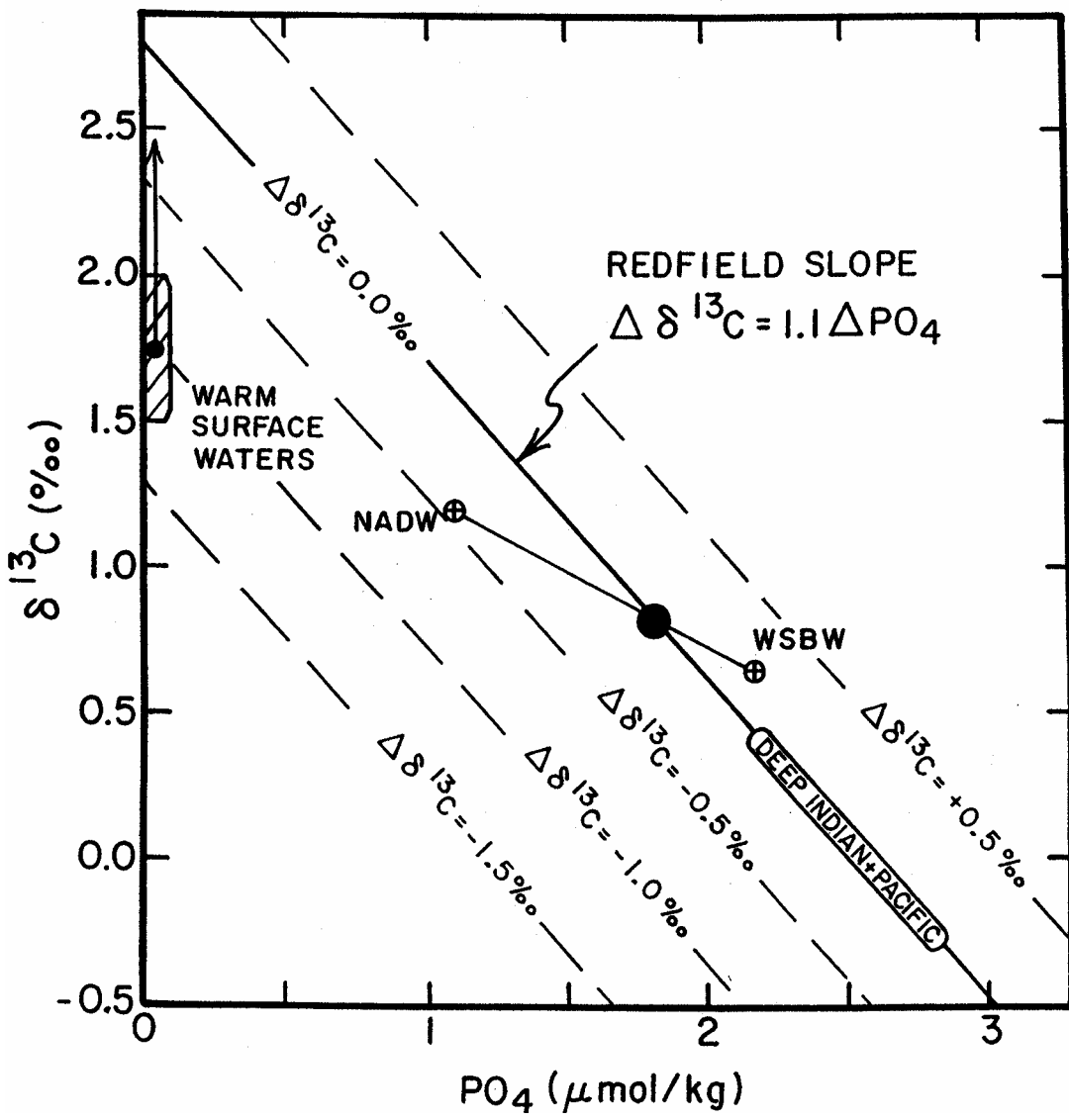


Figure 49. Relationship between $\delta^{13}\text{C}$ and PO_4 for major water types in the world ocean. The contours denote departures from the Redfield slope defined by deep waters in the Pacific and Indian Oceans. The arrow associated with the warm surface ocean results is the approximate correction for the impact of fossil fuel CO_2 . NADW stands for North Atlantic Deep Water and WSBW for Weddell Sea Bottom Water.

Fortunately, two means exist by which ventilation rates during glacial time can be reconstructed. One involves radiocarbon measurements on shells of foraminifera from deep-sea sediments and the other radiocarbon measurements on ^{230}Th dated benthic corals. Before discussing how these reconstructions are carried out, a few words must be said about today's radiocarbon distribution and what it tells us. Sections with water depth of the radiocarbon to carbon ratio in the ΣCO_2 for the western basins of the Atlantic and Pacific Oceans are shown in figure 50. The $^{14}\text{C}/\text{C}$ ratios are referenced to that for atmospheric CO_2 prior to the impacts of fossil fuel burning and nuclear testing. The units are ‰ (parts per thousand). The use of a Δ instead of δ denotes that corrections based on the $^{13}\text{C}/^{12}\text{C}$ ratio have been made for $^{14}\text{C}/^{12}\text{C}$ ratio differences caused by isotope fractionation during chemical reactions.

As can be seen, all the ocean values are negative. This is to be expected because ^{14}C atoms are created in the atmosphere. The highest oceanic $\Delta^{14}\text{C}$ values (~-50‰) are found in surface waters from the temperate regions and the lowest (-240‰) in the deep North Pacific. The values are set by competing processes. CO_2 exchange between the ocean and atmosphere and mixing within the sea tend to homogenize the $^{14}\text{C}/\text{C}$ values. Radioactive decay within the sea tends to create differences. The more remote the reservoir from communication with the atmosphere, the greater the toll taken by radiodecay. It is for this reason that the radiocarbon distribution in the ocean tells us something about the rate of ventilation of the deep sea. The more rapid the ventilation, the smaller the difference between the $^{14}\text{C}/\text{C}$ ratios in surface and deep waters. In today's ocean, the $\Delta^{14}\text{C}$ values for deep water in the Atlantic are less negative than those for the Pacific and Indian Oceans. One reason is that much of the deep water production occurs in the northern Atlantic. The other is that deep water forming in the northern Atlantic has a higher $^{14}\text{C}/\text{C}$ ratio than that forming in the Antarctic.

While not offering a complete set of information about the distribution of radiocarbon in the glacial ocean, measurements on foraminifera from deep-sea cores

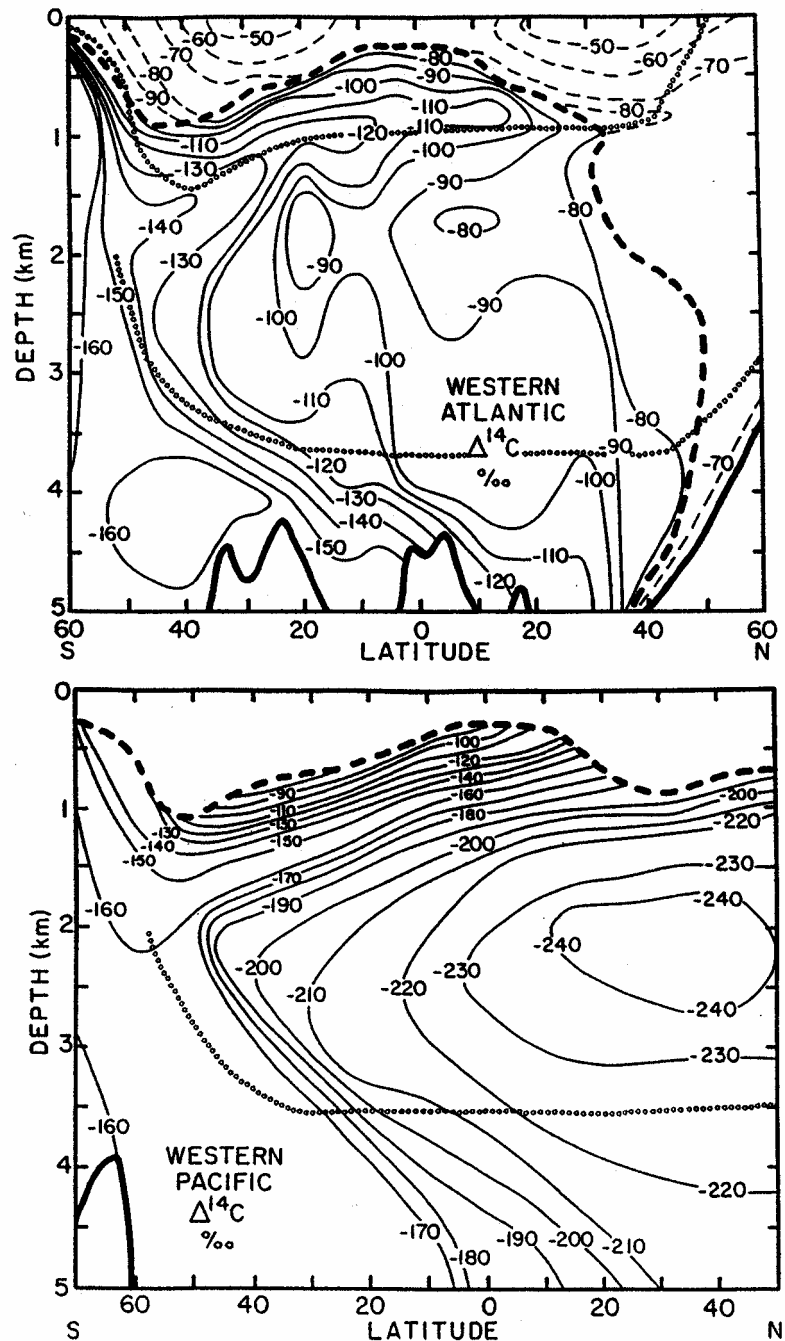


Figure 50. Sections showing the distribution of $\Delta^{14}\text{C}$ values in the western Atlantic and western Pacific Oceans at the time of the GEOSECS survey (1972-4). The bold dashed lines show the limit to which ^{14}C produced during nuclear weapons' tests has penetrated into the sea. The contours above this boundary are based on a far more limited set of measurements on prenuclear samples.

allow the difference between the $^{14}\text{C}/\text{C}$ ratio in surface and bottom water at a given site to be reconstructed for times in the past. This is accomplished by comparing the $^{14}\text{C}/\text{C}$ ratio in planktonic foraminifera with that in benthic foraminifera from same sediment sample. These radiocarbon measurements can be expressed as apparent ages; ‘apparent’ because as a result of mixing among water masses, they are not true measures of isolation time. As shown in figure 51, for tropical Atlantic today’s age difference is currently about 350 years, and for the tropical Pacific about 1600 years.

Measurements on coexisting glacial age benthic and planktonic foraminifera have been made on only a few cores. The results from one of the Atlantic cores are reproduced in figure 52. A summary of age differences for four Atlantic cores and one Pacific core is given in table 5. While no significant glacial to Holocene difference exists for the Pacific, the age difference for the Atlantic during glacial time is twice today’s. This strongly suggests that while perhaps weaker during glacial time, the Atlantic’s conveyor was still a major conduit for radiocarbon into the deep sea.

The second method involves measuring the ^{14}C to C ratio in ^{230}Th dated benthic corals (see below). In this case, the actual radiocarbon content of the coral at the time of its growth can be reconstructed.

CO₃ Concentration

The solubility of CaCO₃ in sea water increases with pressure. Because of this, calcitic shells which fall to the ocean’s abyssal plains have a greater tendency to dissolve than those which fall onto the flanks of undersea mountains (i.e., ridges and plateaus projecting well above the sea floor). Indeed, this tendency shows up in the composition of sediments. Those which mantle the abyssal plains are nearly free of CaCO₃ while those which mantle the ridges and plateaus are rich in CaCO₃. Traverses of sediment composition with water depth reveal a transition zone several hundred meters in width over which the CaCO₃ content progressively drops from the $88 \pm 8\%$ value which characterizes ridges and plateaus to the near zero value which characterizes abyssal plains

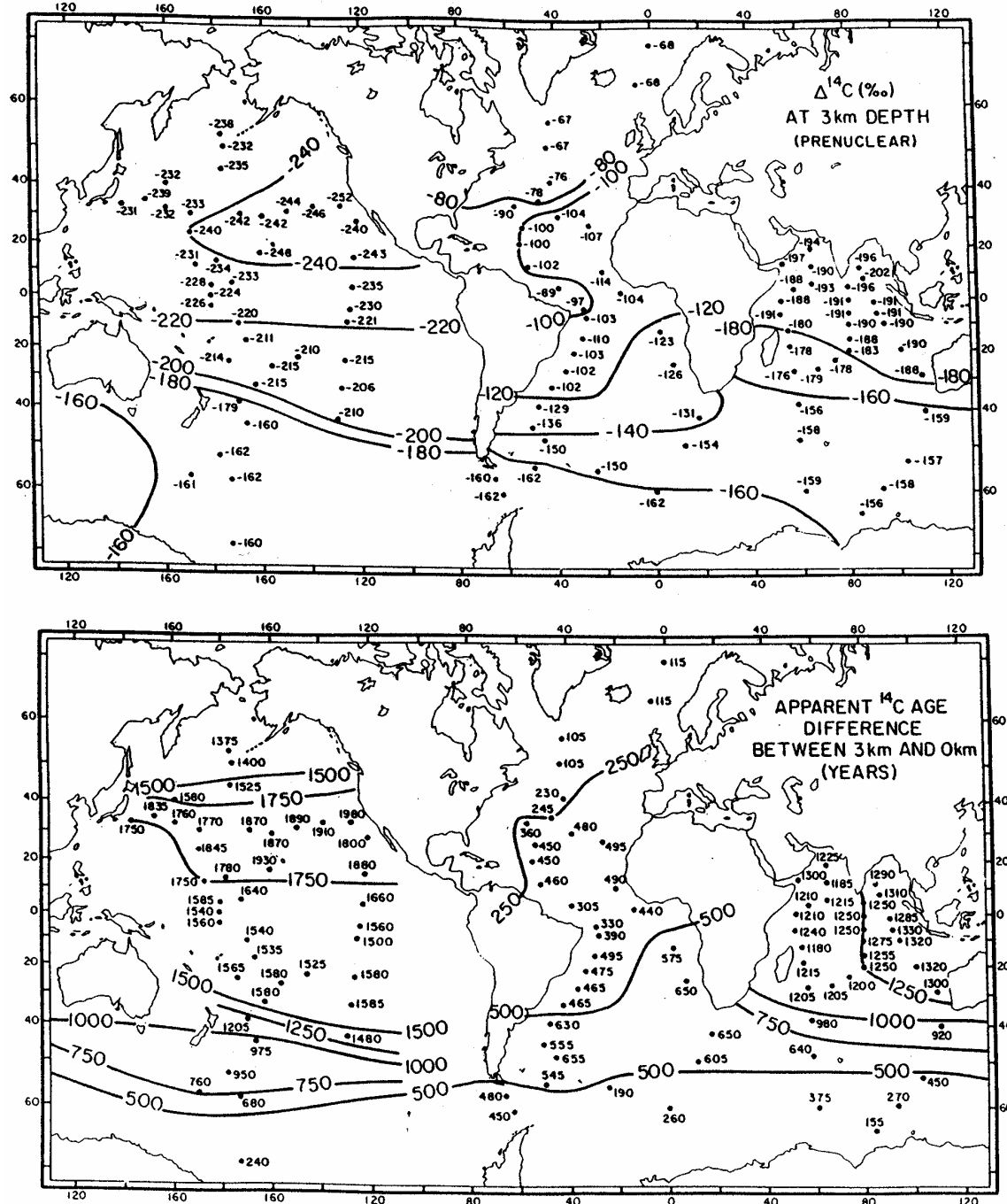


Figure 51. The map in the upper panel shows the distribution of $\Delta^{14}\text{C}$ values at a depth of 3 kilometers in today's ocean. The map in the lower panel shows the age difference calculated from the ratio of the $^{14}\text{C}/\text{C}$ ratio for 3 km water and that for overlying surface water.

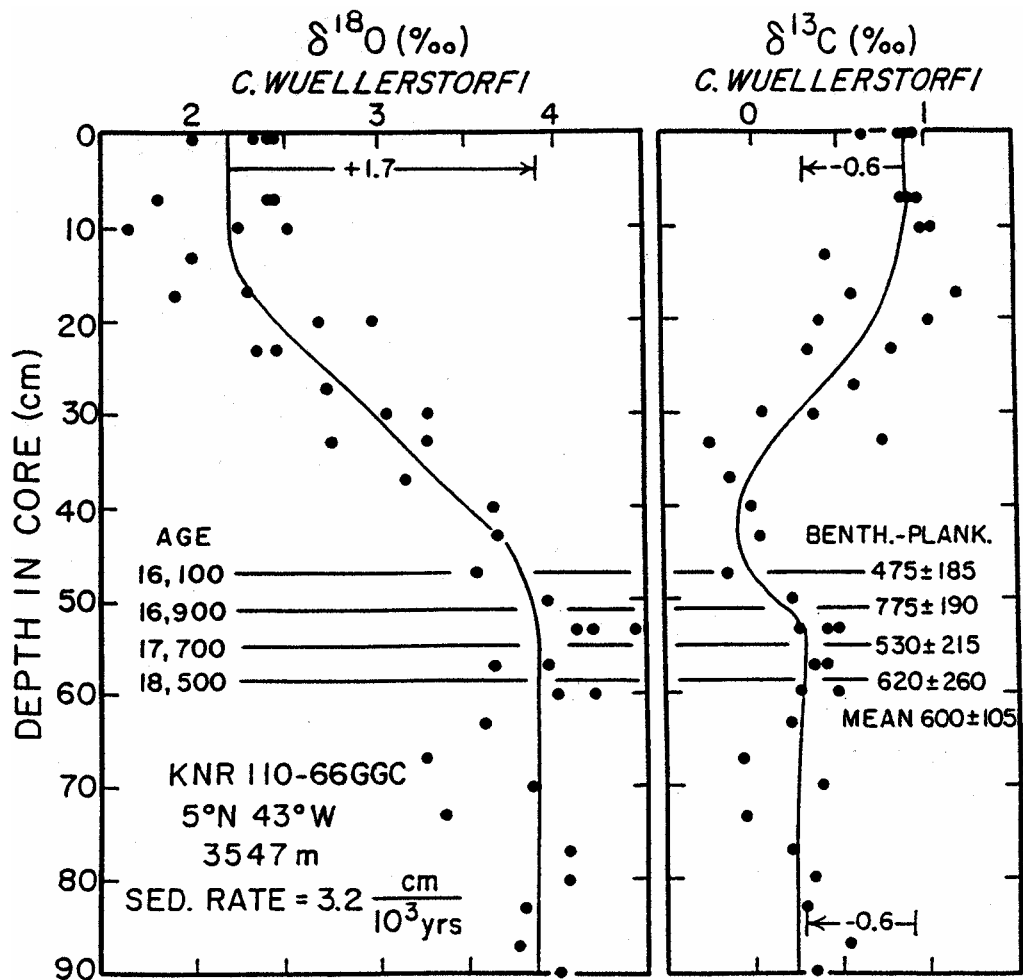


Figure 52. Radiocarbon age differences between coexisting benthic and planktonic foraminifera from full glacial horizons in a core from the Ceura Rise in the western Atlantic. The average difference of 600 years can be compared with that of 350 years based on water samples from today's ocean.

Table 5. Summary of the age differences obtained for coexisting benthic and planktonic foraminifera shells from glacial horizons of deep sea cores.

Location	Core	Latitude	Longitude	Water depth, km	Number of Pairs	Mean Benth-Plank Age, Years	Today's Age, Years
Atlantic	V28-122	12°N	79°W	1.8*	3	195±140	300
Atlantic	K110-82	4°N	43°W	2.8	5	780±220	350
Atlantic	K110-66	5°N	43°W	3.5	4	600±105	350
Atlantic	K110-50	5°N	43°W	4.0	5	705±150	400
Pacific	S50-37	19°N	116°E	2.1	4	1670±105	1600

*Sill depth of Caribbean

(see figure 53). The top of this transition zone is often referred to as the lysocline. The depth of this horizon is close to, but not identical to, that of the water column saturation horizon (see figure 54). The degree of undersaturation increases with depth below the saturation horizon driving up the rates of dissolution and taking an ever greater toll on the sediments calcite. The situation is complicated by the release of respiration CO_2 into the sediment pore waters. This release lowers the carbonate ion concentration permitting calcite dissolution to occur at depths shallower than the saturation horizon.

Sediments from depths corresponding to the transition zone provide a means of the CO_3^{\pm} ion content reconstructing the ocean's deep waters. For example, if at a given site, the extent of dissolution during glacial time were greater than today's, the CO_3^{\pm} ion concentration was likely lower. On the other hand, if the extent of dissolution were less, then the CO_3^{\pm} ion concentration was likely higher. As the saturation CO_3^{\pm} ion concentration increases about 15×10^{-6} moles per liter per 100 atm of additional pressure (i.e., per km water depth), a change in lysocline depth of let's say 0.5 km would suggest a CO_3^{\pm} ion concentration change of 7×10^{-6} moles/liter. It must be kept in mind that as the Ca^{++} concentration in sea water is nearly uniform with geographic location depth and also on the time scale of several glacial cycles, only changes in CO_3^{\pm} concentration need be considered.

Now one might ask, of what importance is the CO_3^{\pm} ion content of deep sea water to climate? The answer is that the higher the CO_3 ion content of deep water, the lower the CO_2 partial pressure in the atmosphere. To a rough approximation the product $[\text{CO}_3^{\pm}]_{\text{DEEP SEA}} \times p_{\text{CO}_2}^{\text{atm}}$ remains constant. The next question which comes to mind is what controls the CO_3^{\pm} ion concentration in the deep sea? The answer is that it is controlled by an interaction between the rate of supply of the ingredients needed for the manufacture of CaCO_3 (i.e., CaO and CO_2) and the rate of manufacture of CaCO_3 by marine organisms.. In today's ocean, organisms manufacture CaCO_3 several times faster than the ingredients are being supplied. Material balance between the input of ingredients

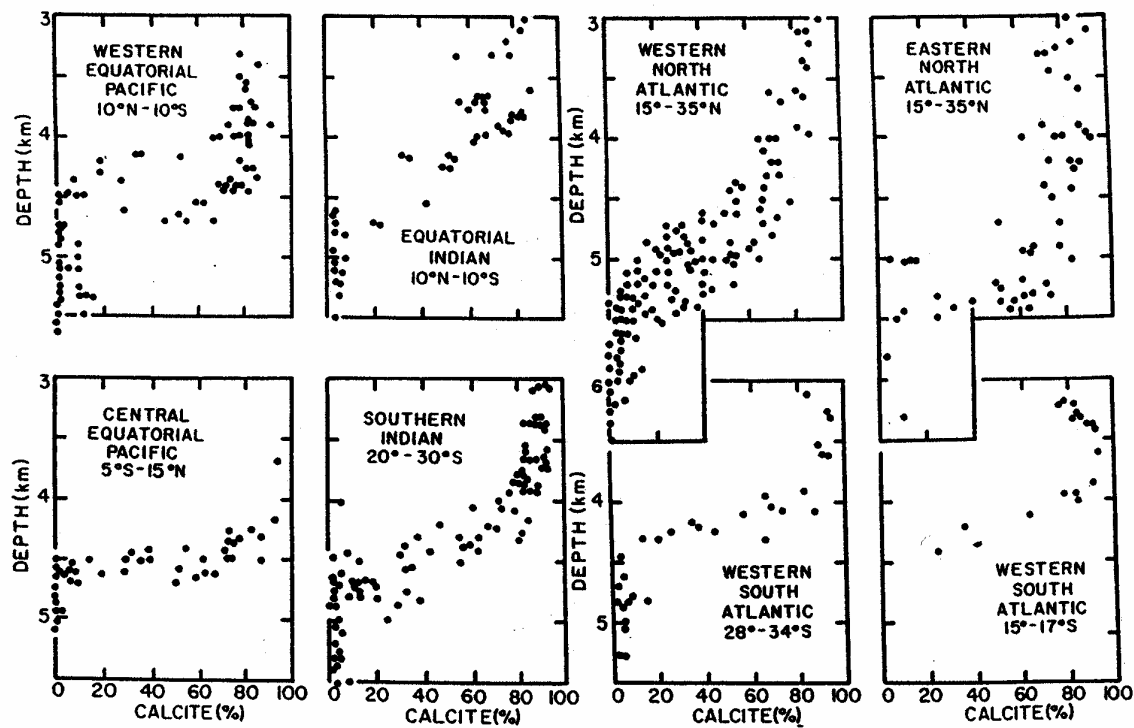


Figure 53. Plots of percent CaCO₃ for core top samples as a function of water depth for various regions of the ocean. Based on a compilation provided by Pierre Biscaye of the Lamont-Doherty Earth Observatory.

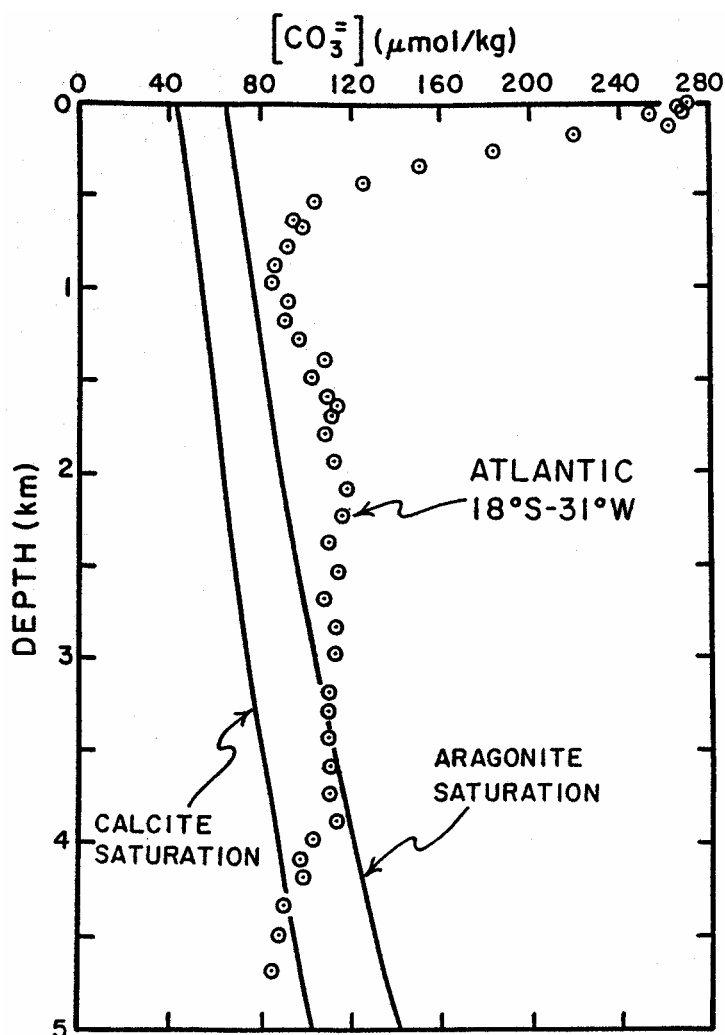


Figure 54. Plot of carbonate ion concentration versus water depth for a GEOSECS station in the western South Atlantic (open circles). The concentration of carbonate ion remains fairly constant through the North Atlantic Deep Water mass. It is higher in this water mass than in the underlying wedge of Antarctic Bottom Water and in the overlying tongue of Antarctic Intermediate Water. The saturation carbonate ion concentration (as shown by solid lines) increase with depth because of the pressure effect (calcium and carbonate ions occupy less volume when dissolved in sea water than when locked in CaCO_3). The saturation horizon for aragonite lies at about 3.3 km, and that for calcite at about 4.3 km. These results were obtained as part of the GEOSECS program (Takahashi, et al 1980).

and the burial of CaCO_3 in sediments is maintained by dissolution. The $\text{CO}_3^{\bar{}} \text{ ion}$ concentration of the deep sea is continually driven toward that value where the rate of burial of CaCO_3 just matches the rate of supply of the ingredients to the sea. In other words, the fraction of the sea floor bathed in undersaturated water adjusts so that just the right fraction of the raining CaCO_3 is dissolved. If the system gets out of balance such that the amount of CaCO_3 accumulating on the sea floor exceeds the ingredient supply, then the $\text{CO}_3^{\bar{}} \text{ ion}$ in the ocean will be drawn down and the lysocline will move to shallower depths. This shoaling will continue until the balance between loss and supply is restored. At the present rate of CaCO_3 production in the sea, the time constant for restoration of balance is about 5000 years.

In today's ocean, a sizable difference exists between the $\text{CO}_3^{\bar{}} \text{ ion}$ content of deep water in the Atlantic Ocean ($\sim 112 \mu\text{mol/kg}$) and that in the Pacific and Indian Oceans ($\sim 84 \mu\text{mol/kg}$). Because of this $28 \mu\text{mol/kg}$ concentration difference, the lysocline depth resides about two kilometers deeper in the Atlantic than in the Pacific and Indian Oceans.

Quantitative reconstruction of the depth of the transition zone at times in the past is not a simple matter. It requires the determination of the fraction of the calcite rained to the sea floor which survives dissolution. Unfortunately, the criteria used to judge the state of preservation of the calcite remain semi-quantitative. Several are used. One approach is to measure the ratio of fragments to whole foraminifera shells; the logic being that as dissolution proceeds, the individual chambers making up the shell become disconnected creating fragments. Another indicator is the ratio of the shells of a dissolution-prone species to shells of a dissolution-resistant species. The assessment of the relative vulnerability of species to solution and fragmentation comes from depth traverses of recent sediment. As it is reasonably safe to assume that the ratio of one species to another falling to the sea floor does not vary over the small area chosen for the study, the changes in ratio seen at successively greater water depth can be attributed to differential vulnerability to dissolution. Finally, Pat Lohmann developed a method of

assessing the thickness of the walls of foraminifera shells, the idea being that they would thin as dissolution proceeded. He did this by picking and then weighing 50 or so whole shells of a given species from a narrow size range. By making measurements on core-top samples from a range of water depths, Lohmann showed that this method could be calibrated against pressure-normalized carbonate ion concentration.

A potentially quantitative index of calcite dissolution is the percentage CaCO_3 in the sediment. Clearly, as the calcite dissolves, the CaCO_3 content of the sediment must drop. In the ideal situation, where the rain rate of calcitic and of noncalcitic material are constant geographically, the amount of calcite lost to dissolution could be calculated from the percent CaCO_3 in the sediment. For each region of interest, the calcite content of the sediment from above the transition zone is used as the reference for the calculation of the amount of dissolution which has occurred in cores from within the transition zone. The degree of dissolution can then be read from a graph akin to that in the insert in figure 55. However, the fact that CaCO_3 contents of superlysocline sediment average about 90% ocean raises a serious problem. Quite large amounts of dissolution create only very small changes in the percent CaCO_3 . For example, consider a sediment had a calcite content of 90%. Were this sediment to lose half of its calcite to dissolution, its CaCO_3 content would drop to only 82%. Because of this, small changes from glacial to interglacial in the ratio of the rain rate of calcite to the rain rate of the non-calcitic diluent would lead to substantial biases in estimates of the extent of dissolution during glacial time.

In addition, a chemical complication must be considered. It has to do with the CO_2 released within the sediment by respiration. It drives down its $\text{CO}_3^{=}$ ion content of the pore water. Because of this, calcite dissolves at depths shallower than the saturation horizon. As we shall see, this process has some important consequences.

Despite all these potential complications, a strong glacial to interglacial signal is observed. In both the Pacific and Indian Oceans, the extent of dissolution experienced by

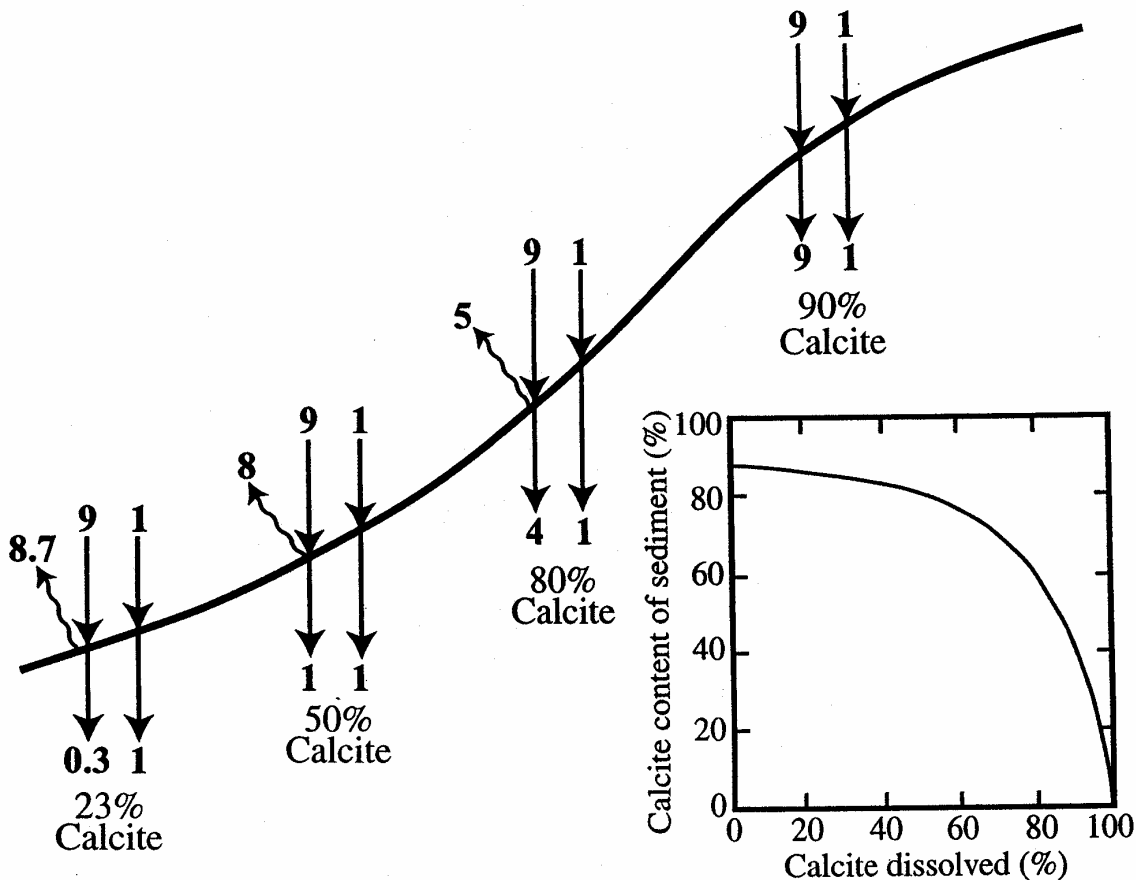


Figure 55. A diagrammatic view of changes in the extent of solution and the percent calcite in the sediment with water depth. In each example, the right hand arrows give the rain rate and accumulation rate of non CaCO_3 debris and the left hand arrows, the rain rate and accumulation rate of calcite. The wavy arrows represent the solution rate of calcite. As can be seen from the graph on the lower right, the fraction of calcite in the sediment gives a misleading view of the fraction of the raining calcite which dissolves, for large amounts of dissolution are required before the calcite content drops significantly.

glacial-age sediments deposited within the depth range corresponding to today's transition zone was clearly smaller. The lysocline in these two oceans appears to have been about 600 meters deeper during glacial time (see figure 56). All the indicators mentioned above agree on this. For the Atlantic, the opposite was true; the extent of dissolution was greater during glacial time suggesting that the lysocline was several hundred meters shallower. The overall impression we get is that the current upward step in the depth of the transition from the Atlantic to the Pacific was smaller or during glacial time. This reduction in interocean lysocline elevation difference is consistent with conclusions drawn from measurements of barium in benthic forams which show a much reduced barium (and hence presumably also alkalinity) difference between the oceans. However, taken at face value, the glacial to interglacial changes in deep ocean CO_3^{\pm} ion concentration appear to be too small to be of much help in explaining the change atmospheric CO_2 content. But as will be described in the next section, the lysocline depth could be a misleading index of deep ocean CO_3^{\pm} ion concentration. A somewhat different picture is obtained from estimates of wall thicknesses based on shell weights. The advantage of this method is that it covers a much larger range of water depths than the other methods which depend on large extents of CaCO_3 dissolution and hence are restricted to the deepest waters. The surprise was that unlike today's ocean, where the carbonate ion concentration is in most places nearly constant with water depth, large gradients in carbonate ion concentration existed in the glacial ocean.

Paleo pH

Boron isotope studies carried out at SUNY Stonybrook by Gary Hemming demonstrate the possibility that the isotope ratio of ^{11}B to ^{10}B in boron incorporated into the shells of foraminifera might provide an index of the pH of past oceans. This elegant idea goes as follows. As boron has an ocean residence time measured in many millions of years, neither its concentration nor its bulk isotopic composition could have changed significantly between glacial and interglacial time. However, as there is a 20‰ difference

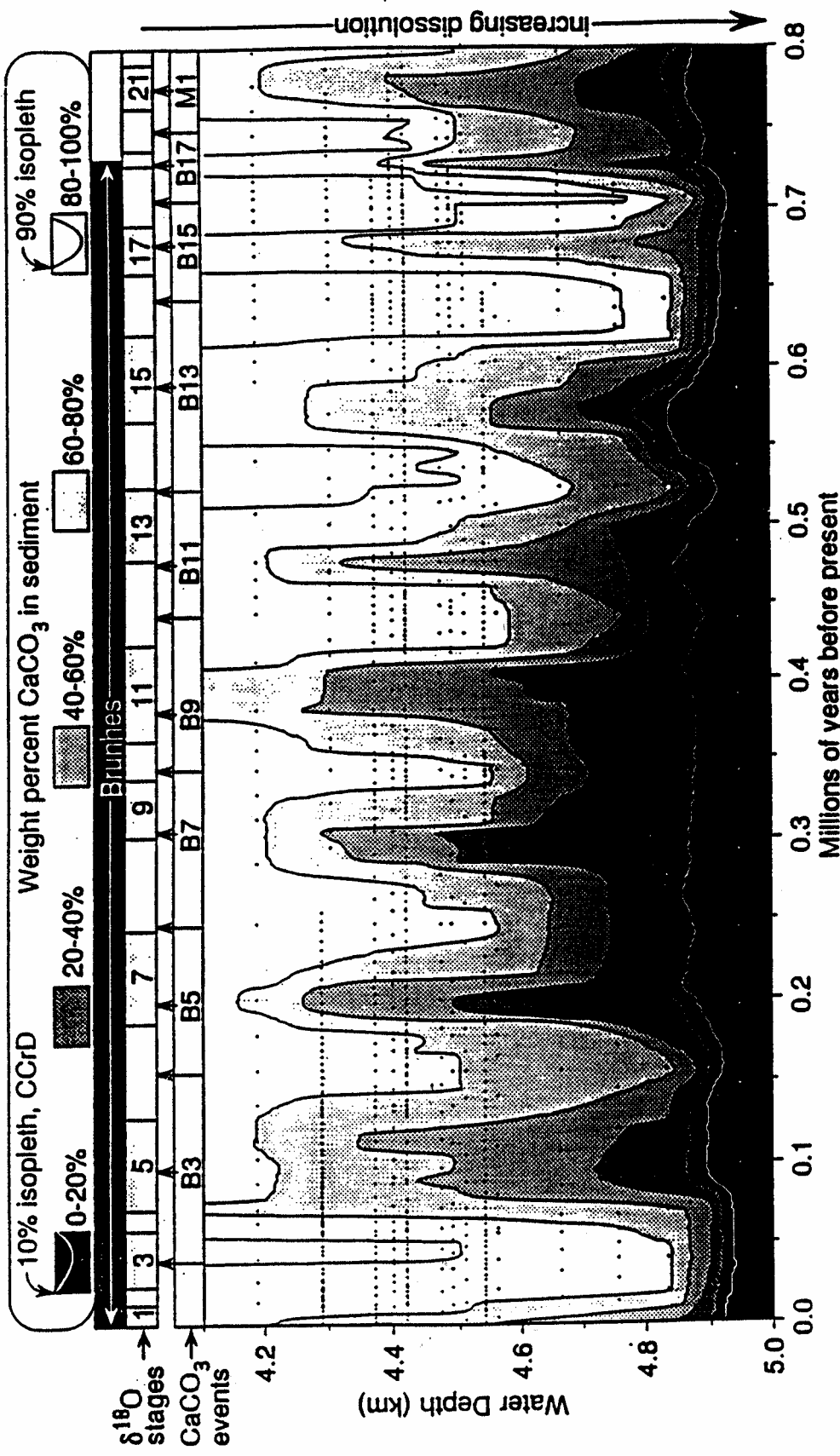


Figure 56. CaCO_3 content of equatorial Pacific sediments over the last 800,000 years as reconstructed by Farrell and Prell from a set of 15 cores covering the depth range 4100 to 5000 meters. The contours show how the depth of given percent CaCO_3 horizons has changed with time. A puzzling feature of this record is that while the depths of isopleths representing high CaCO_3 contents undergo large glacial to interglacial changes, those for isopleths representing low CaCO_3 show little change. This results in a great widening during interglacials of the transition zone separating CaCO_3 -rich from CaCO_3 -poor sediments. My explanation for this rather strange situation is that during interglacials chemical erosion of glacial sediments buffers the CaCO_3 content, preventing the full shift in isopleth depth from occurring.

between the isotopic composition of charged and uncharged species of borate, changes in ocean pH will result in changes in the isotopic composition of both species (figure 57). Were sea water to become more acid, the isotopic composition of the neutral species would approach that for bulk sea water borate. Were sea water to become more basic, the isotopic composition of the charged borate species would approach that of bulk borate. The assumption is that only the charged borate species is incorporated into the calcite lattice. If so, then the ^{11}B to ^{10}B ratio in foraminifera shells should record pH.

In an attempt to harness this technique, Gary Hemming and Abhijit Sanyal compared the boron isotope ratio in foraminifera of glacial and Holocene age, using samples from sediment cores in both the Atlantic and the Pacific Oceans. For planktonic forams, they obtained results suggesting that glacial surface waters were 0.2 ± 0.1 pH units more basic than Holocene waters. This result is consistent with that of 0.15 pH units required to accompany the decrease in atmospheric CO₂. For benthic foraminifera, they found isotopic differences corresponding to 0.3 ± 0.1 pH units more basic than Holocene waters. The exciting thing about the latter result is that it suggested that the glacial to Holocene increase in atmospheric CO₂ content was entirely the result of changes in the amount of CaCO₃ dissolved in the sea (more in glacial and less in Holocene). Were this the case, the pH of deep water would have to have been 0.3 pH units higher during glacial time just as obtained from the boron isotope measurements! The reason the expected pH change in deep water (0.30) is larger than that expected for surface water (0.15) is the CO₃²⁻ ion content of warm surface is currently roughly twice that in deep water.

There is, however, a fly in the ointment. Laboratory calibrations conducted on planktic foraminifera cultured at various pHs and inorganic calcite precipitated at various pHs, although following the expected $\delta^{11}\text{B}$ trend, reveal species to species offsets (figure 58). As these offsets are as large as the glacial to Holocene $\delta^{11}\text{B}$ changes, there is concern that the benthic results are also subject to large vital effects.

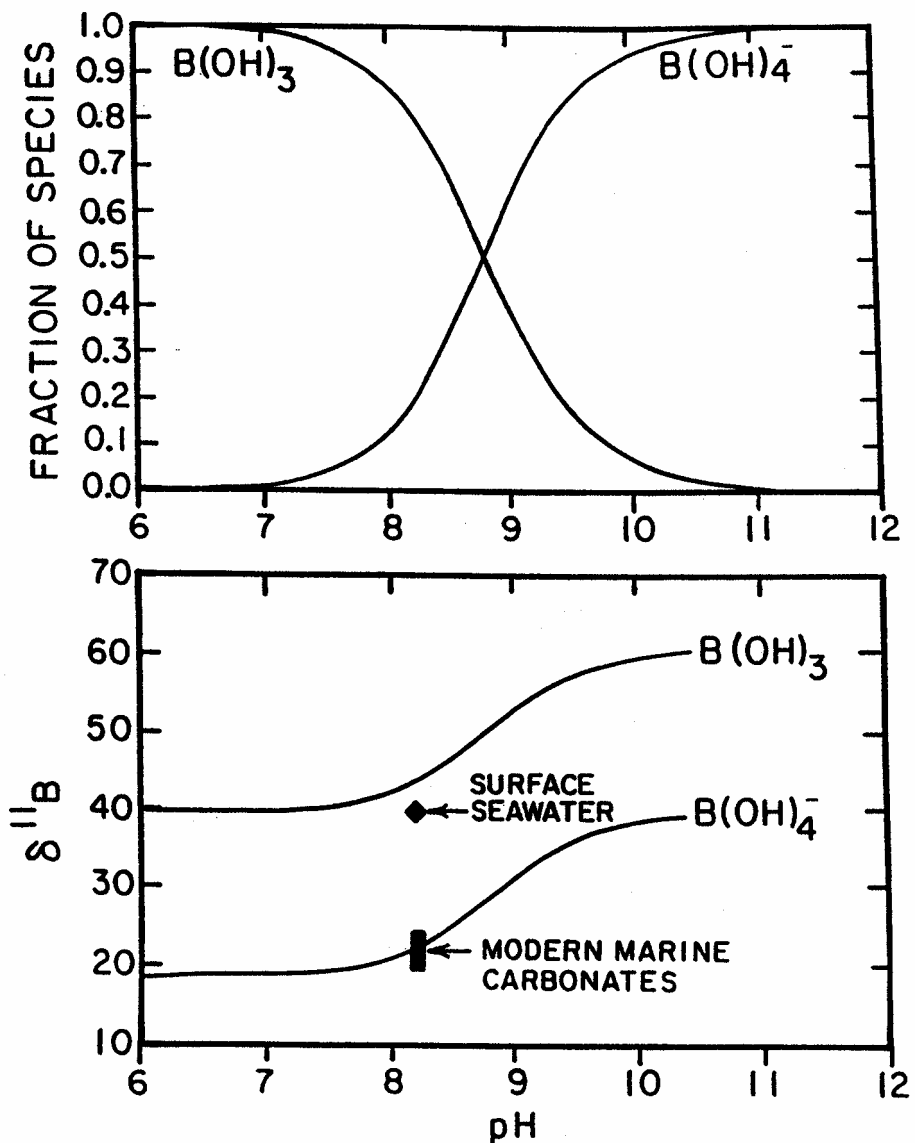


Figure 57. Like that of ΣCO_2 , the speciation of borate dissolved in sea water changes with pH. At high pHs, the charged borate species dominates and at low pHs, the neutral species dominates. The two are in equal abundance at a pH of about 8.75. The isotopes of boron are not distributed uniformly between these two chemical forms. Rather, the heavy isotope, ^{11}B , is depleted by about 22‰ in the charged species relative to the neutral species. As it is the charged borate which becomes incorporated into marine calcite, its isotopic composition is preserved in the sedimentary record. The isotopic composition of this species depends on pH. The higher the pH, the closer this value will be to the isotopic composition of bulk borate in sea water. It is for this reason that the isotopic record in foraminifera offers a means to test the idea that it was a higher rain rate of organic matter to the sea floor during glacial time which caused the atmosphere's CO_2 content to drop. The higher CO_3^{2-} ion content of deep sea water required by this scenario would be accompanied by a higher pH and hence a higher ^{11}B to ^{10}B ratio in the shells of benthic foraminifera.

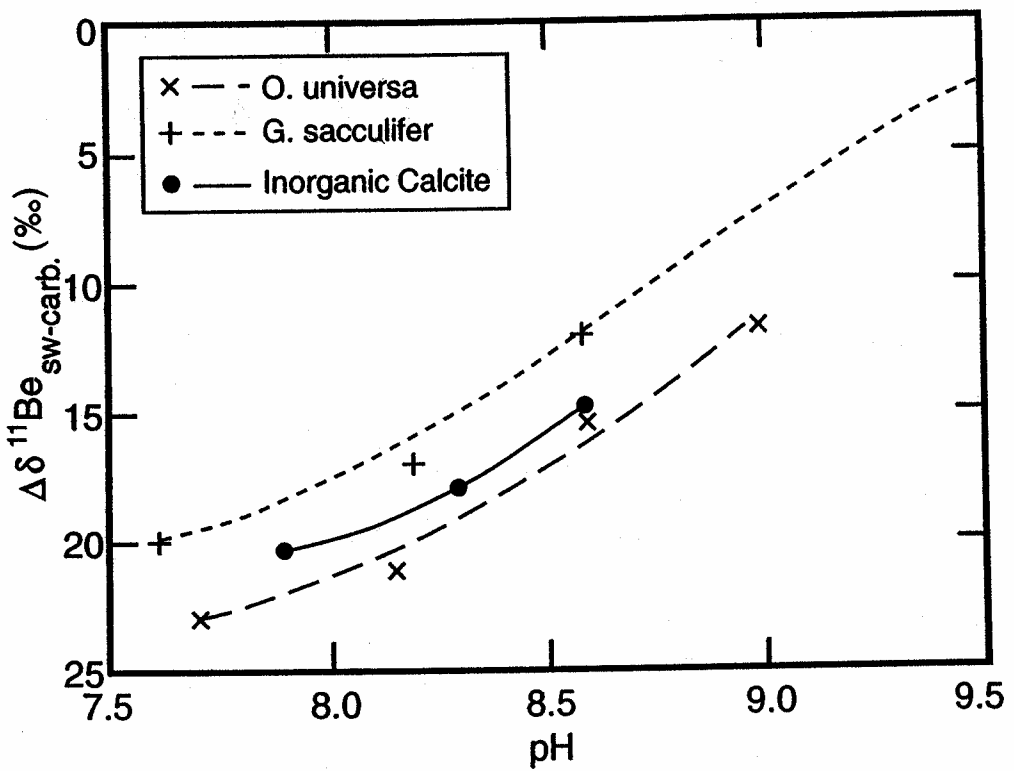


Figure 58. Comparison of the boron isotope ratio trends with pH for two species of planktonic foraminifera shells cultured in the laboratory. Although both follow the expected trend, there is a large offset between them. Such 'vital' effects complicate the application of the boron isotope paleo pH method. Laboratory results on inorganically precipitated calcite are shown for comparison.

The boron isotope results create a huge problem for they are in clear conflict with the conclusions drawn from the glacial to interglacial change in lysocline depth. While the latter evidence calls on only a modest change in the carbonate ion content of deep water, the former requires a whopping change. If the boron isotope-based change of 0.3 pH units is to be believed, the $\text{CO}_3^{=}$ ion content of glacial deep water must have been twice as great as today's. This would have saturated the entire oceanic water column with respect to calcite. CaCO_3 should have accumulated everywhere on the sea floor. But clearly the sediments tell us that this didn't happen.

Does this mean that the boron isotope paleo pHs of Hemming and Sanyal must be tossed in the waste basket? Not necessarily. David Archer, while a research scientist at Columbia's Lamont-Doherty, came up with an explanation as to how the lysocline might be displaced well above the saturation horizon. His argument runs as follows. Assume that for some reason during glacial time the rain rate of organic matter (relative to that of CaCO_3) to the sea floor was much greater than today's. If so, the reduction of the $\text{CO}_3^{=}$ ion concentration caused by the release of respiration CO_2 to the sediment pore waters would have been correspondingly increased (see figure 59). This increase would have raised the extent of dissolution and thereby unbalanced the ocean's calcite budget; i.e., the supply of ingredients for the manufacture of calcite would have outstripped the rate of burial of calcite. This consequent rise in the $\text{CO}_3^{=}$ ion concentration would have eventually compensated for the extra respiration CO_2 , restoring the balance between input and loss. Hence the shoaling of the lysocline caused by the increase in the production of respiration CO_2 would have been compensated by a deepening of the saturation horizon!

While the Archer hypothesis does provide a way to make compatible the lysocline and boron isotope evidence, it is not without its problems. What is responsible for the required rise in the rain rate of organic matter to the sea floor? One suggestion is that the ocean's dissolved silica reached a far greater fraction of surface waters than it does today.

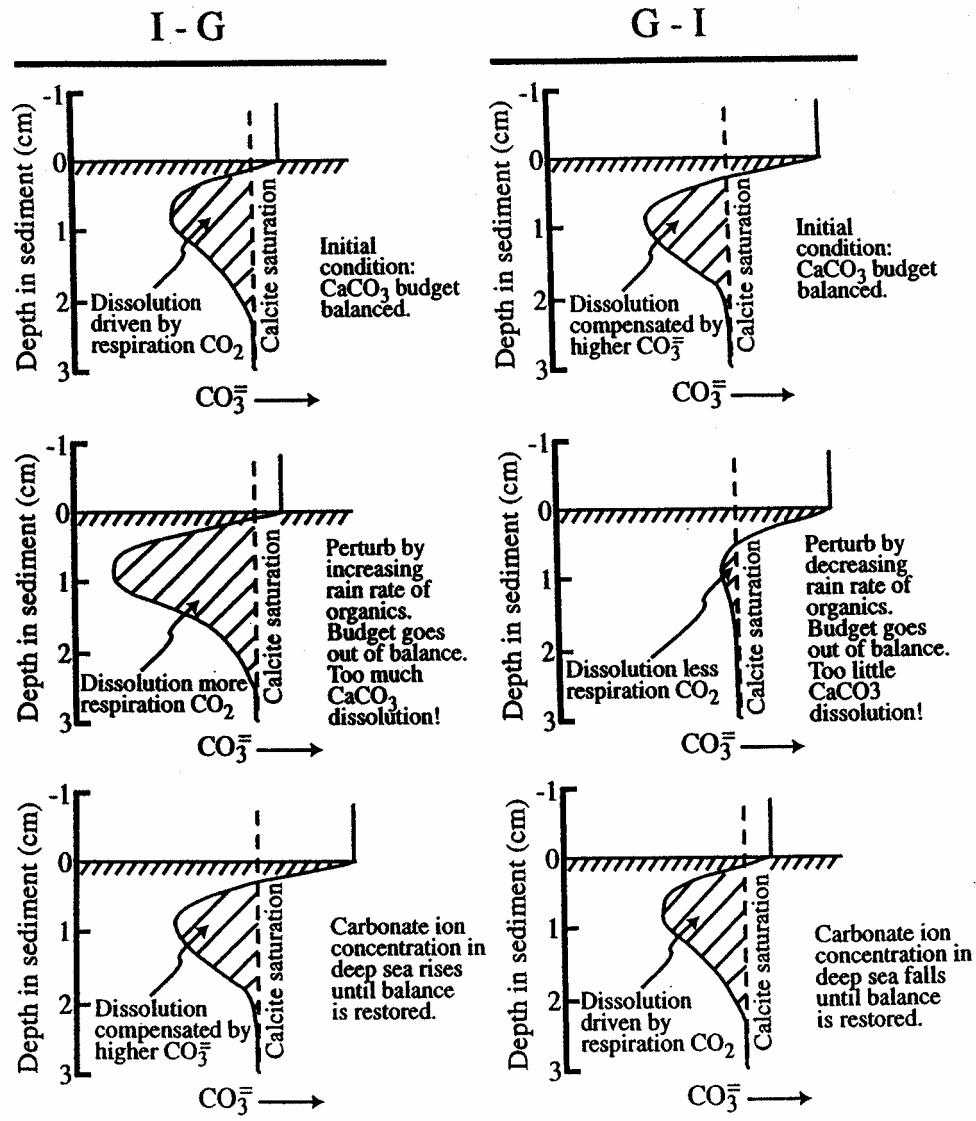


Figure 59. Shown here on the left is the sequence of events envisioned by Archer and Maier-Reimer (1994) for the transition from interglacial to glacial conditions. An increase in respiration CO_2 release to the sediment pore waters enhances calcite dissolution, thereby unbalancing the CaCO_3 budget. This imbalance leads to a buildup in $\text{CO}_3^{=}$ ion concentration in the deep sea until it compensates for the extra respiration CO_2 . On the right is the sequence of events envisioned for the transition from glacial to interglacial conditions. The input of excess respiration CO_2 to the sediments ceases, thereby reducing the rate of calcite dissolution. This leads to a reduction in carbonate ion concentration which continues until steady state is reestablished.

If so, diatoms would replace CaCO_3 producing organisms, and in so doing, increase the rain of organic matter relative to CaCO_3 . However, no sedimentary evidence has been found which supports this hypothesis. Further, to be effective, this increase would have to encompass all the areas where CaCO_3 currently accumulates. For were it not geographically uniform, huge ‘bumps’ in the depth of the glacial lysocline would have been created. None have been identified. Another flaw tarnishes Archer’s clever scheme. At the end of glacial time when the extra flux of CO_2 into sediment pore waters was shut down, the deep ocean would have been left with a large CO_3^{\equiv} ion excess. The accumulation of CaCO_3 in sediments below the glacial lysocline would have gradually disposed of the CO_3^{\equiv} excess. However, in so doing it would have created a layer of CaCO_3 about three centimeters thick over the entire abyssal sea floor. In all likelihood this CaCO_3 would have been bioturbated into the underlying red clay. Currently no trace of this CaCO_3 remains. Abyssal plain sediment has less than 0.2 percent CaCO_3 . It is very difficult to imagine that in a brief period of 10,000 years this CaCO_3 could have been so efficiently dissolved.

CLOCKS

INTRODUCTION

If we are ever to solve the knotty problem of how the Earth's climate machine gets pushed back and forth between conditions akin to today's and those of the last full glacial, we must be able to precisely correlate events which took place at various places on the globe. Fortunately, radioisotope clocks permit this to be done. These clocks provide a chronologic framework upon which the climatic records can be hung. Three radioisotopes are of particular importance: ^{14}C , ^{230}Th and ^{40}K . In addition, the so-called cosmogenic isotopes, ^{10}Be , ^{26}Al and ^{36}Cl have in recent years assumed an important role. Because the disintegration rates of radio isotopes are immutable, ages derived from them are inherently absolute. However, as each of these clocks is subject to its own particular set of "geochemical" biases, one isotope clock must be checked against another and against ages based on annual layer counting (in ice, sediments and trees) and on planetary periodicities (precession, obliquity and eccentricity).

THE RADIOCARBON CLOCK

The most widely applied radioisotope method is that based on the decay of ^{14}C , a radioisotope with a half life of 5730 years. Radiocarbon ages provide a detailed chronology for the last 40 thousand years for deep sea sediments, bog and lake deposits and glacial moraines.

Radiocarbon is produced in the atmosphere by cosmic rays. Protons whipped up to great speeds by the galactic magnetic field smash into atmospheric nuclei knocking loose neutrons. The fate of most of these neutrons is to penetrate the nucleus of a nitrogen atom and bump out a proton thereby converting the stable ^{14}N into radioactive ^{14}C . On average radiocarbon atoms created in this way survive for 8270 years before succumbing to radioactive decay (see figure 1). During their lifetimes, ^{14}C atoms become dispersed through the Earth's active carbon reservoirs. In particular they "tag"

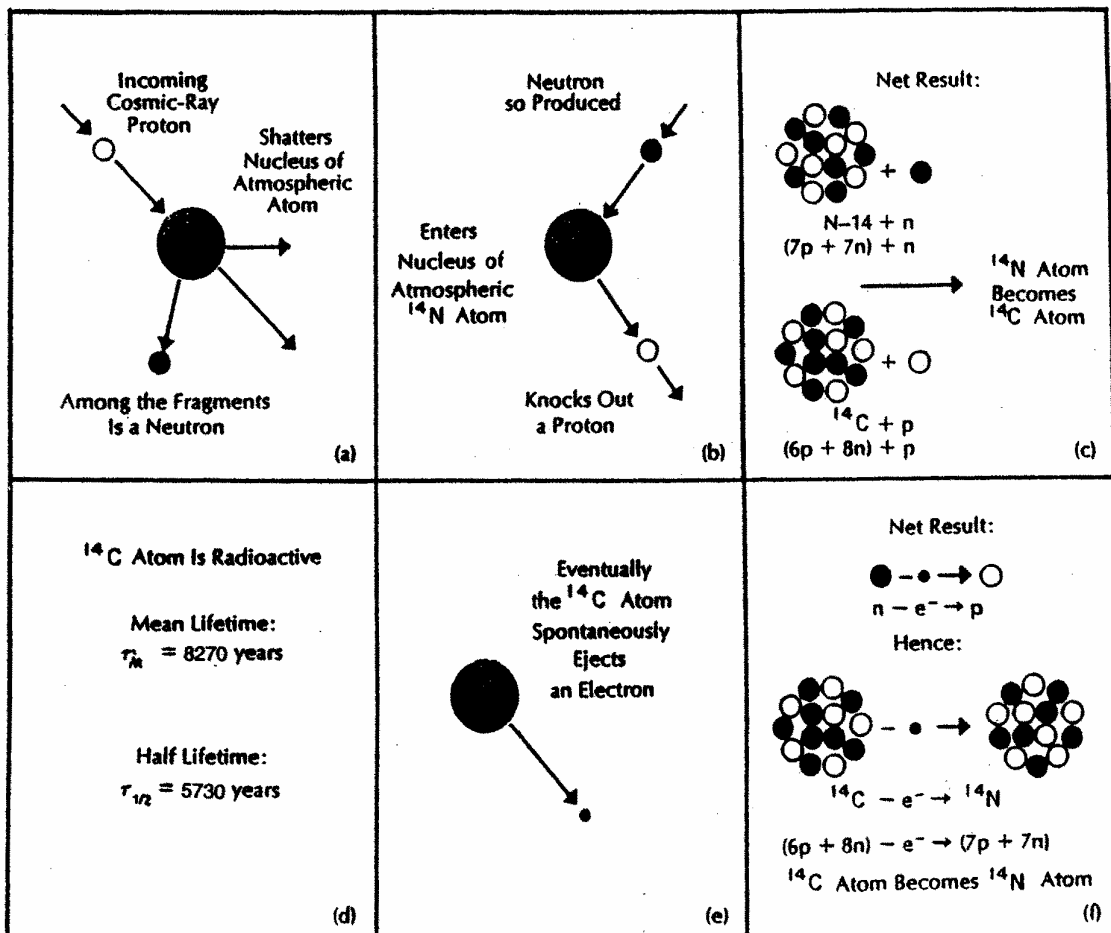


Figure 1. The "life cycle" of a carbon-14 atom. Created in the atmosphere by the collision of a neutron with a nitrogen atom, the average ^{14}C atom "lives" for 8270 years. Its existence is terminated by the ejection of an electron which returns the atom to its original form, ^{14}N .

carbon dioxide molecules in the atmosphere and bicarbonate ions dissolved in the Earth's surface waters. As CO_2 and HCO_3^- are the sources of the carbon fixed during photosynthesis and of that incorporated into CaCO_3 shells, fossil remains provide an archive of datable material.

Three problems must be confronted by those who apply the radiocarbon method. The first has to do with an assumption basic to the method, namely that the $^{14}\text{C}/\text{C}$ ratio in atmospheric CO_2 has remained constant with time. However, the fact that radiocarbon ages differ from those obtained for materials whose calendar age has been independently established tells us that the radiocarbon content of atmospheric CO_2 has changed with time. Fortunately, much of the complication introduced by these fluctuations is avoided through the use of so-called radiocarbon years. Ages in radiocarbon years are calculated assuming that the $^{14}\text{C}/\text{C}$ ratio in atmospheric CO_2 was always the same as it was in the year 1850. The zero year on this time scale is 1950 in honor of the completion of the first radiocarbon age determination in Willard Libby's University of Chicago laboratory. Radiocarbon years are also based on his original estimate of radiocarbon's half life, i.e., 5568 years instead of on the best current estimate, i.e., 5730 years. The important point is that even though radiocarbon years do not exactly match calendar years, their use permits precise correlation and sequencing of events from throughout the world. We will return to the problem of converting radiocarbon years to calendar years later in this section.

The second problem has to do with the difference between the $^{14}\text{C}/\text{C}$ ratio in atmospheric CO_2 (hence also in organic matter synthesized by plants which obtain their carbon from the atmosphere) and that in the HCO_3^- of natural waters (and hence in the CaCO_3 produced from this carbon). Because the rate of exchange of CO_2 between the atmosphere and surface waters is finite, the $^{14}\text{C}/\text{C}$ ratio in HCO_3^- is always somewhat less than that in atmospheric CO_2 . In the case of the ocean, this radiocarbon deficiency is the result of radiodecay and in the case of continental waters, it is the result of the

Table 1. ^{13}C normalization of radiocarbon concentrations: The radiocarbon distribution in contemporary materials is influenced both by the incomplete mixing of radiocarbon atoms among the active carbon reservoirs and by isotope separations during chemical reactions. Because it depends on the mass difference, the separation between ^{14}C and ^{12}C is exactly twice that between ^{13}C and ^{12}C . Hence, the influence of isotope fractionation can be eliminated using measurements of the ^{13}C to ^{12}C ratio in the samples carbon. The examples in the table represent the situation which existed in 1850 before the onset of large scale burning of fossil fuels. Without the correction for isotope separations during chemical reactions, the radiocarbon content of wood and shell (at least that formed in mid and low latitude surface ocean water) turns out, by chance, to be the same. The reason is that the deficiency of radiocarbon in surface ocean HCO_3^- created by radiocarbon decay is by chance balanced by the enrichment of ^{14}C through isotope separation. To avoid confusion, radiocarbon results are always corrected for differences created by isotope separation. These separation-corrected results are expressed in $\Delta^{14}\text{C}$ units (see below).

	$\frac{^{13}\text{C}/^{12}\text{C}}{^{13}\text{C}/^{12}\text{C std}}$	$\delta^{13}\text{C}$ ‰	$\frac{^{14}\text{C}/^{12}\text{C}}{^{14}\text{C}/^{12}\text{C std}}$	$\delta^{14}\text{C}$ ‰	$\Delta^{14}\text{C}$ ‰
Atmospheric CO_2	.993	-7	1.036	+36	0
Wood	.975	-25	1.000	0	0
Surface Ocean ΣCO_2	1.002	+2	1.000	0	-54
Shell	1.002	+2	1.000	0	-54

where

$$\delta^{13}\text{C} = \left[\frac{^{13}\text{C}/^{12}\text{C sample} - ^{13}\text{C}/^{12}\text{C standard}}{^{13}\text{C}/^{12}\text{C standard}} \right] 1000$$

$$\delta^{14}\text{C} = \left[\frac{^{14}\text{C}/\text{C sample} - ^{14}\text{C}/\text{C standard}}{^{14}\text{C}/\text{C standard}} \right] 1000$$

$$\Delta^{14}\text{C} = \delta^{14}\text{C} - 2(\delta^{13}\text{C} + 25) \left(1 + \frac{\delta^{14}\text{C}}{1000} \right)$$

dissolution of ancient limestone. Radiocarbon measurements on CaCO_3 from deep sea sediments, coral reefs and from lake sediments must be corrected for this so-called reservoir effect.

The most reliable of these corrections is for material (mainly shells and coral) formed in surface waters of the tropical and temperate ocean (see table 1). About 400 years must be subtracted from their ^{14}C ages in order to correct for the deficiency of ^{14}C in surface ocean HCO_3^- . This correction is accurate to perhaps ± 160 years. Larger corrections are required for materials formed in the polar oceans and in lakes. Not only are these corrections larger but they are subject to a wider range of uncertainty. In the case of lake and bog deposits, this correction can often be circumvented by dating fragments of terrestrial plant matter blown into the lake. This is possible because the AMS (see table 2) method requires only a fraction of a milligram of carbon. Hence, a single pine needle or leaf stem can be dated.

The third problem has to do with contamination with younger carbon. Such contamination can be mechanical (for example, rootlet intrusion) or chemical (for example, humic acid infiltration). The impact of a given amount of contamination with recent carbon becomes twice as great for each half life the dating range is extended; for example, contamination with a given amount of recent carbon has 16 times more serious consequences for a sample 34,000 years in age than for a sample 11,000 years in age (i.e., 4 half lives younger). Again the advent of AMS has been a great help in this regard for it allows small amounts of material less prone to contamination to be hand picked or chemically extracted. Nevertheless, radiocarbon dates on materials beyond 45,000 years in age, while technically possible, are of questionable reliability. As such samples contain less than 0.5% of their original radiocarbon, contamination becomes an insuperable problem.

ANNUAL CLOCKS

For a few places on earth absolute chronologies have been developed based

Table 2. Radiocarbon Measurement Methods

Decay counting method

Libby's method for measuring radiocarbon involves detection of the beta particles ejected when ^{14}C atoms undergo radioactive decay. One gram of carbon from a sample 2 half-lives old (i.e., about 11,000 years old) produced about 3 decay events per minute. Hence in order to measure the 10,000 events required in order to achieve a precision of 1%, the sample would have to be counted for about 2 days.

Atom counting method

In the early 1980s, a method was developed which permitted radiocarbon atoms themselves to be measured. One milligram of carbon 2 half-lives old contains about 15 million ^{14}C atoms. Thus for a sample of this size, only one atom in about 1,000 need be detected in order to reach the 10,000 events required for 1% precision. This is now done routinely by a technique called Accelerator Mass Spectrometry (AMS). The measurement can be made in less than one hour.

simply on counting annual bands. Despite their limited applicability, these chronologies offer an absolute calibration for the radiocarbon scale. Of greatest importance is the record kept by trees. Because of the strong seasonality, trees grown at mid and high latitudes produce easily identified annual rings. Further, as the thickness of the ring formed in a given year depends on environmental conditions, a unique sequence of thicknesses develops for a given species of tree in a given region. This signature permits the construction of an overlapping sequence of fossil logs (see figure 2) which after thorough replication provides a continuous chronology good to a single year! Through a lifetime effort by the late Bernt Becker, such a sequence has been created from oak logs recovered from alluvial deposits in the river valleys of southern Germany. It now extends back to 7938 BC (i.e., 9888 calendar years before 1950). Precise radiocarbon measurements on wood from these trees permits the radiocarbon age scale to be converted to absolute ages. The difference between the radiocarbon time scale and the absolute time scale obtained from radiocarbon measurements on ring dated wood is shown in figure 3.

No oaks older than 7938 BC have been found. Presumably they were unable to grow in Germany because the winters were too cold. Instead pine forests covered the area. But fortunately, a pine chronology has been created which overlaps the early portion of that based on the oaks allowing the combined chronology to be extended to about 11,500 calendar years. Before his death in 1994, Becker had convinced himself and his collaborators that a firm tie between the oak and pine chronologies had been established. This was done by comparing the thickness signatures during a two hundred-year period of overlap. This correlation was strengthened by highly precise ^{14}C measurements carried out by Bernt Kromer at Heidelberg University on both oak and pine samples spanning the period of overlap.

A second approach is to make use of annually layered (i.e., varved) sediments. While more problematic than trees, these sediments offer the potential to extend the ^{14}C

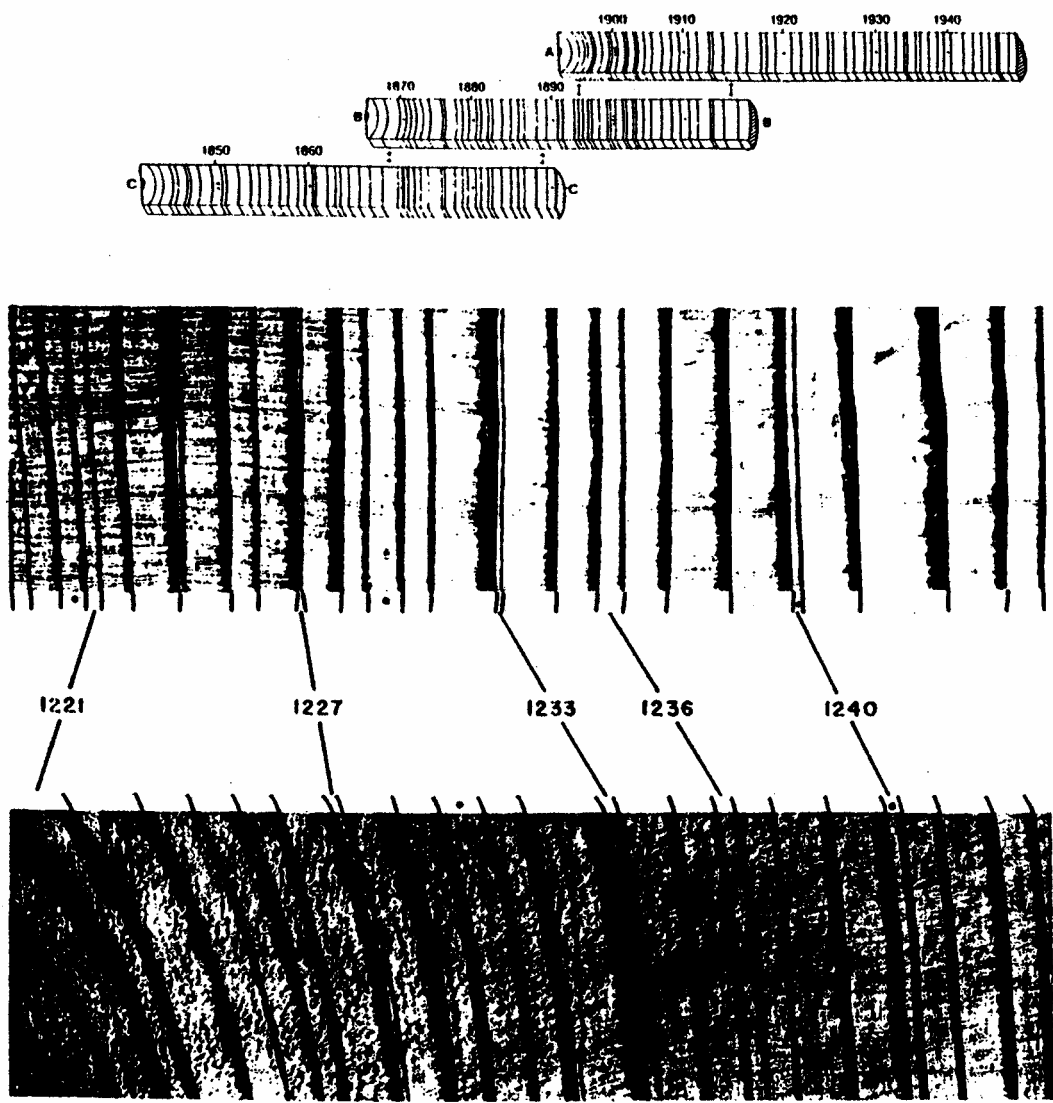


Figure 2. The lower panel shows actual photographs of ring sequences from two neighboring trees and the correlation between them. The upper panel show how the overlap between records can be used to build a master chronology.

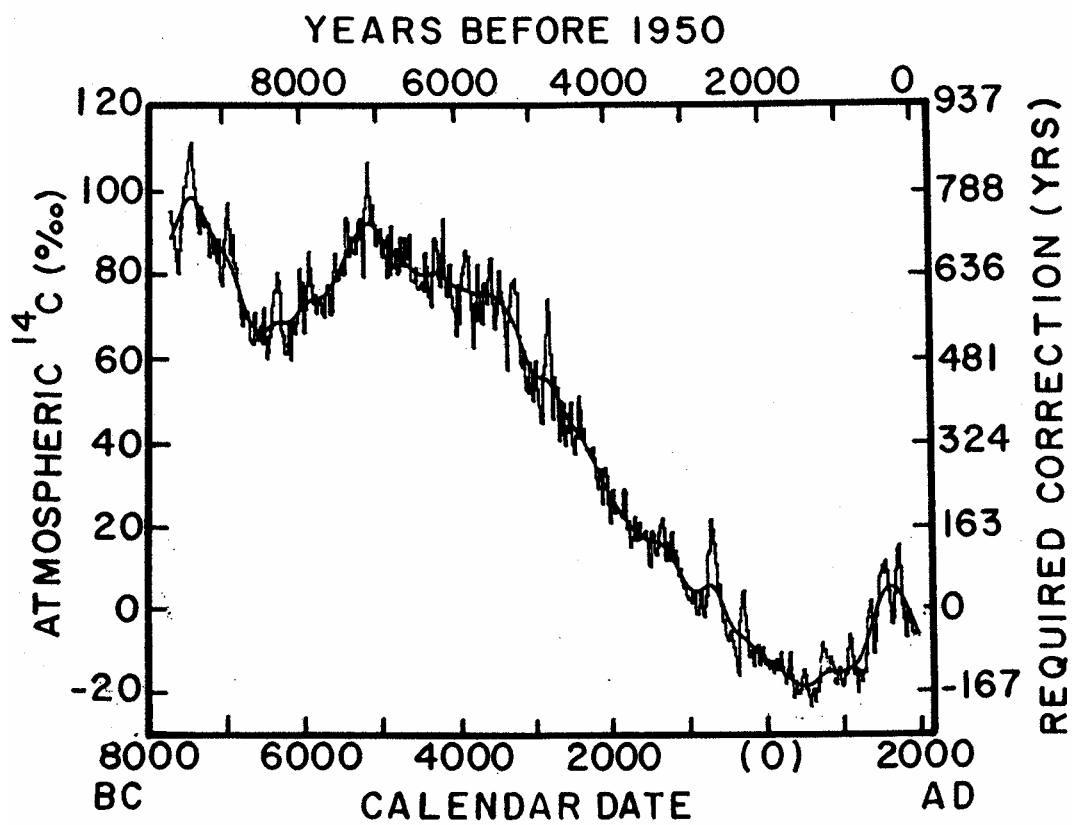


Figure 3. Atmospheric $\Delta^{14}\text{C}$ values in per mil reconstructed from Becker's master oak chronology for the past 9600 yr. The time scale (in year A.D. or B.C.) was derived from dendrochronologically dated wood, with each data point covering 20 yr. Data from Stuiver and Pearson, 1986; Stuiver and Becker, 1986; Pearson et al., 1986; Linick et al., 1985; Stuiver et al., 1986a; Kromer et al., 1986; and Linick et al., 1986. The scale on the right shows the correction required to convert radiocarbon ages to calendar ages. For example objects with ages in the range 6000 to 7000 thousand calendar years yield radiocarbon ages averaging about 600 years too young.

calibration beyond the limit so far achieved using fossil trees (i.e., through the Younger Dryas cold excursion back into the preceding Bolling-Allerod warm interstadial). As radiocarbon measurements on macrofossils found in the sediments can be used to 'splice' these varve records onto the master tree-ring chronology, it is not necessary to find a record with annual layering extending right up to the present. If, over the period of overlap between the varve and dendro records, the number of varves counted for the interval between a pair of radiocarbon ages matches the number of dendro years between these same ^{14}C ages, then it can be demonstrated that the sediment layering is indeed annual, and assurance is given that no serious bias results from false or missing years.

To me, the most interesting of these records is that for sediments from the Cariaco Basin off Venezuela. From about 14,000 years ago to the present its deep waters (isolated from the Caribbean Sea by a shallow sill) were anaerobic. In the absence of benthic organisms capable of stirring the sediment, the annual cycle of sediment composition is preserved. While a graduate student at the University of Colorado, Conrad Hughen, counted the layers in the lower portion of this sequence and also obtained 50 or so ^{14}C ages on planktonic foraminifera shells which allowed him to splice his record onto that for the German tree-ring series. In this way, he was able to extend the reconstruction of the atmospheric ^{14}C to C record back beyond the Younger Dryas into the preceding Bolling-Allerod warm period. As discussed in the section on 'Records,' he came up with an astounding discovery.

Most famous among the varved lake records is that constructed for a series paleolakes extending over several hundred kilometers along the eastern margin of Sweden. The sequence follows the path of retreat of the Scandinavian ice sheet. For each lake, the record begins with deglaciation and extends through the period when ice margin remained in the lake's immediate vicinity. The records from individual lakes are then correlated using varve thickness signatures in exactly the same way as tree section chronologies are constructed (see figure 4). This method works particularly well for

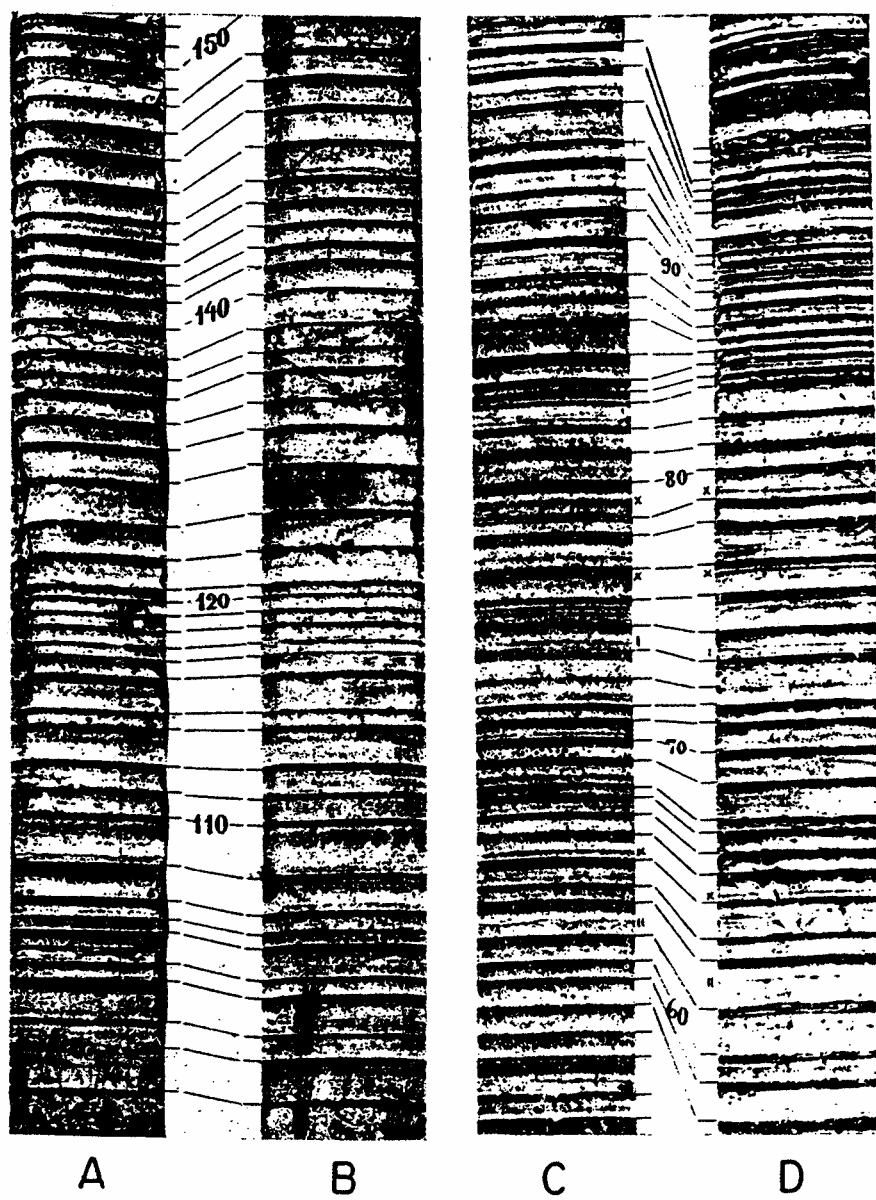


Figure 4. Photographs of annually-varved sediments of Swedish lakes. Each varve consists of a dark winter layer and a light summer layer. Sections A and B were taken 750 meters from one another in the same lake. Sections C and D are from localities separated by 45 kilometers (Sauramo, 1929).

these particular lakes because the thickness of the layer deposited during a given year depends on the extent of glacial melting and hence on regional summer temperature. Unfortunately, material datable by radiocarbon is largely absent.

The third annual layer sequence of importance is that kept in Greenland ice. Seasonality is imprinted in ice in a number of ways. First of all, it shows up visually. During the summer period of intense sunlight, a hoar frost layer forms in the snow (sunlight which penetrates into the snow pack raises the temperature causing water vapor to migrate to the surface where it refreezes). These layers persist yielding more coarsely crystalline layers in the lithified ice. As shown in figure 5, seasonal couplets are also seen in the $^{18}\text{O}/^{16}\text{O}$ ratio in the ice (reflecting the annual cycle in air temperature), and in impurities in the ice reflecting seasonality in dust and sea salt inputs. In the GRIP and GISP II cores from Greenland's Summit, annual layers can be readily resolved back to about 40,000 years ago. The reason for this limit is that the deeper a layer is buried the more it has thinned by lateral spreading (see figure 6). This thinning eventually becomes so severe that the annual layers can no longer be reliably identified. Below about 40,000 years in the summit Greenland ice cores, the annual layers become difficult to identify and hence the year counts more tentative. Unfortunately, this beautiful annually layered sequence cannot be used in a direct way to calibrate the radiocarbon method. The reason is that two problems prevent reliable radiocarbon dating, one technical and the other geochemical. The technical problem relates to the rarity of CO_2 in ice. Even by the most sensitive AMS methods, 8 kilograms of ice must be processed to get enough carbon for analyses. Even then, contamination during extraction rears its ugly head! The geochemical problem is twofold. First, Devendra Lal and coworkers in La Jolla and Tucson have shown that ice contains extra ^{14}C atoms generated by cosmic ray bombardment of oxygen nuclei in the snow pack. The second has to do with the presence of radiocarbon-free dust grains from ancient limestone. This fine calcite may partially dissolve. At this point, the prospects for obtaining sufficiently accurate ^{14}C ages

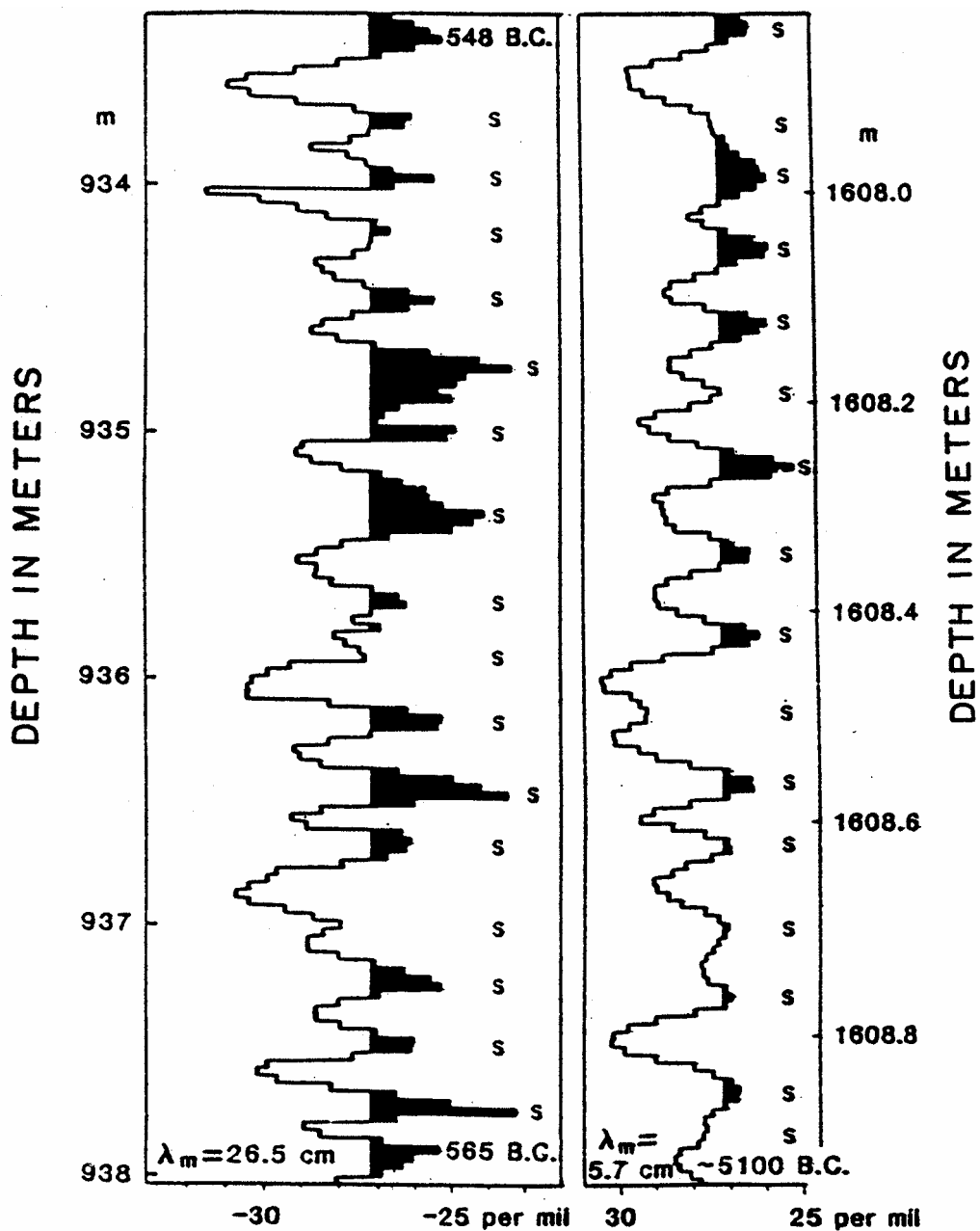


Figure 5. Demonstration of how both the layer thickness and the amplitude of the seasonal cycle in oxygen isotope ratio shrink as the ice is buried more deeply. The average thickness of an annual layer drops from 26.5cm at 2500 calendar years (i.e., 550 BC) to 5.7cm at 7000 calendar years (i.e., 5050 BC).

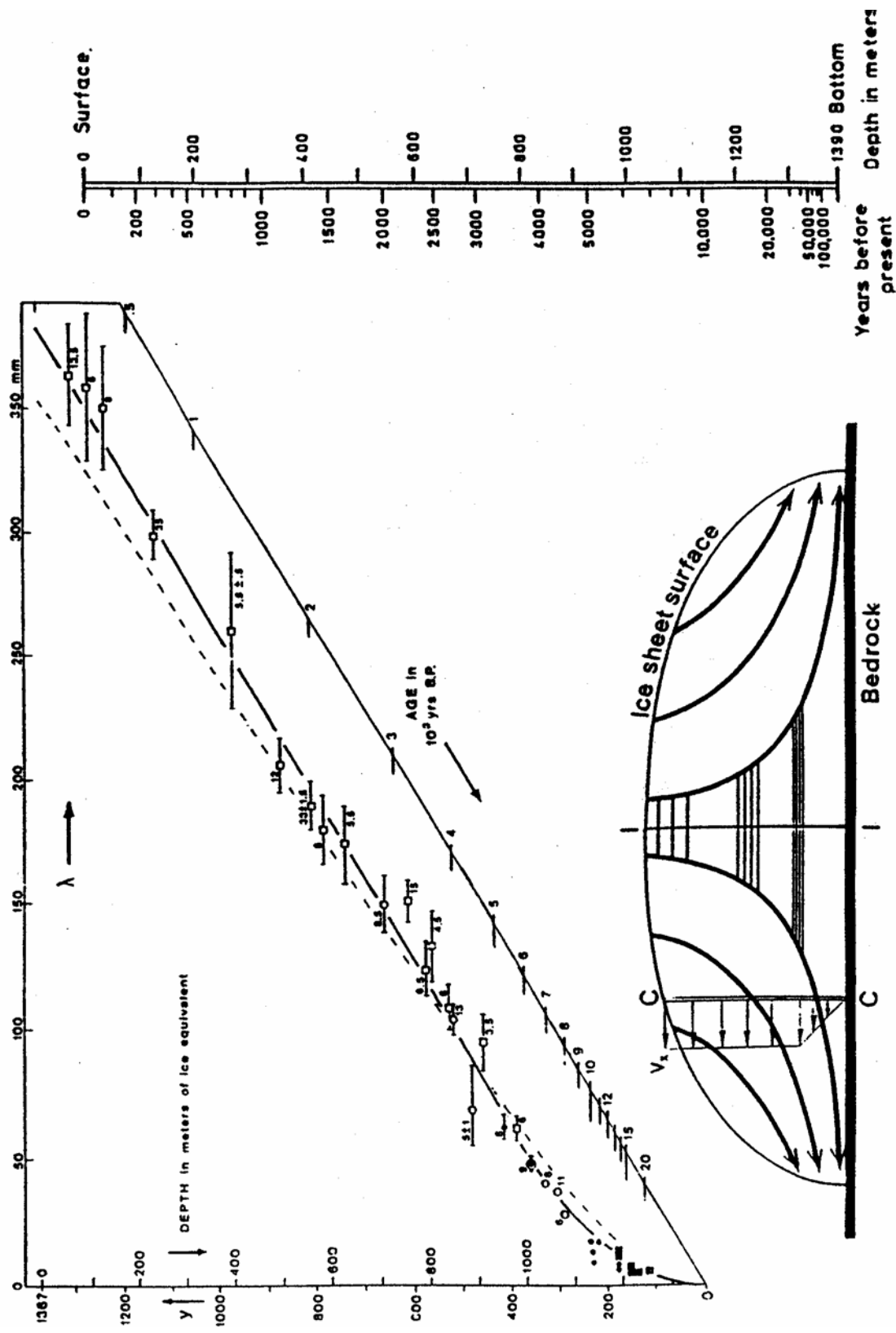


Figure 6. As shown at the lower left layers in the ice thin as they spread laterally. The extent of thinning can be determined from the change in the thickness of seasonal couplets. Measurements of this type are shown for the Camp Century Greenland ice core in the upper left part of the diagram. This thinning leads to a great distortion in the age versus depth relationship (see nomograph on the right hand side).

on the CO₂ trapped in ice are dim. However, an indirect means exists for applying the ice core chronology to the absolute calibration of the radiocarbon time scale. Three events very clearly marked in the ice core also appear in lake records that can be dated by radiocarbon (i.e., the beginning of the Bolling-Allerod warm episode, the beginning of the Younger Dryas cold episode, and the end of the Younger Dryas cold episode. Radiocarbon dates on the beginning of the Bolling-Allerod come out to be about 12,700 years. The ice core age is 14,400. Hence at this time, the radiocarbon scale is off by 1700 years. Radiocarbon dates for the beginning of the Younger Dryas come out to be about 11,000 years. The ice core age is 12,700 years. Again, the radiocarbon age is 1700 years too young. Finally, the radiocarbon age for the end of the Younger Dryas is about 10,000. The ice core age is 11,500 years. So the offset is perhaps a bit smaller, 1500 rather than 1700 years.

THE URANIUM-THORIUM CLOCK

Long lived ²³⁸U decays to form ²³⁰Th, an isotope with a half life of 77,000 years (see table 3). This “parent-daughter” pair holds the potential for dating back to several hundred thousands of years. Corals are ideal for its application. One reason is that, unlike most marine organisms, corals incorporate uranium atoms into their aragonitic mineral lattice in nearly the same ratio to calcium atoms as they exist in sea water. Thus, so long as the aragonite does not recrystallize, the uranium atoms and their thorium daughter products should remain firmly bound. Further, because uranium is quite soluble in sea water, coraline aragonite contains about three parts per million, giving rise to easily measured amounts of ²³⁰Th.

More important to the suitability of corals as a chronometer is the fact that when formed they are entirely free of the element thorium. The absence of thorium reflects the extreme insolubility of this element in sea water. Unlike uranium atoms which reside in the sea for several hundred thousand years before being removed to the sediment, thorium atoms reside in the sea for no more than 100 years. The reason is that they

Table 3. Geochemistry of ^{234}U

In addition to ^{238}U and ^{230}Th , a third isotope ^{234}U is involved in coral dating. It fits into the decay sequence as follows:

Isotope	Half Life	
^{238}U	4.47×10^9 years	emits an α particle to become
^{234}U	244,000 years	emits an α particle to become
^{230}Th	77,000 years	emits an α particle to become ...

At birth, ^{234}U atoms receive a strong jolt supplied by the launch of an alpha particle by its parent, ^{238}U . This so-called recoil knocks them loose from their position in the mineral lattice making ^{234}U atoms more susceptible to leaching into passing waters. For this reason, most natural waters including seawater, have a ^{234}U to ^{238}U activity ratio greater than unity.

For sea water the excess ^{234}U activity is 15% (i.e. $A^{234}\text{U}/A^{238}\text{U} = 1.15$). Once incorporated into a coral this excess will decay away in accord with the 244,000 year half life of ^{234}U . This decay must be accounted for in the calculation of ^{230}Th ages. This is done through the use of the following equation

$$\frac{A_{230}}{A_{234}} = \frac{A_{238}}{A_{234}} \left(1 - e^{-\lambda_0 t} \right) + \left(1 - \frac{A_{238}}{A_{234}} \right) \left(\frac{\lambda_0}{\lambda_0 - \lambda_4} \right) \left[1 - e^{-\lambda_0 - \lambda_4 t} \right],$$

Where A denotes specific activities(e.g., dpm/g) with subscripts 238, 234, and 230 referring to ^{238}U , ^{234}U , and ^{230}Th , respectively; λ_0 and λ_4 are decay constants of ^{230}Th and ^{234}U ; and t is the sample age which can be calculated by iteration from the measured $^{230}\text{Th}/^{234}\text{U}$ and $^{234}\text{U}/^{238}\text{U}$ activity ratios.

Table 3 con't.

Examples of the concentrations and the radioactivities of these three isotopes for corals of three different ages are as follows:

NEWLY FORMED CORAL

	CONCENTRATION 10^{-6} gm/gm gm	CONCENTRATION atoms/gm	ACTIVITY disintegrations/min
^{238}U	3.2	8.09×10^{15}	2.40
^{234}U	-	5.11×10^{11}	2.76
^{230}Th	-	0.00×10^{11}	0.00

124,000 YEAR OLD CORAL

^{238}U	3.2	8.09×10^{15}	2.40
^{234}U	-	4.91×10^{11}	2.65
^{230}Th	-	0.95×10^{11}	1.71

ANCIENT CORAL

^{238}U	3.2	8.09×10^{15}	2.40
^{234}U	-	4.44×10^{11}	2.40
^{230}Th	-	1.33×10^{11}	2.40

become firmly attached to particles and are efficiently carried to the sediments beneath the sea. In coastal surface waters where particles are abundant, removal occurs in a year or less. So low is the ^{230}Th content of newly formed coral and so sensitive the mass spectrometric technique, that age measurements accurate to a decade can be made on young corals.

The coral clock works in a very simple way. Initially corals are free of ^{230}Th . With time, the content of ^{230}Th rises until its rate of radioactive decay exactly matches that of its parent uranium. The extent to which growth toward steady state has been accomplished provides a precise measure of the coral's age.

Because of these geochemical peculiarities, corals are a near perfect hour glass (i.e., it initially contains an inexhaustible supply of sand [i.e., ^{238}U] in its upper chamber and with less than 1 year's worth of sand [i.e., ^{230}Th] in its lower chamber). Further, when stored in suitable environments, the hour glass is leak proof, no extra sand gets in and no sand escapes. Under these circumstances, the ^{230}Th to ^{238}U ratio in a fossil coral provides a very accurate measure of the time elapsed since the coral formed.

When dating corals, the concentration of a third isotope, ^{234}U (see table 3), must be measured. ^{234}U is produced by the decay of ^{238}U . In turn it decays to form ^{230}Th . The kick received by the parent ^{238}U atom when it ejects an α particle makes its daughter ^{234}U susceptible to chemical leaching. Hence natural waters, including sea water, are enriched in ^{234}U relative to ^{238}U . Because of this corals form with an excess of ^{234}U . As the coral ages, this excess decreases in accord with ^{234}U 's half life of 244,000 years. One of the most valuable checks on the requirement that the fossil coral have been stored in a suitable environment is to determine whether or not the age corrected $^{234}\text{U}/^{238}\text{U}$ ratio in corals is the same as in today's sea water. Diagenetic alteration of the coral generally leads to higher than expected ^{234}U to ^{238}U ratios.

Because of the perfection of their ^{230}Th clocks, corals became the obvious candidate for extending the calibration radiocarbon clock beyond the tree ring limit. The

difficulty is that from 35,000 years ago (the practical limit for precise ^{14}C dating) to 11,000 years ago (the limit of the tree ring chronology), the sea stood more than 40 meters below today's level. The missing water was bound into the ice sheets of the last glacial period. Because of this, it has proven very difficult to obtain corals in this age range. A breakthrough in this regard came when Richard Fairbanks, of Columbia University's Lamont-Doherty Earth Observatory, managed to recover a series of corals ranging in radiocarbon age from 8000 to 19,000 years from borings made off the coast of Barbados. His colleagues, Bard and Hamelin, applied the highly accurate mass spectrometric method, developed at Caltech by Wasserburg and his associates, to these corals. While the ^{230}Th method had been used for dating corals since the early 1960s, only in 1985 when Edwards, Wasserburg and Chen demonstrated that direct atom counting using mass spectrometry provided results ten times more precise than the traditional alpha particle counting technique, did it become possible for this method to meet the challenge of calibrating the radiocarbon time scale. The Fairbank's team was astounded by the results they obtained. Beyond 10,000 years the difference between the ^{14}C and ^{230}Th ages grew larger and larger reaching 3,000 years during peak glacial time (see figure 7). A coral dating 18,600 years by radiocarbon yielded a radiothorium age of 21,900 years.

In defense of case that the departure is real, Bard and his colleagues point to ^{230}Th ages obtained on corals with ^{14}C ages falling within the tree ring calibration range. The coral results agree with those based on tree rings. In addition, Fairbank's corals are remarkably well preserved. Stored below the sea surface ever since their formation, they have escaped the ravages of caused by contact with corrosive ground waters. The finest septa remain undissolved. No conversion of aragonite to calcite has occurred. The age corrected ^{234}U to ^{238}U ratios are spot on the sea water values. Finally, the differences found in coral for times corresponding to the beginning and end of the Younger Dryas and the beginning of Bolling-Allerod are consistent with the differences between the

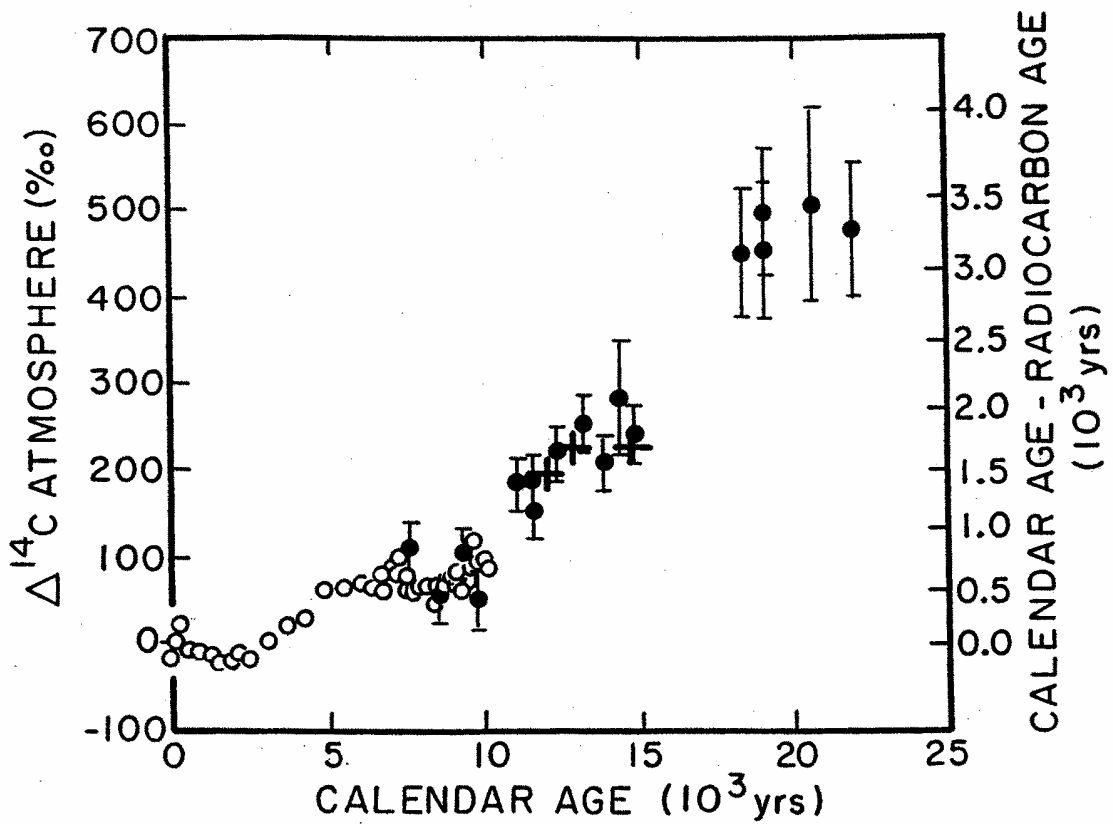


Figure 7. Difference between the ^{230}Th age and the ^{14}C age (calculated using the 5730 year half life with a subtraction of 400 years for the apparent age of surface ocean carbon) for corals from Barbados (solid circles) as obtained by Bard et al (1990). Also shown (open circles) are differences between tree ring and ^{14}C age (calculated using the 5730 year half life).

The three large (+s) are the results obtained for the three sharp climate boundaries mentioned earlier in this section (i.e., the beginning of the Bolling-Allerod warm episode, the beginning of the Younger Dryas cold episode, and the end of the YD). The calendar ages for these events were obtained by counting annual layers in the Summit Greenland ice cores and the radiocarbon ages by dating macrofossils from lake sediments.

macrofossil radiocarbon ages and ice core calendar-year ages for this event (see figure 7). This adds up to a very impressive case in favor of the coral-based calibration.

Recent measurements by Bill Thompson, while a graduate student at Lamont-Doherty, convincingly demonstrate that corals which have spent much of their history above sea level are subject to a curious diagenetic effect. They somehow incorporate both excess ^{230}Th and excess ^{234}U atoms. A correction for this anomaly can be made by extrapolating along the empirically determined slope for the ratio of these excess atoms on a $^{234}\text{U}/^{238}\text{U}$ versus $^{230}\text{Th}/^{234}\text{U}$ isotope development plot (see figure 8). While almost certainly related to the ejection of ^{230}Th and ^{234}U from coral as the result of alpha particle-induced recoils accompanied by re-absorption, the exact pathways followed remain obscure. As no conversion of aragonite to calcite has occurred in corals displaying this anomaly, it does not appear that re-crystallization is involved. In the absence of a correction for this addition, coral ages are too old. As shown by Thompson (see figure 9), the correction is far from insignificant.

^{230}Th and ^{14}C measurements on cave stalagmites offer a means to extend the Barbados calibration further back in time. Warren Beck of the University of Arizona and David Richards of the University of Bristol conducted a series of such measurements on a stalagmite from an underwater cave in the Bahamas. Prior to the flooding associated with the melting of the glacial ice caps, this cave was above sea level and hence underwent calcite deposition from prior to 45,000 years to 11,000 years ago. A series of 278 ^{14}C measurements and 81 ^{230}Th measurements document the evolution of both sets of ages over this time period. Stalagmites, however, suffer from two drawbacks not affecting corals. First of all, while the reservoir correction is reasonably well established for the surface ocean water in which corals grow, the CO_2 in cave waters is partly derived from the decay of soil organic matter and partly from dissolution of previously formed CaCO_3 . Hence the reservoir correction is larger and also less certain. Second, while corals are initially free of thorium, the Barbados stalagmite contains a small amount.

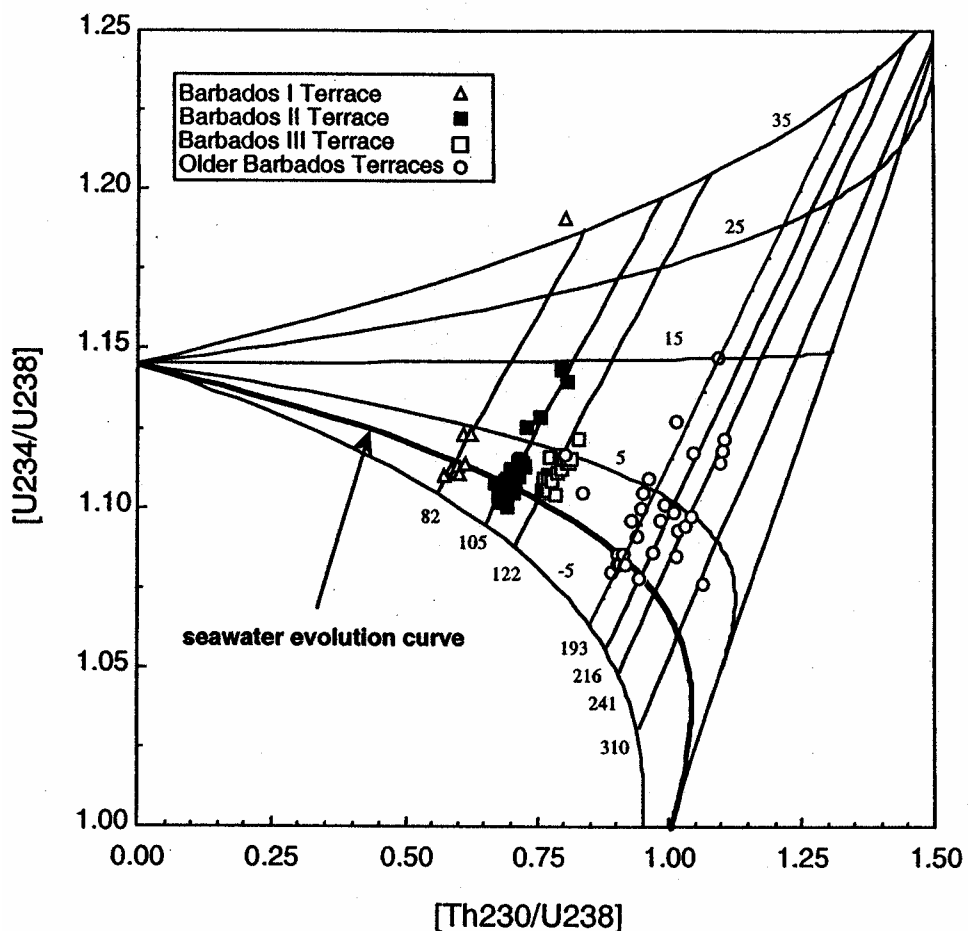


Figure 8. Measured U-series isotope ratios of Barbados corals plotted on an open-system diagram. Open-system evolution curves are labeled with their percent excess ^{234}U . The sub-vertical lines are open-system isochrons labeled with their ages in ka. Closed-system evolution from an initial $^{234}\text{U}/^{238}\text{U}$ ratio of modern seawater (1.145) is indicated by the bold curve. If the uranium isotopic composition of the ocean has not changed with time, and the corals have remained a closed system, all coral isotope measurements should plot on this line.

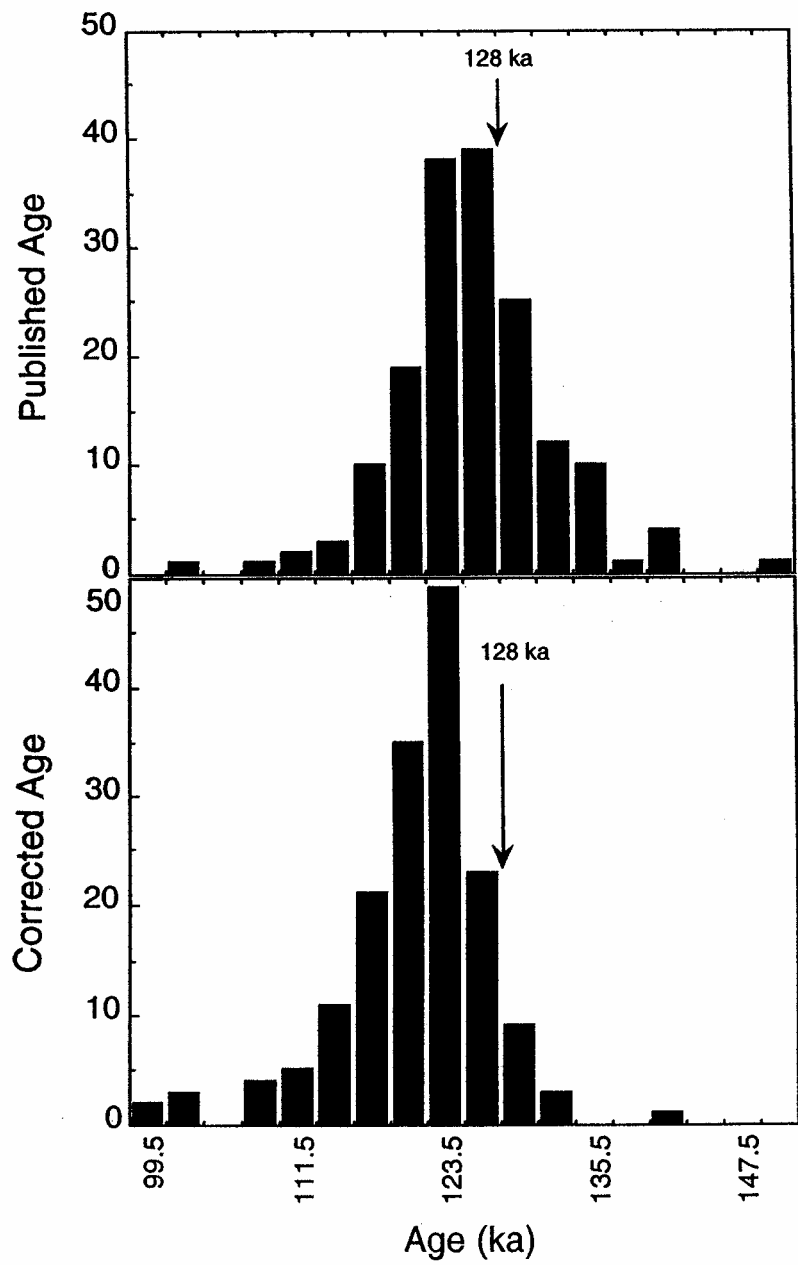


Figure 9. Histograms of last interglacial coral ages. In this summary of 166 coral ages, nearly one third of the published ages are older than the June 65°N insolation peak at 128 ka. However, when corrected for the addition of secondary ^{230}Th and ^{234}U , these corals tell a different story, with 92% of the ages younger than 128 ka.

Based on the overlap with the Barbados record, Beck and Richards were able to establish both the initial ^{14}C to C ratio and the initial ^{230}Th to ^{232}Th ratio. They assumed that these ratios applied to the entire time span recorded by the stalagmite. In this way, they established the radiocarbon-calendar age offset back to perhaps 35,000 calendar years (see figure 10). Beyond 35,000 years, the reliability of ^{14}C dates on calcite comes into question. So little of the original ^{14}C remains that contamination with tiny amounts of recent carbon lead to serious under estimates of the ages.

What might have caused the temporal changes in $^{14}\text{C/C}$ ratio required to explain the offset between the radiocarbon and calendar time scales? Two possibilities exist. One has to do with changes in the production rate of radiocarbon in the atmosphere. The other has to do with changes in the efficiency with which the earth's radiocarbon is mixed into the deep ocean reservoir. It turns out that observations exist which allow the second of these possibilities to be ruled out as a major player.

Measurements on ocean water HCO_3^- from various depths and geographic locations show that prior to the onset of anthropogenic perturbations (i.e. prior to about 1850 AD) surface ocean water HCO_3^- had on the average a 5% lower radiocarbon to carbon ratio than atmospheric CO_2 . For deep water the ratios ranged from 10% lower than atmospheric in the tropical Atlantic to 22% lower in the tropical Pacific. As the spread in $^{14}\text{C/C}$ ratio within the sea depends on the rate of deep water formation, it is possible that climate-related changes in these so-called ventilation rates are responsible for the deviations in the radiocarbon age from calendar ages. An important point to keep in mind in this regard is that, as roughly 80% of the carbon in the combined ocean-atmosphere reservoir resides in the deep sea, the major impact of mixing rate changes will be on the $^{14}\text{C/C}$ ratio in upper ocean and atmosphere carbon. For example, if the deep sea were to become totally isolated, all the Earth's radiocarbon would eventually be confined to in the upper reservoir and its $^{14}\text{C/C}$ ratio would rise by about a factor of five. As the deviations in the radiocarbon time scale are all in a direction requiring higher

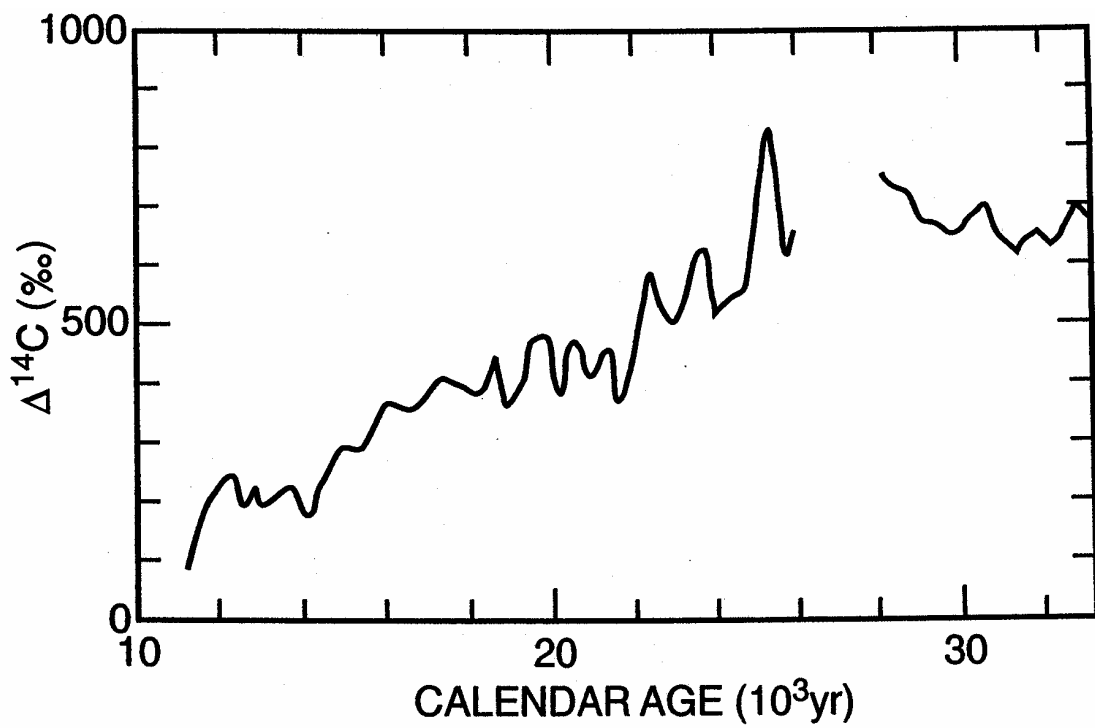


Figure 10. Reconstructed ^{14}C to C ratio (expressed in Δ units) for the period 11,000 to 33,000 calendar years as reconstructed from ^{14}C and ^{230}Th measurements on a stalagmite from a now submerged cave in the Bahamas (Beck et al., 2001).

$^{14}\text{C}/\text{C}$ ratios in upper ocean and atmosphere carbon, the possibility that they are the result of a glacial age slowdown in the ventilation rate of the deep sea must be taken seriously.

How is it then that this possibility can be rejected? The reason is that a means has been devised to determine the surface to deep ocean $^{14}\text{C}/\text{C}$ ratio difference during late glacial time (i.e., 22,000 to 15,000 calendar years ago). It takes advantage of the fact that two distinct kinds of microscopic shells are found in deep sea sediments. One type is manufactured by planktonic foraminifera living in surface water. The other is manufactured by benthic foraminifera living on the sea floor. Hence one type records the $^{14}\text{C}/\text{C}$ ratio for surface ocean water and the other $^{14}\text{C}/\text{C}$ ratio for deep ocean water. The important point is that when the organisms which inhabit them die, planktonic shells fall to the sea floor joining their benthic cousins. Despite the fact that both shell types lose radiocarbon by radiodecay, the age difference between the planktonic foraminifera and the coexisting benthic foraminifera does not change with time. Hence each layer of shell-bearing deep-sea sediment bears a record of the surface to deep difference in radiocarbon for the overlying water column.

As it would take about 300,000 of these tiny shells to yield the gram of carbon required by the traditional decay-counting method of ^{14}C dating, the exploitation of this record awaited the discovery of the atom-counting method of radiocarbon dating which allows the job to be done with just 300 shells. The results of measurements of benthic-planktonic shell pairs hand picked from glacial horizons reveal that the $^{14}\text{C}/\text{C}$ difference between surface and deep water was on the average just slightly greater than today's. These results (see figure 11 for summary) suggest that the surface to deep radiocarbon difference was enough larger during glacial time to create only a 200 or so year discordance between the radiocarbon and calendar time scales. In other words, it is by no means large enough to account for the 2,000- to 3,000-year discordance required to explain the $^{14}\text{C} - ^{230}\text{Th}$ age difference observed for late glacial Barbados corals.

Thus the discrepancy must be the result of a change in the rate of radiocarbon

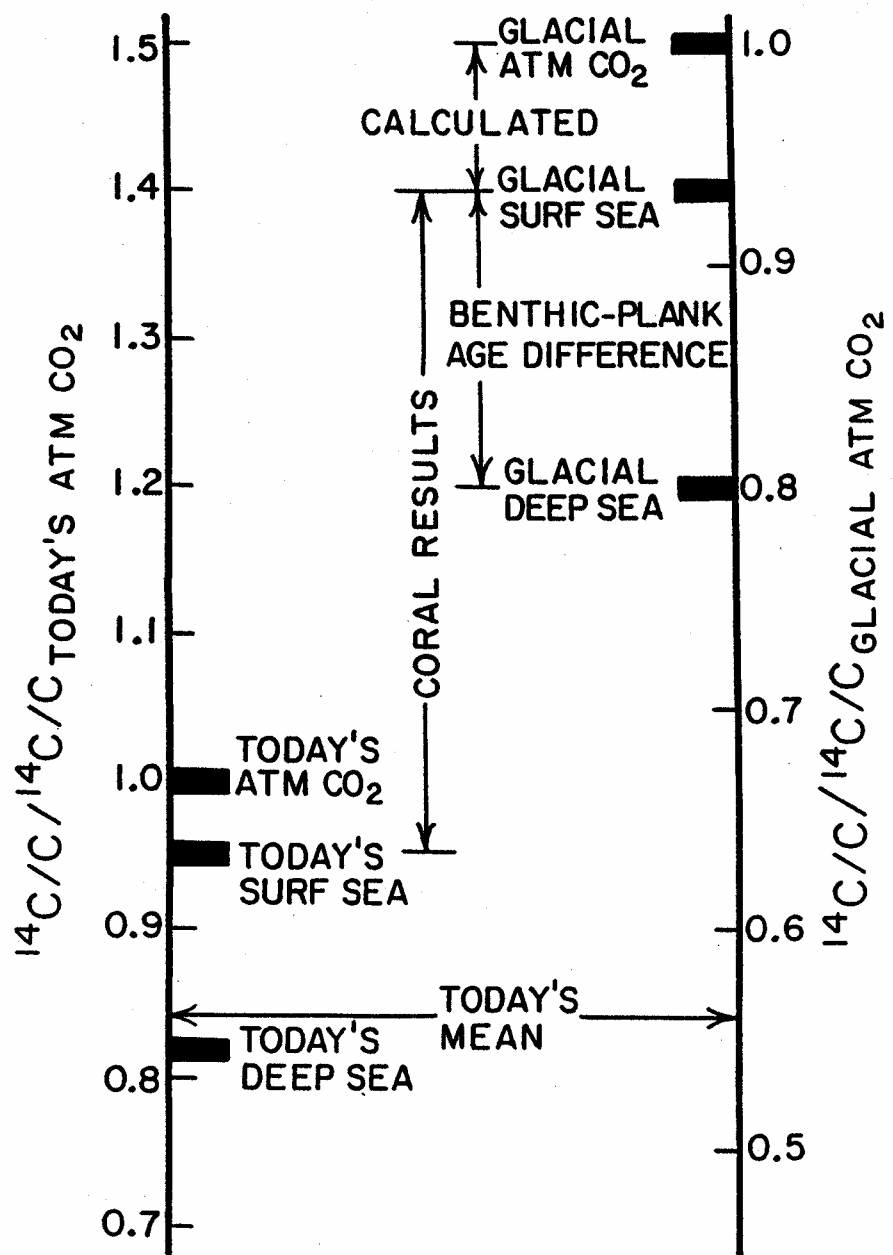


Figure 11. Comparison of the radiocarbon distribution for today's ocean (i.e. that existing prior to anthropogenic impacts of fossil fuel burning and nuclear testing) with that reconstructed for glacial time. The difference between the ^{14}C to C ratio in the tropical waters of the glacial ocean and today's is based on ^{230}Th and ^{14}C measurements on glacial age corals. The surface sea to deep sea radiocarbon difference for the glacial tropical ocean is based on measurements of paired planktonic and benthic foraminifera samples hand picked from glacial horizons in deep sea sediments. The air-sea difference is calculated using the atmospheric CO_2 content measured in bubbles from glacial age ice.

production. To explain the coral results, the Earth's inventory of radiocarbon must have been about 1.4 times higher during peak glacial time than in the year 1850. In order to explain the trend in the discrepancy between the ^{14}C and absolute age scale, during the last 18,000 years the Earth's radiocarbon inventory has been steadily decreasing. Clearly for this to have happened, the number of cosmic ray protons smashing into our atmosphere must have been decreased. While it is clear that these fast moving particles have their origin in distant regions of our galaxy, the processes which accelerate them and shoot them in our direction remain a mystery. But because of the vast scale of our galaxy astrophysicists consider it unlikely that their numbers should change on time scales as short as 10,000 years. Hence the assumption is made that no change has occurred in the number of these particles streaming toward our solar system.

The important point is that not all the protons aimed by the Galaxy at Earth reach our atmosphere. The reason is that their courses are altered by the interaction of two magnetic fields, one created by the ions streaming out from the Sun (i.e. the solar wind) and the other by fluid motions in the Earth's core (the Earth's dipole field). We know for sure that neither of these magnetic fields has maintained a constant strength. Historic observations show that the number of ions streaming out from the Sun's surface varies with the number of Sun spots and that these spots undergo 11 and 22-year cycles. Further, during a period from 1645 to 1715, referred to as the Maunder Minimum, no spots were present. Geologic observations demonstrate not only that the Earth's magnetic field has undergone reversals from positive to negative polarity but also that between the times of these reversals the strength of the field has fluctuated.

Information about the strength of the Earth's magnetic field at times in the past can be obtained from volcanic rocks and potsherds. By measuring the magnetic field of these objects before and after heating to temperatures above the Curie point, an estimate of the field strength at the time (and site) which the volcanic rock or the potsherd was created can be made. It is also possible to get a sense of the time history of the Earth's

magnetic field intensity by making measurements on marine sediments. Estimates of the amount of radiocarbon on Earth over the last 50,000 years based on these paleomagnetic results is shown in figure 12. While not in total agreement with the observed trends in the Earth's radiocarbon inventory, the match is sufficiently good that most scientists accept that the Earth magnetic field change is primarily responsible for the deviations between the radiocarbon and calendar time scales.

The pronounced rise in the age offset centered at 40,000 years is associated with what is referred to as the Laschamp paleomagnetic event which is thought to be the result of an aborted reversal of the Earth's magnetic field (i.e., the field dropped to near zero intensity and then reformed with the same polarity).

CLOCKS READING MORE THAN 50,000 YEARS

In addition to serving as a means of calibrating the radiocarbon method, ^{230}Th is one of the main contributors to dating events beyond the range of radiocarbon. Two approaches have been used. The first is the one we have just discussed, namely to use the ingrowth of ^{230}Th in corals. The ages of three points on the sea level record established in this way played a key role in demonstrating the tie between the Earth's orbital cycles and its climate. One of these, the 124,000-year age obtained on corals formed during the peak of the last interglaciation, proves to be a king pin in the master chronology for the ice ages.

The ^{230}Th in-growth method has also been used to determine the ages of CaCO_3 deposits on the continents. These deposits form in caves, in faults, in springs and in saline lakes. Because fresh waters rarely have as low a Th to U ratio as does sea water, the situation for these deposits is often more complicated than that for corals. Often the uranium content is lower and thorium content higher than in the sea. Unlike coral hour glasses which initially have no sand in their bottoms, fresh water CaCO_3 hour glasses often have sizable initial readings. In other words, ^{230}Th is built in as they form. Fortunately a means exists to assess the amount of this initial ^{230}Th and correct for its

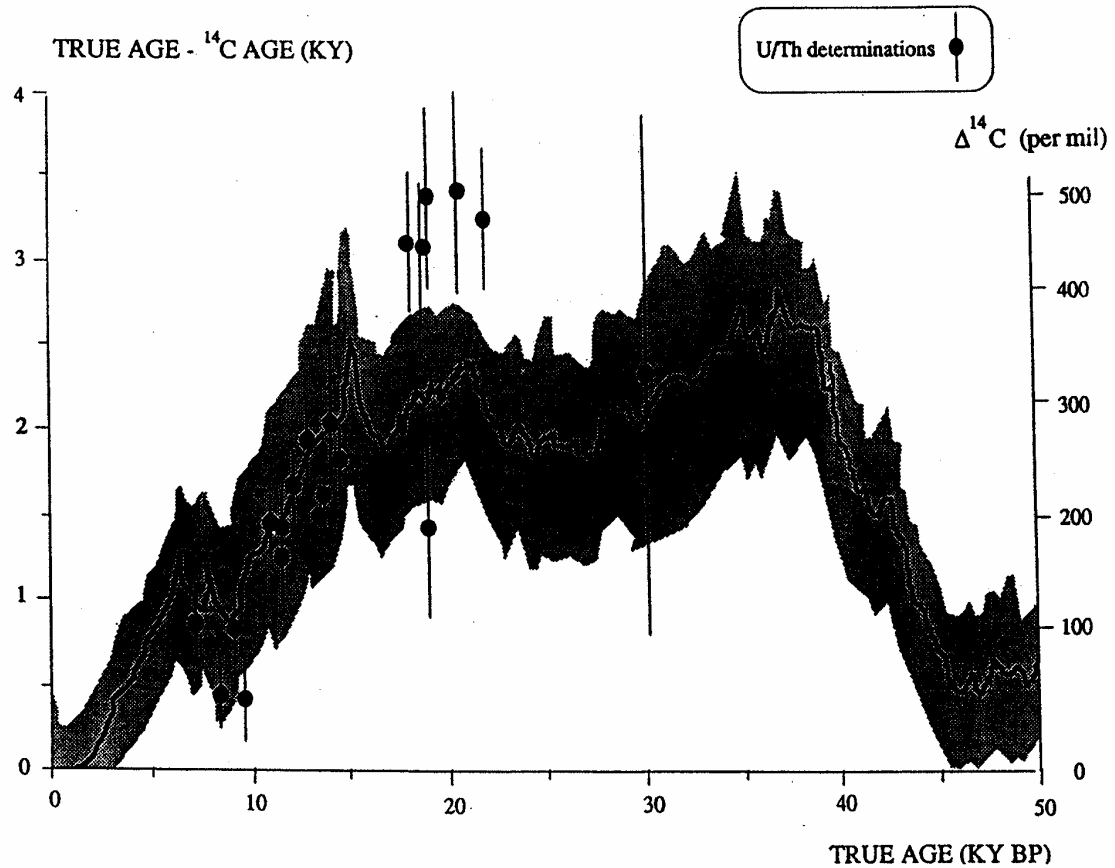


Figure 12. Comparison of observed deviation of radiocarbon ages from radiothorium ages compared with those expected from reconstructions of the Earth's magnetic field strength (Laj et al., 1990).

presence. The trick is to make measurements on a number of different samples of the same age. Such measurements reveal differences in the ratio of ^{232}Th to ^{238}U from piece to piece of CaCO_3 presumably as the result of differing modes of growth. These differences permit isochron diagrams akin to that shown in figure 13, to be constructed. If, as in this example the ratio of $^{230}\text{Th}/^{234}\text{U}$ increases linearly with the ratio of $^{232}\text{Th}/^{234}\text{U}$, then by extrapolating this line to the origin, the $^{230}\text{Th}/^{234}\text{U}$ ratio for a hypothetical sample which formed entirely free of ^{232}Th (and hence also of ^{230}Th) can be obtained. Based on this ratio, a correction for initial ^{230}Th can be made and then the age can be calculated in the same manner as for corals.

The second approach to harnessing ^{230}Th for dating is very different from the first. Instead of utilizing the ingrowth of ^{230}Th in materials with initial ^{230}Th to ^{238}U activity ratios much less than unity, focus is placed on the decay of ^{230}Th in materials which formed with initial ^{230}Th to ^{238}U activity ratios much greater than unity. Nearly all open ocean sediments fall into this latter category. While they have uranium contents consistent with their mineralogy (i.e. a few parts per million in the silicate fraction) they have unusually large contents of ^{230}Th . The reason is that the ^{230}Th produced by the uranium dissolved in the sea is trapped on particles and carried to the sea floor. Because of the rather large amount of uranium dissolved in the sea this removal process endows recently deposited marine sediments with a high ^{230}Th to ^{238}U activity ratios.

In an ideal world the rate of sediment accumulation and the rate of ^{230}Th delivery would remain constant with time. If this case, then the ratio of the excess ^{230}Th content of a horizon at some depth in a deep sea core to that at the core top fixes its age (an example is given in figure 14). Unfortunately, these ideal conditions are rarely met. Rather, the rate of accumulation of sediment almost everywhere on the sea floor changes with climate. Because of this, the ^{230}Th raining to the sea floor is diluted with varying amounts of sediment and the assumption of constant initial ^{230}Th concentration is not valid. This complication has yet to be satisfactorily overcome, hence ^{230}Th ages

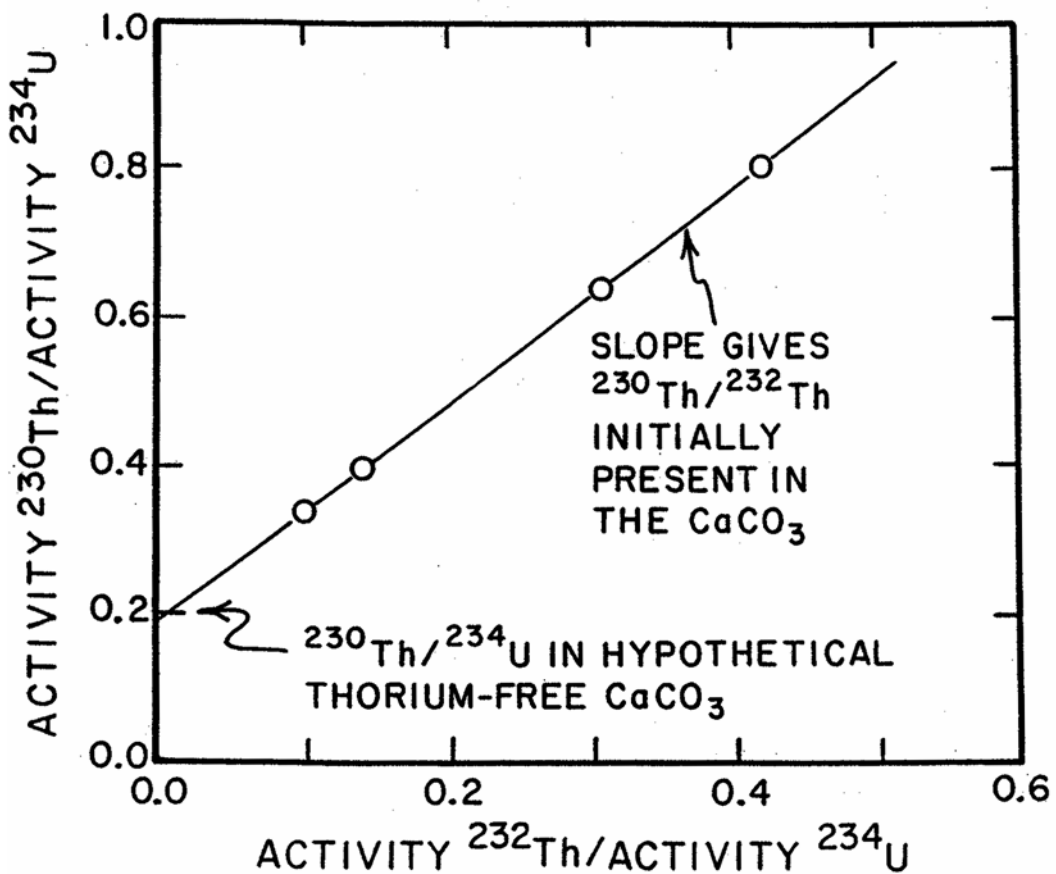


Figure 13. Hypothetical set of results for uranium and thorium measurements on separate pieces of "dirty" CaCO_3 . Differing ^{232}Th to ^{234}U ratios allow an isochron to be constructed. The slope of this isochron yields the ratio of ^{230}Th to ^{232}Th in the thorium incorporated when the carbonate was deposited. More important, the intercept of this line with the origin gives the ^{230}Th to ^{234}U ratio for a hypothetical "clean" CaCO_3 . From this ratio, the age of the "dirty" samples can be calculated.

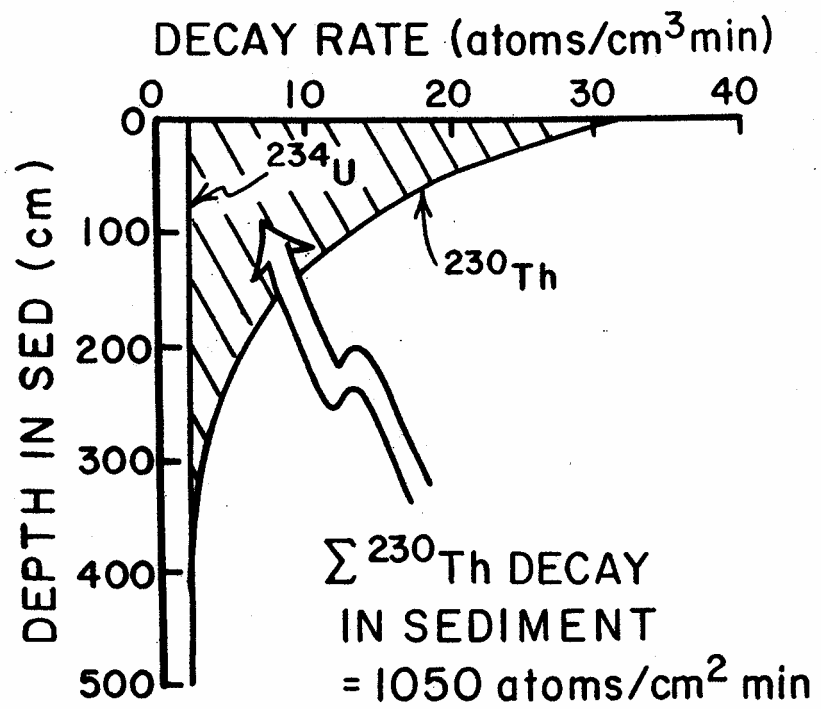


Figure 14. Distribution of ^{230}Th with depth in an ideal deep sea core with a constant sedimentation rate and with an amount of excess ^{230}Th matching the production in the overlying water column.

obtained by this method remain approximate. However during the 1950's and early 1960's when the Urey's ^{18}O method was first being applied to marine foraminifera, ^{230}Th ages provided the only available means to tie these records to the astronomical timing of Milankovitch forcing. In hindsight the ages obtained in this way were sufficiently accurate to provide a quite good picture of the relationship between insolation forcing and climate response.

A great hope for avoiding the difficulties created by changing sedimentation rates was to measure ^{231}Pa along with ^{230}Th in marine sediments. ^{231}Pa is also created by the decay of uranium (in this case ^{235}U) dissolved in the sea. Like thorium, protactinium is a chemically reactive element and soon becomes attached to particles and is removed to the sea floor. So marine sediments form with a high of ^{231}Pa to ^{235}U activity ratios. The idea was that since the ^{235}U to ^{238}U ratio in the sea remains constant with time, so also would the ^{231}Pa to ^{230}Th ratio in newly formed marine sediment. Unlike the concentration of ^{230}Th alone, the ratio of these two isotopes should be independent of the rate of accumulation of sediment on the sea floor. This hope was voided by an unforeseen difficulty. It turns out that the geographic pattern of removal of ^{231}Pa from sea water to the sea floor is different than that for ^{230}Th . The reason is that waters adjacent to the margins of the ocean have far more particles passing through them than do waters in the open ocean. Hence ^{230}Th or ^{231}Pa atoms created in the particle starved open ocean might survive removal until carried by currents to the high particle rain rate zone at the edges of the sea. As ^{231}Pa has a somewhat smaller affinity for particles than ^{230}Th , a greater fraction of the ^{231}Pa atoms produced in the open sea reach the margins. Because of this, the $^{231}\text{Pa}/^{230}\text{Th}$ ratio in recently formed continental margin sediments is several times higher than would be expected and that for open ocean sediments is several times lower. Further, the interplay between open ocean and ocean margin removal is influenced by climate. Hence the initial ^{231}Pa to ^{230}Th ratio for the sediment accumulating at any given spot in the ocean floor cannot be assumed to remain constant

with time.

While the use of ^{231}Pa in conjunction with ^{230}Th as a means of dating marine sediments did not pan out as hoped, this isotope has provided an excellent cross check on the ^{230}Th ages of corals. Newly formed corals should be ^{231}Pa free. As is the case for ^{230}Th , the amount of this isotope increases with time until it reaches steady state with the parent ^{235}U in the coral (see figure 15). As summarized in table 4, the concordancy between results obtained on corals by the ^{230}Th and by the ^{231}Pa method raises confidence in the validity of these uranium series ages.

As already mentioned, a study by Lamont-Doherty's Bill Thompson reveals that corals collected above sea level often contain excess ^{230}Th and therefore yield anomalously high ages. The failure to account for this excess led to what I believe to be a false conclusion, namely, that the rise in sea level associated with the termination of the penultimate glaciation occurred prior to the northern hemisphere summer insolation maximum centered at 128,000 years ago. Once Thompson's correction for this excess was applied, the ages for the interglacial high sea stand collapsed on a value averaging 124,000. Hence, as was the case following the most recent termination, the sea level maximum postdates the summer insolation maximum.

THE POTASSIUM-ARGON CLOCK

Beyond the range of accurate U-series dating (i.e. beyond about 300,000 years) the only conventional radiochronometer which has generated highly reliable absolute ages for glacial events is that based on the decay of ^{40}K to ^{40}Ar in minerals of volcanic origin. The idea is that, as argon is a gas, it will be excluded when minerals crystallize from magmas. Thus volcanic minerals such as sanidine ($\text{KAl}_2\text{Si}_3\text{O}_8$), which have lattice sites designed to accommodate potassium, are obvious candidates for use in dating.

One problem faced in application of this method is that the basalt flows and ash horizons suitable for dating are only rarely found in close association with the climate records of prime interest. Fortunately a way around this severe limitation has been found.

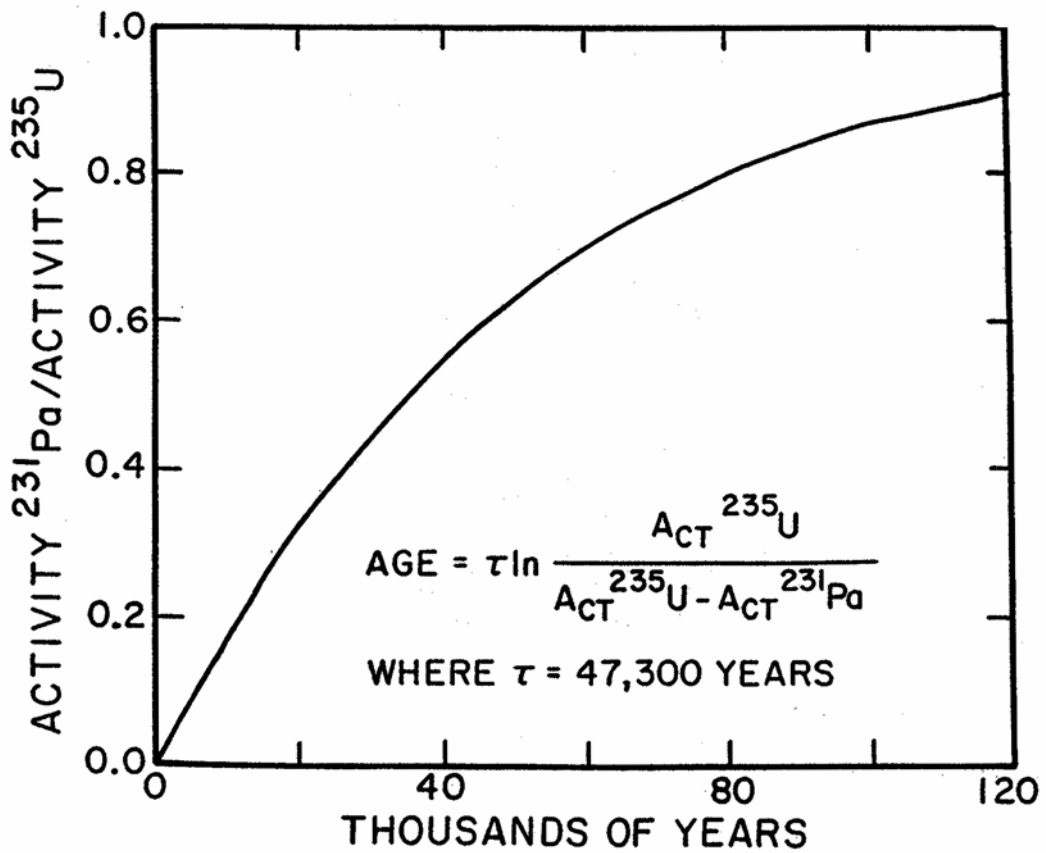


Figure 15. Curve showing the pattern of in-growth of ^{231}Pa in a coral.

Table 4. Comparison of ^{230}Th and ^{231}Pa ages on corals from Barbados (Ku, 1968). The ^{230}Th ages are calculated using a half life of 75,200 years and the ^{231}Pa ages using a half life of 34,300 years.

Terrace	<u>Activity Ratios</u>						
	U ppm	Th ppm	$\text{U}^{234}/\text{U}^{238}$	$\text{Th}^{230}/\text{U}^{234}$	$\text{Pa}^{231}/\text{U}^{235}$	Th^{230} Age $\times 10^3$ yr.	Pa^{231} Age $\times 10^3$ yr.
(Living)	$3.07 \pm .03$	$<.01$	$1.14 \pm .01$	$<.002$	$<.002$	$<.2$	$<.1$
1	$2.63 \pm .02$	$<.01$	$1.11 \pm .01$	$.52 \pm .01$	$.798 \pm .017$	79 ± 2	79 ± 4
2	$2.62 \pm .03$	$<.01$	$1.13 \pm .01$	$.63 \pm .01$	$.877 \pm .018$	105 ± 3	104 ± 8
3	$3.27 \pm .04$	$.01$	$1.10 \pm .01$	$.69 \pm .01$	$.912 \pm .018$	125 ± 5	120 ± 10

The ^{40}K - ^{40}A method has been used to the determination of the age of reversals in the Earth's magnetic field. Reversals have global imprints. They are recorded in deep sea muds, in loess, and in lake and bog sediments. Thus, the age of this a given reversal has only to be determined precisely in one place. Then this date can be applied worldwide.

Because of the importance of magnetic reversals to plate tectonic reconstructions, much effort has been expended in establishing the age of not only the last of these reversals but also of as many of the earlier ones as possible. This effort has been concentrated in places like Iceland where stacks of basalt flows extending back several million years in age are to be found. By determining the age of the last basalt flow to have been extruded before a reversal and that of the first flow to have been extruded after a reversal, geochronologists have closely constrained the times of these reversals. The best estimate of the age of the last magnetic reversal, i.e., the Brunhes-Matuyama event, is 780,000 years. Like the 124,000-year age for the high sea stand of the last interglacial, this date serves as a kingpin in the chronology of major climatic cycles about which this book is concerned. One reason is that it comes near the beginning of the sequence of ~100,000-year duration glacial cycles.

Like all radioisotope methods, that based on the decay of ^{40}K is subject to geochemical biases. Two must be considered. One has to do with tiny amounts of ^{40}Ar incorporated into the mineral when it formed. The other has to do with the subsequent escape of the ^{40}Ar produced within the mineral. A clever experimental technique has been devised which largely circumvents both of these potential sources of error. This method involves the irradiation of the mineral with neutrons in an atomic reactor. The neutrons convert ^{39}K atoms into ^{39}Ar atoms. Then the mineral is subjected to step wise heating. The argon released during each stage of heating is analyzed isotopically. The secret is that during heating the ^{40}Ar trapped in the mineral when it formed is released over a different temperature range than the ^{40}Ar produced within the mineral by radioactive decay of ^{40}K . Further, if the mineral has been subject to diffusive loss of

^{40}Ar , the ^{39}Ar produced by neutron irradiation will be released over a different temperature range than that for the radiogenic ^{40}Ar alerting the analyst to the problem. Thus only minerals which show constant $^{40}\text{Ar}/^{39}\text{Ar}$ ratios over a range of temperature steps can be deemed to be reliable clocks.

IN SITU PRODUCTION CLOCKS

One important record for which the available dating techniques have provided surprisingly little information is that produced by mountain glaciers. Moraines marking the extent of repeated expansions of the glaciers on mountains in all parts of the world have a very important story to tell; they record local temperature changes at all latitudes (including the equator). They potentially offer the best insight into the degree of synchronicity between climate changes in the northern and southern hemispheres. The problem is that the vast majority of these moraines have defied precise dating. Only in those few places where the glaciers descended into areas of high precipitation rich in vegetative cover has the wood or peat needed for radiocarbon dating been found. In desert areas, where the moraines are best preserved and most accurately mapped, few radiocarbon dates are available.

A new approach is being taken. It involves the measurements of cosmic ray spallation products accumulated in blocks of rock left behind by retreating glaciers. Just as cosmic rays crash into and smash the nuclei of atoms in our atmosphere, they also crash into and smash the nuclei of atoms in rocks exposed at the Earth's surface. Six isotopes, ^3H , ^{10}Be , ^{14}C , ^{22}Ne , ^{26}Al and ^{36}Cl , produced during these collisions can now be accurately measured; the first and fourth by conventional gas mass spectrometry and the rest by accelerator mass spectrometry.

To be a candidate for such dating a rock must have remained shielded from cosmic rays (i.e., covered by several meters of material) until it was plucked up by a passing glacier. In other words, when dumped from a retreating glacier it must have been free of the isotopes produced by cosmic ray spallation. In addition, once dumped, the

rock must have remained uncovered, unmoved and unbroken. In such a rock the amount of any one of these isotopes provides a measure of the time elapsed since it was implaced.

While these methods are potentially extremely powerful, much has yet to be learned before this potential can be fully realized. The production rate of each isotope from each element present in rocks must be precisely established as a function of latitude and elevation. Changes in production rate induced by temporal variations in magnetic field strength must be taken into account. Geochemical problems such as the loss of ^3He by diffusion through the host mineral, contamination through absorption of the ^{10}Be and ^{26}Al carried to the rock in precipitation must be assessed. Finally, account must be taken of shielding by seasonal cover with snow and of erosion which may have gradually worn away its outer layers. The secret will be to measure several of these isotopes in a number of rocks from the same glacial event. Inconsistencies will point up the problems and allow them to be overcome.

PLANETARY CLOCKS

As was the case for ages obtained by radiocarbon, cross-checks are needed in order to provide confidence that the possible geochemical problems connected with the ^{230}Th and ^{40}Ar methods have not biased the ages. Fortunately, a means has been found which not only permits this to be done but also permits a continuum of ages to be obtained for deep sea cores between the two king pin ages (i.e., 124,000 years for the peak of the last time of interglaciation and 780,000 years the time of the last magnetic reversal). This cross-check is absolute for the same reason as holds for annual layers; i.e., time is kept by planetary motions. Three of these motions are of interest: the wobble of the Earth about its spin axis (precession), the change in the inclination of the plane of the Earth's orbit relative to mean gravitational plane of the solar system (obliquity), and the change in the degree of circularity of the Earth's orbit (eccentricity). The first of these is caused by the pull of the Sun and moon on the Earth's equatorial bulge. The other two

are caused by the pull of the major planets on the Earth. Together these changes produce cycles in the strength of the seasons. As we shall see, these seasonality changes pace climate changes. The imprint of these cycles is especially clear in the $^{18}\text{O}/^{16}\text{O}$ record kept by foraminifera shells of deep sea sediments. Spectral analysis of these records reveals power at a period of 23,000 years expected from the Earth's precession and at a period of 41,000 years expected from the change in the tilt of the orbit. Spectral analysis permits the signal associated with each of these two periods to be extracted from the $^{18}\text{O}/^{16}\text{O}$ record. These extracted signals can then be matched with the astronomical record of seasonality. The latter has been determined with extremely high precision based on measurements of the masses and orbits of the planets (see figure 16). Three time horizons are used to constrain the match between Earth record and astronomical forcing, today, 124,000 years ago and 780,000 years ago. Then the computer is allowed to make small adjustments in the sedimentation rate record between these time points so as to achieve the best possible match for both the 23,000-year period and the 41,000-year period changes. The result is indeed impressive. The amazing aspect is that the envelope of the amplitudes in the Earth's response to the 23,000-year cyclicity conforms exactly to envelop expected changes in the roundness (i.e. eccentricity) of the Earth's orbit on 100,000-year time scale. Because of this excellent match, paleoclimatologists are confident that for the last million years the marine sediment chronology is accurate to a few percent.

SUNDIALS

In addition to the clocks discussed above, a number of non-nuclear dating methods have been proposed. To me, they are sundials rather than clocks. In a pinch they might give an approximate age, but if a real clock is available, it should be used instead. One such method has to do with defects in a variety of materials caused by the radiations given off during decay of naturally occurring radioisotopes either inside or surrounding the mineral of interest. Another is the racemization of amino acids contained

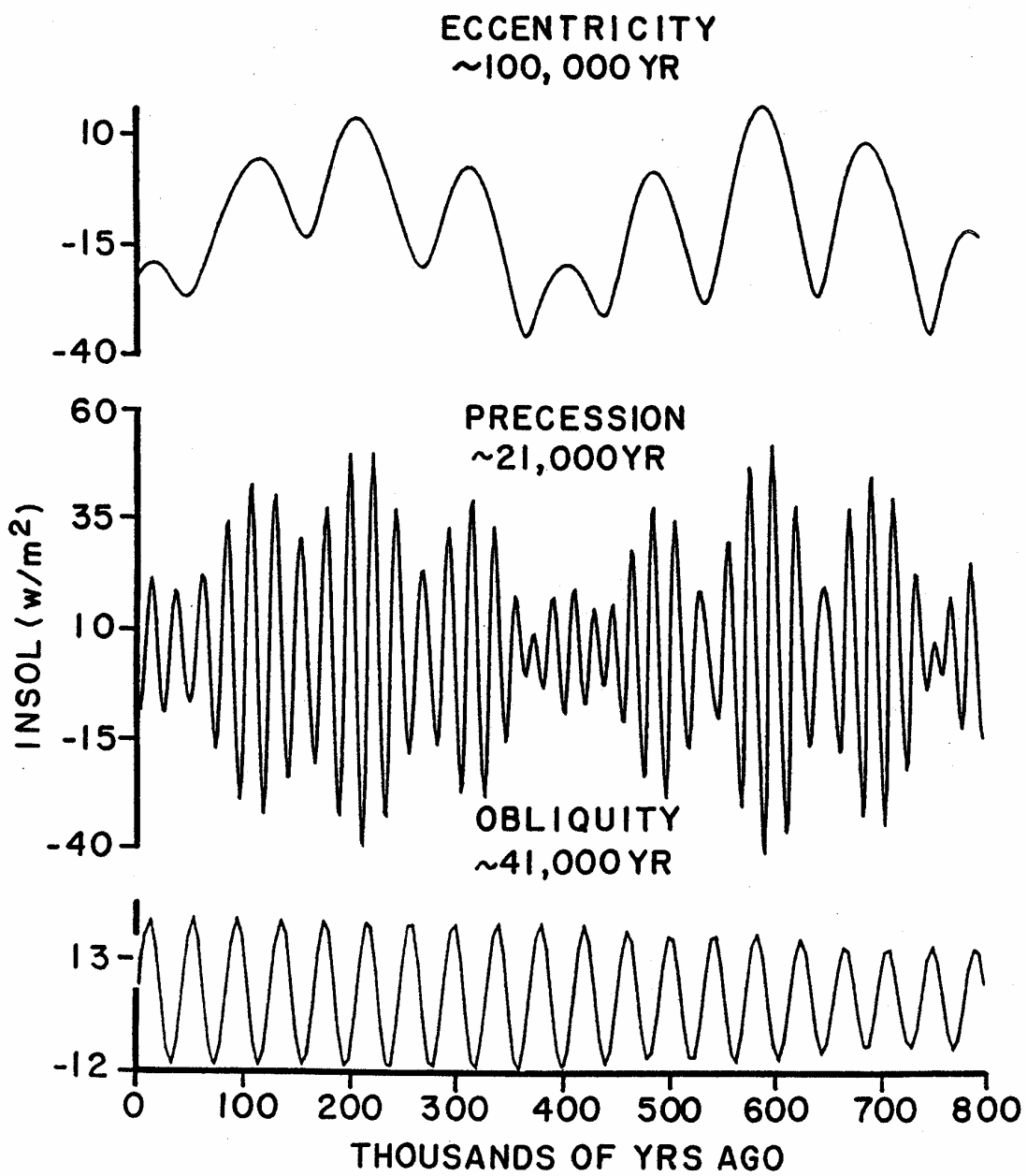


Figure 16. June insolation changes at 65°N caused by changes in the eccentricity of the Earth's orbit (100,000 and 450,000 year cycles), by changes in the phasing between the Earth's distance and tilt seasonality (19,000 and 23,000 year cycles) and by changes in the tilt of the Earth's axis (41,000 year cycle).

in sediment, shell and bone. Still another is the gradual thickening of hydration rims on volcanic glass. Like ^{230}Th in marine sediments, none of these methods is up to the task of providing the accuracy needed if we are to improve our already quite sophisticated knowledge of the chronology of glacial events. But unlike ^{230}Th in marine sediments which played an important role in the development of our knowledge of the chronology of climate changes over the last million years, these sundials appeared too late in the game to have had an important impact on the historical development of the subject.

RECORDS

FIFTY-FIVE MILLION YEARS OF POLAR COOLING

The glacial cycles on which this book focuses were confined to the last two thirds of a million years. These cycles mark the culmination of a progressive cooling of the polar regions which began about 55 million years ago. Hence it is appropriate to launch this section by briefly reviewing what is known about the decline in temperatures which set the stage for the big glaciations of late Quaternary time.

The discovery of the fossilized remains of animals thought to be incapable of surviving subfreezing temperatures provided the first clue that the polar regions were not always so frigid as today. But it was not until the invention, by Harold Urey, of oxygen isotope thermometry that a means became available by which past polar temperature could be quantified. The key lay in the application of this method to the shells of benthic foraminifera recovered from deep sea sediments. If, as seems probable, waters in the deep sea originated as they now do in the coldest regions of the planet, then oxygen isotope measurements on the CaCO_3 shells of benthic foraminifera formed in the deep sea should provide an indication as to how temperatures for the surface waters in the polar ocean changed during the course of the Cenozoic era. As such analyses accumulated, an amazing picture emerged. The $^{18}\text{O}/^{16}\text{O}$ ratio for benthics increased steadily from beginning of Cenozoic time till the present (see figure 1). Taken at face value, this record tells us that the temperature of the deep ocean became progressively colder over the last 55 million years. By contrast, the $^{18}\text{O}/^{16}\text{O}$ ratios for planktonic foraminifera grown in surface waters in the equatorial region show little change, suggesting that tropical temperatures remained more nearly constant.

To convert the oxygen isotope results into deep ocean temperatures requires that a correction be made for the increase in ice volume which must have occurred during the course of the Cenozoic. The ice presently on Greenland and Antarctica is equivalent

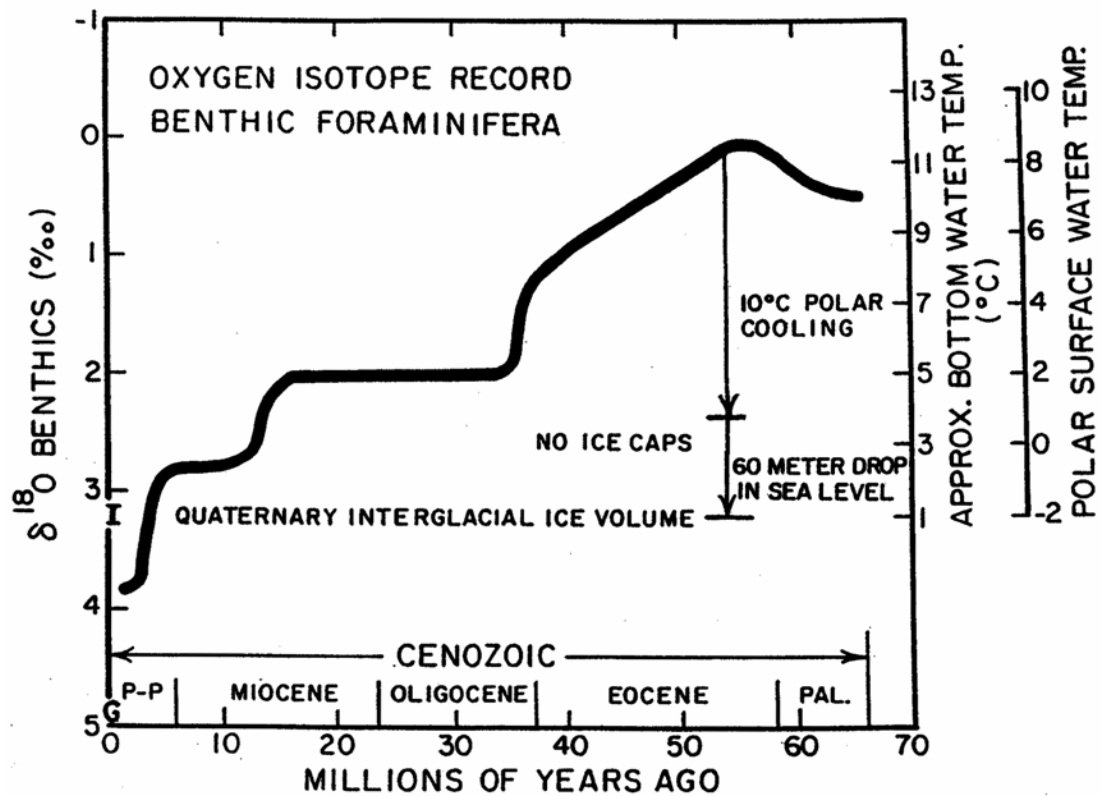


Figure 1. Oxygen isotope trends for the last 66 million years as obtained from the analysis of benthic foraminifera from a large number of borings made in sediments which blanket the floor of the deep sea. The increase of $3.2\text{\textperthousand}$ in the ratio of ^{18}O to ^{16}O from 55 million years ago to the present is the product both of growth of the ice caps on Antarctica and Greenland and a cooling of the deep sea. The contribution of the former can be estimated from the volume and oxygen isotope composition of the present ice caps to be about $0.8\text{\textperthousand}$. The remaining $2.4\text{\textperthousand}$ increase is due to cooling suggesting that 55 million years ago the deep sea was about 10°C warmer than today. The letters I (for interglacial) and G (for glacial) mark range of $\delta^{18}\text{O}$ fluctuations associated with the large glacial cycles of the last three quarters of a million years.

in volume to a layer of ocean water 70 meters thick. As the average $\delta^{18}\text{O}$ value for this ice is about $-45\text{\textperthousand}$, its creation caused the $\delta^{18}\text{O}$ for sea water to rise by about $0.6\text{\textperthousand}$. Since the benthic record suggests that the polar oceans were much warmer during early Cenozoic time, it is likely that no ice caps existed. If so, then between 55 million years ago and now the average $\delta^{18}\text{O}$ for sea water must have increased by $0.8\text{\textperthousand}$ as the result of ice cap growth. The remaining $2.4\text{\textperthousand}$ of the $3.2\text{\textperthousand}$ increase in the $\delta^{18}\text{O}$ for benthic foraminifera between then and now must then be attributed to deep water cooling. This suggests that deep waters cooled by about 10°C over the course of Cenozoic time. As deep ocean waters now have temperatures ranging from 1 to 3°C , 55 million years ago they must have had temperatures in the range 11 to 13°C . This suggests that polar surface waters were no cooler than about 10°C at that time.

We have already seen that during times of peak glaciation temperatures for the polar ice caps dropped by as much as 20°C with only a $3\pm1^\circ\text{C}$ drop in temperature for tropical surface water. Here we see that 55 million years ago temperatures in the polar surface ocean were about 10°C warmer again without any matching change in the temperature of tropical surface waters. Thus paleoclimatic evidence tells us that polar temperatures have undergone much larger swings than have tropical temperatures.

As can be seen in figure 1, much of the decline in bottom water temperatures over the last 55 million years came in three major steps: one at about 36 million years ago, one at about 14 million years ago, and one at about 3 million years ago. Each step involved a cooling of 2° to 3°C . The last of these steps brought the oxygen isotope ratio in benthic foraminifera into its present range. The solid black line in figure 1 depicts the average $\delta^{18}\text{O}$ value for periods long enough to average out fluctuations induced by Milankovitch cycles. As shown by the I and G symbols during the last 650,000 years, the $\delta^{18}\text{O}$ value has swung back and forth from $0.9\text{\textperthousand}$ higher to $0.9\text{\textperthousand}$ lower than this mean. As can be seen from the detailed records in figure 2 during the time period from 2.5 million to 0.7 million years ago, the $\delta^{18}\text{O}$ for benthic forams fluctuated with an

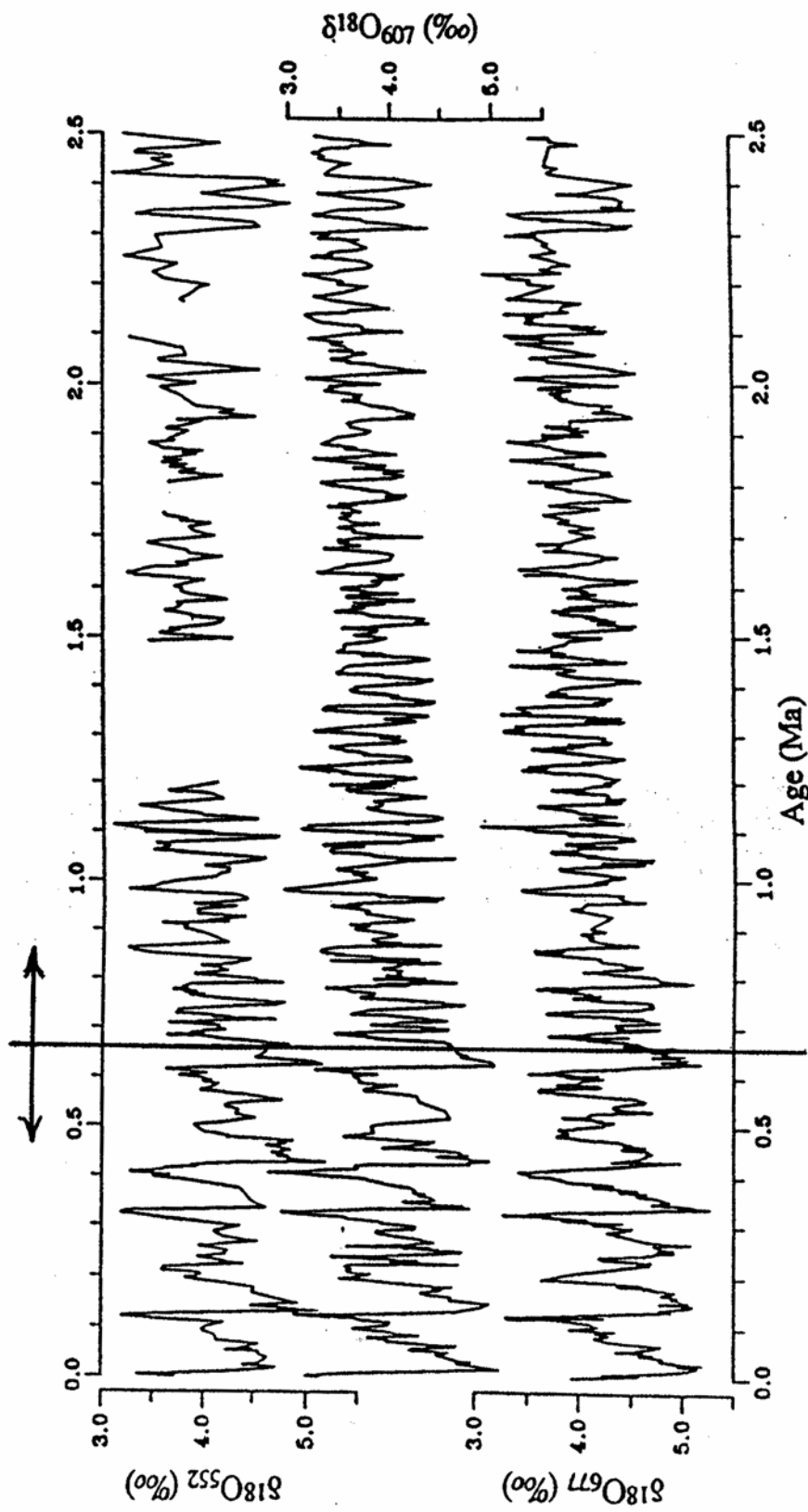


Figure 2. Oxygen isotope records for benthic foraminifera obtained by Maureen Raymo for three deep sea borings. Site 552 is located at 56°N and 23°W in the northern Atlantic. Site 607 is located at 41°N and 33°W in the western basin of the Atlantic. Site 677 is located at 1°N and 84°W in the equatorial Pacific. The vertical line drawn at 650,000 years ago marks the transition from higher frequency-higher amplitude cycles to lower frequency-lower amplitude cycles.

amplitude averaging only about half that for the more recent cycles. It can also be seen that the duration of the earlier cycles was shorter than that of these later cycles. Spectral analyses of the record for the earlier period demonstrates that it was dominated by a periodicity of 41,000 years, while the later period was dominated by periodicity of 100,000 years (see figure 3). So something very important happened to the Earth's climate system about 700,000 years ago. It switched into a new regime characterized by larger amplitude and longer duration fluctuations.

This change in the character of the Earth's climate regime is also recorded in the Chinese loess deposits (see figure 4). The intervals of reduced magnetic susceptibility in the loess record correspond to periods of high dust rain. As the Brunhes-Matuyama reversal in the Earth's magnetic field at 780,000 years ago is preserved in both muds from the deep sea and loess from the continents, the two records can be reliably correlated. The susceptibility variations in loess track very nicely the oxygen isotope variations recorded by benthic foraminifera. As is the case for the ^{18}O record, the character of the loess cycles changes about 700,000 years from smaller amplitude, shorter duration cycles prior to this time, to larger amplitude, longer duration cycles afterward.

As we shall see, changes in the pattern of circulation in the deep sea played a major role in climate change. Evidence obtained by Maureen Raymo and her coworkers from the carbon isotope record kept by benthic forams suggests that a change in ocean operation also took place at about the same time as the change in the character of the climate cycle. As discussed in the section entitled "Indicators", today the ΣCO_2 of waters in the deep Atlantic has a higher $^{13}\text{C}/^{12}\text{C}$ than does the ΣCO_2 in the deep Pacific. We have also seen that the ^{13}C to ^{12}C ratio in the calcite formed by benthic forams provides a record of how the difference between the carbon isotope composition of ΣCO_2 in the two oceans has changed with time. Reproduced by the solid curves in figure 5 are carbon isotope records for a core from the northern Atlantic and from a core from the equatorial Pacific. The former is situated in the region where North Atlantic deep water

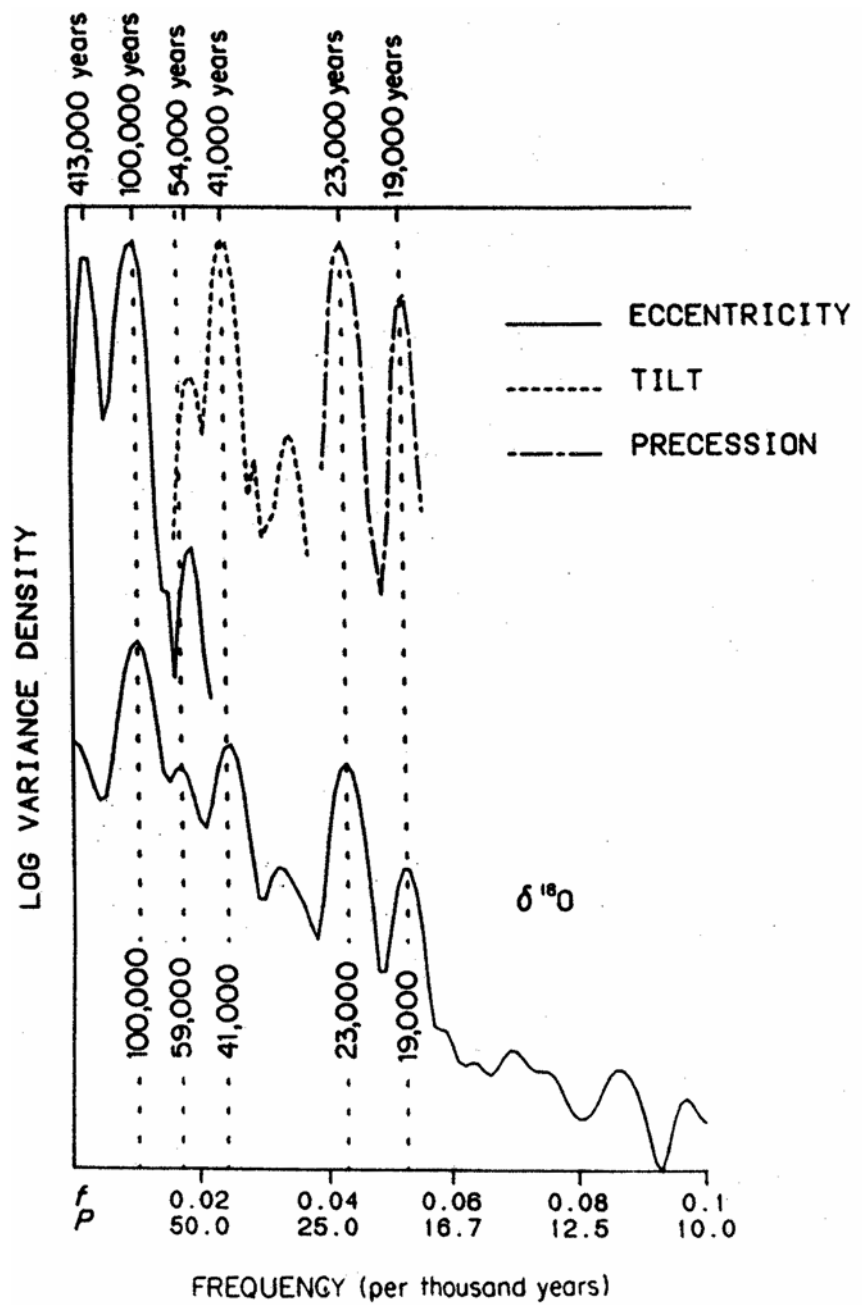


Figure 3. Variance spectra for the marine oxygen isotope of the last 700,000 years (lower curve) compared with spectra for the orbital elements of seasonality (Imbrie, 1985).

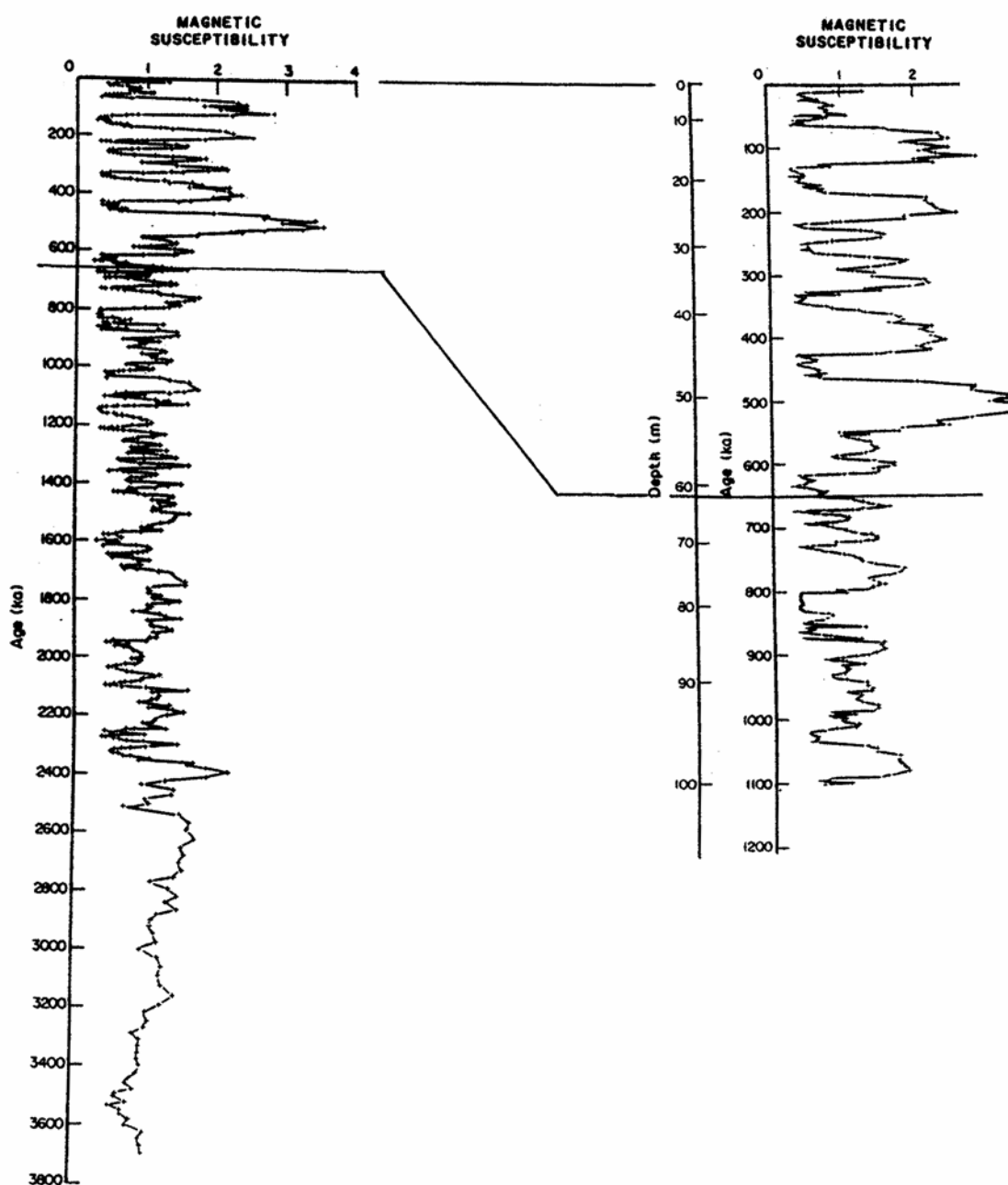


Figure 4. The Xifeng China loess record: On the left is shown the record for the last 3.8 million years and on the right the expanded record for the last 1.1 million years. The magnetic susceptibility has been shown to be inversely proportional to the accumulation rate.

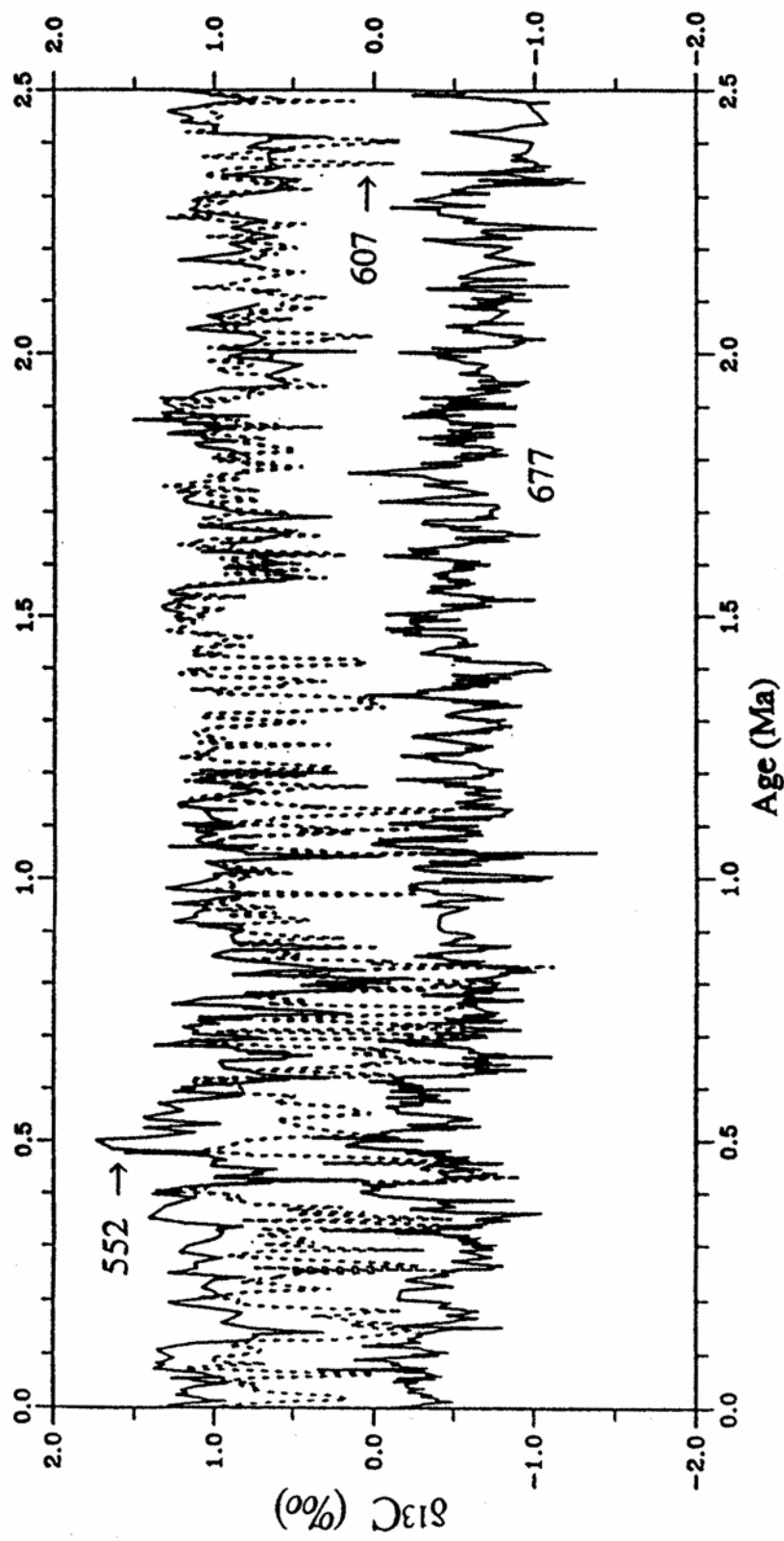


Figure 5. Carbon isotope records obtained by Maureen Raymo on benthic foraminifera for the three deep sea cores whose oxygen isotope records are displayed in figure 2. The uppermost of the three curves is for site 552 in the northern Atlantic and represents the isotope composition of new water descending into the deep Atlantic. The lowermost of the three records is for site 677 in the equatorial Pacific Ocean and represents old deep water. The dashed curve is for site 607 in the western basin of the Atlantic. As can be seen for the early part of the record, the western Atlantic site more nearly tracks the $\delta^{13}\text{C}$ value for northern source water, while during the latter part of the $\delta^{13}\text{C}$ for the western Atlantic it swings back and forth between that for the Pacific value and that for the northern Atlantic.

forms; the latter is situated in the middle of the ocean's largest water reservoir, i.e., the deep Pacific Ocean. These records show that while fluctuations have occurred at both sites, a nearly uniform $\delta^{13}\text{C}$ difference of 1.5‰ has been maintained between them for the last 2.5 million years. The dashed curve is the $^{13}\text{C}/^{12}\text{C}$ record for a third core from the western basin of the northern Atlantic. During the first third of the record, it tracks that for the core from the northern Atlantic, reflecting the fact that the Atlantic was flooded with deep water formed at its northern end. During the middle part of the record, excursions toward the Pacific values are seen suggesting that bottom waters from the Antarctic penetrated far northward in the deep Atlantic. During the most recent third of the record, the $\delta^{13}\text{C}$ values for the western Atlantic core begin a regular swing back and forth between the value characterizing northern Atlantic source water and that characterizing Pacific deep water. When compared with the benthic oxygen isotope records (see figure 6), it can be seen that during times of peak glaciation, the deep western Atlantic was flooded with waters rich in the Pacific end member, and during times of peak interglaciation, it was flooded with waters rich in the northern Atlantic end member. What this record appears to be telling us is that North Atlantic Deep Water, which dominates today's Atlantic, flowed strongly during most of the period from 2.5 to 1.5 million years ago. Subsequently, it was subject to weakenings which allowed waters from the Antarctic to penetrate far northward in the Atlantic. During the last 0.7 million years, these weakenings correspond to times of peak glaciation.

So we see that about seven tenths of a million years ago a series of major cycles in operation of the Earth's climate system was initiated which impacted the polar ice caps, continental dust transport, and deep ocean circulation. What brought about this transition remains a mystery. We can only speculate that the progressive cooling of the polar regions eventually pushed the Earth system over the brink into a new regime. During the intense glacial maxima which characterized this new cycle, a large ice cap formed, the continents were unusually dusty and production of deep water in the North Atlantic

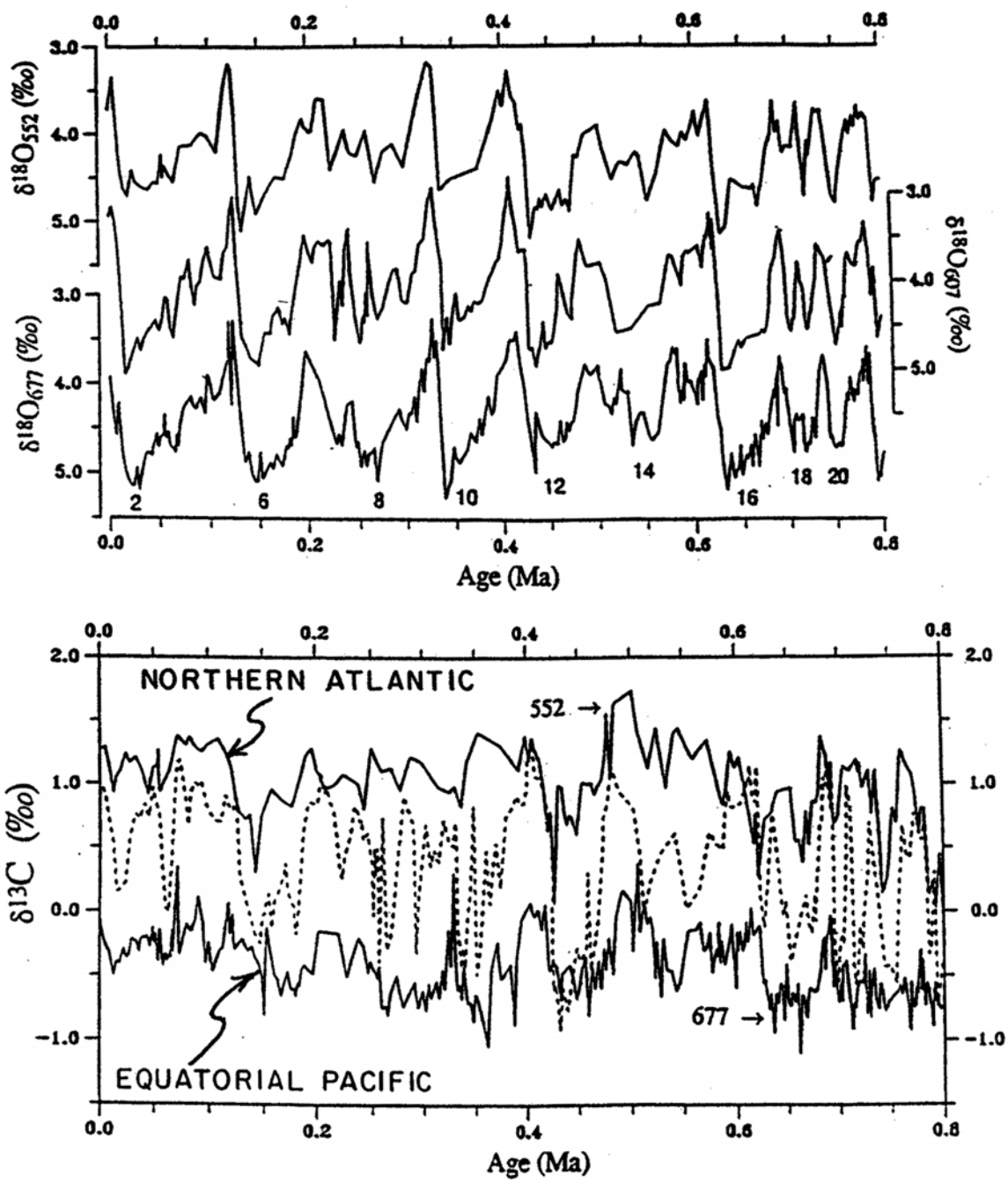


Figure 6. Expanded version of the records in figures 2 and 5 covering the last 0.8 million years. As can be seen during the oxygen isotope warm periods, the carbon isotope ratio for site 607 (dashed curve) lies closer to that for northern Atlantic source water, while during oxygen isotope cold periods, it lies closer to the value for the deep Pacific.

was greatly weakened.

The larger amplitude and longer duration climate cycle which has been in operation during the last two thirds of a million years ago has a distinctly asymmetric shape; long intervals of progressive cooling were terminated by abrupt warmings which brought the system to its full interglacial condition. Our knowledge of these cycles comes mainly from oxygen isotope measurements made on foraminifera shells from deep sea cores. As was discussed in the section entitled “Indicators”, the oxygen isotope variations reflect changes in both ice volume and temperature. As was discussed in the section entitled “Clocks”, the time scale for these variations is constrained by three absolute dates: that for the core top (0 thousand years), that for the peak of the last interglacial (124 thousand years), and that for the time of the last magnetic reversal (780 thousand years). As you recall, the 124,000-year age comes from the ^{230}Th - ^{234}U measurements on coral grown during a time when the sea stood several meters higher than now, and the 780,000-year age comes from ^{40}A - ^{40}K measurements on lava flows bracketing the last magnetic reversal. Initially, the ages for the rest of the record were obtained by interpolation assuming that the sedimentation rate for the intervals between these fixed points remained constant. This approach was later improved upon through correlation with the astronomical time scale.

As can be seen from the oxygen isotope records in figure 6, the long periods of gradual cooling are modulated by ripples. Spectral analyses reveals that these ripples have periodicities close to 41,000 and to 23,000 years. These periods are the same as those associated with the Earth’s orbital parameters. Clearly, changes in the Earth’s orbital parameters have paced Earth climate. They alter the distribution by season of the receipt of solar radiation at any point on Earth’s surface; but the physical links remain obscure. As these periods appear in the oxygen isotope record, the chronology for deep sea sediments can be tuned against the astronomical time scale. The fact that the

modifications in chronology required by this tuning are quite small lends strong support to the reliability of the time scale.

MILANKOVITCH CYCLES

Before continuing with the discussion of the asymmetrical cycle which has run for of the last seven tenths of a million years, it is worthwhile to explore in more detail the orbital cycles which cause the distribution between seasons of the solar radiation received at any point on the planet to change. In recognition of the Yugoslavian mathematician who, during the 1920s and 1930s, first worked out the magnitude of these changes, they are referred to as Milankovitch cycles .

The amount of sunlight reaching any given place on Earth changes during the course of the year for two reasons. The first is because Earth's spin axis is not perpendicular to the plane of its orbit. Rather, it is inclined to the perpendicular by an average of 23° . This causes the Northern Hemisphere to face toward the Sun during one half of the year and the Southern Hemisphere during the other half (see figure 7). Our calendar is geared to the switch between these two situations. The Northern Hemisphere begins its half year of preferential heating on March 21st. On June 21st, the amount of sunlight received by the Northern Hemisphere reaches a maximum. On September 21st, the period of preferential Northern Hemisphere heating comes to an end. We refer to this contribution to seasonality as the tilt component.

The other source of seasonality has to do with the fact that the Earth's orbit is elliptical. The Sun is located at one of the two foci of this ellipse. Because of this, the Sun-Earth distance lengthens and shortens during the course of the year (see figure 7). The further the Earth is from the Sun, the less energy it receives. We refer to this contribution to seasonality as the distance component.

As the tilt influence is the larger, the distance component can be viewed as a modulator of seasonality. Clearly this modulation must have opposite sense in the two hemispheres, for when the Earth is at the long end of the ellipse, if one hemisphere

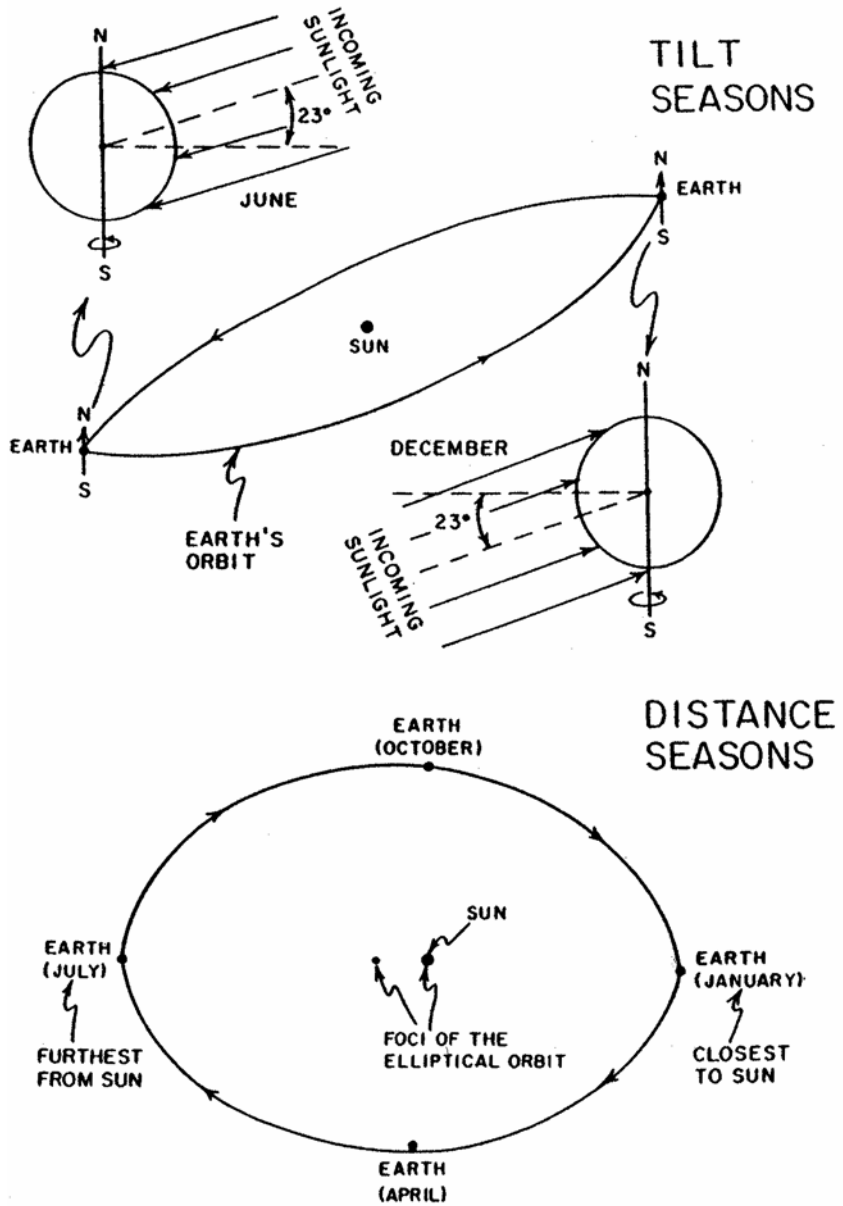


Figure 7. Seasonality and its cyclic changes: Shown in this diagram are the elements of the Earth's motion that influence the seasonal contrast in the amount of radiation received at any point on the globe. The primary cause of seasons is the tilt of the Earth's axis with respect to its orbit about the Sun. As shown in the upper panel, this tilt leads to the highest illumination of the Northern Hemisphere during the month of June and to the highest illumination of the Southern Hemisphere during the month of December. Our calendar is set so that June 21st and December 21st correspond to the days on which maximum radiation falls on the Northern Hemisphere and on the Southern Hemisphere, respectively. A second contribution to seasonality stems from the fact that the Earth's orbit is elliptical. Because of this the Earth-Sun distance changes during the course of the year. As shown in the lower panel, currently the Earth is closest to the Sun early in January and farthest from the Sun early in July. Thus the Earth as a whole currently receives less sunlight during July than during January.

is experiencing a tilt summer, the other must be experiencing a tilt winter. Hence in one hemisphere, the distance component reduces the magnitude of the seasonal contrast, and in the other, it enhances it. Today, the Earth reaches that point in its orbit most distant from the Sun during Northern Hemisphere summer. Because of this, today the seasonal contrast in solar heating is somewhat smaller for the Northern Hemisphere than for the Southern Hemisphere (see figure 8).

Because the Earth's spin axis precesses, the phasing between the distance and tilt components of seasonality gradually shifts (see figure 9). For example, one half precession cycle from now, the Northern rather than the Southern Hemisphere will experience stronger than average seasonality. Since it takes the Earth 27,000 years to complete a precession cycle, one would expect this to occur in 13,500 years. However, the time required to repeat a given phasing between the tilt and distance seasonality is somewhat shorter than this. The difference has to do with the fact that the Earth's orbit swings around in space. The long end of the ellipse makes one full revolution around the sun each 105,000 years (i.e., one revolution for every four precessional cycles). Although a little complicated to picture, this cart wheeling of the orbit causes synchronicity between the distance and tilt seasonality to repeat, once each 23,000 years rather than once each 27,000 years.

The situation is, however, more complicated. Both the magnitude of the tilt and distance components to seasonality undergo cyclic change. The tilt of the spin axis rocks back and forth from about 24 degrees to about 22 degrees with a period of 41,000 years (see figure 10). The reason is that the tilt of the Earth's orbit relative to the plane of Jupiter's orbit undergoes periodic change. During the last half million years, the eccentricity of the Earth's orbit has ranged from close to 0.00 (i.e., perfectly round) to almost 0.05. These changes in eccentricity have periodicities of about 100,000 and about 450,000 years (see figure 10). Both the changes in tilt and in eccentricity have globally symmetrical impacts; one creates stronger tilt-induced seasons; the other

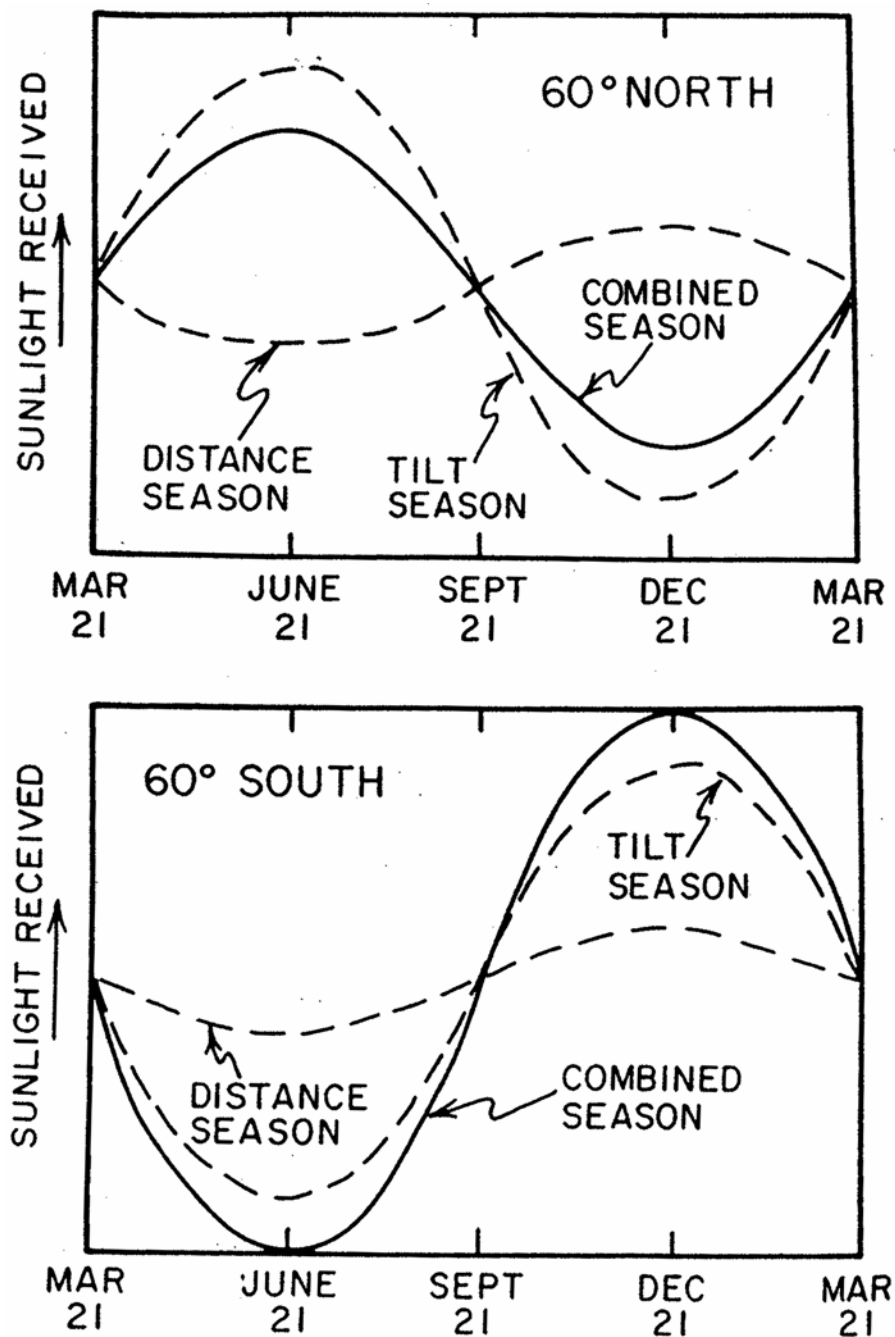


Figure 8. Comparison of the seasonal cycles of solar illumination at 60°N and 60°S: In the Southern Hemisphere the tilt and distance seasons currently reinforce one another. In the Northern Hemisphere they currently oppose one another.

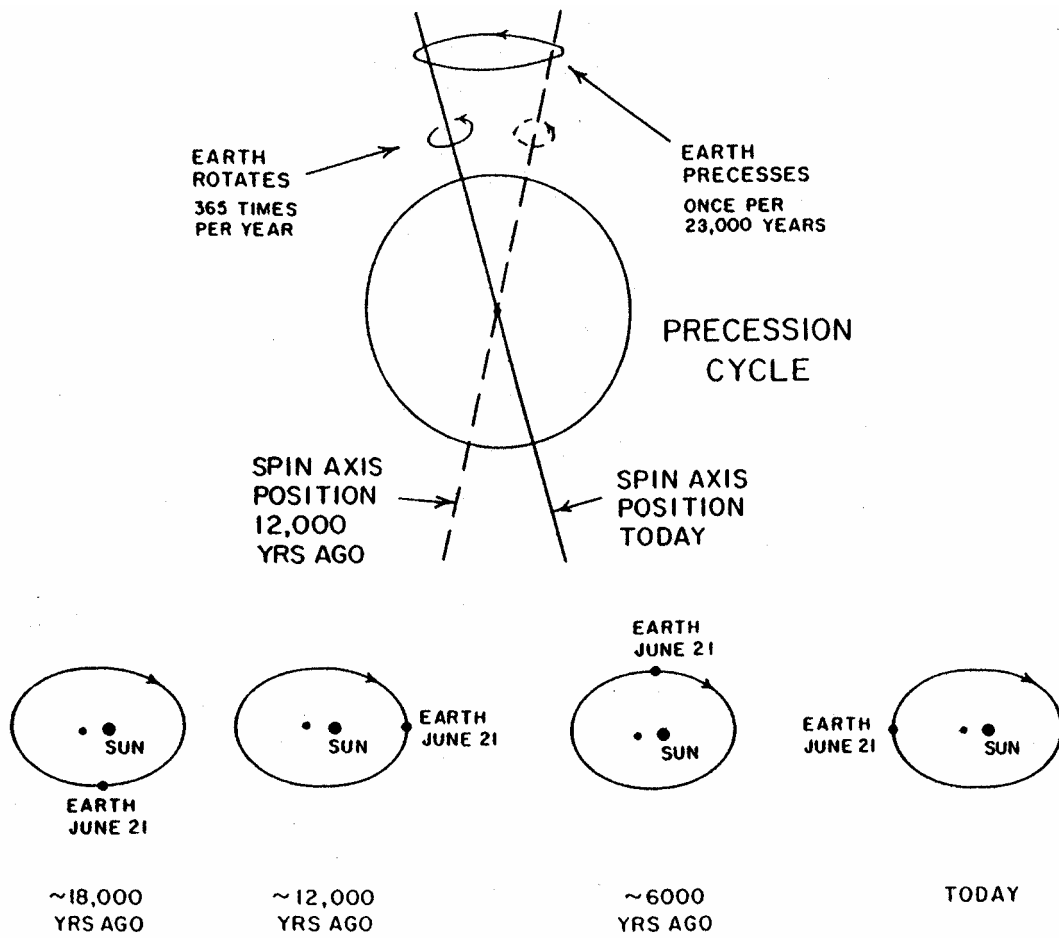


Figure 9. Like that of a top, the Earth's spin axis precesses: It takes about 23,000 years for one complete precession cycle (see text for details). The effect of this motion is to change the point on the Earth's orbit where maximum northern-hemisphere illumination (i.e., June 21) occurs. Today it occurs at the "long" end of the ellipse, reducing summer illumination in the Northern Hemisphere a bit. One-half precession cycle ago (i.e., ~12,000 years ago) it occurred at the "short" end of the ellipse, increasing summer illumination a bit. The precession of the Earth's axis is related to pull by the Sun and Moon on the equatorial bulge produced by the Earth's rotation. Just as the Earth's gravity seeks to tip over a spinning top, the Sun's and Moon's gravity seeks to remove the tilt of the Earth's axis. As does a top, the Earth compensates for this pull by precessing.

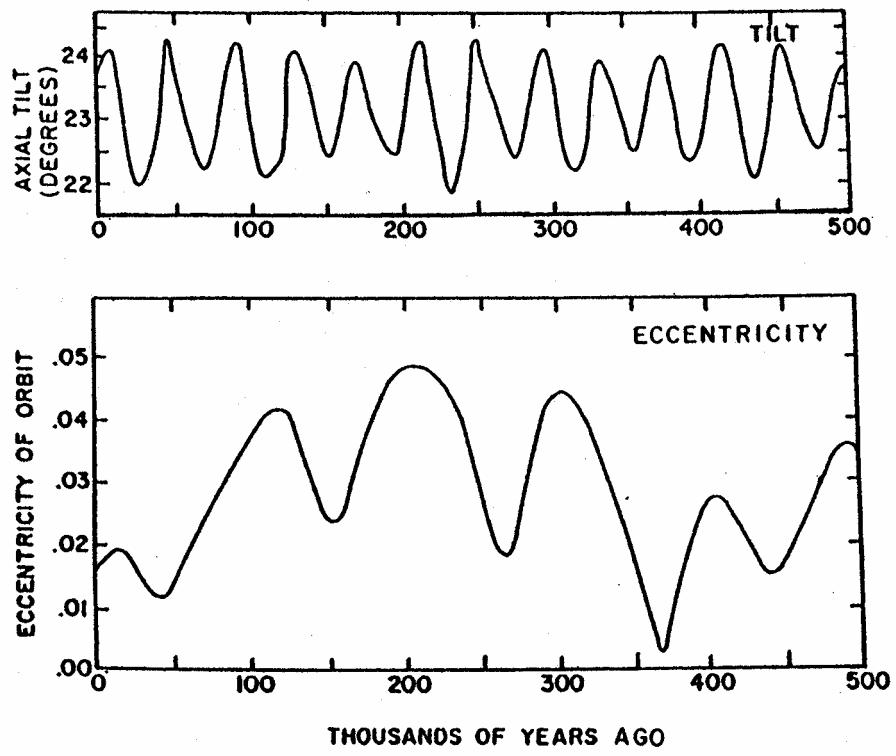


Figure 10. The tilt of the Earth's spin axis and the eccentricity of its orbit as a function of time in the past: These records are reconstructed from calculations based on the law of gravitation and the present-day orbits and masses of the planets.

creates stronger distance-induced seasons. The two impacts have, however, quite different latitude dependencies; the tilt changes are felt more strongly at high latitudes while the eccentricity changes are felt equally at all latitudes. The latter is easily understood because as the Earth-Sun distance increases or decreases, the amount of radiation received at all points on Earth will change by the same percentage. To understand the role of tilt consider the situation where earth's axis had no tilt. In this case, its poles would receive no radiation at all and its equator would receive the maximum possible insolation. With this in mind, it is easy to see that the greater the tilt, the greater the amount of insolation received at the poles and the smaller the amount at the equator.

It is important to emphasize that the timing (and magnitude) of these orbital changes can be computed with high precision. The precession rate of the Earth has been established by observing the change with time of the intersection of the projection of the Earth's spin axis with the canopy of stars. Over the last 4000 years, it has moved through about one sixth of its circular path. The cause of the precession is the attraction by the Sun and the Moon for the equatorial bulge in the Earth's figure created by its spin. The changes in the shape of the Earth's orbit which give rise to variations in tilt and in eccentricity are governed by gravitational interactions among the planets. Basically, the pull on Earth by the large planets Jupiter and Saturn perturbs our orbit. Astronomers have accurately determined the masses and orbital characteristics of the Sun's nine planets. For the same reason NASA scientists can program a space probe to fly past the planet Jupiter at some predetermined time and distance, they can calculate precisely the orbital characteristics of the Earth at any time in the past (or for that matter, at any time in the future). The inaccuracies in these calculations lead to significant errors in seasonality only for times greater than many millions of years. For the interval over which Earth climate has been trapped in its current 100,000-year cycle, the distribution of seasonal heating has been calculated to a gnat's eyebrow.

Calculations covering the last 300,000 years are reproduced in figure 11. Shown are the amounts of heat received at nine latitudes for both the month of June and the month of December. The large amount of information contained in these diagrams takes some time to absorb. First, it must be kept in mind that when integrated over all latitudes and over the entire year, the amount of sunshine reaching the Earth changes only very slightly. Rather, it is the distribution with latitude and season which changes. Next, consider the long term means. For June, the amount of radiation received decreases steadily from north to south. Note that the average of 1035 units received at 40°N exceeds that of 310 units at 40°S by a factor of three. Also note that in June, the amount of heat received at 80°N (1090 units) exceeds by 10% that received at the equator (980 units)!

Having this in mind, let us now look at the variations around these means. The 23,000-year cycle stands out. Thirteen such cycles are present in the last 300,000 years. The amplitude of these peaks changes because they track the eccentricity of the Earth's orbit. Note that triads of strong peaks are centered at 100,000 and at 200,000 years ago. These are times when the 100,000-year cycle in eccentricity produced maxima in the distance component of seasonality.

Now consider the amplitude of these changes. At 80°N, the June radiation goes from a low of 950 units to a high of 1230 units - a range of 25%! Similar percentage changes are seen at all latitudes.

Because the ice sheets of glacial time were located at high latitudes in the Northern Hemisphere and because the mass balance of ice sheets is most sensitive to summer heating, traditionally attention has focused on variations in June radiation received at 65°N. Hence it might be expected that the ice volume changes would follow the seasonality for high northern latitudes with the ice sheets shrinking during times of enhanced summer insolation and expanding during times of reduced summer insolation. However, when the seasonality record for this latitude is placed beside the oxygen

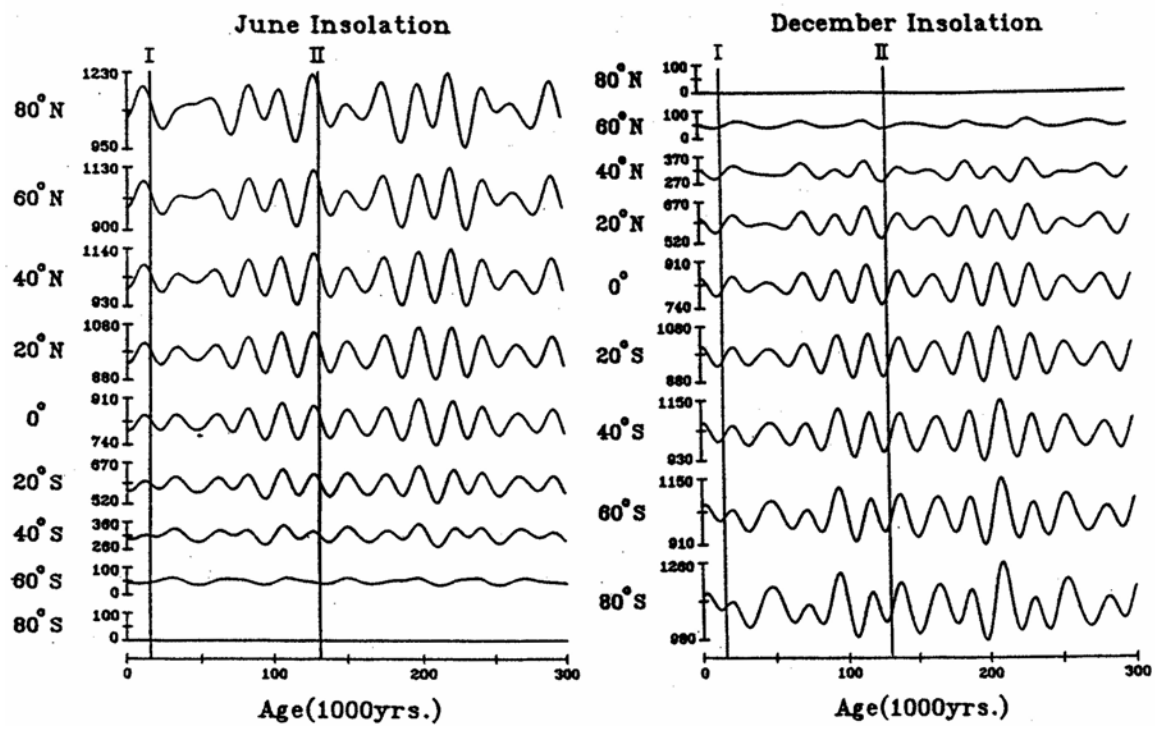


Figure 11. Insolation in June and in December for 9 different latitudes over the last 300,000 years.

isotope record for foraminifera, one's first impression is that they are quite different (see figure 12). However, on closer inspection, one can see that the Earth events do bear a relationship to the seasonality changes. Imbrie and his coworkers clearly demonstrated that the ripples which modulate the 100,000-year long intervals of ice growth nicely conform with seasonality changes. They performed spectral analyses which permitted them to extract from the oxygen isotope records that portion of the variability occurring on a 41,000-year time scale and that portion of the variability happening on a 23,000-year time scale. To their great satisfaction, they found that the amplitude of the oxygen isotope variability associated with the 23,000-year cycle was in proportion to the eccentricity of the Earth's orbit (see figure 13). For example, for the period from 350,000 to 450,000 years ago, when the eccentricity was quite low, the 23,000-year periodicity in climate was very weak; while for the period 180,000 to 220,000 years ago, when the eccentricity was at its highest, the 23,000-year periodicity in climate was very strong. Indeed, the match between expected and observed amplitude is remarkably good. The Imbrie team were equally pleased to find that consistent with near constancy of the tilt cycle the amplitude that of the ^{18}O changes on the 41,000-year time scale was also quite uniform.

The difference between the insolation and oxygen isotope records stems from the existence in Earth climate of a strong 100,000-year-duration asymmetrical sawtooth-like cycle, which is absent in the Milankovitch seasonality curve. In addition to being modulated by the seasonality changes, Earth climate tends to drift toward ever colder conditions. This drift is periodically corrected by an abrupt shift back to full interglacial conditions. The abrupt warmings which mark the termination of each 100,000-year cycle occur at the times of prominent peaks of Northern Hemisphere seasonality. As can be seen in figure 12, the strongest peaks come in triads corresponding to those time periods when the eccentricity is largest. Terminations take place in response to the first in a given triad of strong peaks.

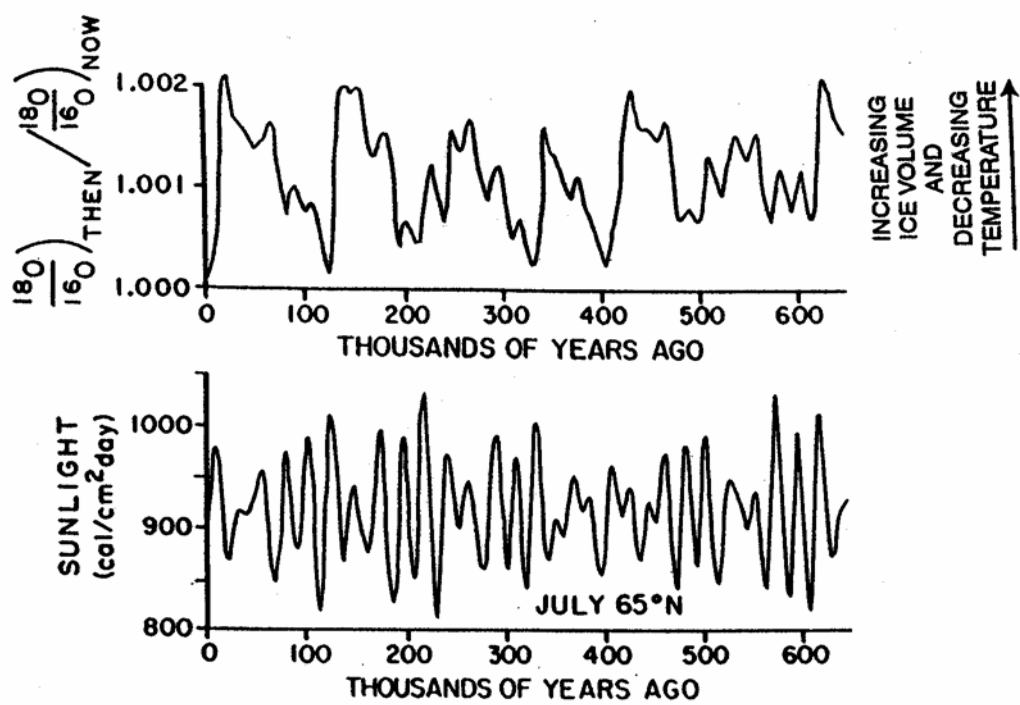


Figure 12. Comparison between the marine ^{18}O record and the July solar-radiation record for 65°N latitude.

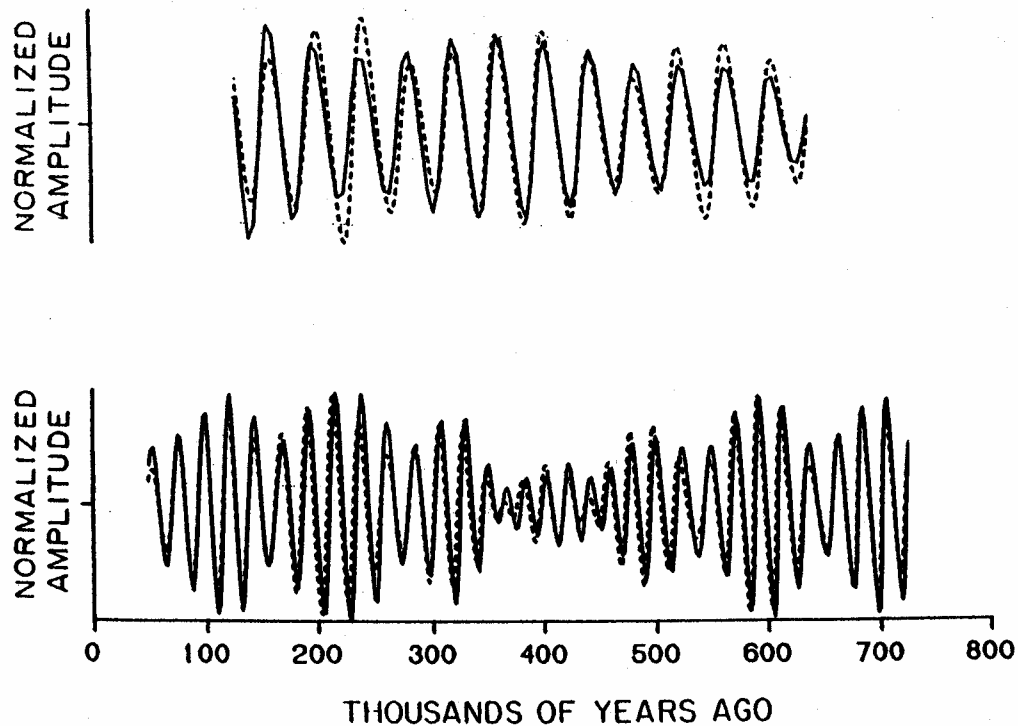


Figure 13. Verification that Earth orbital cycle produces climate changes: In the upper diagram the amplitude history of tilt-induced seasonality changes (dashed curve) is compared with the amplitude history of the variability in the $^{18}\text{O}/^{16}\text{O}$ record associated with the tilt frequency (solid curve). In the lower diagram the amplitude history of the precession-induced seasonality changes (dashed curve) is compared with the amplitude history of the variability in the $^{18}\text{O}/^{16}\text{O}$ record associated with the precession frequency (solid curve). The near-perfect match provides dramatic evidence that Earth climate senses changes in seasonality. The comparison does not extend to the present because the mathematical technique used by Imbrie to isolate the variability in the ^{18}O record associated with a given frequency does not work near the "ends" of the record.

The impression drawn from this is that the Earth system is currently engaged in an internal oscillation characterized by long periods of drift toward ever colder conditions. These drifts are brought to an end by the onset of an instability which causes the system to jump back to its warm state. The seasonality changes appear to exert two influences on this cycle. First, they modulate the periods of coldward drift. Second, they pace the terminations. Apparently, as the ice caps grow ever larger, the climate system becomes ever more vulnerable to self correction. This vulnerability appears to be greatest during periods of strong Northern Hemisphere seasonal contrast. If this view is correct, then three quarters of a million years ago the climate system began this self oscillation. Before that time, the seasonality changes appear to have modulated a more nearly stationary climate. Of course, this analysis is speculative in that nothing has been said about the actual physical connection between seasonality and climate.

THE RECORD IN ANTARCTIC ICE

Over the course of two decades, Russian scientists succeeded in drilling through the entire ice column at the Vostok Station in Antarctica (see insert figure 14). The record encompasses four full glacial cycles. Not only has a stable isotope record (in this case H/D instead of $^{18}\text{O}/^{16}\text{O}$) been obtained, but also records of dust, of atmospheric CO₂, of atmospheric CH₄, and of the $^{18}\text{O}/^{16}\text{O}$ ratio in atmospheric O₂. The latter is particularly important for it allows the ice core record to be tied to both the benthic foraminifera ^{18}O record and the Milankovitch seasonality variations. The tie between the ^{18}O in atmospheric O₂ and that in ocean H₂O stems from the fact that all the O₂ produced by plants ultimately comes from the sea. Further, atmospheric O₂ molecules are replaced by new ones on a time scale of 2000 years. Hence with only a small lag, the ^{18}O in atmospheric O₂ must follow the changes in ocean ^{18}O associated with the waxing and waning of the ice sheets. Hence the sharp decreases in ^{18}O seen at the end of each cycle must record the melting of the large Northern Hemisphere ice sheets.

The tie to the Milankovitch insolation record is through the strong 23,000-year

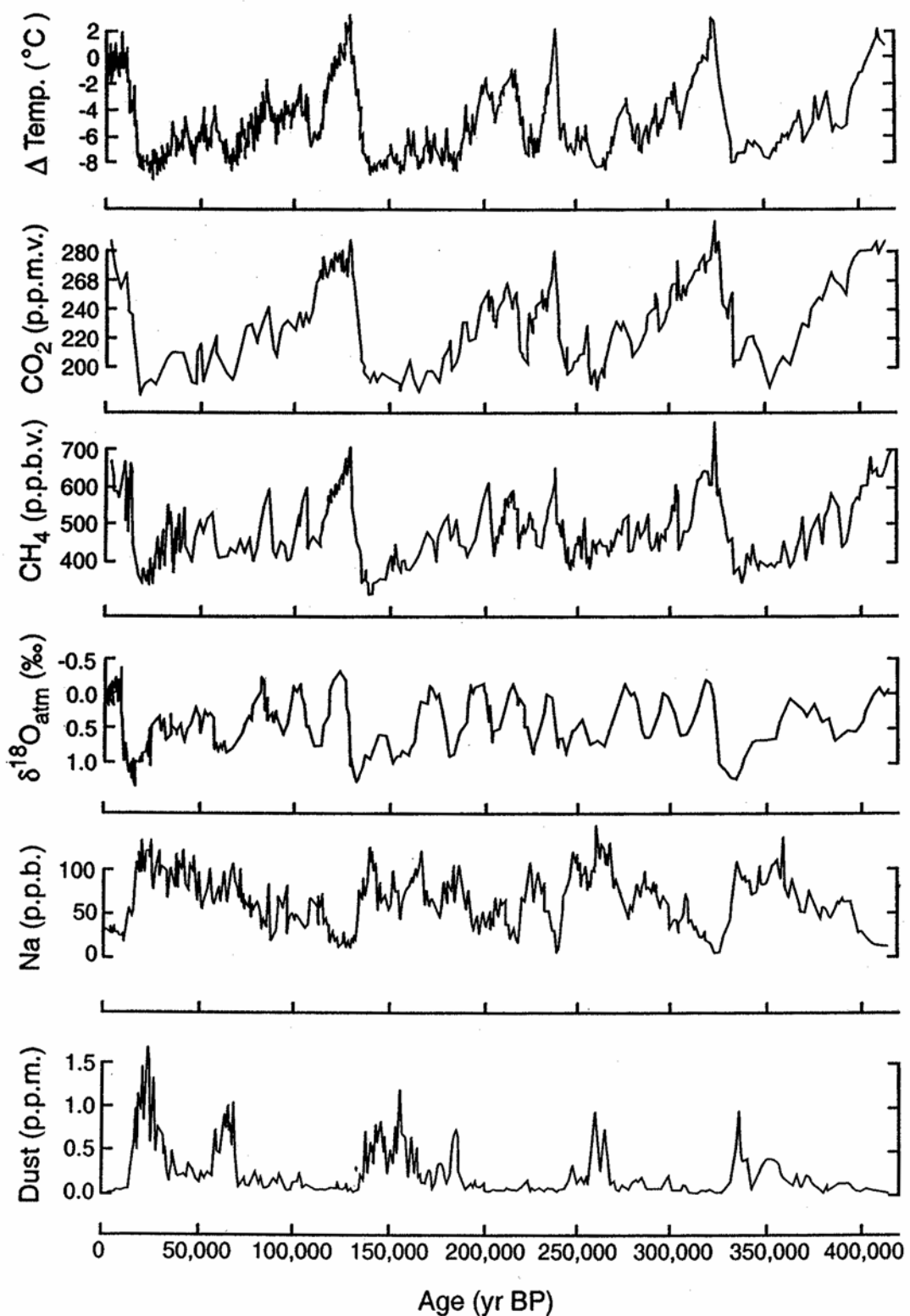


Figure 14. Plots of air temperature based on hydrogen isotope measurements in the ice, of CO_2 , CH_4 and of ^{18}O in O_2 based on measurements on air trapped in the ice and of sodium and dust concentrations in the ice for the long core at the Vostok Station in central Antarctica (Petit et al., 1999).

fluctuations in both methane and the ^{18}O in atmospheric O_2 record. It turns out that atmospheric O_2 has a $\delta^{18}\text{O}$ 23 per mil larger than that for ocean H_2O . This offset is a consequence of a fractionation during respiration. Just as the light molecule of CO_2 is preferentially utilized during photosynthesis, so also is the light molecule of O_2 during respiration. What the record shows is that the offset between the $\delta^{18}\text{O}$ in atmospheric O_2 and that in sea water grew and shrank in concert with the Northern Hemisphere summer insolation. While the exact reason for this change has yet to be understood, its existence allows the chronology for the older portions of the Vostok ice record to be tuned to match the absolute planetary time scale.

It is interesting to note that the records for D to H, CO_2 and CH_4 follow one another quite well. Also, the peak interglacial and peak glacial values of all three properties repeat remarkably well from cycle to cycle. However, the modulations of the decline from peak interglacial to peak glacial have somewhat different characteristics. Unlike the methane and ^{18}O in O_2 , the responses for CO_2 and H/D to the 23,000-year insolation cycle are less pronounced. For dust, the largest peaks come at the times of maximum ice sheet size.

To me one of the most interesting features of this record is the sequence of events at each termination. As shown in figure 15, the first thing to happen at each termination is a collapse of the very large dust inputs to the Antarctic ice cap. Then, H/D, CO_2 and CH_4 commence their rises. They reach to near their peak values before the ^{18}O in O_2 begins its decline. This seems to be telling us that the southern polar region (H/D and CO_2) and the equatorial zone (CH_4) lead the northern polar regions (^{18}O in O_2) out of the glacial period.

THE LAST 160,000 YEARS

We know much more about the last two major 100,000-year climate cycles than we do about the earlier ones. However, before discussing these cycles, it is useful to explain a system of stratigraphic nomenclature widely used by Quaternary geologists.

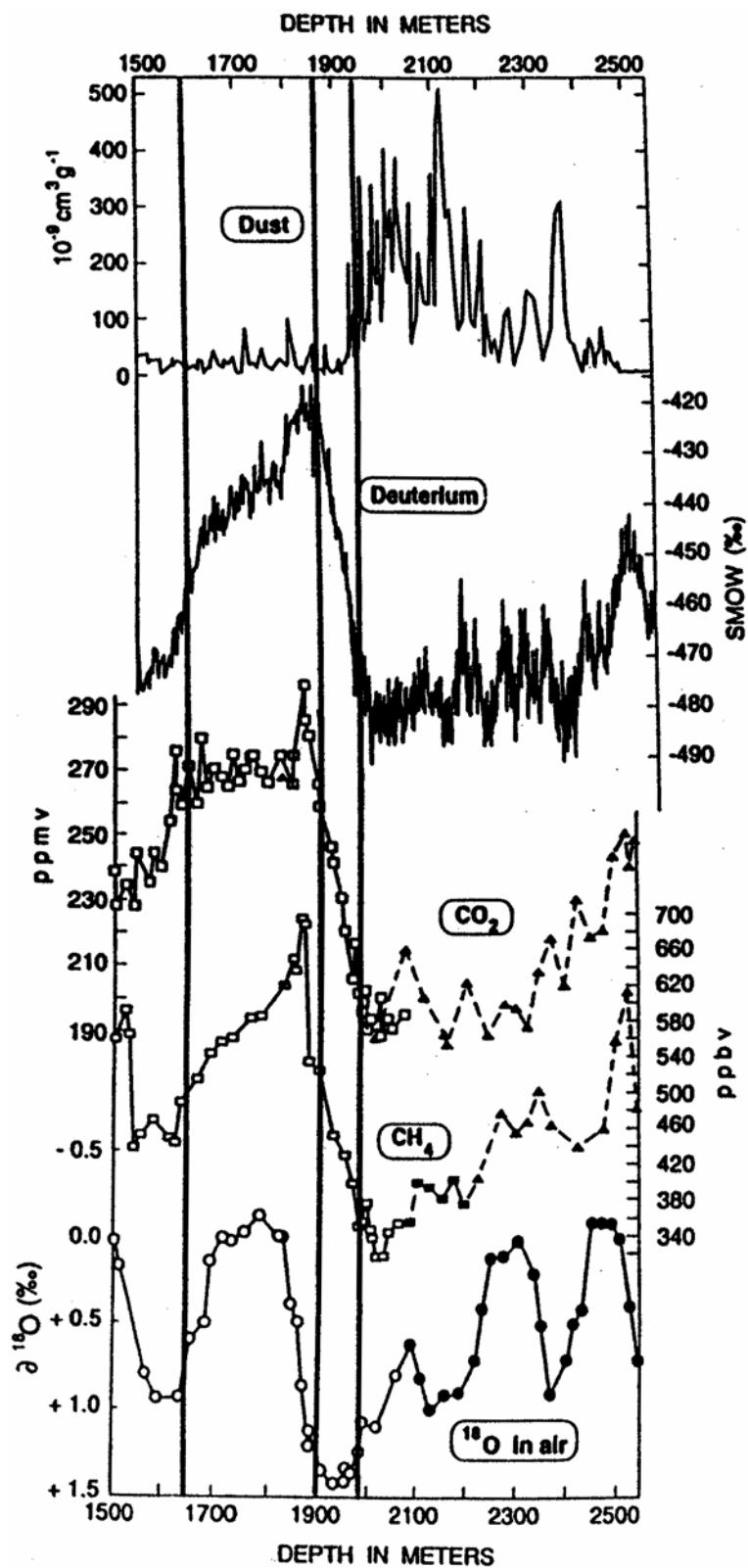


Figure 15. Sequence of events associated with Termination II as recorded in the Vostok Antarctica ice core (as summarized by Broecker and Henderson, 1998). The depth scale (lower) for properties recorded in the air trapped in the ice has been displaced from the depth scale (upper) for the ice itself in order to account for the bubble close-off depth.

In this system, the present interglacial (i.e., the Holocene) is designated as marine isotope stage 1. The last interval of glaciation is subdivided into three stages (2, 3 and 4). Emiliani, who invented this nomenclature, did this in order to set apart the glacial maxima which mark the early (stage 4) and late (stage 2) portions of this cold interval from an intervening interval of moderate cold (stage 3). He used one number (stage 5) to designate the entire last interglacial. This interval has subsequently been subdivided in five subparts. Three of these (i.e., 5e, 5c and 5a) are warm maxima and two (5d and 5b) are intervening intervals of cooler climate. The penultimate glaciation is designated by a single number (i.e., stage 6). For earlier cycles each interglacial is designated by an odd number and each glacial by an even number.

Let us first consider the oxygen isotope ratio record for benthic foraminifera (see figure 16). As we have seen, it changes with both ice volume and deep water temperature. The task of separating these influences is not a simple one for the structure of the time history of deep sea temperature was very unlikely to have been identical to that for ice volume. We know this because sea level (and hence, also ice volume) has been established for three key times. During the peak of the last interglaciation (stage 5e), sea level stood about a few meters higher than now and during stages 5c and 5a, about 16 meters lower. If the 20-meter lowering of sea level between stage 5e (+4 m) and 5c (-16 m) were the only cause for an oxygen isotope change in the deep Pacific benthic $\delta^{18}\text{O}$ record, then a 0.20‰ rise would be expected. The observed increase (see figure 16) is about 0.60‰. The extra 0.40‰ (i.e., 0.60-0.20) requires a 1.5°C cooling of deep Pacific water. In the section entitled “Indicators”, we saw that of the 1.75‰ $\delta^{18}\text{O}$ drop between stage 2 and stage 1, only about 1.1‰ can be accounted for as the result of a reduction in ice volume. The remaining 0.65‰ must have been the result of a warming (by about 2.5°C) of deep sea water. It appears that much of this cooling occurred at the end of stage 5e.

The timing of the remaining 1.0°C of deep Pacific temperature change remains

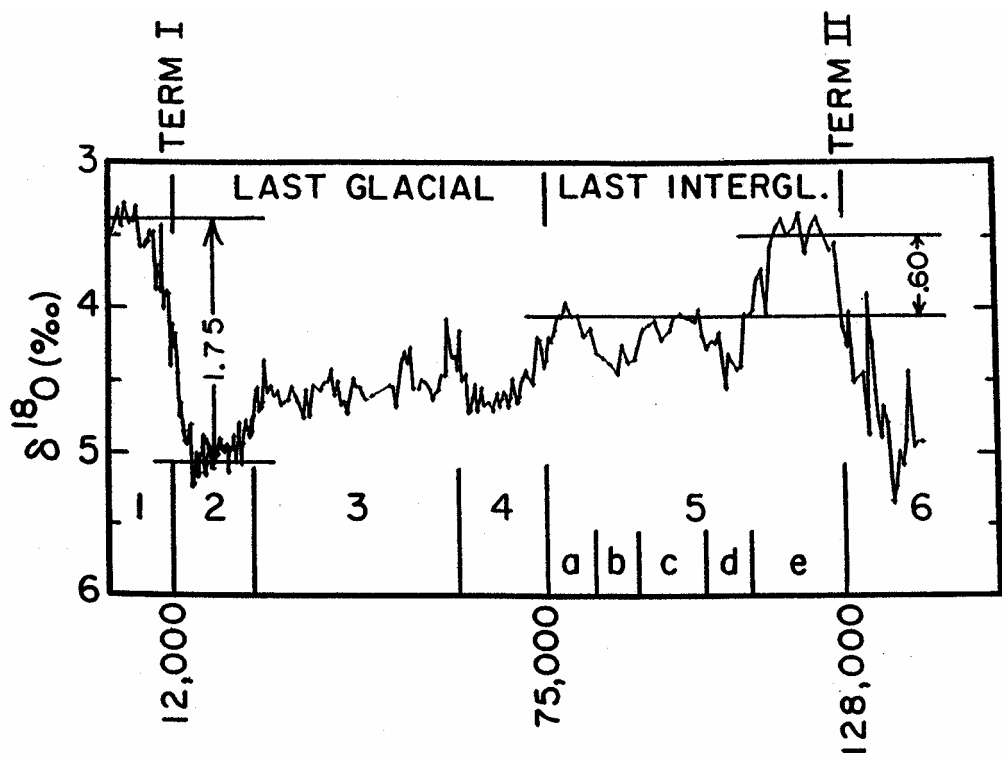


Figure 16. Shackleton's oxygen isotope record for benthic foraminifera from a deep sea core raised from the east equatorial region of the Pacific. The marine isotope stage numbers and the termination positions are shown. Also given are the generally accepted ages for the major boundaries.

uncertain. A logical choice is to place it at the stage 5-4 boundary, i.e., the time of the transition from interglacial to glacial conditions. Support of this placement comes from the $^{13}\text{C}/^{12}\text{C}$ record for high latitude deep sea cores. As reproduced in figure 17, the sharp glacial to interglacial carbon isotope changes which occurred at Terminations II and I are matched by equally sharp changes in the opposite direction at a time corresponding to the stage 5-4 boundary. These ^{13}C results suggest that a major change in the mode of ocean operation occurred about 75,000 years ago. It seems reasonable that this reorganization brought about a temperature change in the deep sea. As the deep water currently produced in the northern Atlantic is about 4°C warmer than that of deep water produced in the Southern Ocean, a reduction in the strength of the northern source would lead to a cooling of the entire deep sea. While the true situation may well be more complicated, this evidence suggests that the deep sea warmed by about 2.5°C during terminations (i.e., at the close of stage 6 and at the close of stage 2) and that the intervening cooling occurred in two steps: one of 1.5°C at the end of stage 5e, and the other of 1.0°C at the end of stage 5a. Based on these assumptions, the ^{18}O record for the last 160,000 years can be separated into an ice volume and a deep ocean temperature component (see figure 18).

One more matter must be dealt with before we proceed with the comparisons between the deep ocean temperature record and the stable isotope-based temperatures, the CO_2 and CH_4 contents of trapped air, and the aluminum content of Vostok ice (see figures 19 and 20). A discrepancy exists between the chronology assigned to Vostok ice core and that assigned to the marine oxygen isotope record. The feature corresponding to Termination II (i.e., the stage 6-5 boundary) is assigned an age of about 140,000 years in the ice core. This is 12,000 years greater than that of 128,000 years assigned to the same feature in the marine record. The time scale adopted for the Vostok core is based on a flow model for the sector of the Antarctic ice cap in which the Vostok site is located. This model is set to match present day accumulation rate of snow. Adjustments in this

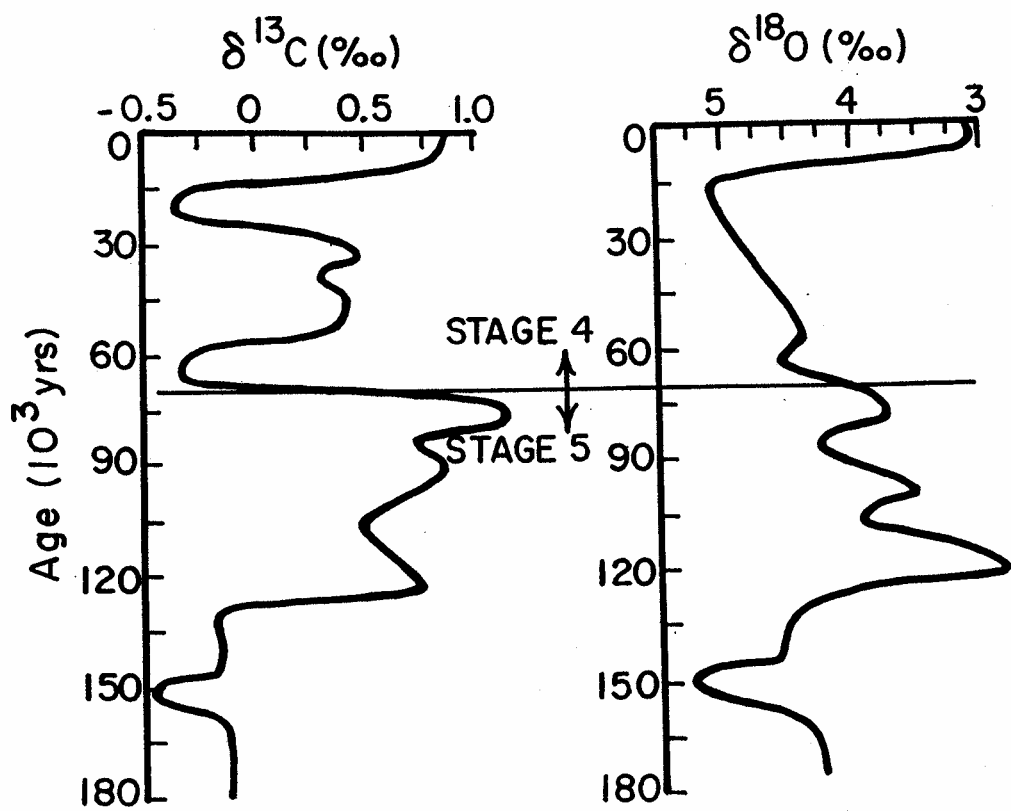


Figure 17. Carbon and oxygen isotope records for benthic foraminifera in core V30-97 (41°N , 33°W , 3.4 km) from the northern Atlantic Ocean (Mix and Fairbanks, 1985).

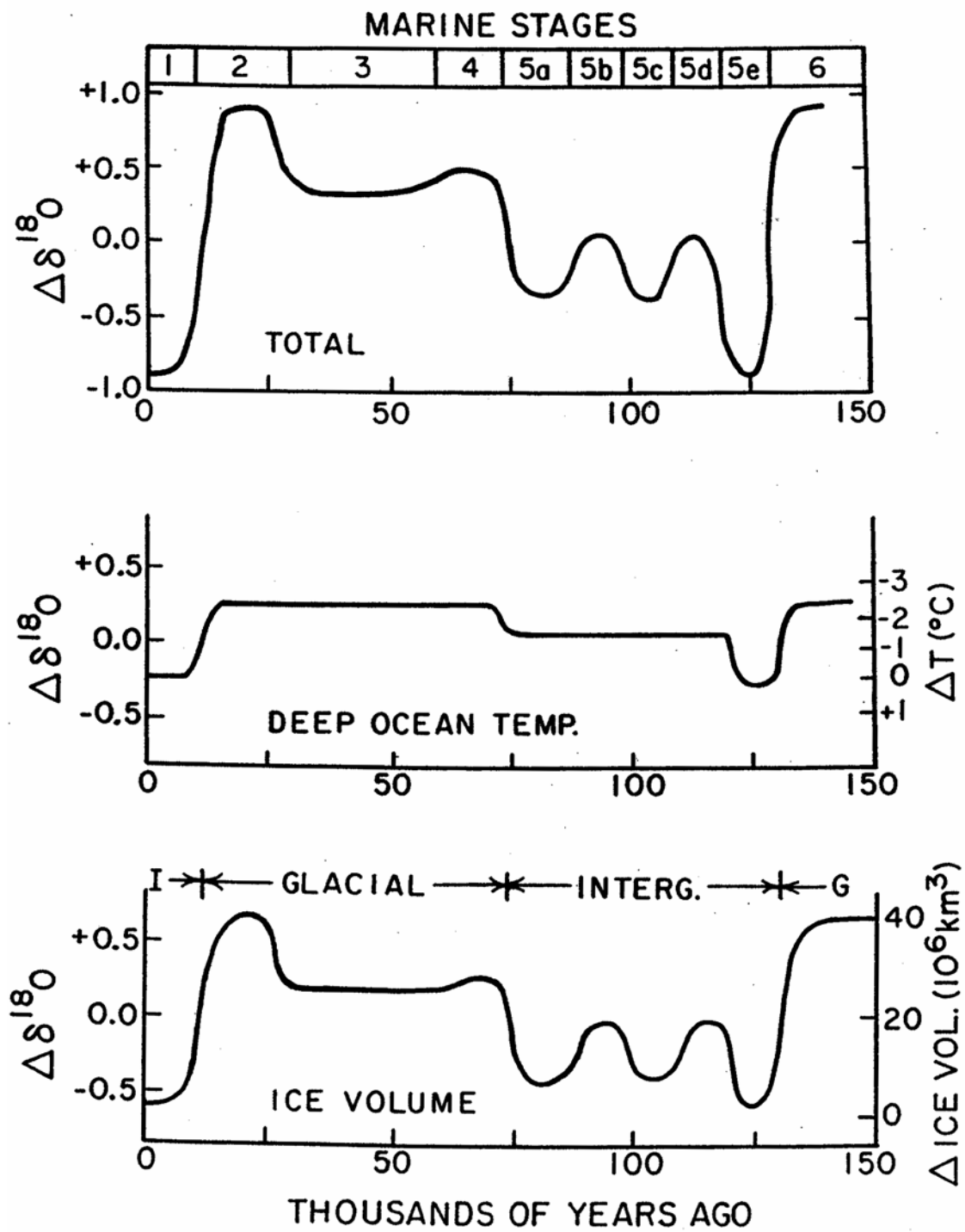


Figure 18. In the upper panel is shown a smoothed version of the oxygen isotope record for benthic foraminifera in the deep Pacific Ocean. In the middle panel, an estimate is given of that part of the ^{18}O signal related to temperature change of deep sea water. In the lower panel, that portion of the ^{18}O change attributable to ice volume is shown.

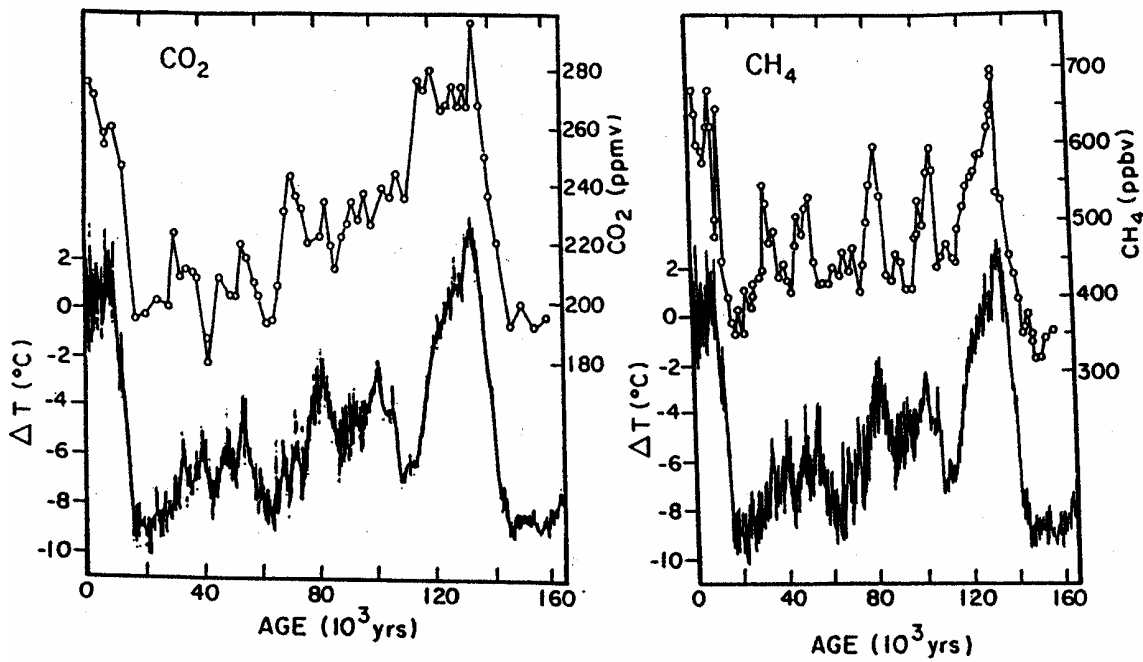


Figure 19. Comparison of the stable isotope record (scale converted to air temperature) with those of CO₂ (left) and CH₄ (right). A correction has been made for the small offset between the gas record and the solid record.

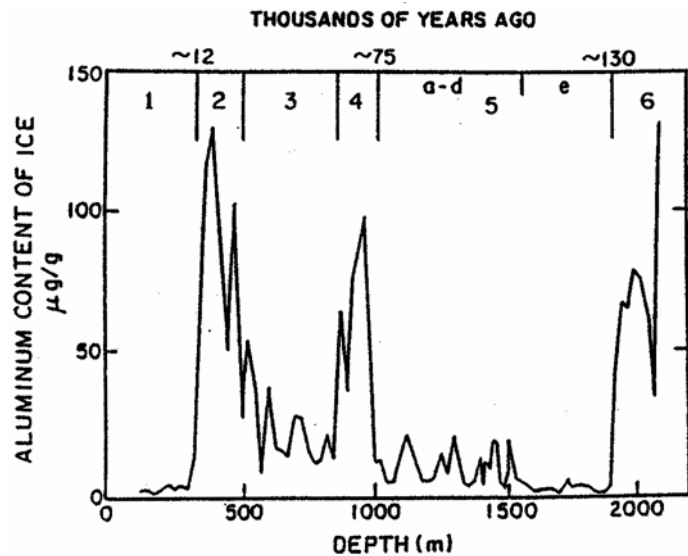


Figure 20. The aluminum content of the Vostok ice core as a function of depth. As the aluminum is contained entirely in silicate mineral grains, this record provides a measure of the dust content of the ice and hence also of dust accumulation rate.

rate are made based on air temperatures reconstructed from the stable isotope record, the assumption being that the snowfall is in proportion to the water vapor content of the air over the site. Since the stable isotope record provides an estimate of air temperature, the water vapor content and, in turn, the rate of snow accumulation can be computed. The major function of the flow model is to correct for the foreshortening of the ice record caused by lateral flow. The snow which accumulates in the interior of the Antarctic continent must eventually flow to the edges of the cap where ablation occurs by melting and by calving. Because of this, as it is buried ever deeper in the cap, every cylinder of ice becomes shorter and fatter (and is displaced laterally toward the ice sheet edge). At the depth in the Vostok ice core of Termination II, the extent of this foreshortening is calculated to be a little over a factor of two. In other words, a layer which had a thickness of 5 cm thick just after the completion of the lithification process is thinned to about 2 cm at a depth of 2000 meters. The reason that the correction is relatively small is that as the ice beneath the Vostok Station is about 4000 meters thick. Hence Termination II does not lie in the region near the bedrock where the thinning reaches tenfold or more. So, why the time scale discrepancy? One answer might be that it would not be surprising if the flow model were in error by $\pm 10\%$.

However, this difference cannot be passed off quite so easily. Although averaging about 124,000 years, a number of ^{230}Th ages on corals representing the stage 5e high sea stand yield ages of greater than 128,000 years, suggesting that the peak in sea level was reached prior to the time of the peak in Northern Hemisphere summer radiation. Indeed, if these older ages are correct, then the chronology applied to the marine ^{18}O record would have to be correspondingly altered.

At the time of this revision (July, 2002), no consensus had been reached. For this to happen, two complications will have to be resolved. One has already been mentioned. The Vostok record suggests a several thousand-year lag between the warming of Antarctica and the melting of the northern ice sheets. Another complication is that it has

been shown that many corals have suffered diagenetic alteration which adds ^{230}Th and ^{234}U in nearly equal activity proportions making the uncorrected ages anomalously high. If it is assumed that the $^{234}\text{U}/^{238}\text{U}$ ratio in sea water was the same during the last interglacial as it is today, then a correction can be made by sliding down the 1:1 ^{230}Th to ^{234}U slope until the isochron is reached. When this is done, most of the corals representing the last interglacial high sea stand drop into the 118,000 to 125,000-year range. However, there are a few corals for which no correction is needed (and one on which concordant $^{231}\text{Pa}/^{235}\text{U}$ ages have been obtained) that are older than 128,000 years.

Oxford University's Gideon Henderson came up with a means of directly dating the deep sea sediments ^{18}O record by the ^{230}Th in-growth method. The interglacial sections of sediment in deep sea cores from adjacent to the Bahamas contain aragonite needles produced by calcareous algae which thrive in the bank's shallow waters. As this aragonite contains 6 ppm uranium and little thorium, it is ideal for dating. Henderson obtained ages for the period of the interglacial ^{18}O minimum consistent with those for the majority of high sea stand corals (after correction for diagenetic additions of ^{230}Th and ^{234}U). But he also obtained age on the sediment deposited during the Termination II ^{18}O drop which predates the rise toward the Northern Hemisphere summer insolation peak.

One might ask, isn't this a tempest in a teapot? Does several thousand years make that big a difference? In fact, it does because to some people it puts in question the pacing of terminations by insolation cycles. Indeed, one might argue that the 100,000-year cycle is internal to the Earth. Many oscillators show the slow drift and abrupt correction behavior characteristic of the 100,000-year cycle. Perhaps, the termination of the Earth's drift toward ever colder conditions is sometimes pre-triggered by insolation perturbations, but at others runs its entire course. So it is extremely important to resolve this dating issue.

Comparing the Vostok ice core records in figure 14 with the oxygen isotope record for benthic foraminifera, one sees that while all four records share the same

rhythms, pronounced differences exist. The most obvious of these is that the 23,000-year periodicity imprints itself more strongly on the ice core methane record than in the other records. Another difference is seen in the width and shape of 5e CO₂ and CH₄ peaks in these two records; while the CO₂ peak is wide and flat, the CH₄ peak is narrow and sharp.

Putting aside these differences, the first order features of these four records tell us that, at least on the 100,000-year time scale, the size of the Northern Hemisphere ice sheets, the air temperature in Antarctica, the ocean driven CO₂ changes, and the land driven CH₄ change proceeded in harmony. Despite the pronounced differences in the history of seasonality records for the two hemispheres, the Southern Hemisphere's climate (as expressed by the Antarctic stable isotope record) matches quite well that for the Northern Hemisphere (as represented by the benthic ¹⁸O record). Climate in both hemispheres appears to be paced by Northern Hemisphere seasonality.

It was already shown in the section entitled "Indicators" that evidence for the synchronicity between Northern and Southern Hemisphere climate does not rest entirely on the Antarctic stable isotope and dust records. Strong support is added from the record of glaciation on high mountains. The change between the last glacial maximum and the Holocene was not only synchronous on the two sides of the equator, it was also symmetrical. To me this makes clear that the cooling in the Southern Hemisphere was not driven by the albedo change created by the ice sheets of the Northern Hemisphere. Rather, the Southern Hemisphere cooling appears to have been just as large as that in the Northern Hemisphere.

While adequate evidence exists to demonstrate that during the peak of the last glaciation mountain snowlines throughout the world stood about one kilometer lower than now and that the retreat of these snowlines to their present position occurred during Termination I, little direct dating exists to demonstrate that this synchronicity extends to earlier portions of the record. However, support for long-term synchronicity comes from

the CaCO_3 record in marine sediments adjacent to the coast of New Zealand (see figure 21). The ^{18}O record on benthic foraminifera from this core permits a direct tie to be made to the volume of the Northern Hemisphere ice sheets. The CaCO_3 content of the core shows wide variations which correlate extremely well with the ^{18}O record. These variations are interpreted to be the result of varying extents of dilution with silicate material supplied by rivers draining the mountainous region of New Zealand's South Island. During episodes of major mountain glaciation, the large amount of debris supplied to the rivers was carried directly out to sea, greatly increasing the rate of sedimentation and thereby diluting the more nearly uniform rain of marine CaCO_3 . By contrast, during times, such as now, of lesser mountain glaciation, not only was less debris generated, but that which is generated is trapped in the lakes impounded behind the moraines left behind during the retreat from the previous glacial maximum. If this logic is correct, then the match between the ^{18}O maxima (representing major Northern Hemisphere glaciations) and the CaCO_3 minima (representing major New Zealand mountain glaciation) requires a synchronicity between climate changes in the two hemispheres.

We have already discussed evidence that dust transport in Asia was much higher during times of large ice volume than during times of small ice volume. The Vostok ice core record confirms that the same holds true for the Southern Hemisphere. As shown in figure 20, during marine stages 6, 4, and 2, dust accumulation rates reached values an order of magnitude higher than those for stages 1 and 5e. This record shows a larger contrast between conditions during marine stage 3 and those during marine stages 2 and 4 than any other climate indicator.

THE LAST TERMINATION

Key to understanding of what drove the glaciations of the last three quarters of a million years are the terminations which brought each of the 100,000-year cycles to an abrupt end. As the last of these events occurred during a time span easily assessable to

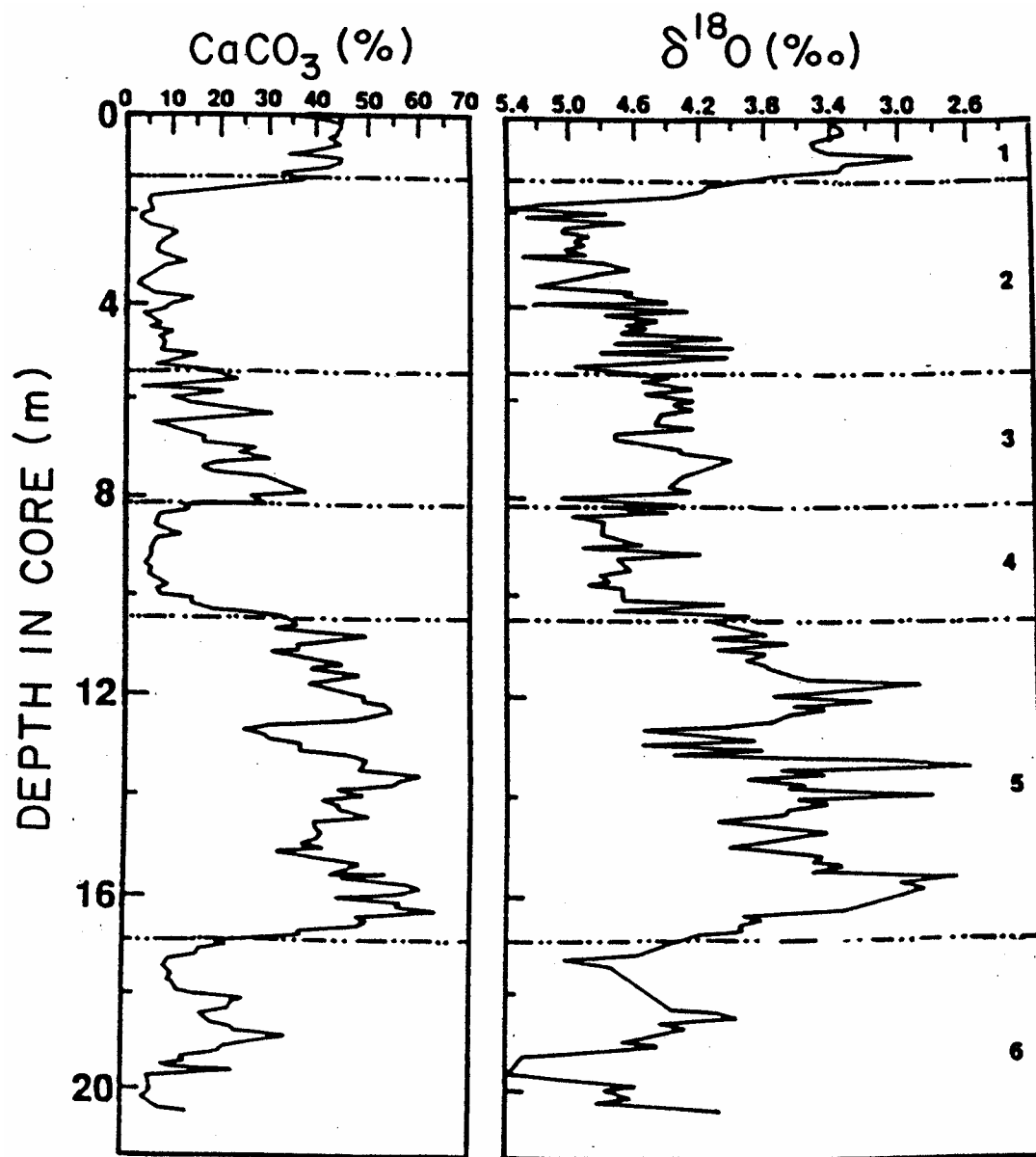


Figure 21. Records of CaCO_3 content and oxygen isotope ratios in benthic foraminifera for DSDP core 594 (45°S , 176°E). Times of low CaCO_3 content are thought to be the result of dilution with debris generated by intense glaciation of the Alps of southern New Zealand. As can be seen, they correspond to times of high benthic ^{18}O (hence times of major Northern Hemisphere glaciation). The numbers denote Emiliani's marine stages.

radiocarbon dating, precise correlation of events taking place throughout the world can be achieved. A summary of the main features of this transition is shown in figure 22.

As late as 18,000 years ago, peak glacial conditions prevailed. Both continental ice sheets and mountain glaciers stood at or close to their maximum extents. The oxygen isotope ratios and dust contents of polar ice still had their full glacial values. Sea level stood 110 or so meters lower than today. The CO₂ and CH₄ contents of the air trapped in polar ice remained at the low values characterizing full glacial time. The surface waters of the Atlantic off the British Isles were populated by the planktonic foraminifera *N. pachyderma* (l.c.), now found only in polar waters. The non-glaciated portions of northern Europe were treeless. The nutrient distribution in the deep sea showed its full glacial pattern. Loess accumulated rapidly in central China and other dust prone areas. Then rather abruptly just after 14,500 ¹⁴C years ago, glaciers throughout the world began to retreat; polar temperatures began to rise; atmospheric dustiness began to diminish; CO₂ and CH₄ began to rise; in other words, the termination was in progress. In the northern Atlantic basin, this first phase of the termination manifested itself as catastrophic break up of the large valley glaciers which extended northward from the Alps. Within a period of a few hundred years, the valleys became ice free. This event is recorded in the sediments of lakes formed in depressions left behind by the retreating ice. However, as recorded by pollen in these sediments, climatic conditions remained too harsh to permit the valleys to be reforested. Then suddenly about 12,800 ¹⁴C years ago, a major warming event took place in the northern Atlantic region which created climatic conditions rivaling those of the present. Trees replaced shrubs. Seemingly the interglacial had arrived. But then about 11,000 ¹⁴C years ago, cold conditions abruptly returned and prevailed for 1200 years (i.e., the Younger Dryas). Then close to 10,000 ¹⁴C years ago, this cold snap came to an abrupt end. Since then, interglacial conditions have remained in place. It must be mentioned that no equivalent of the Younger Dryas cold snap appears to punctuate earlier terminations. As is discussed below, it appears to be a

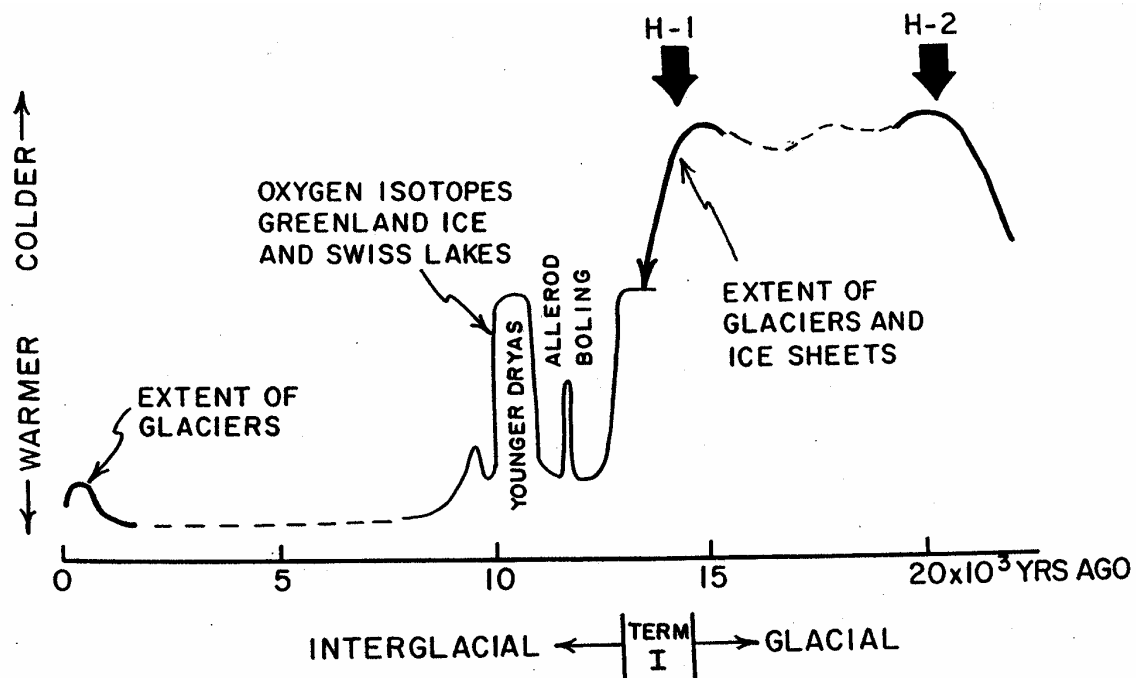


Figure 22. George Denton's view of the events surrounding the last termination: The termination began about 14,500 Libby years ago when mountain glaciers and ice sheets alike commenced a dramatic retreat. This retreat left in its wake thousands of closed topographic depressions, many of which are still occupied by lakes. Oxygen isotope and pollen records kept by the sediment in these lakes reveal that cold conditions prevailed for about a millennium and then quite suddenly it became warmer; trees replaced the shrubs. This warming completed the two-step termination. Events of interest both preceded and followed the termination. The glacial maximum which preceded the termination had two humps separated by an interval during which the ice front fluctuated close to its maximum. The warm period following the termination was punctuated by a major cold event (the Younger Dryas). Most puzzling are the two Heinrich events which flank the glacial maximum. They are recorded as layers of ice rafted material in sediments extending all the way across the northern Atlantic. One (H-2) occurred in coincidence with the onset of the glacial maximum. The other (H-1) coincides with the end of the glacial maximum. Whether these events played an active role in climate changes of this time interval or are merely rapid advances of the eastern margin of the Laurentian ice-driven sheet triggered by colder global climates remains to be demonstrated.

one-time event triggered by a sudden and very large release of meltwater stored in proglacial Lake Agassiz.

So abrupt and short lasting were the changes marking the onset of the Bølling Allerød and the onset and ending of the Younger Dryas that they are properly recorded only in rapidly accumulating sediment or ice. Most of the deep sea sediments, upon which the oxygen isotope records are based, accumulate at only two to three centimeters per thousand years. Core top radiocarbon ages of several thousand years demonstrate that benthic organisms stir marine sediments to a depth of between 6 and 10 centimeters. Hence in such sediments abrupt events are smoothed beyond recognition. While quite adequate for studies aimed depicting climate changes on the time scales of the Milankovitch cycles, these low accumulation-rate sediments do not have sufficient fidelity to properly record of the events which occurred during the last termination. Fortunately, in some places on the ocean floor, sediments accumulate at much higher rates and hence record more nearly the true character of the changes. Under most circumstances, lake and bog sediments accumulate at sufficiently high rates to obviate any blurring by organisms. Of course, no mechanism for blurring exists in ice. It is these high fidelity records we shall now discuss.

The temperature history for the basin of the northern Atlantic is based on four quite independent pieces of evidence (see figure 23). The first of these is the oxygen isotope record for the Greenland ice cores. The main factor controlling for the $^{18}\text{O}/^{16}\text{O}$ ratio in Greenland snow is air temperature. For high latitudes, the coefficient relating the $\delta^{18}\text{O}$ to temperature is $0.7\text{‰}/^{\circ}\text{C}$. Using this coefficient, the magnitude of the warmings at the onset of the onset of the Bølling Allerød and at the end of the Younger Dryas are about 6°C . However, independent estimates based on bore hole thermometry and on the extent of enrichment of ^{15}N in N_2 by thermal diffusion suggest that a more appropriate coefficient is $0.35\text{‰}/^{\circ}\text{C}$ making the magnitude of the warming twice as great. Based on modeling results, the reason for the lower coefficient appears to be that unlike the present

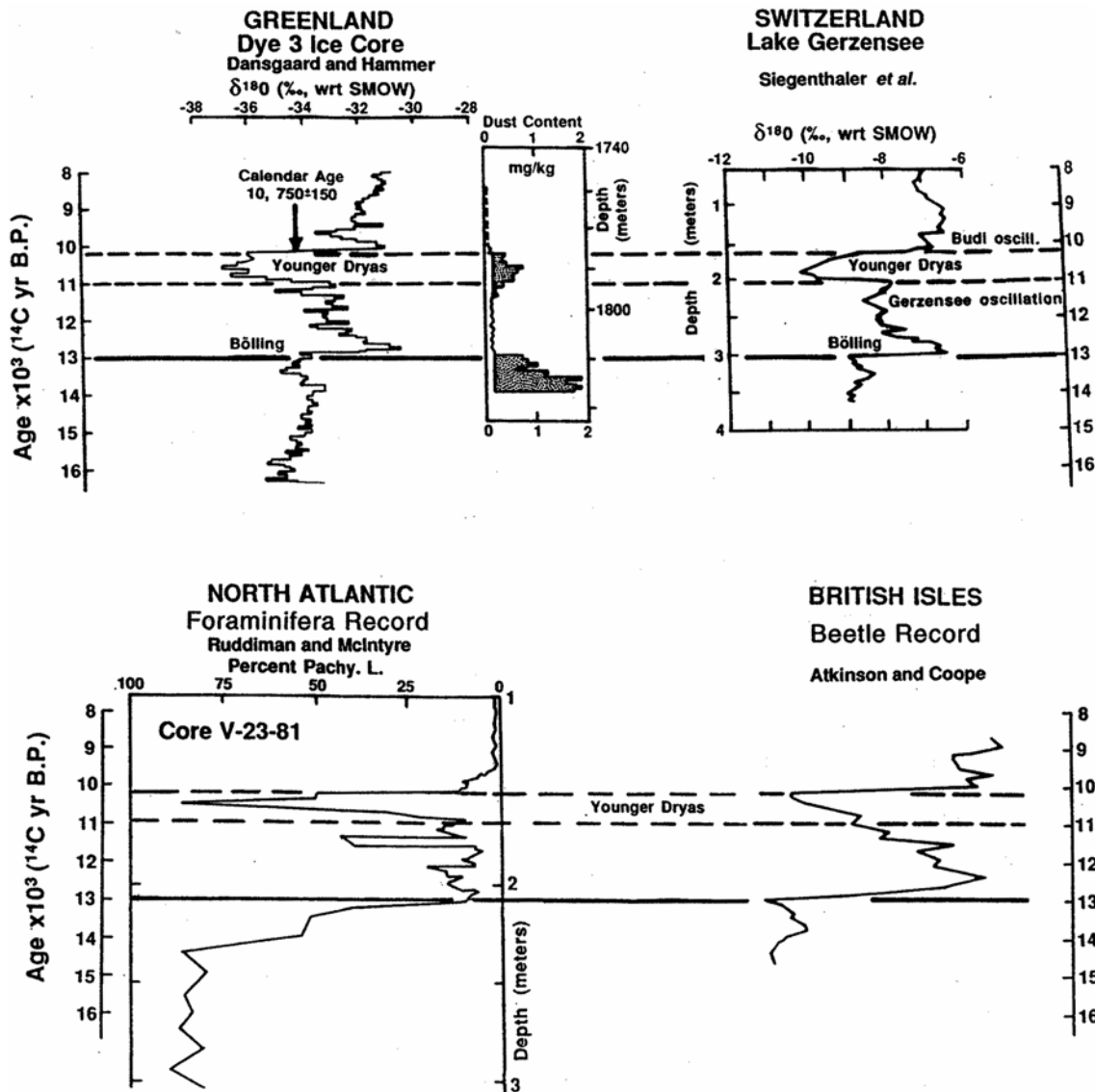


Figure 23. Comparison of four temperature records for the period of deglaciation. The upper two panels are based on oxygen isotope measurements, one for Greenland ice and the other for CaCO_3 from Swiss lake sediment. The lower two panels are based on the species composition, one for northern Atlantic planktonic foraminifera shells and the other for British beetle carapaces. Also shown is the dust record for Greenland ice which shows that storminess must also have dramatically changed.

when snowfall is spread reasonably well over the entire year during the cold glacial and the cold Younger Dryas, the winter air was too cold to yield appreciable snow and hence summer snow dominated. Hence, while the use of the $0.7\text{\%}/^\circ\text{C}$ coefficient provides a better estimate of the shift in average temperature for the times of snowfall, during warm periods this temperature is closer to the mean annual value and during cold periods it is closer to the summer value.

The second piece of evidence comes from the $^{18}\text{O}/^{16}\text{O}$ record for CaCO_3 in the sediments of a small Swiss lake called Gerzensee. The record is nearly identical to that for the Dye 3 core (see figure 23). While the primary cause for the change in the $\delta^{18}\text{O}$ value in Gerzensee CaCO_3 is the dependence of $\delta^{18}\text{O}$ in precipitation on temperature, as discussed earlier, at high latitudes the coefficient relating modern $\delta^{18}\text{O}$ of precipitation and air temperature is $0.67\text{\%}/^\circ\text{C}$. From this value must be subtracted the $+.23\text{\%}/^\circ\text{C}$ change in the fractionation factor between the oxygen in CaCO_3 and that in the lake water in which it formed yielding a net change of $0.44\text{\%}/^\circ\text{C}$, i.e., $(0.67-0.23\text{\%}/^\circ\text{C})$. As the observed change in the $\delta^{18}\text{O}$ for Gerzensee CaCO_3 at the end of the Younger Dryas is about $+3\text{\%}$, the inferred warming is 7°C . While perhaps consistent with the ice core estimate, a warming of this magnitude should show up as a major change in the plant community on the land surrounding the lake. As shown in figure 24, the change in the composition of the pollen is quite small. The reason for this seeming discordancy is not known. Perhaps, as is believed to be the case for Greenland, the apparent coefficient relating temperature and the $\delta^{18}\text{O}$ in precipitation was altered due to changes in the seasonality of precipitation. But in order to bring the ^{18}O based ΔT into line with that based on pollen, the coefficient would have to have been larger rather than smaller during glacial time.

The third record is that for beetle remains in the British Isles. As discussed in the section on “Indicators”, today's distribution of beetle species appears to be controlled mainly by air temperature. The beetle species present in the British Isles during the

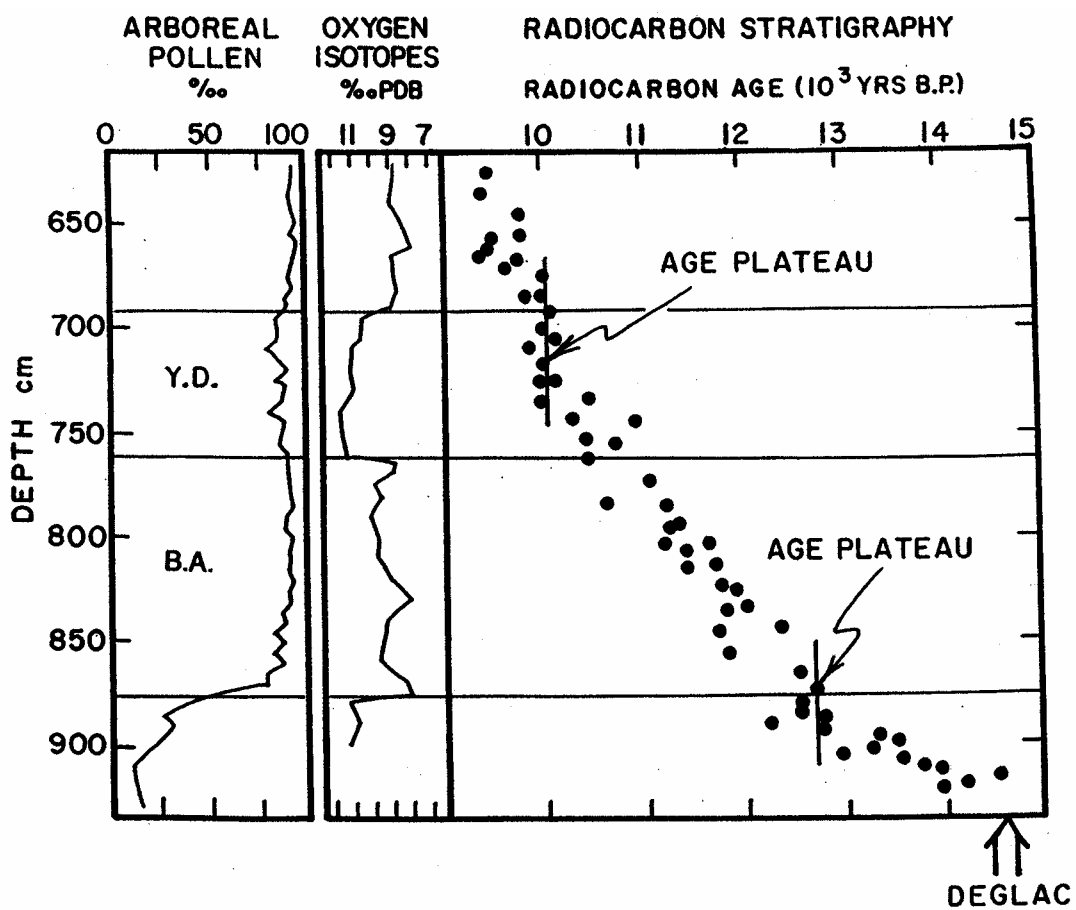


Figure 24. Comparison of the pollen diagram (proportions of tree pollen versus shrub pollen) and the oxygen isotope record for CaCO_3 in sediment from Rotsee, a small lake near Lucerne; Lotter, 1991). Also shown are radiocarbon results on terrestrial macrofossils.

deglaciation interval show changes which nicely parallel those for the isotope records. Although semi-quantitative, the beetle record suggests temperature changes as large or even larger than those derived from isotope measurements.

The fourth piece of evidence comes from the planktonic foraminifera speciation record in deep sea sediments off the British Isles (see Figure 23). Again, the changes have a pattern identical to that in the other three records. The planktonic foraminifera, *N. pachyderma* (left coiling), which dominated the waters off the British Isles during late glacial time and during the Younger Dryas has been absent from this area during the Holocene time. Today *N. pachyderma* is found only in the very cold waters in the sea around Greenland. It is the only species of foraminifera which survives in ice-laden waters.

Independent time scales for three of these records have been constructed based on radiocarbon measurements. In the case of the beetle and lake CaCO₃ records, these determinations were made on organic matter formed by terrestrial plants. In the case of the deep sea sediments, they were made on foraminifera shells. As discussed in the section entitled “Clocks”, radiocarbon dating cannot be done on ice; rather, the time scale is based on annual couplets counts. The offset between the calendar year chronology for the Greenland ice cores and the radiocarbon chronology is about the same as that between the ²³⁰Th and radiocarbon chronologies for corals (see “Clocks” section).

A problem associated with the radiocarbon chronology must be mentioned. Both the abrupt warmings at the onset of the Bølling Allerød and at the close of the Younger Dryas during what are referred to as plateaus in the radiocarbon time scale. Shown in figure 24 is a record of radiocarbon age versus depth in sediments from a small Swiss lake named Rotsee. As these determinations were made on land-plant macrofossils (i.e., seeds, needles, leaves...) sieved from the sediment, variable reservoir corrections do not confuse the situation. Further, as these plateaus have now also been found in the records for several lakes and also in tree ring sequences, they cannot be the result of abnormal

sedimentation in Rotsee. Rather, they represent periods of time when the radiocarbon content of the atmosphere was dropping at about the same rate that radiocarbon decays. Because of this, samples formed at the beginning of the plateau lose just the right amount of radiocarbon by decay, so that at the time of the end of the plateau, they still have a $^{14}\text{C}/\text{C}$ ratio equal to that in the atmosphere. These several hundred-year long periods of declining atmospheric ^{14}C could be the product of changing production of radiocarbon by cosmic rays or of changing rates of ventilation of the deep sea.

Conrad Hughen, while a graduate student at the University of Colorado, obtained evidence for a sharp rise in the radiocarbon content of surface ocean ΣCO_2 (and hence also for atmospheric CO_2) initiated at the onset of Younger Dryas time (see figure 25). He also showed that this rise was very likely the result of a shutdown in the production of deep water in the northern Atlantic (the route which today accounts for about 75 percent of the delivery of ^{14}C to the deep sea). He did this by tying the varve counted record in the Cariaco Basin (off Venezuela in the Caribbean Sea) to the European tree ring chronology. As the ^{14}C age for the onset of this rise corresponds closely to that for the abrupt onset of the Younger Dryas (marked by a sharp color change in Cariaco Basin sediment), it very likely has the same cause as the cooling. Jim Teller at the University of Manitoba has documented that a large release of stored melt water from proglacial Lake Agassiz gushed through the St. Lawrence lowlands into the northern Atlantic at the time of the abrupt younger Dryas onset. As discussed below, the consequent, sudden decrease in salinity is just what is needed to trigger a reorganization of the ocean's deep circulation system. This reorganization is thought to have triggered to the global climate change associated with the Younger Dryas.

These two ^{14}C -age plateaus complicate the task of precisely correlating events which took place in other parts of the world with the northern Atlantic's abrupt warmings. For example, an event with a radiocarbon age of 10,000 ^{14}C years could have occurred toward the beginning of the plateau as much as 250 years before the abrupt ending of the

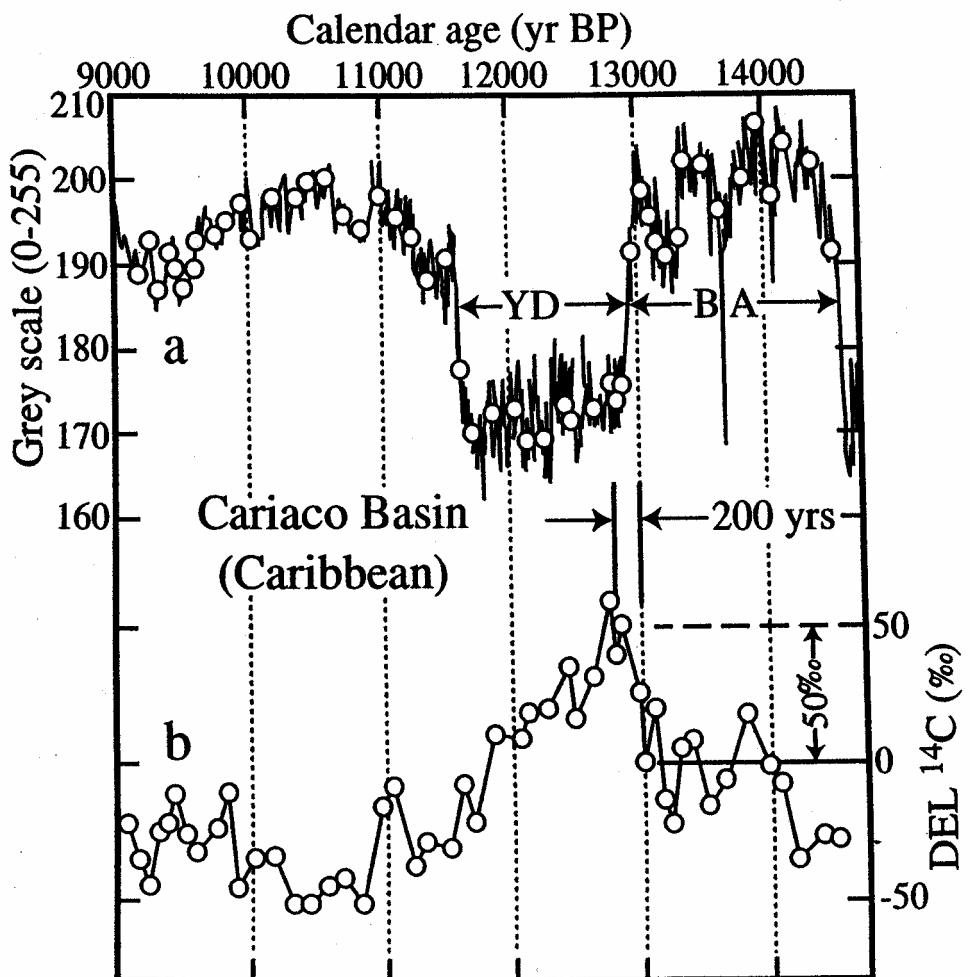


Figure 25. The gray scale record for a sediment core from the Caribbean Sea's Cariaco Basin allows the position of the Younger Dryas event to be precisely defined. As the sediment in this time interval is annually layered, radiocarbon measurements on planktonic foraminifera (open circles) allow the changes in the $\Delta^{14}\text{C}$ for surface waters to be reconstructed. As can be seen, a 50‰ rise in ^{14}C to C ratio occurred during the first 200 years of the Younger Dryas. This rise is followed by a decline in ratio during the remainder of the Younger Dryas (Hughen et al., 1998).

Younger Dryas, or 150 years after the abrupt ending of the Younger Dryas. Further, the radiocarbon age plateaus at 12,800 and 10,000 ^{14}C years ago prevent the use of radiocarbon dating to determine the duration of these warmings. Fortunately, a better means to do this is available. The annual layering in the Greenland ice cores allows the duration of both abrupt warmings to be estimated. As shown in figure 26, at the end of the Younger Dryas, both the warming and the drop in dust content occurred in a period of a few decades. This finding was confirmed in the GRIP and GISP II ice cores from Greenland's Summit locale; snow accumulation rates (figure 27) and electrical conductivity measurements (figure 28) reveal just how sharp was the termination of the Younger Dryas cold.

The ice core record demonstrates that it was not only the climate in Greenland which changed abruptly. Rather, it also provides evidence that the frequency of intense storms in Asian deserts and the warmth and wetness of the tropics underwent abrupt changes at the same times. Pierre Biscaye of Columbia's Lamont-Doherty Earth Observatory used the isotopic fingerprints provided by the neodymium and strontium in Greenland dust to pin down that its source was Asian deserts. Jeff Severinghaus used ^{15}N measurements to show that abrupt increases in methane at the onsets of these warms occurred within a few decades of Greenland's abrupt warmings (see figure 29). A strong case can be made that during the cold times the methane present in the atmosphere was generated largely in the tropics (i.e., wetlands in the vast boreal regions of the Northern Hemisphere were either frozen or buried beneath the glacial ice sheets). As the average methane molecule survives in the atmosphere only about a decade before being oxidized to CO_2 and H_2O , the concentration of this gas quickly responds to shifts in climate.

While perhaps not as iron clad as the evidence from Greenland ice, the documentation by George Denton that a prominent re-advance of New Zealand's Franz Joseph Glacier occurred within no more than a century or two of the onset of the Northern Hemisphere's Younger Dryas (see figure 30) suggests that this cold snap was

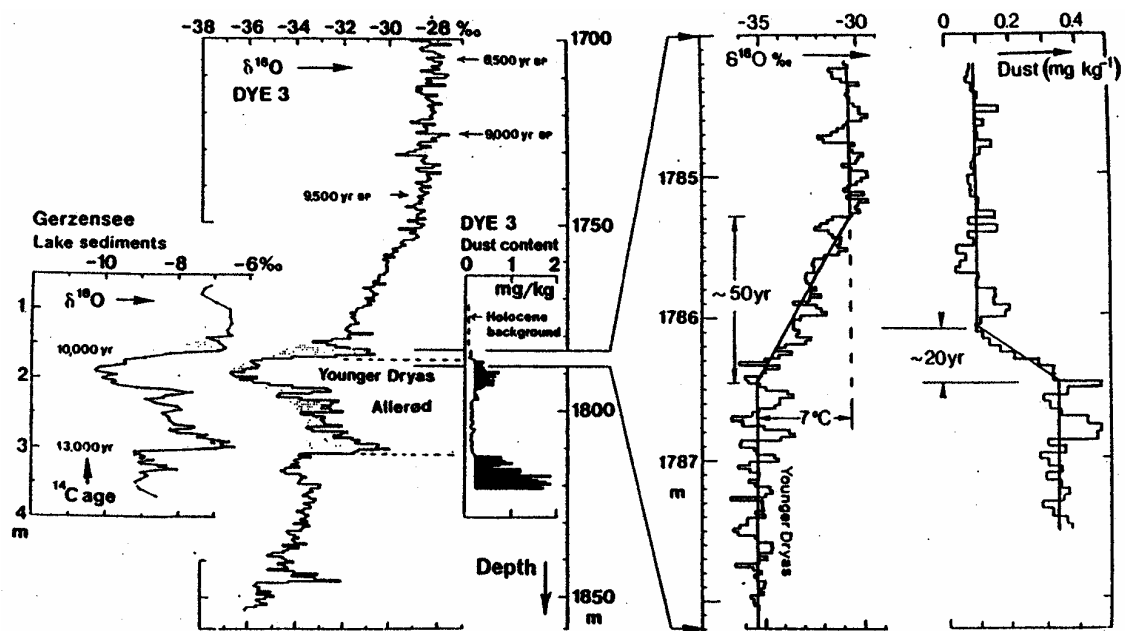


Figure 26. Oxygen isotope and dust records obtained by Dansgaard and Hammer for the Dye 3 Greenland ice core for the period of deglaciation. Shown in detail on the right is the transition marking the end of the Younger Dryas.

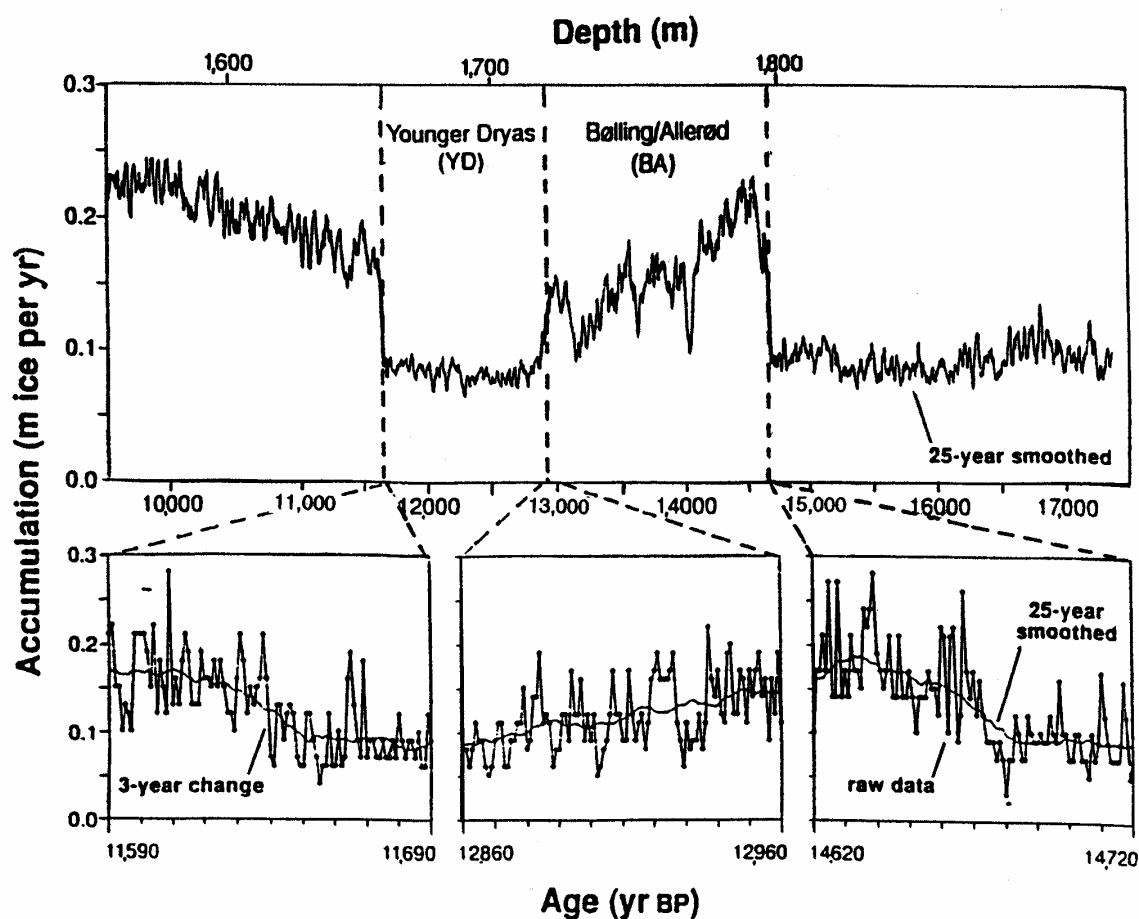


Figure 27. Accumulation rate of snow during Bølling-Allerød and Younger Dryas time as reconstructed by Alley et al. from annual layer thicknesses measured in the GISP II ice core from the Summit Greenland locale. Also shown are blowups for the abrupt warmings at the onset of the Bølling Allerød and the end of the Younger Dryas.

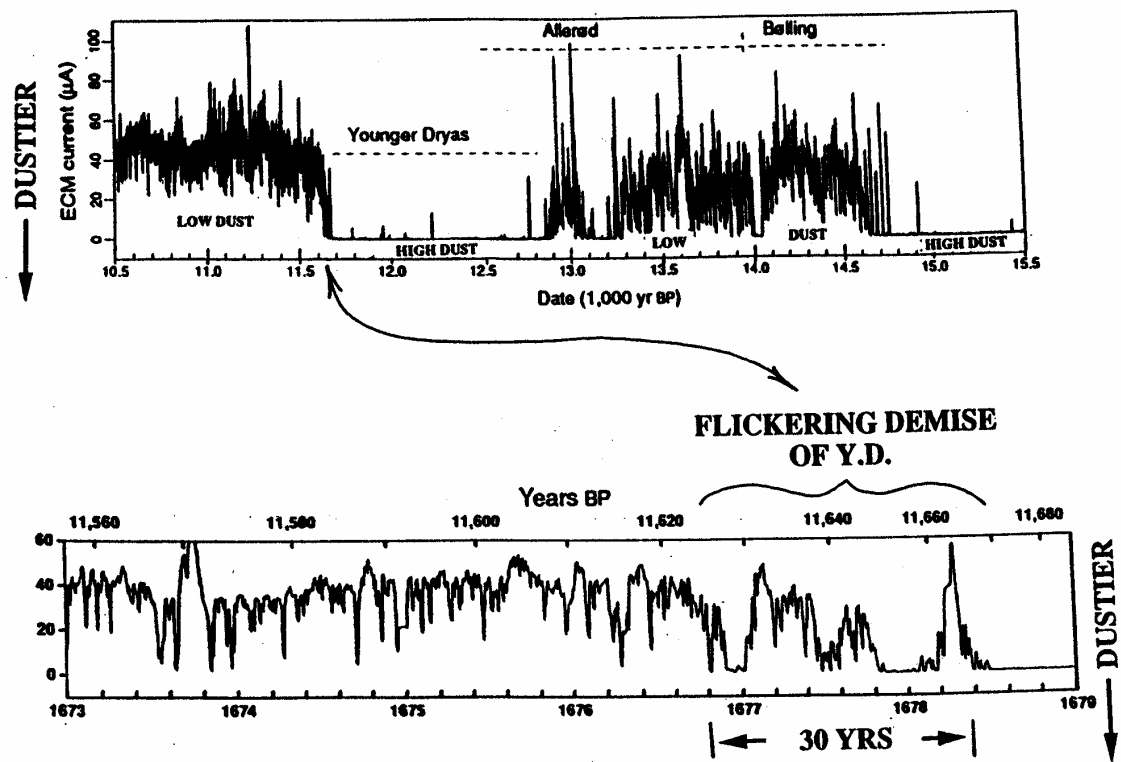


Figure 28 Electrical conductivity record for the Bølling-Allerød and Younger Dryas time obtained by Taylor et al. for the GISP II core from the Summit locale in Greenland. The conductivity is supplied by acid protons; during dusty intervals, the acidity is neutralized by CaCO_3 particles causing the conductivity to drop sharply. A blow up of the time interval representing the end of the Younger Dryas is also shown.

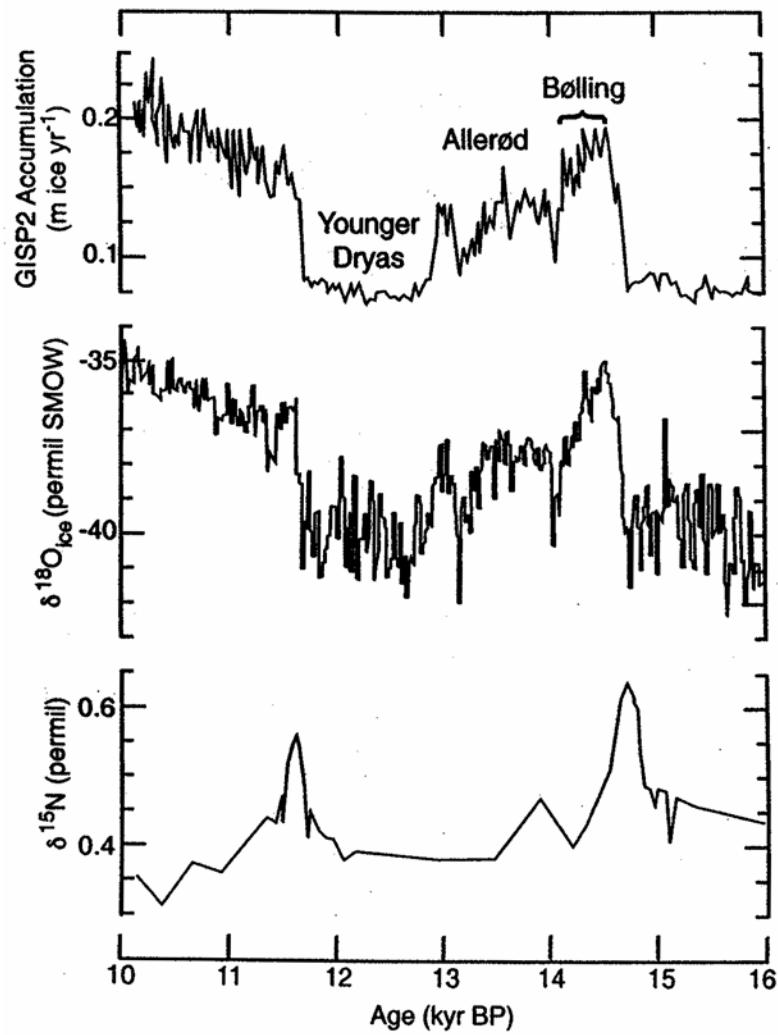


Figure 29. Records of ice accumulation rate of the ^{18}O to ^{16}O ratio in the ice and of the ^{15}N to ^{14}N ratio in N_2 for the deglaciation interval in the GISP II ice core. As can be seen, the peaks in $\delta^{15}\text{N}$ occur at the times of the abrupt warmings marking the onset of the warm Bølling Allerød and the termination of the cold Younger Dryas. They are the result of the enrichment of $^{15}\text{N}^{14}\text{N}$ molecules in the cold basal firn by thermal diffusion. As it takes a century or so for the firn to warm, this peak is short-lived (Severinghaus and Brook, 1999).

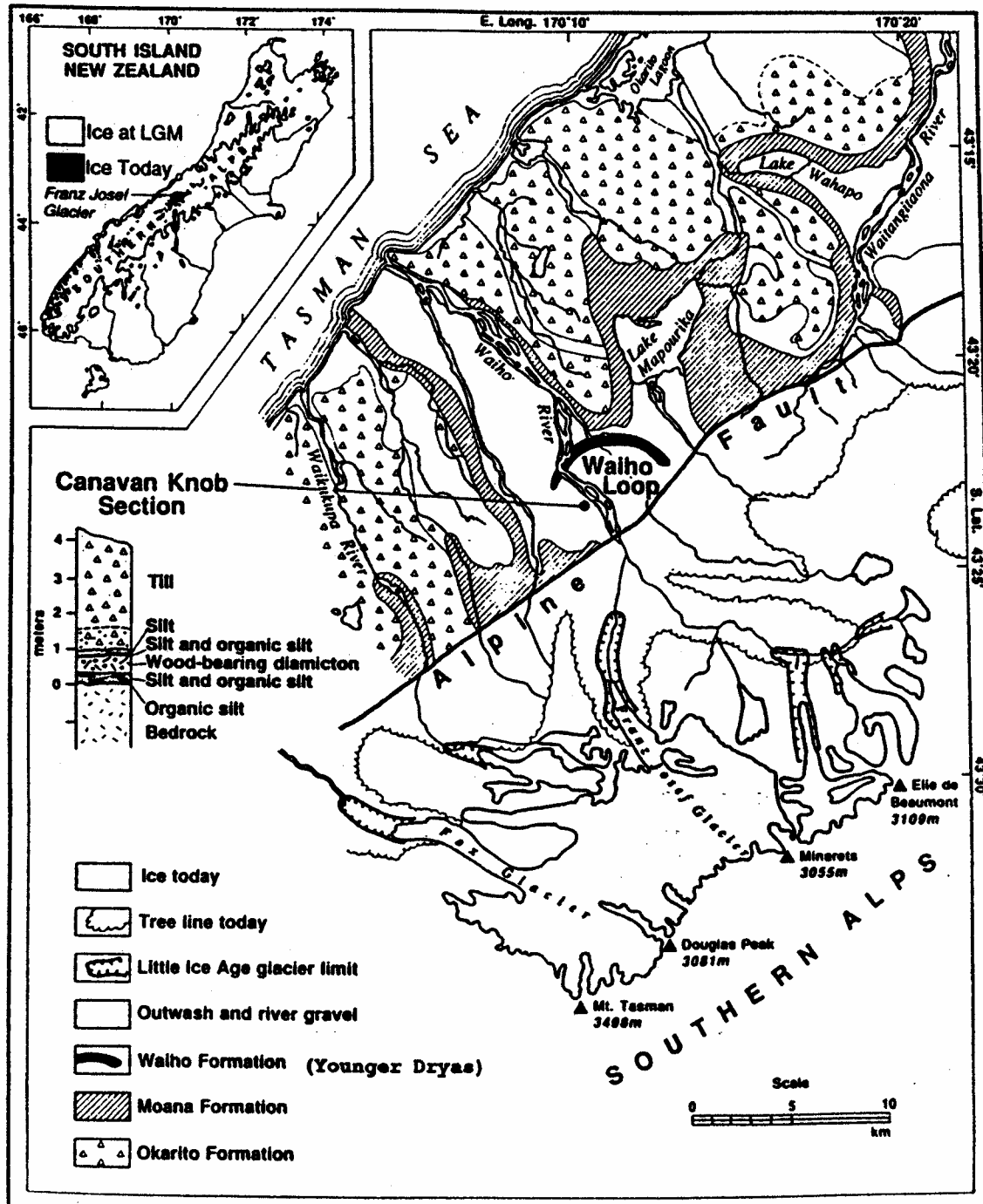


Figure 30. Map showing the extent of the Franz Josef glacier during the Little Ice age and during the Younger Dryas. Denton and Hendy have obtained 37 radiocarbon dates for the diamictite which marks the onset of the YD. The average of these ages is 11,050 Libby years, in good agreement with that for the beginning of the Younger Dryas in northern Europe.

global in extent.

It turns out that global is an overstatement. There is an important exception, namely, the record in Antarctic ice where there is a prominent plateau in the stable isotope warming marking the end of the last glaciation from the Vostok and the Dome C ice cores (see figure 31). Originally this feature was correlated with the Younger Dryas, but then when methane records became available allowing the records in Antarctic ice to be precisely correlated with those in Greenland ice, it was clear that this correlation was incorrect. Rather, the plateau corresponds to the warm Bølling-Allerød period and the steep warming which follows the plateau to the Younger Dryas (see figure 32). As discussed below, it was this finding that led to the concept of the bipolar seesaw.

One might take issue with focusing attention on the air temperature record for the northern Atlantic. Instead one might look to the record of ice volume as more meaningful. Shown in figure 33 is the sea level record from Barbados, obtained by Richard Fairbanks, which shows sea level had begun to rise by 15,000 ^{14}C years ago. During the next 3000 years, it rose about 20 meters, reaching 95 meters below present sea level. Then, about 12,000 ^{14}C years ago, sea level appears to have spurted from 95 to 75 meters below present, a rise of 20 meters in only a hundred or so years. This spurt was followed by an interval of modest rise which brought sea level to -55 meters at 10,000 ^{14}C years ago. At this time, another sudden spurt took place bringing sea level to -40 meters. The inclusion of the ^{230}Th based time scale in Figure 33 reminds us of the substantial difference between ^{14}C years and calendar years during this time interval. For example, the steep sea level rise dated by radiocarbon at about 12,000 Libby years occurred about 14,000 calendar years ago.

While the second of these two intervals of rapid sea level rise comes on the heels of the Younger Dryas warming, the first falls well within the Bølling-Allerød warm interval rather than just after the dramatic warming at 12,800 ^{14}C years. The somewhat

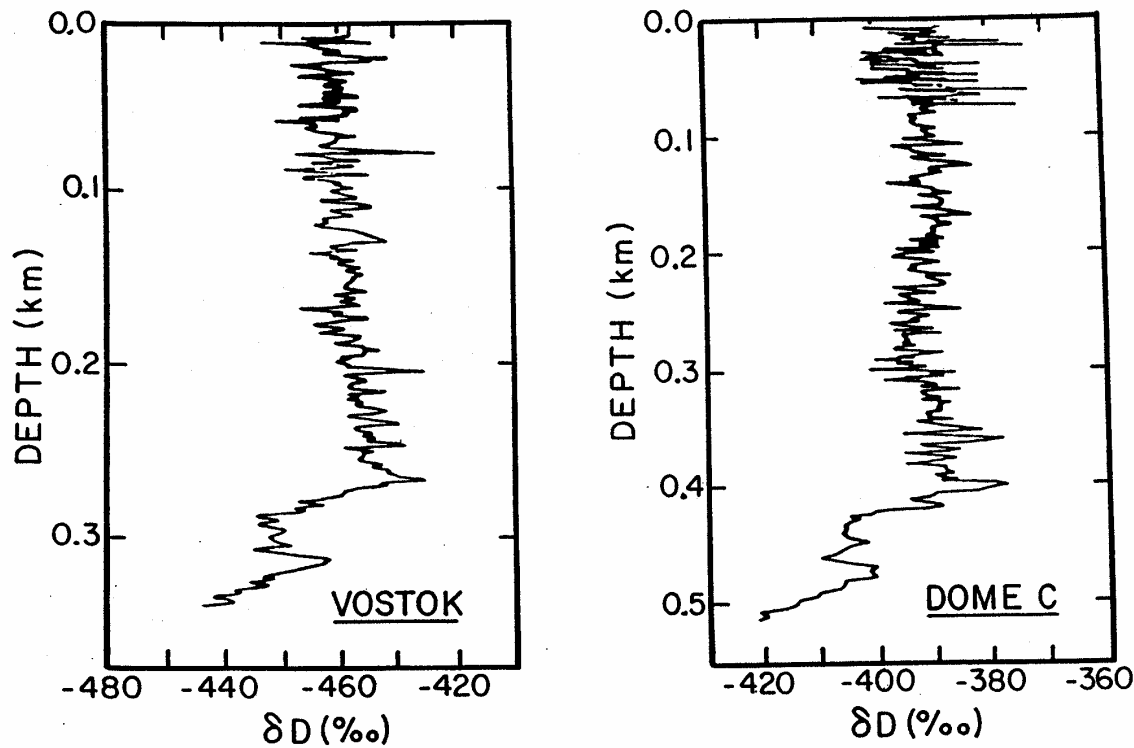


Figure 31. Hydrogen isotope measurements by Jean Jouzel on the Vostok and Dome C Antarctica ice cores for the last ~15,000 years. In each, there is a small reversal followed by a plateau. While once explained as a reflection of the Younger Dryas, this plateau is now documented to reflect the Bølling-Allerød warm. The sharp warming after the plateau corresponds to Younger Dryas time.

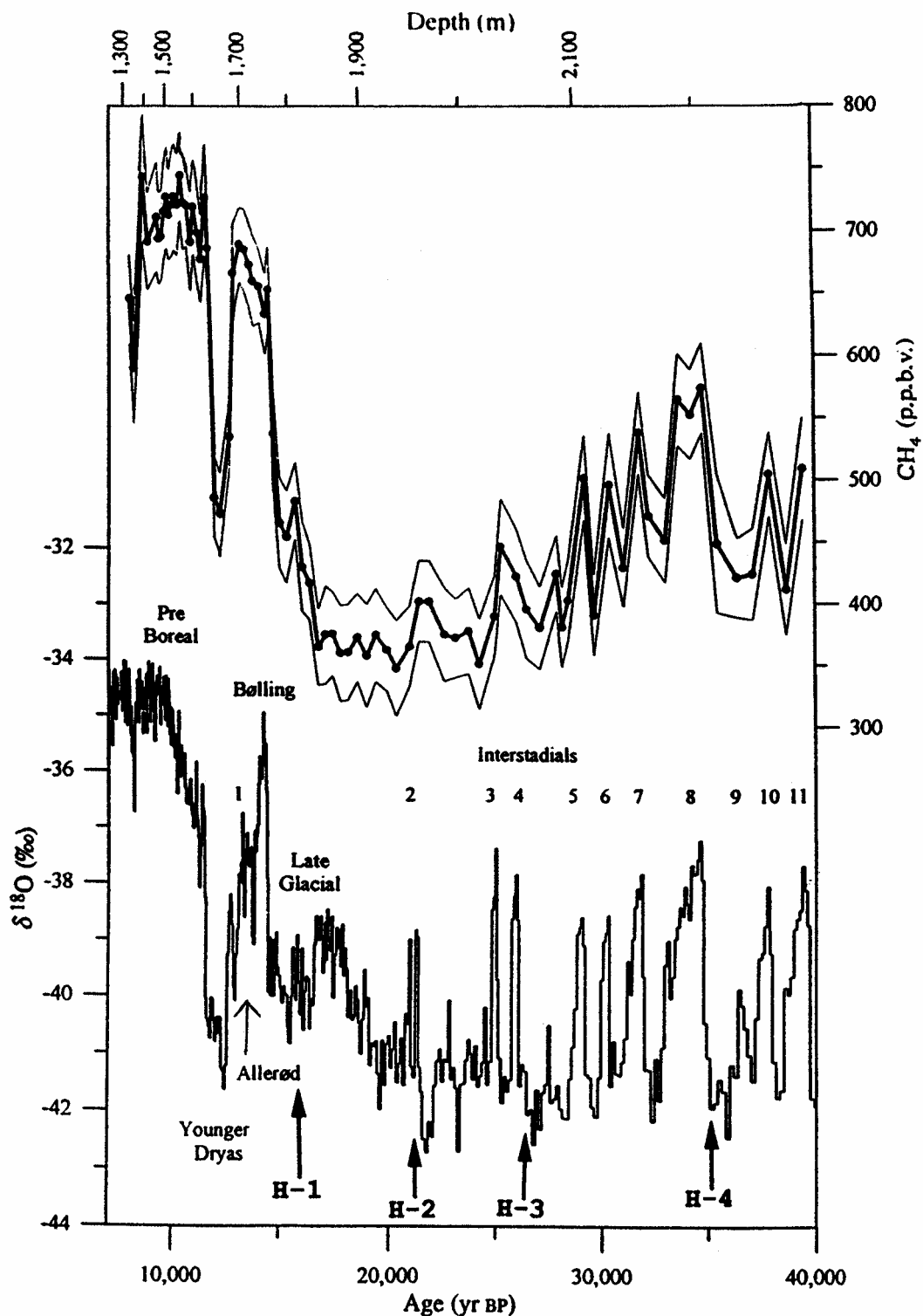


Figure 32. Jerome Chappellaz's record of the methane content of air trapped in the GRIP ice core from the Summit locale in Greenland and its correlation with the Dansgaard-Oeschger events as recorded by ^{18}O in the ice. Each oxygen isotope cold phase is accompanied by a 15 to 20 percent drop in methane content.

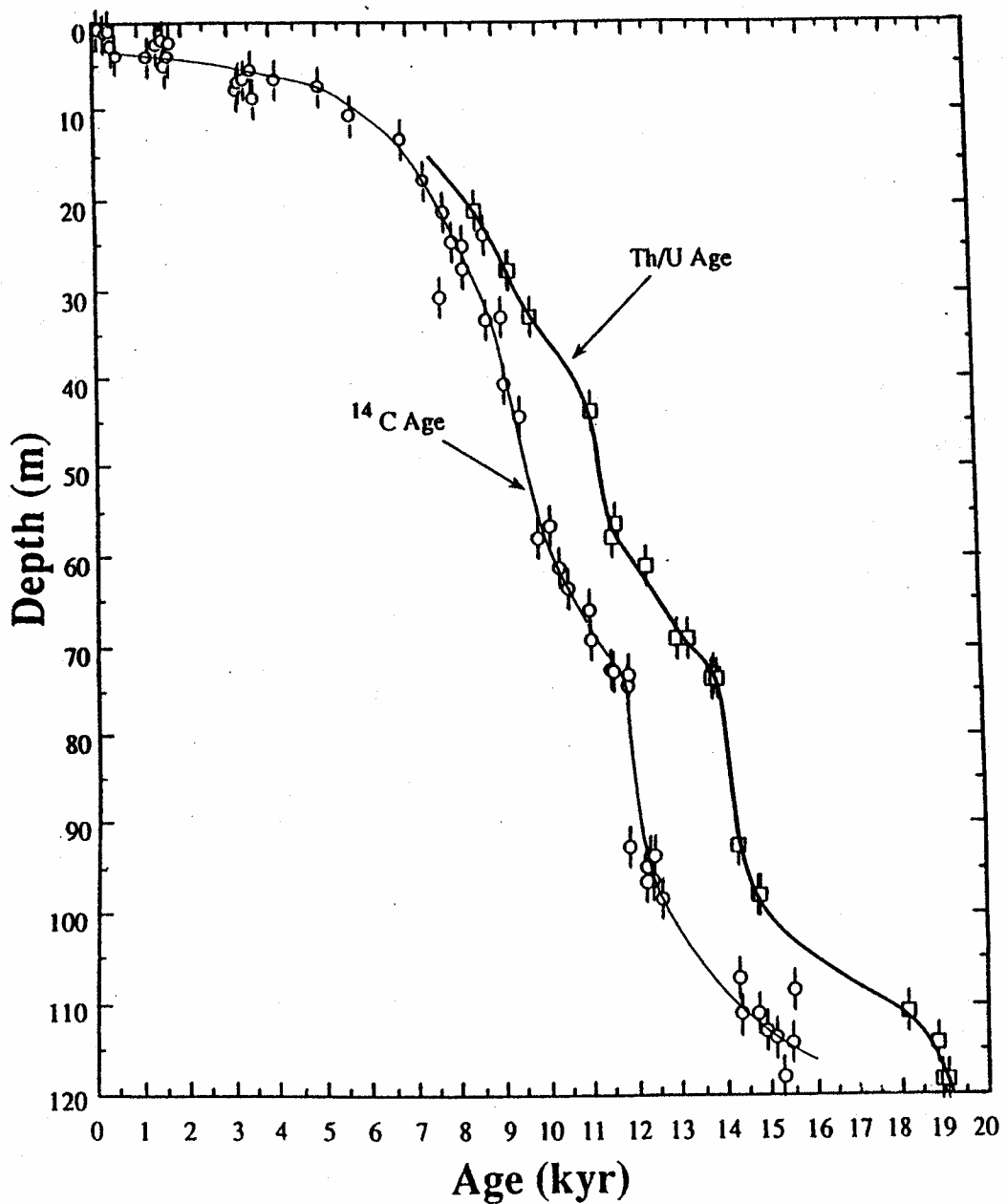


Figure 33. Radiocarbon and radiothorium ages obtained by Bard et al. for Barbados corals as a function of water depth. The record suggests an abrupt rise in sea level at about 12,000 Libby years and perhaps another just after 10,000 Libby years.

odd timing of the first of these rapid rises has caused doubt to be cast on the existence of this sudden sea level rise. The basis for this doubt is that rise is not recorded at a single site. Rather, the coral which precedes it comes from one core and the coral which postdates it comes from another core at a different locale. Perhaps post-growth collapse of the coral column rather than an abrupt rise in sea level accounts for the observed depth offset.

The exact timing of the ocean circulation change from its glacial to its interglacial mode is less well documented. The ^{13}C record for benthic foraminifera from a core from the Bermuda area in North Atlantic (see figure 34) suggests that the change commenced after 12,400 years age (at the time of the first meltwater event?) and was interrupted by a return to glacial conditions during the Younger Dryas. A benthic ^{13}C record from the opposite end of the Atlantic (see figure 35) appears to tell a similar story but as can be seen, the radiocarbon results for the latter are shifted to higher ages. Until a great deal more work has been done, not only the chronology but also the implications to ocean circulation of these ^{13}C records will remain open to a range of interpretations.

In other places where evidence for the Younger Dryas event is muted or perhaps absent, the major climate change occurred close to 13,000 ^{14}C years ago. Two examples are: the size of closed basin lake, Lahontan (figure 36) and the salinity of the Red Sea (figure 37). Both water bodies lie in desert regions. Lake Lahontan covered much of the state of Nevada during glacial time. During Holocene time, only small remnants (Pyramid Lake, Walker Lake, and Honey Lake) remain. Radiocarbon dating of algal carbonates deposited along shorelines of this once large lake provide a chronology for the extent of wetness of this region. The lake stood at a level intermediate between its highest stand and today's low stand, during the period about 20,000 to about 15,000 ^{14}C years ago. About 14,500 ^{14}C years ago, it rose to its highest level and then about 13,000 ^{14}C years ago the lake underwent a dramatic desiccation.

During glacial time, the Red Sea was hypersaline. This conclusion is based on the

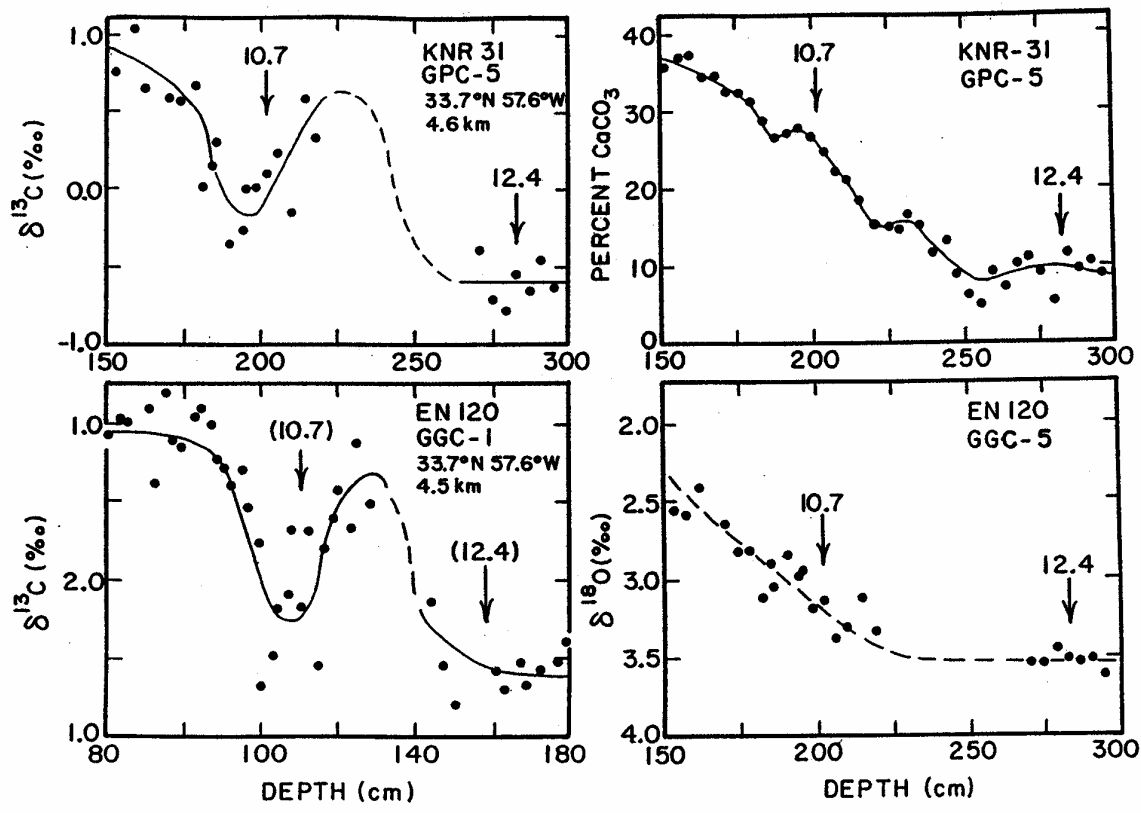


Figure 34. Carbon isotope records for benthic foraminifera, *C. wuellerstorfi*, for two cores from nearly identical locations in the western basin of the north Atlantic. The difference in depth scales is likely the result of a combination of stretching of the section by the piston cores (GPC-5) and compression of the section by the gravity cores (GGC-1). The gaps in the records represent an interval where the abundance of *C. wuellerstorfi* is too low to provide adequate samples. As the records of many properties of these two cores correlate perfectly, the radiocarbon dates of 10,700 and 12,400 Libby years obtained on core GPC-5 can be applied to GGC-1 as well. Also shown are the CaCO_3 and benthic oxygen isotope records for one of these cores (GPC-5). The CaCO_3 and isotope results were obtained by Lloyd Kergwin and the radiocarbon dates by Glen Jones at Woods Hole Oceanographic.

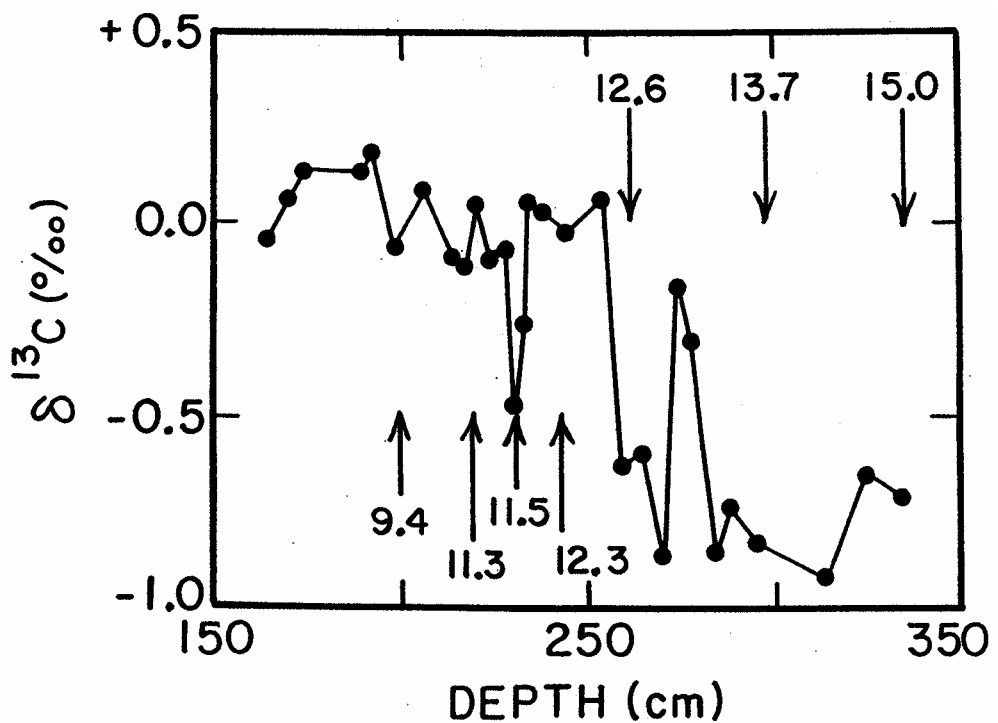


Figure 35. Carbon isotope ratios on benthic foraminifera, *P. wuellerstorfi*, from core RC11-83 (41.6°S, 9.8°E, 4.7 km). Radiocarbon measurements were obtained on planktonic foraminifera, *G. bulloides*, a reservoir correction of 600 years has been applied. The record suggests that the change in $^{13}\text{C}/^{12}\text{C}$ ratio occurred about 12,500 Libby years ago. It can also be seen that no change corresponding to the Younger Dryas event is to be seen. These results were obtained by Charles and Fairbanks.

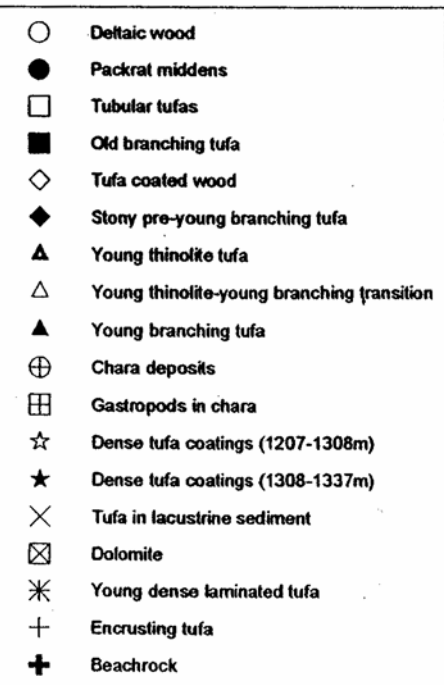
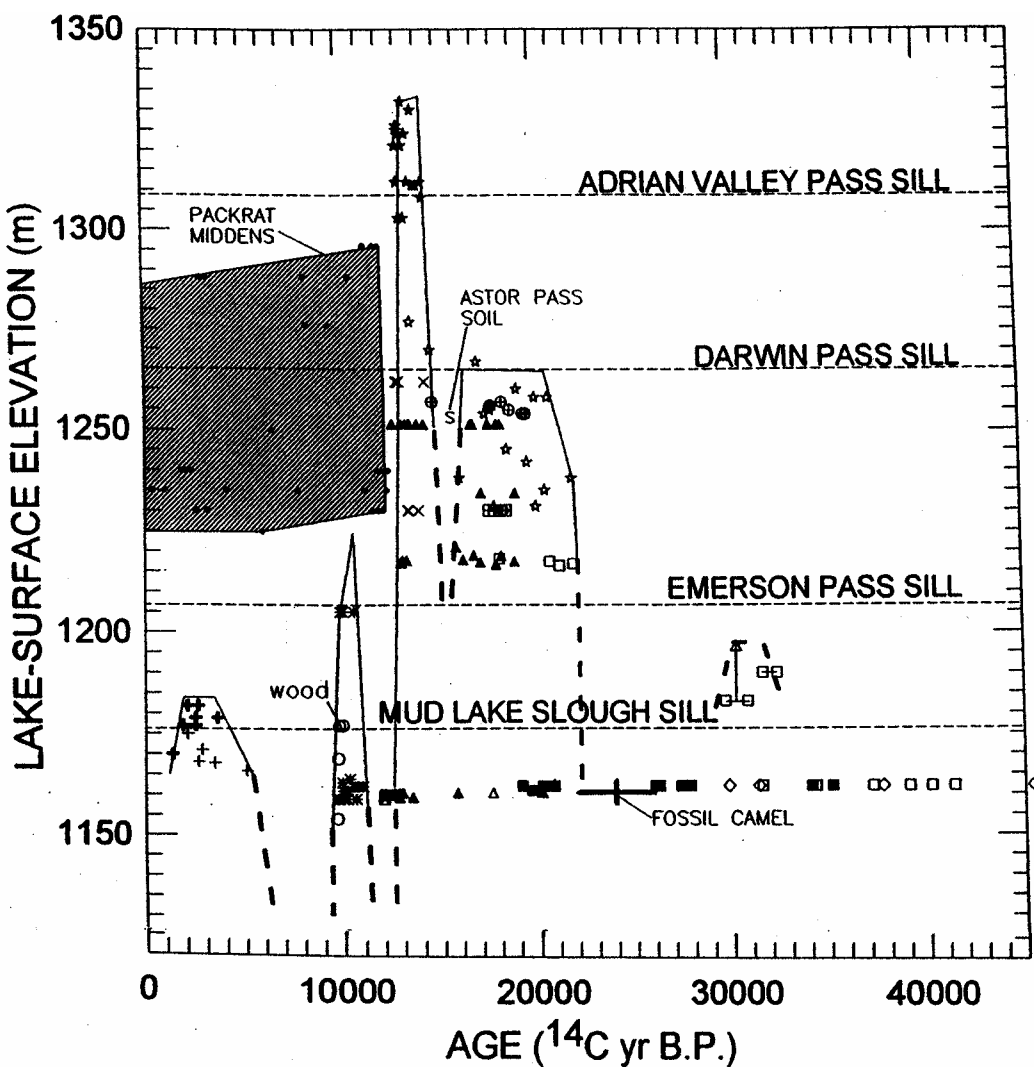


Figure 36. Radiocarbon dating of materials from the Lake Lahontan basin in Nevada reveal that during glacial time conditions were much wetter than now with the wettest phase coming at the time of the onset of the deglaciation (i.e., about 14,000 ^{14}C years ago). This wet period was brought to an end by a dramatic desiccation which occurred about 13,000 years ago. These results were compiled by Larry Benson of the USGS.

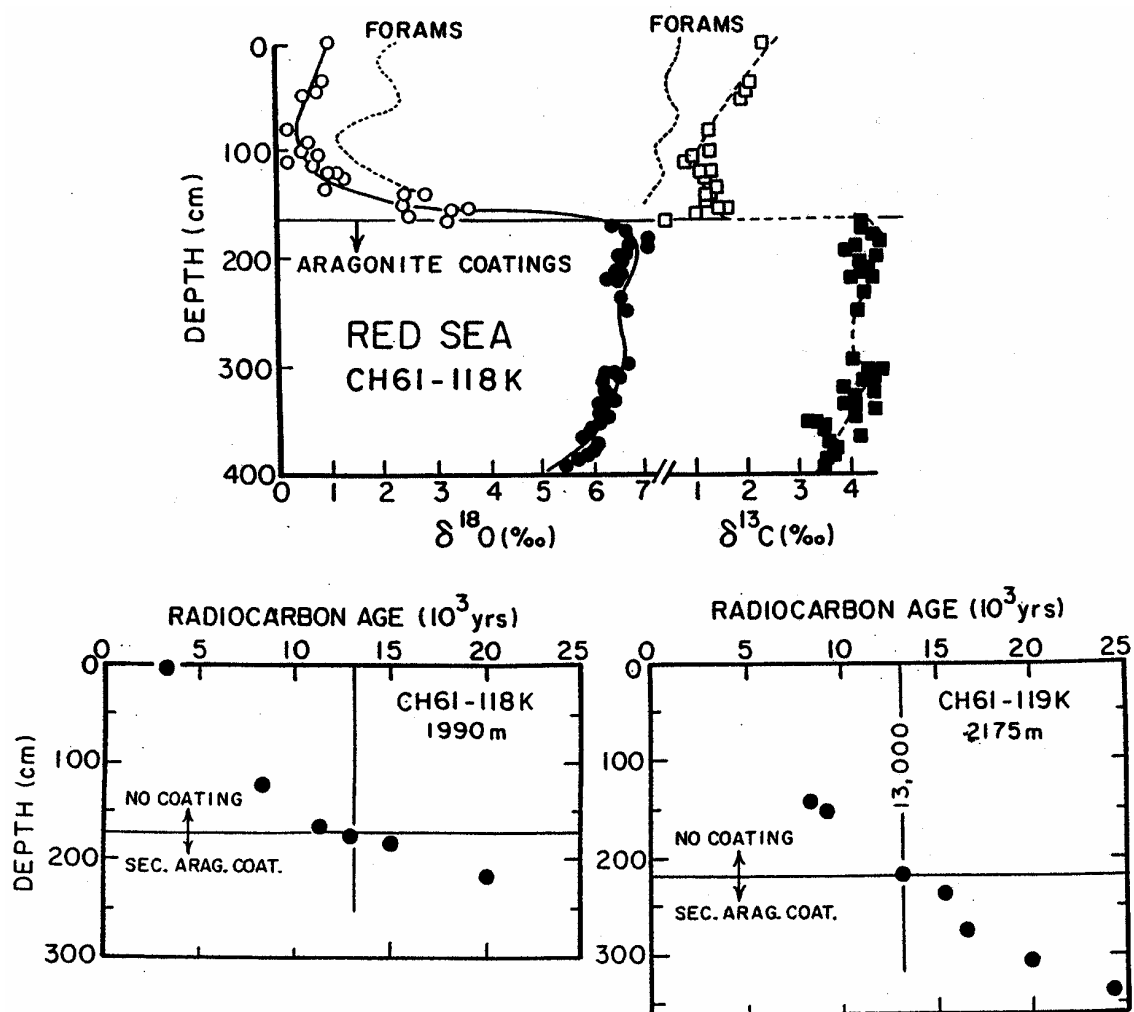


Figure 37. The upper diagram reproduces the oxygen and carbon isotope results on pteropods from the Red Sea sediment cores (Deuser and Degens, 1969). The open circles are for measurements on pteropods free of secondary coatings and the closed circles for those on pteropods heavily encrusted with secondary aragonite. The lower diagrams show ^{14}C ages (corrected for a 400-yr age for surface-water) versus depth in two Red Sea cores. In both, the transition from hypersaline to present-day conditions occurred about 13,000 ^{14}C years ago.

absence of planktonic foraminifera in glacial-age sediments, the presence of thick secondary calcite encrustations on glacial pteropods and the enrichment of ^{18}O in the CaCO_3 in pteropod shells. The very high $^{18}\text{O}/^{16}\text{O}$ ratios in glacial age pteropods suggest that a large percentage of the water spilling into the Red Sea from the Indian Ocean was lost by evaporation. Radiocarbon dates show that period of hypersalinity came to an abrupt end about 13,000 years ago. Two explanations come to mind. First, the rising sea level enhanced the interchange of water between the Indian Ocean and the Red Sea, thereby preventing a large buildup of salt. The other, which I favor, is that more arid conditions of glacial time suddenly gave way to less arid conditions.

Sediment coring and seismic profiling conducted in Africa's Lake Victoria make clear that during late glacial time this now large equatorial lake was completely dry. During this dry period a soil formed on older lake beds. It is found in each piston core and can be traced as a reflection horizon in the seismic profiles across the entire lake. As indicated by dating of the basal lake sediment lying above this soil, the lake came back into existence about 13,000 ^{14}C years ago.

Taken together, all the existing evidence suggests that during late glacial time the tropics were less wet than now and the extra tropical deserts were less dry. The transition to present conditions came at or very close to the time of the onset of the Bølling-Allerød warm.

DANGAARD-OESCHGER EVENTS

The Younger Dryas event is not the only event punctuating the climatic record of the northern Atlantic basin. With the exception of intervals of peak interglaciation, the record is riddled with them. The Younger Dryas stands out because it postdates the last termination. Since then, except for a brief cold blip at 8200 years ago, climate in the northern Atlantic region has been extremely quiet (see figure 38). During the glacial period abrupt climate changes were the rule rather than the exception. These glacial-age Younger Dryas-like events were first documented in the ^{18}O record from the Camp

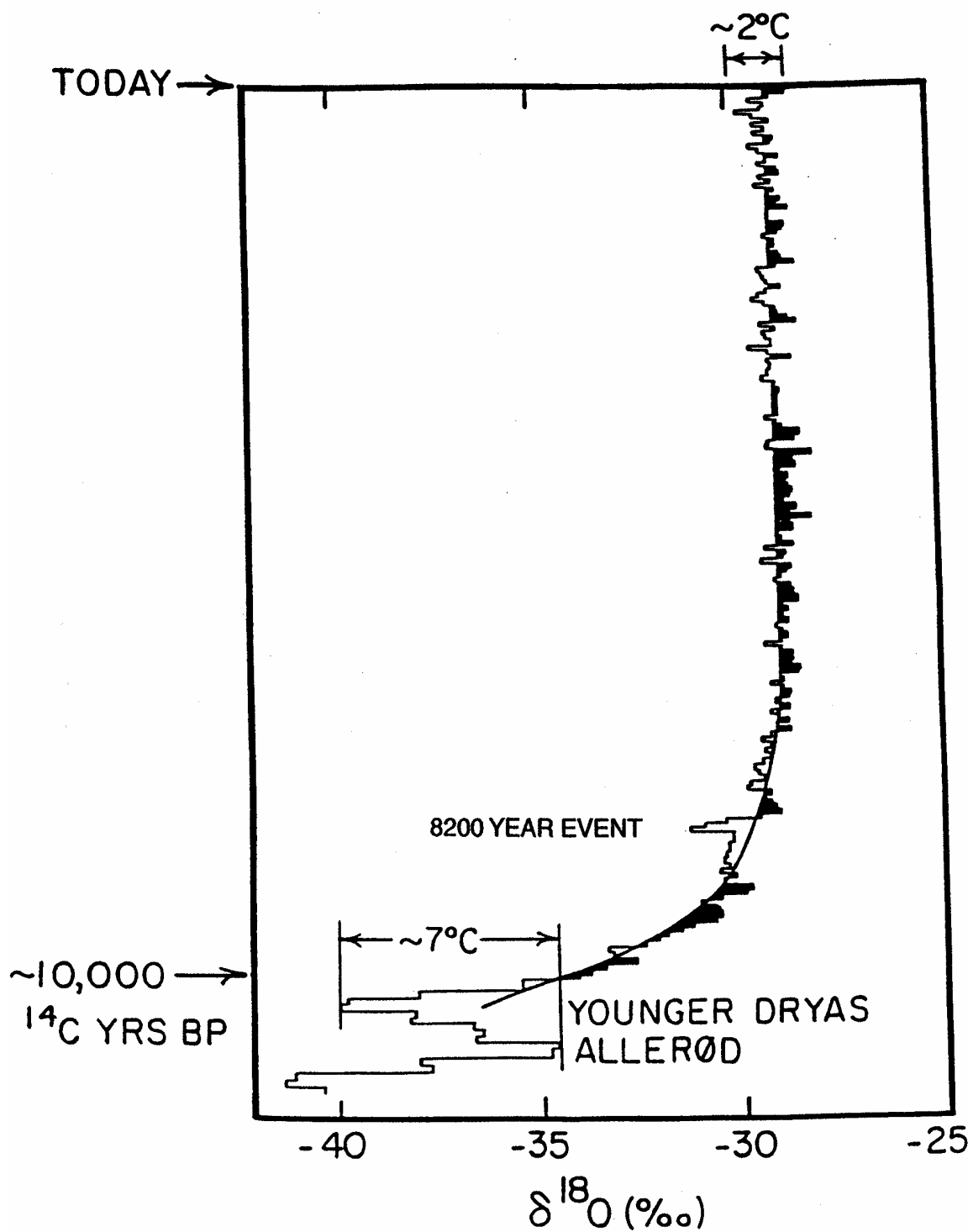


Figure 38. Oxygen isotope recorded obtained by Dansgaard and his coworkers for the Camp Century ice core from northern Greenland. Except for a small event at 8200 calendar years before present, following the end of the Younger Dryas, the record is 'event' free. The air temperature has remained nearly constant for the last 8000 or so years.

Century Greenland ice core by Dansgaard and his coworkers in the early 1970s. However, their existence did not receive much attention until a decade later when the record from a second long Greenland ice core became available. Not only were the same ^{18}O events present but they were shown to have associated dust and CO₂ changes. This caught everyone's attention. As shown in figures 39 and 40, each event was initiated by an abrupt $\delta^{18}\text{O}$ shift of 4 to 5‰. Using the standard 0.7‰/°C slope for the temperature dependence of polar precipitation, this corresponds to about 6 to 7°C warming of air temperature. Were the 0.35‰/°C relationship established for the interglacial to glacial change adopted, these temperature shifts would become twice as large. However, as the actual dependence of ^{18}O on temperature probably falls somewhere in between the two extremes, only maxima and minima estimates can be given for these temperature changes. The duration of each event averages about 750 years. Each oxygen isotope event is accompanied by an equally sudden fourfold shift in the dust and sea-salt content of the ice.

The discovery by Stauffer and his coworkers that these events were accompanied by 50 μatm swings in atmospheric CO₂ content (see figure 39) focused attention on ocean circulation changes as a cause for these events, for only the ocean's biological pump could bring about such large and rapid excursions. This led me to propose that changes in the mode of the Atlantic's thermohaline circulation were responsible for these so-called Dansgaard-Oeschger events. Measurements on air trapped in Antarctic ice showed, by contrast, uniformly low glacial values. The failure to find these CO₂ changes in the Byrd Antarctica ice core led to the realization that the shifts to higher CO₂ seen in Greenland were likely the result of the reaction of acids and CaCO₃ in the ice leading to anomalously high CO₂ contents. However, the idea that the abrupt Greenland temperature changes were caused by flips in the Atlantic's thermohaline circulation has found considerable observational and modeling support.

Two new ice cores from the Summit site in the center of the Greenland ice sheet

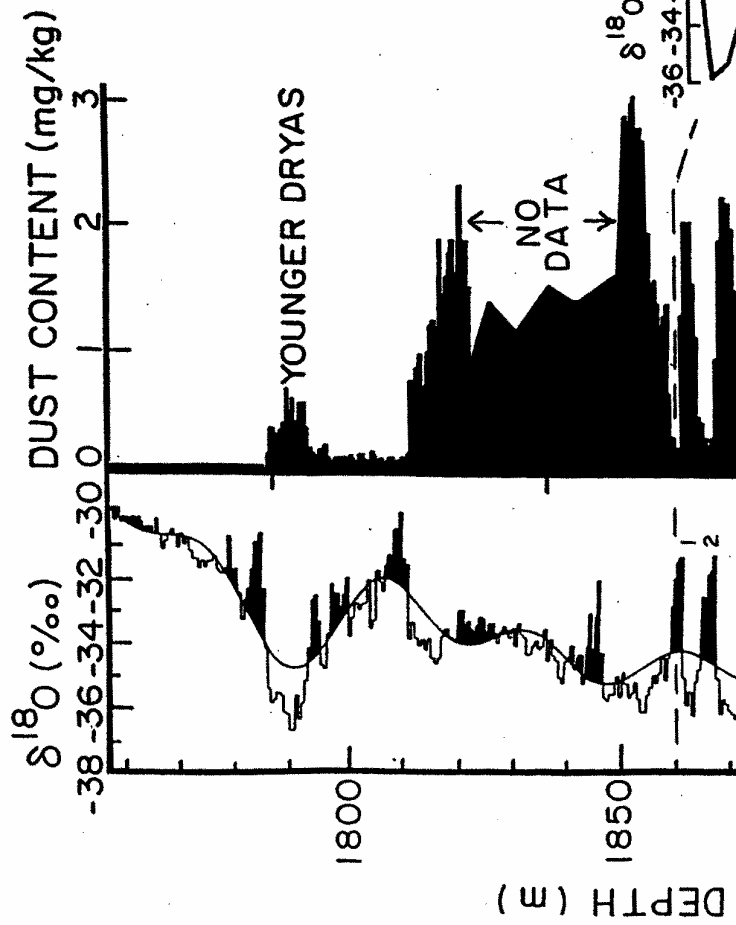
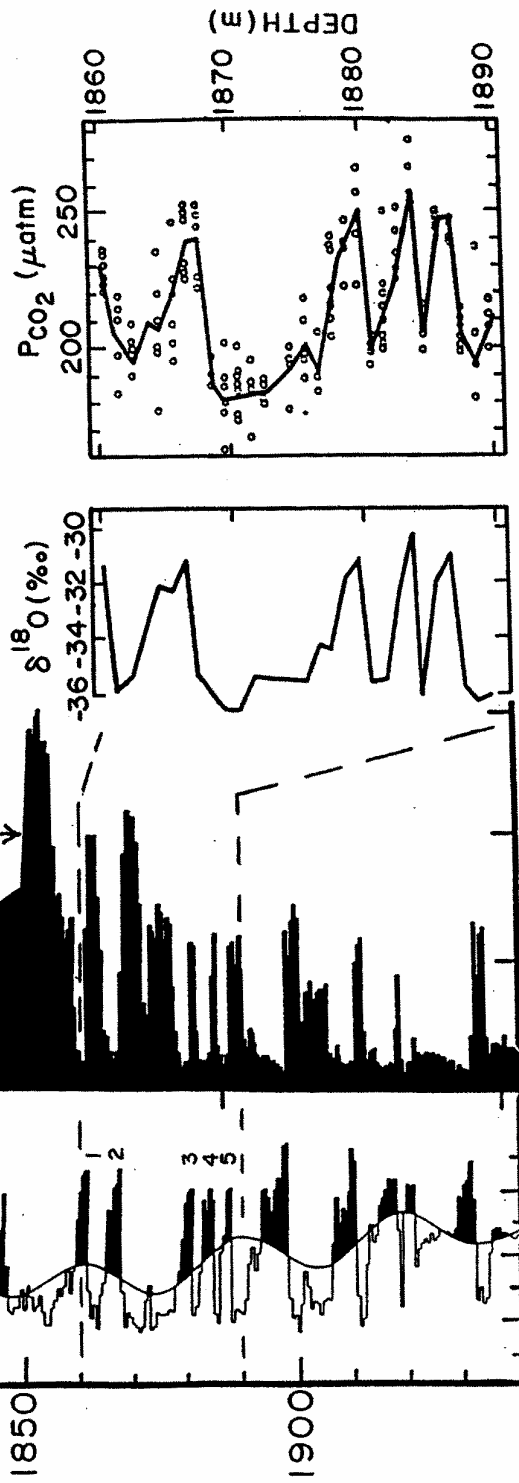


Figure 39. Oxygen isotope and dust records for the Dye 3 Greenland ice core covering the time period ~45,000 to ~8,000 years BP (Hamner et al., 1985). Also shown are $\text{CO}_2 - \delta^{18}\text{O}$ records made by Stauffer and his coworkers in Bern, Switzerland for the portion of the record between 1860 and 1890 meters depth. The CO_2 maxima were subsequently shown to be anomalous, the result presumably of a reaction of acids with CaCO_3 .



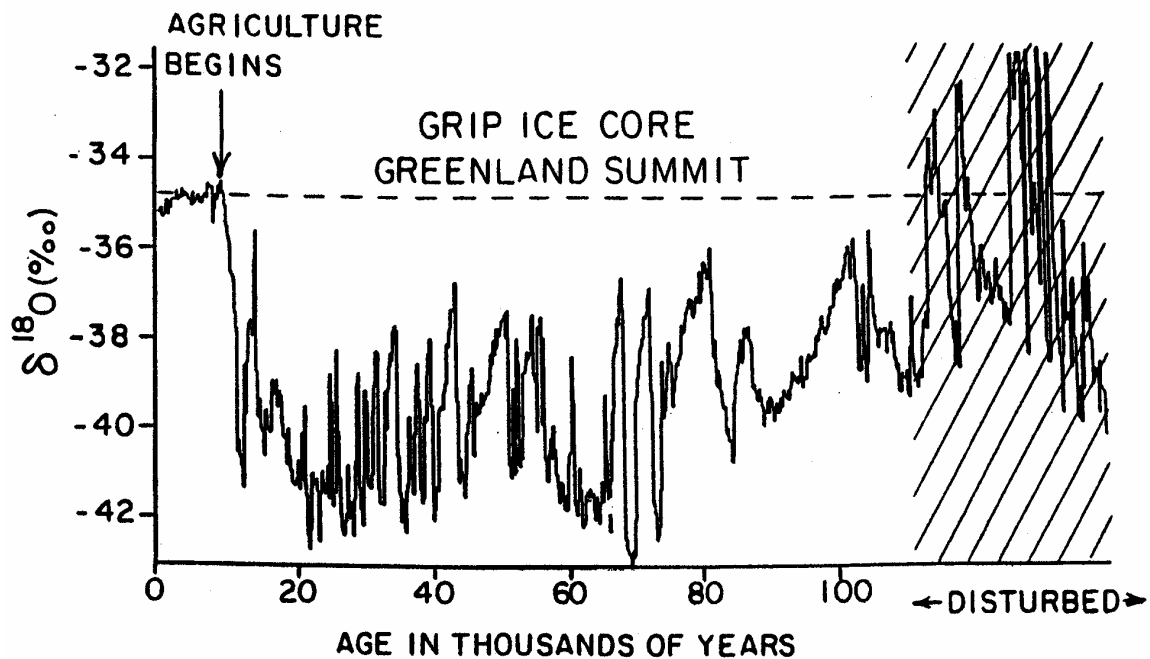


Figure 40. Oxygen isotope record obtained by Willie Dansgaard and his Copenhagen colleagues on the GRIP ice core from the Summit locale in Greenland. The record for the lower 200 meters of this core is very different from that for the neighboring GISP II core. In both cores, this lower portion contains tilted layers and drag folds. Hence beyond 110,000 years of the record should be disregarded.

not only reproduce the event structure found in the Camp Century (northern Greenland) and Dye 3 (southern Greenland) ice cores but they also extend the record back in time (see figure 40). The results from the first of these cores (drilled by a European team) stunned the climate community by revealing a number of events in what appeared to represent the peak of the last interglaciation (i.e., marine stage 5e) suggesting that, unlike the present interglacial, the last interglacial was riddled with large and abrupt jumps in climate. However, when the results from a second core (drilled by an American Team) became available, serious doubts regarding the validity of the lower 200 meters of the record arose. The reason was that the details of the record for this portion were quite different in the two cores. The incredible agreement down to the minutest detail found for the upper 90% of the records from the two cores (drilled 30 km apart) was absent for the period beyond about 110,000 years. Careful examination of the ice revealed that in the lower portion of both cores, the layering was tilted by as much as 20° and frequent folds appeared. The conclusion is that this portion of the ice is highly deformed raising the distinct possibility that layers might be repeated and intervals of time might be missing. Rather, the events initially believed to have punctuated the peak of the last interglacial more likely are the product of tectonic shingling with ice whose age is likely even older than the last interglacial.

While the lower portion of these records is controversial, that portion representing the last glacial period is pristine. Clearly, during the last glacial period, the climate over Greenland experienced large and abrupt jumps akin to those bounding the Younger Dryas. If these earlier events had the same origin as the Younger Dryas, then they should have produced a similar geographic pattern of impacts, i.e., the changes in oxygen isotopic composition of the CaCO₃ of European lakes and in the species of beetles living in Britain. Unfortunately, the lakes and bogs on which oxygen isotope beetle records were obtained came into existence after 14,500 years ago. Before this, the basins were covered by ice.

The surprise came when Jim Kennett of the University of California at Santa Barbara obtained a long core from the Santa Barbara Basin. He stunned us all by showing that all the events seen in the Greenland core were reproduced in the largely anaerobic sediments of this 500-meter deep coastal basin. The events showed up as large changes in ^{18}O and ^{13}C in both benthic and planktonic foraminifera, in the relative abundance of benthics species, and in the degree of preservation of annual layering. Similar records now have been obtained in continental margin sediments in the Indian Ocean's Arabian Sea and in the Caribbean Sea's Cariaco Basin. They also show up prominently in an alkenone record from a deep-sea core from the vicinity of Bermuda. In this case, the surface water temperature shifted back and forth by about 4°C . Finally, as shown by Gerard Bond, the Dansgaard-Oeschger events are represented by ice-rafting maxima in sediments from the northern Atlantic. The locations of these records are shown in figure 41.

HEINRICH EVENTS

Now let us turn our attention to the curious set of very curious layers found in deep sea cores from the northern Atlantic. Named for their discoverer, Hartmut Heinrich, these layers are distinctive for several reasons (see table 1 and figure 42 for summary). First, unlike ambient glacial sediment, all six layers are nearly free of foraminifera, suggesting that either the productivity of these organisms dropped dramatically or that the layers were deposited extremely rapidly. Those few foram shells that are present are *N. pachyderma* (left coiling) species which dwells only in very cold water. The oxygen isotope ratios for *N. pacyderma* from these layers are 1 to 2‰ more negative than those for the *N. pacyderma* from the over and underlying ambient glacial sediment, suggesting that a low salinity lid capped the water column. Second, in four of the six layers, 20 or so percent of the ice-rafted debris is detrital limestone. In contrast, the ambient glacial sediment is nearly free of detrital carbonate. Third, the $^{40}\text{Ar} - ^{40}\text{K}$ ratios for the fine-grained clay minerals contained in the four detrital carbonate-bearing layers are

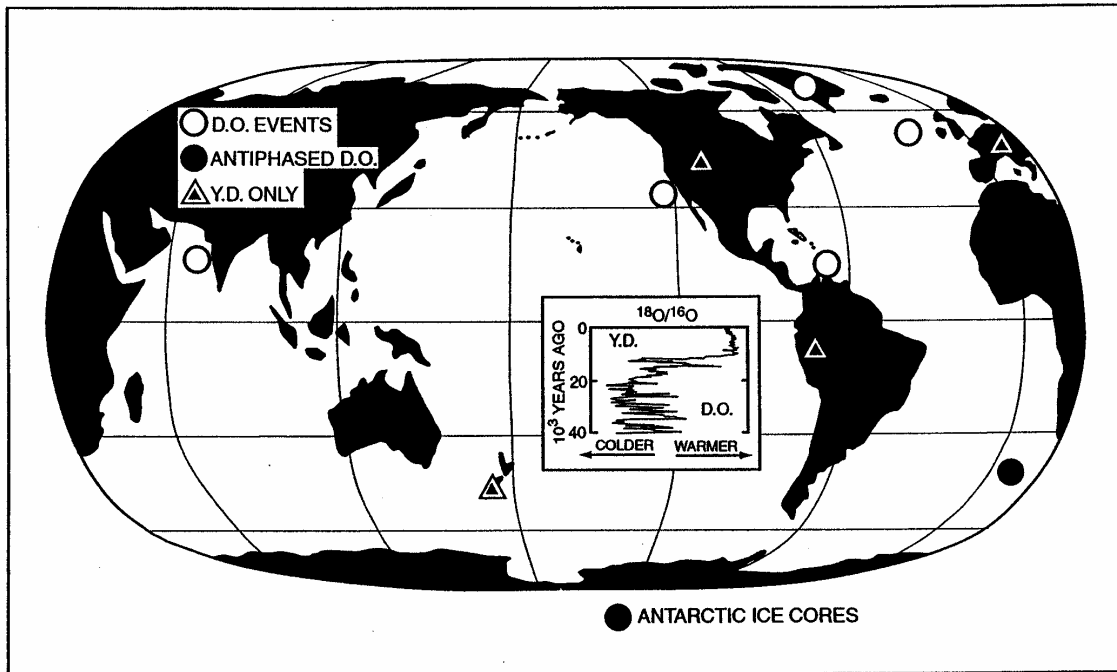


Figure 41. Map showing the locations where the abrupt climate changes (i.e., Dansgaard-Oeschger events) have been documented in records kept in marine sediments or polar ice (white and black dots). The triangles show those locations where the last of these events (i.e., the Younger Dryas) is recorded by major advances of mountain glaciers. While for most of the globe, these events are in phase, in parts of the Southern Ocean and of the Antarctic ice cap, they are clearly antiphased. This switch in phasing at high southern latitudes appears to reflect a seesawing of deep-ocean ventilation between the northern Atlantic and the perimeter of the Antarctic continent.

Table. 1. Comparison of the composition of the material in Heinrich layers with that of the adjacent glacial sediment.

PROPERTY	AMBIENT GLACIAL SEDIMENT	HEINRICH LAYERS	REASON FOR DIFFERENCE
FORAMINIFERA SHELLS (> 159 µm)			
Abundance	High	Low	Low productivity and/or high sed. rate
$^{18}\text{O}/^{16}\text{O}$	High	Low	Melt water
Species	Variable	All <i>pachy</i> (<i>l.c.</i>)	Cold ocean
LITHIC FRAGMENTS (>150 µm)			
Quartz	~80%	~80%	—
Det. CaCO_3	<2%	~20%	Icebergs from eastern Canada
FINE-GRAINED MATERIAL			
Clays	Smectite present	Smectite absent	No debris from Iceland
K-Ar age clays	0.44 billion	0.90 billion	Icebergs from eastern Canada
K-Ar age ind. amphibole grains	Large range	1.7 billion	Icebergs from Churchill Province northeast Canada
Pb isotopes ind. feldspar grains	Large range	2.7 billion crust 1.7 billion metamorph.	Icebergs from Churchill Prov. northeast Canada

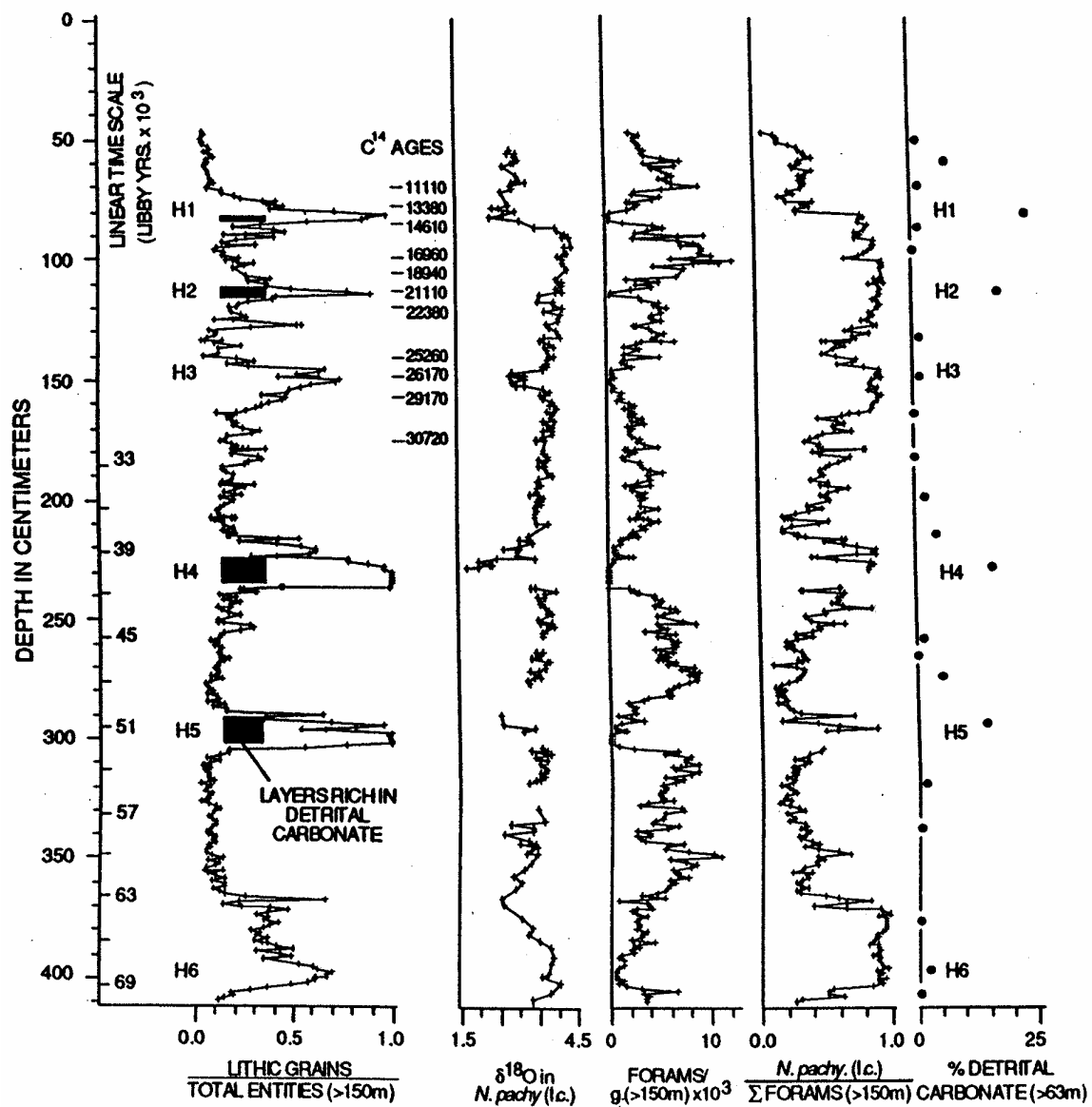


Figure 42. Detailed records covering the last glacial period in ODP core 609 (50°N, 24°W). The left hand panel shows the Heinrich events as originally defined (i.e., ratio of lithic fragments to foraminifera shells in the >150 μm size fraction). Shown by black bars are the layers bearing detrital limestone. Also shown are the radiocarbon ages. In the other four panels are shown respectively: the $\delta^{18}\text{O}$ record for *N. pachyderma* (l.c.), the number of foraminifera shells per gram of sediment, the ratio of *N. pachyderma* (l.c.) to total foraminifera shells, and the percent detrital limestone fragments in the lithic fraction.

unexpectedly high corresponding to ages of 900 million years. For comparison, the ratios obtained for clay minerals from ambient glacial-age sediment correspond to ages of 440 million years.

As shown in figure 42, six Heinrich layers are present in the sediment representing the last full glacial period. They are designated H-1 through H-6 counting down core. Event H-6 (age ~65,000 years) is just above the boundary marking the transition from interglacial to glacial conditions. Event H-1 (^{14}C age ~14,500 years) marks the onset of the transition between the last glacial and the present interglacial (i.e., in other words, Termination I). The other four layers, H5, H4, H3 and H2, have ages of ~54,000, ~40,000, ~27,000 and ~21,000 years respectively.

Lamont-Doherty Earth Observatory's Gerard Bond has established a regional pattern for these deposits. As shown in figure 43, they form a belt extending from the Labrador Sea all the way across the Atlantic to France. The thickness of the detrital carbonate layer thins from west to east. The trans-Atlantic portion of this belt is centered at about 45°N . For each event, the geographic extent of the decreased foraminifera abundance and low $\delta^{18}\text{O}$ values is greater than that of detrital carbonate; a halo of low foram sediment extends to the north and to the south of the belt of detrital carbonate. For H-6 and H-3, the detrital carbonate belt is confined to the Labrador Sea while the low foram sediment can be traced all the way across the Atlantic.

This evidence suggests that the Heinrich layers were the product of large armadas of icebergs discharged into the ocean from that portion of the Laurentian ice cap centered over the northern Hudson Bay and Baffin Island. Potassium-argon ages on individual amphibole grains (figure 44) and lead isotope measurements on individual feldspar grains (figure 45) co-existing with limestone grains in Heinrich layers (#5, #4, #2 and #1) demonstrate that most of the ice-rafted silicates in these layers come from the Churchill province of the Canadian shield. This part of the North American craton formed about 2.7 billion years ago and was metamorphosed about 1.8 billion years ago. The reheating

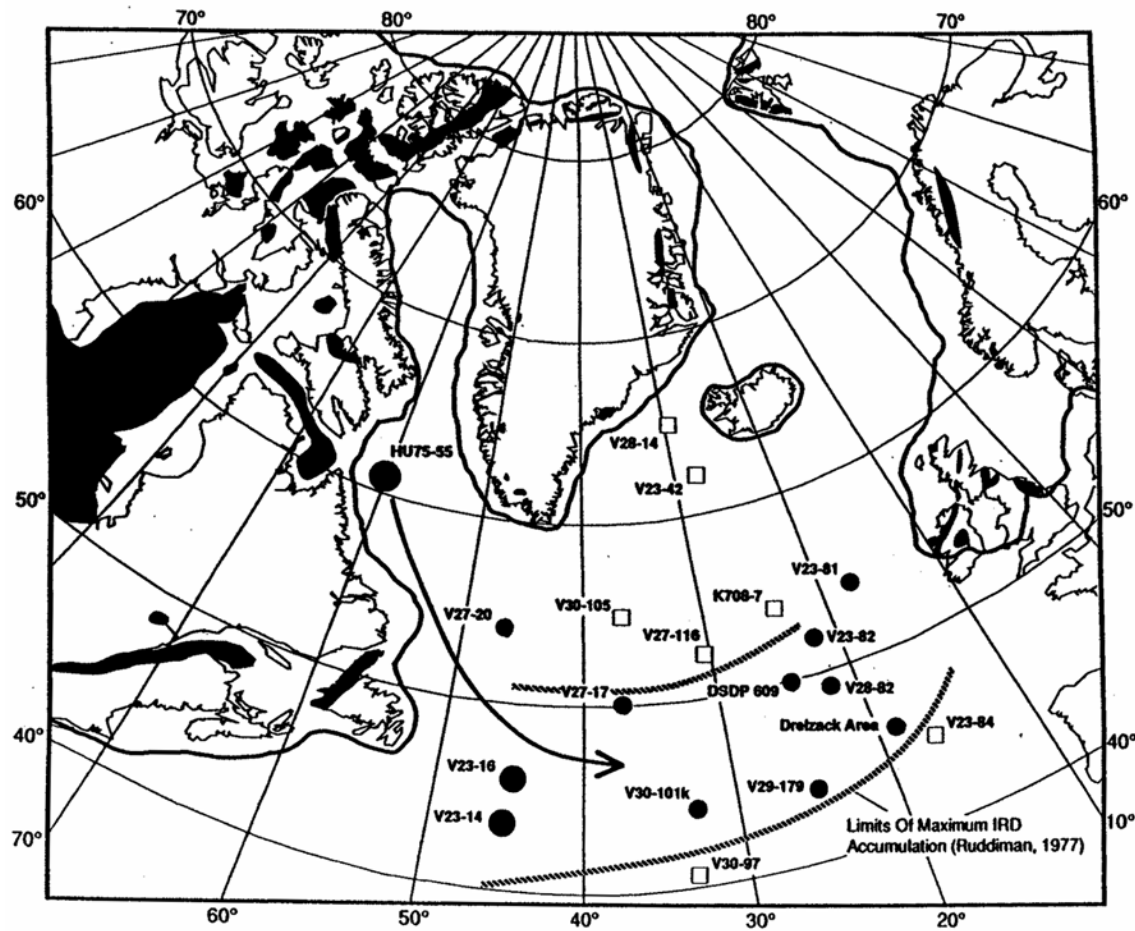


Figure 43. Location of cores in which detrital limestone-bearing Heinrich layers have been identified (closed circles) and of cores in which they are absent (open squares). The size of the circles is proportional to the thickness of the layers. The black patches denote occurrences of sedimentary limestones. The solid line shows the maximum size of the glacial ice sheets. The arrow shows the likely path taken by the Heinrich layer-producing icebergs.

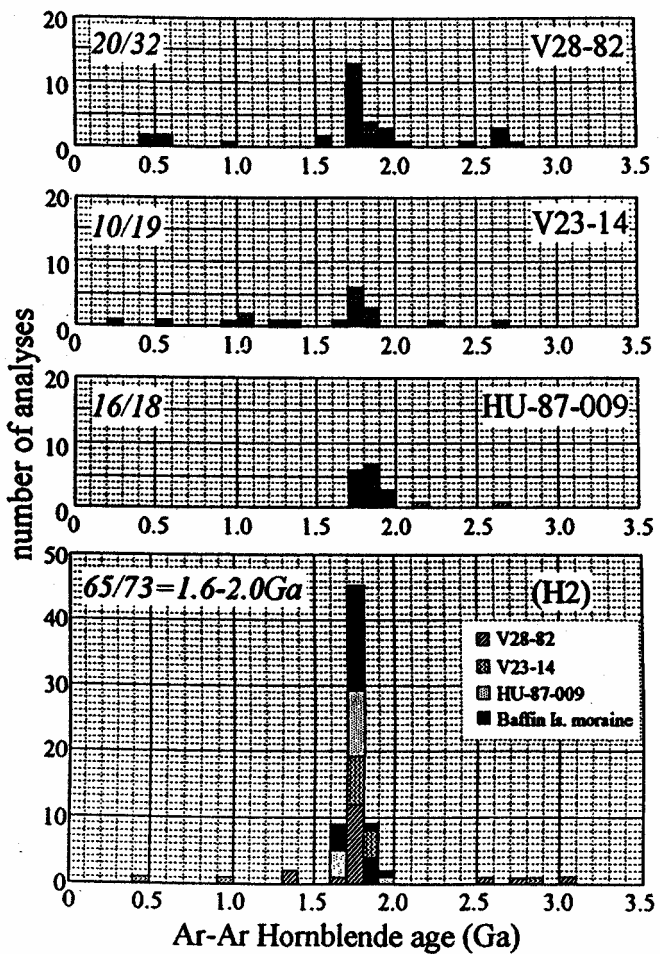


Figure 44. Potassium-argon ages on individual amphibole grains from the coarse fraction (ice-raftered debris) of glacial-age sediment from the northern Atlantic Ocean. The upper three panels depict the results for grains from ambient glacial sediment above and below Heinrich layer #2 for a core from the eastern Atlantic (V28-82), a core from the western Atlantic (V23-14) and a core from the Labrador Sea (HU-87-009). The lower panel shows the results for grains from Heinrich layer #2 on all three of these cores and also from a moraine on Baffin Island. As can be seen, the grains from the Heinrich layer are dominated by the 1.7 ± 0.2 billion-year metamorphic age of Churchill Province Archean rocks. The conclusion to be drawn from this is that the ice-raftered debris in the Heinrich layers comes exclusively from the northern part of Hudson Bay while that in the ambient sediment, although rich in the same material, comes from other terrains as well.

caused the K-Ar clock to be reset. It also redistributed the lead, adding variable amounts of radiogenic lead to the uranium-free feldspars (see figure 45). Similar measurements on feldspars and amphiboles from the detrital carbonate-free Heinrich layers (i.e., #3 and #6) suggest sources more akin to those for the ice-rafted debris in ambient glacial sediment (i.e., a mixture of sources with quite different geological ages).

A further indication of a major difference between Heinrich layers with and without detrital limestone grains comes from measurements of uranium series isotopes. No detectable excess of ^{230}Th exists in Heinrich layers #1, #2, #4 and #5 layers. By contrast, Heinrich layers of ^{230}Th #3 and #6 have excesses comparable to those found in ambient glacial sediment. The most likely explanation is that the four detrital carbonate-bearing layers were deposited very rapidly, perhaps in response to surges in the lobe of the Laurentian ice sheet centered over northern Hudson Bay. It is interesting to note that the two anomalous events (i.e., #3 and #6) mark the onset of stage 2 and stage 4 ice growth (see figure 46) and also the onset of two major Antarctic dust events coincident with these episodes of Northern Hemisphere ice sheet growth (see figure 47).

Evidence is accumulating that Heinrich events also have global footprints. The first indication came from a sediment core from Florida's Luke Tulane. Eric Grimm led a team which analyzed the pollen in this core. They were amazed to find that the oak savannah conditions of ambient glacial time were periodically interrupted by intervals when pine pollen underwent large increases presumably heralding wetter conditions. Preliminary radiocarbon dating suggests that there was one such pine event for each Heinrich event.

Helge Arz in his studies of continental-rise cores off Brazil's savannah region found that ambient high CaCO_3 sediment was interrupted by six injections of large amounts of continental detritus. He attributes these events to Heinrich event-associated rainy periods in the normally dry savannah. Arz also studied a continental margin core from the equator off western Africa and found by contrast that six Heinrich-related dry

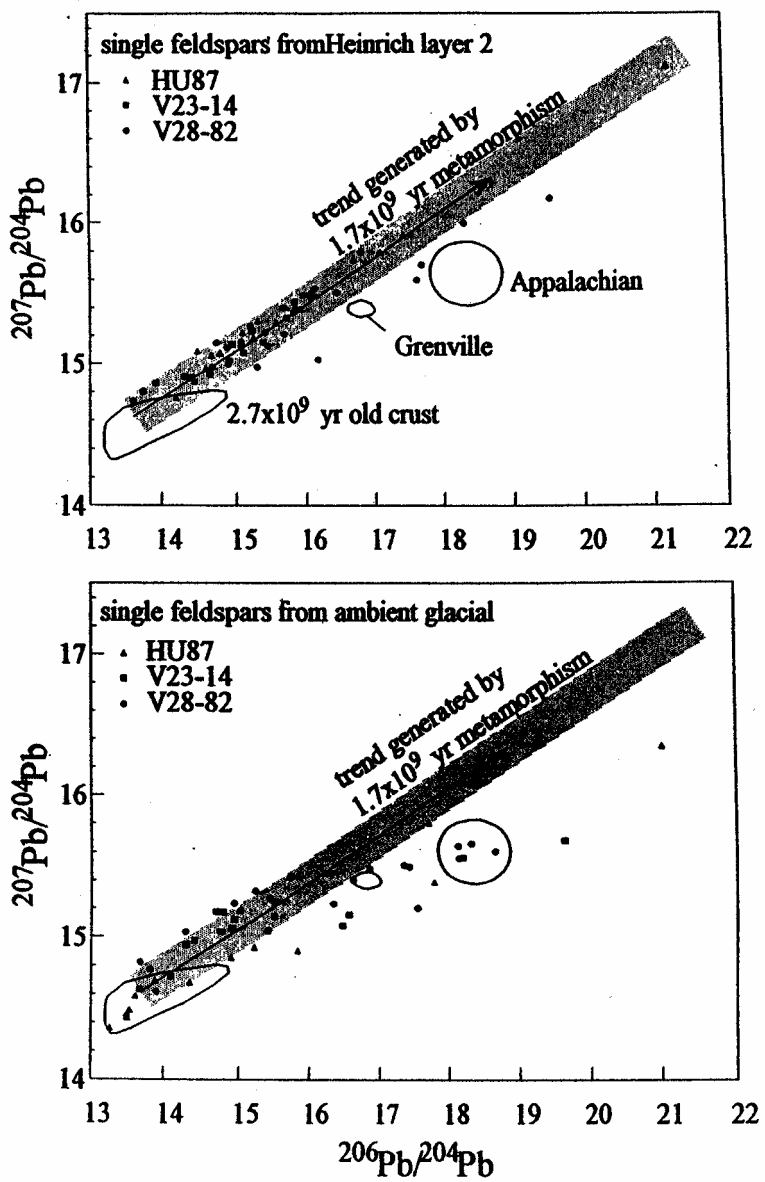


Figure 45. Lead isotope measurements by LDEO's Sidney Hemming and Roberto Gwiazda on single feldspar grains from Heinrich layer 2 reveal that most of these grains have Churchill Province signature, i.e., they were formed 2.7 billion years ago and then received variable amounts of additional radiogenic lead during a metamorphic event about 1.7 billion years ago. It was during this metamorphism that the K-Ar clocks of the amphibole grains were reset to zero. By contrast, the feldspars from ambient glacial sediment above and below H2 show a wide range of origins.

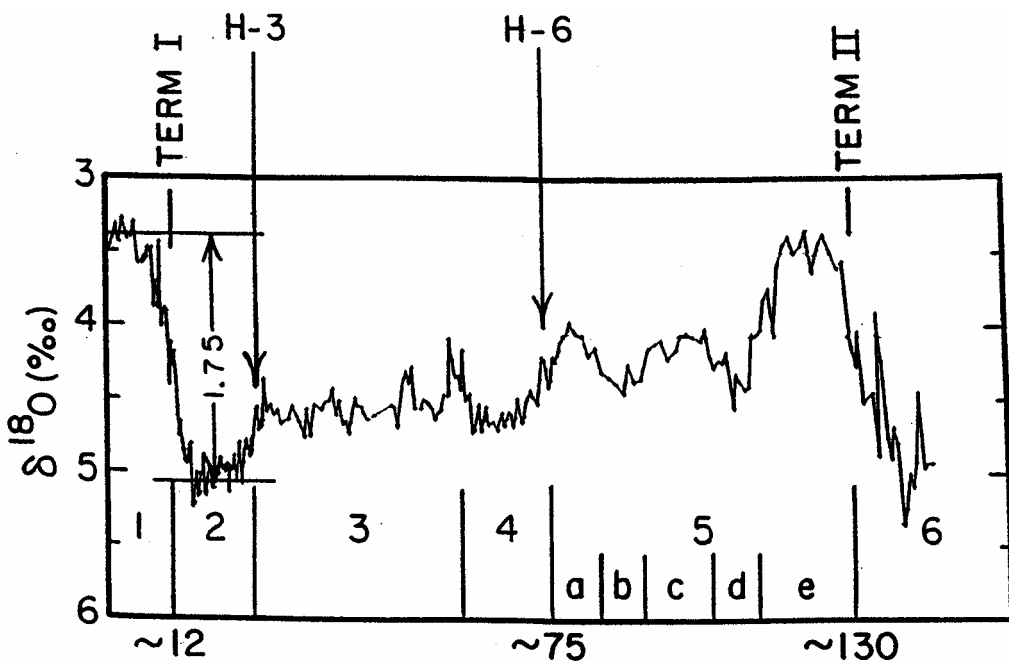


Figure 46. Placement of Heinrich events #3 and #6 in Shackleton's oxygen isotope record for benthic foraminifera from the eastern equatorial Pacific. As can be seen, they mark the onsets of periods of rapid ice sheet growth.

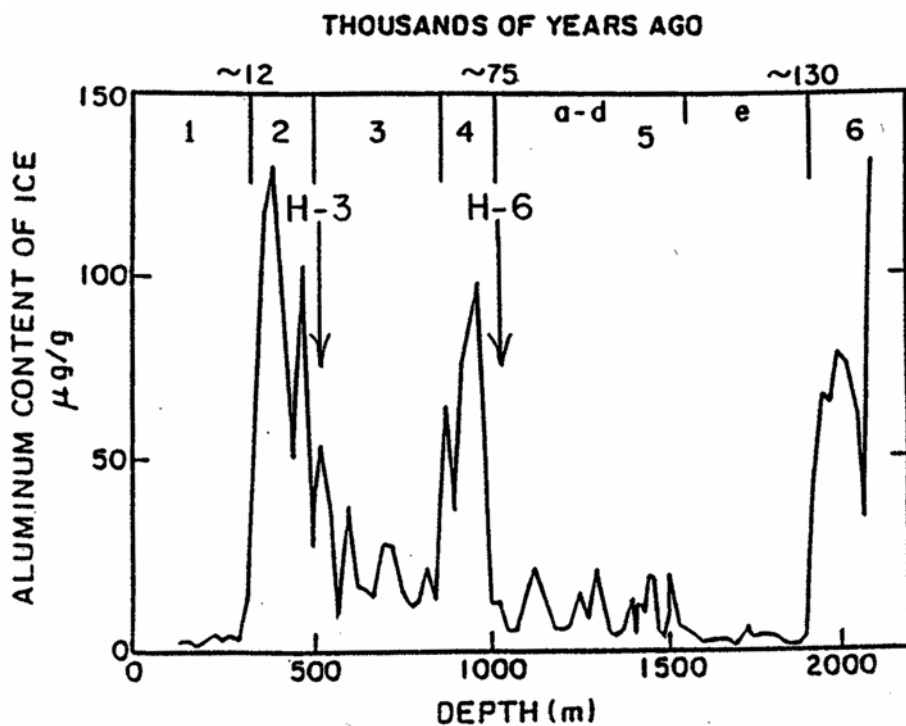


Figure 47. Placement of Heinrich events #3 and #6 in the de Angeles et al. aluminum record for the Vostok Antarctica ice core. They mark the onsets of major dust episodes

events punctuated glacial time. As is the case in the Lake Tulane Florida record, no evidence for the impacts of Dansgaard-Oeschger events is to be seen in either of Arz's records.

In separate studies, Edouard Bard and Isabel Cacho Lascorz demonstrated that the time intervals correlating with Heinrich events were significantly colder than the glacial ambient in the eastern Atlantic (off France and Portugal) and in the western Mediterranean. In both studies, alkenones were employed as paleothermometers. In Cacho Lascorz's Mediterranean study, these extreme colds were confirmed with Mg/Ca ratios on planktonic foraminifera and by pollen blown off the adjacent European land mass.

The locales where impacts of Heinrich events clearly stand out are shown in the map in figure 48. Note that Dansgaard-Oeschger events dominate the record in some places and Heinrich events in others. Examples of these records are shown in figure 49.

RELATIONSHIP BETWEEN DANSGAARD-OESCHGER AND HEINRICH EVENTS

The question naturally arises as to the relationship between Heinrich and Dansgaard-Oeschger events. The problem is that the D-O events seen so prominently in the Greenland ice cores are not prominent in the marine record from the northern Atlantic. Nor are Heinrich events prominent in the ice core record. Only when Lamont-Doherty's Gerard Bond carefully examined very detailed records of color, foraminifera speciation and abundance of ice rafted debris was he able to correlate the two records. Reproduced in figure 50 is his comparison between the gray scale record for a core from the northeastern Atlantic and two ^{18}O records for Greenland ice cores. For the first time, Bond was able to demonstrate the existence of D-O cycles on the marine record. Bond used this correlation to place the Heinrich in the Greenland ice core record (see figure 51). As would be expected, from their positioning in the ocean record, the Heinrich events occur during ^{18}O minima (cold peaks). There also appears to be a tendency for

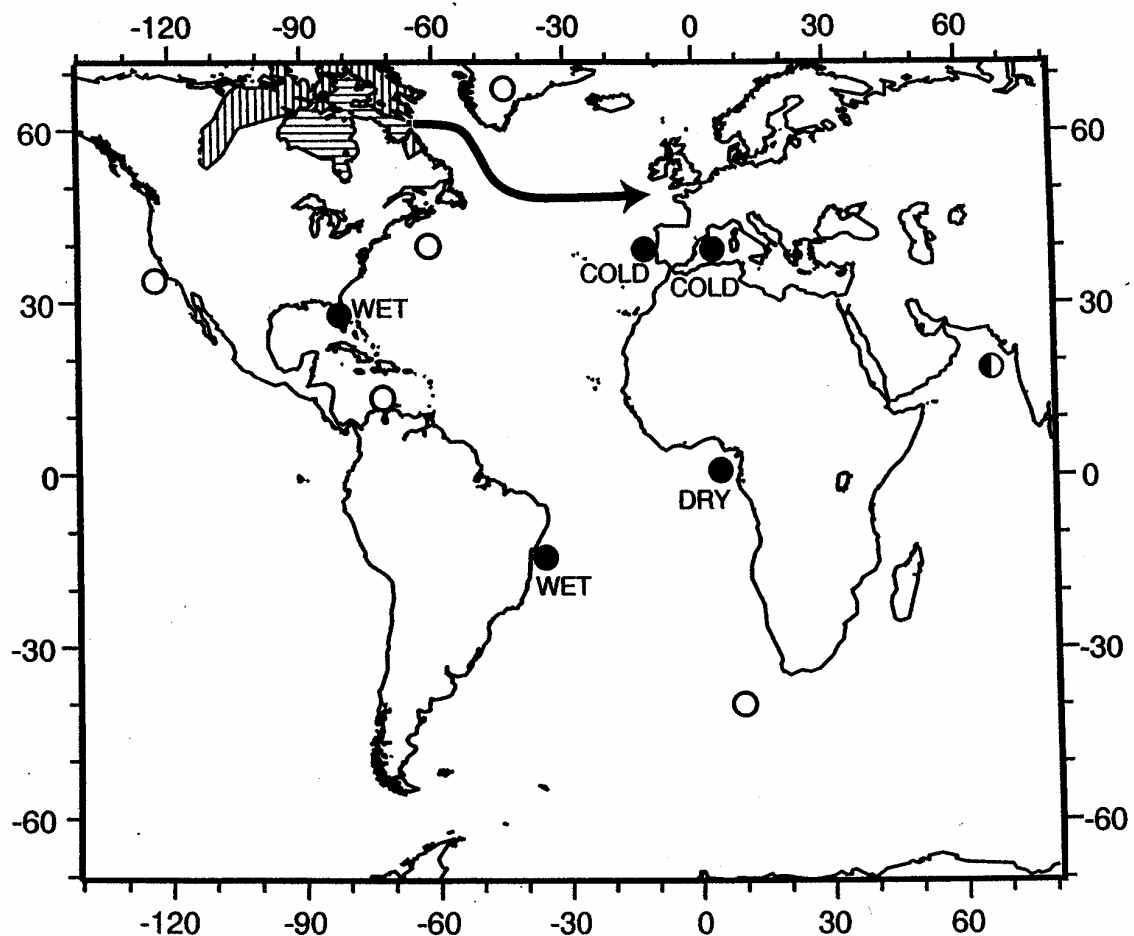


Figure 48. Map showing sites where the climatic impacts of H events dominate (black circles) and sites where those of DO events dominate (white circles). The black arrow shows pathway followed by the Heinrich armadas, the patch with vertical lines is the area where Churchill province crystalline rocks outcrop and the horizontal lines indicate the Paleozoic limestone underlying Hudson Bay and Strait.

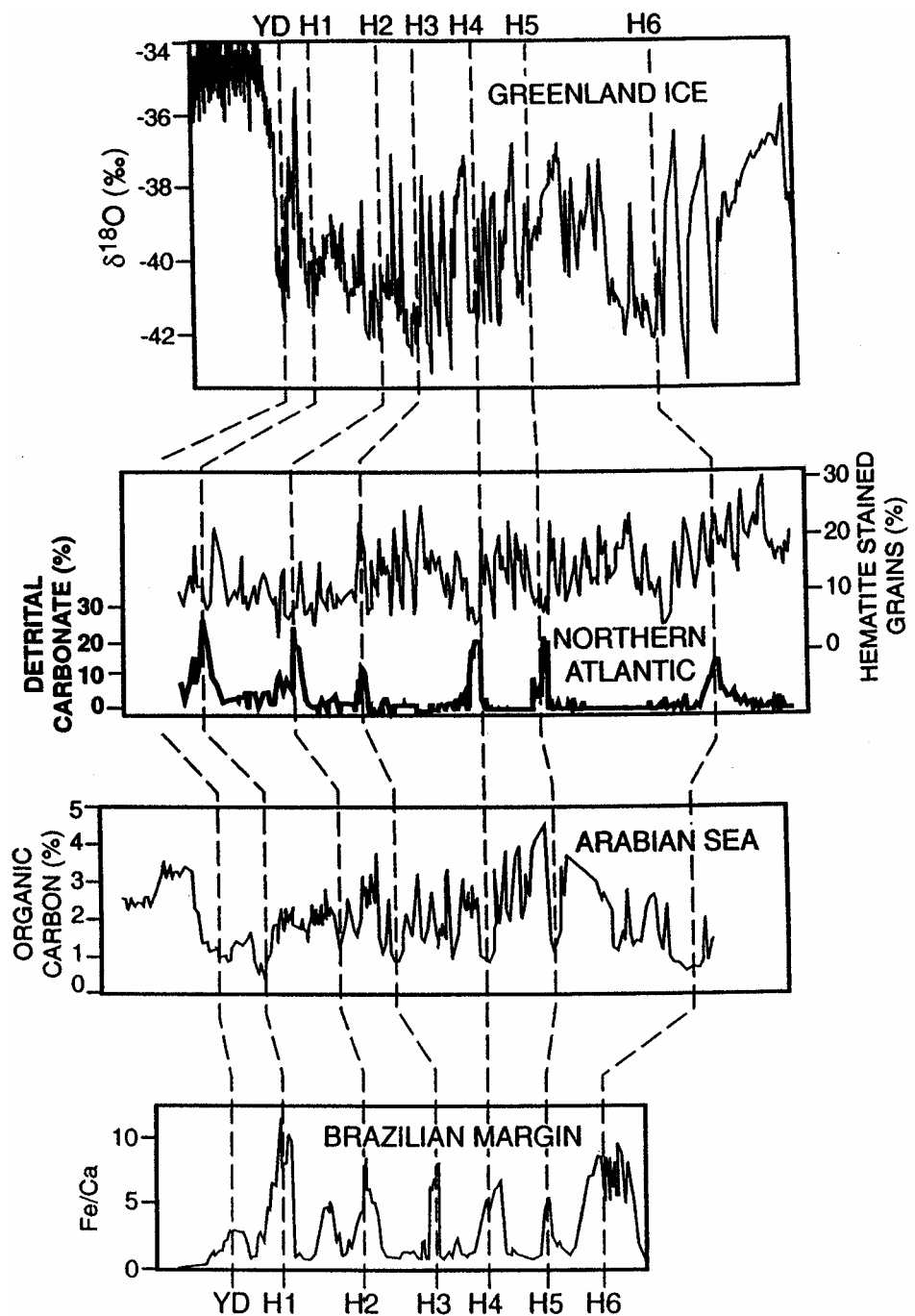


Figure 49. Comparison of four records showing a range in the ratio of the climatic impacts of Heinrich events to those of Dansgaard-Oeschger events. On the top is the Summit Greenland $\delta^{18}\text{O}$ record in which DO events dominate. In the center are records of ice rafting in the northern Atlantic Ocean (Bond et al., 1999) and of organic matter in the Arabian Sea (Schulz et al., 1998). In these records, the impacts of both H and DO events are apparent. At the bottom is the record of lithic input off Brazil in which only Heinrich events are seen (Arz et al., 1998). Time and depth scales are deliberately left off, but the Heinrich events are approximately 16, 22, 30, 38, 45, 65 ka.

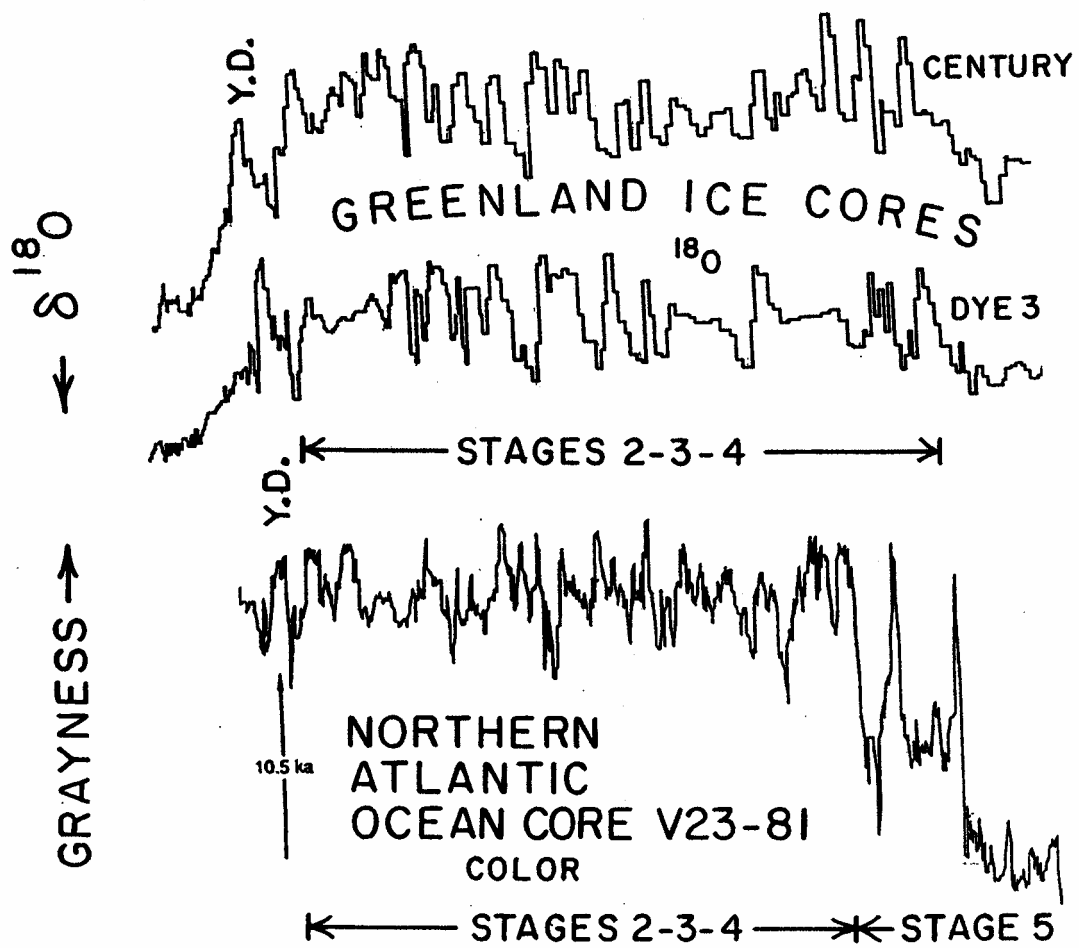


Figure 50. Comparison between the oxygen isotope records for the Greenland ice cores (Dansgaard et al.) and Bond's gray-scale record for northern Atlantic core V23-81.

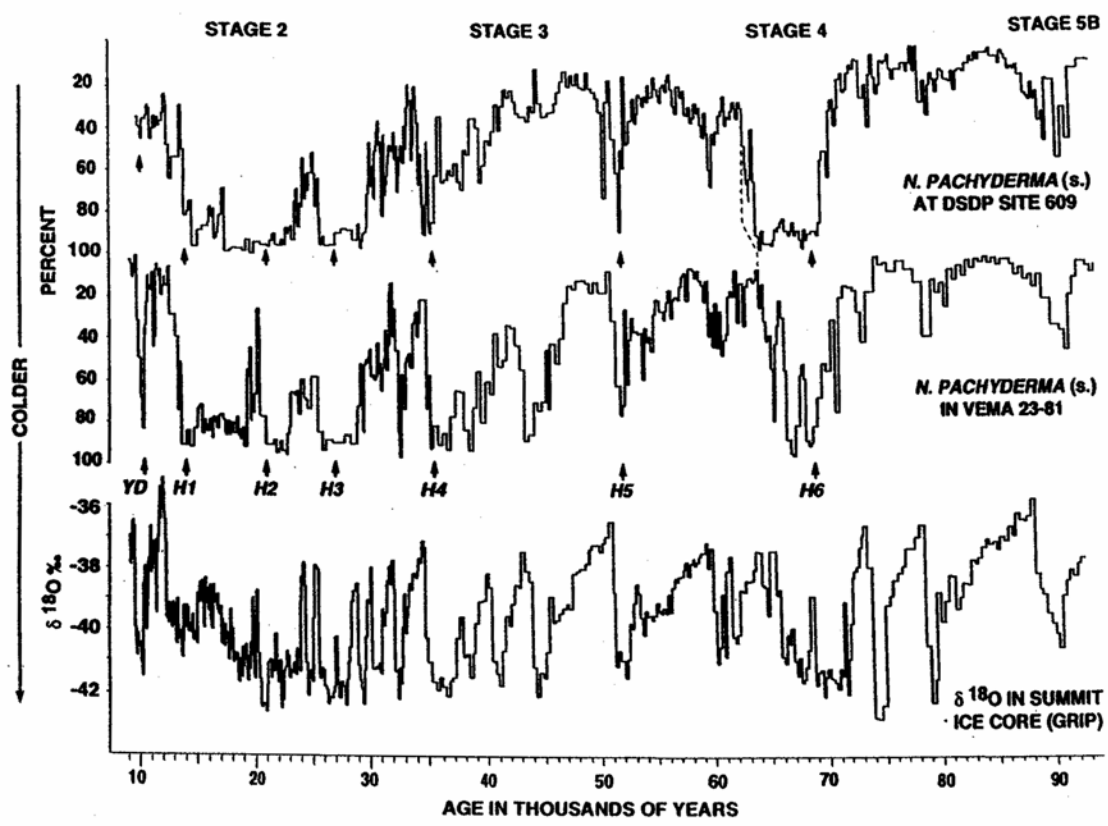


Figure 51. Gerard Bond's correlation between the Greenland ice core ^{18}O record and the planktonic foraminifera record for northern Atlantic marine sediment.

magnitude of ^{18}O maxima associated with D-O cycles to decrease during the course of the interval separating successive Heinrich events (see figure 52).

THE 1500-YEAR CYCLE

As part of his quest to reconstruct the record of ice rafting in the northern Atlantic, Lamont-Doherty's Gerard Bond noted a curious pattern in the composition of the lithic fragments in his sediment samples. These fragments were dropped from melting icebergs. He noted that the proportion of red-coated (i.e., iron-stained) grains underwent a cyclic change from highs of 16 to 18 percent to lows of 2 to 4 percent. Despite large changes in the absolute abundance of lithic grains from glacial to interglacial, Bond found that the compositional cycle ran uninterrupted through the entire record from Termination II to the present. Although the width of the cycle ranges from 1200 to 1800 years, when Bond averaged ten or so successive cycles, the mean duration turned out to be close to 1500 years during both times of glaciation and times of interglaciations. Even the range in amplitude did not change. The persistence and regularity of this composition cycle was, to say the least, puzzling. Bond noted that today icebergs bearing the iron-stained grains are on the average launched poleward of those bearing unstained grains. Thus he reasoned that icebergs bearing the red grains would reach the sites of his piston cores in greater numbers during cold periods than during warm periods. Hence, he postulated that the 1500-year cycle involved an alternate warming and cooling of the northern Atlantic. He also demonstrated that the most recent of these cycles corresponds to the Medieval Warm (800 to 1300 AD) – Little Ice Age (1350 to 1850 AD) oscillation.

Bond compounded the surprise when, as senior author on a paper published in December 2001 in *Science*, he made a convincing case that the 1500-year cycle is paced by the Sun. The argument is based on a similarity between the lithic-grain composition record and the records of the production rate of both ^{14}C and of ^{10}Be (see figure 53). The ^{14}C reconstruction is based on the tree-ring measurements discussed in the section on

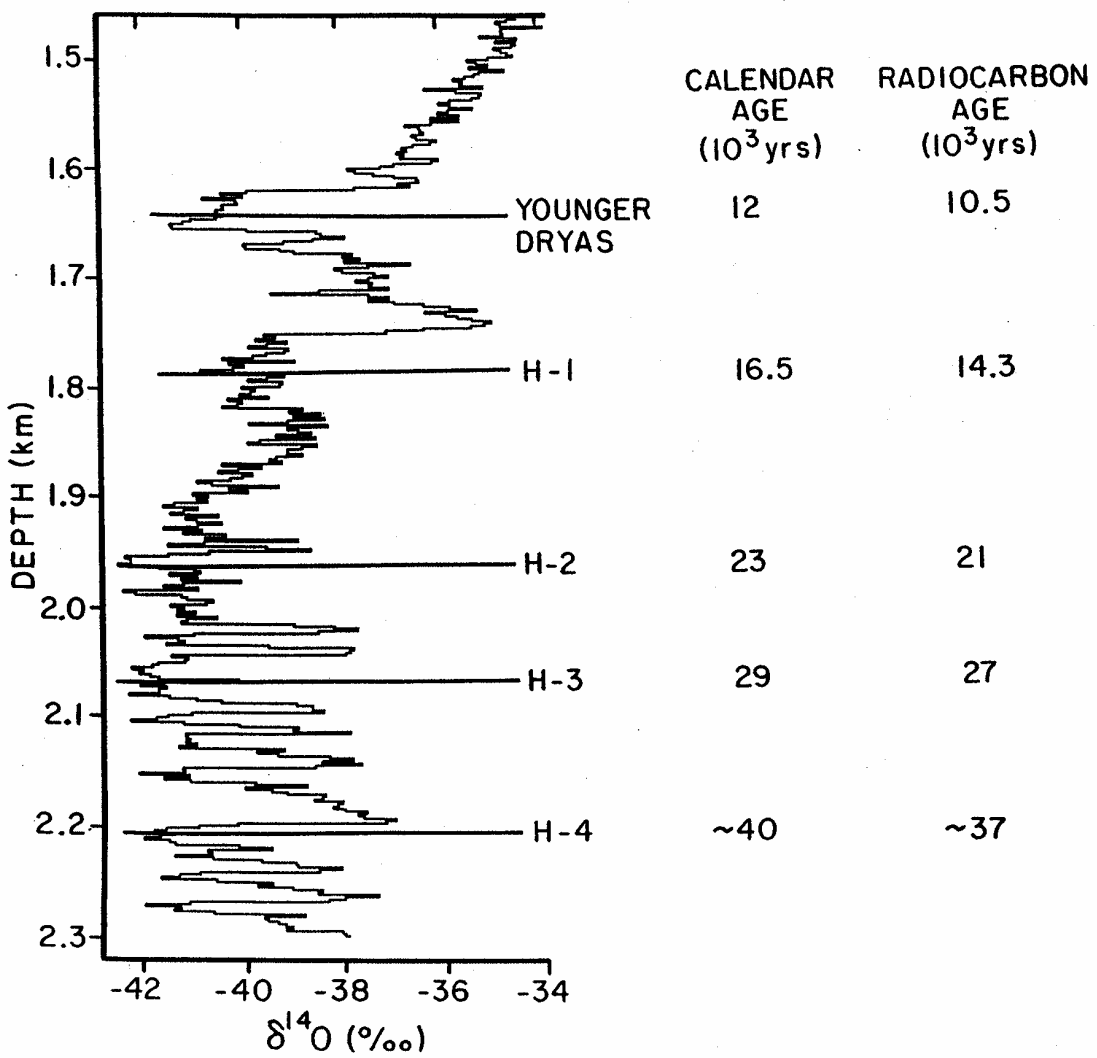


Figure 52. Gerard Bond's placement of the last four Heinrich events in the Greenland ice core record. The correlation between the ocean ice core records was accomplished by matching features shown in figure 47. The correlation conforms to the independent time scales for the marine record (^{14}C) and for the ice core record (annual layer counting).

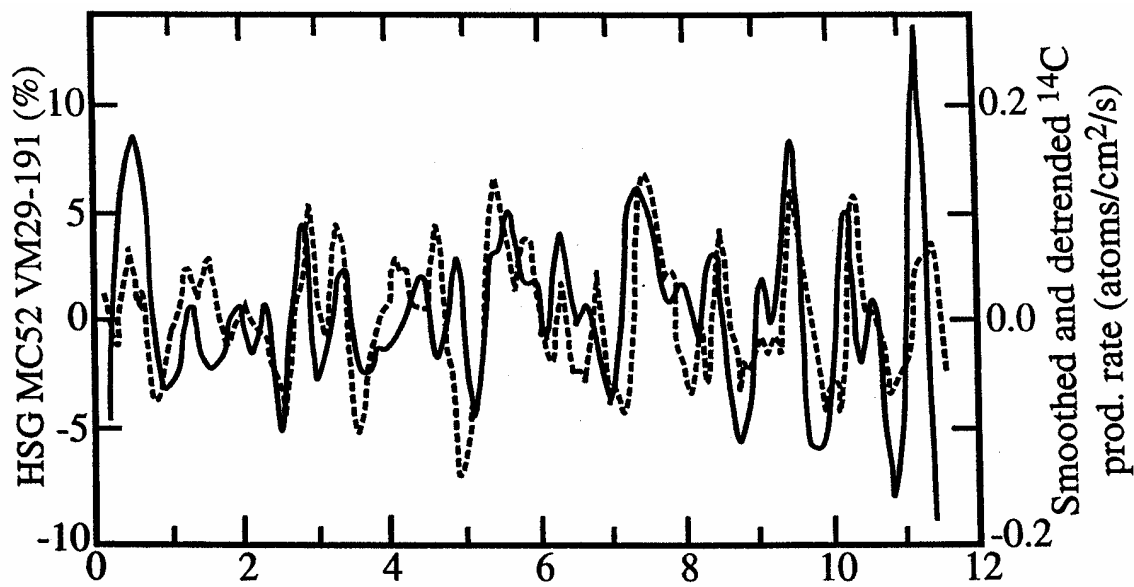


Figure 53. Comparison between the fluctuations in the fraction of red-coated lithic grains (dashed curve) with that of cosmogenic nuclide production (solid curve) in the Earth's atmosphere. This correspondence provides powerful evidence that the Holocene's small cyclic temperature changes were paced by changes in solar luminosity (Bond et al., 2001).

‘Clocks.’ The ^{10}Be reconstruction is based on measurements in Greenland ice. As the two records yield nearly the same timing and amplitude for the required changes in the influx of cosmic rays, it is difficult to find an alternate explanation.

The next step in the Bond et al.’s logic involves the tie between sunspot activity and the production rate of cosmogenic nuclides. It is well known that streaming forth from the Sun’s spots are ions and that these ions generate a magnetic field which acts as a shield which diverts inbound galactic cosmic rays. An interesting natural experiment occurred when from 1650 to 1715 sunspots disappeared. During this so-called Maunder Minimum interval, the production rates of both ^{14}C and ^{10}Be increased by the amount expected if the heliomagnetic field dropped to zero. Thus it appears safe to say that the reconstructed production rates of ^{14}C and of ^{10}Be provide a record sunspot activity.

The final step in the Bond et al.’s argument is that solar luminosity varies with sunspot activity, the more spots the greater the energy output. This relationship has been quantified by very precise satellite observations of solar energy output over the last two eleven-year sunspot cycles (see figure 54).

Support for Bond’s interpretation that the shifts in lithic composition reflect temperature changes comes from the Swiss Alps. Radiocarbon dating of wood and peat being carried out from beneath the glaciers by summer melt water fall in groupings which match three of Bond’s warm intervals. Based on the change in the elevation of the so-called equilibrium snowline, it has been estimated that the temperature has warmed $0.6 \pm 0.1^\circ\text{C}$ since 1860 when the glaciers extended to their Holocene maximum moraines. Clearly, for the wood and peat to have formed, the glaciers must have been even smaller than now. If there is a problem with the idea that the Sun is driving these Holocene temperature changes, it is that the luminosity changes appear to be too small to account for the Earth impacts. What is more disconcerting is that the Dansgaard-Oeschger events appear to follow the pacing of the 1500-year cycle. As the climate changes associated with these D-O were an order of magnitude larger than those of the Holocene, it becomes

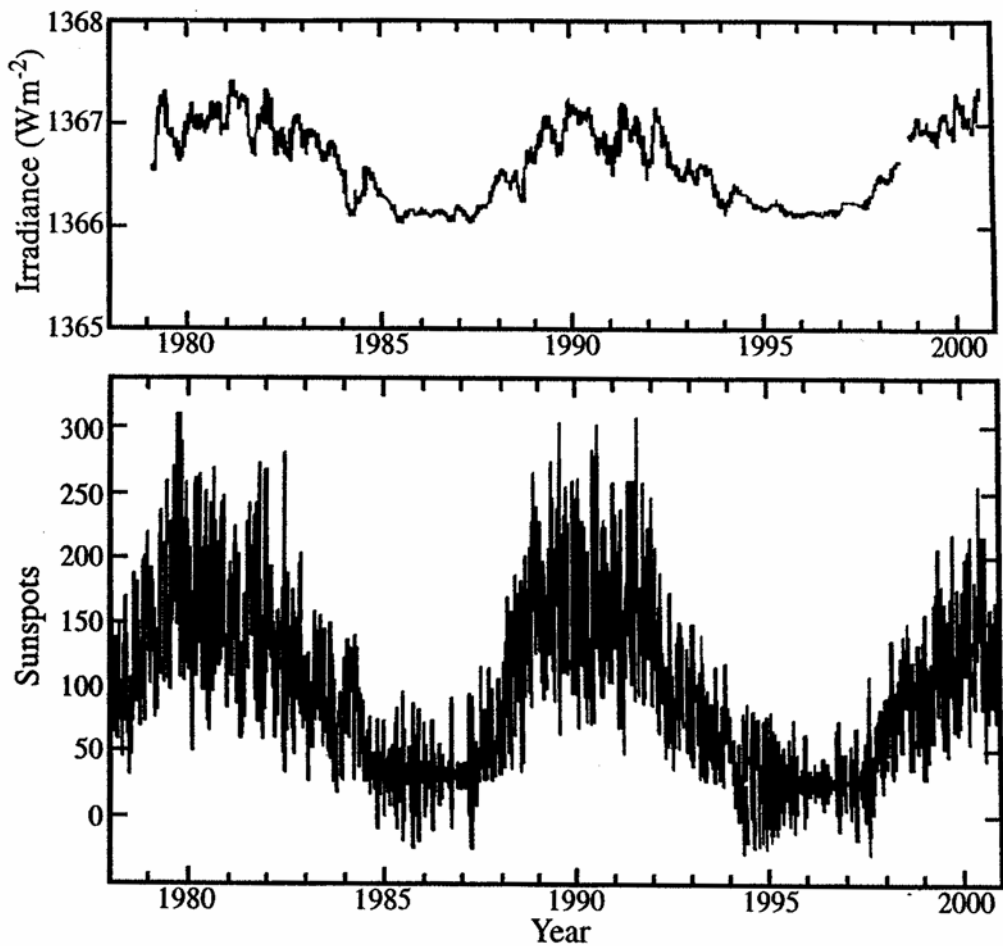


Figure 54. Comparison of the solar irradiance with the sunspot numbers for the last two Schwabe cycles. The irradiance record is a compilation of data from different satellites. During periods of high solar activity there are more sunspots darkening a small part of the solar disk (visible in the negative excursions of the irradiance). However, the brightness of the Sun is increased at the same time, overcompensating the darkening effect of the sunspots.

even harder to understand how they could have been driven by the tiny changes in solar energy output.

MECHANISMS

INTRODUCTION

In addition to tweaking our intellectual curiosity, the record of the large and often abrupt climate shifts of the late Quaternary offers valuable information regarding the sensitivity of the Earth's climate system to nudges. The bottom line is that while the forcings which gave rise to these shifts are known, the joint atmosphere-ocean models in current use are incapable of reproducing the changes the Earth's climate has undergone in response to these forcings. This failure tells us that these simulations lack teleconnections and feedbacks necessary to extend and amplify these forcings. As we are now faced with predicting the consequences of the ongoing increase in the atmosphere's burden of CO₂ and other greenhouse gases, it is imperative that we decipher the physics behind these extenders and amplifiers so that they can be properly included in atmosphere-ocean simulations.

FORCINGS

Three types of forcing appear to be responsible for a sizable fraction of the drifts and jumps in climate which have occurred during the late Quaternary. They are as follows: 1) changes in seasonality associated with the Earth's orbital cycles; 2) reorganizations of the ocean's mode of thermohaline circulation associated with catastrophic inputs of fresh water to the northern Atlantic; and 3) changes in the Sun's energy output associated with sunspot activity.

INSOLATION SEASONALITY CYCLES

As already discussed, while the cyclic changes in the Earth's orbital characteristics lead to a redistribution of heat among the seasons, for the Earth as a whole, there is no significant change in annual insolation receipt. Even when endowed with seasonality, full-scale atmosphere-ocean computer simulations fail to significantly

respond to these so-called Milankovitch cycles. Clearly then, some important characteristics of the climate system are not being adequately replicated in these models.

To date, much of the effort to model the impacts of Milankovitch cycles has been focused on the Northern Hemisphere's ice caps, the idea being that the reflectivity of these caps dictates the climate of the entire planet. However, the documentation that the glaciation of mountains had the same amplitude and timing at 40°S as at 40°N, in my estimation voids this concept. I suspect that the simplified models used for this purpose are capable of replicating the time history of ice sheets only because they are designed and tuned to do so. Models of greater complexity are incapable of initializing ice caps or of terminating those prescribed by the modeler.

To me, the most promising link between seasonality and Earth climate involves monsoonal activity for it certainly influences the atmosphere's moisture content and cloud cover. The activity is driven by the seasonality of heating and hence should respond to Milankovitch cycles. Indeed this is a promising way to explain the strong 23,000-year cycles in atmospheric methane content and in the isotopic composition of atmospheric oxygen. Both are sensitive to the Earth's moisture budget.

THERMOHALINE CIRCULATION REORGANIZATIONS

A wide range of models of the ocean's thermohaline circulation undergo bifurcations from one mode of operation to another. Further, these reorganizations are readily triggered by the addition of fresh water to the northern Atlantic. The reason is that the consequent density reduction in surface waters leads to a shutting down deep water formation (i.e., a disruption of the Atlantic's conveyor-like circulation). As waters in the deep sea are continuously being dedensified by the downward stirring of warm upper ocean water, such a cutoff of deep water formation is soon compensated by a supply of dense water from an alternate high latitude site.

As outlined in the section of "Records," seven such deluges of fresh water entered the northern Atlantic during the course of the last glacial period. Six were associated

with the melting of Heinrich ice armadas and the seventh (i.e., that at the onset of the Y.D.) with a sudden release of melt water stored in proglacial Lake Agassiz. The geologic record clearly demonstrates that the impacts on the atmosphere presumably triggered by these shutdowns were large and also geographically widespread. However, when such shutdowns are triggered in joint ocean-atmosphere models, the atmospheric impacts are restricted to northwestern Europe. Again, this tells us that some essential physics must be missing in these simulations.

In the case of the Younger Dryas, the snowline lowering in New Zealand's South Island has been shown to be nearly the same as that in the Swiss Alps. This appears to require an alteration driven by the convective systems of the equatorial atmosphere and has led some scientists to put aside the idea of an ocean trigger and replace it with an, as yet, undefined tropical trigger. As outlined below in the section on the bipolar seesaw, I feel that the case for an ocean trigger remains strong. The discovery that Heinrich armadas led to important changes in the tropical moisture budget appears to require a rapid link between ocean thermohaline circulation and the dynamics of the tropical atmosphere.

Not only are the impacts of the Y.D. event hemispherically symmetrical and large, they also are very nearly synchronous everywhere. The ice core results show that the abrupt global rise in methane which occurred at the end of the Y.D. commenced within a decade or so after the abrupt warming of Greenland. As this methane increase is very likely the result of the warming and wetting of tropical swamps, it points to the existence of a fast link between the tropics and polar regions. The nature of this link remains unknown.

FLUCTUATIONS IN SOLAR ENERGY OUTPUT

Precise satellite-based measurements of solar luminosity carried out over the last two decades reveal a correlation with sunspot number. Over the course of the 11-year sunspot cycle, there is a variation in solar energy output of about one part in 1300, the

higher the number of spots, the greater the energy output. Unfortunately, the record of sunspots extends back only to the time when Galileo first observed them (i.e., to 1600 AD). However, during the 400-year period of observation there was an interval (1650 to 1715 AD), referred to as the Maunder Minimum, when no sunspots were observed. During this interval, the production rate of ^{14}C and ^{10}Be increased presumably as the result of the weakening of the magnetic field created by the ions shot out from the sunspots. This led to the idea that reconstructions of past ^{14}C and ^{10}Be production rates provide a measure of the Sun's ion emission, and hence also of its paleo sunspot activity. As already described, these reconstructions revealed a quasi 1500-year cycle in cosmic ray bombardment running through the entire Holocene. Furthermore, geologic data reveals that temperatures in high northern latitudes fluctuated in harmony with these production cycles, the cold intervals corresponding to times of increased production of cosmogenic isotopes (and hence of low sunspot activity), and the warm to times of reduced cosmogenic production (and hence high sunspot activity). Thus, it appears that these temperature changes were driven by small changes in solar luminosity.

However, a number of questions must be answered before a relationship between Earth temperature and solar luminosity can be established. One involves the magnitude of the global temperature change. From tree ring and mountain snowline reconstructions, it appears that during the Holocene the 1500-year temperature cycle at high northern latitudes had an amplitude of about 1°C . Unfortunately, the evidence for the rest of the planet is inadequate to determine whether the changes are global or confined to high northern latitudes. Only for the last cold phase (i.e., the Little Ice Age) has the extent been documented to be global. Also, it is not clear how one goes about estimating the luminosity during periods like the Maunder Minimum when sunspot activity was shut down. If luminosity is proportional to sunspot number, then it would not be much lower during periods of no spots than it was during the minima of the 11-year cycles. The reason is that over the last two 11-year cycles, the spot number has gone from a high of

about 240 to a low of about 40. Hence, were the relationship between luminosity and sunspot number linear a drop to zero would only make a very small change. On the other hand, were it proportional to cosmic ray production (i.e., to the heliomagnetic field), then the luminosity would have been substantially lower during periods like the Maunder Minimum than during the minimum of the 11-year cycle. Radiocarbon production increases by a factor of 1.5 between the maxima and the minima of the 11-year sunspot cycle. In contrast, production was roughly twice as high during the Maunder Minimum than during maxima in the 11-year cycle. So, if luminosity follows radiocarbon production, it would be lower during the Maunder Minimum than during the minima in the 11-year cycle. The truth of the matter is that no observation or theory exists which would allow the luminosity during periods such as the Maunder Minimum when sun spots were absent to be estimated. Astrophysicists warn that any attempt to estimate the Sun's liminosity changes during periods such as the Maunder Minimum based on observations of its surface features is very likely to be flawed. The reason is that the longer the time scale, the greater the depths in the Sun's interior which are involved. However, it can be stated that unless the drop in luminosity during these periods was quite large ($\sim 0.5\%$), then it is very difficult to explain the cooling associated with the Little Ice Age. Models fail to produce any significant change in temperature in response to the observed solar luminosity changes.

A great puzzle in this regard involves glacial time. Gerard Bond has shown that his quasi 1500-year cycle in the composition of ice-rafted debris continues uninterrupted through the last glacial period. Furthermore, the Dansgaard-Oeschger cycles which punctuate substantial portions of glacial time have durations averaging 1500 years. As shown by Richard Alley, the entire glacial record in the Greenland ice core can be explained in terms of stochastic resonance. The idea is that if Bond's 1500-year cycle acts as a trigger for the far larger Dansgaard-Oeschger events, then perhaps this trigger does not always kick in. However, if it fails during any given 1500-cycle, it is likely that

it will trigger a response during the subsequent cycle. This behavior constitutes a phenomena known as stochastic resonance.

The mystery is how these seemingly very small fluctuations in solar output can have such immense consequences to the Earth's climate. Some very powerful amplifiers must be operative.

THE BIPOLAR SEESAW

That the competition between deep water formation in the northern Atlantic and in the Southern Ocean has led to abrupt circulation flip flops is reasonably well documented. One piece of evidence is the polar antiphasing of the temperature during the last deglaciation as recorded in Antarctic and Greenland ice. Another is the abrupt rise in the ^{14}C to C ratio in the surface ocean at the onset of the Younger Dryas.

A number of simplified ocean models have been constructed whose thermohaline circulation jumps back and forth between states characterized by stronger and weaker conveyor circulation. In most of these models, the cycle length is set by the ocean's interval dynamics with help from fresh water additions to the northern Atlantic. For example, Stefan Ramstorf and his Potsdam colleagues have a model which nicely responds in accord with Alley's stochastic resonance concept.

Personally I have always leaned toward the idea that the salt budget of the Atlantic played an important role and have envisioned a salt oscillator. During episodes of 'strong' conveyor operation, the Atlantic exports more salt to the Southern Ocean than it gains through vapor loss through the atmosphere. During times of 'weak' conveyor operation, the opposite was the case.

AMPLIFIERS

Observations regarding the concentration of continental dust and of sea salt in Greenland ice strike me as very revealing. First, both of these concentrations are more than an order of magnitude higher during the coldest times of the last glacial period than during the Holocene. Second, both underwent abrupt threefold jumps during the

transitions between the moderately cold and extremely cold phases of the Dansgaard-Oeschger cycles. Together with the evidence from continental loess and from ocean sediments, it is clear that the atmosphere was far dustier during glacial time. The high sea salt content in glacial ice from both Antarctica and Greenland points to storminess rather than rainfall or vegetative cover as the key cause. To me, these records are telling us that the frequency of intense storms was greater during glacial time. A hot clue regarding the cause of these changes comes from the nature of the transitions which separate the extremely cold and moderately cold phases of the Dansgaard-Oeschger events. As we have seen, these transitions occurred in just a few decades. Further, during this transition period, the climate flickered. So, the clue is that we are dealing with some aspect of the system capable of undergoing a major change in one to three years.

We can eliminate glacial extent, sea level and atmospheric CO₂ content as candidates for they are incapable of such rapid change. Also, we seek a property of the system that has an off-on characteristic. While water vapor, snow cover and cloudiness can change with sufficient rapidity, it is difficult to see why operating alone any of the three could have the required on-off property. The only aspect of the climate system I know of which has this capability is the ocean's thermohaline circulation. It could act as follows. Were the Atlantic's conveyor circulation to have been weaker during the intervals of Greenland's intense colds and stronger during the intervals of Greenland's moderate colds, then sea ice cover could be the critical element in the system. During times of weak conveyor circulation, sea ice cover in the northern Atlantic could well have extended to the latitude of southern England. Then when the conveyor popped back into its strong mode, the warmth it carried would have driven the sea ice front back to the north of Iceland. As shown by ocean models, these transitions can occur with sufficient rapidity to be consistent with observation.

If this is indeed the correct pathway toward understanding the very large and often abrupt changes in the loading of atmospheric particulates, then the obvious connection is the atmosphere's winter thermal gradient. The key is that over open water winter air temperatures cannot get much below freezing. However, in regions of sea ice cover like the present day Arctic, winter temperatures can drop to several tens of degrees Celsius below the freezing point. Hence, the extension of sea ice cover shortens the distance separating the ultra cold conditions over winter sea ice and those in the warm tropical zone. The tendency would then be to increase the frequency of winter storms capable of lofting dust from continental deserts and spray from ocean white caps. However, as this tendency has yet to be quantified, this explanation has to be classified as Broecker's hunch.

Clearly, if this scenario is the correct one, then the impacts of the coupling of the Atlantic's conveyor to sea ice cover would be limited to the Northern Hemisphere. To my knowledge, no firm evidence for significant impacts to the Southern Hemisphere atmosphere associated with Dansgaard-Oeschger events has yet been obtained. Only in one place in the Southern Hemisphere (i.e., in the southern Atlantic) has evidence for D-O ocean impacts been identified. However, as this record can be interpreted as a consequence of a change in position of the interface between deep waters of northern Atlantic origin and those of the Southern Ocean origin (i.e., on the strength of conveyor circulation), it does not necessarily implicate the atmosphere. Clearly, future research must be focused on obtaining records which will allow global maps of the magnitude of impacts associated with Dansgaard-Oeschger events and with Heinrich events to be constructed.

WATER VAPOR

Water vapor is the atmosphere's most powerful greenhouse gas. As water molecules spend only days to weeks in the atmosphere before raining out, it is clear that the inventory of this gas can change very rapidly. In most general circulation models the

atmosphere's water vapor inventory changes in accord with the surface ocean temperature (i.e., ~8% per °C). In other words, the relative humidity remains nearly constant. Hence water vapor changes tend to amplify the primary forcing. For example, in the case of excess anthropogenic CO₂, in most models the water vapor feedback amplifies the primary greenhouse forcing by a factor of 2 to 3.

CLOUD COVER

Currently, on any given day, clouds shroud roughly half of our planet. They reflect back to space about one quarter of the incoming solar radiation. It turns out that the impact of an 8 percent change in cloud albedo has about the same impact on the Earth's radiation budget as a doubling of atmospheric CO₂ content. Interactive modeling of cloud cover turns out to be a nightmare, for cloud albedo depends on droplet density, droplet size, cloud thickness and cloud height. So, cloudiness is certainly a wild card in connection with the question as to why small forcings are amplified into large climate changes.

One particularly interesting aspect of cloud albedo is that the number of droplets depends on the availability of cloud condensation nuclei. The more nuclei, the greater the droplet number and hence the smaller the size of the average droplet. The importance to albedo is that, given the same amount of precipitable water, the cloud with many smaller droplets will be more reflective than the cloud with fewer larger droplets. We have already seen that during peak glacial time the amount of sea spray lofted high into the atmosphere was on order of magnitude larger than during interglacial time. Hydroscopic sea salt aerosols make excellent cloud condensation nuclei. Hence, the greater number of droplets generated by these additional nuclei may have contributed to the global cooling of glacial time.

TERMINATIONS

Each of the 100,000-year duration major glacial to interglacial cycles of the late Quaternary ended abruptly. In no more than 5000 years, climate switched from its full

glacial to its full interglacial condition. Many papers have been written putting forth scenarios designed to explain the cause of these so-called terminations. To my way of thinking, none have fully succeeded.

I suspect that these events are part of a drift-correct oscillation. During the course of each major cycle, the planet gets progressively colder. Then, at some point, the system becomes unstable and snaps back to its warm condition. For the last four terminations (i.e., those associated with marine isotope boundaries 10-9, 8-7, 6-5 and 2-1), these reorganizations appear to have been triggered by strong Northern Hemisphere summer insolation peaks. But, in the case of the 12-11 boundary, the Earth's orbit was almost perfectly round yet the termination was just as large and just as abrupt as subsequent ones. This suggests that the 100,000-year cycle is internal to the Earth and that it may not be driven by Milankovitch insolation cycles. Rather, these cycles modulate the cooling interval and pace the timing of the terminations. One can imagine that, as the system drifts toward instability, it is somehow pushed over the brink by an interval of exceptionally strong Northern Hemisphere summer insolation. In the absence of such an insolation nudge, the cycle is ended when instability is achieved. So, in a sense, the insolation peaks cause the cycle to pre-trigger.

Those who have pondered this phenomena seek to identify some aspect of the system which might have the required long-time constant. The favorite candidates have to do with the Northern Hemisphere ice sheets. Either their geographic extent or their loading of the underlying mantle may eventually create an instability. The problem is that the exact nature of this instability eludes us.

SUMMARY

The record kept in ice and in high accumulation-rate sediments clearly demonstrates that the Earth's climate has undergone large and abrupt changes. Evidence is building that some of these changes were paced by changes in insolation both due to cycles internal to the Sun and to changes in seasonal distribution related to the Earth's

orbital cycles. In a number of cases it seems clear that reorganizations of the ocean's thermohaline circulation triggered the atmospheric change. The fact that during both peak glacial time and the Younger Dryas cold snap mountain snowlines simultaneously descended just as much at 40°S as they did at 40°N requires that the cooling of the planet was driven by modifications in the operation of the great equatorial convective heat and moisture engine. Further, since the forcings for these changes appear to be too weak to do the job, powerful amplifiers must have been at work. It appears that these amplifiers were much stronger during times of glaciation than during times of interglaciation. Despite these intriguing clues, we have a long way to go before we can claim to understand how our climate system responds to nudges.

FOSSIL FUEL CO₂

While this book is concerned with the climate changes associated with glacial cycles, it would be unfortunate were I not to mention the implications of what we have learned to the near future. Most important in this regard is the global warming expected from the ongoing buildup of CO₂ and other greenhouse gases in our atmosphere. Championed by MIT's Richard Lindzen, detractors claim that this warming will be minor and therefore we need not take any expensive actions to stem this buildup. With population increasing and with the world's poor becoming less poor, energy consumption is bound to increase. In the absence of a minor miracle, this energy will come largely from burning fossil fuels. I believe that unless some drastic action is taken, by early in the next century, we will have quadrupled the atmosphere's CO₂ content (i.e., from the pre-industrial 280 ppm to ~1100 ppm). Compared to the minuscule changes in solar luminosity (a few parts in 1000), this rise will alter the radiation balance by 15 to 40 parts in 1000. To assume that such a change will not lead to significant impacts on wildlife, agriculture, water availability.... in my estimation is ludicrous.

The models used to estimate the impacts of excess CO₂ yield near linear responses. Yet, over the past few hundred-thousand years, the Earth's climate has

undergone numerous sudden large jumps. Hence, we can not exclude this possibility of such jumps in response to the ongoing greenhouse warming.

In summary, climate has proven itself to be an angry beast. We are in the process of provoking this beast with greenhouse gases. It is my feeling that we must do everything possible to reduce the magnitude of this poke!

BIBLIOGRAPHY
TABLE OF CONTENTS

1) Mountain glaciation	1
2) Dust and loess	3
3) Closed basin lakes.....	6
4) Rock varnish	10
5) Ice volume and sea level	11
6) Stable isotopes in ice.....	13
7) Carbon dioxide in polar ice.....	18
8) Methane in polar ice.....	20
9) Isotopes of O ₂ and N ₂ in ice.....	22
10) Oxygen isotopes in deep sea sediments	22
11) Carbon isotopes in deep sea sediments.....	26
12) Cadmium, zinc and barium in foraminifera.....	29
13) Alkenone thermometry	32
14) Strontium-calcium thermometry	34
15) Magnesium-calcium thermometry	36
16) Continental paleothermometers	38
17) CaCO ₃ dissolution	39

BIBLIOGRAPHY
TABLE OF CONTENTS
(continued)

18) Boron isotope paleoacidity	43
19) Radiocarbon dating	45
20) Uranium series dating	48
21) Cosmogenic isotope dating.....	53
22) Luminescence dating	55
23) Milankovitch seasonality cycles	56
24) The 100,000-year cycle.....	58
25) The Bølling Allerød-Younger Dryas	59
26) Heinrich events	64
27) Dansgaard-Oeschger events.....	68
28) The 1500-year cycle.....	70
29) Global water budget.....	71
30) Ocean thermohaline circulation	73

1) Mountain glaciation

- Klute, F., **1921**, *Zeitschrift fer Geographie*, 27, 199-203; Earliest summary of glacial snowline lowering for mountains throughout the world.
- Selling, O.H., **1948**, *Bishop Museum Special Publication* 39, Honolulu; Mountain vegetation in Hawaii during the last glacial.
- Osmaston, H.A., **1965**, Ph.D. thesis, Oxford University, Worcester College; Snowline lowering on the mountains of tropical Africa.
- Denton, G.H. and Stuiver, M., **1967**, *Geological Society of America Bulletin*, 78, 485-510; Chronology of Alaskan mountain glaciation.
- Suggate, R.P. and Moar, N.T., **1970**, *New Zealand Journal of Geology and Geophysics*, 13, 742-746; Chronology for the last glaciation of the New Zealand Alps.
- Denton, G.H., **1974**, *Geological Society of America Bulletin*, 85, 871-892; Glacial snowline lowering in Alaska.
- Herd, D.G. and Naeser, C.W., **1974**, *Geology*, 2, 603-604; Mountain snowline lowering in the tropical Andes.
- Van der Hammen, T., **1974**, *Journal of Biogeography*, 1, 3-26; Mountain vegetation during glacial time in the tropical Andes.
- Porter, S.C., **1975**, *Quaternary Research*, 5, 27-47; Glacial snowline lowering in the New Zealand Alps.
- Hope, G.S., **1976**, *Journal of Ecology*, 64, 627-664; Mountain vegetation in New Guinea during glacial time.
- Mercer, J.H., **1976**, *Quaternary Research*, 6, 125-166; Glacial snowline lowering in the southern Andes.
- Porter, S.C., **1977**, *Journal of Glaciology*, 18, 101-116; Mountain snowline lowering in the Cascade Range.
- Porter, S.C., **1979**, *Geological Society of America Bulletin*, Pt. II, 90, 980-1093; Glacial snowline lowering in Hawaii.
- Porter, S.C., **1981**, *Quaternary Research*, 16, 263-292; Glacial snowline lowering in the Chilean lake district.
- Hamilton, A.C., **1982**, *Environmental History of East Africa*, Academic Press, New York; Mountain vegetation in tropical Africa during glacial time.
- Clapperton, C.M., **1983**, *Quaternary Science Reviews*, 2, 83-155; Summary of the glaciation of the Andes.
- Porter, S.C., Pierce, K.L., and Hamilton, T.D., **1983**, In: Wright, H.F. Jr. (ed.), *Late Quaternary Environments of the United States, Vol. I, The Late Pleistocene*, Porter, S.C.(ed.), University of Minnesota Press, Minneapolis, 71-111; Glacial snowline lowering in the western United States.

- Schubert, C., **1984**, Erdwissenschaftliche Forschung, 18, 269-278; Glaciation of the Venezuelan Andes.
- Calhoun, E.A., **1985**, *Quaternary Research*, 24, 39-59; Glacial snowline lowering in Tasmania.
- Nelson, C.S., Hendy, C.H., Jarrett, G.R., and Cuthbertson, A.M., **1985**, *Nature*, 318, 361-363; Correlation of New Zealand alpine glaciation with the northern hemisphere ice-cap chronology, based on measurements from a single deep sea core.
- Rind, D. and Peteet, D., **1985**, *Quaternary Research*, 24, 1-22; A summary of evidence for snowline lowering and vegetation changes for tropical mountains.
- Clapperton, C.M., **1987**, In: Gardiner, V., (ed.), *International Geomorphology 1986 Part II*, J. Wiley & sons, 843-870; Glacial snowline lowering in the Ecuadorian Andes.
- Schlüchter, C., **1988**, *Bull. de l'Association française pour l'étude du Quaternaire*, 141-145; The chronology for the deglaciation of the Swiss Alps.
- Broecker, W.S. and Denton, G.H., **1990**, *Quaternary Science Reviews*, 9, 305-341; Implications of a global snowline lowering during glacial time to glacial theory.
- Schubert, C. and Clapperton, C.M., **1990**, *Quaternary Science Reviews*, 9, 123-135; Glaciation of the northern Andes.
- Kuhle, M., **1991**, *GeoJournal*, 25, 133-231; Snowline lowering in high Asia.
- Rodbell, D.T., **1992**, *Boreas*, 21, 43-52; Snowline lowering in the Peruvian Andes.
- Espizua, L.D., **1993**, *Quaternary Research*, 40, 150-162, Quaternary glaciations in the Rio Mendoza Valley, Argentine Andes.
- Denton, G.H. and Hendy, C.H., **1994**, *Science*, 264, 1434-1437; Documentation of a Younger Dryas glacial advance in the New Zealand Alps.
- Thompson, L.G. et al., **1995**, *Science*, 269, 46-50, Late glacial stage and Holocene tropical ice core records from Huascarán, Peru.
- Thompson, L.G. et al., **1998**, *Science*, 282, 1858-1864, A 25,000-year tropical climate history from Bolivian ice cores.
- Greene, A.M., Broecker, W.S., and Rind, D., **1999**, *Geophysical Research Letters*, 26, 1909-1912, Swiss glacier recession since the Little Ice Age: Reconciliation with climate records.
- Maisch, M.A. et al., in press **1999**, NFP 31-Teilprojekt Nr. 4031-033412, Universität Zürich, vdf Hochschulverlag AG, ETH Zürich, 385 pp., *Die Gletscher der Schweizer Alpen*.
- Kaser, G., **1999**, *Global and Planetary Change*, 22, 93-103, A review of the modern fluctuations of tropical glaciers.

Orvis, K.H., and Horn, S.P., **2000**, *Quaternary Research*, 54, 24-37, Quaternary glaciers and climate on Cerro Chirripó, Costa Rica.

Rodbell, D.T., and Seltzer, G.O., **2000**, *Quaternary Research*, 54, 328-338, Rapid ice margin fluctuations during the Younger Dryas in the Tropical Andes.

Strelin, J.A., and Malagnino, **2000**, *Quaternary Research*, 54, 339-347, Late-glacial history of Lago Argentino, Argentina, and age of the Puerto Bandera Moraines.

Barrows, T.T., Stone, J.O., Fiffield, L.K., and Cresswell, R.G., **2001**, *Quaternary Research*, 55, 179-189, Late Pleistocene glaciation of the Kosciuszko Massif, Snowy Mountains, Australia.

Bischoff, J.L., and Cummins, K., **2001**, *Quaternary Research*, 55, 14-24, Wisconsin glaciation of the Sierra Nevada (79,000-15,000 yr. BP.) as recorded by rock flour in sediments of Owens Lake, California.

Porter, S.C., in press **2001**, *Quaternary Science Reviews* 20-10, Snowline depression in the tropics during the last glaciation.

2) Dust and loess

Broecker, W.S., Turekian, K.K., and Heezen, B.C., **1958**, *American Journal of Science*, 256, 503-517; Glacial to interglacial change in the accumulation rate of silicate material off the bulge of Africa.

Kukla, J., **1961**, *Vestnik Ustredniho Ustavu Geologickeho*, 36, 369-372; The lithology of Central European loess.

Liu, T.S. and Chang, T.H., **1962**, *Acta Geologica Sinica*, 42, 1-14; The Huangtu loess in China.

Folger, D.W., **1970**, *Deep-Sea Research*, 17, 337-352; The wind transport of land derived debris into the North Atlantic.

Kukla, J., **1970**, *Geologiska Foereningens Stockholm Foerhandlingar*, 92, 148-180; The correlation between the record in European loess and that in the deep sea.

Hays, J.D. and Perruzza, A., **1972**, *Quaternary Research*, 2, 355-362; The accumulation rate of wind blown sediment off the bulge of Africa.

Parmenter, C., and Folger, D.W., **1974**, *Science*, 185, 695-698; Eolian biogenic detritus in equatorial Atlantic deep sea sediments.

Kukla, G., **1975**, In: Butzer, K.W. and Isaac, G.L., eds., *After the Australopithecines*, Mouton Publishers, The Hague, 99-188; Loess stratigraphy of Central Europe.

Kukla, G., **1977**, *Earth Science Reviews*, 13, 307-374; Correlation of the European loess record with the oxygen isotope record for deep sea sediments.

Fink, J. and Kukla, G.J., **1977**, *Quaternary Research*, 7, 363-371; European interglacials as read from the soils in Central European loess.

Hammer, C.U., **1977**, *Symposium Isotopes et impuretés dans les neiges et glaces. Actes du colloque de Grenoble, août/Septembre 1975*, (IAHS-AISH Publication No. 118), 365-370; Continental dust in Greenland ice.

Thompson, L.G., **1977**, *International Symposium on Isotopes and Impurities in Snow and Ice*, IAHS Publication 118, 351-364; Concentration, particle size, and particle composition of dust in the Camp Century Greenland ice core.

Kukla, G., **1978**, *Transactions of the Nebraska Academy of Sciences*, VI, 57-93; The classification of European glacial stages.

Hammer, C.U., Clausen, H.B., Dansgaard, W., Gundestrup, N., Johnsen, S.J., and Reeh, N., **1978**, Continental dust in Greenland ice.

Thompson, L.G., Mosley-Thompson, E., Petit, J.R., **1981**, *International Association of Hydrological Sciences Publication 131* (Symposium at Canberra 1979 - Sea level, ice and climatic change), 227-234; Particulate matter in the Dome C Antarctica ice core.

Petit, J.-R., Briat, M., and Royer, A., **1981**, *Nature*, 293, 391-394; Aluminum and microparticle record for the Dome C Antarctica ice core.

Briat, M., Royer, A., Petit, J.R., and Lorius, C., **1982**, *Annals of Glaciology* 3, 27-31. Mineralogy of the dust in Antarctic ice cores.

Heller, F. and Liu, T.S., **1982**, *Nature*, 300, 431-433; Magnetostratigraphy of the Chinese loess.

Burbanks, E.W. and Li, J.J., **1985**, *Nature*, 316, 429-431; Paleoclimatic significance of Chinese loess.

Kukla, G., **1987**, *Quaternary Science Review*, 6, 191-219; Loess stratigraphy of Central China.

Kukla, G., Heller, F., Ming, L.X., Chun, X.T., Sheng, L.T., and Sheng, A.Z., **1988**, *Geology*, 16, 811-814; Magnetic susceptibility as an indicator of dust accumulation rates in Chinese loess.

Harvey, L.D.D., **1988**, *Nature*, 334, 333-335, Climatic impact of ice-age aerosols.

Ram, M., Gayley, R.I., and Petit, J.-R., **1988**, *Journal of Geophysical Research*, 93, 8378-8382; Particle size record for dust grains in the Dome C Antarctica ice core.

Gaudichet, A., De Angelis, M., Lefevre, R., Petit, J.R., Korotkevitch, Y.S., and Petrov, V.N., **1988**, *Geophysical Research Letters*, 15, 1471-1474; Mineralogy of Antarctic ice core dust.

Tiedemann, R., Sarnthein, M., and Stein, R., **1989**, In: Ruddiman, W., Sarnthein, M., et al., *Proceedings of the Ocean Drilling Program, Scientific Results*, 108, 241-277; Long term history of Saharan dust as read from ODP cores off Africa.

Petit, J.R., Mounier, L., Jouzel, J., Korotkevitch, Y.S., Kotlyakov, V.I., and Lorius, C., **1990**, *Nature*, 343, 56-58; 160,000 year long dust record in the Vostok Antarctica ice core.

Sirocko, F., and Lange, H., **1991**, *Marine Geology*, 97, 105-119, Clay-mineral accumulation rates in the Arabian Sea during the late Quaternary.

Grousset, F.E., Biscaye, P.E., Revel, M., Petit, J.-R., Pye, K., Joussaume, S., and Jouzel, J., **1992**, *Earth and Planetary Science Letters*, 111, 175-182; Use of Nd and Sr isotope signatures to demonstrate that Patagonia is the source of glacial age dust in Antarctic ice.

Taylor, K.C., Lamorey, G.W., Doyle, G.A., Alley, R.B., Grootes, P.M., Mayewski, P.A., White, J.W.C., Barlow, L.K., **1993**, *Nature*, 361, 432-436; The electrical conductivity record for the GISP II ice core.

Taylor, K.C., Hammer, C.U., Alley, R.B., Clausen, H.B., Dahl-Jensen, D., Gow, A.J., Gundestrup, N.S., Kipfstuhl, J., Moore, J.C., and Waddington, E.D., **1993**, *Nature*, 377, 540-552; Comparison of the electrical conductivity records in the GISP2 and GRIP ice cores.

Mayewski, P.A., Meeker, L.D., Whitlow, S., Twickler, M.S., Morrison, M.C., Alley, R.B., Bloomfield, P., and Taylor, K., **1993**, *Science*, 261, 195-197; The calcium record in the GISP 2 ice core.

Zhisheng, A. et al., **1993**, *Quaternary Research*, 39, 45-54, Episode of strengthened summer monsoon climate of Younger Dryas age on the Loess Plateau of Central China.

Mayewski, P.A., Meeker, L.D., Whitlow, S., Twickler, M.S., Morrison, M.C., Bloomfield, P., Bond, G.C., Alley, R.B., Gow, A.J., Grootes, P.M., Meese, D.A., Ram, M., Taylor, K.C., and Wumkes, **1994**, *Science*, 263, 1747-1751; The dust and sea salt record in the GISP 2 ice core

Ram, M. and Gayley, R.I., **1994**, *Geophysical Research Letters*, 21, 437-440; The particle content record in Greenland ice.

Rea, D.K., **1994**, *Reviews of Geophysics*, 32, 159-195, The paleoclimatic record provided by Eolian deposition in the deep sea: The geologic history of wind.

Bloemendal, J., Liu, X.M. and Rolph, T.C., **1995**, *Earth and Planetary Science Letters*, 131, 371-380, Correlation of the magnetic susceptibility stratigraphy of Chinese loess and the marine oxygen isotope record: chronological and palaeoclimatic implications.

Xiao, J. et al., **1995**, *Quaternary Research*, 43, 22-29, Grain size of quartz as an indicator of winter monsoon strength of the Loess Plateau of Central China during the last 130,000 yr.

Yung, Y.L. et al., **1996**, *Science*, 271, 962-963, Dust: A diagnostic of the hydrologic cycle during the last glacial maximum.

Biscaye, P.E. et al., **1997**, *Journal of Geophysical Research*, 102, 26,765-26,781, Asian provenance of glacial dust (stage 2) in the Greenland ice Sheet Project 2 Ice Core, Summit, Greenland.

De Angelis, M. et al., **1997**, *Journal of Geophysical Research*, 102, 26,681-26,698, Primary aerosol (sea salt and soil dust) deposited in Greenland ice during the last climatic cycle: Comparison with east Antarctic records.

Mayewski, P.A. et al., **1997**, *Journal of Geophysical Research*, 102, 26,345-26,366, Major features and forcing of high-latitude northern hemisphere atmospheric circulation using a 110,000-year-long glaciochemical series.

Jickells, T.D. et al., **1998**, *Global Biogeochemical Cycles*, 12, 311-320, Air-borne dust fluxes to a deep water sediment trap in the Sargasso Sea.

Hesse, P.O., and McTainsh, G.H., **1999**, *Quaternary Research*, 52, 343-349, Last glacial maximum to early Holocene wind strength in the mid latitudes of the Southern Hemisphere from Aeolian dust in the Tasman Sea.

Oba, T., and Pedersen, T.F., **1999**, *Paleoceanography*, 14, 34-41, Paleoclimatic significance of eolian carbonates supplied to the Japan Sea during the last glacial maximum.

Tegen, I., and Rind, D., **2000**, *Journal of Geophysical Research*, 105, 7199-7212, Influence of the latitudinal temperature gradient on soil dust concentration and deposition in Greenland.

Broecker, W.S., **2001**, 12th Symposium on Global Change Climate Variations, 14-19 January 2001, Albuquerque, NM, by AMS, Boston, MA, 175-176, A dusty past.

Mason, J.A., **2001**, *Quaternary Research*, 56, 79-86, Transport direction of Peoria Loess in Nebraska and implications of loess sources on the Central Great Plains.

3) Closed basin lakes

Russell, I.C., **1885**, *U.S. Geological Survey Monograph*, 11, 287p; The geologic history of Lake Lahontan.

Russell, I.C., **1889**, *U.S. Geological Survey 8th Annual Report*, 261-394; The geological history of Mono Lake.

Gilbert, G.K., **1890**, *U.S. Geological Survey Monograph 1*, 375p; The geologic history of Lake Bonneville.

Gale, H.S., **1914**, *U.S. Geological Survey Bulletin*, 580-L, 251; Stratigraphy of saline deposits in the California desert.

Broecker, W.S. and Orr, P.C., **1958**, *Geological Society of America Bulletin*, 69, 1009-1032; The radiocarbon chronology of Lake Lahontan and Bonneville shorelines.

Flint, R.F. and Gale, W.A., **1958**, *American Journal of Science*, 256, 689-714; Radiocarbon stratigraphy of dry Searles Lake California.

Eardley, A.J. and Gvosdetsky, V., **1960**, *Geological Society of America Bulletin*, 71, 1323-1344; Pluvial record from Great Salt Lake, Utah.

Broecker, W.S. and Kaufman, A., **1965**, *Geological Society of America Bulletin*, 76, 537-566; The radiocarbon chronology for Lakes Lahontan and Bonneville.

Kaufman, A., **1971**, *Geochimica et Cosmochimica Acta*, 35, 1269-1281; Uranium series dating of Dead Sea basin carbonates.

Butzer, K.W., Isaac, G.L., Richardson, J.L., Washbourn-Kamau, C., **1972**, *Science*, 175, 1069-1076; Pluvial record from East African Lake levels.

Neev, D. and Hall, J.K., **1977**, In: Greer, D.C., ed., *Desertic Terminal Lakes*, 53-60; Pluvial record from the Dead Sea.

Street, F.A. and Grove, A.T., **1979**, *Quaternary Research*, 12, 83-118; Global summary of the pluvial record from lakes.

Stuiver, M. and Smith, G.I., **1979**, In: Smith, G.I., ed., *Subsurface Stratigraphy and Geochemistry of Late Quaternary Evaporites, Searles Lake, California, U.S. Geological Survey Professional Paper 1043*, 68-75; Pluvial record from Searles Lake, California.

Smith, G.I., **1984**, *Quaternary Research*, 22, 1-17; Pluvial record from Searles Lake, California.

Gillespie, R., Street-Perrott, F., and Switsur, R., **1984**, *Nature*, 306, 680-683; Pluvial record from Ethiopian Lake levels.

Bischoff, J.L., Rosenbauer, R.J., Smith, G.I., **1985**, *Science*, 227, 1222-1224; Uranium series dating of sediments from Searles Lake.

Currey, D.R. and Oviatt, C.G., **1985**, In: Kay, P.A. and Diaz, H.F., eds., *Problems and Prospects for Predicting Great Salt Lake Levels: Proceedings of a Conference*, Salt Lake City, 1985, University of Utah, 9-24; The pluvial history of Lake Bonneville.

Thompson, R.S., Benson, L., and Hattori, E.M., **1986**, *Quaternary Research*, 25, 1-9; A lower limit on the time of the desiccation of Lake Lahontan.

Benson, L.V. and Thompson, R.S., **1987**, *Quaternary Research*, 28, 69-85; The radiocarbon chronology for Lake Lahontan.

Lao, Y. and Benson, L., **1988**, *Quaternary Research*, 30, 165-176; Uranium series dating of Lake Lahontan shoreline carbonates.

Winograd, I.J., Szabo, B.J., Coplen, T.B., and Riggs, A.C., **1988**, *Science*, 242, 1275-1280; The oxygen isotope record for the Devil's Hole calcite vein.

Benson, L.V. and Paillet, F.L., **1989**, *Quaternary Research*, 32, 262-275; The relationship between lake level and area for Lake Lahontan.

Benson, L.V., Currey, D.R., Dorn, R.I., Lajoie, Oviatt, C.G., Robinson, S.W., Smith, G.I., and Stine, S., **1990**, *Palaeogeography, Palaeoclimatology, Palaeoecology*, 78, 241-286; Comparison of the pluvial histories of four closed basin lakes in the Great Basin.

Hostetler, S. and Benson, L.V., **1990**, *Climate Dynamics*, 4, 207-217; Paleoclimatic implications of the high stand of Lake Lahontan.

Oviatt, C.G., Currey, D.R., and Miller, D.M., **1990**, *Quaternary Research*, 33, 291-305; The pluvial history of Lake Bonneville.

Stine, S. and Stine, M., **1990**, *Nature*, 345, 705-708; Pluvial history of Lago Cardiel at 49°S in the Patagonian desert.

Benson, L.V., **1991**, *Journal of Paleolimnology*, 5, 115-126; Dating of the last high stand of Lake Lahontan.

Allen, B.D., and Anderson, R.Y., **1993**, *Science*, 260, 1920-1923, Evidence from western North America for rapid shifts in climate during the last glacial maximum.

Anderson, R.S., **1993**, *Quaternary Research*, 40, 351-359; Vegetation history of Potato Lake in Central Arizona.

Benson, L., **1993**, *Quaternary Research*, 39, 163-174; Timing of the last high stand of Lake Lahontan.

- Roberts, N., Taleb, M., Barker, P., Damnatl, B., Icole, M., and Williamson, D., **1993**, *Nature*, 366, 146-148; Evidence for a Younger Dryas influence on the lake levels in East Africa.
- Benson, L., **1994**, *Palaeogeography, Palaeoclimatology, Palaeoecology*, 109, 55-87; The tufas of Lake Lahontan.
- Coplen, T.B., Winograd, I.J., Landwehr, J.M., and Riggs, A.C., **1994**, *Science*, 263, 361-365; Water table fluctuations in Devil's Hole.
- Phillips, F.M., Campbell, A.R., Smith, G.I., and Bischoff, J.L., **1994**, *Geology*, 22, 1115-1118; The relationship between the timing of fluctuation in Searles Lake with Dansgaard-Oeschger events in Greenland.
- Szabo, B.J., Kolesar, P.T., Riggs, A.C., Winograd, I.J., and Ludwig, K.R., **1994**, *Quaternary Research*, 41, 59-69; Water table fluctuations in Devil's Hole.
- Rhode, D., and Madsen, D.B., **1995**, *Quaternary Research*, 44, 246-256, Late Wisconsin/early Holocene vegetation in the Bonneville Basin.
- Benson, L.V. et al., **1996**, *Science*, 274, 746-749, Climatic and hydrologic oscillations in the Owens Lake Basin and adjacent Sierra Nevada, California.
- Johnson, T.C. et al., **1996**, *Science*, 273, 1091-1093, Late Pleistocene desiccation of Lake Victoria and rapid evolution of Cichlid fishes.
- Li, J. et al., **1996**, *Palaeogeography, Palaeoclimatology, Palaeoecology*, 123, 179-203, A 100 ka record of water tables and paleoclimates from salt cores, Death Valley, California.
- Lin, J.C. et al., **1996**, *Geochimica et Cosmochimica Acta*, 60, 2817-2832, New $^{230}\text{Th}/\text{U}$ and ^{14}C ages from Lake Lahontan carbonates, Nevada, USA, and a discussion of the origin of initial thorium.
- Szabo, B.J., Bush, C.A., and Benson, L.V., **1996**, *Quaternary Research*, 45, 271-281, Uranium-series dating of carbonate (tufa) deposits associated with Quaternary fluctuations of Pyramid Lake, Nevada.
- Bischoff, J.L. et al., **1997**, *Quaternary Research*, 48, 313-325, Climatic oscillations 10,000-155,000 yr. B.P. at Owens Lake, California reflected in glacial rock flour abundance and Lake Salinity in Core OL-92.
- Menking, K.M. et al., **1997**, *Quaternary Research*, 48, 58-68, Climatic/hydrologic oscillations since 155,000 yr. B.P. at Owens Lake, California, reflected in abundance and stable isotope composition of sediment carbonate.
- Stein, M. et al., **1997**, *Geochimica et Cosmochimica Acta*, 61, 3975-3992, Strontium isotopic, chemical and sedimentological evidence for the evolution of Lake Lisan and the Dead Sea.
- Benson, L.V. et al., **1998**, *Quaternary Research*, 50, 113-127, Continuous lake-sediment records of glaciation in the Sierra Nevada between 52,600 and 12,500 ^{14}C yr. B.P.

- Benson, L.V. et al., **1998**, *Quaternary Research*, 49, 1-10, Correlation of late-Pleistocene lake-level oscillations in Mono Lake, California, with North Atlantic climate events.
- Broecker, W.S. et al., **1998**, *Quaternary Research*, 50, 12-20, Antiphasing between rainfall in Africa's rift valley and North America's Great Basin.
- Caballero, M. and Guerrero, B.O., **1998**, *Quaternary Research*, 50, 69-79, Lake levels since about 40,000 years ago at Lake Chalco, near Mexico City.
- Ku, T.-L. et al., **1998**, *Quaternary Research*, 50, 261-275, U-series chronology of Lacustrine deposits in Death Valley, California.
- Lin, J.C. et al., **1998**, *Quaternary Research*, 59, 11-23, A reassessment of U-Th and ^{14}C ages for late-glacial high-frequency hydrological events at Searles Lake, California.
- Lowenstein, T.K. Li, J., and Brown, C.B., **1998**, *Chemical Geology*, 150, 223-245, Paleotemperatures from fluid inclusions in halite: Method verification and a 100,000 year paleotemperature record, Death Valley, CA.
- Quade, J. et al., **1998**, *Quaternary Research*, 49, 129-148, Black mats, spring-fed streams, and late-glacial-age recharge in the Southern Great Basin.
- Hodell, D.A. et al., **1999**, *Quaternary Research*, 52, 369-380, Paleoclimate of Southwestern China for the past 50,000 yr. inferred from lake Sediment records.
- Lowenstein, T.K. et al., **1999**, *Geology*, 27, 3-6, 200 k.y. paleoclimate record from Death Valley salt core.
- Oviatt, C.G. et al., **1999**, *Quaternary Research*, 52, 180-184, Reinterpretation of the Burmester core, Bonneville Basin, Utah.
- Schramm, A., Stein, M., and Goldstein, S.L., **2000**, *Earth and Planetary Science Letters*, 175, 27-40, Calibration of the ^{14}C time scale to >40 ka by ^{234}U - ^{230}Th dating of Lake Lisan sediments (last glacial Dead Sea).
- Betancourt, J.L. et al., **2000**, *Science*, 389, 1542-1546, A 22,000-year record of monsoonal precipitation from Northern Chile's Atacama Desert.
- Prokopenko, A.A. et al., **2001**, *Quaternary International*, 80-81, 59-68, The detailed record of climatic events during the past 75,000 yrs. B.P. from the Lake Baikal drill core BDP-93-2.
- Prokopenko, A.A. et al., **2001**, *Quaternary Research*, 55, 123-132, Biogenic silica record of the Lake Baikal response to climatic forcing during the Brunhes.
- Johnson, T.C. et al., **2002**, *Science*, 296, 113-132, A high-resolution paleoclimate record spanning the past 25,000 years in southern east Africa.

4) Rock varnish

Potter, R.M. and Rossman, G.R., **1979**, *Chemical Geology*, 25, 79-94, The manganese-

and iron-oxide mineralogy of desert varnish.

Raymond Jr., R., Reneau, S.L., and Harrington, C.D., **1991**, *Scanning Microscopy*, 5, 37-46, Elemental relationships in rock varnish as seen with scanning electron microscopy and energy dispersive x-ray elemental line profiling.

Reneau, S.L., Hagan, R.C., Harrington, C.D., and Raymond Jr., R., **1991**, *Scanning Microscopy*, 5, 47-54, Scanning electron microscopic analysis of rock varnish chemistry for cation-ratio dating: An examination of electron beam penetration depths.

Reneau, S.L., Raymond Jr., R., and Harrington, C.D., **1992**, *American Journal of Science*, 191, 684-723, Elemental relationships in rock varnish stratigraphic layers, Cima Volcanic Field, California: Implications for varnish development and the interpretation of varnish chemistry.

Reneau, S.L., **1993**, *Quaternary Research*, 40, 309-317, Manganese accumulation in rock varnish on a desert piedmont, Mojave Desert, California, and application to evaluation varnish development.

Fleisher, M., Liu, T., Broecker, W.S. and Moore, W., **1999**, *Geophysical Research Letters*, 26, 103-106, A clue regarding the origin of rock varnish.

Liu, T. and Broecker, W.S., **2000**, *Geology*, 28, 183-186, How fast does rock varnish grow?

Liu, T., Broecker, W.S., Bell, J.W., and Mandeville, C.W., **2000**, *Palaeogeography, Palaeoclimatology, Palaeoecology*, 16, 423-433, Terminal Pleistocene wet event recorded in rock varnish from Las Vegas Valley, southern Nevada.

Broecker, W.S. and Liu, T., **2001**, *GSA Today*, 11, 4-10, Rock varnish: Recorder of desert wetness.

Moore, W., Liu, T., Broecker, W.S., and Wright, A., **2001**, *Geophysical Research Letters*, 28, 4475-4478, Factors influencing ^{7}Be accumulation on rock varnish.

5) Ice volume and sea level

Ku, T.-L., **1968**, *Journal of Geophysical Research*, 73, 2271-2276, Protactinium 231 method of dating coral from Barbados Island.

Mesolella, K.J. et al., **1969**, *Journal of Geology*, 77, 250-274, The astronomical theory of climatic change: Barbados data.

Matthews, R.K., **1973**, *Journal of Quaternary Research*, 3, 147-153, Relative elevation of late Pleistocene high sea level stands: Barbados uplift rates and their implications.

Bloom, A.L. et al., **1974**, *Quaternary Research*, 4, 185-205, Quaternary sea level fluctuations on a tectonic coast: New $^{230}\text{Th}/^{234}\text{U}$ dates from the Huon Peninsula, New Guinea.

Denton, G.H., and Hughes, T.J., **1981**, *The last Great Ice Sheets*, 484 pp., John Wiley and Sons, New York.

- Pickett, J.W. et al., **1985**, *Quaternary Research*, 24, 103-114, Evidence of high sea level during isotope stage 5c in Queensland, Australia.
- Somayajulu, B.L.K., Broecker, W.S., and Goddard, J., **1985**, *Quaternary Research*, 24, 235-239, Dating Indian corals by U-decay-series methods.
- Chappell, J., and Shackleton, N.J., **1986**, *Nature*, 324, 137-140, Oxygen isotopes and sea level.
- Edwards, R.L. et al., **1987**, *Science*, 236, 1547-1553, Precise timing of the last interglacial period from mass spectrometric determination of thorium-230 in corals.
- Nakada, M., and Lambeck, K., **1988**, *Nature*, 333, 36-40, The melting history of the late Pleistocene Antarctic ice sheet.
- Fairbanks, R.G., **1989**, *Nature*, 342, 637-642, A 17,000-year glacio-eustatic sea level record: Influence of glacial melting rates on the Younger Dryas event and deep-ocean circulation.
- Pickett, J.W. et al., **1989**, *Quaternary Research*, 31, 392-395, A review of age determinations on Pleistocene corals in Eastern Australia.
- Bard, E., Hamelin, B., and Fairbanks, R.G., **1990**, *Nature*, 346, 456-458, U/Th ages obtained by mass spectrometry in corals from Barbados: Sea level during the past 130,000 years.
- Ku, T.-L., Ivanovich, M., and Luo, S., **1990**, *Quaternary Research*, 33, 129-147, U-series dating of last interglacial high sea stands: Barbados revisited.
- Schrag, D.P., and DePaolo, D.J., **1993**, *Paleoceanography*, 8, 1-6, Determination of $\delta^{18}\text{O}$ of seawater in the deep ocean during the last glacial maximum.
- Stein, M. et al., **1993**, *Geochimica et Cosmochimica Acta*, 57, 2541-2554, TIMS U-series dating and stable isotopes of the last interglacial event in Papua New Guinea.
- Peltier, W.R., **1994**, *Science*, 265, 195-201, Ice age paleotopography.
- Stirling, C.H. et al., **1995**, *Earth and Planetary Science Letters*, 135, 115-130, High-precision U-series dating of corals from Western Australia and implications for the timing and duration of the last interglacial.
- Bard, E. et al., **1996**, *Nature*, 382, 241-244, Deglacial sea-level record from Tahiti corals and the timing of global meltwater discharge.
- Chappell, J. et al., **1996**, *Earth and Planetary Science letters*, 141, 227-236, Reconciliation of late Quaternary sea levels derived from coral terraces at Huon Peninsula with deep sea oxygen isotope records.
- Schrag, D.P., Hampton, G., and Murray, D.W., **1996**, *Science*, 272, 1930-1932, Pore fluid constraints on the temperature and oxygen isotopic composition of the glacial ocean.

Slowey, N.C., Henderson, G.M., and Curry, W.B., **1996**, *Nature*, 383, 242-244, Direct U-Th dating of marine sediments from the two most recent interglacial periods.

Edwards, R.L. et al., **1997**, *Science*, 276, 782-786, Protactinium -231 dating of carbonates by thermal ionization mass spectrometry: Implications for Quaternary climate change.

Peltier, W.R., **1998**, *Reviews Geophysics*, 36, 603-689, Postglacial variations in the level of the sea: Implications for climate dynamics and solid Earth geophysics.

Esat, T.M. et al., **1999**, *Science*, 283, 197-201, Rapid fluctuations in sea level recorded at Huon Peninsula during the penultimate deglaciation.

Hanebuth, T., Stattegger, K. and Grootes, P.M., **2000**, *Science*, 288, 1033-1035, Rapid flooding of the Sunda Shelf: A late-glacial sea-level record.

Guilderson, T.P. et al., **2000**, *G³*, 1, 2000GC00098, Late Pleistocene sea level variations derived from the Argentine Shelf.

Henderson, G.M., and Slowey, N.C., **2000**, *Nature*, 404, 61-66, Evidence from U-Th dating against Northern Hemisphere forcing of the penultimate deglaciation.

Yokoyama, Y. et al., **2000**, *Nature*, 406, 713-716, Timing of the Last Glacial Maximum from observed sea-level minima.

Cabioch, G., and Ayliffe, L.K., **2001**, *Quaternary Research*, 56, 357-365, Raised coral terraces at Malakula, Vanuatu, Southwest Pacific, indicate high sea level during marine isotope stage 3.

Lambeck, K., and Chappell, J., **2001**, *Science*, 292, 679-686, sea level change through the last glacial cycle.

Gallup, C.D. et al., **2002**, *Science*, 295, 310-313, Direct determination of the timing of sea level change during Termination II.

Schrag, D.P. et al., **2002**, *Quaternary Science Reviews*, 21, 331-342, The oxygen isotopic composition of seawater during the Last Glacial Maximum.

6) Stable isotopes in ice

Dansgaard, W., **1953**, *Tellus*, 5, 461-469; Oxygen isotopes in rain and water vapor.

Friedman, I., **1953**, *Geochimica et Cosmochimica Acta*, 4, 89-103; Deuterium content of natural waters.

Epstein, S. and Mayeda, T., **1953**, *Geochimica et Cosmochimica Acta*, 4, 213-224; Oxygen isotopes in natural waters.

Dansgaard, W., **1954**, *Geochimica et Cosmochimica Acta*, 6, 241-260; Oxygen isotopes in fresh water.

Epstein, S., **1956**, *National Academy of Science, Nuclear Science Series*, Report No. 19, 20-25; Oxygen isotopes in fresh water and ice.

Gonfiantini, R. and Picciotto, E., **1959**, *Nature*, 184, 1557-1558; Oxygen isotopes in Antarctic snow.

Picciotto, E., De Maere, X., and Friedman, I., **1960**, *Nature*, 187, 857-859; Temperature dependence of the isotopic composition of Antarctic snows.

Craig, H., **1961**, *Science*, 133, 1702-1703; Isotopic variations in meteoric waters.

Lorius, C., **1961**, *Ann. de Geophys.*, 17, 378-387; Deuterium in Antarctic snow.

Dansgaard, W., **1961**, *Medd. om Gronland*, 165, 1-120; Oxygen isotope variations in natural waters.

Gonfiantini, W., Togliatti, V., Tongiorgi, E. De Breuck, W., and Picciotto, E., **1963**, *Journal of Geophysical Research*, 68, 3791-3798; Oxygen isotope changes with season in Antarctic snow.

Ehhalt, D., Knot, K., Nagel, J.F., and Vogel, J.C., **1963**, *Journal of Geophysical Research*, 68, 3775-3780; Deuterium and oxygen 18 in precipitation.

Lorius, C., **1963**, *Comité National Francois des Recherches Antarctiques*, 8, 1-102; Deuterium in Antarctic snow.

Dansgaard, W., **1964**, *Tellus*, 16, 437-468; Isotope systematics in high latitude precipitation.

Friedman, I., Redfield, A.C., Schoen, B., and Harris, J., **1964**, *Reviews of Geophysics*, 2, 177-224; Deuterium content of natural waters.

Dansgaard, W. and Tauber, H., **1969**, *Science*, 166, 499; The oxygen isotope record from Camp Century Greenland.

Dansgaard, W., Johnsen, S.J., Møller, J., and Langway, C.C. Jr., **1969**, *Science*, 166, 377; Oxygen isotope record for the Camp Century Greenland ice core.

Epstein, S., Sharp, R.P., and Gow, A.J., **1970**, *Science*, 168, 1570; Stable isotope record for the Bryd Station Antarctica ice core.

Dansgaard, W., Johnsen, S.J., Clausen, H.B., and Langway, C.C., **1971**, In: Turekian, K.K. (ed.), *Late Cenozoic Ice Ages*, 37, Yale University Press; Oxygen isotope

record for the Camp Century Greenland ice core.

Paterson, W.S.B., Koerner, R.M., Fisher, D., Johnsen, S.J., Clausen, H.B., Dansgaard, W., Bucher, P., and Oeschger, H., **1977**, *Nature*, 266, 508-511; Oxygen isotope record for the Devon Ice cap core.

Hammer, C.U., Clausen, H.B., Dansgaard, W., Gundestrup, N., Johnsen, S.J., and Reeh, N., **1978**, *Journal of Glaciology*, 20, 3-26; the use of annual layers to establish the chronology of the ice core ^{18}O record.

Lorius, C., Merlivat, L., Jouzel, J., and Pourchet, M., **1979**, *Nature*, 280, 644-648; Detailed ^{18}O record for the last ~30,000 years from the Dome C Antarctica ice core.

Koerner, R.M., **1979**, *Journal of Glaciology*, 22, 25-41; Oxygen isotope record for cores from the Queen Elizabeth Island ice caps.

Dansgaard, W., Clausen, H.B., Gundestrup, N., Hammer, C.U., Johnsen, S.F., Kristinsdottir, P.M., and Reeh, N., **1982**, *Science*, 218, 1273-1277; Oxygen isotope record for the Dye 3 Greenland ice core.

Jouzel, J., Merlivat, Ll., and Lorius, C., **1982**, *Nature*, 299, 688-691; Evidence for higher glacial atmospheric humidity from the deuterium excess in Antarctic ice.

Lorius, C., Jouzel, J., Ritz, C., Merlivat, L., Barkov, N.I., Korotkevich, Y.S., and Kotlyakov, V.M., **1985**, *Nature*, 316, 591-596; Oxygen isotope record from the Vostok Antarctica ice core.

Dansgaard, W., Clausen, H.B., Gundestrup, N., Johnsen, S.J., and Rygner, C., **1985**, *American Geophysical Union Geophysical Monograph* 33, 71-76; Comparison of the Camp Century and Dye 3 oxygen isotope records.

Jouzel, J., Lorius, C., Petit, J.R., Genthon, C., Barkov, N.I., Kotlyakov, V.M., and Petrov, V.M., **1987**, *Nature*, 329, 403; Stable isotope record for the last 160,000 years in the Vostok Antarctica ice core.

Reeh, N., Thomsen, H.H., and Clausen, H.B., **1987**, *Palaeogeography, Palaeoclimatology, Palaeoecology*, 58, 229-234; Oxygen isotope profiles from ice cap sections exposed on the western margin of Greenland.

Dansgaard, W. and Oeschger, H., **1989**, In: Oeschger, H. and Langway, C.C., Jr. (eds.), *The Environmental Record in Glaciers and Ice Sheets*, John Wiley and Sons, New York, 287-318; Review paper on ice core studies.

Dansgaard, W., White, J.W.C., and Johnsen, S.J., **1989**, *Nature*, 339, 532-534; Evidence from the Dye 3 Greenland ice core in support of a very abrupt end for the Younger Dryas cold episode.

- Jouzel, J., Raisbeck, G., Benoist, J.P., Yiou, F., Lorius, C., Raynaud, D., Petit, J.R., Barkov, N.I., Korotkevitch, Y.S., and Kotlyakov, V.M., **1989**, *Quaternary Research*, 31, 135-150; Comparison of the stable isotope records for the ice cores from Antarctica.
- Thompson, L.G. et al., **1989**, *Science*, 246, 474-477, Holocene-Late Pleistocene climatic ice core records from Qinghai-Tibetan Plateau.
- Reeh, N., Oerter, H., Letréguilly, Miller, H., and Hubberten, H.-W., **1991**, *Palaeogeography, Palaeoclimatology, Palaeoecology*, 90, 373-383; A detailed ^{18}O record for the Pakitsoa outcrop of the Greenland ice cap.
- Sowers, T., Bender, M., Raynaud, D., Korotkevich, Y.S., and Orchardo, J., **1991**, *Paleoceanography*, 6, 679-696; The oxygen isotope record for O_2 from air trapped in the Vostok Antarctica ice core.
- Johnsen, S.J., Clausen, H.B., Dansgaard, W., Fuhrer, K., Gundestrup, N., Hammer, C.U., Iversen, P., Jouzel, J., Stauffer, B., and Steffensen, J.P., **1992**, *Nature*, 359, 311-313.
- Dansgaard, W. et al., **1993**, *Nature*, 364, 218-220, Evidence for general instability of past climate from a 250-kyr. ice-core record.
- Greenland Ice-core Project (GRIP) members, **1993**, *Nature*, 364, 203-207; First report on the complete oxygen isotope and calcium records from the Summit Greenland GRIP ice core.
- Grootes, P.M., Stuiver, M., White, J.W.C., Johnsen, S., and Jouzel, J., **1993**, *Nature*, 366, 1993; Comparison of the oxygen isotope records for the GISP 2 and GRIP ice cores from the Summit located in Greenland.
- Jouzel, J., Barkov, N.I., Barnola, J.M., Bender, M., Chappellaz, J., Genthon, C., Kotlyakov, V.M., Lipenkov, V., Lorius, C., Petit, J.R., Raynaud, D., Raisbeck, G., Ritz, C., Sowers, T., Stievenard, M., Yiou, F., and Yiou, P., **1993**, *Nature*, 364, 407-412; Extension of the Vostok Antarctica ice core record from about 140,000 years ago to about 200,000-years ago.
- Sowers, T., Bender, M., Labeyrie, L., Martinson, D., Jouzel, J., Raynaud, D., Pichon, J.J., and Korotkevich, Y.S., **1993**, *Paleoceanography*, 8, 737-766; Use of the ^{18}O record in O_2 from the air trapped in Vostok ice to correlate the Antarctic and marine climate records.
- Bender, M., Sowers, T., Dickson, M.-L., Orchardo, J., Grootes, P., Mayewski, P.A., and Meese, D.A., **1994**, *Nature*, 372, 663-666; Climate correlations between the Greenland and Antarctica ice core records based on the ^{18}O to ^{16}O ratio in O_2 contained in trapped air.
- Bender, M., Sowers, T., and Labeyrie, L., **1994**, *Global Biogeochemical Cycles*, 8, 363-376; Variation over the last 130,000 years in the ^{18}O to ^{16}O ratio in O_2 contained in the air trapped in Vostok Antarctica ice.
- Charles, C.D., Rind, D., Jouzel, J., Koster, R.D., and Fairbanks, R.G., **1994**, *Science*, 263, 508-511; Use of the GISS atmospheric circulation model to assess the source of

moisture reaching the Greenland ice cap.

Souchez, R. et al., **1994**, *Geophysical Research Letters*, 21, 693-696, Stable isotopes in the basal silty ice preserved in the Greenland ice sheet at Summit; environmental implications.

Jouzel, J. et al., **1995**, *Climate Dynamics*, 11, 151-161, The two-step shape and timing of the last deglaciation in Antarctica.

Stuiver, M., Grootes, P.M., and Braziunas, T.F., **1995**, *Quaternary Research*, 44, 341-354, The GISP2 $\delta^{18}\text{O}$ climate record of the past 16,500 years and the role of the Sun, ocean and volcanoes.

Thompson, L.G. et al., **1995**, *Science*, 269, 46-50, Late glacial stage and Holocene tropical ice core records from Huascarán, Peru.

Yiou, P. et al., **1995**, *Geophysical Research Letters*, 22, 2179-2182, rapid oscillations in Vostok and GRIP ice cores.

Grootes, P.M., and Stuiver, M., **1997**, *Journal of Geophysical Research*, 102, 26,455-26,470, Oxygen 18/16 variability in Greenland snow and ice with 10^{-3} - 10^{-5} -year time resolution.

Johnsen, S.J. et al., **1997**, *Journal of Geophysical Research*, 102, 26,397-26,410, The $\delta^{18}\text{O}$ record along the Greenland ice core project deep ice core and the problem of possible Eemian climatic instability.

Jouzel, J. et al., **1997**, *Journal of Geophysical Research*, 102, 26,471-26,487, Validity of the temperature reconstruction from water isotopes in ice cores.

Stuiver, et al., P.M., **1997**, *Quaternary Research*, 48, 259-266, Is there evidence for solar forcing of climate in the GISP2 oxygen isotope record?

Thompson, L.G. et al., **1997**, *Science*, 276, 1821-1825, Tropical climate instability: The last glacial cycle from a Qinghai-Tibetan ice core.

Steig, E.J. et al., **1998**, *Science*, 282, 92-95, Synchronous climate changes in Antarctica and the North Atlantic.

Thompson, L.G. et al., **1998**, *Science*, 282, 1858-1864, A 25,000-year tropical climate history from Bolivian ice cores.

Henderson, K.A., Thompson, L.G., and Lin P.-N., **1999**, *Journal of Geophysical Research*, 104, 31,053-31,065, Recording of El Niño in ice core $\delta^{18}\text{O}$ records from Nevado Huascarán, Peru.

Stuiver, M., and Grootes, P.M., **2000**, *Quaternary Research*, 53, 277-284, GISP2 oxygen isotope ratios.

Thompson, L.G. et al., **2000**, *Science*, 289, 1916-1919, A high-resolution millennial record of the South Asian monsoon from Himalayan ice cores.

Blunier, T., and Brook, E.J., **2001**, *Science*, 291, 109-112, Timing of millennial-scale climate change in Antarctica and Greenland during the last glacial period.

Grootes, P.M. et al., **2001**, *Quaternary Research*, 56, 289-298, The Taylor Dome Antarctic ^{18}O record and globally synchronous changes in climate.

Jouzel, J. et al., **2001**, *Geophysical Research Letters*, 28, 3199-3202, A new 27 ky high resolution East Antarctic climate record.

7) Carbon dioxide in polar ice

Scholander, P.F., Hemmingsen, E.A., Coachman, L.K., and Nutt, D.C., **1961**, *Journal of Glaciology*, 3, 813-822; The earliest attempt to extract information concerning past atmospheric CO₂ content from ice; it was not successful.

Matsuo, S. and Miyake, Y., **1966**, *Journal of Geophysical Research*, 71, 5235-5241; Another unsuccessful attempt.

Alder, B., Geiss, J., Groegler, N., and Renaud, A., **1969**, *Meddr Grønland*, 177, 100-107; Yet another unsuccessful attempt.

Raynaud, D. and Delmas, R., **1977**, *Isotopes and Impurities in Snow and Ice*, Grenoble 1975, IUGG Meeting, IAHS Publication No. 118, 377-381; Yet another unsuccessful attempt.

Berner, W., Stauffer, B., and Oeschger, H., **1978**, *Nature*, 276, 53-55; Yet another unsuccessful attempt.

Delmas, R.J., Ascencio, J.-M., and Legrand, M., **1980**, *Nature*, 284, 155-157; Successful attempt to obtain information about past atmosphere carbon dioxide contents of air trapped in ice cores.

Berner, W., Oeschger, H., and Stauffer, B., **1980**, *Radiocarbon*, 22, 227-235; Successful attempt to obtain information about past atmospheric carbon dioxide contents from air trapped in ice cores.

Neftel, A., Oeschger, H., Schwander, J., Stauffer, B., and Zumbrunn, R., **1982**, *Nature*, 295, 220-223; First set of measurements clearly demonstrating that the CO₂ content of the atmosphere was about two thirds its 1850 value during the last glacial period.

Stauffer, B., Hofer, H., Oeschger, H., Schwander, J., and Siegenthaler, U., **1984**, *Annals of Glaciology*, 5, 160-164; Discovery of millennial time scale CO₂ changes in the glacial portion of the Dye 3 Greenland ice core record.

Schwander, J. and Stauffer, B., **1984**, *Nature*, 311, 45-47; The closure of air bubbles during the lithification of ice.

Oeschger, H., Stauffer, B., Finkel, R. and Langway, C.C., Jr., **1985**, In: E. Sundquist and W.S. Broecker (eds.), *The Carbon Cycle and Atmospheric CO₂: Natural Variations Archean to Present*, Geophysical Monograph 32, American Geophysical Union, Washington, D.C., 132-142; Review of CO₂ measurements in ice.

Friedli, H., Lotscher, H., Oeschger, H., Siegenthaler, U., and Stauffer, B., **1986**, *Nature*, 324, 237-238; Carbon isotopic composition of CO₂ from polar ice.

Barnola, J.M., Raynaud, D., Korotkevich, Y.S., and Lorius, C., **1987**, *Nature*, 329, 408-414; CO₂ record for the last 160,000 years from the Vostok Antarctica ice core.

Neftel, A., Oeschger, H., Staffelbach, T., and Stauffer, B., **1988**, *Nature*, 331, 609-611; Detailed CO₂ record for the last 50,000 years from the Byrd Station Antarctica ice core.

Staffelbach, T., Stauffer, B., Sigg, A., and Oeschger, H., **1991**, *Tellus*, 43B, 91-96; More CO₂ measurements on ice cores.

Leuenberger, M., Siegenthaler, U., and Langway, C.C., **1992**, *Nature*, 357, 488-490; Carbon isotope ratios in CO₂ from Antarctic ice.

Blunier, T. et al., **1995**, *Nature*, 374, 46-49, Variations in atmospheric methane concentration during the Holocene epoch.

Battle, M. et al., **1996**, *Nature*, 383, 231-235, Atmospheric gas concentrations over the past century measured in air from firn at the South Pole.

Etheridge, D.M. et al., **1996**, *Journal of Geophysical Research*, 101, 4115-4128, Natural and anthropogenic changes in atmospheric CO₂ over the last 1000 years from air in Antarctic ice and firn.

Haan, D., Martinerie, P., and Raynaud, D., **1996**, *Geophysical Research Letters*, 17, 2235-2238, Ice core data of atmospheric carbon monoxide over Antarctica and Greenland during the last 200 years.

Anklin, M. et al., **1997**, *Journal of Geophysical Research*, 102, 26,539-26,545, CO₂ record between 40 and 8 kyr. B.P. from the Greenland Ice Core Project ice core.

Blunier, T. et al., **1997**, *Geophysical Research Letters*, 24, 2683-2686, Timing of the Antarctic Cold Reversal and the atmospheric CO₂ increase with respect to the Younger Dryas event.

Smith, H.J. et al., **1997**, *Geophysical Research Letters*, 24, 1-4, The CO₂ concentration of air trapped in GISP2 ice from the Last Glacial Maximum-Holocene transition.

Blunier, T. et al., **1998**, *Nature*, 394, 739-743, Asynchrony of Antarctic and Greenland climate change during the last glacial period.

Stauffer, B. et al., **1998**, *Nature*, 392, 59-62, Atmospheric CO₂ concentration and millennial-scale climate change during the last glacial period.

Fischer, H. et al., **1999**, *Science*, 283, 1712-1714, Ice core records of atmospheric CO₂ around the last three glacial terminations.

Indermühle, A. et al., **1999**, *Nature*, 398, 121-126, Holocene carbon-cycle dynamics based on CO₂ trapped in ice at Taylor Dome, Antarctica.

Petit, J.R. et al., **1999**, *Nature*, 399, 429-436, Climate and atmospheric history of the past 420,000 years from the Vostok ice core, Antarctica.

Smith, H.J. et al., **1999**, *Nature*, 400, 248-250, Dual modes of the carbon cycle since the Last Glacial Maximum.

Indermühle, A. et al., **2000**, *Geophysical Research Letters*, 27, 735-738, Atmospheric CO₂ concentration from 60 to 20 kyr. B.P. from the Taylor Dome ice core, Antarctica.

Cuffey, K.M., and Vimeux, F., **2001**, *Nature*, 412, 523-526, Covariation of carbon dioxide and temperature from the Vostok ice core after deuterium-excess correction.

Monnin, E. et al., **2001**, *Science*, 291, 112-114, Atmospheric CO₂ concentrations of the last glacial termination.

8) Methane in polar ice

Craig, H. and Chou, C.C., **1982**, *Geophysical Research Letters*, 9, 1221-1224; Measurements on air extracted from ice cores showing that the atmosphere's methane content doubled since 1650 A.D.

Khalil, M.A.K. and Rasmussen, R.A., **1982**, *Chemosphere* 11, 877; Measurements on air extracted from ice cores showing that the atmosphere's methane content doubled over the last 200 years.

Rasmussen, R.A. and Khalil, M.A.K., **1984**, *Journal of Geophysical Research*, 89, 11599; Measurements on air extracted from ice cores showing that the atmosphere's methane content doubled over the last 200 years.

Stauffer, B., Fischer, G., Neftel, A., and Oeschger, H., **1985**, *Science*, 229, 1386-1388; Measurements on air extracted from ice cores showing that the atmosphere's methane content doubled over the last 200 years.

Pearman, G.I., Etheridge, D., de Silva, F., and Fraser, P.J., **1986**, *Nature*, 320, 248-250; Measurements on air extracted from ice cores showing that the atmosphere's methane content doubled over the last 200 years.

Stauffer, B., Lochbronner, E., Oeschger, H., and Schwander, J., **1988**, *Nature*, 332, 812-814; Measurements showing that the methane content of the atmosphere was half as high during glacial time as it was during pre-industrial time.

Raynaud, D., Chappellaz, J., Barnola, J.M., Korotkevich, Y.S., and Lorius, C., **1988**, *Nature*, 333, 655-657; Measurements showing that the methane content of the atmosphere was half as high during glacial time as it was during pre-industrial time.

Chappellaz, J., Barnola, J.M., Raynaud, D., Korotkevich, Y.S., and Lorius, C., **1990**, *Nature*, 345, 127-131; Methane record for the last 160,000 years from the Vostok Antarctica ice core.

Chappellaz, J., Blunier, T., Raynaud, D., Barnola, J.M., Schwander, J., and Stauffer, B., **1993**, *Nature*, 366, 443-445; Atmospheric methane variations correlated with Dansgaard-Oeschger events.

Brook, E.J. Sowers, T., and Orchardo, J., **1996**, *Science*, 273, 1087-1091, Rapid variations in atmospheric methane concentration during the past 110,000 years.

Chappellaz, J. et al., **1997**, *Journal of Geophysical Research*, 102, 26,547-26,557, CH_4 and $\delta^{18}\text{O}$ of O_2 records from Antarctic and Greenland ice: A clue for stratigraphic disturbance in the bottom part of the Greenland Ice Core Project and the Greenland ice Sheet project 2 ice cores.

Severinghaus, J.P. et al., **1998**, *Nature*, 391, 141-146, Timing of abrupt climate change at the end of the Younger Dryas interval from thermally fractionated gases in polar ice.

Brook, E.J. et al., **1999**, In: *Mechanisms of Global Climate Change at Millennial Time Scales*, Geophysical Monograph 112, 165-175, Atmospheric methane and millennial-scale climate change.

Petit, J.R. et al., **1999**, *Nature*, 399, 429-436, Climate and atmospheric history of the past 420,000 years from the Vostok ice core, Antarctica.

Severinghaus, J.P., and Brook, E.J., **1999**, *Science*, 286, 930-934, Abrupt climate change at the end of the last glacial period inferred from trapped air in polar ice.

Brook, E.J. et al., **2000**, *Global Biogeochemical Cycles*, 14, 559-572, On the origin and timing of rapid changes in atmospheric methane during the last glacial period.

Dällenbach, A. et al., **2000**, *Geophysical Research Letters*, 27, 1005-1008, Changes in the atmospheric CH_4 gradient between Greenland and Antarctica during the Last Glacial and the transition to the Holocene.

9) Isotopes of O₂ and N₂ in ice

Craig, H., Horibe, Y., and Sowers, T., **1988**, *Science*, 242, 1675-1678, Gravitational separation of gases and isotopes in polar ice caps.

Sowers, T. et al., **1992**, *Journal of Geophysical Research*, 97, 15,683-15,697, $\delta^{15}\text{N}$ of N₂ in air trapped in polar ice: A tracer of gas transport in the firn and a possible constraint on ice age-gas age differences.

Bender, M. et al., **1994**, *Nature*, 372, 663-666, Climate correlations between Greenland and Antarctica during the past 100,000 years.

Battle, M. et al., **1996**, *Nature*, 383, 231-235, Atmospheric gas concentrations over the past century measured in air from firn at the South Pole.

Severinghaus, J.P. et al., **1998**, *Nature*, 391, 141-146, Timing of abrupt climate change at the end of the Younger Dryas interval from thermally fractionated gases in polar ice.

Severinghaus, J.P., and Brook, E.J., **1999**, *Science*, 286, 930-934, Abrupt climate change at the end of the last glacial period inferred from trapped air in polar ice.

Brook, E.J. et al., **1999**, In: *Mechanisms of Global Climate Change at Millennial Time Scales*, Geophysical Monograph 112, American Geophysical Union, 165-175, Atmospheric methane and millennial-scale climate change.

Brook, E.J. et al., **1999**, *Global Biogeochemical Cycles*, 14, 559-572, On the origin and timing of rapid changes in atmospheric methane during the last glacial period.

Severinghaus, J.P., and Grachev, A., **2001**, *G³*, 2, #2000GC000146, Thermal fractionation of air in polar firn by seasonal temperature gradients.

10) Oxygen isotopes in deep sea sediments

Urey, H.C., **1948**, *Science*, 108, 489-496; First paper putting forth the potential of oxygen isotopes for geothermometry.

McCrea, J.M., **1950**, *Journal of Chemical Physics*, 18, 849-857; Early calibration of the oxygen isotope paleotemperature scale for CaCO₃.

Silverman, S.R., **1951**, *Geochimica et Cosmochimica Acta*, 2, 26-42; Early summary of oxygen isotope applications in geology.

Epstein, S., Buchsbaum, R., Lowenstam, H., and Urey, H.C., **1951**, *Geological Society America Bulletin*, 62, 417-425; Experimental determination of the oxygen isotope temperature scale for CaCO₃.

Urey, H.C., Lowenstam, H.A., Epstein, S., and McKinney, C.R., **1951**, *Geological Society America Bulletin*, 62, 399-416; First paleotemperature estimates based on oxygen isotope measurements on marine shells.

Emiliani, C., **1954**, *American Journal of Science*, 252, 149-158; First use of benthic foraminifera to obtain paleotemperatures for the deep ocean.

Emiliani, C., **1955**, *The Journal of Geology*, 63, 538-577; Classic paper showing for the first time the late Quaternary oxygen isotope cycles in foraminifera shells.

Emiliani, C., **1958**, *Journal of Geology*, 66, 264-275; First late Quaternary ¹⁸O record for a core from outside the tropics.

Shackleton, N.J., **1965**, *Journal of Scientific Instrumentation*, 642, 689-692; Demonstration that precise oxygen isotope measurements could be made on much smaller samples opening the way for detailed measurements on benthic foraminifera.

Emiliani, C., **1966**, *Journal of Geology*, 74, 109-126; A generalized oxygen isotope curve for the last 425,000 years.

Shackleton, N.J., **1967**, *Nature (London)*, 215, 15-17; A new calibration of the oxygen isotope thermometer for marine foraminifera.

Shackleton, N.J., **1967**, *Nature*, 215, 15-17; First demonstration of the true amplitude of the glacial to interglacial change in the oxygen isotope ratios in benthic foraminifera.

Donk, J. van and Mathieu, G., **1969**, *Journal of Geophysical Research*, 74, 3396-3407; Oxygen isotope record for Arctic sediments, last glacial and Holocene.

Broecker, W.S. and van Donk, J., **1970**, *Reviews of Geophysics and Space Physics*, 8, 169-198; A revised time scale for the marine ¹⁸O record for the last 200,000 years and a discussion of the relationship with Milankovitch cycles.

Shackleton, N.J. and Opdyke, N.D., **1973**, *Quaternary Research*, 3, 39-55; Oxygen isotope record back to the last magnetic reversal.

Duplessy, J.C., Chenouard, L., and Vila, F., **1975**, *Science*, 188, 1208-1209; Late Quaternary oxygen isotope record for the Norwegian Sea.

Shackleton, N.J. and Opdyke, N.D., **1976**, *Geological Society of America Memoir 145*,

449-464; Oxygen isotope record for Pacific planktonic foraminifera for the last million years.

Hays, J.D., Lozano, J., Shackleton, N., and Irving, G., **1976**, In: Cline, R.M. and Hays, J.D. (eds.), *Investigation of late Quaternary paleoceanography and paleoclimatology: Geol. Soc. America Mem. 145*; Late Quaternary oxygen isotope record for Antarctic sediments.

Hays, J.D., Imbrie, J., and Shackleton, N.J., **1976**, *Science*, 194, 1121-1132; Classic paper showing that spectral frequencies recovered from deep sea oxygen isotope records match those expected from Milankovitch forcing.

Shackleton, N.J., **1977**, *Philosophical Transactions of Royal Society London*, B280, 169-182; Review paper on oxygen isotope measurements on Quaternary marine foraminifera.

Kellogg, T.B., Duplessy, J.C., and Shackleton, N.J., **1978**, *Boreas*, 7, 61-73; Oxygen isotope record for planktonic foraminifera from the Norwegian Sea.

Duplessy, J.C., **1981**, In: J. Gribben (ed.), *Climatic Change*, Cambridge University Press, New York, 46-67; Review paper on oxygen isotopes in marine sediments.

Duplessy, J.C., **1982**, *Nature (London)*, 295, 494-498; Glacial to interglacial oxygen isotope changes in the northern Indian Ocean.

Shackleton, N.J., Imbrie, J., and Hall, M.A., **1983**, *Earth and Planetary Science Letters*, 65, 233-244; Very detailed oxygen isotope record for benthic foraminifera from the Pacific Ocean for the last 160,000 years

Thunell, R.C. and Williams, D.F., **1983**, *Palaeogeography, Palaeoclimatology, Palaeoecology*, 44, 23-39; Oxygen isotope record for the Mediterranean Sea.

Mix, A.C. and Ruddiman, W.R., **1984**, *Quaternary Research*, 21, 1-20; Oxygen isotopes and ice volume.

Pisias, N.G., Martinson, D.G., Moore, T.C., Jr., Shackleton, N.J., Prell, W., Hays, J., and Boden, G., **1984**, *Marine Geology*, 56, 119-136; High resolution oxygen isotope record for the last 300,000 years.

Broecker, W.S., **1986**, *Quaternary Research*, 26, 121-134; Oxygen isotope constraints on surface ocean temperature.

Labeyrie, L.D., Pichon, J.J., Labracherie, M., Ippolito, P., Duprat, J., and Duplessy, J.C., **1986**, *Nature*, 322, 701-706; Planktonic and benthic oxygen isotope records for the Antarctic covering the last 60,000 years.

Labeyrie, L., Duplessy, J.C., and Blanc, P.L., **1987**, *Nature*, 327, 477-482; Variation in deep water temperatures for the last 125,000 years.

Martinson, D.G., Pisias, N.G., Hays, J.D., Imbrie, J., Moore, T.C., Jr., and Shackleton, N.J., **1987**, *Quaternary Research*, 27, 1-29; Orbitally tuned oxygen isotope chronology for the last 300,000 years.

Shackleton, N.J., **1987**, *Quaternary Science Reviews*, 6, 183-190; Relationship between ice volume and the oxygen isotope record in benthic foraminifera.

Duplessy, J.C. et al., **1993**, *Paleoceanography*, 8, 341-350, Oxygen isotope records and salinity changes in the northeastern Atlantic Ocean during the last 18,000 years.

Nelson, C.S. et al., **1993**, *Paleoceanography*, 8, 435-458, Oceanographic and climatic changes over the past 160,000 years at deep sea drilling project site 594 off southeastern New Zealand, Southwest Pacific Ocean.

Shackleton, N.J. et al., **1993**, *Paleoceanography*, 8, 141-148, High-resolution stable isotope stratigraphy from bulk sediment.

Raymo, M.E., **1994**, *Annual Reviews of Earth Planetary Science*, 22, 353-383, The initiation of Northern Hemisphere glaciation.

Bigg, G.R., **1995**, *Paleoceanography*, 10, 283-290, Aridity of the Mediterranean Sea at the last glacial maximum: A reinterpretation of the $\delta^{18}\text{O}$ record.

Billups, K., and Spero, H.J., **1996**, *Paleoceanography*, 11, 217-238, Reconstructing the stable isotope geochemistry and paleotemperatures of the equatorial Atlantic during the last 150,000 years: Results from individual foraminifera.

Labeyrie, L. et al., **1996**, *Paleoceanography*, 11, 57-76, Hydrographic changes of the Southern Ocean (southeast Indian sector) over the last 230 kyr.

Linsley, B.K., **1996**, *Nature*, 380, 234-237, Oxygen-isotope record of sea level and climate variations in the Sulu Sea over the past 150,000 years.

Spero, H.J., and Lea, D.W., **1996**, *Marine Micropaleontology*, 28, 231-246, Experimental determination of stable isotope variability in *Globigerina bulloides*: implications for paleoceanographic reconstructions.

Stott, L.D., and Tang, C.M., **1996**, *Paleoceanography*, 11, 37-56, Reassessment of foraminifral-based tropical sea surface $\delta^{18}\text{O}$ paleotemperatures.

Martinez, J.I., De Deckker, P., and Chivas, A.R., **1997**, *Marine Micropaleontology*, 32, 311-340, New estimates for salinity changes in the Western Pacific Warm Pool during the Last Glacial Maximum: oxygen-isotope evidence.

Keigwin, L.D., **1998**, *Paleoceanography*, 13, 323-339, Glacial-age hydrography of the far northwest Pacific Ocean.

Schmiedl, G. et al., **1998**, *Paleoceanography*, 13, 447-458, Impact of climatic changes on the benthic foraminiferal fauna in the Ionian Sea during the last 330,000 years.

Vidal, L., Labeyrie, L., and van Weering, T.C.E., **1998**, *Paleoceanography*, 13, 245-251, Benthic $\delta^{18}\text{O}$ records in the North Atlantic over the last glacial period (60-10 kyr): Evidence for brine formation.

Lynch-Stieglitz, J., Curry, W.B., and Slowey, N., **1999**, *Paleoceanography*, 14, 360-373, A geostrophic transport estimate for the Florida current from the oxygen isotope composition of benthic foraminifera.

Lynch-Stieglitz, J., Curry, W.B., and Slowey, N., **1999**, *Nature*, 402, 644-648, Weaker Guf Stream in the Florida Straits during the last Glacial Maximum.

Matsumoto, K., Lynch-Stieglitz, J., and Anderson, R.F., **2001**, *Paleoceanography*, 16, 445-454, Similar glacial and Holocene Southern Ocean hydrography.

11) Carbon isotopes in deep sea sediments

Shackleton, N.J., **1977**, In: Andersen N.R. and Malahoff, A. (eds.), *Fate of Fossil Fuel CO₂ in the Oceans*, Plenum, NY, 401-427; First demonstration of a glacial to interglacial change in deep water $^{13}\text{C}/^{12}\text{C}$ and proposal that it reflected a change in the amount of carbon stored in wood and humus.

Boyle, E.A. and Keigwin, L.D., **1982**, *Science*, 218, 784-787; Deep circulation in the Atlantic over the last 200,000 years.

Shackleton, N.J., Imbrie, J., and Hall, M.A., **1983**, *Earth and Planetary Science Letters*, 65, 233-244; First record clearly showing a change in the surface water - deep water $^{13}\text{C}/^{12}\text{C}$ ratio difference through the last two glacial cycles.

Shackleton, N.J., Hall, M.A., Line, J., and Shuxi, C., **1983**, *Nature*, 306, 319-322; The relationship between the surface to deep ocean $^{13}\text{C}/^{12}\text{C}$ ratio difference and atmospheric CO₂ content.

Duplessy, J.C., Shackleton, N.J., Matthews, R.K., Prell, W., Ruddiman, W.F., Caralp, M., and Hendy, C., **1984**, *Quaternary Research*, 21, 225-243; Distribution of $^{13}\text{C}/^{12}\text{C}$ ratios in the deep sea during the last interglacial.

McCorkle, D.C., Emerson, S.R., and Quay, P.D., **1985**, *Earth and Planetary Science Letters*, 74, 13-26; Carbon isotope ratios in pore water from marine sediments.

Boyle, E. and Keigwin, L.D., **1987**, *Nature*, 330, 35-40; Evidence for the impact of the Younger Dryas event on deep water circulation in the Atlantic.

Oppo., D.W. and Fairbanks, R.G., **1987**, *Earth and Planetary Science Letters*, 86, 1-15; Circulation in the deep Atlantic over the last 25,000 years.

Curry et al., **1988**, *Paleoceanography*, 3, 317-342; The magnitude of the glacial to interglacial $^{13}\text{C}/^{12}\text{C}$ change in the ocean.

Sayles, F.L. and Curry, W.B., **1988**, *Geochimica et Cosmochimica Acta*, 52, 2963-2978; Carbon isotope ratios in pore waters from marine sediments.

Oppo, D.W. and Fairbanks, R.G., **1989**, *Paleoceanography*, v, 333-351; The carbon isotope record for the tropical Atlantic and Caribbean Sea over the last 22,000 years as recorded by planktonic foraminifera.

Charles, C.D. and Fairbanks, R.G., **1990**, In: Bleil, U. and Thiede, J. (eds.), *Geological History of the Polar Oceans: Arctic Versus Antarctic*, Kluwer Academic Publishers, Netherlands, 512-538; Glacial to interglacial ^{13}C change in benthic and planktonic foraminifera from the Southern Ocean.

McCorkle, D.C. and Keigwin, L.D., Corliss, B.H., Emerson, S.R., **1990**, *Paleoceanography*, 5, 161-185; The influence of sediment pore water ΣCO_2 on the carbon isotope composition of benthic foraminifera.

Oppo, D.W. and Fairbanks, R.G., **1990**, *Paleoceanography*, 5, 277-288; A 130,000-year record of carbon isotopes in benthic foraminifera from the Caribbean Sea.

Raymo, M.E., Ruddiman, W.F., Shackleton, N.J., and Oppo, D.W., **1990**, *Earth and Planetary Science Letters*, 97, 353-368; Atlantic-Pacific carbon isotope differences over the last 2.5 million years.

Spero, H.J., Lerche, I., and Williams, D.F., **1991**, *Paleoceanography*, 6, 639-655; The influence of vital effects on the carbon isotope composition of planktonic foraminifera.

Zahn, R., Rushdi, A., Pisias, N.G., Bornhold, B.D., Blaise, B., and Karlin, R., **1991**, *Earth and Planetary Science Letters*, 103, 116-132; Carbon isotope record for benthic foraminifera from the northern Pacific Ocean.

Oppo, D.W. and Lehman, S.J., **1993**, *Science*, 259, 1148-1152; Carbon isotope record for benthic foraminifera from the northern Atlantic Ocean.

Charles, C.D., Wright, J.D., and Fairbanks, R.G., **1993**, *Paleoceanography*, 8, 691-697; Evidence for the influence of the air-sea thermodynamic effect on the carbon isotope composition of ocean ^{13}C .

Mackensen, A., Hubberten, H.-W., Bickert, T., Fischer, G., and Fütterer, D.K., **1993**, *Paleoceanography*, 8, 587-610; Vital effects on the carbon isotope composition of benthic foraminifera from the Southern Ocean.

Lynch-Stieglitz, J. and Fairbanks, R.G., **1994**, *Nature*, 369, 308-310; The joint use of Cd and ^{13}C data for benthic foraminifera to isolate the air-sea thermodynamic influence on the carbon isotope distribution in the sea.

- Lynch-Stieglitz, J., Fairbanks, R.G., and Charles, C.D., **1994**, *Paleoceanography*, 9, 7-29; Intermediate waters in the glacial Southern Ocean as reconstructed from ^{13}C measurements in benthic foraminifera.
- McCorkle, D.C. and Keigwin, L.D., **1994**, *Paleoceanography*, 9, 197-208; A test of the validity of ^{13}C reconstructions based on benthic foraminifera.
- Naqvi, W.A., Charles, C.D., and Fairbanks, R.G., **1994**, *Earth and Planetary Science Letters*, 121, 99-110, Carbon and oxygen isotopic records of benthic foraminifera from the Northeast Indian Ocean: implications on glacial-interglacial atmospheric CO_2 changes.
- Sarnthein, M., Winn, K., Jung, S.J.A., Duplessy, J.-C., Labeyrie, L., Erlenkeuser, H., and Ganssen, G., **1994**, *Paleoceanography*, 9, 209-267; A compilation of 95 benthic ^{13}C records from the eastern Atlantic covering the last 30,000 years.
- Beveridge, N.A.S., and Elderfield, H., **1995**, *Paleoceanography*, 10, 643-660, Deep thermohaline circulation in the low-latitude Atlantic during the last glacial.
- Oppo, D.W., and Lehman, S.J., **1995**, *Paleoceanography*, 10, 901-910, Suborbital timescale variability of North Atlantic Deep Water during the past 200,000 years.
- Sarnthein, M. et al., **1995**, *Paleoceanography*, 10, 1063-1094, Variations in Atlantic surface ocean paleoceanography, $50^\circ\text{-}80^\circ\text{N}$: A time-slice record of the last 30,000 years.
- Slowey, N.C., and Curry, W.B., **1995**, *Paleoceanography*, 10, 715-732, Glacial-interglacial differences in circulation and carbon cycling within the upper western North Atlantic.
- Charles et al., **1996**, *Earth and Planetary Science Letters*, 142, 19-27, Climate connections between the hemisphere revealed by deep sea sediment core/ice core correlations.
- Lynch-Stieglitz, J., van Green, A., and Fairbanks, R.G., **1996**, *Paleoceanography*, 11, 191-201, Intercean exchange of glacial North Atlantic Intermediate Water: Evidence from Subantarctic Cd/Ca and carbon isotope measurements.
- Mackensen, A. et al., **1996**, *Paleoceanography*, 11, 203-215, decoupling of $\delta^{13}\text{C}_{\Sigma\text{CO}_2}$ and phosphate in recent Weddell Sea deep and bottom water: Implications for glacial Southern Ocean paleoceanography.
- Ortiz, J.D. et al., **1996**, *Geochimica et Cosmochimica Acta*, 60, 4509-4523, Deep-dwelling planktonic foraminifera of the northeastern Pacific ocean reveal environmental control of oxygen and carbon isotopic disequilibria.
- Spero, H.J., and Lea, D.W., **1996**, *Marine Micropaleontology*, 28, 231-246, Experimental determination of stable isotope variability in *Globigerina bulloides*: implications for paleoceanographic reconstructions.
- Curry, W.B., and Oppo, D.W., **1997**, *Paleoceanography*, 12, 1-14, Synchronous, high-frequency oscillations in tropical sea surface temperatures and North Atlantic Deep Water production during the last glacial cycle.

Ninnemann, U.S., and Charles, C.D., **1997**, *Paleoceanography*, 12, 560-567, Regional differences in Quaternary Subantarctic nutrient cycling: Link to intermediate and deep water ventilation.

Oppo, D.W., Horowitz, M., and Lehman, S.J., **1997**, *Paleoceanography*, 12, 51-63, Marine core evidence for reduced deep water production during Termination II followed by a relatively stable substage 5e (Eemian).

Spero, H.J. et al., **1997**, *Nature*, 390, 497-500, Effect of seawater carbonate concentration on foraminiferal carbon and oxygen isotopes.

Keigwin, L.D., **1998**, *Paleoceanography*, 13, 323-339, Glacial-age hydrography of the far northwest Pacific Ocean.

McCorkle, D.C., Heggie, D.T., and Veeh, H.H., **1998**, *Paleoceanography*, 13, 30-34, Glacial and Holocene stable isotope distributions in the southeastern Indian Ocean.

Mulitza, S. et al., **1998**, *Earth and Planetary Science Letters*, 155, 237-249, Late Quaternary $\delta^{13}\text{C}$ gradients and carbonate accumulation in the western equatorial Atlantic.

Matsumoto, K., and Lynch-Stieglitz, J., **1999**, *Paleoceanography*, 14, 149-163, Similar glacial and Holocene deep water circulation inferred from southeast Pacific benthic foraminiferal carbon isotope composition.

Ninnemann, U.S., Charles, C.D., Hodell, D.A., **1999**, In: *Mechanisms of Global Climate Change at Millennial Time Scales*, Geophysical Monograph 112, 99-111, Origin of global millennial scale climate events: Constraints from the Southern Ocean deep sea sedimentary record.

12) Cadmium, zinc and barium in foraminifera

Chow, T.J. and Goldberg, E.D., **1960**, *Geochimica et Cosmochimica Acta*, 20, 192-198; The marine geochemistry of barium.

Boyle, E.A., Sclater, F., and Edmond, J.M., **1976**, *Nature*, 263, 42-44; Measurements of cadmium in sea water.

Chan, L.H., Edmond, J.M., Stallard, R.F., Broecker, W.S., Chung, Y.C., Weiss, R.F., and Ku, T.L., **1976**, *Earth & Planetary Science Letters*, 32, 258-267; Distribution of barium in the deep Pacific.

Chan, L.H., Drummond, D., Edmond, J.M., and Grant, B., **1977**, *Deep Sea Research*, 24, 613-649; Distribution of barium in the deep Atlantic.

Bruland, K.W., Knauer, G.A., and Martin, J.H., **1978**, *Limnology Oceanography*, 23, 618-625; Cadmium distribution in the northeast Pacific.

- Bruland, K.W., **1980**, *Earth & Planetary Science Letters*, 47, 176-198; Distribution of cadmium in the ocean.
- Boyle, E.A., **1981**, *Earth and Planetary Science Letters*, 53, 11-35; Cadmium concentration in foraminiferal tests.
- Knauer, G.A. and Martin, J.H., **1981**, *Journal of Marine Research*, 39, 65-76; Phosphorus and cadmium cycling in the northeast Pacific.
- Boyle, E.A. and Keigwin, L.D., **1982**, *Science*, 218, 784-787; Glacial to interglacial change in the cadmium content of deep Atlantic water.
- Hester, K. and Boyle, E., **1982**, *Nature*, 298, 260-262; Distribution coefficient for barium between sea water and the CaCO_3 in benthic foraminifera.
- Boyle, E.A. and Keigwin, L.D., **1985**, *Earth and Planetary Science Letters*, 76, 135-150; Comparison of cadmium records in benthic foraminifera from Atlantic and Pacific cores.
- Boyle, E.A., **1986**, *Geochimica et Cosmochimica Acta*, 50, 265-276; Cadmium record for the east equatorial Pacific.
- Boyle, E.A. and Keigwin, L.D., **1987**, *Nature*, 330, 35-40; Demonstration of a Younger Dryas increase in the cadmium content of the deep western Atlantic.
- Bishop, J.K.B., **1988**, *Nature*, 332, 341-343; Barite crystals in marine organic matter.
- Boyle, E.A., **1988**, *Paleoceanography*, 3 (4), 471-489; A summary of cadmium comparisons between deep water and benthic foraminifera.
- Keigwin, L.D. and Boyle, E.A., **1989**, *Palaeogeography, Palaeoclimatology, Palaeoecology*, 73, 85-106; Cadmium concentrations and carbon isotope ratios in planktonic foraminifera from high latitude surface waters.
- Lea, D. and Boyle, E., **1989**, *Nature*, 338, 751-753; Barium content of benthic foraminifera.
- Lea, D.W. and Boyle, E.A., **1990a**, *Nature*, 347, 269-272; Glacial to interglacial change in the barium content of deep Atlantic waters.
- Lea, D.W. and Boyle, E.A., **1990b**, *Paleoceanography*, 5, 719-742; Distribution of barium in the glacial deep ocean.
- Lea, D.W. and Boyle, E.A., **1991**, *Geochimica et Cosmochimica Acta*, 55, 3321-3331; Barium in planktonic foraminifera.

- McCorkle, D.C. and Klinkhammer, G.P., **1991**, *Geochimica et Cosmochimica Acta*, 55, 161-168; Measurements of cadmium concentration and carbon isotope ratios in the pore waters of deep sea sediments.
- Boyle, E.A., **1992**, *Annual Review of Earth and Planetary Sciences* 20, 245-287; Distributions of cadmium and carbon isotope ratios in the glacial ocean.
- Frew, R.D. and Hunter, K.A., **1992**, *Nature*, 360, 144-146; A kink in the modern ocean cadmium-phosphate trend.
- Lea, D.W. and Spero, H.J., **1992**, *Geochimica et Cosmochimica Acta*, 56, 2673-2680; Barium uptake by planktonic foraminifera culture.
- van Geen, A., Luoma, S.N., Fuller, C.C., Anima, R., Clifton, H.E., and Trumbore, S., **1992**, *Nature*, 358, 54-56; Upwelling history off California as determined by cadmium measurements in foraminifera shells.
- Lea, D.W., **1993**, *Global Biogeochemical Cycles*, 7, 695-710; Culture experiments for the uptake of barium by planktonic foraminifera shells.
- Lea, D.W. and Spero, H.J., **1994**, *Paleoceanography*, 9, 445-452; Relationship between the distributions of barium and alkalinity in the modern ocean.
- Ohkouchi, N., Kawahata, H., Murayama, M., Okada, M., Nakamura, T., and Taira, A., **1994**, *Earth and Planetary Science Letters*, 124, 185-194; Cadmium for benthic foraminifera from the North Pacific.
- Oppo, D.W. and Rosenthal, Y., **1994**, *Paleoceanography*, 9, 661-675; Cadmium-calcium and carbon isotope records for the Cape Basin over the last 700,000 years.
- Bertram, C.J. et al., **1995**, *Paleoceanography*, 10, 563-578, Cadmium/calcium and carbon isotope reconstructions of the glacial northeast Atlantic Ocean.
- Boyle, E.A., Labeyrie, L., and Duplessy, J.-C., **1995**, *Paleoceanography*, 10, 881-900, Calcitic foraminiferal data confirmed by cadmium in aragonitic *Hoeglundina*: Application to the last glacial maximum in the northern Indian Ocean.
- Frew, R.D., **1995**, *Geophysical Research Letters*, 22, 2349-2352, Antarctic Bottom Water formation and the global cadmium to phosphorus relationship.
- Lea, D.W., **1995**, *Paleoceanography*, 10, 733-747, A trace metal perspective on the evolution of Antarctic Circumpolar Deep Water chemistry.
- McCorkle, D.C. et al., **1995**, *Paleoceanography*, 10, 699-714, Evidence of a dissolution effect on benthic foraminiferal shell chemistry: $\delta^{13}\text{C}$, Cd/Ca, Ba/Ca and Sr/Ca results from the Ontong Java Plateau.
- van Geen, A., and Husby, D.M., **1996**, Cadmium in the California current system: Tracer of past and present upwelling.
- Martin, P.A., and Lea, D.W., **1998**, *Paleoceanography*, 13, 572-585, Comparison of water mass changes in the deep tropical Atlantic derived from Cd/Ca and carbon

isotope records: Implications for changing Ba composition of deep Atlantic water masses.

Mashiotta, T.A., Lea, D.W., and Spero, H.J., **1997**, *Geochimica et Cosmochimica Acta*, 61, 4053-4065, Experimental determination of cadmium uptake in shells of the planktonic foraminifera *Orbulina universa* and *Globigerina bulloides*: Implications for surface water paleoreconstructions.

Roenthal, Y., Boyle, E.A., and Labeyrie, L., **1997**, *Paleoceanography*, 12, 787-796, Last glacial maximum paleochemistry and deepwater circulation in the Southern Ocean: Evidence from foraminiferal cadmium.

Rickaby, R.E.M., and Elderfield, H., **1999**, *Paleoceanography*, 14, 293-303, Planktonic foraminiferal Cd/Ca: Paleonutrients or paleotemperature?

Elderfield, H., and Rickaby, R.E.M., **2000**, *Nature*, 405, 305-310, Oceanic Cd/P ratio and nutrient utilization in the glacial Southern Ocean.

Ellwood, M.J., and Hunter, K.A., **2000**, *Paleoceanography*, 15, 506-514, Variations in the Zn/Si record over the last interglacial glacial transition.

Marchitto, T.M., Jr., Curry, W.B., and Oppo, D.W., **2000**, *Paleoceanography*, 15, 299-306, Zinc concentrations in benthic foraminifera reflect seawater chemistry.

Oppo, D.W., and Horowitz, M., **2000**, *Paleoceanography*, 15, 147-160, Glacial deep water geometry: South Atlantic benthic foraminiferal Cd/Ca and $\delta^{13}\text{C}$ evidence.

Rickaby, R.E.M., Greaves, M.J., and Elderfield, H., **2000**, *Geochimica et Cosmochimica Acta*, 64, 1229-1236, Cd in planktonic and benthic foraminiferal shells determined by thermal ionisation mass spectrometry.

Marchitto, T.M., Jr., Oppo, D.W., and Curry, W.B., in press, **2002**, *Paleoceanography*, Paired benthic foraminiferal Cd/Ca and Zn/Ca evidence for a greatly increased presence of Southern Ocean Water in the glacial North Atlantic.

13) Alkenone thermometry

Marlowe, I.T., **1984**, Ph.D. Thesis, University of Bristol, 273 pp.; Lipids as paleoclimatic indicators.

Prahl, F.G. and Wakeham, S.G., **1987**, *Nature*, 330, 367-369; Calibration of the alkenone paleotemperature method.

Prahl, F.G., Muehlhausen, L.A., and Zahnle, D.L., **1988**, *Geochimica et Cosmochimica Acta*, 52, 2303-2310.

- Sikes, E.L., Farrington, J.W., and Keigwin, L.D., **1991**, *Earth and Planetary Science Letters*, 104, 36-47; Calibration of alkenone paleothermometry.
- Conte, M.H., Eglinton, G., and Madureira, L.A.S., **1992**, *Org. Geochemistry*, 19, 287-298; Alkenone paleotemperatures in the eastern North Atlantic.
- Eglinton, G., Bradshaw, S.A., Rosell, A., Sarnthein, M., Pflaumann, U., and Tiedemann, R., **1992**, *Nature*, 356, 423-426.
- Conte, M.H., and Eglinton, G., **1993**, *Deep Sea Research*, 10, 1935-1961; Alkenone systematics in the eastern North Atlantic.
- Prahl, F.G., Collier, R.B., Dymond, J., Lyle, M., and Sparrow, M.A., **1993**, *Deep Sea Research*, 40, 2061-2076; Alkenone paleothermometry in the northeastern Pacific.
- Rostek, F., Ruhland, G., Bassinot, F.C., Müller, P.J., Labeyrie, L.D., Lancelot, Y., Bard, E., **1993**, *Nature*, 364, 319-321; Alkenone paleotemperatures for the last 150,000 years for an equatorial Indian Ocean core.
- Sikes, E.L., and Volkman, J.K., **1993**, *Geochimica et Cosmochimica Acta*, 57, 1883-1889; Calibration of alkenone thermometry in polar waters.
- Fluegge, A., **1994**, M.S. Thesis, Indiana University, 72 pp.; Alkenone temepratures for a core from the eastern equatorial Pacific.
- Rosell, A., **1994**, Ph.D. Thesis, University of Bristol, 164 pp.; Alkenone paleotemperatures for a core from the northeastern Atlantic.
- Rosell-Melé, A. et al., **1995**, *Geochimica et Cosmochimica Acta*, 59, 3099-3107, Atlantic core-top calibration of the U_{37}^K index as a sea-surface palaeotemperature indicator.
- Prahl, F.G. et al., **1995**, *Paleoceanography*, 10, 763-773, Assessment of sea-surface temperature at 42°N in the California current over the last 30,000 years.
- Bard, E., Rostek, F., and Sonzogni, C., **1997**, *Nature*, 385, 707-710, Interhemispheric synchrony of the last deglaciation inferred from alkenone palaeothermometry.
- Ikehara, M. et al., **1997**, *Geophysical Research Letters*, 24, 679-682, Alkenone sea surface temperature in the Southern Ocean for the last two deglaciations.
- Rosell-Melé, A. et al., **1997**, *Quaternary Research*, 47, 344-355, Temperature and salinity effects on Alkenone ratios measured in surface sediments from the Indian Ocean.
- Epstein, B.L. et al., **1998**, *Paleoceanography*, 13, 122-126, An effect of dissolved nutrient concentrations on alkenone-based temperature estimates.

Sonzogni, C., Bark, E., and Rostek, F., **1998**, *Quaternary Science Reviews*, 17, 1185-1201, Tropical sea-surface temperatures during the last glacial period: a view based on alkenones in Indian Ocean sediments.

Bard, E., **1999**, *Science*, 284, 1133-1134, Ice age temperatures and geochemistry.

Cacho, I. et al., **1999**, *Paleoceanography*, 14, 698-705, Dansgaard-Oeschger and Heinrich event imprints in Alboran Sea paleotemperatures.

Cayre, O., and Bard, E., **1999**, *Quaternary Research*, 52, 337-342, Planktonic foraminiferal and alkenone records of the last deglaciation from the eastern Arabian Sea.

Kirst, G.J. et al., **1999**, *Quaternary Research*, 52, 92-103, Late Quaternary temperature variability in the Benguela current system derived from alkenones.

Pelejero, C., and Grimalt, J.O., **1999**, *Paleoceanography*, 14, 224-231, High-resolution U^{237} temperature reconstructions in the South China Sea over the past 220 kyr.

Sachs, J.P., and Lehman, S.J., **1999**, *Science*, 286, 756-759, Subtropical North Atlantic temperatures 60,000 to 30,000 years ago.

Sicre, M.-A. et al., **1999**, *Geophysical Research Letters*, 26, 1735-1738, Alkenones in the Northwestern Mediterranean Sea: Interannual variability and vertical transfer.

Budziak, D. et al., **2000**, *Paleoceanography*, 15, 307-321, Late Quaternary insolation forcing on total organic carbon and C_{37} alkenone variations in the Arabian Sea.

Calvo, E. et al., **2001**, *Earth and Planetary Science Letters*, 188, 509-519, New insights into the glacial latitudinal temperature gradients in the North Atlantic. Results from U^{237} sea surface temperatures and terrigenous inputs.

Conte, M.H. et al., **2001**, *Geochimica et Cosmochimica Acta*, 65, 4275-4287, The alkenone temperature signal in western North Atlantic surface waters.

14) Strontium-calcium thermometry

Kinsman, D.J.J. and Holland, H.D., **1969**, *Geochimica et Cosmochimica Acta*, 33, 1-17; Early measurements of the strontium content of marine carbonates.

Thompson, G. and Livingston, H.D., **1970**, *Earth and Planetary Science Letters*, 8, 439-442.

Weber, J.N., **1973**, *Geochimica et Cosmochimica Acta*, 37, 2173-2190.

Brass, G.W. and Turekian, K.K., **1974**, *Earth and Planetary Science Letters*, 23, 141-148.

Smith, S.V., Buddemeier, R.W., Redalje, R.C., and Houcke, J.E., **1979**, *Science*, 204, 404-407; First demonstration that Sr to Ca ratios in corals depend on growth temperature.

Tsunogai, S. and Watanabe, Y., **1981**, *Geochemistry Journal*, 15, 95-107.

Beck, J.W., Edwards, R.L., Ito, E., Taylor, F.W., Recy, J., Rougerie, F., Joannot, P., and Henin, C., **1992**, *Science*, 257, 644-647; Demonstration that Sr to Ca ratios in coral as measured by isotope dilution strongly correlate with water temperature.

de Villiers, A., Shen, G.T., and Nelson, B.K., **1994**, *Geochimica et Cosmochimica Acta*, 58, 197-208; Exploration of possible biases in Sr-Ca paleotemperatures for corals related to growth rate and non uniformity of the Sr to Ca in the sea.

Guilderson, T.P., Fairbanks, R.G., and Rubenstone, J.L., **1994**, *Science*, 263, 663-665; Application of the Sr to Ca method to paleothermometry of Barbados corals spanning the period of deglaciation.

de Villiers, S., Nelson, B.K., and Chivas, A.R., **1995**, *Science*, 269, 1247-1249, Biological controls on coral Sr/Ca and $\delta^{18}\text{O}$ reconstructions of sea surface temperatures.

McCulloch, M. et al., **1996**, *Earth and Planetary Science Letters*, 138, 169-178, High resolution windows into early Holocene climate: Sr/Ca coral records from the Huon Peninsula.

Shen, C.-C. et al., **1996**, *Geochimica et Cosmochimica Acta*, 60, 3849-3858, The calibration of D[Sr/Ca] versus sea surface temperature relationship for *Porites*, corals.

Alibert, C., and McCulloch, M.T., **1997**, *Paleoceanography*, 12, 345-363, Strontium/calcium ratios in modern *Porites*, corals from the Great Barrier Reef as a proxy for sea surface temperature: Calibration of the thermometer and monitoring of ENSO.

Beck, J.W. et al., **1997**, *Nature*, 385, 705-707, Abrupt changes in early Holocene tropical sea surface temperature derived from coral records.

de Villiers, **1999**, *Earth and Planetary Science Letters*, 171, 623-634, Seawater strontium and Sr/Ca variability in the Atlantic and Pacific Oceans

Martin, P.A. et al., **1999**, *G³*, 1, #1999GC000006, Variation of foraminiferal Sr/Ca over Quaternary glacial-interglacial cycles: Evidence for changes in mean ocean Sr/Ca?

Schrag, D.P., **1999**, *Paleoceanography*, 14, 97-102, Rapid analysis of high-precision Sr/Ca ratios in corals and other marine carbonates.

Stoll, H.M., and Schrag, D.P., **2000**, *G³*, 1, #1999GC000015, Coccolith Sr/Ca as a new indicator of coccolithophorid calcification and growth rate.

Shen, C.-C. et al., **2001**, *Earth and Planetary Science Letters*, 190, 197-209, High precision glacial-interglacial benthic foraminiferal Sr/Ca records from the eastern equatorial Atlantic Ocean and Caribbean Sea.

15) Magnesium-calcium thermometry

Chave, K.E., **1954**, *Journal of Geology*, 62, 266-283, Aspects of the biogeochemistry of magnesium 1. Calcareous marine organisms.

Katz, A., **1973**, *Geochimica et Cosmochimica Acta*, 37, 1563-1586, The interaction of magnesium with calcite during crystal growth at 25-90°C and one atmosphere.

Savin, S.M. and Douglas, R.G., **1973**, *Geological Society of America Bulletin*, 84, 2327-2342, Stable isotope and magnesium geochemistry of recent planktonic foraminifera from the South Pacific.

Bender, M.L., Lorens, R.B., and Williams, D.F., **1975**, *Micropaleontology*, 21, 448-459, Sodium, magnesium, and strontium in the tests of planktonic foraminifera.

Cronblad, H.G. and Malmgren, B.A., **1981**, *Nature*, 291, 61-64, Climatically controlled variation of Sr and Mg in Quaternary planktonic foraminifera.

Delaney, M.L., Bé, and Boyle, E.A., **1985**, *Geochimica et Cosmochimica Acta*, 49, 1327-1341, Li, Sr, Mg, and Na in foraminiferal calcite shells from laboratory culture, sediment traps, and sediment cores.

Nürnberg, D., **1995**, *Journal Foraminifera Research*, 25, 350-368, Magnesium in tests of *Neogloboquadrina pachyderma* sinistral from high northern and southern latitudes.

Nürnberg, D., Bijma, J., and Hemleben, C., **1996**, *Geochimica et Cosmochimica Acta*, 60, 803-814, Assessing the reliability of magnesium in foraminiferal calcite as a proxy for water mass temperatures.

Brown, S.J. and Elderfield, H., **1996**, *Paleoceanography*, 11, 543-551, Variations in Mg/Ca and Sr/Ca ratios of planktonic foraminifera caused by postdepositional dissolution: Evidence of a shallow Mg-dependent dissolution.

Rosenthal, Y., Boyle, E.A., and Slowey, N., **1997**, *Geochimica et Cosmochimica Acta*, 61, 3633-3643, Temperature control on the incorporation of magnesium,

strontium, fluorine, and cadmium into benthic foraminiferal shells from Little Bahama Bank: Prospects for thermocline paleoceanography.

Hastings, D.W., Russell, A.D., and Emerson, S.R., **1998**, *Paleoceanography*, 13, 161-169, Foraminiferal magnesium in *Globigerinoides sacculifer* as a paleotemperature proxy.

Lea, D.W., Mashiotta, T.A., and Spero, H.J., **1999**, *Geochimica et Cosmochimica Acta*, 63, 2369-2379, Controls on magnesium and strontium uptake in planktonic foraminifera determined by live culturing.

Mashiotta, T.A., Lea, D.W., and Spero, H.J., **1999**, *Earth and Planetary Science Letters*, 170, 417-432. Glacial-interglacial changes in Subantarctic sea surface temperature and $\delta^{18}\text{O}$ -water using foraminiferal Mg.

Dwyer, G.S. et al., **2000**, *G³*, 1, #2000GC000046, Changes in North Atlantic deep-sea temperature during climatic fluctuations of the last 25,000 years based on ostracode Mg/Ca ratios.

Elderfield, H., and Ganssen, G., **2000**, *Nature*, 405, 442-445, Past temperature and $\delta^{18}\text{O}$ of surface ocean waters inferred from foraminiferal Mg/Ca ratios.

Lea, D.W., Pak, D.K., and Spero, H.J., **2000**, *Science*, 289, 1719-1724, Climate impact of late Quaternary equatorial Pacific sea surface temperature variations.

Lear, C.H., Elderfield, H., and Wilson, P.A., **2000**, *Science*, 287, 269-272, Cenozoic deep-sea temperatures and global ice volumes from Mg/Ca in benthic foraminiferal calcite.

Nürnberg, and Müller, A., and Schneider, R.R., **2000**, *Paleoceanography*, 15, 124-134, Paleo-sea surface temperature calculations in the equatorial east Atlantic from Mg/Ca ratios in planktic foraminifera: A comparison to sea surface temperature estimates from U₃₇^{K'}, oxygen isotopes, and foraminiferal transfer function.

Rosenthal, Y. et al., **2000**, *Paleoceanography*, 15, 135-145, Incorporation and preservation of Mg in *Globigerinoides sacculifer*: Implications for reconstructing the temperature and $^{18}\text{O}/^{16}\text{O}$ of seawater.

Toyofuku, T. et al., **2000**, *Paleoceanography*, 15, 456-464, Evaluation of Mg/Ca thermometry in foraminifera: Comparison of experimental results and measurements in nature.

Dekens, P.S. et al., **2002**, *Geochemistry, Geophysics, Geosystems*, 3(4), 10.1029/2001GC000200, Core top calibration of Mg/Ca in tropical foraminifera: Refining paleotemperature estimation.

16) Continental paleothermometers

Mazor, E., 1972, *Geochimica et Cosmochimica Acta*, 35, 1321-1336, Paleotemperatures and other hydrological parameters deduced from noble gases dissolved in groundwaters, Jordan Rift Valley, Israel.

Deák, J., 1979, In: *Isotope Hydrology 1978 (Proc. Symp. Vienna)*, 1, IAEA, Vienna, 221-249, Environmental isotopes and water chemical studies for groundwater research in Hungary.

Heaton, T.H.E., 1984, *Hydrology Science Journal*, 29, 29-47, Rates and sources of ^4He accumulation in groundwater.

Heaton, T.H.E., Talma, A.S., and Vogel, J.C., 1986, *Quaternary Research*, 25, 79-88; Paleotemperatures based on stable isotope ratios and gas content of glacial age ground water in South Africa.

Phillips, F.M., Peeters, L.A., Tansey, M.K., and Davis, S.N., 1986, *Quaternary Research*, 26, 179-193; Paleotemperatures based on noble gas composition of glacial age water from a southwestern U.S. aquifer.

Schwarcz, H.P., 1986, In: Fritz, P. and Fontes, J.Ch. (eds.), *Handbook of Environmental Isotope Geochemistry*, Elsevier, Amsterdam, 2, 271-303; Geochronology and isotopic geochemistry of speleothems.

Atkinson, T.C., Briffa, K.R., and Coope, G.R., 1987, *Nature*, 325, 587-592; Temperature record for Britain over the last 22,000 years based on beetle remains.

Winograd, I.J., Szabo, B.J., Coplen, T.B., and Riggs, A.C., 1988, *Science*, 242, 1275-1280; Oxygen isotope chronology for a vein calcite in southern Nevada.

Benson, L.V., Currey, D.R., Dorn, R.I., Lajoie, K.R., Oviatt, C.G., Robinson, S.W., Smith, G.I., and Stine, S., 1990, *Palaeogeography, Palaeoclimatology, Palaeoecology*, 78, 241-286; Chronology for closed basin lakes in the US's Great Basin.

Stute, M., Sonntag, C., Deák, J., and Schlosser, P., 1992, *Geochimica et Cosmochimica Acta*, 56, 2051-2067, Helium in deep circulating groundwater in the Great Hungarian Plain: Flow dynamics and crustal and mantle He fluxes

Stute, M., Schlosser, P., Clark, J.F., and Broecker, W.S., 1992, *Science*, 256, 1000-1003; Paleotemperatures based on noble gas concentrations in water from the Carrizo aquifer in Texas.

Stute, M., Clark, J.F., Schlosser, P., Broecker, W.S., and Bonani, G., 1995, *Quaternary Research*, 43, 209-220, A high altitude continental paleotemperature record derived from noble gases dissolved in groundwater from the San Juan Basin, New Mexico.

Stute, M. et al., 1995, *Science*, 269, 379-383, Cooling of tropical Brazil (5°C) during the last glacial maximum.

Clark, J.F. et al., **1997**, *Water Resource Research*, 33, 281-290, An isotope study of the Floridan Aquifer in southeastern Georgia; Implications for groundwater flow and paleoclimate.

Stute, M., and Schlosser, P., **1999**, In: Cook, P., and Herceg, A. (eds.), *Environmental Tracers in Subsurface Hydrology*, Kluwer Academic Publishers, 349-377, Atmospheric noble gases.

17) CaCO_3 dissolution

Arrhenius, G., **1952**, *Swedish Deep Sea Expedition (1947-1948) Reports*, 5, 1-227; Analysis of CaCO_3 content, foram fragment to whole foram ratios and planktonic to benthic foram ratios with depth in a series of equatorial Pacific cores.

Peterson, M.N.A., **1966**, *Science*, 154, 1542-1544; The first demonstration that the long-term exposure of calcite crystals to sea water on deep sea moorings offered valuable information regarding the depth dependence of dissolution rates and the depth of the horizon of calcite saturation.

Pytkowicz, R.M. and Fowler, G.A., **1967**, *Geochemical Journal.*, VI, 169-182; Discussion of the effect of pressure on carbonate ion pairs, on the relative solubilities of calcite and aragonite, and on rates of solution of these phases.

Ruddiman, W.F. and Heezen, B.C., **1967**, *Deep Sea Research*, 14, 801-808; Down core studies in the equatorial Atlantic Ocean showing the change in preservation of solution sensitive foraminifera with climate.

Berger, W.H., **1968**, *Deep Sea Research*, 15, 31-43; Application of the selective preservation of the shells of various species of foraminifera to the distribution of calcite dissolution in sediments from the floor of the Pacific Ocean.

Hays, J.D., Saito, T., Opdyke, N.D., and Burckle, L.H., **1969**, *Geological Society of America Bulletin*, 8, 1481-1514; Calcium carbonate cycles in long equatorial Pacific cores.

Berger, W.H., **1970**, *Marine Geology*, 8, 111-138; Geographic distribution of dissolution patterns in the deep Pacific.

Broecker, W.S., **1971**, In: Turekian, K.K.(ed.), *The Late Cenozoic Glacial Ages*, Yale Univ. Press, New Haven, CT, 239-265; A discussion of the factors influencing of the calcium carbonate budget in the ocean and an examination of the record of budgetary changes kept in deep sea cores.

Parker, F.L. and Berger, W.H., **1971**, *Deep Sea Research*, 18, 73-107; The influence of partial dissolution on the distribution of foraminifera shells in the recent

sediments of the South Pacific.

Millero, F.J. and Berner, R.A., **1972**, *Geochimica et Cosmochimica Acta*, 36, 92-98; A discussion of the effect of pressure on carbonate equilibria in seawater based on the partial molar volumes.

Hays, J.D., Perruzza, A., **1972**, *Quaternary Research*, 2, 355-362; Demonstration that the changing dilution of calcium carbonate with wind-borne dust from Africa is the cause of the calcium carbonate cycles in cores from the east flank of the mid-Atlantic Ridge.

Ben-Yaakov, S., Ruth, S.E., and Kaplan, I.R., **1974**, *Science*, 184, 982-984; The application *in situ* saturometry to determine the relationship between the lysocline depth and calcite saturation depth..

Broecker, W.S. and Broecker, S., **1974**, In: Hay, W.W. (ed.), *Society of Economic Paleontologists and Mineralogists Special Publication 20*, 44-57; Demonstration that the boundary between sediments experiencing large-scale calcite dissolution and minimal calcite dissolution is quite sharp on the west flank of the East Pacific Rise and that this horizon was deeper during glacial time.

Gardner, J.V., **1975**, In: Sliter, W.V., Be, A.W.H., and Berger, W.H. (eds.), *Dissolution of Deep Sea Carbonates*, Cushman Foundation for Foraminiferal Res. Special Publication 13, 129-141; Evidence for glacial to interglacial changes in the extent of dissolution of the calcite accumulating in the eastern equatorial Atlantic.

Biscaye, P.E., Kolla, V., and Turekian, K.K., **1976**, *Journal of Geophysical Research*, 81, 2595-2603; Contains a map showing the percent CaCO₃ in recent Atlantic Ocean sediments.

Kolla, V., Be, A.W.H., and Biscaye, P.E., **1976**, *Journal of Geophysical Research*, 81, 2605-2616; Contains a map showing the percent CaCO₃ in recent Indian Ocean sediments.

Berger, W.H., Adelseck, C.G., Jr., and Mayer, L.A., **1976**, *Journal of Geophysical Research*, 81, 2617-2627; Contains a map showing the percent CaCO₃ in recent Pacific Ocean sediments.

Sundquist, E., Richardson, D.K., Broecker, W.S., and Peng, T.-H., **1977**, In: Andersen, N.R. and Malahoff, A.(eds.), *The Fate of Fossil Fuel CO₂ in the Oceans*, Plenum Press, New York, 429-454; An attempt to reconstruct the events which created the core top CaCO₃-rich layer just beneath the present day lysocline on the west flank of the East Pacific Rise.

Takahashi T. and Broecker, W.S., **1977**, In: Andersen, N.R. and Malahoff, A.(eds.), *The*

Fate of Fossil Fuel CO₂ in the Oceans, Plenum Press, New York, 455-478; A discussion of the interaction between the potential dissolution rate of calcite, the rain rate of other phases for three different assumptions regarding the rate limiting step for dissolution. Also a means of distinguishing among these possible models is discussed.

Sayles, F.L., **1980**, *Marine Chemistry*, 9, 223-235; Solubility of calcite.

Emerson, S. and Bender, M., **1981**, *Journal of Marine Research*, 39, 139-162; A discussion of the role of bioturbated organic material to the dissolution of calcite.

Kier, R.S., **1984**, *Marine Geology*, 59, 227-250; Transient dissolution.

Farrell, J.W. and Prell, W.L., **1989**, *Paleoceanography*, 4, 447-466, Climatic change and CaCO₃ preservation: An 800,000-year bathymetric reconstruction from the central equatorial Pacific Ocean.

Archer, D., Emerson, S., and Reimers, C., **1989**, *Geochimica et Cosmochimica Acta*, 45, 2169-2175; Calcite dissolution driven by respiration CO₂.

Archer, D.E., **1991**, *Paleoceanography*, 6, 561-571; The influences of rain rate and dissolution intensity on calcite accumulation in the equatorial Pacific.

Archer, D., **1991**, *Journal of Geophysical Research*, 96, 17,037-17,050; The influence of organic matter rain in the depth of the lysocline.

Broecker, W.S., Klas, M., Clark, E., Bonani, G., and Wolfli, W., **1991**, *Paleoceanography*, 6, 593-608; Chemical erosion in the equatorial Pacific.

Farrell, J.W. and Prell, W.L., **1991**, *Paleoceanography*, 6, 485-498, Pacific CaCO₃ preservation and δ¹⁸O since 4 Ma: Paleoceanic and paleoclimatic implications.

Emerson, S. and Archer, D., **1992**, *Paleoceanography*, 7, 319-331; A model for calcite dissolution during glacial time.

Oxburgh, R. and Broecker, W.S., **1993**, *Palaeogeography, Palaeoclimatology, Palaeoecology*, 103, 31-39; Chemical erosion in the equatorial Pacific.

Hales, B., Emerson, S., and Archer, D., **1994**, *Deep Sea Research*, 41, 695-719; Microelectrode measurements of pore water O₂ and pH permit quantification of respiration-induced calcite dissolution.

Archer, D. and Maier-Reimer, E., **1994**, *Nature*, 367, 260-263; A pore water respiration model explaining the glacial to interglacial change in atmospheric CO₂ content.

Lohmann, G.P., **1995**, *Paleoceanography*, 10, 445-457, A model for variation in the chemistry of planktonic foraminifera due to secondary calcification and selective dissolution.

Broecker, W.S., and Sanyal, A., **1997**, *Paleoceanography*, 12, 530-532, Magnitude of the CaCO_3 dissolution events marking the onset of times of glaciation.

Broecker, W.S., and Clark, E., **1999**, *Paleoceanography*, 14, 596-604, CaCO_3 Size distribution: A paleo carbonate ion proxy.

Broecker, W.S. et al., **1999**, *Paleoceanography*, 14, 13-22, Core-top ^{14}C ages as a function of water depth on the Ontong-Java Plateau.

Broecker, W.S. et al., **1999**, *Paleoceanography*, 14, 744-752, Evidence for a reduction in the carbonate ion content of the deep sea during the course of the Holocene.

Broecker, W. S., and Sutherland, S., **2000**, *Geochemistry, Geophysics, Geosystems*, 1, 2000GC000039, The distribution of carbonate ion in the deep ocean: Support for a post-Little Ice Age change in Southern Ocean ventilation.

Broecker, W.S., and Clark, E., **2001**, *Paleoceanography*, 16, 531-534, An evaluation of Lohmann's foraminifera-weight index.

Broecker, W.S., and Clark, E., **2001**, *Geochemistry, Geophysics, Geosystems*, 2, 2001GC000185, A dramatic Atlantic dissolution event at the onset of the last glaciation.

Broecker, W.S., and Clark, E., **2001**, *Paleoceanography*, 16, 669-671, Reevaluation of the CaCO_3 size-index paleocarbonate ion proxy.

Broecker, W.S., Lynch-Stieglitz, J., and Clark, E., **2001**, *Geochemistry, Geophysics, Geosystems*, 2, 2001GC000177, What caused the atmosphere's CO_2 content to rise during the last 8000 years?

Broecker, W.S. et al., **2001**, *Geochemistry, Geophysics, Geosystems*, 2, 2001GC000151, Record of sea-floor CaCO_3 dissolution in the equatorial Pacific.

Broecker, W.S., and Clark, E., **2002**, *Geochemistry, Geophysics, Geosystems*, 3(2), 10.1029/2001GC000210, A major dissolution event at the close of MIS 5e in the western equatorial Atlantic.

Broecker, W.S., and Clark, E., **2002**, *Geochemistry, Geophysics, Geosystems*, 3(3), 10.1029/2001GC000231, Carbonate ion concentration in glacial-age deep waters of the Caribbean Sea.

Broecker, W.S., in press, **2002**, In: Turekian, K.K. and Holland, H.D. (eds.), *Treatise on*

Geochemistry, Elsevier Science Limited, Oxford, England, The Oceanic CaCO_3 Cycle.

18) Boron isotope paleoacidity

Kakihana, H., Kotaka M., Satoh, S., Nomura, M., and Okamoto, M., **1977**, *Bulletin of the Chemical Society of Japan*, 50, 158-163; Theoretical calculation of the isotope fractionation between the charged and uncharged aqueous boron species.

Palmer, M.R., Spivack, A.J., and Edmond, J.M., **1987**, *Geochimica et Cosmochimica Acta*, 51, 2319-2323; Boron isotope fractionation between sea water and marine clays.

Spivack, A.J., Palmer, M.R., and Edmond, J.M., **1987**, *Geochimica et Cosmochimica Acta*, 51, 1939-1949; The sedimentary cycle of boron isotopes.

Spivack, A.J. and Edmond, J.M., **1987**, *Geochimica et Cosmochimica Acta*, 51, 1033-1043; Boron isotope exchange between sea water and the oceanic crust.

Vengosh, A., Kolodny, Y., Starinsky, A., Chivas, A.R., and McCulloch, M.T., **1991**, *Geochimica et Cosmochimica Acta*, 55, 2901-2910; Boron isotope fractionation between sea water and marine carbonates.

Hemming, N.G. and Hanson, G.N., **1992**, *Geochimica et Cosmochimica Acta*, 56, 537-543; Relationship of boron isotope fractionation between sea water and marine carbonates to pH.

Spivack, A.J., You, C.-F., and Smith, H.J., **1993**, *Nature*, 363, 149-151; Application of boron isotopes in foraminifera shells to the estimation of the long term trend in oceanic pH.

Ishikawa, T. and Nakamura, E., **1993**, *Earth and Planetary Science Letters*, 117, 567-580; Boron isotope systematics in marine sediments.

Chaussidon, M. and Jambon, A., **1994**, *Earth and Planetary Science Letters*, 121, 277-291; Boron isotopic composition of oceanic basalts.

Hemming, N.G., and Hanson, G.N., **1994**, *Chemical Geology* (Isotope Geoscience Section), 114, 147-156; The negative ion method of boron isotope measurement.

Gaillardet, J., and Allègre, C.J., **1995**, *Earth and Planetary Science Letters*, 136, 665-676; Boron isotopic compositions of corals: Seawater or diagenesis record?

Sanyal, A., Hemming, N.G., Hanson, G.N., and Broecker, W.S., **1995**, *Nature*, 373, 234-236; Isotope composition of boron in foraminifera shells as an indicator of the glacial to interglacial change in oceanic pH.

Sanyal et al., **1996**, *Paleoceanography*, 11, 513-517, Oceanic pH control on the boron isotopic composition of foraminifera: Evidence from culture experiments.

Sanyal, A., Hemming, N.G., and Broecker, W.S., **1997**, *Global Biogeochemical Cycles*, 11, 125-133, Changes in pH in the eastern equatorial Pacific across stage 5-6 boundary based on boron isotopes in foraminifera.

Spivack, A.J., and Youk, C.-F., **1997**, *Earth and Planetary Science Letters*, 152, 113-122, Boron isotopic geochemistry of carbonates and pore waters, Ocean Drilling Program Site 851.

Hemming, N.G., Guilderson, T.P. and Fairbanks, R.G., **1998**, *Global Biogeochemical Cycles*, 12, 581-586, Seasonal variations in the boron isotopic composition of coral: A productivity signal?

Hemming, N.G., Reeder, R.J., and Hart, S.R., **1998**, *Geochimica et Cosmochimica Acta*, 62, 2915-2922, Growth-step-selective incorporation of boron on the calcite surface.

Palmer, M.R., Pearson, P.N., and Cobb, S.J., **1998**, *Science*, 282, 1468-1471, Reconstructing past ocean pH-depth profiles.

Sanyal, A., and Bijma, J., **1999**, *Paleoceanography*, 14, 753-759, A comparative study of the northwest Africa and eastern equatorial Pacific upwelling zones as sources of CO₂ during glacial periods based on boron isotope paleo-pH estimation.

Lemarchand, D. et al., **2000**, *Nature*, 408, 951-954, The influence of rivers on marine boron isotopes and implications for reconstructing past ocean pH.

Sanyal, A. et al., **2000**, *Geochimica et Cosmochimica Acta*, 64, 1551-1555, Seawater pH control on the boron isotopic composition of calcite: Evidence from inorganic calcite precipitation experiments.

Zeebe, R.E. et al., **2001**, *Marine Chemistry*, 73, 113-124, A theoretical study of the kinetics of the boric acid-borate equilibrium in seawater.

Sanyal et al., **2001**, *Paleoceanography*, 14, 515-519, Empirical relationship between pH and the boron isotopic composition of *Globigerinoides sacculifer*: Implications for the boron isotope paleo-pH proxy.

Pearson, P.N. and Palmer, M.R., **2000**, *Nature*, 406, 695-699, Atmospheric carbon dioxide concentrations over the past 60 million years.

19) Radiocarbon dating

Libby, W., **1952**, *Radiocarbon Dating*, University of Chicago Press; Book describing the discovery of the radiocarbon dating method.

Suess, H.E., **1955**, *Science*, 120, 467-473; Demonstration of a decline of atmospheric ^{14}C content over the last century due to fossil fuel CO₂.

de Vries, Hl., **1958**, *K. Ned. Akad. Wet.*, B61, 94-102; First demonstration of natural atmospheric radiocarbon content changes.

Suess, H.E., **1961**, *Proceedings of an informal conference, Problems related to Interplanetary Matter*, Highland Park, Illinois, 90-95; Secular variations in atmospheric ^{14}C content.

Lingenfelter, R.E., **1963**, *Reviews of Geophysics* 1, 35-55; Radiocarbon production by neutrons.

Suess, H.E., **1965**, *Journal of Geophysical Research*, 70, 5937-5952; Secular variations in atmospheric radiocarbon.

Suess, H.E., **1967**, In: *Radioactive Dating and Methods of Low-Level Counting*, Vienna, IAEA, 143-151; Radiocarbon calibration based on bristlecone pine series.

Suess, H.E., **1970**, In: *Radiocarbon Variations and Absolute Chronology*, ed., I.U. Olsson, Proceedings XII Nobel Symposium, New York, Wiley, 303-311; Radiocarbon calibration based on bristlecone pine series.

Lingenfelter, R.E. and Ramaty, R., **1970**, In: Olsson, I.H. (ed.), *Radiocarbon Variations and Absolute Chronology*, Wiley, New York, 513-537; Astrophysical and geophysical causes for radiocarbon change in production rate.

Stuiver, M., **1971**, In: Turekian, K.K. (ed.), *The late Cenozoic Glacial Ages*, Yale University Press, New Haven, CT, 57-70; Evidence for changes in the atmospheric ^{14}C content.

Stuiver, M., **1978**, *Nature*, 273, 271-274; Radiocarbon time scale tested against other chronometers.

Stuiver, M., **1980**, *Nature*, 286, 868-871; Changes in the radiocarbon content of the atmosphere during the current millennium.

Suess, H.E., **1980**, *Radiocarbon*, 22, 200-209; Atmospheric ^{14}C changes due to sunspot cycles.

Stuiver, M. and Quay, P.D., **1980**, *Science*, 207, 11-19; Relationship between ^{14}C production and sunspot activity.

Linick, T.W., Suess, H.E., and Becker, B., **1985**, *Radiocarbon*, 27, 20-32; Radiocarbon measurements on the German oak series.

Lal, D., **1985**, In: *The Carbon Cycle and Atmospheric CO₂: Natural Variations Archean to Present*, Geophysical Monograph 32, AGU, 221-233; Long term changes in atmospheric ^{14}C content.

Stuiver, M. and Pearson, G.W., **1986**, *Radiocarbon*, 28, 805-838; High precision radiocarbon calibration back to 2500 B.P.

Stuiver, M. and Reimer, P.J., **1986**, *Radiocarbon*, 28, 1022-1030; A computer program to radiocarbon age correction.

Stuiver, M. and Becker, B., **1986**, *Radiocarbon*, 28, 863-910; High precision radiocarbon calibration 3800 to 4500 B.P.

Kromer, B., Rhein, M., Bruns, M., Schoch-Fischer, H., Münnich, K.O., Stuiver, M., and Becker, B., **1986**, *Radiocarbon*, 28, 954-960; Tree ring calibration for 8000 to 10,000 years B.P.

Pearson, G.W., Pilcher, J.R., Baillie, M.G.L., Corbett, D.M., and Qua, F., **1986**, *Radiocarbon*, 28, 911-934; Radiocarbon measurements on the Irish oak series.

Pearson, G.W. and Stuiver, M., **1986**, *Radiocarbon*, 28, 839-862; Precision calibration of the radiocarbon time scale 2500 to 4500 B.P.

Stuiver, M., Kromer, B., Becker, B., and Ferguson, C.W., **1986**, *Radiocarbon*, 28, 969-979; Radiocarbon calibration back to 13,300 B.P.

Becker, B. and Kromer, B., **1986**, *Radiocarbon*, 28, 961-968; Extension of the tree ring calibration 8800 to 10,100 B.P.

Damon, P.E. and Linick, T.W., **1986**, *Radiocarbon*, 28, 266-278; Geomagnetic and heliomagnetic induced changes in radiocarbon production rate.

Linick, T.W., Long, A., Damon, P.E., and Ferguson, C.W., **1986**, *Radiocarbon*, 28, 943-953; Radiocarbon measurements on bristlecone pine.

Stuiver, M. and Braziunas, T.F., **1989**, *Nature*, 338, 405-408; Atmospheric ^{14}C content and sunspot cycles.

Bard, E., Hamelin, B., Fairbanks, R.G., and Zindler, A., **1990**, *Nature*, 345, 405-410; Uranium series - radiocarbon age differences are glacial age corals.

Mazaud, A., Laj, C., Bard, E., Arnold, M., and Tric, E., **1991**, *Geophysical Research Letters*, 18, 1885-1888; The influence of the geomagnetic field on radiocarbon production over the last 80,000 years.

Stuiver, M. and Braziunas, T.F., **1991**, *Quaternary Research*, 35, 1-24; Variations in the atmospheric $^{14}\text{C}/^{12}\text{C}$ during Holocene time.

Bard, E., Fairbanks, R.G., Arnold, M., and Hamelin B., **1992**, In: Bard, E. and Broecker, W.S. (eds.), *The Last Deglaciation: Absolute and Radiocarbon Chronologies*, Springer-Verlag, NY, NATO ASI Series, 2, 103-112; radiocarbon-radiothorium age comparisons on coral.

Kromer, B., and Becker, B., **1992**, In: Bard, E. and Broecker, W.S. (eds.), *The Last Deglaciation: Absolute and Radiocarbon Chronologies*, Springer-Verlag, NY, NATO ASI Series, 2, 3-12; Tree ring calibration at 10,000 BP.

Bard, E., Arnold, M., Fairbanks, R.G., and Hamelin, B., **1993**, *Radiocarbon*, 35, 191-199; Comparison of ^{14}C and uranium series ages on corals.

Becker, B. and Kromer, B., **1993**, *Palaeogeography, Palaeoclimatology, Palaeoecology*, 103, 67-71; Extension of the tree ring calibration of the ^{14}C method back to 11,400 calendar years.

Edwards, R.L., Beck, J.W., Burr, G.S., Donahue, D.J., Chappell, J.M.A., Bloom, A.L., Druffel, E.R.M., and Taylor, F.W., **1993**, *Science*, 260, 962-968; Comparison of ^{14}C and uranium series ages on corals.

Stuiver, M. and Braziunas, T.F., **1993**, *The Holocene*, 3,4, 289-305; Periodicities in ^{14}C production.

Adkins, J.F. et al., **1998**, *Science*, 280, 725-728, Deep-sea coral evidence for rapid change in ventilation of the deep North Atlantic 15,400 years ago.

Bard, E., **1998**, *Geochimica et Cosmochimica Acta*, 62, 2025-2038, Geochemical and geophysical implications of the radiocarbon calibration.

Hughen, K.A. et al., **1998**, *Nature*, 391, 65-68, Deglacial changes in ocean circulation from an extended radiocarbon calibration.

Kromer, B., and Spurk, M., **1998**, *Radiocarbon*, 40, 1117-1125, Revision and tentative extension of the tree-ring based ^{14}C calibration, 9200-11,855 cal BP.

Stuiver, M. et al., **1998**, *Radiocarbon*, 40, 1126-1159, Intcal98 radiocarbon age calibration, 24,000-0 cal BP.

Voelker, A.H.L. et al., **1998**, *Radiocarbon*, 40, 517-534, Correlation of marine ^{14}C ages from the Nordic seas with the GISP2 isotope record: Implications for radiocarbon calibration beyond 25 ka BP.

Beck, J.W. et al., **2001**, *Science*, 292, 2453-2458, Extremely large variations of atmospheric ^{14}C concentration during the last glacial period.

Bond, G. et al., **2001**, *Science*, 294, 2130-2152, Persistent solar influence on North Atlantic climate during the Holocene.

Broecker, W.S., in press, **2002**, In: Turekian, K.K. and Holland, H.D. (eds.), *Treatise on Geochemistry*, Elsevier Science Limited, Oxford, England, Radiocarbon.

20) Uranium series dating

Pettersson, H., **1937**, *Anz. Akad. Wiss. Wien, Math-Naturwiss.*, 127-128; First measurements of uranium series isotopes in marine sediments.

Piggot, C.S. and Urry, W.D., **1942**, *Geological Society of America Bulletin*, 53, 1187-1210; First time scale for deep sea sediments based on uranium series measurements.

Isaac, N. and Picciotto, E., **1953**, *Nature*, 171, 742-743; First direct measurement of ^{230}Th in deep sea sediments.

Kröll, V. St., **1953**, *Nature*, 171, 742; ^{226}Ra measurements in deep sea sediments.

Kröll, V. St., **1954**, *Deep-Sea Research*, 1, 211-215; Use of ^{226}Ra measurements to determine deep sea sedimentation rates.

Barnes, J.W., Lang, E.J., and Potratz, H.A., **1956**, *Science*, 124, 175-176; First paper on uranium series dating of corals.

Volchok, H.L. and Kulp, J.L., **1957**, *Geochimica et Cosmochimica Acta*, 11, 219-246; ^{226}Ra based estimates of sediment accumulation rates.

Goldberg, I.D. and Koide, M., **1958**, *Science*, 128, 1003; First application of direct measurement of ^{230}Th to the determination of sediment accumulation rates in the deep sea.

Sackett, W.M., **1960**, *Science*, 132, 1761-1762; First measurement of ^{231}Pa in marine sediments.

Koczy, F.F., **1961**, *Science*, 133, 978-979; ^{230}Th to ^{232}Th ratio in deep sea sediment.

Miyake, Y. and Sugimura, Y., **1961**, *Science*, 133, 1823; ^{230}Th based sedimentation rates for western Pacific sediments.

Rosholt, J.N., Emiliani, C., Geiss, J., Koczy, F.F., and Wangersky, P.J., **1961**, *Journal of Geology*, 69, 162-185; First application of the $^{231}\text{Pa}/^{230}\text{Th}$ method for dating deep sea sediments.

Goldberg, E.D. and Koide, M., **1962**, *Geochimica et Cosmochimica Acta*, 26, 417-450; $^{230}\text{Th}/^{232}\text{Th}$ measurements on deep sea sediments.

Rosholt, J.N., Emiliani, C., Geiss, J., Koczy, F.F., and Wangersky, P.J., **1962**, *Journal of Geophysical Research*, 67, 2907-2911; ^{231}Pa to ^{230}Th radiodating of a Caribbean core.

Goldberg, E.D. and Koide, M., **1963**, *Earth Sciences and Meteoritics*, North-Holland Publishing Company, 90-102; Uranium series based accumulation rates for Indian Ocean sediment.

Sackett, W.M. and Potratz, H.A., **1963**, *U.S. Geological Survey Professional Paper 260-BB*, 1053-1066; First application of uranium series dating of corals.

Ku, T.L., **1965**, *Journal of Geophysical Research*, 70, 3457-3474; First measurement of ^{234}U to ^{238}U ratios in deep sea sediments.

Sackett, W.M., **1965**, *Symposium on Marine Geochemistry*, ed., D.R. Schink and Corless, J.T., Univ. Rhode Island, 29-40; ^{230}Pa based sediment accumulation rates.

Thurber, D.I., Broecker, W.S., Blanchard, R.L., and Potratz, H.A., **1965**, *Science*, 149, 55-58; Uranium series dating of submerged reefs in Enewetak Atoll.

Ku, T.L. and Broecker, W.S., **1966**, *Science*, 151, 448-450; ^{230}Th measurements as a means of establishing the chronology of deep sea climatic record back to 320,000 years.

Veeh, H.H., **1966**, *Journal of Geophysical Research*, 71, 3379-3386; First uranium series ages on coral reefs showing that sea level stood higher during the last interglacial.

Broecker, W.S., Thurber, D.L., Goddard, J., Ku, T.L., Matthews, R.K., and Mesolella, K.J., **1968**, *Science*, 159, 297-300; First paper on uranium series dating of Barbados raised coral reefs.

Ku, T.-L., **1968**, *Journal of Geophysical Research*, 73, 2271-2276; Crosschecks on ^{230}Th ages for raised Barbados reefs by the ^{231}Pa method.

Ku, T.L., Broecker, W.S., and Opdyke, N., **1968**, *Earth and Planetary Science Letters*, 4, 1-16; Comparison of ^{230}Th based sedimentation rates for deep sea sediments with those based on magnetic reversals.

Broecker, W.S. and Ku, T.L., **1969**, *Science*, 166, 404-406; Uranium series measurements in Caribbean Sea sediments.

- Mesolella, K.J., Matthews, R.K., Broecker, W.S., and Thurber, D.L., **1969**, *Journal of Geology*, 77, 250-274; The relationship between the Barbados sea level record and Milankovitch cycles.
- Broecker, W.S. and van Donk, J., **1970**, *Review of Geophysics and Space Physics*, 8, 169-198; Chronology for deep sea core ^{18}O record compared to Milankovitch seasonality cycle chronology.
- Veeh, H.H. and Veevers, J.J., **1970**, *Nature*, 226; First comparison between U series and radiocarbon ages for a glacial age coral.
- Bender, M.L., Taylor, F.W., and Matthews, R.K., **1973**, *Quaternary Research*, 3, 142-146; Helium dating of raised coral reefs on Barbados back to 500,000 years.
- Bloom, A.L., Broecker, W.S., Chappell, J.M.A., Matthews, R.K., and Mesolella, K.J., **1974**, *Quaternary Research*, 4, 185-205; Uranium series ages for coral reefs 5-9, 41, 61, 85, 107, and 118-142 thousand years in age, exposed on the rapidly uplifting New Guinea coast.
- Ku, T.-L. and Kern, J.P., **1974**, *Geological Society of America Bulletin*, 85, 1713-1716; Uranium series ages for solitary corals from a raised terrace in San Diego.
- Ku, T.-L., Kimmel, M., Easton, W.H., and O'Neil, T.J., **1974**, *Science*, 183, 959-962; Uranium series age for the last interglacial coral reef on Hawaii.
- Stearns, H.T., **1974**, *Geological Society of America Bulletin*, 85, 795-804; Significance of uranium series ages on raised coral reefs in Hawaii.
- Neumann, A.C. and Moore, W.S., **1975**, *Quaternary Research*, 5, 215-224; Uranium series ages for the last interglacial coral reef in the Bahamas.
- Ku, T.L., **1976**, *Annual Review of Earth and Planetary Sciences*, 4, 347-379; Review article on uranium series dating.
- Marshall, J.F. and Thom, B.G., **1976**, *Nature*, 263, 120-121; Uranium series ages for last interglacial coral reefs in eastern Australia.
- Mangini, A., **1978**, *Meteor Forschungsergeb.*, 29, 1-5; Uranium series measurements on core from African continental rise.
- Turekian, K.K. and Cochran, J.K., **1978**, In: Chester, J.P. and R. (eds.), *Chemical Oceanography*, Academic Press, New York, 7, 313-360; Review article on methods used to date marine sediments.
- Omura, A., Emerson, W.K., and Ku, T.-L., **1979**, *The Nautilus*, 93, 184-189; Uranium series dating of solitary corals from raised terraces in Baja, California.
- Veeh, H.H., Schwebel, D., van de Graff, W.J.E., and Denman, P.D., **1979**, *Journal of the Geological Society of Australia*, 26, 285-292; Uranium series ages for the last interglacial age coral reef in western Australia.

- Anderson, R.F., Bacon, M.P., and Brewer, P.G., **1983**, *Earth and Planetary Science Letters*, 66, 73-90; Removal of ^{230}Th and ^{231}Pa from open ocean waters.
- Dodge, R.E., Fairbanks, R.G., Benninger, L.K., and Maurrasse, F., **1983**, *Science*, 219, 1423-1425; Uranium series ages for raised coral reefs on the island of Haiti.
- Harmon, R.S., Mitterer, R.M., Kriausakul, N., Land, L.S., Schwarcz, H.P., Garrett, P., Larson, G.J., Vacher, H.L., and Rowe, M., **1983**, *Palaeogeography, Palaeoclimatology, Palaeoecology*, 44, 41-70; Uranium series age for the last interglacial reef on Bermuda.
- Somayajulu, B.L.K., Broecker, W.S., and Goddard, J., **1985**, *Quaternary Research*, 24, 235-239; Uranium series age for the last interglacial coral reef in India.
- Szabo, B.J., Tracey, J.I., Jr., and Gotter, E.R., **1985**, *Quaternary Research*, 23, 54-61; Uranium series ages for submerged coral reefs on the Enewetak Atoll.
- Taylor, F.W., Jouannic, C., and Bloom, A.L., **1985**, *Journal of Geology*, 93, 419-438; Uranium series ages for raised coral reefs in the New Hebrides Islands.
- Kaufman, A., **1986**, *Quaternary Research*, 25, 55-62; A summary of alpha spectrometric ages for raised coral reefs of last interglacial age.
- Yang, H.-S., Nozaki, Y., Sakai, H., **1986**, *Geochimica et Cosmochimica Acta*, 50, 81-89; ^{230}Th to ^{231}Pa ratios in surface sediments.
- Edwards, R.L., Chen, J.H., and Wasserburg, G.J., **1987**, *Earth and Planetary Science Letters*, 81, 175-192; First demonstration that far more precise uranium series age measurements can be achieved by mass spectrometry.
- Edwards, R.L., Chen, J.H., Ku, T.-L., and Wasserburg, G.J., **1987**, *Science*, 236, 1547-1553; Uranium series dating of last interglacial corals by mass spectrometry.
- Pickett, J.W., Ku, T.-L., Thompson, C.H., Roman, D., Kelley, R.A., and Huang, Y.P., **1989**, *Quaternary Research*, 31, 392-395; Uranium series dating of last interglacial coral reefs in eastern Australia.
- Bard, E., Hamelin, B., Fairbanks, R.G., and Zindler, A., **1990**, *Nature*, 345, 405-409; Comparison between radiocarbon and uranium series ages on glacial age Barbados corals.
- Bard, E., Hamelin, B., and Fairbanks, R.G., **1990**, *Nature*, 346, 456-458; Additional uranium series ages for Barbados corals by the mass spectrometry method.
- Ku, T.-L., Ivanovich, M., and Luo, S., **1990**, *Quaternary Research*, 33, 129-147; Improved precision of the chronology of Barbados corals by the alpha spectrometry method.
- Bard, E., Fairbanks, R.G., Hamelin, B., Zindler, A., and Hoang, C. T., **1991**, *Geochimica et Cosmochimica Acta*, 55, 2385-2390; ^{234}U systematics in fossil coral.

- Chappell, J. and Polach, H., **1991**, *Nature*, 349, 147-149; Radiocarbon dating of corals from a 52 meter deep boring in New Guinea.
- Hamelin, B., Bard, E., Zindler, A., and Fairbanks, R.G., **1991**, *Earth and Planetary Science Letters*, 106, 169-180; ^{234}U systematics in fossil coral.
- Hoang, C.T. and Taviani, **1991**, *Quaternary Research*, 35, 264-273; Uranium series dating of last interglacial corals on islands in the Red Sea.
- Woodroffe, C.D., Short, S.A., Stoddart, D.R., Spencer, T., and Harmon, R.S., **1991**, *Quaternary Research*, 35, 246-263; Uranium series ages on last interglacial coral reefs on the slowly uplifting Cook Islands.
- Henderson, G.M., Cohen, A.S., and O'Nions, R.K. **1993**, *Earth and Planetary Science Letters*, 115, 65-73, $^{234}\text{U}/^{238}\text{U}$ ratios and ^{230}Th ages for Hateruma Atoll corals: Implications for coral diagenesis and seawater $^{234}\text{U}/^{238}\text{U}$ ratios.
- Stein, M. et al., **1993**, *Geochimica et Cosmochimica Acta*, 57, 2541-2554, TIMS U-series dating and stable isotopes of the last interglacial event in Papua New Guinea.
- Gallup, C.D., Edwards, R.L., and Johnson, R.G., **1994**, *Science*, 263, 796-800, The timing of high sea levels over the past 200,000 years.
- Szabo, B.J., Ludwig, K.R., Muhs, D.R., and Simmons, K.R., **1994**, *Science*, 266, 93-96; Uranium series dating of the Devil's Hole calcite.
- Gallup, C.D. et al., **1995**, *EOS*, 76, 291-292, Constraints on past changes in the marine $\delta^{234}\text{U}$ value from Northern Nicaragua rise, Caribbean sea cores.
- Stirling, C.H. et al. **1995**, *Earth and Planetary Science Letters*, 135, 115-130, High-precision U-series dating of corals from Western Australia and implications for the timing and duration of the Last Interglacial.
- Bard, E. et al., **1996**, *Geophysical Research Letters*, 23, 1473-1476, Pleistocene sea levels and tectonic uplift based on dating of corals from Sumba Island, Indonesia.
- Slowey, N.C., Henderson, G.M., and Curry, W.B., **1996**, *Nature*, 383, 242-244, Direct U-Th dating of marine sediments from the two most recent interglacial periods.
- Edwards, R.L. et al., **1997**, *Science*, 276, 782-786, Protactinium-231 dating of carbonates by thermal ionization mass spectrometry: Implications for Quaternary climate change.
- Winograd, I.J. et al., **1997**, *Quaternary Research*, 48, 141-154, Duration and structure of the past four interglaciations.
- Bard, E et al., **1998**, *Radiocarbon*, 40, 1085-1092, Radiocarbon calibration by means of mass spectrometric $^{230}\text{U}/^{234}\text{U}$ and ^{14}C ages of corals. An updated data base including samples from Barbados, Mururoa, and Tahiti.
- Stirling C.H. et al., **1998**, *Earth and Planetary Science Letters*, 160, 745-762, Timing and duration of the Last Interglacial: Evidence for a restricted interval of widespread coral reef growth.

Esat, T.M. et al., **1999**, *Science*, 283, 197-201, Rapid fluctuations in sea level recorded at Huon Peninsula during the penultimate deglaciation.

Henderson, G.M., Slowey, N.C., and Haddad, G.A., **1999**, *Earth and Planetary Science Letters*, 169, 99-111, Fluid flow through carbonate platforms: Constraints from $^{234}\text{U}/^{238}\text{U}$ and Cl- in Bahamas pore-waters.

Cheng, H. et al., **2000**, *Chemical Geology*, 169, 17-33, The half lives of uranium-234 and thorium-230.

Henderson, G.M., and Slowey, N.C., **2000**, *Nature*, 402, 61-66, Evidence from U-Th dating against northern-hemisphere forcing of the penultimate deglaciation.

Wang, Y.J. et al., **2001**, *Science*, 294, 2345-2348, A high-resolution absolute-dated Late Pleistocene monsoon record from Hulu Cave, China.

21) Cosmogenic isotope dating

Lingenfelter, R.E., **1963**, *Reviews Geophysics*, 1, 35-55, Production of ^{14}C by cosmic ray neutrons.

Craig, H., and Poreda, R.J., **1986**, *Proceedings National Academy Sciences*, 83, 1970-1974, Cosmogenic ^3He in terrestrial rocks: The summit lavas of Maui.

Kurz, M.D., **1986**, *Nature*, 320, 435-439, Cosmogenic helium in a terrestrial igneous rock.

Lal, D., **1986**, In: Hurford, A.J., Jäger, E., and Ten Cate, J.A.M. (eds.), *Dating Young Sediments*, CCOP Technical Secretariat, Bangkok, 285-297, On the study of continental erosion rates and cycles using cosmogenic ^{10}Be and ^{26}Al and other isotopes.

Lal, D., **1987a**, *Instr. Meth. Phys. Res.*, B29, 238-245, Cosmogenic nuclides produced in situ in terrestrial solids.

Lal, D., **1987b**, *Chemical Geology (Isotope Geoscience Section)*, 66, 89-98, Production of ^3He in terrestrial rocks.

Lal, D., **1988a**, *Annual Reviews Earth Planetary Science*, 16, 355-388, In situ produced cosmogenic isotopes in terrestrial rocks.

Lal, D., **1988b**, In: *Proceedings 45th Solar-Terrestrial Relationships and the Earth Environment in the Last Millennia*, Bologna, Italy: Soc. Ital. Fis., 216-233, Theoretically expected variations in the terrestrial cosmic-ray production of isotopes.

Jull, A.J.T. et al., **1989**, *Radiocarbon*, 31, 719-724, Spallogenic ^{14}C in high-altitude rocks and in Antarctic meteorites.

Nishizumi, K. et al., **1989**, *Journal of Geophysical Research*, 94, 17,907-17,915, Cosmic ray production rates of ^{10}Be and ^{26}Al in quartz from glacially polished rocks.

Cerling, T.E., **1990**, *Quaternary Research*, 33, 148-156, Dating geomorphic surfaces using cosmogenic ^3He .

Phillips, F.M. et al., **1990**, *Science*, 248, 1529-1532, Cosmogenic chlorine-36 chronology for glacial deposits at Bloody Canyon, eastern Sierra Nevada.

Yiou, F. et al., **1991**, *Geochimica et Cosmochimica Acta*, 55, 2269-2283, Examination of surface exposure ages of Antarctic moraines using in situ ^{10}Be and ^{26}Al .

Brown, E.T. et al., **1992**, *Geophysical Research Letters*, 19, 369-372, Effective attenuation lengths of cosmic rays producing ^{10}Be and ^{26}Al in quartz: Implications for exposure age dating.

Jull, A.J.T. et al., **1992**, *Radiocarbon*, 34, 737-744, Measurements of cosmogenic ^{14}C produced by spallation in high-altitude rocks.

Zreda, M.G., and Phillips, F.M., **1994**, In: Beck, C. (ed.), *Dating in Exposed and Surface Contexts*, Univ. New Mexico Press, Albuquerque, NM, 161-183, Surface exposure dating by cosmogenic chlorine-36 accumulation.

Zreda, M.G. et al., **1993**, *Geology*, 21, 57-60, Cosmogenic ^{36}Cl dating of a young basaltic eruption complex, Lathrop Wells, Nevada.

Cerling, T.E., and Craig, H., **1994**, *Annual Reviews Earth Planetary Science*, 22, 273-317, Geomorphology and in-situ cosmogenic isotopes.

Cerling, T.E., and Craig, H., **1994**, *Geochimica et Cosmochimica Acta*, 58, 249-255, Cosmogenic ^3He production rates from 39°N to 46°N latitude, western USA and France.

Cerling, T.E., Poreda, R.J., and Rathburn, S.L., **1994**, *Geology*, 22, 227-230, Cosmogenic ^3He and ^{21}Ne age of the Big Lost River Flood, Snake River Plain, Idaho.

Gosse, J.C. et al., **1995**, *Science*, 268, 1329-1333, Beryllium-10 dating of the duration and retreat of the last Pinedale glacial sequence.

Brook, E.J. et al., **1996**, *Geology*, 24, 207-210, Cosmogenic nuclide exposure ages along a vertical transect in western Norway: Implications for the height of the Fennoscandian ice sheet.

Ivy-Ochs, S. et al., **1996**, *Eclogae geol. Helv.*, 89, 1049-1063, the exposure age of an Egesen moraine at Julier Pass, Switzerland, measured with the cosmogenic radionuclides ^{10}Be , ^{26}Al and ^{36}Cl .

Phillips, F.M. et al., **1996**, *Science*, 274, 749-751, Chronology for fluctuations in late Pleistocene Sierra Nevada glaciers and lakes.

Ivy-Ochs, S. et al., **1998**, In: *Zeitschrift für Gletscherkunde und Glazialgeologie*, University Wagner, Innsbruck, 34, 57-70, The age of the Köfels event, relative ^{14}C and cosmogenic isotope dating of an early Holocene landslide in the central Alps (Tyrol, Austria).

Kubik, P.W. et al., **1998**, *Earth and Planetary Science Letters*, 161, 231-241, ^{10}Be and ^{26}Al production rates deduced from an instantaneous event within the dendro-calibration curve, the landslide of Köfels, Ötztal Valley, Austria.

Schafer, J.M. et al., **1999**, *Earth and Planetary Science Letters*, 167, 215-226, Cosmogenic noble gas studies in the oldest landscape on earth: surface exposure ages of the Dry Valleys, Antarctica.

Briner, J.P., Swanson, T.W., and Caffee, M., **2001**, *Quaternary Research*, 56, 148-154, Late Pleistocene cosmogenic ^{36}Cl glacial chronology of the southwestern Ahklun Mountains, Alaska.

Gosse, J.C. and Phillips, F.M., **2001**, *Quaternary Science Reviews*, 20, 1475-1560, Terrestrial in situ cosmogenic nuclides: Theory and application.

Schäfer, J.M. et al., **2002**, *Earth and Planetary Science Letters*, 194, 287-297, The limited influence of glaciations in Tibet on global climate over the past 170,000 yr.

22. Luminescence dating

Wintle, A.G. and Huntley, D.J., **1980**, *Canadian Journal of Earth Science*, 17, 348-360, Thermoluminescence dating of ocean sediments.

Wintle, A.G., **1985**, *Nature*, 313, 99-105, Lighting up the past with lasers.

Mejdahl, V., **1986**, *Radiation Protection Dosimetry*, 17, 219-227, Thermoluminescence dating of sediments.

Aitken, M.J., **1990**, *Radiation Protection Dosimetry*, 34, 55-60, TLD methods in archaeometry, geology and sediment studies.

Aitken, M.J., **1992**, *Science Reviews*, 11, 127-131, Optical dating.

Mejdahl, V. and Christiansen, H.H., **1994**, *Quaternary Geochronology (Quaternary Science Reviews)*, 13, 403-406, Procedures used for liminescence dating of sediments.

Murray, A.S., Olley, J.M., and Caicheon, G.G., **1995**, *Quaternary Science Reviews*, 14, 365-371, Measurement of equivalent doses in quartz from contemporary water-lain sediments using optically stimulated liminescence.

Duller, G.A.T., **1996**, *Progress in Physical Geography*, 20, 127-145, Recent developments in luminescence dating of Quaternary sediments.

Krbetschek, M.R., Götze, J., Dietrich, A., and Trautmann, T., **1997**, *Radiation Measurements*, 27, 695-748, Spectral information from minerals.

Prescott, J.R. and Robertson, G.B., **1997**, *Radiation Measurements*, 27, 893-922, Sediment dating by liminescence: A review.

Wintle, A.G., **1997**, *Radiation Measurements*, 27, 769-817, Luminescence dating: Laboratory procedures and protocols.

Aitken, M.J., **1998**, 267 S., University Press, Oxford, *An introduction to optical dating*.

Olley, J.M., Caicheon, G.G., and Murray, A.S., **1998**, *Quaternary Science Reviews*, 17, 1033-1040, The distribution of apparent dose as determined by optically stimulated luminescence in small aliquots of fluvial quartz: Implications for dating young sediments.

Murray, A.S. and Wintle, A.G., **2000**, *Radiation Measurements*, 33, 57-73, Luminescence dating of quartz using an improved single-aliquot regenerative-dose protocol.

Banerjee, D., Murray, A.S., Bøtter-Jensen, L., and Lang, A., **2001**, *Radiation Measurements*, 33, 73-93, Equivalent dose estimation using a single aliquot of polymineral fine grains.

23) Milankovitch seasonality cycles

Croll, J., **1867**, *Philosophical Magazine*, 33, 119-131; The possible influence of the eccentricity of the Earth's orbit on climate.

Croll, J., **1867**, *Philosophical Magazine*, 33, 426-445; The possible influence of the obliquity of the ecliptic on climate.

Milankovitch, M., **1920**, *Théorie mathématique des phénomènes thermiques produits par la radiation solaire*, Gauthier-Villars, Paris; The intensity of incoming solar radiation as a function of latitude and season.

Milankovitch, M., **1938**, In: Gutenberg, B., (ed.), *Handbuch der Geophysik*, 9, Berlin, 593-698; The influence of axial tilt and precession as the cause of glacial cycles.

Emiliani, C., **1955**, *Journal of Geology*, 63, 538-578; First demonstration that the oxygen isotope record in deep sea cores contained Milankovitch frequencies.

Broecker, W.S., Thurber, D.L., Goddard, J., Ku, T., Matthews, R.K., and Mesolella, K.J., **1968**, *Science*, 159, 1-4; Demonstration that sea level cycles followed the 23,000-year precession cycle.

Vernekar, A.D., **1972**, *Meteorological Monographs*, 12, American Meteorological Society, Boston; Improved calculation of orbital-induced seasonality cycles.

Hays, J.D., Imbrie, J., and Shackleton, N.J., 1976, *Science*, 194, 1121-1132; Rigorous demonstration that the oxygen isotope record contains the Milankovitch frequencies.

Imbrie, J. and Imbrie, J.Z., **1980**, *Science*, 207, 943-953; Model showing how Milankovitch cycles might produce the observed glacial cycles.

Imbrie, J., **1985**, *Journal of the Geological Society of London*, 142, 417-432; A theoretical framework for the Pleistocene ice ages.

Broecker, W.S. and Denton, G.H., **1990**, *Quaternary Science Reviews*, 9, 305-341; Demonstration that abrupt changes in ocean circulation play a key role in the tie between Milankovitch cycles and climate.

Berger, A., Loutre,M.F.,and Laskar, J., **1992**, *Science*, 255, 560-566; Stability of the orbital frequencies.

Imbrie, J., Boyle, E.A., Clemens, S.C., Duffy, A., Howard, W.R., Kukla, G., Kutzbach, J., Martinson, D.G., McIntyre, A., Mix, A.C., Molino, B., Morley, J.J., Peterson, L.C., Pisias, N.G., Prell, W.L., Raymo, M.E., Shackleton, N.J. and Toggweiler, J.R., **1992**, *Paleoceanography*, 7, 701-738; Linear responses to Milankovitch forcing.

Imbrie, J., Berger, A., and Shackleton, N.J., **1993**, In: Eddy, J.A. and Oeschger, H. (eds.), *Global Changes in the Perspective of the Past*, John Wiley & Sons Ltd., New York, 263-277; A review of the role of orbital forcing in climate change.

Bassinot, F.C. et al., **1994**, *Earth and Planetary Science Letters*, 126, 91-108, The astronomical theory of climate and the age of the Brunhes-Matuyama magnetic reversal.

Berger, A. and Loutre, M.F., **1994**, In: Boutron, Cl. (ed.), *Topics in Atmospheric and Interstellar Physics and Chemistry*, Les Editions de Physique, Les Ulis, France, 33-61, Long-term variations of the astronomical seasons.

Berger, A. and Loutre, M.F., **1994**, In: Duplessy, J.-C. and Spyridakis, M.-T. (eds.), *Long-Term Climatic Variations*, NATO ASI Series, 122, Springer-Verlag, Berlin Heidelberg, 108-151, Precession, Eccentricity, obliquity, insolation and paleoclimates.

Hagelberg, T.K., Bond, G. and deMenocal, P., **1994**, *Paleoceanography*, 9, 545-558; Evidence for climate forcing by the split precession cycle.

Jiang, X. and Peltier, W.R., **1996**, *Earth and Planetary Science Letters*, 139, 17-32, Ten million year histories of obliquity and precession: The influence of the ice-age cycle.

Muller, R.A. and MacDonald, G.J., **1997**, *Science*, 277, 215-218, Glacial cycles and astronomical forcing.

Kent, D.V. and Olsen, P.E., **1999**, *Journal of Geophysical Research*, 104, 12,831-12,841, Astronomically tuned geomagnetic polarity timescale.

Olsen, P.E. and Kent, D.V., **1999**, *Phil. Trans. R. Soc. Lond. A*, 357, 1761-1786, Long-period Milankovitch cycles from the Late Triassic and Early Jurassic of eastern North America and their implications for the calibration of the Early Mesozoic time-scale and the long-term behaviour of the planets.

Ridgwell, A.J., Watson, A.J. and Maureen E. Raymo, **1999**, *Paleoceanography*, 14, 437-440, Is the spectral signature of the 100 kyr glacial cycle consistent with a Milankovitch origin?

24) The 100,000-year cycle

Raymo, M.E., **1997**, *Paleoceanography*, 12, 577-585, The timing of major climate terminations.

Broecker, W.S. and Henderson, G.M., **1998**, *Paleoceanography*, 13, 352-364, The sequence of events surrounding Termination II and their implications for the cause of glacial-interglacial CO₂ changes.

Shackleton, N.J., **2000**, *Science*, 289, 1897-1902, The 100,000-year ice-age cycle identified and found to lag temperature, Carbon dioxide, and orbital eccentricity.

25) The Bølling Allerød-Younger Dryas

Kennett, J.P. and Shackleton, N.J., **1975**, *Science*, 188, 147-150; Evidence for the discharge of pre Younger Dryas meltwater via the Mississippi River into the Gulf of Mexico.

Eicher, U., Siegenthaler, U., and Wegmüller, **1981**, *Quaternary Research*, 15, 160-170; Oxygen isotope and pollen evidence for the Bølling Allerød-Younger Dryas oscillation from the sediments of a small lake in the vicinity of Grenoble, France.

Leventer, A., Williams, D.F., and Kennett, J.P., **1982**, *Earth and Planetary Science Letters*, 59, 11-17; Further evidence for the pre Younger Dryas Mississippi meltwater event.

Leventer, A., Williams, D.F., and Kennett, J.P., **1983**, *Marine Geology*, 53, 23-40; Still more.

Mangerud, J., Lie, S.E., Furnes, H., Kristiansen, I.L., and Lømo L., **1984**, *Quaternary Research*, 21, 85-104; Discovery of the mid Younger Dryas Vedde ash bed.

Siegenthaler, U., Eicher, U., Oeschger, H., and Dansgaard, W., **1984**, *Annals of Glaciology*, 5, 149-152; Comparison of the late glacial oxygen isotope records for sediments in a small Swiss lake with that for the Dye 3 Greenland ice core.

Kennett, J.P., Elmstrom, K., and Penrose, N., **1985**, *Palaeogeography, Palaeoclimatology, Palaeoecology*, 50, 189-216; A higher resolution oxygen isotope record for the Mississippi meltwater event.

Mott, R.J., Grant, D.R., Stea, R., and Occhietti, **1986**, *Nature*, 323, 247-250; Evidence for the Younger Dryas event in Atlantic Canada.

Rind, D., Peteet, D., Broecker, W., McIntyre, A., and Ruddiman, W., **1986**, *Climate Dynamics*, 1, 3-33; Comparison of the observed geographic distribution of Younger Dryas impacts with that predicted by a G.C.M. model which assumes the CLIMAP-based temperature change for the northern Atlantic Ocean.

Atkinson, T.C., Briffa, K.R., and Coope, G.R., **1987**, *Nature*, 325, 587-592; Evidence based on beetle remains for a Younger Dryas cooling in the British Isles.

Bard, E., Arnold, M., Duprat, J., Moyes, J., and Duplessy, J.-C., **1987**, *Climate Dynamics*, 1, 101-112; Dealing with the impacts of bioturbation on the

radiocarbon dates for foraminifera from deep sea cores for the deglacial time interval.

Chinzei, K., Fujioka, K., Kitazato, H., Koizumi, I., Oba, T., Oda, M., Okada, H., Sakai, T., and Tanimura, Y., **1987**, *Marine Micropaleontology*, 11, 273-291; Evidence for the Younger Dryas in the marine record off central Japan.

Heusser, C.J. and Rabassa, J., **1987**, *Nature*, 328, 609-611; Evidence for a Younger Dryas cooling as recorded in Tierra del Fuego bog pollen.

Shane, L.C., **1987**, *Boreas*, 16, 1-20; Evidence for a Younger Dryas cooling as recorded in central Ohio bog pollen.

Teller, J.T., **1987**, In: Ruddiman, W. and Wright, H.E., (eds.) *The Last Deglaciation in North America and Adjacent Oceans: Responses and Mechanisms*, Geological Society of America, The Geology of North America, K-3, 39-69; Diversion of meltwater from the Mississippi to the St. Lawrence drainage.

Broecker, W.S., Andree, M., Wolfli, W., Oeschger, H., Bonani, G., Kennett, J., and Peteet, D., **1988**, *Paleoceanography*, 3, 1-19; A case in support of a meltwater diversion as the trigger for the onset of the Younger Dryas.

Kallel, N., Labeyrie, L.D., Arnold, M., Okada, H., Dudley, W.C., and Duplessy, J.-C., **1988**, *Oceanologia Acta*, 12, 369-375; Evidence from Younger Dryas impacts in the northern Pacific Ocean.

Bard, E., Fairbanks, R., Arnold, M., Maurice, P., Duprat, J., Moyes, J., and Duplessy, J.-C., **1989**, *Quaternary Research*, 31, 381-391; Use of the oxygen isotope record in planktonic foraminifera to estimate sea level changes during the last deglaciation.

Broecker, W.S., Kennett, J.P., Flower, B.P., Teller, J.T., Trumbore, S., Bonani, G., and Wolfli, W., **1989**, *Nature*, 341, 318-321; Meltwater routing from the Laurentian ice sheet during the last deglaciation.

Fairbanks, R.G., **1989**, *Nature*, 342, 637-642; Sea level rise during the last deglaciation as recorded in Barbados corals.

Labracherie, M., Labeyrie, L.D., Duprat, J., Bard, E., Arnold, M., Pichon, J.-J., and Duplessy, J.-C., **1989**, *Paleoceanography*, 4, 629-638; The deglaciation as recorded in sediments from the Southern Ocean.

Lotter, A.F. and Zbinden, H., **1989**, *Eclogae geol. Helv.*, 82/1, 191-202; Detailed pollen and oxygen isotope record for Rotsee (Lucerne, Switzerland) showing the abruptness of the climate changes at 12,700 and 10,000 Libby years ago.

Teller, J.T., **1989**, *Quaternary Research*, 32, 12-23; Timing of the diversion of the outflow from proglacial Lake Agassiz to the St. Lawrence drainage.

Ammann, B. and Lotter, A.F., **1989**, *Boreas*, 18, 109-126; Summary of pollen and oxygen isotope records from small lakes on the Swiss Plateau.

Berger, W.H., **1990**, *Palaeogeography, Palaeoclimatology, Palaeoecology*, 89, 219-237; A discussion of the possible causes for the Younger Dryas.

Engstrom, D.R., Hansen, B.C.S., and Wright, H.E., Jr., **1990**, *Science*, 250, 1383-1385; Evidence in support of a Younger Dryas cooling in Alaska.

Fairbanks, R.G., **1990**, *Paleoceanography*, 5, 937-948; The relationship between the deglacial record of sea level rise as recorded in Barbados corals and air temperature change as recorded in the Greenland ice cap.

Jansen, E. and Veum, T., **1990**, *Nature*, 343, 612-616; Implication of the carbon isotope record during the last deglaciation for planktic and benthic foraminifera from the northern Atlantic sediments.

Keigwin, L.D., and Jones, G.A., **1990**, *Paleoceanography*, 5, 1009-1023; Evidence for Younger Dryas impacts in the Gulf of California.

Linsley, B.K. and Thunell, R.C., **1990**, *Paleoceanography*, 5, 1025-1039; Evidence for Younger Dryas impacts in planktonic foraminifera assemblages in the Sulu Sea.

Peteet, D.M., Vogel, J.S., Nelson, D.E., Southon, J.R., Nickmann, R.J., and Heusser, L.E., **1990**, *Quaternary Research*, 33, 219-230; Evidence for a Younger Dryas impact on the pollen assemblage as recorded in an Alpine New Jersey swamp.

Deckker, P.D., Corrège, T., and Head, J., **1991**, *Geology*, 19, 602-605; A search for Younger Dryas impacts in tropical Australia.

Kudrass, H.R., Erlenkeuser, H., Vollbrecht, R., and Weiss, W., **1991**, *Nature*, 349, 406-409; Younger Dryas impacts on the oxygen isotope composition of planktonic foraminifera from the Sulu Sea.

Lotter, A.F., **1991**, *Quaternary Research*, 35, 321-330; An attempt to establish the absolute age of the Younger Dryas based on annually layered sediments in Swiss lake Rotsee.

Walker, I.R., Mott, R.J., and Smol, J.P., **1991**, *Science*, 253, 1010-1012; Pollen evidence for a Younger Dryas cooling in Atlantic Canada.

Charles, C.D. and Fairbanks, R.G., **1992**, *Nature*, 355, 416-419; Evidence for changes in the flux of NADW to the Southern Ocean during the deglacial period.

Lehman, S.J. and Keigwin, L.D., **1992**, *Nature*, 356, 757-762; Evidence for abrupt climate changes from marine sediment in the northern Atlantic basin during the deglacial period.

Alley, R.B., Meese, D.A., Shuman, C.A., Gow, A.J., Taylor, K.C., Grootes, P.M., White, J.W.C., Ram, M., Waddington, E.D., Mayewski, P.A., and Zielinski, G.A., **1993**, *Nature*, 362, 527-529; Twofold lower snow accumulation rates during the Younger Dryas at the Summit Greenland locale.

Goslar, T., Kuc, T., Ralska-Jasiewiczowa, M., Różański, K., Arnold, M., Bard, E., van Geel, B., Pazdur, M.F., Szeroczynska, K., Wicik, B., Wieckowski, K., and Walanus, A., **1993**, *Quaternary Science Reviews*, 12, 287-294; Evidence for a Younger Dryas shift in the oxygen isotope composition CaCO₃ from Lake Gosciaz, Poland.

Hajdas, I., Ivy, S.D., Beer, J., Bonani, G., Imboden, D., Lotter, A.F., Sturm, M., and Suter, M., **1993**, *Climate Dynamics*, 9, 107-116; Comparison of radiocarbon and varve-based ages for the Younger Dryas in Swiss Lake Soppensee.

Mathewes, R.W., **1993**, *Quaternary Science Reviews*, 12, 321-332; Pollen-based evidence for a Younger Dryas cooling in the Pacific Northwest.

Mathewes, R.W., Heusser, L.E., and Patterson, R.T., **1993**, *Geology*, 21, 101-104; Pollen-based evidence for a Younger Dryas cooling in British Columbia.

Mayewski, P.A., Meeker, L.D., Whitlow, S., Twickler, M.S., Morrison, M.C., Alley, R.B., Bloomfield, P., and Taylor, K., **1993**, *Science*, 261, 195-197; Evidence for a pronounced increase in dustiness of the air over Greenland during the Younger Dryas.

Taylor, K.C., Lamorey, G.W., Doyle, G.A., Alley, R.B., Grootes, P.M., Mayewski, P.A., White, J.W.C., and Barlow, L.K., **1993**, *Nature*, 361, 432-436; Abruptness of the changes in acidity of the Greenland ice at the times of abrupt warming (i.e., at 12,700 and 10,000 Libby years).

Denton, G.H. and Hendy, C.H., **1994**, *Science*, 264, 1434-1437; Documentation of an advance of New Zealand's Franz Josef Glacial at the onset of Younger Dryas time.

Kennett, J.P. and Ingram, B.L., **1995**, *Nature*, 377, 510-514, A 20,000-year record of ocean circulation and climate change from the Santa Barbara basin.

Peteet, D., **1995**, *Quaternary International*, 28, 93-104, Global Younger Dryas?

Van der Hammen, T. and Hooghiemstra, H., **1995**, *Quaternary Science Reviews*, 14, 841-851, The El Abra Stadial, a Younger Dryas equivalent in Colombia.

de Vernal, A., Hillaire-Marcel, C., and Bilodeau, G., **1996**, *Nature*, 381, 774-777, Reduced meltwater outflow from the Laurentide ice margin during the Younger Dryas.

Duplessy, J.C., Labeyrie, L.D., and Paterne, M., **1996**, In: Andrews, J.T., Austin, W.E.N., Bergsten, H. and Jennings, A.E. (eds.), *Late Quaternary Palaeoceanography of the North Atlantic Margins*, Geological Society Special Publications 111, 167-175, North Atlantic sea surface conditions during the Younger Dryas cold event.

Elias, S.A., **1996**, *Quaternary Research*, 46, 311-318, Late Pleistocene and Holocene seasonal temperatures reconstructed from fossil beetle assemblages in the Rocky Mountains.

Hughen, K.A. et al., **1996**, *Nature*, 380, 51-54, Rapid climate changes in the tropical Atlantic region during the last deglaciation.

Thunell, R.C. and Miao, Q., **1996**, *Quaternary Research*, 46, 72-77, Sea surface temperature of the western equatorial Pacific Ocean during the Younger Dryas.

Clapperton, C.M. et al., **1997**, *Quaternary Research*, 47, 13-28, A Younger Dryas icecap in the equatorial Andes.

Lin, H.-L. et al., **1997**, *Paleoceanography*, 12, 415-427, Late Quaternary climate change from $\delta^{18}\text{O}$ records of multiple species of planktonic foraminifera: High-resolution records from the anoxic Cariaco Basin, Venezuela.

Broecker, W.S., **1998**, *Paleoceanography*, 13, 119-121, Paleocean circulation during the last deglaciation: A bipolar seesaw?

Yu, Z. and Eicher, U., **1998**, *Science*, 282, 2235-2238, Abrupt climate oscillations during the last deglaciation in central North America.

Lotter, A.F. et al., **2000**, *Palaeogeography, Palaeoclimatology, Palaeoecology*, 159, 349-361, Younger Dryas and Allerød summer temperatures at Gerzensee (Switzerland) inferred from fossil pollen and cladoceran assemblages.

Maslin, M.A. and Burns, S.J., **2000**, *Science*, 290, 2285-2287, Reconstruction of the Amazon Basin effective moisture availability over the past 14,000 years.

Moore, T.C. et al., **2000**, *Paleoceanography*, 15, 4-18, Younger Dryas interval and outflow from the Laurentide.

Zheng, Y. et al., **2000**, *Paleoceanography*, 15, 528-536, Intensification of the northeast Pacific oxygen minimum zone during the Bölling-Alleröd warm period.

Clark, P.U. et al., **2001**, *Science*, 293, 283-287, Freshwater forcing of abrupt climate change during the last glaciation.

Pendall, E. et al., **2001**, *Quaternary Research*, 55, 168-178, Multiproxy record of Late Pleistocene—Holocene climate and vegetation changes from a peat bog in Patagonia.

26) Heinrich events

Heinrich, H., **1988**, *Quaternary Research*, 29, 142-152; Discovery and description of six layers rich in ice-raftered debris in the sediment cores from the Dreizack seamount in the northeastern Atlantic.

Broecker, W., Bond, G., Klas, M., Clark, E., and McManus, J., **1992**, *Climate Dynamics*, 6, 265-273; Confirmation of Heinrich's finding in ODP core 609 from the northern Atlantic.

Andrews, J.T. and Tedesco, K., **1992**, *Geology*, 20, 1087-1090; Discovery of thick detrital carbonate-rich Heinrich equivalents in the Labrador Sea off Hudson Straits.

Bond, G., Heinrich, H., Broecker, W., Labeyrie, L., McManus, J., Andrews, J., Huon, S., Jantschik, R., Clasen, S., Simet, C., Tedesco, K., Klas, M., Bonani, G., and Ivy, S., **1992**, *Nature*, 360, 245-249; Summary of findings with regard to the geographic distribution composition and origin of Heinrich layers.

Bond, G., Broecker, W., Johnsen, S., McManus, J., Labeyrie, L., Jouzel, J., and Bonani, G., **1993**, *Nature*, 365, 143-147; Correlation between the climate record in northern Atlantic marine sediment and in Greenland ice.

Grimm, E.C., Jacobson, G.L., Jr., Watts, W.A., Hansen, B.C.S., and Maasch, K.A., **1993**, *Science*, 261, 198-201, A 50,000-year record of climatic oscillations from Florida and its temporal correlation with the Heinrich events.

Grousset, F.E., Labeyrie, L., Sinko, J.A., Cremer, M., Bond, G., Duprat, J., Cortijo, E., and Huon S., **1993**, *Paleoceanography*, 8, 175-192, Patterns of ice-raftered debris in the glacial North Atlantic (40-55°N).

MacAyeal, D.R., **1993a**, *Paleoceanography*, 8, 767-773, A low-order model of the Heinrich event cycle.

MacAyeal, D.R., **1993b**, *Paleoceanography*, 8, 775-784, Binge/purge oscillations of the Laurentide Ice Sheet as a cause of the North Atlantic's Heinrich events

Oerlemans, J., **1993**, *Nature*, 364, 783-785, Evaluating the role of climate cooling in iceberg production and the Heinrich events.

Alley, R.B. and MacAyeal, D.R., **1994**, *Paleoceanography*, 9, 503-511; Mechanism for entrainment of Heinrich debris in ice sheets.

Andrews, J.T., Erlenkeuser, H., Tedesco, K., Aksu, A.E., and Jull, A.J.T., **1994**, *Quaternary Research*, 41, 26-34; Additional evidence regarding Heinrich correlated debris layers in the Labrador Sea.

Broecker, W.S., **1994**, *Nature*, 372, 421-424; Iceberg discharges as triggers for global climate change.

François, R. and Bacon, M.P., **1994**, *Deep-sea Research*, 41, 315-334, Heinrich events in the North Atlantic: Radiochemical evidence.

Paillard, D. and Labeyrie, L., **1994**, *Nature*, 372, 162-164, Role of the thermohaline circulation in the abrupt warming after Heinrich events.

Bond, G.C. and Lotti, R., **1995**, *Science*, 267, 1005-1010; Detailed record of iceberg discharges into the northern Atlantic.

Andrews, J.T. et al., **1995**, *Paleoceanography*, 10, 943-952, A Heinrich-like event, H-0 (DC-0): Source(s) for detrital carbonate in the North Atlantic during the Younger Dryas chronozone.

Dowdeswell, J.A. et al., **1995**, *Geology*, 23, 301-304, Iceberg production, debris rafting, and the extent and thickness of Heinrich layers (H1, H2) in North Atlantic sediments.

Johnson, R.G. and Lauritzen, S.E., **1995**, *Palaeogeography, Palaeoclimatology, Palaeoecology*, 117, 123-137, Hudson Bay – Hudson Strait Jökulhlaups and Heinrich events: a hypothesis.

Maslin, M., Shackleton, N.J., and Pflaumann, U., **1995**, *Paleoceanography*, 10, 527-544, Surface temperature, salinity and density changes in the northeastern Atlantic during the last 45,000 years: Heinrich events, deep water formation and climatic rebounds.

Gwiazda, R.H., Hemming, S.R., and Broecker, W.S., **1996a**, *Paleoceanography*, 11, 77-93, Tracking the sources of icebergs with lead isotopes: The provenance of ice-rafted debris in Heinrich layer 2.

Gwiazda, R.H., Hemming, S.R., and Broecker, W.S., **1996b**, *Paleoceanography*, 11, 371-378, Provenance of icebergs during Heinrich event 3 and their contrast to their sources during other Heinrich episodes.

Gwiazda, R.H., Hemming, S.R., and Broecker, W.S., Onstott, T., and Mueller, C., **1996c**, *Journal of Glaciology*, 42, 440-446, Evidence from $^{40}\text{Ar}/^{39}\text{Ar}$ ages for a Churchill province source of ice-rafted amphiboles in Heinrich layer 2.

Jennings, A.E. et al., **1996**, In: Andrews, J.T. (ed.), *Late Quaternary Palaeoceanography of the North Atlantic Margins*, 3, 29-49, Geological Society Special Publication, Shelf erosion and glacial ice proximity in the labrador Sea during and after Heinrich events (H-3 or H-4 to H-0) as shown by foraminifera.

Stoner, J.S., Channell, J.E.T., and Hillaire-Marcel, C., **1996**, *Paleoceanography*, 11, 309-325, The magnetic signature of rapidly deposited detrital layers from the deep Labrador Sea: Relationship to North Atlantic Heinrich layers.

Van Kreveld, S. et al., **1996**, *Marine Geology*, 131, 21-48, Biogenic carbonates and ice-rafted debris (Heinrich Layer) accumulation in deep-sea sediments from a northeast Atlantic piston core.

Cortijo, E. et al., **1997**, *Earth and Planetary Science Letters*, 146, 29-45, Changes in sea-surface hydrology associated with Heinrich event 4 in the North Atlantic Ocean between 40° and 60°N.

Alley, R.B., **1998**, *Nature*, 392, 335-336, Icing the North Atlantic.

Andrews, J.T., **1998**, *Journal of Quaternary Sciences*, 13, 3-16, Abrupt changes (Heinrich events) in late Quaternary North Atlantic marine environments: A history and review of data and concepts.

Grousset, F.E., **1998**, *Oceanis*, 24, 1-18, Les évènements de Heinrich.

Hemming, S.R. et al., **1998**, *Earth and Planetary Science Letters*, 164, 317-333, Provenance of Heinrich layers in core V28-82, northeastern Atlantic: $^{40}\text{Ar}/^{39}\text{Ar}$ ages of ice-rafted hornblende, Pb isotopes in feldspar grains, and Nd-Sr-Pb isotopes in the fine sediment fraction.

Hunt, A.G. and Malin, P.E., **1998**, *Nature*, 393, 155-158, Possible triggering of Heinrich events by ice-load-induced earthquakes.

MacCabe, M., Knight, J., McCarron, S., **1998**, *Journal of Quaternary Sciences*, 13, 549-568, Evidence for Heinrich event 1 in the British Isles.

McManus, J.F. et al., **1998**, *Earth and Planetary Science Letters*, 155, 29-43, Radiometrically determined sedimentary fluxes in the sub-polar North Atlantic during the last 140,000 years.

Cacho, I. et al., **1999**, *Paleoceanography*, 14, 698-705, Dansgaard-Oeschger and Heinrich event imprints in Alboran sea temperatures.

Cayre, O. et al., **1999**, *Paleoceanography*, 14, 384-396, Paleoceanographic reconstructions from planktonic foraminifera off the Iberian margin: Temperature, salinity, and Heinrich events.

Hostetler, S.W. et al., **1999**, *Journal of Geophysical Research*, 104, 3947-3952, Atmospheric transmission of North Atlantic Heinrich events.

Seidov, D. and Maslin, M., **1999**, *Geology*, 27, 23-26, North Atlantic deep water circulation collapse during Heinrich events.

Veiga-Pires, C.C. and Hillaire-Marcel, C., **1999**, *Paleoceanography*, 14, 187-199, U and Th isotope constraints on the duration of Heinrich events H0-H4 in the southeastern Labrador Sea.

Bard, E. et al., **2000**, *Science*, 289, 1221-1324, Hydrological impact of Heinrich events in the subtropical Northeast Atlantic.

Grousset, F.E. et al., **2000**, *Geology*, 28, 123-126, Were the North Atlantic Heinrich events triggered by the behavior of the European ice sheets?

Hemming, S.R. et al., **2000**, *Quaternary Research*, 54, 372-383, Evidence from $^{40}\text{Ar}/^{39}\text{Ar}$ ages of individual hornblende grains for varying Laurentide sources of iceberg discharges 22,000 to 10,500 ^{14}C yr B.P.

Hemming, S.R. et al., **2000**, *Canadian Journal of Earth Sciences*, 37, 879-890, $^{40}\text{Ar}/^{39}\text{Ar}$ and Pb-Pb study of individual hornblende and feldspar grains from southeastern Baffin Island glacial sediments: Implications for the Provenance of the Heinrich layers.

Thouveny, N. et al., **2000**, *Earth and Planetary Science Letters*, 180, 61-75, Rock-magnetic detection of distal ice rafted debris: Clue for the identification of Heinrich layers on the Portuguese margin.

Bard, E., **2001**, *Geochemistry, Geophysics, Geosystems*, 3, #50, 1-12, Comparison of alkenone estimates with other temperature proxies.

Broecker, W.S. and Hemming, S.R., **2001**, *Science*, 294, 2308-2309, Climate swings come into focus.

Cacho, I. et al., **2001**, *Paleoceanography*, 16, 40-52, Variability of the western Mediterranean Sea surface temperature during the last 25,000 years and its connection with the Northern Hemisphere climatic changes.

Grousset, F.E. et al., **2001**, *Paleoceanography*, 16, 240-259, Zooming in on Heinrich layers.

Shackleton, N., **2001**, *Science*, 291, 58-59, Climate change across the hemispheres.

Hemming, S.R. et al., **2002**, *Chemical Geology*, 182, 583-603, $^{40}\text{Ar}/^{39}\text{Ar}$ ages and $^{40}\text{Ar}^*$ concentrations of fine-grained sediment fractions from North Atlantic Heinrich layers.

Huon, S., Grousset, F.E. et al., in press, **2002**, *Geochimica et Cosmochimica Acta*, Sources of fine organic matter in the North Atlantic Heinrich layers.

27) Dansgaard-Oeschger events

Dansgaard, W. et al., **1982**, *Science*, 218, 1273-1277, A new Greenland deep ice core.

Dansgaard, W. et al., **1984**, In: Hansen, J.E. and Takahashi, T. (eds.), *Climate Processes and Climate Sensitivity*, *Geophys. Monogr.*, 29, Maurice Ewing vol. 5, Am. Geophys. Union, Washington, D.C., 288-298, North Atlantic climatic oscillations revealed by deep Greenland ice cores.

Dansgaard, W., **1985**, *Palaeogeography, Palaeoclimatology, Palaeoecology*, 50, 185-187, Greenland ice core studies.

Reeh, N., Thomsen, H.H., and Clausen, H.B., **1987**, *Palaeogeography, Palaeoclimatology, Palaeoecology*, 58, 229-234, The Greenland ice-sheet margin – a mine of ice for paleo-environmental studies.

Bond, G. et al., **1992**, *Nature*, 360, 245-249, Evidence for massive discharges of icebergs into the North Atlantic ocean during the last glacial period.

Johnsen, S.J. et al., **1992**, *Nature*, 359, 311-313, Irregular glacial interstadials recorded in a new Greenland ice core.

Bond, G. et al., **1993**, *Nature*, 365, 143-147, Correlations between climate records from North Atlantic sediments and Greenland ice.

Chappellaz, J. et al., **1993**, *Nature*, 366, 443-445, Synchronous changes in atmospheric CH_4 and Greenland climate between 40 and 8 kyr BP.

Greenland Ice-core Project (GRIP) Members, **1993**, *Nature*, 364, 203-207, Climate

instability during the last interglacial period recorded in the GRIP ice core.

Grootes, P.M. et al., **1993**, *Nature*, 366, 552-555, Comparison of oxygen isotope records from the GISP2 and GRIP Greenland ice cores.

Taylor, K.C. et al., **1993**, *Nature*, 366, 549-552, Electrical conductivity measurements from the GISP2 and GRIP Greenland ice cores.

Keigwin, L.D. and Jones, G.A., **1994**, *Journal of Geophysical Research*, 99, 12,397-12,410, Western North Atlantic evidence for millennial-scale changes in ocean circulation and climate.

Mayewski, P.A. et al., **1994**, *Science*, 263, 1747-1751, Changes in atmospheric circulation and ocean ice cover over the North Atlantic during the last 41,000 years.

Bond, G. and Lotti, R., **1995**, *Science*, 267, 1005-1010, Iceberg discharges into the North Atlantic on millennial time scales during the last glaciation.

Cortijo, E. et al., **1995**, *Paleoceanography*, 10, 911-926, Sedimentary record of rapid climatic variability in the North Atlantic Ocean during the last glacial cycle.

Maslin, M.A., Shackleton, N.J., and Pflaumann, U., **1995**, *Paleoceanography*, 10, 527-544, Surface water temperature, salinity, and density changes in the northeast Atlantic during the last 45,000 years: Heinrich events, deep water formation, and climatic rebounds.

Thomas, E. et al., **1995**, *Paleoceanography*, 10, 545-562, Northeastern Atlantic benthic foraminifera during the last 45,000 years: Changes in productivity seen from the bottom up.

Behl, R.J. and Kennett, J.P., **1996**, *Nature*, 379, 243-246, Brief interstadial events in the Santa Barbara basin, NE Pacific, during the past 60 kyr.

Brook, E.J., Sowers, T., and Orchardo, J., **1996**, *Science*, 273, 1087-1091, Rapid variations in atmospheric methane concentration during the past 110,000 years.

Saltzman, E.S., Whung, P.-Y., and Mayewski, P.A., **1997**, *Journal of Geophysical Research*, 102, 26,649-26,657, Methanesulfonate in the Greenland Ice Sheet Project 2 ice core.

Blunier, T. et al., **1998**, *Nature*, 394, 739-743, Asynchrony of Antarctic and Greenland climate change during the last glacial period.

Schultz, H., von Rad, U., and Erlenkeuser, H., **1998**, *Nature*, 393, 54-57, Correlation between Arabian Sea and Greenland climate oscillations of the past 110,000

years.

Stauffer, B. et al., **1998**, *Nature*, 392, 59-62, Atmospheric CO₂ concentration and millennial-scale climate change during the last glacial period.

Brook, E.J. et al., **1999**, In: *Mechanisms of Global Climate Change at Millennial Time Scales*, *Geophysical Monograph*, 112, 165-175, Atmospheric methane and millennial-scale climate change.

Brook, E. et al., **2000**, *Global Biogeochemical Cycles*, 14, 559-572, On the origin and timing of rapid changes in atmospheric methane during the last glacial period.

Dallenbach, A. et al., **2000**, *Geophysical Research Letters*, 27, 1005-1008, Changes in the atmospheric CH₄ gradient between Greenland and Antarctica during the Last Glacial and the transition to the Holocene.

Hendy, I.L. and Kennett, J.P., **2000**, *Paleoceanography*, 15, 30-42, Dansgaard-Oeschger cycles and the California current system: Planktonic foraminiferal response to rapid climate change in Santa Barbara Basin, Ocean Drilling Program hole 893A.

Indermühle, A. et al., **2000**, *Geophysical Research Letters*, 27, 735-738, Atmospheric CO₂ concentration from 60 to 20 kyr BP from the Taylor Dome ice core, Antarctica.

Shackleton, N.J., Hall, M.A. and Vincent, E., **2000**, *Paleoceanography*, 15, 565-569, Phase relationships between millennial-scale events 64,000-24,000 years ago.

Blunier, T. and Brook, E.J., **2001**, *Science*, 291, 109-112, Timing of millennial-scale climate change in Antarctica and Greenland during the last glacial period.

Broecker, W.S., **2001**, In: *preprint volume of the 12th Symposium on Global Change Climate Variations*, January 14-19, 2001, Albuquerque, New Mexico, AMS, Boston, MA, 175-176, A Dusty Past.

28) The 1500-year cycle

Eddy, J.A., **1976**, *Science*, 192, 1189-1202, The Maunder Minimum.

Stuiver, M. and Braziunas, T.F., **1993**, *The Holocene*, 3, 289-305, Sun, ocean climate and atmospheric ¹⁴CO₂: An evaluation of causal and spectral relationships.

Keigwin, L.D., **1996**, *Science*, 274, 1504-1508, The Little Ice Age and Medieval Warm Period in the Sargasso Sea.

Bond, G. et al., **1997**, *Science*, 278, 1257-1266, A pervasive millennial-scale cycle in North Atlantic Holocene and glacial climates.

Hormes, A., Schlüchter, and Stocker, T.F., **1998**, *Radiocarbon*, 40, 809-817, Minimal extension phases of Unteraarglacier (Swiss Alps) during the Holocene based on ¹⁴C analysis of wood.

Domack, E.W. and Mayewski, P.A., **1999**, *The Holocene*, 9, 247-251, Bi-polar ocean linkages: Evidence from late-Holocene Antarctic marine and Greenland ice-core records.

Beer, J., Mende, W., and Stellmacher, R., **2000**, *Quaternary Science Reviews*, 19, 403-415, The role of the sun in climate forcing.

deMenocal, P. et al., **2000**, *Quaternary Science Reviews*, 19, 347-361, Abrupt onset and termination of the African Humid Period: Rapid climate responses to gradual insolation forcing.

deMenocal, P. et al., **2000**, *Science*, 288, 2198-2202, Coherent high- and low-latitude climate variability during the Holocene Warm Period.

Keeling, C.D. and Whorf, T.P., **2000**, *PNAS*, 97, 3814-3819, The 1,800-year oceanic tidal cycle: A possible cause of rapid climate change.

Keigwin, L.D. and Boyle, E.A., **2000**, *PNAS*, 97, 1243-1346, Detecting Holocene changes in thermohaline circulation.

Wunsch, C., **2000**, *Paleoceanography*, 15, 417-424, On sharp spectral lines in the climate record and the millennial peak.

Bond, G. et al., **2001**, *Science*, 294, 2130-2136, Persistent solar influence on North Atlantic climate during the Holocene.

Hormes, A., Müller, B.U., and Schlüchter, C., **2001**, *The Holocene*, 11, 255-265, The Alps with little ice: evidence for eight Holocene phases of reduced glacier extent in the Central Swiss Alps.

29) Global water budget

Weyl, P.K., **1968**, *Meteorological Monograph*, 8, 37-62; The importance of trans central America water vapor transport to thermohaline circulation in the Atlantic.

Baumgartner, A. and Reichel, E., **1975**, *Die Weltwasserbilanz*, Oldenbourg, Verlag, München, 179 p.; An assessment from measurements of the global fresh water budget.

Sarachik, E.S., **1978**, *Dynamics of the Atmospheric Oceans*, 2, 455-469; A one-dimensional atmosphere-ocean model for calculating the tropical sea surface temperature.

Warren, B.A., **1983**, *Journal Marine Research*, 41, 327-347; Fresh water transfer from Atlantic to Pacific and its prevention of deep water formation in the northern Pacific.

Oort, A.H., **1983**, *NOAA Professional Paper 14*; Global humidity distribution.

Peixoto, J.P. and Oort, A.H., **1983**, In: *Variations in the Global Water Budget*, D. Reidel, Hingham, Mass., 5-65; Water vapor transport through the atmosphere.

Lal, M. and Ramanathan, V., **1984**, *Journal of the Atmospheric Sciences*, 41, 2238-2249; Moist convection and water vapor content of the tropical atmosphere.

Betts, A.K. and Ridgway, W., **1989**, *Journal of the Atmospheric Sciences*, 46, 2621-2641; Extension of the Saracheck model for convection over the tropical ocean.

Ramanathan, V. et al., **1989**, *Science*, 243, 57-63, Cloud-radiative forcing and climate: Results from the Earth radiation budget experiment.

Raval, A. and Ramanathan, V., **1989**, *Nature*, 342, 758-761, Observational determination of the greenhouse effect.

Broecker, W.S., Peng, T.-H., Jouzel, J., and Russell, G., **1990**, *Climate Dynamics*, 4, 73-79, The magnitude of global fresh-water transports of importance to ocean circulation.

Lindzen, R.S., **1990**, *Bulletin of the American Meteorological Society*, 71, 288-299; The role of atmospheric water vapor in global warming.

Miller, J.R. and Russell, G.L., **1990**, *Paleoceanography*, 5, 397-407, Oceanic freshwater transport during the last glacial maximum.

Del Genio, A.D., Lacis, A.A., and Ruedy, R.A., **1991**, *Nature*, 351, 382-385; Simulation of water vapor changes induced by a CO₂ warming.

Hastenrath, S., **1991**, *Climate Dynamics of the Tropics*, Kluwer Academic Publishers, Dordrecht, Netherlands; Tropical moisture.

Kelly, K.K., Tuck, A.F., and Davies, T., **1991**, *Nature*, 353, 244-247, Wintertime asymmetry of upper tropospheric water between the Northern and Southern Hemispheres.

- Ramanathan, V. and Collins, W., **1991**, *Nature*, 351, 27-32, Thermodynamic regulation of ocean warming by cirrus clouds deduced from observations of the 1987 El Niño.
- Betts, A.K. and Ridgway, W., **1992**, *Journal of Geophysical Research*, 97, 2529-2534; Application of tropical boundary layer model to simulate glacial conditions.
- Wallace, J.M., **1992**, *Nature*, 357, 230-231; Relationship between deep convection and tropical sea surface temperature.
- Zaucker, F. and Broecker, W.S., **1992**, *Journal of Geophysical Research*, 97, 2765-2773, The influence of atmospheric moisture transport on the fresh water balance of the Atlantic Drainage Basin: General circulation model simulations and observations.
- Del Genio, A.D., Kovari, W. Jr., and Yao, M.-S., **1994**, *Geophysical Research Letters*, 21, 2701-2704; Seasonal variations in upper troposphere water vapor.
- Fu, R., Del Genio, A.D., and Rossow, W.B., **1994**, *Journal of Climate*, 7, 1092-1108; Relationship between sea surface temperature and deep convection in the tropical atmosphere.
- Zaucker, F., Stocker, T.F., and Broecker, W.S., **1994**, *Journal of the Geophysical Research*, 99, 12,443-12,457, Atmospheric freshwater fluxes and their effect on the global thermohaline circulation.
- Zhu, Y. and Newell, R.E., **1994**, *Geophysical Research Letters*, 21, 1999-2002, Atmospheric rivers and bombs.
- Pierrehumbert, R.T., **1995**, *Journal of the Atmospheric Sciences*, 52, 1784-1806, Thermostats, radiator fins, and the local runaway greenhouse.
- Broecker, W.S., **1997**, *Global Biogeochemical Cycles*, 11, 589-597, Mountain glaciers: Recorders of atmospheric water vapor content?
- Chýlek, P. and Geldart, D.J.W., **1997**, *Geophysical Research Letters*, 24, 2015-2018, Water vapor dimers and atmospheric absorption of electromagnetic radiation.
- Pierrehumbert, R.T., **1998**, *Geophysical Research Letters*, 25, 151-154, Lateral mixing as a source of subtropical water vapor.
- Schmittner, A., Appenzeller, C., and Stocker, T.F., **2000**, *Geophysical Research Letters*, 27, 1163-1166, Enhanced Atlantic freshwater export during El Niño.

30) Ocean thermohaline circulation

Stommel, H., **1961**, *Tellus*, 13, 324-328; Model showing that the ocean might have more than one stable mode of thermohaline circulation.

Weyl, P., **1968**, *Meteorological Monograph*, 8, 37-62; First proposal that water vapor transport through the atmosphere from the Atlantic to the Pacific Ocean might influence thermohaline circulation.

Stommel, H., **1980**, *Proc. National Academy Science USA*, 77, 2377-2381; Importance of the asymmetry of heat and water vapor fluxes to thermohaline circulation.

Welander, P., **1981**, *Dynamics of the Atmospheres and Oceans*, 5, 269-280; Simple salt-heat oscillators with reference to ocean thermohaline circulation.

Welander, P., **1982**, *Dynamics of the Atmospheres and Oceans*, 6, 233-242; More of same.

Welander, P., **1986**, In: Willebrand, J., and Anderson, D.L.T. (eds.), *Large-scale transport processes in ocean and atmosphere*, D. Reidel, Dordrecht, 379 pp.; More of same.

Bryan, F., **1986**, *Nature*, 323, 301-304; Role of high latitude salinity in variations of thermohaline circulation.

Gordon, A.L., **1986**, *Journal of Geophysical Research*, 91, 5037-5046; Intercean exchange of thermocline water and its influence on thermohaline circulation.

Manabe, S. and Stouffer, R.J., **1988**, *Journal of Climate*, 1, 841-866; Demonstration that two modes of thermohaline circulation can be induced in an ocean GCM by the same atmospheric forcing.

Birchfield, G.E., **1989**, *Climate Dynamics*, 4, 57-71; The interacting influences of salt and heat in a simple ocean model.

Maier-Reimer, E. and Mikolajewicz, U., **1989**, In: Ayala-Castañares, A., Wooster, W., and Yáñez-Arancibia (eds.) *Oceanography 1988*, Universidad Nacional Autónoma de México Press, Mexico City, 87-100; Demonstration that small doses of excess fresh water from the St. Lawrence drainage shut down the Atlantic's conveyor circulation in the Hamburg OGCM.

Broecker, W.S., Peng., T.-H., Trumbore, S., Bonani, G., and Wolfli, W., **1990**, *Biogeochemical Cycles*, 4, 103-117; Conceptual model of a soft oscillator operating in the Atlantic which might be responsible for the Dansgaard-Oeschger events.

Broecker, W.S., **1991**, *Oceanography*, 4, 79-89; Summary of today's global thermohaline circulation and how it may have changed in the past.

Stocker, T.F., Wright, D.G., and Broecker, W.S., **1992**, *Paleoceanography*, 7, 529-541; Influence of high latitude surface forcing on the thermohaline in a simple basin-averaged ocean circulation model.

Maier-Reimer, E., Mikolajewicz, U, and Hasselmann, K., **1993**, *Journal of Physical Oceanography*, 23, 731-757; Thermohaline circulation in the Hamburg Ocean GCM and its sensitivity to surface forcing.

Manabe, S. and Stouffer, R.J., **1993**, *Nature*, 364, 215-218; Response of the thermohaline circulation in a joint atmosphere-ocean GCM to an increase in atmospheric carbon dioxide.

Boyle, E. and Weaver, A., **1994**, *Nature*, 372, 41-42, Ocean circulation: Conveying past climates.

Manabe, S. and Stouffer, R.J., **1994**, *Journal of Climate*, 7, 5-23; Response of the thermohaline circulation in a joint atmosphere-ocean GCM to an increase in atmospheric carbon dioxide.

Döscher, R., Böning, C.W., and Herrmann, P, **1994**, *Journal of Physical Oceanography*, 24, 2306-2320; A model study of the response in North Atlantic circulation to surface forcing.

Mikolajewicz, U. and Maier-Reimer, E., **1994**, *Journal of Geophysical Research*, 99, 22,633-22,644; The sensitivity of conveyor circulation in the Hambrug OGCM to mixed boundary conditions.

Rahmstorf, S., **1994**, *Nature*, 372, 82-85; Two different Atlantic conveyor modes in a coupled atmosphere-ocean model.

Weaver, A.J. and Hughes, T.M.C., **1994**, *Nature*, 367, 447-450; Interglacial instabilities in the thermohaline circulation in a simple model.

Zaucker, F., Stocker, T.F., and Broecker, W.S., **1994**, *Journal of Geophysical Research*, 99, 12,443-12-457; Atmospheric fresh water fluxes and their influence on thermohaline circulation in a basin-averaged ocean circulation model.

Rahmstorf, S., **1995**, *Nature*, 378, 145-149, Bifurcations of the Atlantic thermohaline circulation in response to changes in the hydrological cycle.

Rahmstorf, S. and Willebrand, J., **1995**, *Journal of Physical Oceanography*, 25, 787-805, The role of temperature feedback in stabilizing the thermohaline circulation.

Rahmstorf, S., **1996**, *Journal of Physical Oceanography*, 26, 1100-1105, Comments on
“Instability of the thermohaline circulation with respect to mixed boundary
conditions: Is it really a problem for realistic models?”

Fanning, A.F. and Weaver, A.J., **1997**, *Paleoceanography*, 12, 307-320, Temporal-
geographical meltwater influences on the North Atlantic Conveyor: Implications
for the Younger Dryas.

Tziperman, E., **1997**, *Nature*, 386, 592-595, Inherently unstable climate behaviour due to
weak thermohaline ocean circulation.

Ganopolski, A. et al., **1998**, *Nature*, 391, 351-356, Simulation of modern and glacial
climates with a coupled global model of intermediate complexity.

Weaver, A.J. et al., **1998**, *Nature*, 394, 847-853, Simulated influence of carbon dioxide,
orbital forcing and ice sheets on the climate of the Last Glacial Maximum.

Tziperman, E., **2000**, *Journal of Physical Oceanography*, 30, 90-104, Proximity of the
present-day thermohaline circulation to an instability threshold.

Ganopolski, A. and Rahmstorf, S., **2001**, *Nature*, 409, 153-158, Rapid changes of glacial
climate simulated in a coupled climate model.

Broecker, W.S., in press, **2002**, *Israel Journal of Chemistry*, Constraints on the Glacial
Operation of the Atlantic Ocean’s Conveyor Circulation.